APPLIED AERODYNAMICS

APPLIED AERODYNAMICS

BY

LEONARD BAIRSTOW, F.R.S., C.B.E.,

EXPERT ADVISER ON AERODYNAMICS TO THE AIR MINISTRY: MEMBER OF THE ADVISORY COMMITTEE
FOR AERONAUTICS, AIR INVENTIONS COMMITTEE, ACCIDENTS INVESTIGATION COMMITTEE,
AND ADVISORY COMMITTEE ON CIVIL AVIATION; LATE SUPERINTENDENT OF THE
AERODYNAMICS DEPARTMENT OF THE NATIONAL PHYSICAL LABORATORY

WITH ILLUSTRATIONS AND DIAGRAMS

LONGMANS, GREEN AND CO.

39 PATERNOSTER ROW, LONDON
FOURTH AVENUE & 30TH STREET, NEW YORK
BOMBAY, CALCUTTA, AND MADRAS

1920

PREFACE

THE work aims at the extraction of principles of flight from, and the illustration of the use of, detailed information on aeronautics now available from many sources, notably the publications of the Advisory Committee for Aeronautics. The main outlines of the theory of flight are simple, but the stage of application now reached necessitates careful examination of secondary features. This book is cast with this distinction in view and starts with a description of the various classes of aircraft, both heavier and lighter than air, and then proceeds to develop the laws of steady flight on elementary principles. Later chapters complete the detail as known at the present time and cover predictions and analyses of performance, aeroplane acrobatics, and the general problems of control and stability. The subject of aerodynamics is almost wholly based on experiment, and methods are described of obtaining basic information from tests on aircraft in flight or from tests in a wind channel on models of aircraft and aircraft parts.

The author is anxious to acknowledge his particular indebtedness to the Advisory Committee for Aeronautics for permission to make use of reports issued under its authority. Extensive reference is made to those reports which, prior to the war, were issued annually; it is understood that all reports approved for issue before the beginning of 1919 are now ready for publication. To this material the author has had access, but it will be understood by all intimately acquainted with the reports that the contents cannot be fully represented by extracts. The present volume is not an attempt at collection of the results of research, but a contribution to their application to industry.

For the last year of the war the author was responsible to the Department of Aircraft Production for the conduct of aerodynamic research on aeroplanes in flight, and his thanks are due for permission to make use of information acquired. For permission to reproduce photographs acknowledgment is made to the Admiralty Airship Department, Messrs. Handley Page and Co., the British and Colonial Aeroplane Co., the Phœnix Dynamo Co., Messrs. D. Napier and Co., and H.M. Stationery Office.

L. BAIRSTOW.

HAMPTON WICK,
October 6th, 1919.

CONTENTS

CHAPTER I

GENERAL DESCRIPTION OF STANDARD FORMS OF AIRCRAFT

CHAPTER II

THE PRINCIPLES OF FLIGHT

CHAPTER III

GENERAL DESCRIPTION OF METHODS OF MEASUREMENT IN AERODYNAMICS AND THE PRINCIPLES UNDERLYING THE USE OF INSTRUMENTS AND SPECIAL APPARATUS

CHAPTER IV

DESIGN DATA FROM THE AERODYNAMICS LABORATORIES

CHAPTER V

AERIAL MANOEUVRES AND THE EQUATION OF MOTION

CHAPTER VI

AIRSCREWS

CHAPTER VII

FLUID MOTION

CHAPTER VIII

DYNAMICAL SIMILARITY AND SCALE EFFECTS

CHAPTER IX

THE PREDICTION AND ANALYSIS OF AEROPLANE PERFORMANCE

CHAPTER X

THE STABILITY OF THE MOTIONS OF AIRCRAFT

APPENDIX

LIST OF PLATES

FOURTEEN TONS OF MATTER IN FLIGHT

CHAPTER I

INTRODUCTION

IN the opening references to aircraft as represented by photographs of modern types, both heavier-than-air and lighter-than-air, attention will be more especially directed to those points which specifically relate to the subject-matter of this book, *i.e.* to applied aerodynamics. Strictly interpreted, the word " aerodynamics " is used only for the study of the forces on bodies due to their motion through the air, but for many reasons it is not convenient to adhere too closely to this definition. In the case of heavier-than-air craft one of the aerodynamic forces is required to counterbalance the weight of the aircraft, and is therefore directly related to a non-dynamic force. In lighter-than-air craft, size depends directly on the weight to be carried, but the weight itself is balanced by the buoyancy of a mass of entrapped hydrogen which again has no dynamic origin. As the size of aircraft increases, the resistance to motion at any predetermined speed increases, and the aerodynamic forces for lighter-than-air craft depend upon and are conditioned by non-dynamic forces.

The inter-relation indicated above between aerodynamic and static forces has extensions which affect the external form taken by aircraft. One of the most important items in aircraft design is the economical distribution of material so as to produce a sufficient margin of strength for the least weight of material. Accepting the statement that additional resistance is a consequence of increased weight, it will be appreciated that the problem of external form cannot be determined solely from aerodynamic considerations. As an example of a simple type of compromise may be instanced the problem of wing form. The greatest lift for a given resistance is obtained by the use of single long and narrow planes, the advantage being less and less marked as the ratio of length to breadth increases, but remaining appreciable when the ratio is ten. Most aeroplanes have this " aspect ratio " more nearly equal to six then ten, and instead of the single plane a double arrangement is preferred, the effect of the doubling being an appreciable loss of aerodynamic efficiency. The reasons which have led to this result are partly accounted for by a special convenience in fighting which accompanies the use of short planes, but a factor of greater importance is that arising from the strength desiderata. The weight of wings of large aspect ratio is greater for a given lifting capacity than that of short wings, and the external support necessary in all types of aeroplane is more difficult to achieve with aerodynamic economy for a single than for a double plane. Aerodynamically, a limit is fixed to the weight

APPLIED AERODYNAMICS
carried by a wing at a chosen speed, and for safe alighting the tendency has been to fix this speed at a little over forty miles an hour. This gives a lower limit to the wing area of an aeroplane which has to carry a specified weight. The general experience of designers has been that this limit is a serious restriction in the design of a monoplane, but offers very little difficulty in a biplane. In a few cases, three planes have been superposed, but the type has not received any general degree of acceptance. For small aeroplanes, the further loss of aerodynamic efficiency in a triplane has been accepted for the sake of the greater rapidity of manœuvre which can be made to accompany reduced span and chord, whilst in very large aeroplanes the chief advantage of the triplane is a reduction of the overall dimensions. Up to the present time it appears that an advantage remains with the biplane type of construction, although very good monoplanes and triplanes have been built.

The illustration shows that aircraft have entered the stage of " engineering " as distinct from " aerodynamical science " in that the final product is determined by a number of considerations which are mutually restrictive and in which the practical knowledge of usage is a very important factor in the attainment of the best result.

Although air is the fluid indicated by the term " aerodynamics," it has been found that many of the phenomena of fluid motion are independent of the particular fluid moved. Advantage has been taken of this fact in arranging experimental work, and in a later chapter a striking optical illustration of the truth of the above observation is given. The distinction between aerodynamics and the dynamics of fluid motion tends to disappear in any comprehensive treatment of the subject.

In the consideration of aerial manœuvres and stability the aerodynamics of the motion must be related to the dynamics of the moving masses. It is usual to assume that aircraft are rigid bodies for the purposes indicated, and in general the assumption is justifiable. In a few cases, as in certain fins of airships which deflect under load, greater refinement may be necessary as the science of aeronautics develops.

It will readily be understood that aerodynamics in its strict interpretation has little direct connection with the internal construction of aircraft, the important items being the external form and the changes of it which give the pilot control over the motion. As the subject is in itself extensive, and as the internal structure is being dealt with by other writers, the present book aims only at supplying the information by means of which the forces on aircraft in motion may be calculated.

The science of aerodynamics is still very young, and it is thirteen years only since the first long hop on an aeroplane was made in public by Santos Dumont. The circuit of the Eiffel Tower in a dirigible balloon preceded this feat by only a short period of time. Aeronautics attracted the attention of numerous thinkers during past centuries, and many historical accounts are extant dealing with the results of their labours. For many reasons early attempts at flight all fell short of practical success, although they advanced the theory of the subject in various degrees. The present epoch of aviation may be said to have begun with the publication of the

experiments made by Langley in America in the period 1890 to 1900. The apparatus used was a whirling arm fitted with various contrivances for the measurement of the forces on flat plates moved through the air at the end of the arm.

One line of experiment may perhaps be described briefly. A number of plates of equal area were made and arranged to have the same total weight, after which they were constrained to remain horizontal and to fall down vertical guides at the end of the whirling arm. The time of fall of the plates through a given distance was measured and found to depend, not only on the speed of the plate through the air, but also on its shape. At the same speed it was found that the plates with the greatest dimension across the wind fell more slowly than those of smaller aspect ratio. For small velocities of fall the time of fall increased markedly with the speed of the plate through the air. By a change of experiment in which the plates were held on the whirling arm at an inclination to the horizontal and by running the arm at increasing speeds the value of the latter when the plate just lifted itself was found. Repetition of this experiment showed that a particular inclination gave less resistance than any other for the condition that the plate should just be airborne.

From Langley's experiments it was deduced that a plate weighing two pounds per square foot could be supported at 35 m.p.h. if the inclination was made eight degrees. The resistance was then one-sixth of the weight, and making allowance for other parts of an aeroplane it was concluded that a total weight of 750 lbs. could be carried for the expenditure of 25 horsepower. Early experimenters set themselves the task of building a complete structure within these limitations, and succeeded in producing aircraft which lifted themselves.

Langley put his experimental results to the test of a flight from the top of a houseboat on the Potomac river. Owing to accident the aeroplane dived into the river and brought the experiment to a very early end.

In England, Maxim attempted the design of a large aeroplane and engine, and achieved a notable result when he built an engine, exclusive of boilers and water, which weighed 180 lbs. and developed 360 horsepower. To avoid the difficulties of dealing with stability in flight, the aeroplane was made captive by fixing wheels between upper and lower rails. The experiments carried out were very few in number, but a lift of 10,000 lbs. was obtained before one of the wheels carried away after contact with the upper rail.

For some ten years after these experiments, aviation took a new direction, and attempts to gain knowledge of control by the use of aeroplane gliders were made by Pilcher, Lilienthal and Chanute. From a hill built for the purpose Lilienthal made numerous glides before being caught in a powerful gust which he was unable to negotiate and which cost him his life. In the course of his experiments he discovered the great superiority of a curved wing over the planes on which Langley conducted his tests. By a suitable choice of curved wing it is possible to reduce the resistance to less than half the value estimated for flat plates of the same carrying capacity. The only control attempted in these early gliding experiments

was that which could be produced by moving the body of the aeronaut in a direction to counteract the effects of the wind forces.

In the same period very rapid progress was made in the development of the light petrol motor for automobile road transport, and between 1906 and 1908 it became clear that the prospects of mechanical flight had materially improved. The first achievements of power-driven aeroplanes to call for general attention throughout the world were those of two Frenchmen, Henri Farman and Bleriot, who made numerous short flights which were limited by lack of adequate control. These two pioneers took opposite views as to the possibilities of the biplane and monoplane, but in the end the first produced an aeroplane which became very popular as a training aeroplane for new pilots, whilst the second had the honour of the first crossing of the English Channel from France to Dover.

The lack of control referred to, existed chiefly in the lateral balance of the aeroplanes, it being difficult to keep the wings horizontal by means of the rudder alone. The revolutionary step came from the Brothers Wright in America as the result of a patient study of the problems of gliding. A lateral control was developed which depended on the twisting or warping of the aeroplane wings so that the lift on the depressed wing could be increased in order to raise it, with a corresponding decrease of lift on the other wing. As the changes of lift due to warping were accompanied by changes of drag which tended to turn the aeroplane, the Brothers Wright connected the warp and rudder controls so as to keep the aeroplane on a straight course during the warping. The principle of increasing the lift on the lower wing by a special control is now universally applied, but the rudder is not connected to the wing flap control which has taken the place of wing warping. From the time of the Wrights' first public flights in Europe in 1908 the aviators of the world began to increase the duration of their flights from minutes to hours. Progress became very rapid, and the speed of flight has risen from the 35 m.p.h. of the Henri Farman to nearly 140 m.p.h. in a modern fighting scout. The range has been increased to over 2000 miles in the bombing class of aeroplane, and the Atlantic Ocean has recently been crossed from Newfoundland to Ireland by the Vickers' " Vimy " bomber.

As soon as the problems of sustaining the weight of an aeroplane and of controlling the motion through the air had been solved, many investigations were attempted of stability so as to elucidate the requirements in an aeroplane which would render it able to control itself. Partial attempts were made in France for the aeroplane by Ferber, Seé and others, but the most satisfactory treatment is due to Bryan. Starting in 1903 in collaboration with Williams, Bryan applied the standard mathematical equations of motion of a rigid body to the disturbed motions of an aeroplane, and the culmination of this work appeared in 1911. The mathematical theory remains fundamentally in the form proposed by Bryan, but changes have been made in the method of application as the result of the development of experimental research under the Advisory Committee for Aeronautics. The mathematical theory is founded on a set of numbers obtained from experiment, and it is chiefly in the determination of these numbers that

development has taken place in recent years. Some extensions of the mathematical theory have been made to cover flight in a natural wind and in spiral paths.

Experimental work on stability on the model scale at the National Physical Laboratory was co-ordinated with flying experiments at the Royal Aircraft Factory, and the results of the mathematical theory of stability were applied by Busk in the production of the B.E. 2c. aeroplane, which, with control on the rudder only, was flown for distances of 60 or 70 miles on several occasions. By this time, 1914, the main foundations of aviation as we now know it had been laid. The later history is largely that of detailed development under stress of the Great War.

The history of airships has followed a different course. The problem of support never arose in the same way as for aeroplanes and seaplanes, as balloons had been known for many years before the advent of the airship. The first change from the free balloon was little more than the attachment of an engine in order to give it independent motion through the air, and the power available was very small. The spherical balloon has a high resistance, its course is not easily directed, and the dirigible balloon became elongated at its earliest stages. The long cigar-shaped forms adopted brought their own special difficulties, as they too are difficult to steer and are inclined to buckle and collapse unless sufficient precautions are taken. Steering and management has been attained in all cases by the fitting of fins, both horizontal and vertical, to the rear of the airship envelope, and the problem of affixing fins of sufficient area to the flexible envelope of an airship has imposed engineering limitations which prevent a simple application of aerodynamic knowledge.

The problem of maintenance of form of an airship envelope has led to several solutions of very different natures. In the non-rigid airship the envelope is kept inflated by the provision of sufficient internal pressure, either by automatic valves which limit the maximum pressure or by the pilot who limits the minimum. The interior of the envelope is divided by gastight fabric into two or three compartments, the largest of which is filled with hydrogen, and the smaller ones are fully or partially inflated with air either from the slip stream of an airscrew or by a special fan. As the airship ascends into air at lower pressure the valves to the air chambers open and allow air to escape as the hydrogen expands, and so long as this is possible loss of lift is avoided. The greatest height to which a non-rigid airship can go without loss of hydrogen is that for which the air chambers or balloonets are empty, and hence the size of the balloonets is proportioned by the ceiling of the airship.

If the car of an airship is suspended near its centre, the envelope at rest has gas forces acting on it which tend to raise the tail and head. The underside of the envelope is then in tension on account of the gas lift, whilst the upper side is in compression. As fabric cannot withstand compression, sufficient internal pressure is applied to counteract the effect of the lift in producing compression.

The car of the non-rigid airship is attached by cables to the underside of the envelope, and as these are inclined, an inward pull is exerted which

tends to neutralise the tension in the fabric. For some particular internal pressure the fabric will tend to pucker, and special experiments are made to determine this pressure and to distribute the pull in the cables so as to make the pressure as small as possible before puckering occurs. The experiment is made on a model airship which is inverted and filled with water. The loads in the cables, their positions and the pressure are all under control, and the necessary measurements are easily made. The theory of the experiment is dealt with in a later chapter.

In flight the exterior of the envelope is subjected to aerodynamic pressures which are intense near the nose, but which fall off very rapidly at points behind the nose. From a tendency of the nose to blow in under positive pressure, a change occurs to a tendency to suck out at a distance of less than half the diameter of the airship behind the nose, and this suction, in varying degrees, persists over the greater part of the envelope. At high speeds the tendency of the nose to blow in is very great as compared with the internal pressure necessary to retain the form of the rest of the envelope, and a reduction in the weight of fabric used is obtained if the nose is reinforced locally instead of maintaining its shape by internal pressure alone. In one of the photographs of this chapter the reinforcement of the nose is very clearly shown.

The problem of the maintenance of form of a non-rigid airship is appreciably simplified if the weight to be carried is not all concentrated in one car.

In the semi-rigid airship the envelope is still of fabric maintained to form by internal pressure, but between the envelope and car is interposed a long girder which distributes the concentrated load of the car over the whole surface of the envelope. This type of airship has been used in France, but has received most development in Italy; it is not used in this country.

Rigid airships depend upon a metal framework for the maintenance of their form, and in Germany were developed to a very high degree of efficiency by Count Zeppelin. The largest airships are of rigid construction and have a gross lift of nearly seventy tons. The framework is usually of a light aluminium alloy, occasionally of wood, and in the future steel may possibly be used. The structure is a light latticework system of girders running along and around the envelope and braced by wires into a stiff frame. In modern types a keel girder is provided inside the envelope at the bottom, which serves to distribute the load from the cars and also furnishes a communication way. The number of cars may be four or more, and the bending under the lift of the hydrogen is kept small by a careful choice of their positions. Some of the transverse girders are braced inside the envelope by a number of radial wires, the centres of which are joined by a wire running the whole length of the airship along its axis. In the compartments so produced the gas-containers are floated, and the lift is transferred to the rigid frame by the pressure on a netting of small cord.

The latticework is covered by fabric in order to produce a smooth unbroken surface and so keep down the resistance. Speeds of 75 m.p.h. have been reached in the latest British types of rigid airship, and the return

journey of many thousands of miles across the Atlantic has been made by the R 34 airship.

The duties for which the aeroplane and seaplane, non-rigid and rigid airships are suitable probably differ very widely. The heavier-than-air craft have a distinct superiority in speed and an equally distinct inferiority in range. The heavier-than-air craft must have an appreciable speed at first contact with the ground or sea, whilst airships are very difficult to handle in a strong wind. It is to be expected that each will find its position in the world's commerce, but the hurried growth of the aeronautical industry under the stimulus of war conditions has led to a state without precedent in the history of locomotion in that the means of production have developed far more rapidly than the civil demands.

In Britain, in particular, the progress of aeronautics has been assisted by the publications and work of the Advisory Committee for Aeronautics, and the country has now a very extensive literature on the subject. The Advisory Committee for Aeronautics was formed on April 30, 1909, by the Prime Minister " For the superintendence of the investigations at the National Physical Laboratory, and for general advice on the scientific problems arising in connection with the work of the Admiralty and War Office in aerial construction and navigation." The committee has worked in close co-operation with Service Departments, which have submitted for discussion and subsequent publication the results of research on flying craft. The Royal Aircraft Factory has conducted systematic research on the aerodynamics of aeroplanes, and the Admiralty Airship department has taken charge of all lighter-than-air craft. Standard tests on aircraft have also been carried out at Martlesham Heath and the Isle of Grain by the Air Ministry. The collected results were published annually until the outbreak of war in 1914, and are now being prepared for publication up to the present date. These publications form by far the greatest volume of aeronautical data in any country of the world, and from them a large part of this book is prepared.

In January, 1910, M. Eiffel described a wind channel which he had erected in Paris for the determination of the forces on plates and aeroplane wings, the first results being published later in the same year. The volumes containing Eiffel's results formed the first important contribution to the technical equipment of an aeronautical drawing office, and are well known throughout Britain. The aerodynamic laboratory was a private venture, and experiments for designers were carried out without charge, but with the rights of publication of the results.

For the Italian Government, Captain Crocco was at work on the aerodynamics of airships, and published papers on the subject of the stability of airships in April, 1907. He has since been intimately connected with the development of Italian airships. The chief aerodynamics laboratory, prior to 1914, in Germany was the property of the Parseval Airship Company, but was housed in the Göttingen University under the control of Professor Prandtl. Some particularly good work on balloon models was carried out and the results published in 1911, but in 1914 the German Government started a National laboratory in Berlin under

the direction of Prandtl, of which no results have been obtained in this country. Some of the German writers on stability were following closely along parallel lines to those of Bryan in Britain, and had, prior to 1914, arrived at the idea of maximum lateral stability.

The other European laboratory of note was at Koutchino near Moscow, with D. Riabouchinsky as director. This laboratory appears to have been a private establishment, and played a very useful part in the development of some of the fundamental theories of fluid motion. The practical demand on the time of the experimenters appears to have been less severe than in the more Western countries.

A National Advisory Committee for Aeronautics was formed at Washington on April 2, 1915, by the President of the United States. Reports of work have appeared from time to time which largely follow the lines of the older British Committee and add to the growing stock of valuable aeronautical data.

Before dealing with specific cases of aircraft it may be useful to compare and contrast man's efforts with the most nearly corresponding products of nature. Between the birds and the man-carrying aeroplane there are points of similarity and difference which strike an observer immediately. Both have wings, those in the bird being movable so as to allow of flapping, whilst those in the aeroplane are fixed to the body. Both the bird and the aeroplane have bodies which carry the motive power, in one case muscular and in the other mechanical. Both have the intelligence factor in the body, the aeroplane as a pilot. The aeroplane body is fitted with an airscrew, an organ wholly unrepresented in bird and animal life, the propulsion of the bird through the air as well as its support being achieved by the flapping of its wings. In both cases the bodies terminate in thin surfaces, or tails, which are used for control, but whilst the aeroplane has a vertical fin the bird has no such organ. The wings of a bird are so mobile at will that manœuvres of great complexity can be made by altering their position and shape, manœuvres which are not possible with the rigid wings of an aeroplane. In addition to the difference between airscrew and flapping wings, aeroplanes and birds differ greatly in the arrangements for alighting, the skids and wheels of the aeroplane being totally dissimilar to the legs of the bird.

The study of bird flight as a basis for aviation has clearly had a marked influence on the particular form which modern aeroplanes have taken, and no method of aerodynamic support is known which has the same value as that obtained from wings similar to those of birds. The fact that flapping motion has not been adopted, at least for extensive trial, appears to be due entirely to mechanical difficulties. In this respect natural development indicates some limitation to the size of bird which can fly. The smaller birds fly with ease and with a very rapid flapping of the wings ; larger birds spend long periods on the wing, but general information indicates that they are soaring birds taking advantage of up currents behind cliffs or a large steamer. With the still larger birds, the emu and ostrich, flight is not possible. The history of bird-life is in strict accordance with the mechanical principle that structures of a similar nature get

relatively weaker as they get larger. Man, although he has steel and a large selection of other materials at his disposal, has not found anything so much better than the muscle of the bird as to make the problem of supporting large weights by flapping flight any more promising than the results for the largest birds. In looking for an alternative to flapping the screw propeller as developed for steamships has been modified for aerial use, and at present is the universal instrument of propulsion.

The adoption of rigid wings in large flying machines in order to obtain sufficient strength also brought new methods of control. Mechanical principles relating to the effect of size on the capacity for manœuvre show that recovery from a disturbance is slower for the larger construction. The gusts encountered are much the same for birds and aeroplane, and the slowness of recovery of the aeroplane makes it improbable that the beautiful evolutions of a bird in countering the effects of a gust will ever be imitated by a man-carrying aeroplane. In one respect the aeroplane has a distinct advantage : its speed through the air is greater than that of the birds, and speed is itself one of the most effective means of combating the effect of gusts.

Further reference to bird flight is foreign to the purpose of this book, which relates to information obtained without special attention to the study of bird flight.

The airship envelope and the submarine have more resemblance to the fishes than to any other living creatures. Generally speaking, the form of the larger fishes provides a very good basis for the form of airships. It is curious that the fins of the fish are usually vertical as distinct from the horizontal tail feathers of the bird, and the fins over and under the central body have no counterpart in the airship. Both the artificial and living craft obtain support by displacement of the medium in which they are submerged, and rising and falling can be produced by moderate changes of volume. The resemblance between the fishes and airships is far less close than that between the birds and aeroplanes.

General Description of Particular Aircraft

A number of photographs of modern aircraft and aero engines are reproduced as typical of the subject of aeronautics. They will be used to define those parts which are important in each type. The details of the motion of aircraft are the subject of later chapters in which the conditions of steady motion and stability are developed and discussed.

The Aeroplane.—The frontispiece shows a large aeroplane in flight. Built by Messrs. Handley Page & Co., the aeroplane is the heaviest yet flown and weighs about 30,000 lbs. when fully loaded. Its engines develop 1500 horsepower and propel the aeroplane at a speed of about 100 miles an hour. It is of normal biplane construction for its wings, the special characteristics being in the box tail and in the arrangement of its four engines. Each engine has its own airscrew, the power units being divided into two by the body of the aeroplane, each half consisting of a pair of engines arranged back to back. One airscrew of each pair is working in

the draught of the forward screw, and this tandem arrangement is as yet somewhat novel.

Biplane (Fig. 1).—Fig. 1 shows a single-seater fighting scout, the S.E. 5, much used in the later stages of the war. Its four wings are of equal length, and form the two planes which give the name to the type. The lower wings are attached to the underside of the body behind the airscrew and engine cowl, whilst the upper wings are joined to a short centre section supported from the body on a framework of struts and wires. Away from the body the upper and lower planes are supported by wing struts and wire bracing, and the whole forms a stiff girder. In flight the load from the wings is transmitted to the body through the wing struts and the wires from their upper ends to the underside of the body. These wires are frequently referred to as lift wires. The downward load on the wings which accompanies the running of the aeroplane over rough ground is taken by " anti-lift " wires, which run from the lower ends of the wing struts to the centre section of the upper plane.

In the direction of motion of the aeroplane in flight are a number of bracing wires from the bottom of the various struts to the top of the neighbouring member. These wires stiffen the wings in a way which maintains the correct angle to the body of the aeroplane, and are known as incidence wires. The bracing system is redundant, *i.e.* one or more members may break without causing the collapse of the structure.

The wings of each plane will be seen from the photograph to be bent upwards in what is known as a dihedral angle, the object of which is to assist in obtaining lateral stability. For the lateral control, wing flaps are provided, the extent of which can be seen on the wings on the left of the figure. On the lower flap the lever for attachment of the operating cable is visible, the latter being led into the wing at the front spar, and hence by pulleys to the pilot's cockpit. The positions of the front and rear spars are indicated by the ends of the wing struts in the fore and aft direction, and run along the wings parallel to the leading edges.

The body rests on the spars of the bottom plane, and carries the engine and airscrew in the forward end. The engine is water-cooled, and the necessary radiators are mounted in the nose immediately behind the air-screw. Blinds, shown closed, are required in aeroplanes which climb to great heights, since the temperature is then well below the freezing-point of water, and unrestricted flow of air through the radiator during a glide would lead to the freezing of the water and to loss of control of the engine. The blinds can be adjusted to give intermediate degrees of cooling to correspond with engine powers intermediate between gliding and the maximum possible.

Alongside the body and stretching back behind the pilot's seat is one of the exhaust pipes which carry the hot gases well to the rear of the aeroplane. The pilot's seat is just behind the trailing edge of the upper wing. Above the exhaust pipe and near the front of the body is a cover over the cylinders on one side of the engine, the cover being used to reduce the air resistance.

The airscrew is in the extreme forward position on the aeroplane, and
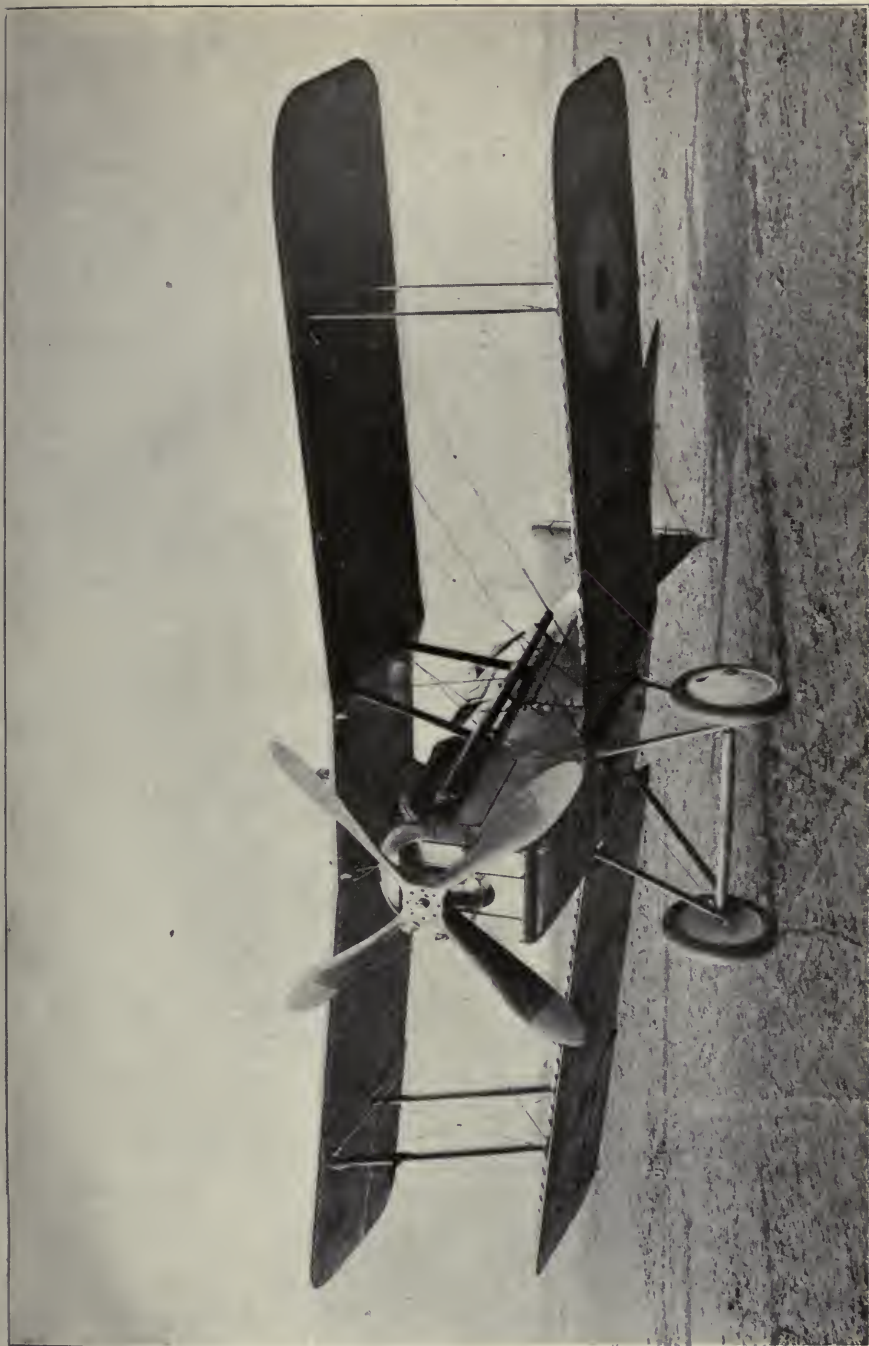
Fig. 1.—Fighting biplane scout.
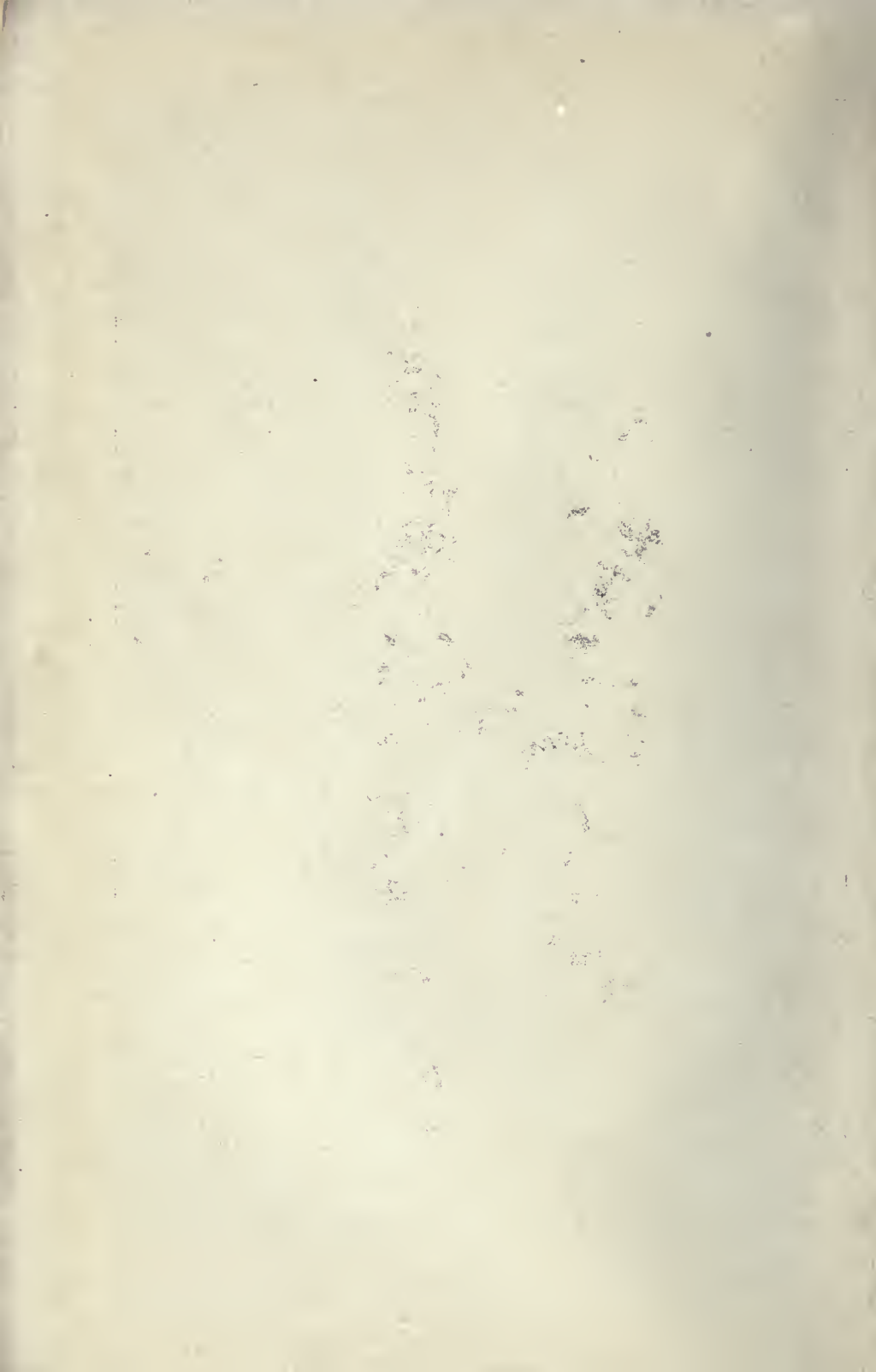
Fig. 2.—High-speed monoplane.

has four blades. The diameter is fixed in this case by the high speed of the airscrew shaft, and not, as in many cases, by the ground clearance required for safety when running over the ground.

Below the body and under the wings of the lower plane is the landing chassis. The frame consists of a pair of vee-shaped struts based on the body and joined at the bottom ends by a cross tube. The structure is supported by a diagonal cross-bracing of wires. The wheels and axle are held to the undercarriage by bindings of rubber cord so as to provide flexibility. The shocks of landing are taken partly by this rubber cord and partly by the pneumatic tyres on the wheels. With the aeroplane body nearly horizontal the wheel axle is ahead of the centre of gravity of the aeroplane, so that the effect of the first contact with the ground is to throw up the nose, increasing the angle of incidence and drag. If the speed of alighting is too great the lift may increase sufficiently to raise the aeroplane off the ground. The art of making a correct landing is one of the most difficult parts to be learnt by a pilot.

The tail of the aeroplane is not clearly shown in this figure, and description is deferred.

With an engine developing 210 horsepower and a load bringing the gross weight of the aeroplane to 2000 lbs., the aeroplane illustrated is capable of a speed of over 130 m.p.h. and can climb to a height of 20,000 feet. The limit to the height to which aircraft can climb is usually called the " ceiling."

Monoplane (Fig. 2).—The most striking difference from Fig. 1 is the change from two planes to a single one, and in order to support the wings against landing shocks, a pyramid of struts or " cabane " has been built over the body. From the apex of the pyramid bracing wires are carried to points on the upper sides of the front and rear spars. The lower bracing wires go from the spars to the underside of the body, and each is duplicated.

On the right wing near the tip is a tube anemometer used as part of the equipment for measuring the speed of the aeroplane. In biplanes the anemometer is usually fixed to one of the wing struts, as the effect of the presence of the wing on the reading is less marked than in the case now illustrated.

In this type of aeroplane, made by the British & Colonial Aeroplane Coy., the engine rotates, and the airscrew has a somewhat unusual feature in the " spinner " which is attached to it. The airscrew has two blades only, and this type of construction has been more common than the four-bladed type for reasons of economy of timber. The differences of efficiency are not marked, and either type can be made to give good service, the choice being determined in some cases by the speed of rotation of the airscrew shaft of an available engine.

The undercarriage is very similar to that shown in Fig. 1. On one of the front struts is a small windmill which drives a pump for the petrol feed. Windmills are now frequently used for auxiliary services, such as the electrical heating of clothing and the generation of current for the wireless transmission of messages.

The tail is clearly visible, and underneath the extreme end of the body

is the tail-skid. This skid is hinged to the body, and is secured by rubber cord at its inner end, so as to decrease the shock of contact with the ground.

The horizontal plane at the tail is seen to be divided, the front part or tailplane being fixed, whilst the rear part or elevator is movable at the pilot's wish. The control cables go inside the fuselage at the root of the tail plane. Underneath, the tail plane is seen to be braced to the body; above, the bracing wires are attached to the fin, which, like the tail plane, is fixed to the body. The rudder is hidden behind the fin, but the rudder lever for attachment of the control cable can be seen about halfway up the fin.

The pilot sits under the " cabane," and his downward view is helped by holes through the wings. Immediately in front of him is a wind screen, and also in this instance a machine-gun, which fires through the airscrew.

Flying-boat (Fig. 3).—The difference of shape from the land types is marked in several directions, as will be seen from the illustration relating to the Phoenix " Cork " flying-boat P. 5. The particular feature which gives its name to the type is the boat structure under the lower wing, and this replaces the wheel undercarriage of the aeroplane in order to render possible alighting on water. The flying boat is shown mounted on a trolley during transit from the sheds to the water. On the underside of the boat, just behind the nationality circles, is a step which plays an important part in the preliminary run on the water. A second step occurs under the wings at the place of last contact with the sea during a flight, but is hidden by the deep shadow of the lower wing.

Underneath the lower wing at the outer struts is a wing float which keeps the wing out of the water in any slight roll. The wing structure is much larger than those of Figs. 1 and 2, and there are six pairs of interplane struts. The upper plane is appreciably longer than the lower, the extensions being braced from the feet of the outer struts. The levers on the wing flaps or ailerons are now very clearly shown; owing to the proximity of waves to the lower wing, ailerons are not fitted to them.

The tail is raised high above the boat and is in the slip streams from the two airscrews. As the centre line of the airscrews is far above the centre of gravity, switching on the engine would tend to make the flying-boat dive, were it not so arranged that the slip-stream effect on the tail is arranged to give an opposite tendency. The fin and rudder are clearly shown, as are also the levers on the rudder and elevators. Besides having a dihedral angle on the wings, small fins have been fitted above the top wings as part of the lateral balance of the flying-boat.

The engines are built on struts between the wings, and each engine drives a tractor airscrew. The engines are run in the same direction, although at an early stage of development of flying-boats the effects of gyroscopic action of the rotatory airscrews were eliminated by arranging for rotation in opposite directions. This was found to be unnecessary.

The tail of the flying-boat has been especially arranged to come into the slip stream of the airscrews, but in aeroplanes this occurs without special provision or desire. Not only does the airscrew increase the air-speed over the tail, but it alters the angle of incidence and blows the tail

Fig. 3.—Large flying boat.
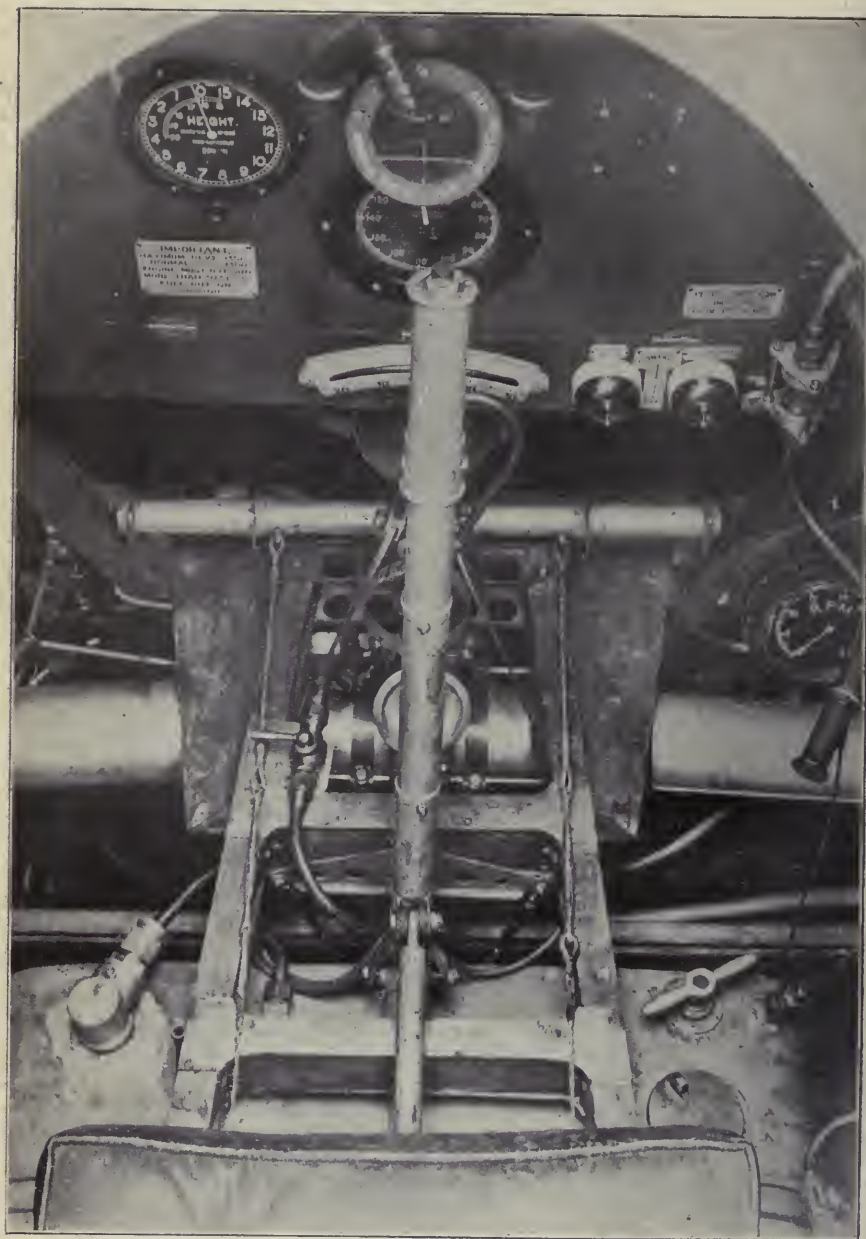
Fig. 4.—Cockpit of an aeroplane.

up or down depending on its setting. There is also a twist in the slip stream which is frequently unsymmetrically placed with respect to the fin and rudder and tends to produce turning. The effects of switching the engine on and off may be very complex.

In order to ease the pilot's efforts many aeroplanes are fitted with an adjustable tail plane, and if they are stable the adjustment can be made so as to give any chosen flying speed without the application of force to the control stick.

Pilot's Cockpit (Fig. 4).—The photograph of the " Panther " was taken from above the aeroplane looking down and forward. At the bottom of the figure is the edge of the seat which rests on the top of the petrol tank. Along the centre of the figure is the control column hinged at the bottom to a rocking shaft so that the pilot is able to move it in any direction. By suitable cable connections it is arranged that fore-and-aft movement depresses or raises the elevators, whilst movement to right or left raises or lowers the right ailerons. Some of the connections can be seen ; behind the control column is a lever attached to the rocking shaft and having at its ends the cables for the ailerons. The cables can be seen passing in inclined directions in front of the petrol tank. On the near side of the control column but partly hidden by the seat is the link which operates the elevators.

In the case of each control the motion of the column required is that which would be made were it fixed to the aeroplane and the pilot held independently and he attempted to pull the aeroplane into any desired position. In other words, if the pilot pulls the stick towards him the nose of the aeroplane comes up, whilst moving the column to the right brings the left wing up.

On the top of the control column is a small switch which is used by the pilot to cut out the engine temporarily, an operation which is frequently required with a rotary engine just before landing.

Across the photograph and a little below the engine control switches is the rudder bar, the hinge of which is vertical and behind the control column. The two cables to the rudder are seen to come straight back under the pilot's seat. In the rudder control the pilot pushes the rudder bar to the right in order to turn to the right.

Several instruments are shown in the photograph. In the top left corner is the aneroid barometer, which gives the pilot an approximate idea of his height. In the centre is the compass, an instrument specially designed for aircraft where the conditions of use are not very favourable to good results. Immediately below the compass and partly hidden by it is the airspeed indicator, which is usually connected to a tube anemometer such as was shown in Fig. 2 on the edge of the wing. Still lower on the instrument board and behind the control column is the cross-level which indicates to a pilot whether he is side-slipping or not. To the right of the cross-level are the starting switches for the engine, two magnetos being used as a precautionary measure. Below and to the right of the rudder bar is the engine revolution-indicator.

ENGINES

Air-cooled Rotary Engine (Fig. 5a).—In this type of engine, the B.R. 2, the airscrew is bolted to the crank case and cylinders, and the whole then rotates about a fixed crankshaft. The cylinders, nine in number, develop a net brake horsepower of about 230 at a speed of 1100 to 1300 revolutions per minute. The cylinders are provided with gills, which greatly assist the cooling of the cylinder due to their motion through the air. Without any forward motion of the aeroplane, cooling is provided by the rotation of the cylinders, and an appreciable part of the horsepower developed is absorbed in turning the engine against its air resistance. Air and petrol are admitted through pipes shown at the side of each cylinder, and both the inlet and exhaust valves are mechanically operated by the rods from the head of the cylinder to the crank case. The cam mechanism for operating the rods is inside the crank case. The hub for the attachment of the airscrew is shown in the centre.

A type of engine of generally similar appearance has stationary cylinders and is known as "radial." It is probable that the cooling losses in a radial engine are less than those in a rotary engine of the same net power, but no direct comparison appears to have been made. The effectiveness of an engine cannot be dissociated from the means taken to cool its cylinders. The resistance of cylinders in a radial engine and radiators in a water-cooled engine should be estimated and allowed for before comparison can be made with a rotary engine, the losses of which have already been deducted in the engine test-bed figures. For engines with stationary cylinders test-bed figures usually give brake horsepower without allowance for aerodynamic cooling losses.

Vee-type Air-cooled Engine (Fig. 5b).—The engine shown has twelve cylinders, develops about 240 horsepower and is known as the R.A.F. 4d. The cylinders are arranged above the crank case in two rows of six, with an angle between them, hence the name given to the type. In order to cool the cylinders a cowl has been provided, so that the forward motion of the aeroplane forces air between the cylinders and over the cylinder heads. At the extreme left of the photograph is the airscrew hub, and in this particular engine the airscrew is geared so as to turn at half the speed of the crankshaft, the latter making 1800 to 2000 r.p.m. To the right of and below the airscrew hub is one of the magnetos with its distributing wires for the correct timing of the explosions in the several cylinders. At the bottom of the photograph are the inlet pipes, carburettors, petrol pipes and throttle valves.

Water-cooled Engine (Fig. 6).—Water-cooled engines have been used more than any other type in both aeroplanes and airships. The two photographs of the Napier 450 h.p. engine show what an intricate mechanism the aero engine may be. The cylinders are arranged in three rows of four, each one being surrounded by a water jacket. The feed-pipes of the water-circulating system can be seen in Fig. 6b going from the water pump at the bottom of the picture to the lower ends of the cylinder jackets, whilst above them are the pipes which connect the
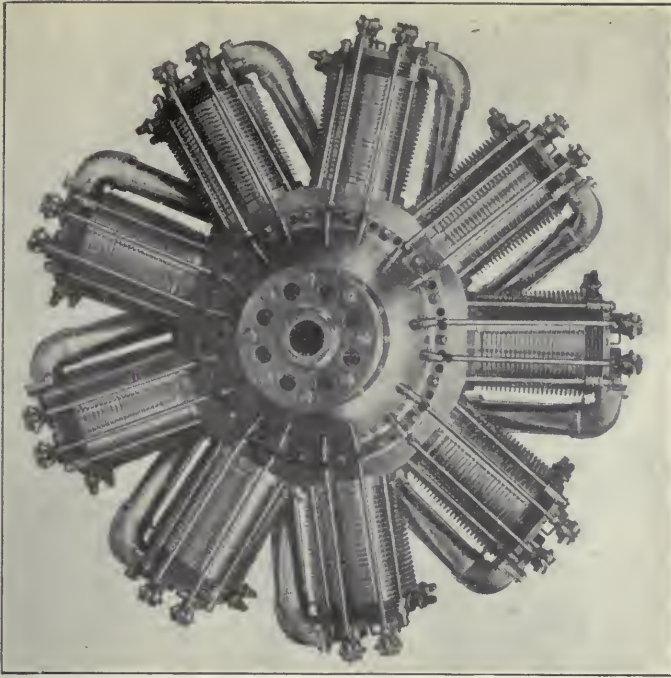
Fig. 5 (a).—Rotary engine.
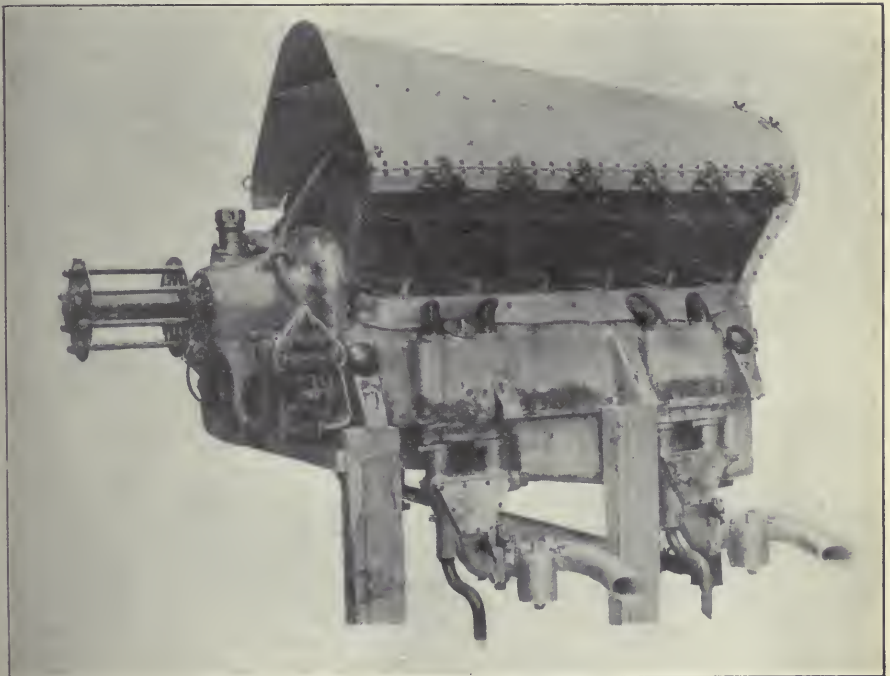
Fig. 5 (b).—Air-cooled stationary engine.

(b)

(a)
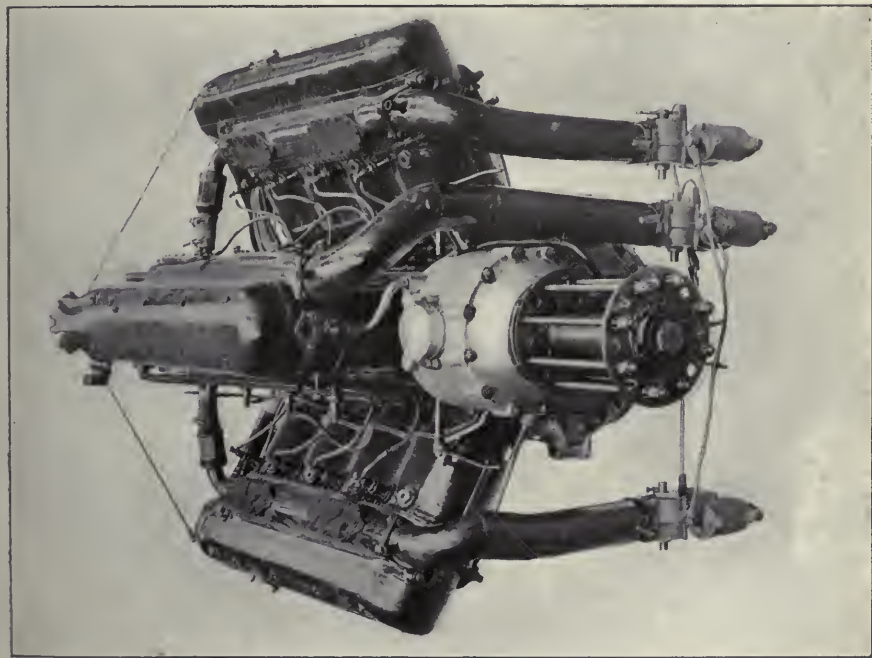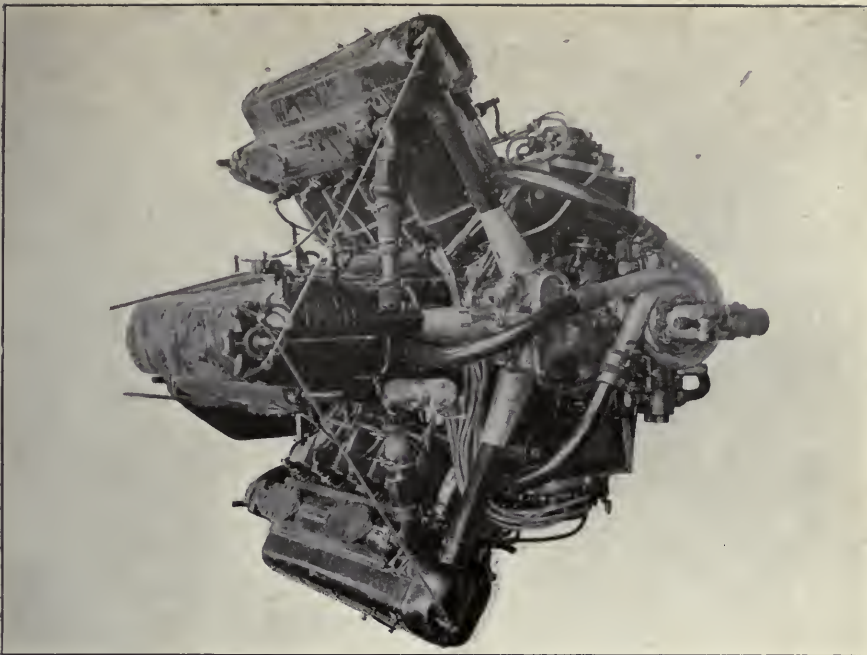
Fig. 6.—Water-cooled engine.

Fig. 7.—Rigid airship.
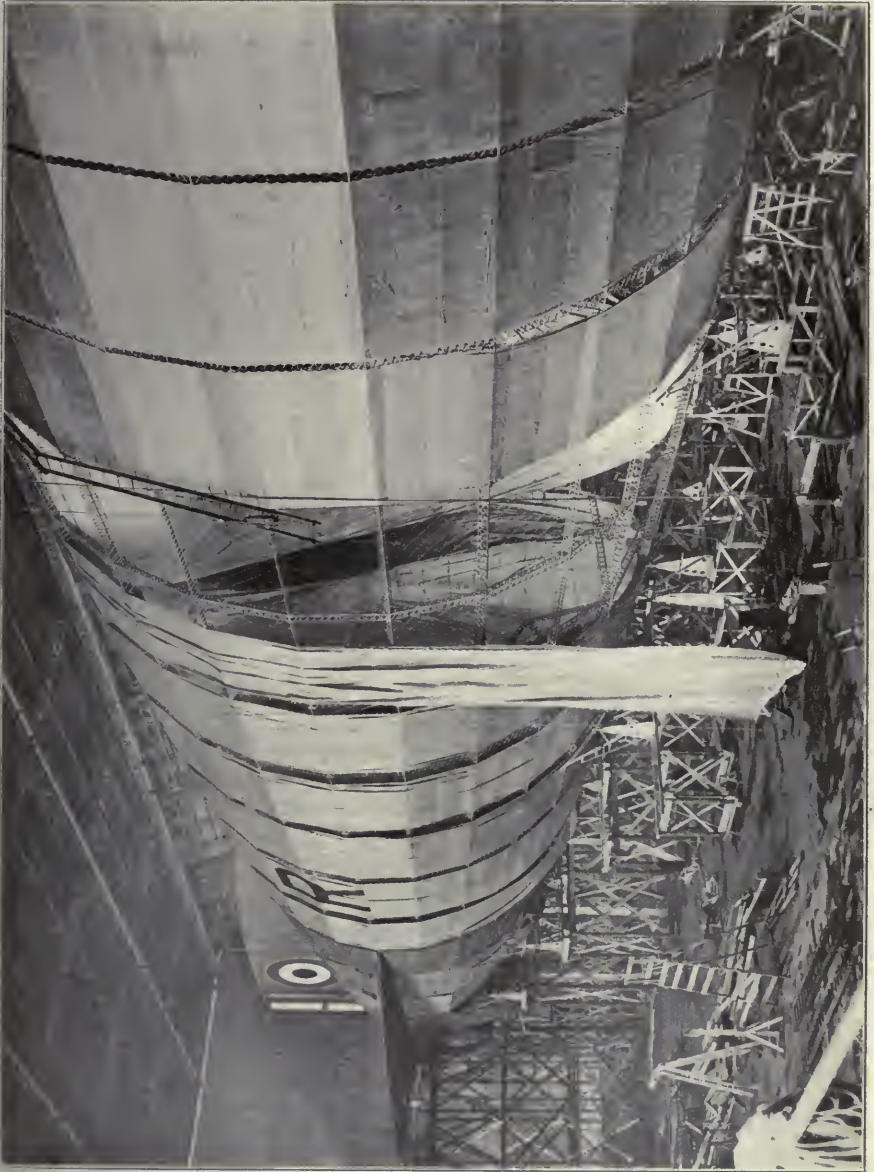
Fig. 8.—Nearly completed rigid airship.

outlets for the hot water and transmit the latter to the radiator. The camshafts which operate the inlet and exhaust valves run along the tops of the cylinders, and are carefully protected by covers; the inclined shafts, ending in gear cases at the top, connect the camshafts with the crankshaft of the engine.

The inlet pipes for the air and petrol mixture are shown in Fig. 6a; they are three in number, each feeding four cylinders and having its own carburetter. The magnetos are shown in Fig. 6b, on either side of the engine, with the distributing leads taken to supporting tubes along the engine. The same illustration also shows the location of the sparking plugs and the other end of the magneto connecting wires.

The airscrew is geared 0·66 to 1, and runs at about 1300 r.p.m.; the hub to which it is attached is clearly shown in Fig. 6a.

The engine is well known as the " Napier Lion," and was especially designed for work at altitudes of 10,000 feet and over. It represents the furthest advance yet made in the design of the aero-motor.

AIRSHIPS

The Rigid Airship (Figs. 7 and 8).—Rigid airships have been made with a total lift of nearly 70 tons, a length of 650 feet, and a diameter of envelope of about 80 feet. They are capable of extended flight, being afloat for days at a time whilst travelling many thousands of miles. The speeds reached with a horsepower of 2000 are a little in excess of 75 miles an hour. A photograph of a recent rigid airship is shown in Fig. 7. The sections of the envelope are polygonal, and the central part of the ship cylindrical. The head and tail are short and give the whole a form of low resistance. Still later designs have a much reduced cylindrical middle body and consequent longer head and tail, with an appreciably lower resistance.

To the rear of the airship are the fins which give stability and control, and in the instance illustrated the four fins are of equal size. The control surfaces, elevators and rudders, are attached at the rear edges of the fixed fins.

The airship has three cars; each contains an engine for the driving of a pair of airscrews. For the central car the airscrews are very clearly shown, but for the front and rear cars they have been turned into a horizontal position to assist the landing, and are seen in projection on the side of the cars, so that detection in the figure is much more difficult than for those of the central car. Below each of the end cars is a bumping bag to take landing shocks, whilst rope ladders connect the cars with a communication way in the lower part of the envelope.

Valves are shown at intervals along the ships, one for each of the gas containers, and serve to prevent an excess of internal pressure due to the expansion of the hydrogen. As arranged for flight, rigid airships can reach a height of 20,000 feet before the valves begin to operate. Fig. 8, R 34, shows the gas containers hanging loosely to the metal frame, which is just being fitted with its outer coverings. In the centre of the figure the skeleton is clearly visible, and consists of triangular girders running along

the ship and rings running round it. Two types of ring are visible, one of which is wholly composed of simple girders, whilst the second has king-posts as stiffeners on the inside. From the corners of this second frame radial wires pass to the centre of the envelope and form one of the divisions of the airship. The centres of the various radial divisions are connected by an axial wire, which takes the end pressure of the gas bags in the case of deflation of one of them or of inclination of the airship. The cord netting against which the gas bags rest can be seen very clearly. The airship is one built for the Admiralty by Messrs Beardmore.

The Non-rigid Airship (Fig. 9).—The non-rigid type of construction is essentially different from that described above, the shape of the envelope being maintained wholly by the internal gas pressure. The N.S. type of airship illustrated in Fig. 9 has a gross weight of 11 tons, and with 500 h.p. travels at a little more than 55 m.p.h. The length is 262 feet, and the maximum width of the envelope 57 feet. Fig. 9b gives the best idea of the cross-section of this type of airship, and shows three lobes meeting in well-defined corners. The type was originated in Spain by Torres Quevedo and developed in Paris by the Astra Company. It contains an internal triangular stiffening of ropes and fabric between the corners. The satisfactory distribution of loads on the fabric due to the weight of the car and engines is possible with this construction without necessitating suspension far below the lower surface of the envelope. Fig. 9c, taken from below the airship, shows the wires from the car to the junction of the lobes at the bottom of the envelope, and these take the whole load under level-keel conditions. To brace the car against rolling, wires are carried out on either side and fixed to the lobes at some distance from the plane of symmetry of the airship. The principle of relief of stress by distribution of load has been utilised in this ship, the car and engine nacelles being supported as separate units. Communication is permitted across a gangway which adds nothing of value to the distribution of load.

The engines are two in number, situated behind the observation car, and each is provided with its own airscrew. Beneath the engines and also below the car are bumping bags for use on alighting.

As the shape of the airship is dependent on the internal gas pressure, special arrangements are made to control this quantity, and the fabric pipes shown in Fig. 9c show how air is admitted for this purpose to enclosed portions of the envelope. The envelope is divided inside by gastight fabric, so that in the lower lobes both of the fore and rear parts of the airship, small chambers, or balloonets, are formed into which air can be pumped or from which it can be released. The position of these balloonets can be seen in Fig. 9c, at the ends of the pair of long horizontal feed pipes ; they are cross connected by fabric tubes which are also clearly visible. The high-pressure air is obtained from scoops lowered into the slip streams from the airscrews, the scoops being visible in all the figures, but are folded against the envelope in Fig. 9a. Valves are provided in the feed pipes for use by the pilot, who inflates or deflates the balloonets as required to allow for changes in volume of the hydrogen due to variations
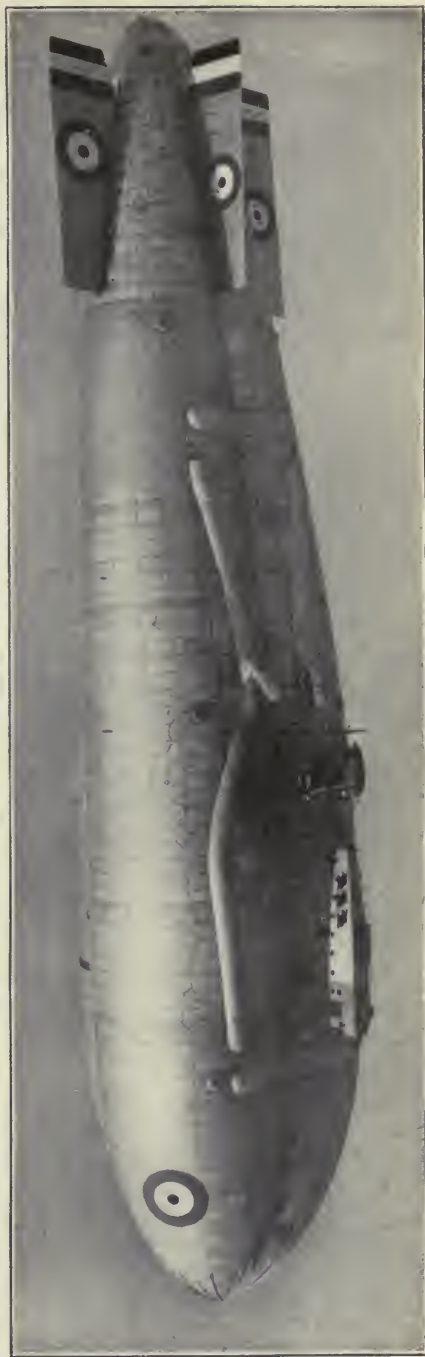
Fig. 9.—Non-rigid airship.

(a)
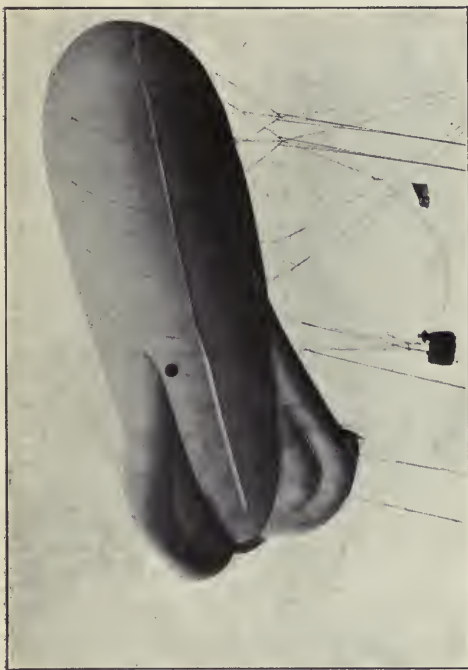
(b)

(c)

Fig. 10.—Kite balloons.

of height. Automatic valves are arranged to release air if the pressure rises above a chosen amount.

The weight of fabric necessary to withstand the pressure of the gas is greatly reduced by reinforcing the nose of the airship as shown in Fig. 9b. The maximum external air force due to motion occurs at the nose of the airship, and at high speeds becomes greater than the internal pressure usually provided. The region of high pressure is extremely local, and by the addition of stiffening ribs the excess of pressure over the internal pressure is transmitted back to a part of the envelope where it is easily supported by a small internal pressure. Occasionally the nose of an airship is blown in at high speed, but with the arrangements adopted the consequences are unimportant, and the correct shape is recovered by an increase of balloonet pressure.

The inflation of one balloonet and the deflation of the other is a control by means of which the nose of the airship can be raised or lowered, and so effect a change of trim, but the usual control is by elevators and rudders. In the N.S. type of airship the rudder is confined to the lower surface, and the upper fin is of reduced size. This, the largest of the non-rigid airships, is the product of the Admiralty Airship Department from their station at Kingsnorth, and has seen much service as a sea-scout.

Kite Balloons (Fig. 10).—The early kite balloon was probably a German type, with a string of parachutes attached to the tail in order to keep the balloon pointing into the wind. The lift on a kite balloon is partly due to buoyancy and partly due to dynamic lift, the latter being largely predominant in winds of 40 or 50 m.p.h. The balloon is captive, and may either be sent aloft in a natural wind or be towed from a ship. Two types of modern kite balloon are shown in Fig. 10, (a) and (b) showing the latest and most successful development. To the tail of the balloon are fixed three fins, which are kept inflated in a wind by the pressure of air in a scoop attached to the lower fin. With this arrangement the balloon swings slowly backwards and forwards about a vertical axis, and travels sideways as an accompanying movement.

The kite wire is shown in Fig. 10b as coming to a motor boat. The second rope which dips into the sea is an automatic device for maintaining the height of the balloon. The general steadiness of the balloon depends on the point of attachment of the kite wire, and the important difference illustrated by the types Fig. 10 (a) and (c) is that the latter becomes longitudinally unstable at high-wind speeds and tends to break away, whilst the former does not become unstable. The general disposition of the rigging is shown most clearly in Fig. 10a, where a rigging band is shown for the attachment of the car and kite line.

CHAPTER II

THE PRINCIPLES OF FLIGHT

(i) The Aeroplane

In developing the matter under the above heading, an endeavour will be made to avoid the finer details both of calculation and of experiment. In the later stages of any engineering development the amount of time devoted to the details in order to produce the best results is apt to dull the sense of those important factors which are fundamental and common to all discussions of the subject. It usually falls to a few pioneers to establish the main principles, and aviation follows the rule. The relations between lift, resistance and horsepower became the subject of general discussion amongst enthusiasts in the period 1896–1900 mainly owing to the researches of Langley. Maxim made an aeroplane embodying his views, and we can now see that on the subjects of weight and horsepower these early investigations established the fundamental truths. Methods of obtaining data and of making calculations have improved and have been extended to cover points not arising in the early days of flight, and one extension is the consideration of flight at altitudes of many thousands of feet.

The main framework of the present chapter is the relating of experimental data to the conditions of flight, and the experimental data will be taken for granted. Later chapters in the book take up the examination of the experimental data and the finer details of the analysis and prediction of aeroplane performance.

Wings.—The most prominent important parts of an aeroplane are the wings, and their function is the supporting of the aeroplane against gravitational attraction. The force on the wings arises from motion through the air, and is accompanied by a downward motion of the air over which the wings have passed. The principle of dynamic support in a fluid has been called the " sacrificial " principle (by Lord Rayleigh, I believe), and stated broadly expresses the fact that if you do not wish to fall yourself you must make something else fall, in this case air.

If AB, Fig. 11; be taken to represent a wing moving in the direction of the arrow, it will meet air at rest at C and will leave it at EE endued with a downward motion. Now, from Newton's laws of motion it is known that the rate at which downward momentum is given to the fluid is equal to the supporting force on the wings, and if we knew the exact motion of the air round the wing the upward force could be calculated. The problem is, however, too difficult for the present state of mathematical knowledge, and our information is almost entirely based on the results of tests on models of wings in an artificial air current.

18

The direct measurement of the sustaining force in this way does not involve any necessity for knowledge of the details of the flow. It is usual to divide the resultant force R into two components, L the lift, and D the drag, but the essential measurements in the air current are the magnitude of R and its direction γ, the latter being reckoned from the normal to the direction of motion. The resolution into lift and drag is not the only useful form, and it will be found later that in some calculations it is convenient to use a line fixed relative to the wing as a basis for resolution rather than the direction of motion.

No matter by what means the results are obtained, it is found that the supporting force or lift of an aeroplane wing can be represented by curves such as those of Fig. 12. The lifting force depends on the angle a (Fig. 11) which the aerofoil makes with the relative wind, and it is interesting to
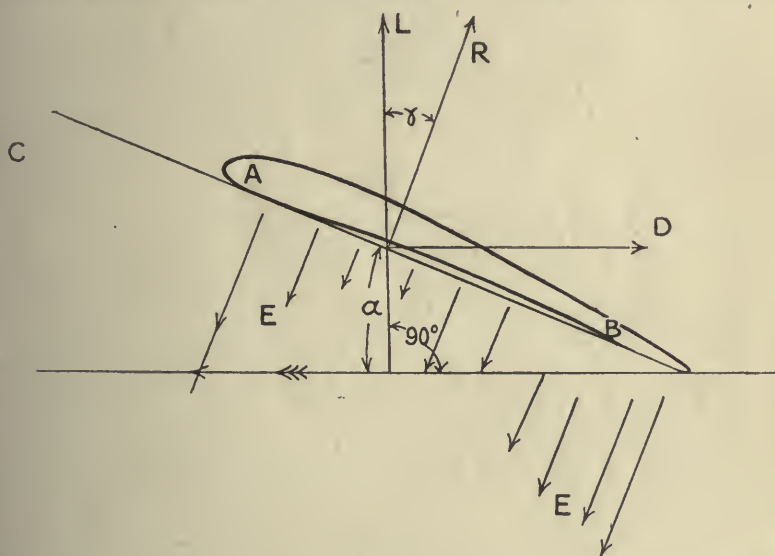
Fig. 11.

find that the lifting force may be positive when a is negative, *i.e.* when the relative wind is apparently blowing on the upper surface. The chord, *i.e.* the straight line touching the wing on the under surface, is inclined downwards at 3° or more before a wing of usual form ceases to lift.

The lift on the wing depends not only on the angle of incidence and of course the area, but also on the velocity relative to the air, and for full-scale aeroplanes the lift is proportional to the square of the speed at the same angle of incidence. Of course in any given flying machine the weight of the machine is fixed, and therefore the lift is fixed, and it follows from the above statement that only one speed of flight can correspond with a given angle of incidence, and that the speed and angle of incidence must change together in such a way that the lift is constant. This relation can easily be seen by reference to Fig. 12. The curve ABCDE is obtained by experiment as follows : A wing (in practice a model of it is used and

multiplying factors applied) is moved through the air at a speed of 40 m.p.h. In one experiment the angle of incidence is made zero, and the measured lift is 340 lbs. This gives the point P of Fig. 12. When the angle of incidence is 5° the lift is 900 lbs., and so on. In the course of such an experiment, there is reached an angle of incidence at which the lift is a maximum, and this is shown at D in Fig. 12 for an angle of incidence of 17° or 18°. For angles of incidence greater than this it is not possible to carry so much load at 40 m.p.h. Without any further experiments it is now possible to draw the remainder of the curves of Fig. 12. At B the lift for 40 m.p.h. has been found to be 610 lbs. At B_1 it will be $610 \times (\frac{50}{40})^2$ lbs.,
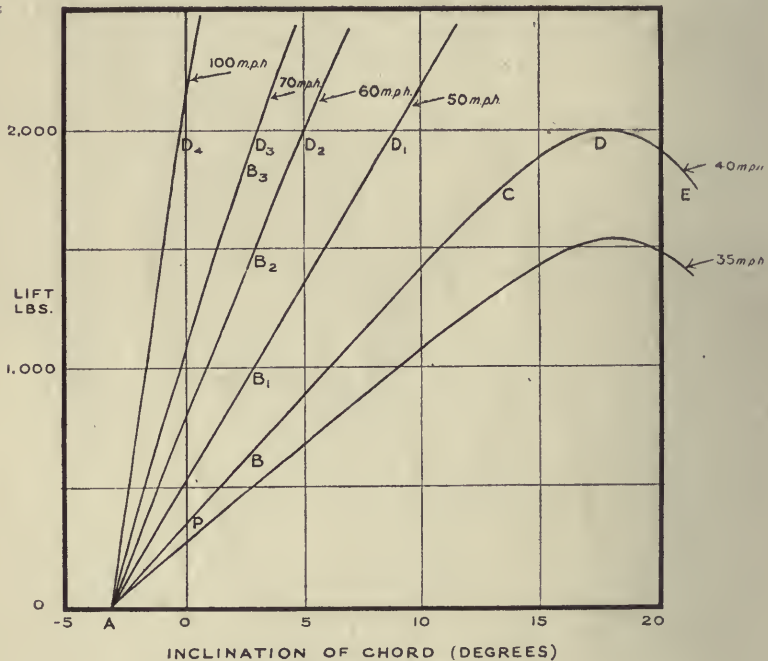
FIG. 12.—Wing lift and speed.

at B_2 $610 \times (\frac{60}{40})^2$ lbs., and so on, the lift for a given angle being proportional to the square of the speed.

Now suppose that the wings for which Fig. 12 was prepared are to be used on an aeroplane weighing 2000 lbs. At 35 m.p.h. the wings cannot be made to carry more than 1530 lbs., and consequently the aeroplane will need to get up a speed of more than 35 m.p.h. before it can leave the ground. At 40 m.p.h., as we see at D, the weight can just be lifted, and this constitutes the slowest possible flying speed of that aeroplane. The angle of incidence is then 17 to 18 degrees. If the speed is increased to 50 m.p.h. the required lift is obtained at an angle of incidence rather less than 9°, and so on, until if the engine is powerful enough to drive the aeroplane at 100 m.p.h. the angle of incidence has a small negative value.

It will be noticed that in this calculation no knowledge is needed of the resistance of the aeroplane or the horsepower of its engine. The angle of incidence for any speed is fixed entirely from the lift curves.

A common size of aeroplane in flying order weighs roughly 2000 lbs. The area of the four wings adopted in order to alight at 40 m.p.h. comes to be approximately 360 sq. feet. Flying at the lower speeds is almost entirely confined to the last few seconds before alighting.

Resistance or Drag.—All the parts of an aeroplane contribute to the resistance, whereas practically the whole of the lift is taken by the wings. The resistance is usually divided into two parts, one due to the wings and the other due to the remainder of the machine. The reason for this is that the resistance of the wings is not even approximately proportional to the square of the flying speed, because of the change of angle of incidence of the wings already shown to occur ; on the other hand, the resistance of each of the other parts is very nearly proportional to the square of the speed.

At low flight speeds the resistance of the wings is by far the greater of the two parts, whilst at higher speeds the body resistance may be appreciably greater than that of the wings.

Drag of the Wings.—The curves for the drag of the wings corresponding with those of Fig. 12 for the lift are given in Fig. 13. The curve marked ABCDE in Fig. 13 is obtained experimentally, usually at the same time as the similarly marked curve of Fig. 12. It shows the drag of the wings when travelling at 40 m.p.h. at various angles of incidence. At 0° the drag is little more than 30 lbs., whilst at 15° it is 300 lbs. B_1 is got from B by increasing the drag at the same angle of incidence in proportion to the square of the speed.

It has already been shown that there can only be one angle of incidence of the main planes for any one speed, and from Fig. 12 the relation between angle and speed for an aeroplane weighing 2000 lbs. was obtained. At a speed of 40 m.p.h. an angle of 17·5° was found, and point E of Fig. 13 shows that the resistance would then be 560 lbs. The points E_1, E_2, E_3 and E_4 similarly show the drag at 50, 60, 70 and 100 m.p.h. If the aeroplane is supposed to be flying slowly, *i.e.* at 40 m.p.h., and the speed be gradually increased, it will be seen that the drag due to the wings diminishes very rapidly at first from 560 lbs. at 40 m.p.h. to 130 lbs. at 50 m.p.h., and reaches a minimum of 99 lbs. at about 60 miles an hour, after which a marked increase occurs. Contrary to almost every other kind of locomotion, a very considerable reduction of resistance may result from increasing the speed of the aeroplane. It will be seen later that the reduction is so great that less horsepower is required at the higher speed.

Drag of the Body, Struts, Undercarriage, etc.—The drag of the aeroplane other than the wings is usually obtained by the addition of the measured resistances of many parts. The actual carrying out of the operation is one of some detail and is referred to later in the book (Chapter IV.). For present purposes it is sufficient to know that as the result of experiment, these additional resistances amount to about 50 lbs. at 40 m.p.h., and vary as the square of the speed, so that at 100 m.p.h. the additional resistances have increased to 312 lbs.

It is now possible to make Table 1 showing the resistance of the aeroplane at various speeds, and to estimate the net horsepower required to propel an aeroplane weighing 2000 lbs. The losses in the organs of propulsion will not be considered at this point, but will be dealt with almost immediately when determining the horsepower available.

A rough idea of the brake horsepower of the engine required for
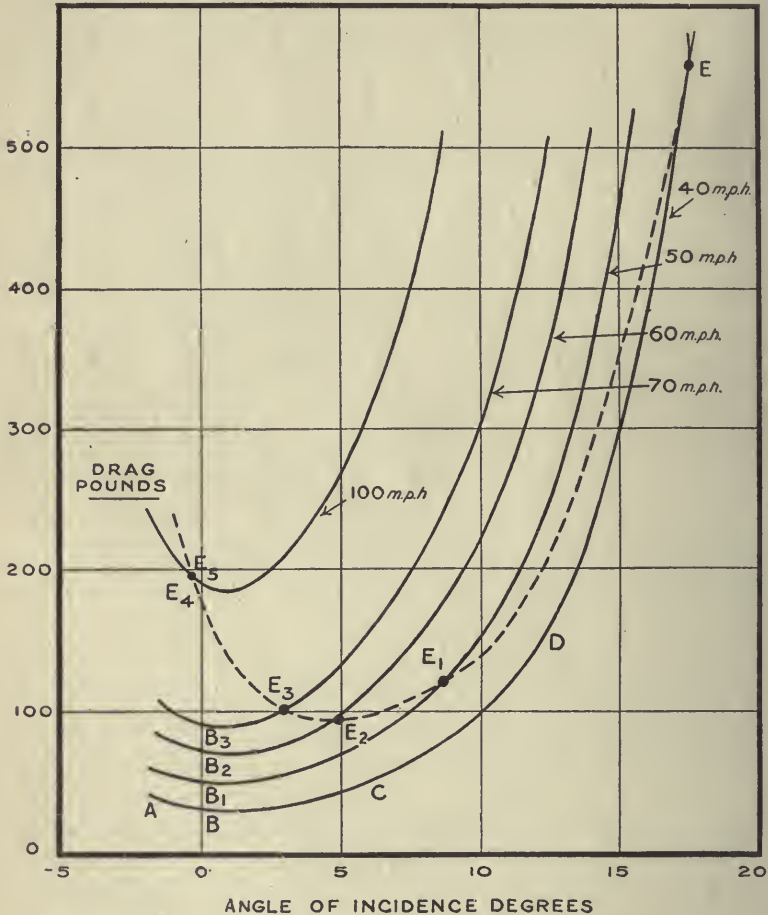
Fig. 13.—Wing drag and speed.

horizontal flight can be obtained by assuming a propeller efficiency of 60 per cent. in all cases. It will then be seen that the aeroplane would just be able to fly with an engine of 45 horsepower at a speed of approximately 50 m.p.h. At 70 m.p.h. the brake horsepower of the engine would need to be nearly 80, whilst to fly at 100 m.p.h. would need no less than 225 horsepower. By various modifications of wing area the horsepower for a given speed can be varied considerably, but the example given illustrates fairly accurately the limits of speed of an

aeroplane of the weight assumed; *e.g.* an engine developing 100 horse-power may be expected to give a flight-speed range of from 40 m.p.h. to 80 m.p.h. to an aeroplane weighing 2000 lbs.

TABLE 1.—AEROPLANE DRAG AND SPEED.

Speed of flight (m.p.h.).	Resistance of wings alone (lbs.).	Resistance of rest of aeroplane (lbs.).	Total resistance (lbs.).	Net horsepower required.*
40	560	50	610	65
50	130	78	208	28
60	97	113	210	34
70	100	153	253	47
100	195	312	507	134

The Propulsive Mechanism.—Up to the present the calculations have referred to the behaviour of the aeroplane, without detailed reference to the means by which motion through the air is produced. It is now proposed to show how the necessary horsepower is estimated in order that the aeroplane may fly. This estimate involves the consideration of the airscrew.

An airscrew acts on the air in a manner somewhat similar to that of a wing, and throws air backwards in a continuous stream in order to produce a forward thrust. The thrust is obtained for the least expenditure of power only when the revolutions of the engine are in a very special relation to the forward speed.

Increase of the speed of revolution without alteration of the forward speed of the aeroplane leads to increased thrust, but the law of increase is complex. Increasing the speed of the aeroplane usually has the effect of decreasing the thrust, again in a manner which it is not easy to express simply. Calculations can be made to show what the airscrew will do under any circumstances, but the discussion will be left to a special chapter.

One simple law can, however, be deduced from the behaviour of air-screws, and is of much the same nature as that already pointed out for the supporting surfaces. It was stated that, if the angle of incidence is kept constant, the lift and drag of a wing increase in proportion to the square of the speed. Now in the airscrew, it will be found that the angle of incidence of each blade section is kept constant if the revolutions are increased in the same proportion as the forward speed, and that under such conditions the thrust and torque both vary as the square of the speed. If from a forward speed of 40 m.p.h. and a rotational speed of 600 r.p.m. the forward speed be increased to 80 m.p.h. and the rotational speed to 1200 r.p.m., the thrust will be increased four times.

Given a table of figures, such as Table 2, which shows the thrust of an airscrew at several speeds of rotation when travelling at 40 m.p.h. through the air, results can be deduced for the thrust at other values of the forward speed in the manner described below.

* By net horsepower is here meant the power necessary to drive the aeroplane if a perfectly efficient means of propulsion existed. The conditions are very nearly satisfied by an aeroplane when gliding.

The figures in Table 2 would be obtained either by calculation or by an experiment. Tests on airscrews are frequently made at the end of a long arm which can be rotated, so giving the airscrew its forward motion. Actual airscrews may be tested on a large whirling arm, or a model airscrew may be used in a wind channel and multiplying factors employed to allow for the change of scale.

TABLE 2.—Airscrew Thrust and Speed.

Forward speed 40 m.p.h.	
Revs. per minute.	Thrust (lbs.).
500	0
800	162
1100	374
1400	620

It will be noticed from Table 2 that the airscrew gives no thrust until rotating faster than 500 r.p.m. At lower speeds than this the airscrew would oppose a resistance to the forward motion, and would tend to be turning as a windmill. When the subject is entered into in more detail it will be found that the number of revolutions necessary before a thrust is produced is determined by the " pitch " of the airscrew. The term " pitch " is obtained from an analogy between an airscrew and a screw, the advance of the latter along its axis for one complete revolution being known as the " pitch." Whilst there are obvious mechanical differences between a solid screw turning in its nut and an airscrew moving in a mobile fluid, the expression has many advantages in the latter case and will be referred to frequently. For the present it is not necessary to know how pitch is defined.

The numbers given in Table 2 correspond with the curve marked ABC in Fig. 14. To deduce those for any other speed, say 60 m.p.h., the first column is multiplied by $\frac{60}{40}$ and the second by $(\frac{60}{40})^2$, giving the following table :—

TABLE 3.—Airscrew Thrust and Speed.

Forward speed 60 m.p.h.	
Revs. per minute.	Thrust (lbs).
750	0
1200	365
1650	842
2100	1400

It will be noticed that the airscrew must now be rotating much more rapidly than before in order to produce a thrust. The remaining curves of Fig. 14 were produced in a similar way, and relate to speeds of the

aeroplane which were considered in the supporting of an aeroplane weigh-
ing 2000 lbs. The thrust necessary to support the aeroplane in the air at
speeds of 40, 50, 60, 70 and 100 m.p.h. has been obtained in Table 1, and
using Fig. 14 it is now possible to obtain the propeller revolutions which
are necessary to produce this required thrust. The points are marked
C, C_1, C_2, C_3 and C_4. To produce a thrust of 610 lbs. at 40 m.p.h. the
propeller must be turning at about 1380 r.p.m., as shown at the point C.
As the speed rises to 50 m.p.h. the engine may be shut down very appre-
ciably, the revolutions being only 930. For higher velocities of flight the
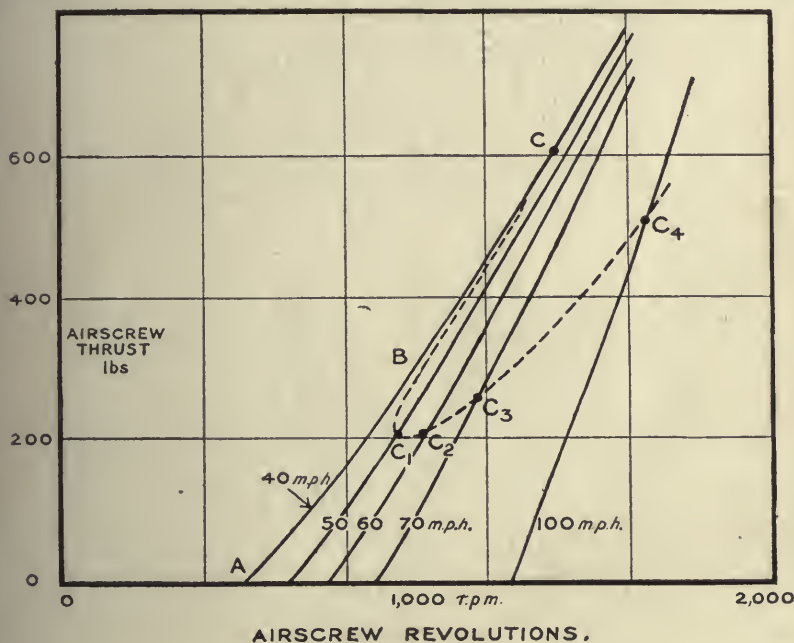
FIG. 14.—Thrust and speed.

necessary revolutions increase steadily, until at 100 m.p.h. the rate of rota-
tion is over 1600 r.p.m. The engine may, however, not be powerful enough
to drive the propeller at these rates, and it is now necessary to estimate,
in a manner similar to that for thrust, how much horsepower is required.
The initial data given in Table 4 are again assumed to have been

TABLE 4.—AIRSCREW HORSEPOWER AND SPEED.

Forward speed 40 m.p.h.

Revs. per minute.	Horsepower.
500	3·0
800	27
1100	76
1400	167

obtained experimentally, and the figures from this table are plotted in Fig. 15 in the curve ABC. To obtain the curve for 60 m.p.h. the first column of Table 4 is multiplied by $\frac{60}{40}$ and the second by $(\frac{60}{40})^3$, obtaining the numbers given in Table 5.

TABLE 5.—AIRSCREW HORSEPOWER AND SPEED.

Forward speed 60 m.p.h.	
Revs. per minute.	Horsepower.
750	10·1
1200	91
1650	256
2100	710
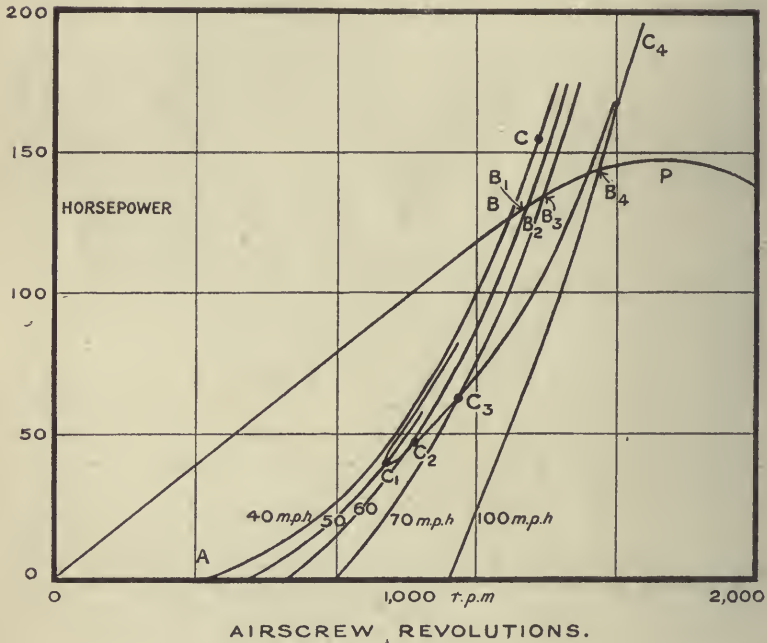
FIG. 15.—Horsepower and speed.

The curves so obtained for various flight speeds indicate zero horse-power before the airscrew has stopped. The speeds are lower than those for which the thrust has become zero, and indicate the points at which the airscrew becomes a windmill. In an aeroplane, however, the resistance to turning of the engine would greatly reduce the speed at which the wind-mill becomes effective below that indicated for no-horsepower, and stoppage of the petrol supply to the engine would often result in the stoppage of the airscrew.

From Figs. 14 and 15 it is now easy to find the brake horsepower of the engine which would be necessary to drive the aeroplane through the air at speeds from 40 to 100 m.p.h. From Fig. 14 it is found that the aeroplane when travelling at 50 m.p.h through the air needs an airscrew speed of 930 r.p.m. To drive the airscrew at this speed is seen from Fig. 15, point C_1, to need 39 horsepower. For other speeds the horsepower is indicated by the points C, C_2, C_3 and C_4, and the collected results are given in Table 6.

TABLE 6.—AEROPLANE HORSEPOWER AND SPEED.

Speed of aeroplane (m.p.h.)	Horsepower of engine necessary for flight.
40	156
50	39
60	48
70	66
100	188

On Fig. 15 a line OP has been drawn which represents the work which a particular engine could do at the various speeds of rotation ; this again is an experimental curve. The engine is supposed to be giving 120 h.p. at 1200 r.p.m. It will be seen, from Fig. 15, that the engine is not powerful enough to drive the aeroplane at either the lowest or the highest speeds for which the calculations have been made. For many purposes the information given in Fig. 15 is more conveniently expressed in the form shown in Fig. 16, where the abscissa is the flight speed of the aeroplane. The curve ABCDE of the latter figure is plotted from the points C, C_1, C_2, C_3 and C_4 of Fig. 15, while the line FGH corresponds with the points B, B_1, B_2, B_3 and B_4. The first curve shows the horsepower required for flight, and the second the horsepower available. From the diagram in this form it is easily seen that the point F represents the slowest speed at which the aeroplane can fly, in this case 40·3 m.p.h., and that H shows the possibility of reaching a speed of nearly 93 m.p.h.

Fig. 16 shows more than this, for it gives the reserve horsepower at any speed of flight. This reserve horsepower is roughly proportional to the speed at which the aeroplane can climb, and the curve shows that the best climbing speed is much nearer to the lower limit of speed than to the upper limit.

General Remarks on Figs. 12–16.—Calculations relating to the flight speed of an aeroplane are illustrated fairly exactly by the curves in Fig. 12–16. As the subject is entered into in detail many secondary considerations will be seen to come in. The difficulties will be found to consist very largely in the determination of the standard curves marked ABCDE in the figures, and the analysis of results to obtain these data constitutes one of the more laborious parts of the process. The complication is very largely one of detail, and should not be allowed to obscure the common basis of flight conditions for all aeroplanes as typified by the curves of Figs. 12–16.

Climbing Flight.—In the more general theory of the aeroplane it is of interest to show how the previous calculations may be modified to include flights other than those in a horizontal plane. The rate at which an aeroplane can climb has already been referred to incidentally in connection with Fig. 16.

It is clear from the outset that the air forces acting on the aeroplane depend on its speed and angle of incidence, and are not dependent on the attitude (or inclination) of the aeroplane relative to the direction of gravity. If the aeroplane is flying steadily, the force of gravity acting on it will always be vertical, whilst the inclination of the wind forces will vary with the attitude of the aeroplane. If the aeroplane is climbing the airscrew thrust will need to be greater than for horizontal flight, whilst if descending the thrust is reduced and may become zero or negative. There is a minimum angle of descent for any aeroplane when
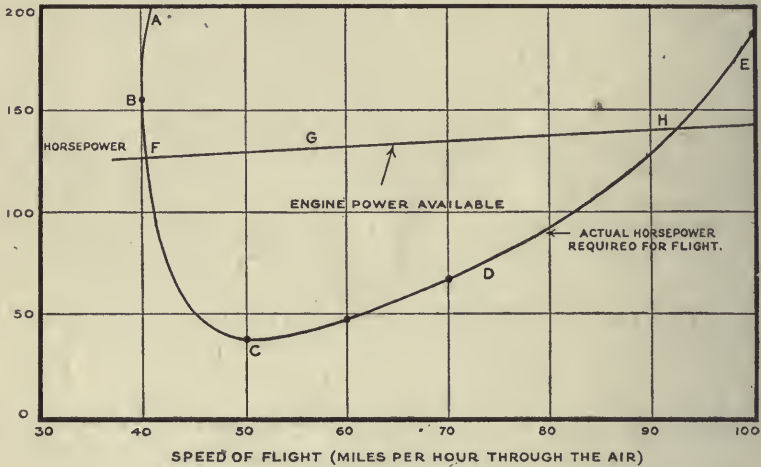
FIG. 16.—Horsepower and speed for level flight.

the airscrew is giving no thrust, and this angle is often referred to as the " angle of glide for the aeroplane." More correctly it should be referred to as the " least angle of glide."

The method of calculation of gliding and climbing flight is illustrated in Fig. 17, which is a diagram of the forces acting on an aeroplane in free flight but with its flight path inclined to the horizontal.

In horizontal flying it will be assumed that the direction of the thrust is horizontal, in which case it directly balances the resistance of the remainder of the aeroplane to motion through the air. In the above diagram this statement means that $T = D$. Similarly the weight of the aeroplane is exactly counterbalanced by the lift on the wings, i.e. $L = W$. The angle of incidence of the wings may be varied by adjustment of the elevator, in which case the thrust would not strictly lie along the wind. If necessary a slight complication of formula could be introduced to meet this case, but the effect of this variation is small, and, in accordance with the idea on

which this chapter is built, is omitted in order to render the main effects more obvious.

Now suppose that the angle of incidence of the aeroplane is kept constant, by moving the elevator if necessary, and that the thrust is altered by opening the throttle of the engine until the aeroplane climbs at an angle θ as shown. Because the angle of incidence has been kept constant the relative wind will still blow along the same line in the aeroplane, now in the position oX', but the thrust will not now exactly balance the resistance or the lift the weight of the aeroplane.

The relations between weight, speed and thrust may be expressed in different ways, but the following is the most instructive. If the force W be resolved along the new axes of D and L into its components W_1 and W_2, it will be seen immediately that L_1 must exactly counterbalance W_2 as
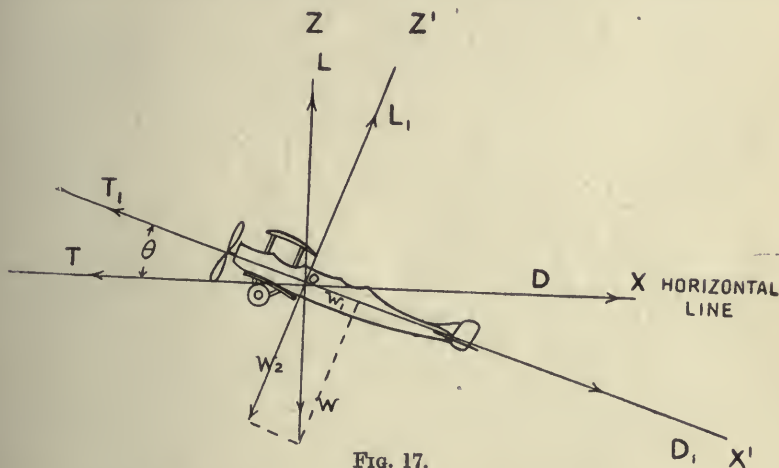
FIG. 17.

for horizontal flight. Since the angle of incidence has not been altered for the climb, it follows that $\dfrac{L}{u^2} = \dfrac{L_1}{u_1{}^2}$, where u is the velocity of the aeroplane through the air in horizontal flight, and u_1 the velocity when climbing. Since $L_1 = W_2$ and W_2 is less than W, it will be seen that the velocity of climbing flight is less than that for horizontal flight if the angle of incidence is unaltered. The relation is easily seen to be

$$\frac{u_1{}^2}{u^2} = \cos \theta \quad . \quad . \quad . \quad . \quad . \quad . \quad . \quad (1)$$

From the balance of forces along the axis of D_1 it is clear that $T_1 = W_1 + D_1$, or the thrust is greater than the drag by a fraction of the weight of the aeroplane. If climbing at 1 in 6 this fraction is $\frac{1}{6}$th. Since at the same attitude drag varies as the square of speed, the relation between thrust, weight and resistance can be put into the form

$$T_1 = W \sin \theta + D \cos \theta \quad . \quad . \quad . \quad . \quad . \quad (2)$$

where D is the aeroplane resistance in horizontal flight.

Equation (2) can now be used to show how diagrams 12 and 13 may be altered to allow for inclined flight. In the first place the ordinates of Fig. 13, which, after addition of the drag of the body, show the value of D for many angles of incidence, need to be decreased by multiplying by $\cos \theta$ to give $D \cos \theta$. The effect of this multiplication is very small as a rule. At 10° the factor is 0·985, and at 20°, 0·940. For a very steep spiral glide at say 45°, the difference between $\cos \theta$ and unity becomes important, $\cos \theta$ being then 0·707.

To the value of $D \cos \theta$ is to be added a term $W \sin \theta$ in order to obtain the thrust of the airscrew when climbing at an angle θ. We may then make a table as below, using figures from Table 1 to obtain the second column.

TABLE 7.—Thrust when climbing.

Speed of flight (m.p.h.).	Drag in horizontal flight × cos θ (lbs.).	W sin θ. θ = 5° (lbs.).	Airscrew thrust when climbing at 5° (lbs.).
40	608	174	782
50	208	174	382
60	210	174	384
70	253	174	427
100	506	174	680

The angle of climb was chosen arbitrarily at 5°, and to complete the investigation of the possibilities of climb Table 7 would be repeated for other angles. Using Figs. 14 and 15 for the airscrew as for horizontal flight, we may now calculate the horsepower required for flight when climbing, and so obtain the figures of Table 8.

TABLE 8.—Horsepower when climbing.

Speed of flight (m.p.h.).	(lbs.). Thrust. From Table 7.	R.p.m. from Fig. 14 and previous column.	Horse-power. From Fig. 15 and previous column.
40	782	1600	—
50	382	1170	85
60	384	1220	95
70	427	1340	116
100	680	1760	—

At the lowest and highest speeds of the table the horsepower required is far greater than that available, and the figures are not within the range of Fig. 16.

We may now proceed to plot the horsepower of Table 8 against speed to obtain a diagram corresponding with Fig. 16. The new curve marked $A_1B_1C_1D_1$ in Fig. 18 compared with ABCDE as reproduced from Fig. 16 shows an increase of nearly 50 h.p. at all speeds due to the climb at 5°. The highest speed of flight is shown by the intersection of $A_1B_1C_1D_1$ with FGH at H_5. FGH is the horsepower available, and is the same as the similarly marked curve of Fig. 16. The highest speed is 78·4 m.p.h., and

since the angle θ is constant along $A_1B_1C_1D_1$ the rate of climb will be greatest at this point for the conditions assumed. Rate of climb, V_c, is commonly estimated in feet per minute, and we then have

$$\text{Max. } V_c \text{ for } \theta = 5° = 88 \times V_{\text{m.p.h.}} \times \sin \theta$$
$$= 88 \times 78\cdot4 \times 0\cdot0875$$
$$= 604 \text{ ft. per min.}$$

The calculations shown in Tables 7 and 8 have been repeated for other angles of climb and one angle of descent to obtain corresponding curves
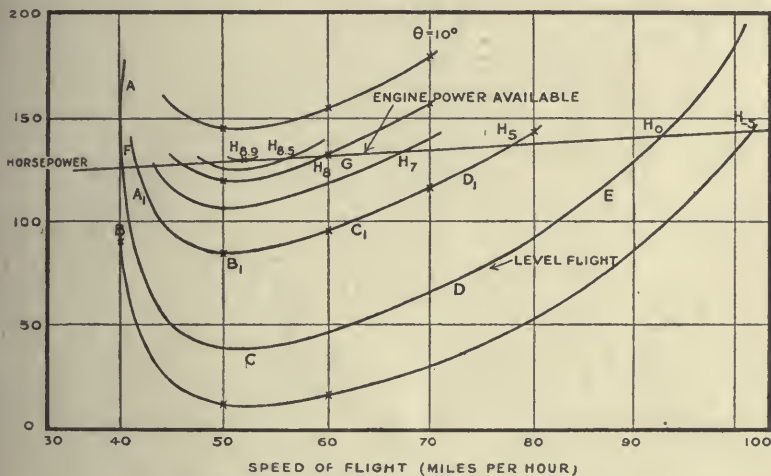
FIG. 18.—Horsepower and speed for climbing flight.

in Fig. 18. The intersections H_{-5}, H_0, etc., then provide data for Table 9 below.

TABLE 9.—RATE OF CLIMB AND SPEED.

Angle of climb.	Maximum flight speed (m.p.h.).	Maximum rate of climb for given angle.
− 5°	101·6	− 783 ft.-min.
0	93	0 ,,
5°	78·4	+ 604 ,,
7°	67·5	+ 725 ,,
8°	59·5	+ 727 ,,
8·5°	56·2	+ 730 ,,
8·9°	51·6	+ 702 ,,
10°	Flight not possible.	

Table 9 shows that the rate of climb varies rapidly with the flight speed in the neighbourhood 100 m.p.h. to 80 m.p.h., but that from 65 m.p.h. to 56 m.p.h. the value of rate of climb varies only from 725 to 730. This illustrates the well-known fact that the best rate of climb of an aeroplane is not much affected by small inaccuracies in the flight speed.

The table shows another interesting detail; the maximum angle of

climb is 8°·9, but the greatest rate of climb occurs at a smaller angle. For reasons connected with the control of the aeroplane an angle of 8° or thereabouts would probably be chosen by a pilot instead of the 8°·5 shown to be the best.

Diving.—By " diving " is meant descent with the engine on, as distinguished from a glide in which the engine is cut off. If the engine be kept fully on it is found that the speed of rotation of the airscrew rises higher and higher as the angle of descent increases. There is, however, an upper limit to the speed at which an aeroplane engine may be run with safety, and in our illustration an appropriate limit would be 1600 r.p.m. The speed of rotation corresponding with H_{-5} was 1550 r.p.m., and it will be seen that the new restriction will come into operation for steeper descent. Fig. 14, if extended, would now enable us to determine the thrust of the airscrew at any speed without reference to the horsepower, but it will be evident that the limits of usefulness of each of the previous figures have been reached, and an extension of experimental data is necessary to cover the higher speeds.

The fact that under certain circumstances forces vary as the square of forward speed of the aeroplane suggests a more comprehensive form of presentation than that of Figs. 12, 13, 14 and 15, and the new curves of Figs. 19 and 20 show an extension of the old information to cover the new points occurring in the consideration of diving. The values of the extended portion are so small that on any appreciable scale it is only possible to show the range corresponding with small angles of incidence and for small values of thrust and horsepower.

<div align="center">TABLE 10.—Airscrew Thrust when Diving.</div>

Speed (m.p.h.).	$\dfrac{n_{\text{r.p.m.}}}{V_{\text{m.p.h.}}}$ $n = 1600$.	Thrust $\overline{V^2_{\text{m.p.h.}}}$ From Fig. 20.
100	16·0	0·0406
120	13·3	0·0088
140	11·4	−0·0095
160	10·0	−0·0180

The curve connecting $\dfrac{\text{thrust}}{V^2_{\text{m.p.h.}}}$ and speed is shown in Fig. 21.

Instead of equation (2) will be used the equation

$$\frac{T_1}{V^2_{\text{m.p.h.}}} = \frac{W \sin \theta}{V^2_{\text{m.p.h.}}} + \frac{D_1}{V^2_{\text{m.p.h.}}} \quad . \quad . \quad . \quad . \quad (3)$$

The use of D_1 instead of $D \cos \theta$ is convenient now since the drag in level flight at high speeds is not determined in any other calculation. In compiling Table 11 some angle of path such as −10° is chosen, and various speeds of flight are assumed. From these speeds the third column is

calculated and gives one of the quantities of Fig. 19. The value $\frac{L_1}{V^2}=0\cdot197$
(Table 11) occurs at an angle of $-0°\cdot16$ (Fig. 19), and from the same figure

ANGLE OF INCIDENCE
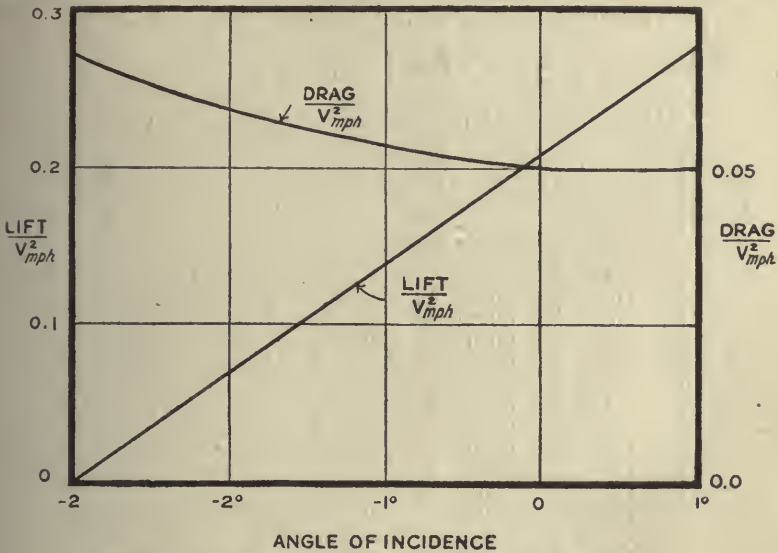
FIG. 19.—Lift and drag of aeroplane at very high speeds.
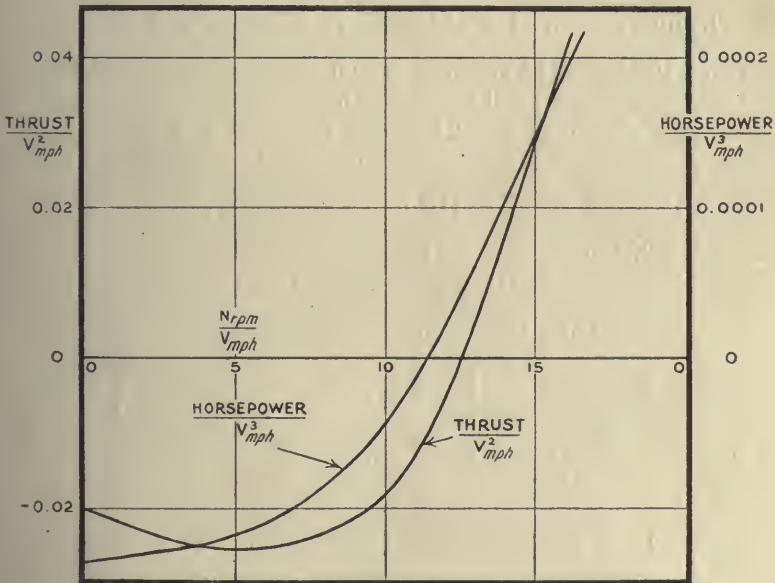
FIG. 20.—Thrust and horsepower of airscrew at very high speeds.

the corresponding value of $\frac{D_1}{V^2}$ is read off as $0\cdot0506$.   Column 5 of

D

Table 11 follows from the known weight of the aeroplane and columns 1 and 2, and the last column of $\frac{T}{V^2}$ is the sum of the preceding columns in accordance with equation (3). The values of $\frac{T}{V^2}$ from Table 11 are plotted in Fig. 21 and marked with the appropriate value

TABLE   .—Angle of Descent and Speed when diving.

θ Angle of path.	Speed (m.p.h.).	$\frac{L_1}{V^2} = \frac{W \cos \theta}{V^2}$	$\frac{D_1}{V^2}$ From col. 3 and Fig. 19.	$\frac{W \sin \theta}{V^2}$	$\frac{T}{V^2}$ by adding cols. 4 and 5.
−10°	100	0·197	0·0506	−0·0348	0·0158
	110	0·163	0·0520	−0·0287	0·0233
−20°	110	0·155	0·0525	−0·0570	−0·0045
	120	0·131	0·0540	−0·0475	+0·0065
−30°	120	0·120	0·0550	−0·0695	−0·0145
	130	0·103	0·0562	−0·0592	−0·0030
	140	0·088	0·0575	−0·0511	+0·0064
−60°	130	0·059	0·0600	−0·1025	−0·0425
	140	0·051	0·0612	−0·0884	−0·0272
	150	0·045	0·0620	−0·0770	−0·0150
−80°	150	0·015	0·0660	−0·0877	−0·0217
	160	0·014	0·0660	−0·0770	−0·0110
−90°	150	0	0·0680	−0·0890	−0·0210
	160	0	0·0680	−0·0784	−0·0104

of θ. The intersection at A of the curve $\theta = -10°$ and the curve $\frac{\text{thrust}}{V_2}$ from Table 10 shows the speed at which the aeroplane must be flying in order that the airscrew shall be giving the thrust required by equation (3).

The results shown in Fig. 21 can be collected in a form which shows how the resistance of an aeroplane is divided between the aeroplane and airscrew. At A the speed is 110 m.p.h. and the value of $\frac{T}{V_2}$ is 0·0240, and hence $T = 290$ lbs. Equation (3) then shows that $D_1 = 290$ lbs. $- W \sin \theta$ $= 290$ lbs. $+348$ lbs. $= 638$ lbs. Repetition of the process leads to Table 12.

TABLE 12.—Speed and Drag when diving.

Angle of descent.	Flight speed (m.p.h.).	Aeroplane drag (lbs.).	Airscrew drag (lbs.).	Wing drag (lbs.).
0	93	437	−437	167
10°	110	638	−290	261
20°	121	789	−105	333
30°	130·5	958	+ 42	427
60°	150·5	1406	+326	700
80°	155	—	—	—
90°	154·5	1618	+382	874

Examination of the table shows that a moderate angle of descent is sufficient to produce a considerable increase of speed. The maximum

flight speed is reached before the path becomes vertical, but the value is little greater than that for vertical descent. The terminal speed of our typical aeroplane is 155 m.p.h. With the limitation placed on the airscrew that its revolutions should not exceed 1600 p.m. it will be noticed from column (4) of Table 12 that the thrust ceases at about 125 m.p.h., and that at higher speeds the airscrew offers a resistance which is an appreciable fraction of the total. At the terminal velocity the total resistance is divided between the airscrew, wings and body in the proportions 19·1 per cent., 43·7 per cent. and 37·2 per cent. respectively.

If the curve of horsepower of Fig. 20 be examined at the terminal velocity it will be found that the value of $\dfrac{\mathrm{T}}{\mathrm{V}^2}$ (−0·016) gives to $\dfrac{n}{\mathrm{V}}$ a value of 10·4, and the horsepower is then negative. This means that the airscrew is tending to run as a windmill, and the horsepower tending to drive
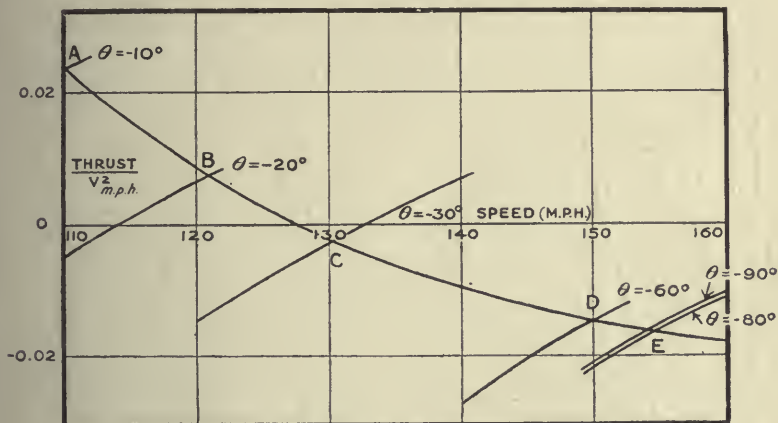
Fig. 21.—Angle of descent and speed in diving.

it is about 150. A speed much less than 155 m.p.h. would provide sufficient power to restart a stopped engine, since 30 h.p. would probably suffice to carry over the first compression stroke. This means of restarting an engine in the air is frequently used in experimental work.

Gliding.—In ordinary flying language " gliding " is distinguished from " diving " by the fact that in the former the engine is switched off. If the revolutions of the airscrew be observed the angle of glide can be calculated as before. There is, however, one special case which has considerable interest, and this occurs when the engine revolutions are just such as to give no thrust from the airscrew. Fig. 20 shows, for our illustration, that the revolutions per minute of the airscrew must then be 12·5 times the speed of the aeroplane in miles per hour. If the revolutions be limited to 1600 p.m. as before, the highest speed permissible is 128 m.p.h. Fig. 20 shows that the engine would then need to develop about 85 horsepower, and would be throttled down but not switched off.

The special interest of glides with the airscrew giving no thrust will

be seen from equation (2) by putting $T_1 = 0$ when the rest of the equation gives

$$\frac{D}{W} = -\tan \theta \quad . \quad . \quad . \quad . \quad . \quad . \quad (4)$$

where D is the drag in horizontal flight at the same angle of incidence as during the glide, and consequently $\dfrac{D}{W}$ is the well-known ratio of lift to
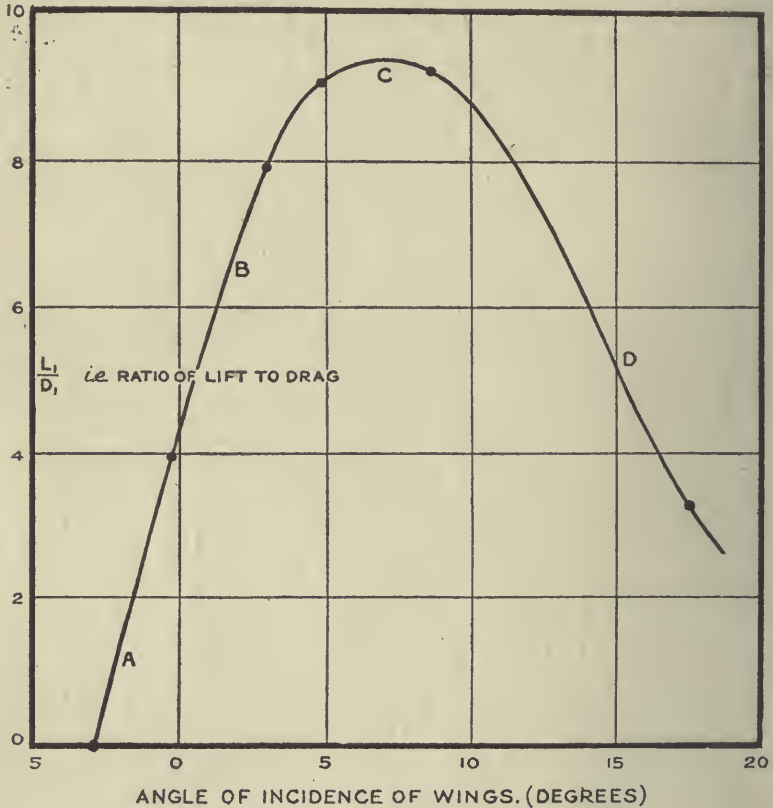
Fig. 22.—Aeroplane efficiency and gliding angle.

drag. This depends only on angle of incidence, and (4) may be generalised to

$$\frac{D_1}{L_1} = \frac{\text{drag}}{\text{lift}} = -\tan \theta \quad . \quad . \quad . \quad . \quad . \quad (5)$$

The negative sign implies downward flight, and we see that the gliding angle θ is a direct measure of the $\dfrac{\text{lift}}{\text{drag}}$ of an aeroplane, i.e. of its aerodynamic efficiency as distinct from that of the airscrew. In practice it is not possible to ensure the condition of no thrust with sufficient accuracy

for the resulting value of $\dfrac{L}{D}$ to be good enough for design purposes. It is better as an experimental method to test with the airscrew stopped and to make allowance for its resistance. The $\dfrac{drag}{lift}$ of the aeroplane and airscrew is then the quantity measured by $-\tan\theta$. The least angle of glide is readily calculated from a curve which shows the ratio of lift to drag for the aeroplane. The curve given in Fig. 22 is obtained from the value of the body drag and the numbers used in plotting Figs. 12 and 13.

The value of drag for the aeroplane is least when the ordinate of the curve in Fig. 22 is greatest, and will be seen to be only $\dfrac{1}{9\cdot3}$ of the lift. If then an aeroplane is one mile high when the engine is throttled down to give no thrust, it will be possible to travel horizontally for 9·3 miles before it is necessary to alight. Should the pilot wish to come down more steeply he could do so either by increasing or decreasing the angle of incidence of his aeroplane. For the least angle of glide Fig. 22 shows the angle of incidence to be about 7 degrees, and by reference to Fig. 12 it will be seen that the flying speed is between 50 and 60 m.p.h., probably about 54 m.p.h. To come down in a straight line to a point 5 miles away from the point vertically under him from a point a mile up, the pilot could choose either the angle of $\frac{1}{2}°$ and a speed of about 90 m.p.h. or an angle of 15° and a speed of about 42 m.p.h. From Fig. 12 it will be seen that 15° is near to the greatest angle at which the aeroplane can fly, and it will be shown later that the control then becomes difficult, and for this reason large angles of incidence are avoided. If a pilot wishes to descend to some point almost directly beneath him, he finds it necessary to descend in a spiral with a considerable " bank " or lateral inclination of the wings of the aeroplane. It is not proposed to analyse the balance of forces on a banked turn at the present stage, but it may here be stated that for the same angle of incidence of the wings an aeroplane descends more rapidly when turning than when flying straight. For an angle of bank of 45° the fall for a given horizontal travel is increased in the ratio of $\sqrt{2}:1$.

Soaring.—In considering the motion of an aeroplane it has so far been assumed that the air itself is either still or moving uniformly in a horizontal direction, so that climbing or descending relative to the air is equal to climbing or descending relative to the earth. The condition corresponds with that of the motion of a train on a straight track which runs up and down hill at various points. If the air be moving the analogy in the case of the train would lead us to consider the motion of the train over the ground when the rails themselves may be moved in any direction without any control being possible by the engine driver. If the rails were to run backwards just as quickly as the train moved forward over them, obviously the train would remain permanently in the same position relative to the ground. If the rails move more quickly backwards than the train moves forward, the train might actually move backwards in spite of the engine driver's efforts. Of course we know that such things do not happen to

trains, but occasionally an aeroplane flying against the wind is blown backwards relative to an observer on the ground. Flying with the wind the pilot may travel at speeds very much greater than those indicated in our earlier calculations. The motion of the aeroplane may be very irregular, just as would be the motion of the train if the rails moved sideways and up and down as well as backwards and forwards, with the difference that the connection between the air and aeroplane is not so rigid as that between a train and its rails. The motion of an aeroplane in a gusty wind is somewhat complicated, but methods of making the necessary calculations have already been developed, and will be referred to at a more advanced stage.

If the rails in the train analogy had been moving steadily upwards with the train stationary on the rails, the train might have been described as soaring. The train would be lifted by the source of energy lifting the rails. Similarly if up-currents occur in the air, an aeroplane may continue to fly whilst getting higher and higher above the ground, without using any power from the aeroplane engine. This case is easily subjected to numerical calculation. Lord Rayleigh and Prof. Langley have shown that soaring may be possible without up-currents, if the wind is gusty or if it has different speeds at different heights. Such conditions occur frequently in nature, and birds may sometimes soar under such conditions. Continued flight without flapping of the wings usually occurs on account of rising currents. These may be due to hot ground, or round the coasts more frequently to the deflection of sea breezes by the cliffs near the shore. Gulls may frequently be seen travelling along above the edges of cliffs, the path following somewhat closely the outline of the coast. Other types of soaring are scarcely known in England.

To calculate the upward velocity of the air necessary for soaring in the case of the aeroplane already considered, it is only necessary to refer back to the gliding angles and speeds of flight. Values obtained from Figs. 12 and 22 are collected in Table 13 for a weight of 2000 lbs.

TABLE 13.—SOARING.

Angle of incidence, from Fig. 12.	Speed of flight (m.p.h.), from Fig. 12.	Gliding angle, from Fig. 22.	Vertical velocity of fall with engine cut off (m.p.h.).
17°·5	40	1 in 3·3	12·1
8°·7	50	1 in 9·2	5·4
5°·0	60	1 in 9·0	6·7
3°·0	70	1 in 7·9	8·8
−0°·2	100	1 in 3·95	25·3

The figures in the last column of Table 13 are readily obtained from those in columns 2 and 3. At 60 m.p.h. and a gliding angle of 1 in 9 the falling speed is $\frac{60}{9}$ m.p.h., *i.e.* 6·7 m.p.h. as in column 4. The least velocity of rising wind is required at a speed just below that of least resistance, and in this case amounts to about 5·4 m.p.h. or nearly 8 feet per second.

Winds having large upward component velocities are known to exist.

In winds having a horizontal component of 20 m.p.h. an upward velocity of 6 or 7 m.p.h. has been recorded on several occasions.* In stronger winds the up-currents may be greater, but in all cases they appear to be local. One well-authenticated test on the climbing speed of an aeroplane shows that a rising current of about 7 miles an hour existed over a distance of more than a mile. The climbing speed of the aeroplane had been calculated by methods similar to those described in the earlier pages of this book and found to be somewhat less than 400 feet per min.; the general correctness of this figure was guaranteed by the average performance of the aeroplane. On one occasion, however, the recording barograph indicated an increase of 1000 feet in a minute, and it would appear that 600 feet per minute of this was due to the fact that the aeroplane was carried bodily upwards by the air in addition to its natural climbing rate. At 60 miles an hour the column traversed per minute is a mile, as already indicated.

The possibility of soaring on up-currents for long distances does not seem to be very great. It will be noticed, from the method of calculation given for Table 13, that the speed of the up-current required for supporting a flying machine at a given gliding angle is proportional to the flying speed. Hence birds having much lower speeds can soar in less strong up-currents than an aeroplane. The local character of the up-currents is evidenced by the tendency for birds when soaring to keep over the same part of the earth.

The Extra Weight a given Aeroplane can carry, and the Height to which an Aeroplane can climb.—So far the calculations have been made for a fixed weight of aeroplane and for an atmosphere as dense as that in the lower reaches of the air. It will often happen that additional weight is to be carried in the form of extra passengers or goods. Also during warfare, in order to escape from hostile aircraft guns, it may be necessary to climb many thousands of feet above the earth's surface. The problem now to be attacked is the method of estimating the effects on the performance of an aeroplane of extra weight and of reduced density. The greatest height yet reached by an aeroplane is about 5 miles, and at such height the barometer stands at less than 10 ins. of mercury; it is clear from the outset that the conditions of flight are then very different from those near the ground. In order to climb to such heights the weight of the aeroplane is kept to a minimum and the reserve horsepower made as great as possible. The problem is easily divisible into two distinct parts, one of which relates to the power required to support the aeroplane in the air of lower density and the other of which deals with the reduction of horsepower of the engine from the same cause. The latter of the two causes is of the greater importance in limiting the height of climb.

It has already been pointed out in connection with Fig. 12 that the lifting force on any aeroplane varies as the square of the speed so long as the angle of incidence is kept constant. Now suppose that the weight

* Report of the Advisory Committee for Aeronautics, 1911–12, p. 315.

of the aeroplane is increased in the ratio $M^2 : 1$ by the addition of load inside the body, *i.e.* where it does not add to the resistance directly. In order that the aeroplane may lift without altering its angle of incidence, it is necessary to increase the speed in the proportion of $M : 1$. This increase will apply with equal exactness to the revolutions of the airscrew, and the simple rule is reached that if an aeroplane has its weight increased in the ratio $M^2 : 1$ and its speeds in the ratio $M : 1$, flying will be possible at the same angle of incidence for both loadings.

From the previous analysis it will be realized that the increase of speed necessary to give the greater lift involves an increase in the resistance proportional to M^2 and to balance this an increase of propeller thrust also proportional to M^2. The method of finding horsepower shows that the increased horsepower is in the ratio of $M^3 : 1$ to the old horsepower. Leaving the variation of density alone for the moment, new calculations for other loads could be made as before. Since Fig. 15 exists for the old loading a simpler method may be followed.

The curves OP and $C_1C_2C_3C_4$ of Fig. 15 are reproduced in Fig. 23 below, with an increase of scale for the airscrew revolutions. The two further curves of Fig. 23 marked 3000 lbs. and 4000 lbs. are produced as shown in Table 14 in accordance with the laws just enunciated.

TABLE 14.—INCREASED LOADING.

Weight = 2000 lbs.		Weight = 3000 lbs.		Weight = 4000 lbs.	
R.p.m. from curve $CC_1C_2C_3C_4$, Fig. 23.	Horsepower from curve $CC_1C_2C_3C_4$, Fig. 23.	R.p.m. from col. (1), by multiplying by $\sqrt{\frac{3000}{2000}}$ *i.e.* by 1·225.	Horsepower, from col. (2), by multiplying by $\left(\frac{3000}{2000}\right)^{3/2}$ *i.e.* by 1·84.	R.p.m. from col. (1), by multiplying by $\sqrt{\frac{4000}{2000}}$ *i.e.* by 1·414.	Horsepower from col. (2), by multiplying by $\left(\frac{4000}{2000}\right)^{3/2}$ *i.e.* by 2·83.
930	40	1140	73	1315	113
950	$\{41, 45\}$	1165	$\{75, 83\}$	1345	$\{116, 127\}$
1000	$\{45, 54\}$	1225	$\{83, 99\}$	1415	$\{127, 153\}$
1050	$\{51, 64\}$	1285	$\{94, 118\}$	1490	144
1100	$\{57, 75\}$	1345	$\{105, 138\}$	—	—
1200	71	1470	131	—	—

Fig. 23 shows that the aeroplane would still fly with a total load of 4000 lbs. At top speed the airscrew speed has fallen from 1525 to 1470 r.p.m. owing to the extra loading. It is easy to calculate the maximum load which might be carried, since Fig. 23 shows that the airscrew would in the limiting case be making about 1400 r.p.m. and delivering 135 horsepower. If, then, we find $\sqrt[3]{\frac{135}{39}}$, *i.e.* 2·28, and multiply 2000 lbs. by this number, 4560 lbs. will be obtained as the limiting load which this aeroplane can carry. It will be seen that each 1000 lbs. of load carried now requires about 30 horsepower.

Corresponding calculations based on Fig. 23 in an exactly analogous way to those of Table 14 on Fig. 16 have been made.   The details are not
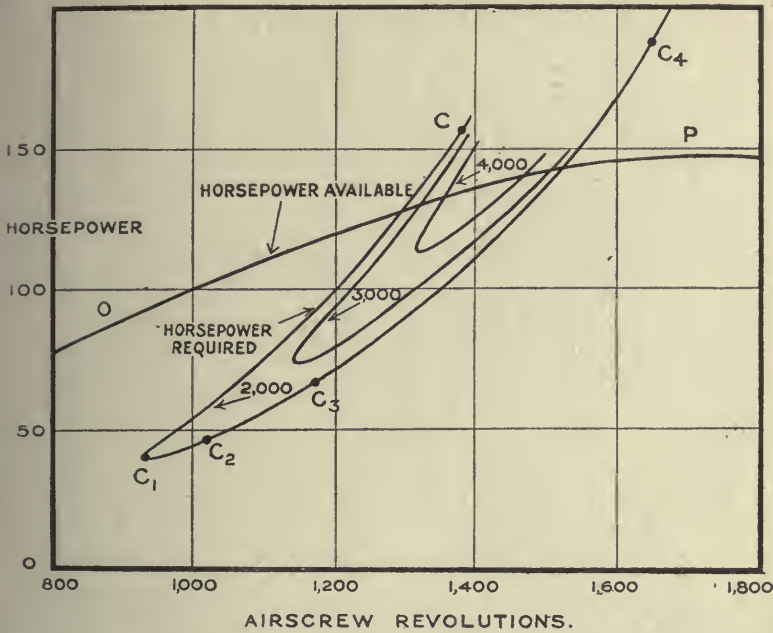
FIG. 23.—Effect of additional weight on horsepower and airscrew revolutions.

given, but the results are shown in Fig. 24, and it can be seen how the speed of flight is affected by the increased loading.
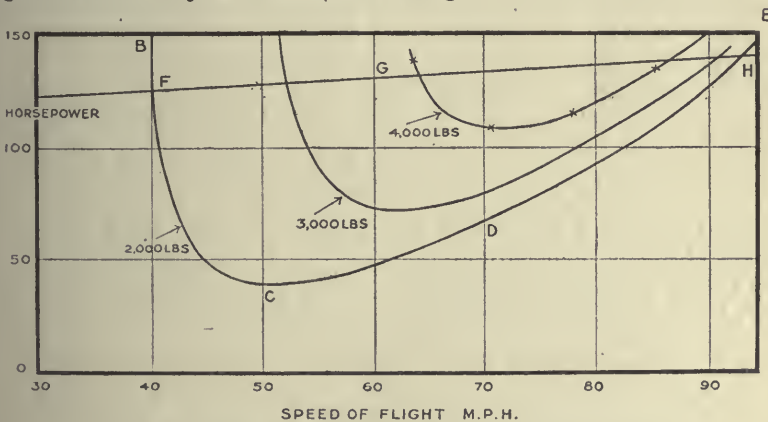
FIG. 24.—Effect of additional weight on the speed of flight.

The curves FGH and BCDE are reproduced from Fig. 16, whilst those marked 3000 lbs. and 4000 lbs. are the results of the new calculations.

The first very noticeable feature of Fig. 24 is the small difference of

top speed due to doubling the load, the fall being from 93 m.p.h. to 86 m.p.h. The effect on the slowest speed of flight is very much greater, for the least possible speed of steady horizontal flight is 64 m.p.h. with a load of 4000 lbs., instead of 40 m.p.h. with a load of 2000 lbs. The difficulties of landing are much increased by this increase of minimum flying speed.

Fig. 24 can be used to illustrate a point in the economics of flight. The subject will not be pursued deeply here, since more comprehensive methods will be developed later. If it be decided that a speed of 90 m.p.h. is desirable for a given service, it is seen that 2000 lbs. can be carried for an expenditure of 129 horsepower, 3000 lbs. for 138 horsepower, and 4000 lbs. for 152 horsepower. If these numbers are expressed as '' horsepower per thousand pounds carried,'' they become 65, 46 and 38, showing a progressive change in favour of the heavy loading. The difference is very great, and obviously of commercial interest. Variation of loading is not the only factor leading to economy, but the impression given above from a particular instance may be accepted as typical of the aeroplane as we now know it.

It should be remembered that the present calculations refer to increased load in an existing aeroplane. Any new design for an original weight of 4000 lbs. would differ from the prototype probably both in size and in the power of its engine.

Flight at Altitudes of 10,000 feet and 20,000 feet.—At a height of 10,000 feet the density of the air is relatively only 0·74 of that near the ground, and we now inquire as to the effect of the change. The experimental law is a simple one, and states that at the same attitude and speed of flight the air force is proportional to the air density.

The new performance at 10,000 ft. may be calculated from that near ground-level by a process somewhat analogous to the one followed for variation of weight. At the same angle of incidence it is possible to produce the same lift in air of different densities by changing the speed, and the law is that σV^2 * is constant during the change.

The power required is not the same since the speed has increased as $\sqrt{\dfrac{1}{\sigma}}$, and hence the horsepower has also increased as $\sqrt{\dfrac{1}{\sigma}}$. We then get the following simple rule for the aeroplane and airscrew, that flight at reduced density is possible at the same angle of incidence if the speed of flight and the speed of rotation of the airscrew are increased in proportion to $\sqrt{\dfrac{1}{\sigma}}$; the horsepower required for flight is also increased in the proportion $\sqrt{\dfrac{1}{\sigma}}$.

Table 15 shows how the calculations are made.

From columns 3 and 4 of Table 15 the curve $A_1B_1C_1$ of Fig. 25 is drawn to represent the horsepower necessary for flight at 10,000 feet. The original curve for unit density is shown as ABC.

* σ is the relative density, while ρ is used for the mass per unit volume of the fluid or absolute density.

TABLE 15.—FLYING AT GREAT HEIGHTS.

Flight near the ground where the relative density is unity.		Flight at 10,000 ft. where the relative density is 0·74.		Flight at 20,000 ft. where the relative density is 0·535.	
R.p.m. from Table 14, column (1).	Horsepower, from Table 14, column (1).	R.p.m. column (1) multiplied by $\frac{1}{\sqrt{\sigma}}$ i.e. by 1·16.	Horsepower, column (2) multiplied by $\frac{1}{\sqrt{\sigma}}$ i.e. by 1·16.	R.p.m. column (1) multiplied by $\frac{1}{\sqrt{\sigma}}$ i.e. by 1·37.	Horsepower column (2) multiplied by $\frac{1}{\sqrt{\sigma}}$ i.e. by 1·37.
930	40	1080	46	1260	54·5
950	$\begin{Bmatrix} 41 \\ 45 \end{Bmatrix}$	1100	$\begin{Bmatrix} 47 \\ 52 \end{Bmatrix}$	1295	$\begin{Bmatrix} 56 \\ 61 \end{Bmatrix}$
1000	$\begin{Bmatrix} 45 \\ 54 \end{Bmatrix}$	1160	$\begin{Bmatrix} 52 \\ 63 \end{Bmatrix}$	1360	$\begin{Bmatrix} 61 \\ 73 \end{Bmatrix}$
1050	$\begin{Bmatrix} 51 \\ 64 \end{Bmatrix}$	1220	$\begin{Bmatrix} 59 \\ 74 \end{Bmatrix}$	—	—
1100	$\begin{Bmatrix} 57 \\ 75 \end{Bmatrix}$	1280	$\begin{Bmatrix} 66 \\ 87 \end{Bmatrix}$	—	—
1200	71	1390	82	—	—

FIG. 25.—Effect of variation of height on horsepower and airscrew revolutions.

Variation of Engine Power with Height.—The horsepower of an engine in an average atmosphere falls off more rapidly than the density and curves of variation have been derived experimentally. For a height of 10,000 ft. the horsepower at any given speed of rotation is found to be 0·69 of that where the density is unity. The curve O_1P_1 of Fig. 25 is obtained from OP by multiplying the ordinates by 0·69. The pair of curves

O_1P_1, $A_1C_1B_1$ now refers to flight at 10,000 ft. and the revolutions of the engine at top speed, *i.e.* at B, will be seen to be a little less than those at the ground. The reserve horsepower for climbing will be seen to be much reduced, and is little more than half that at the low level.

There must come some point in the ascent of an aeroplane at which a new curve for OP will just touch the new curve for ABC, and the density for which this occurs will determine the greatest height to which the aeroplane can climb. This point is technically known as the " ceiling." A repetition of the calculation for a height of 20,000 ft. shows this height as being very near to the ceiling. The drop in airscrew revolutions at top speed (B_{11}) is now well marked.

The corresponding curves for flight speed and horsepower have been calculated and are shown in Fig. 26. The curves for " horsepower required"
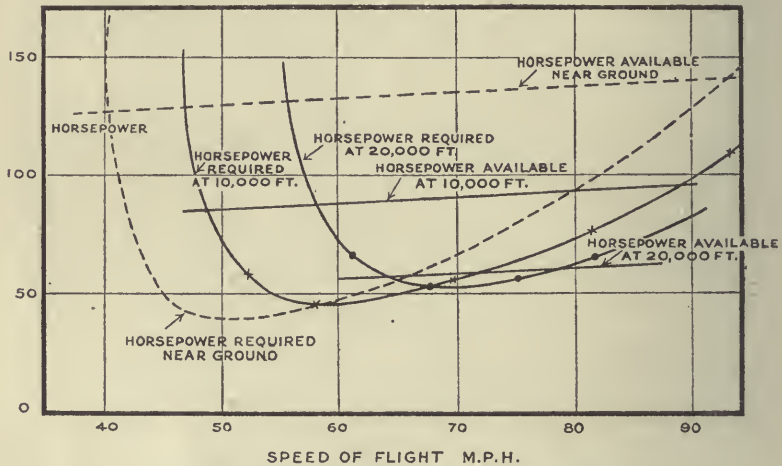
FIG. 26.—Effect of height on the speed of flight.

and speed are obtained from those at ground-level (Fig. 16) by multiplying both abscissae and ordinates by $\dfrac{1}{\sqrt{\sigma}}$. The horsepowers at maximum and minimum speeds are given by the points A_1, B_1, A_{11} and B_{11} of Fig. 25 and fix two points on each curve of horsepower available, and hence fix the maximum and minimum speeds. The speeds at ground-level, 10,000 ft. and 20,000 ft. are found to be 93 m.p.h., 89 m.p.h. and 79 m.p.h., showing a marked fall with increased height.

The increase of the lowest speed of level steady flight is of little importance since landing does not now need to be considered.

Another item in the economics of flight is illustrated by Fig. 26. The load carried is 2000 lbs. at all heights, but at a speed of 90 m.p.h. the horsepowers required are 129 near the ground, 99 at 10,000 ft. and 82 at 20,000 ft., *i.e.* 64, 49 and 41 horsepower per 1000 lbs. of load carried. The intense cold at great heights such as 20,000 ft. must be offset against the

obvious advantages of high flying in reduced size of engine and in petrol consumption.

This completes the general exposition of those properties of an aeroplane which are generally grouped under the heading " Performance." Before passing to the more mathematical treatment of the subject a short account will be given of the longitudinal " balance " of an aeroplane in flight.

Longitudinal Balance.—The function of the tail of an aeroplane is to produce longitudinal balance at all speeds of steady flight. In the search for efficient wings it has been found that the best are associated with a property which does not lend itself to balance of the wings alone. In the earlier part of the chapter we have considered the forces acting on a wing and on an aeroplane without any reference to the couples produced, and the motion of the centre of gravity of the aeroplane is correctly estimated in this way provided the motion can be maintained steady. We now proceed to discuss the couples called into play and the method of dealing with them.

Centre of Pressure.—Fig. 27 shows a drawing of a wing with the position of the resultant force marked on it at various speeds of steady flight. The
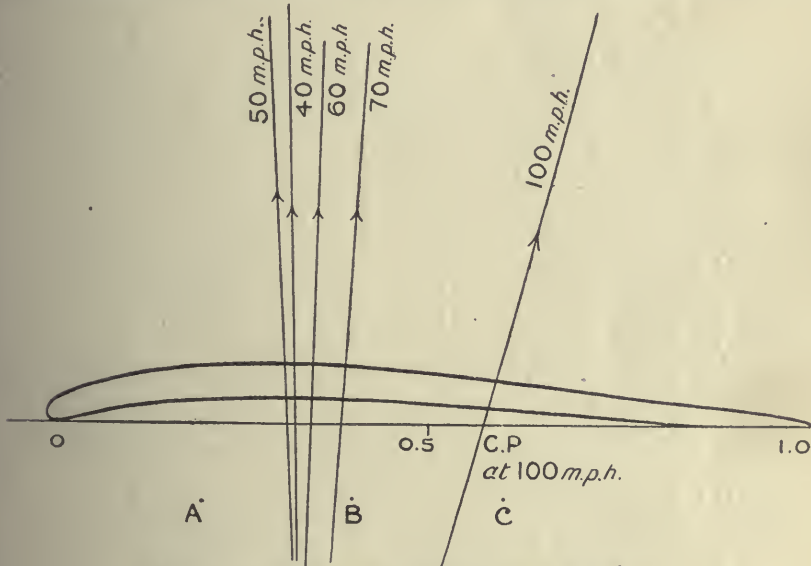
Fig. 27.—Resultant wing force and centre of pressure.

lengths of the lines show the magnitude, and a standard experiment fixes both the magnitude and position. The intersection of the line of the resultant and the chord of the section is called the centre of pressure, and at 100 m.p.h. the intersection, CP of Fig. 27, occurs at 0·58 of the chord from the leading edge. The most forward position of the centre of pressure occurs at about 50 m.p.h., and is situated at 0·32 of the chord from the leading edge.

46   APPLIED AERODYNAMICS

One of the conditions for steady flight requires that the resultant force on the whole aeroplane shall pass through the centre of gravity of the
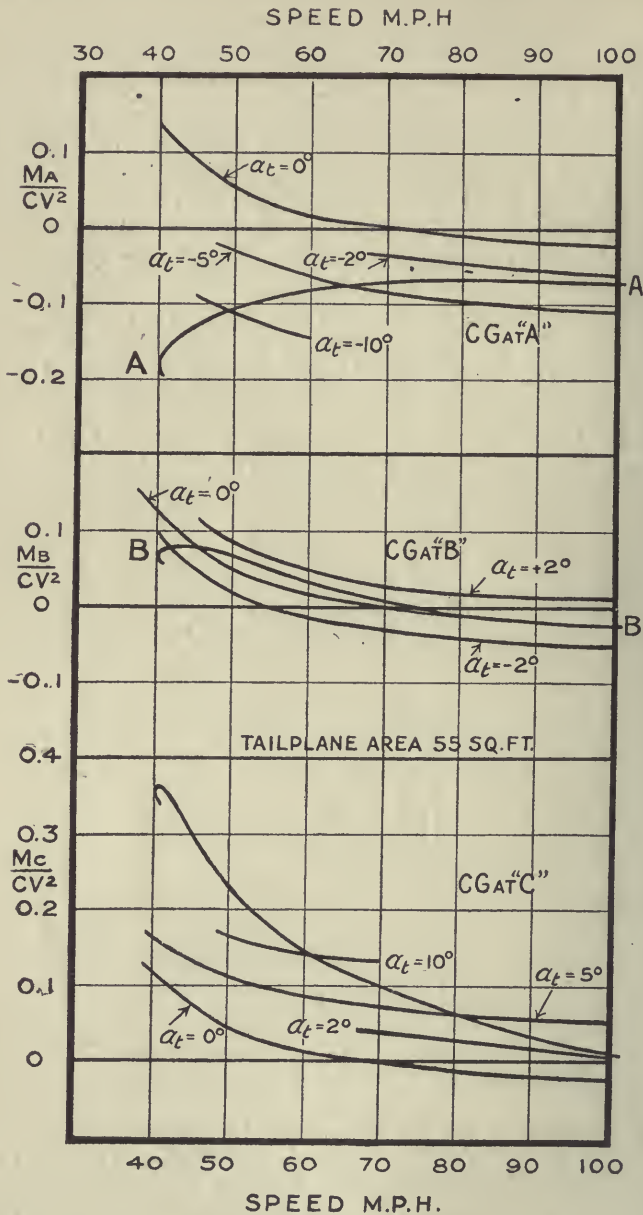
Fig. 28.—Longitudinal balance.

aeroplane, and it is impossible to find any point near the wing for which the condition is satisfied at all speeds. It will be supposed that

the centre of gravity is successively at the points A, B and C of Fig. 27, and it will be shown how to produce the desired effect by means of a tail plane with adjustable angle of incidence. Table 16 shows the values of resultant force and the leverages about the point A in terms of the chord of the aerofoil c, and finally the couple in terms of the previous quantities tabulated.

TABLE 16.—WING MOMENTS.

Flight speed (m.p.h.).	Angle of incidence of wings.	Resultant force (lbs.).	Distance from A.	$\dfrac{M_A}{cV^2}$
40	17°·5	2100	−0·135 c.	−0·177
50	8°·7	2020	−0·125 c.	−0·101
60	4°·9	2020	−0·146 c.	−0·082
70	3°·0	2020	−0·180 c.	−0·074
100	−0°·2	2060	−0·342 c.	−0·070

The moments for the points B and C are obtained by a repetition of the process followed for A. The resulting figures have been used to draw the curves of Fig. 28, which are marked A, B, C.

These couples are to be balanced by the tail plane, and the first point to be considered is the effect of the down current of air from the wings on the air forces acting on the tail plane. The angle through which the air is deflected is called the " angle of downwash," and is denoted by " ϵ ."

Downwash.—In the consideration of wing lift it was seen that the downward velocity of the air is directly related to the lift on the wing. Ex-

Inclination of Chord
of Wing α.
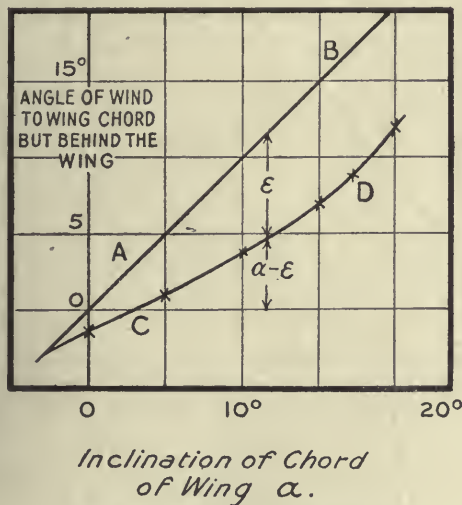
FIG. 29.—Downwash from wings

perimentally it is found to be very nearly proportional to the lift for various angles of incidence, and a typical diagram showing " downwash " is given in Fig. 29.

The upper straight line AB of Fig. 29 shows the angle of the chord of the wings relative to the air in front of the wings, whilst CD shows the angle at the tail. The chord of the tail plane will not usually be parallel to the chord of the wings, and its setting is denoted by a_t. Fig. 30 will make the various quantities clear.
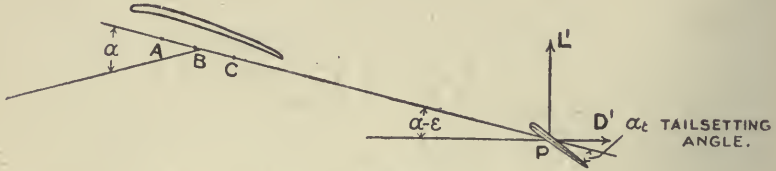
FIG. 30.

For an angle of incidence a at the wings we have at the tail an angle of wind relative to AP of $a - \epsilon$, and the tail plane being set at an angle a_t to AP, for the angle of incidence of the tail plane is given by the relation

$$a' = a - \epsilon + a_t \quad . \quad . \quad . \quad . \quad . \quad . \quad (6)$$

Tail planes are usually symmetrical in form, and the chord is taken as
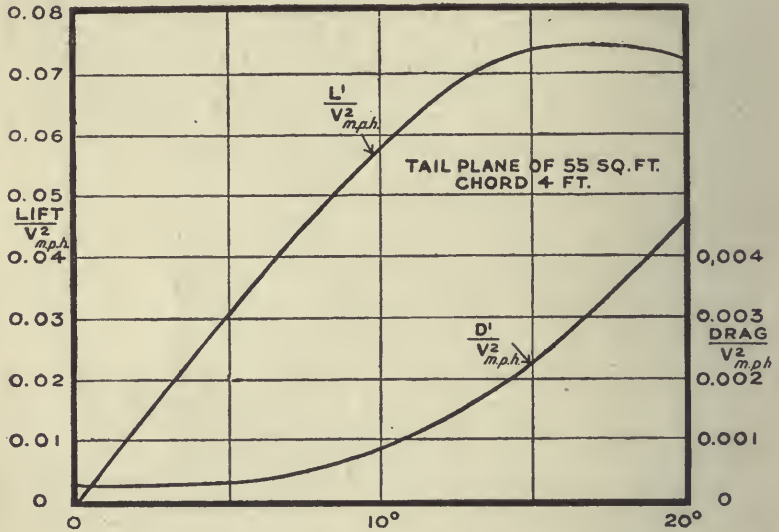
FIG. 31.—Lift and drag of tail plane.

the median line of the section. Fig. 31 shows curves of $\dfrac{\text{tail lift}}{V^2_{\text{m.p.h.}}}$ and $\dfrac{\text{tail drag}}{V^2_{\text{m.p.h.}}}$ for a typical tail plane suitable for an aeroplane weighing 2000 lbs., of 55 sq. feet area and a chord of 4 feet. As nothing is lost in the principle of balance by the omission of terms depending on the change of centre of

pressure of the tail plane, such terms will be ignored, and the force on the tail plane will always be assumed to pass through the point P.

If the distance from A to P be denoted by l_A the equation for moment of the tail about A is

$$\text{moment} = -l_A\{L' \cos (\alpha - \epsilon) + D' \sin (\alpha - \epsilon)\}$$

or more conveniently

$$\frac{\text{moment}}{l_A V^2_{m.p.h.}} = -\left\{\frac{L'}{V^2_{m.p.h.}} \cos (\alpha - \epsilon) + \frac{D'}{V^2_{m.p.h.}} \sin (\alpha - \epsilon)\right\} . \quad . \quad (7)$$

The calculation proceeds as in Table 17.

TABLE 17.—TAIL MOMENTS.

$V_{m.p.h.}$	α	$\alpha - \epsilon$	α'	$\dfrac{L'}{V^2}$	$\dfrac{D'}{V^2}$	$\dfrac{M_A}{cV^2}$
				$\alpha_t = 0, \quad l_A = 2\cdot7c.$		
40	17°·5	8°·6	8°·6	0·0504	0·0006	−0·134
50	8°·7	3°·0	3°·0	0·0181	0·0002	−0·049
60	4°·9	1°·0	1°·0	0·0055	0·0002	−0·015
70	3°·0	0°·0	0°·0	0·0000	0·0002	−0·000
100	−0°·2	−1°·6	−1°·6	−0·0091	0·0002	+0·025

When the aeroplane is in equilibrium the couple given in the last column must be equal to, but of opposite sign to, that on the wings. Couples due to the tail are therefore plotted in Fig. 28 with their sign reversed. The intersections of the various curves then show the speeds of steady flight for various tail settings.

The differences between Figs. 28a, 28b, 28c, correspond with the differences in the position of the centre of gravity, i.e. with A, B and C. They are considerable and important.

Fig. 28a shows that equilibrium is not possible within the flight range 40 m.p.h. to 100 m.p.h. until the tail setting is less than −3°, the speed being then 100 m.p.h. For $\alpha_t = -5°$ the speed for equilibrium is 65 m.p.h., and for $\alpha_t = -10°$, 49 miles per hour.

Fig. 28b shows that the aeroplane is almost in equilibrium at all speeds for the same setting, $\alpha_t = 0$, the statement being most nearly correct at speeds of 70 m.p.h. to 100 m.p.h. To change from 50 m.p.h. to 41 m.p.h. the tail-plane setting needs to be altered from +1° to −2°.

Fig. 28c is to a large extent a reversal of Fig. 28a. The angle of tail setting must exceed +2° to bring the equilibrium position within the flight range 40 m.p.h. to 100 m.p.h At $\alpha_t = +2°$ the speed is 102 m.p.h., for $\alpha_t = +5°$ it is 81 m.p.h., and for $\alpha_t = +10°$ it is 60 m.p.h. To reduce the speed further would need still greater angles, and the tail plane passes its critical angle. It might not be possible in this case to fly steadily at 45 m.p.h. The same might be true for a position of the centre of gravity of the aeroplane further forward than A.

E

If we regard the variation of tail setting as a control, we see that both A and C are positions of the centre of gravity which lead to insensitiveness, whilst position B leads to great sensitivity. An example is then reached of a general conclusion that greatest sensitiveness is obtained for a particular position of the centre of gravity, and that for ordinary wings this point is about 0·4 of the chord from the leading edge. We shall see that this conclusion is not greatly modified if the tail plane be reduced in area.

Consider, now, the aeroplane with its centre of gravity at A, flying at an angle of incidence of 3°·0 and a speed of 70 m.p.h., but with a tail setting of −10°. The wings are then giving a couple −0·08cV², which tends to
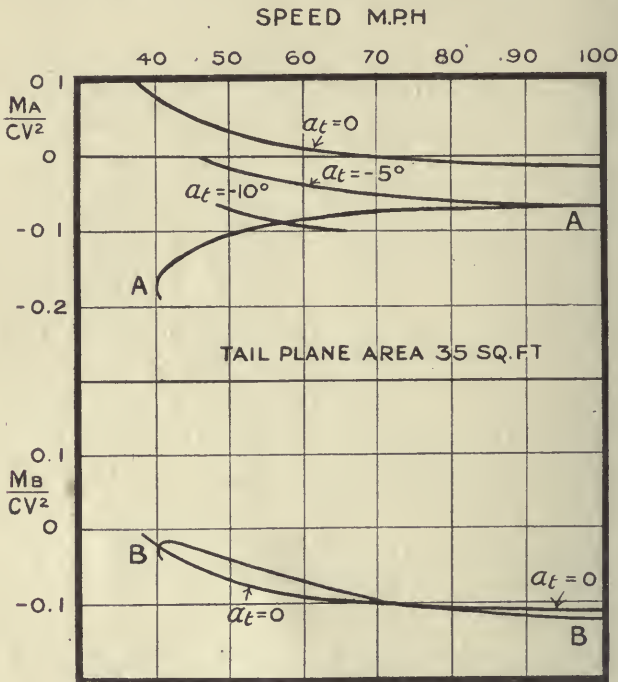
Fig. 32.—Longitudinal balance with small tail plane.

decrease the angle of incidence and to put the aeroplane in a condition suitable for higher speed, whereas the equilibrium position for this tail setting is at a lower speed. The tail is, however, exerting a couple of +0·14cV², and this tends in the opposite direction and overcomes the couple due to the wings. It is almost certain that the aeroplane would be stable and settle down to its speed of 49 m.p.h. if left to itself with the tail plane fixed at −10°.

Fig. 28c shows the reverse case; the wing moment being greater than the tail moment, the aeroplane would be unstable. It is not proposed to discuss stability in detail here, but it should be noted that the simple criteria now employed are only approximate, although roughly correct.

It can now be seen that greatest sensitivity to control occurs when the

stability is neutral; putting the centre of gravity forward reduces the
sensitivity and introduces stability, whilst putting the centre of gravity
back reduces the sensitivity and makes the aeroplane unstable.

Tail Plane of Different Size.—For positions A and B of the centre of
gravity of the aeroplane calculations have been made for a tail area of
35 sq. feet instead of 55. The effect is a reduction of the moment due to
the tail n the proportion of 35 to 55 for the same tail setting and aeroplane
speed. The results are shown in Fig. 32. For neither positions A nor B
is the character of the diagram greatly altered, the chief changes being the
smaller righting couple for a given displacement, as shown by the smaller
angles of crossing as compared with Fig. 28. A tail-setting angle of
−10° with position A now only reduces the speed to 58 m.p.h., and it is
probable that the tail plane would reach its critical angle at lower speeds
of flight.

For position B the diagram shows a smaller restoring couple at low
speeds and a somewhat greater disturbing couple at high speeds.

Small tail planes tend towards instability, but the effect of size is not
so marked as the effect of the centre of gravity changes represented by
A, B and C. The control may not be sufficient to stall the aeroplane when
its centre of gravity is at A. This tends to safety in flight.

Elevators.—Many aeroplanes are fitted with tail planes which can be
set in the air. The motions provided for this purpose are slow, and the
control is normally taken by the elevators. The effect of the motion of
the elevators is equivalent to a smaller motion of the whole tail plane,
and Fig. 33 shows a typical diagram for variation of lift with variation of
angle of elevators, the lift being the only quantity considered of sufficient
importance for reproduction.

The ordinate of Fig. 33 is the value of $\dfrac{\text{lift}}{V^2}$ for a tail plane and elevators
of 55 sq. feet area, of which total the elevators form 40 per cent. The
abscissae are the angles of incidence of the tail plane, and each curve corre-
sponds with a given setting of the elevators. The angle of the elevators
is measured from the centre line of the tail plane, and is positive when
the elevator is down, i.e. making an angle of incidence greater than the
tail plane. For elevator angles between −15° and +15° the curves
are roughly equally spaced on angle, but after that the increase of lift
with further ncrease of elevator angle s much reduced.

The diagram may be used for negative settings by changing the signs
of both angles and of the lift. This follows because the tail plane has a
symmetrical section.

From the diagram at A, it will be seen that an elevator setting of 5°
produces an $\dfrac{L'}{V^2}$ of 0·015, and this would also be produced by a movement of
the whole tail plane and elevators through 2°·6 (B, Fig. 33). For this par-
ticular proportion of elevator to total tail surface the angle moved through
by the elevator is then about twice as great for a given lift as the movement
of the whole tail surface. Variations of tail-plane settings of 10° were seen
to be required (Fig. 28) if the centre of gravity of the aeroplane was far

forward, and this would mean excessive elevator angles, an angle of over
20° being indicated at C for +10°. These elevators are large, and it will
be seen that an aeroplane may be so stable that the controls are not suffi-
cient to ensure flight over the full range otherwise possible. For the centre
of gravity at position B, Fig. 28, the elevator control is ample for all
purposes.
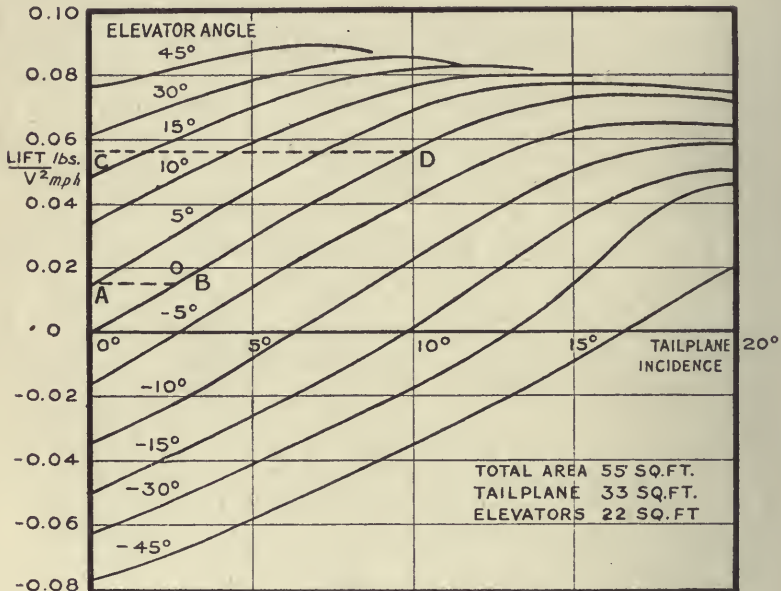
Fig. 33.—Lift of tail plane and elevator for different settings.

Effort necessary to move the Elevators.—The muscular effort required of
the pilot is determined by the moment about the hinge of the forces on the
elevator, and it is to reduce this effort that adjustable tail planes are used.
If it be desired to fly for long periods at a speed of 70 m.p.h. the tail plane
is so set that the moment on the hinge is very small. For large aeroplanes
balancing of controls is resorted to, but there is a limit to the approach
to complete balance, which will ultimately lead to relay control by some
mechanical device. The mmediate scope of this section will be limited
to unbalanced elevators in which the size is fixed at 40 per cent. of the total
tail plane and elevator area.

It has been seen that the lift on the tail is the important factor in longi-
tudinal balance, and so we may usefully plot hinge moments on the basis
of lift produced. In the calculation a total area of 55 sq. feet will be
assumed so as to compare directly with the previous calculations on tail
setting.

The curves of Fig. 34 may be used for negative values of $\frac{L'}{V^2}$ if M_h and
the tail incidence are used with the reversed sign.

As there are now two angles at disposal another condition besides that of zero total moment must be introduced before the problem is definite. The extra condition will be taken to be that which puts the aeroplane " in trim " at 70 m.p.h., this expression corresponding with flight with no force on the control stick. The force on the control stick being due to the moment of the forces on the elevators about its hinge, the condition of " trim " is equivalent to zero h nge moment.
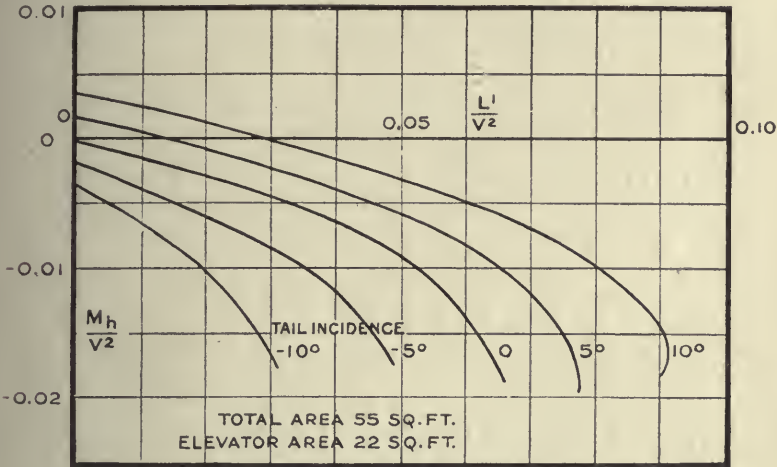
Fig. 34.—Hinge moment of elevators.

For position A of the centre of gravity of the aeroplane the forces on the control stick are worked out in Table 18.

TABLE 18.—Forces on Control Stick.

Speed (m.p.h.).	$\frac{M_A}{cV^2}$ Table 16.	$\frac{L'}{V^2}$	a'	$\frac{M_h}{V^2}$	M_h	Force on pilot's hand.
40	−0·177	−0·065	−0°·9	0·0155	25	12·5 lbs. pull
50	−0·101	−0·037	−6°·5	0·0030	8	4 ,,
60	−0·082	−0·030	−8°·5	0·0010	4	2 ,,
70	−0·074	−0·027	−9°·5	0·0000	0	0 ,,
100	−0·070	−0·026	−11°·1	−0·0010	−10	5 lbs. push

The value of $\frac{M_A}{cV^2}$ is taken from Table 16, and from it $\frac{L'}{V^2}$ for the tail is calculated by dividing by l_A, (2·7 c.). From Fig. 34 we then find that for $\frac{L'}{V^2} = -0·027$ (70 m.p.h.), the hinge moment is zero if the tail incidence is −9°·5. Equation (6) and the figures in column (3) of Table 17 then show the tail setting to be −9°·5, and the angles of incidence at other speeds to be those given in column 4 of Table 18. From columns 3 and 4 of Table 18,

the values of $\dfrac{M_h}{V^2}$ can be determined by use of Fig. 34 (see column (5),

Table 18). M_h is easily calculated from $\dfrac{M_h}{V^2}$, and the force on the pilot's

hand is then calculated by assuming that his hand is 2 feet from the pivot of his control stick. A positive moment at the elevator hinge means a pull on the stick.

Before commenting on the control forces the results of similar calculations for positions B and C of the centre of gravity of the aeroplane are given in Table 19 in comparison with those for A.

TABLE 19.—FORCES ON CONTROL STICK FOR DIFFERENT POSITIONS OF CENTRE OF GRAVITY.

Speed (m.p.h.).	A.	B.	C.
40	12·5 lbs. pull	0	—
50	4 ,,	3 lbs. push	16 lbs. push
60	2 ,,	2 ,,	5 ,,
70	0 ,,	0 ,,	0 ,,
100	5 lbs. push	5 lbs. pull	20 lbs. pull

Consider position C first; at 100 miles per hour the pilot is pulling hard on his control stick. It has already been seen that the aeroplane is unstable with the centre of gravity at C, and one result of this is a tendency to dive without conscious act of the pilot. The result of a dive is an increase of speed, and Table 19 shows that an increase of pull may be expected. At a moderate angle of dive the pull may become so great that the pilot is not strong enough to control his aeroplane, which may then get into a vertical dive or possibly on its back. A skilful pilot can recover his correct flying attitude, but the aeroplane in the condition represented by C is dangerous.

Position A shows the reverse picture; the aeroplane is stable and does not tend to dive without conscious effort by the pilot. It needs to be pushed into a dive, and if the force gets very great owing to increase of speed it automatically stops the process.

The aeroplane which is lightest on its controls is still that with the centre of gravity at B, but it is further clear from Table 19 that an improvement would be obtained by a choice of centre of gravity somewhere between A and B.

(ii) FORCES ON THE FLOAT OF A FLYING BOAT

A diagram illustrating the form of a very large flying boat hull is shown in Fig. 35, the weight of the flying machine being 32,000 lbs. The design of a flying boat hull has to provide for taxying on the water prior to flight and for alighting. When once in the air the problem of the motion of a flying boat differs little from that of an aeroplane, the chief difference

being that the airscrews are raised high above the centre of gravity in order to provide good clearance of the airscrews from waves and any green water which might be thrown up. The present section of this chapter is directed chiefly to an illustration of the forces and couples on a flying boat in the period of motion through the water.

Experiments on flying boat hulls have usually been made on models at the William Froude National Tank at Teddington, but in one instance a flying boat was towed by a torpedo-boat destroyer, and measurements of resistance and inclination made for comparison with the models. The comparison was not complete, but the general agreement between model and full scale was satisfactory. Such phenomena as the depression of the bow due to switching on the engine and " porpoising " are reproduced in the model with sufficient accuracy for the phenomena to be kept under control in the design stages of a flying boat.

In making tests of floats in water, Froude's law of corresponding speeds is used, since the greater part of the force acting on the float arises from
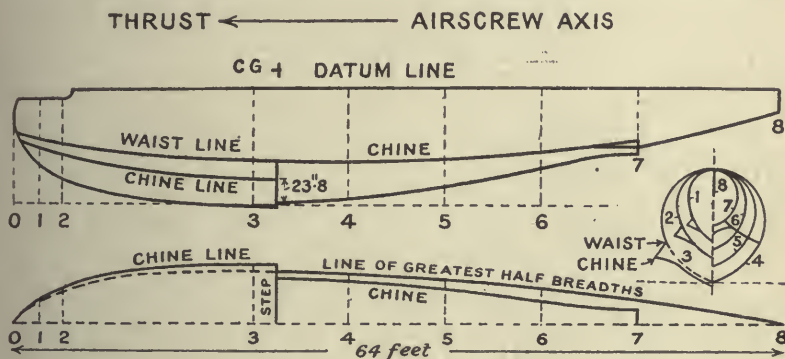
Fig. 35.—Flying boat hull.

the waves produced, and if the law be followed it is known on theoretical grounds that the waves in the model will be similar to those on the full scale. The law states that a scale model should be towed at a speed equal to the speed of the full scale float multiplied by the square root of the scale. A one-sixteenth scale model of a flying boat hull which taxies at 40 m.p.h. will give the same shape of waves at 10 m.p.h. The forces on the full scale are then deduced from those on the model by multiplying by the square of the scale and the square of the corresponding speeds, i.e. by the cube of the scale. Similarly, moments vary as the fourth power of the linear dimensions for tests at corresponding speeds.

As the float is running on the surface of the water, the forces on it depend on the weight supported by the water as well as on the speed and inclination of the float, and this complexity renders a complete set of experiments very exceptional. The full scheme of float experiments which would eliminate the necessity for any reference to the aerodynamics of the superstructure would give the lift, drag and pitching moment of a float for a range of speeds and for a range of weight supported. From

such observations and the known aerodynamic forces and moments on the superstructure for various positions of the elevator, the complete conditions of equilibrium could be worked out in any particular case.

A less complete series of experiments usually suffices. At low air speeds the lift from the wings is not very great, and at the speed of greatest float resistance not so much as one quarter of the total displacement at rest. At higher speeds, but still before the elevators are very effective, the attitude of the wings is fixed by the couples on the float and does not vary greatly. A satisfactory compromise, therefore, is to take the angle of incidence of the wings when the constant value has been reached, and to calculate from it and the known properties of the wings the speed at which the whole load will be air-borne. At lower speeds the air-borne load is taken as proportional to the square of the air speed. After a little experience this part
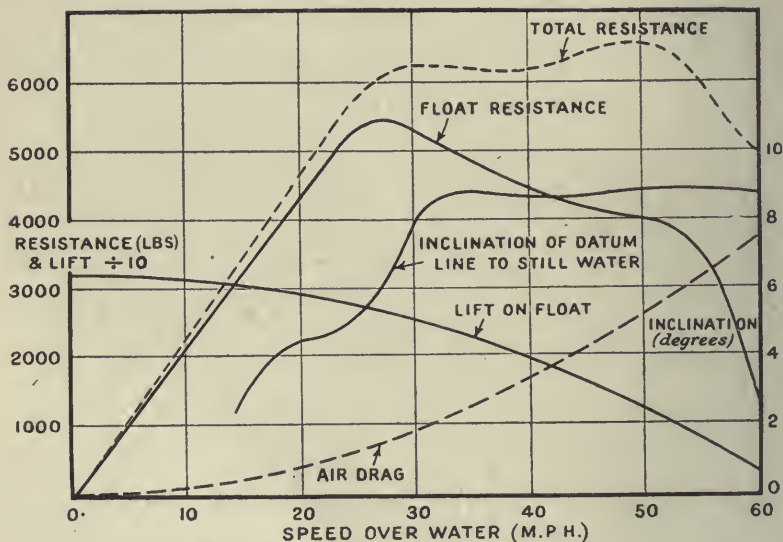
FIG. 36.—Water resistance of a flying boat hull.

of the calculation presents no serious difficulty, and the curve of " lift on float " shown in Fig. 36 is the result for the float under consideration. At rest on the water the displacement was 32,000 lbs. ; at 20 m.p.h., 29,000 lbs. ; at 40 m.p.h., 19,000 lbs., and had become very small at 60 m.p.h.

For the loads shown by the lift curve, the float took up a definite angle of inclination to the water, which is shown in the same figure. The resistance is also shown in one of the curves of Fig. 36. The angle of incidence depends generally on the aerodynamic couple of the superstructure, and the part of this due to airscrew thrust was represented in the tests. By movement of the elevator this couple is variable to a very slight extent at low speeds, but to an appreciable extent at high speeds.

The first noticeable feature of the water resistance of the float is the rapid growth at low speeds from zero to 5400 lbs. at 27 m.p.h., where it is 17 per cent. of the total weight of the flying boat. At higher speeds the

resistance falls appreciably and will of course become zero when the lift on the float is zero. If the aerodynamic efficiency of the flying boat is 8 at the moment of getting off, the air resistance is 4000 lbs., and with negligible error the air resistance at other speeds may be taken as proportional to the square of the air speed, since the attitude is seen to be nearly constant at the higher and more important speeds. By addition of the drags for water and air a curve of total resistance is obtained which reaches a value of a little over 6000 lbs. at a speed of 30 m.p.h., rises slowly to 6600 lbs. at 50 m.p.h., and then falls rapidly to less than 5000 lbs. After the flying boat has become completely air-borne the resistance again increases with increase of speed.

The additional information required to estimate the drag of a seaplane before it leaves the water is thus obtained, and the method of calculation proceeds as for the aeroplane. The drag of the wings is estimated, and to
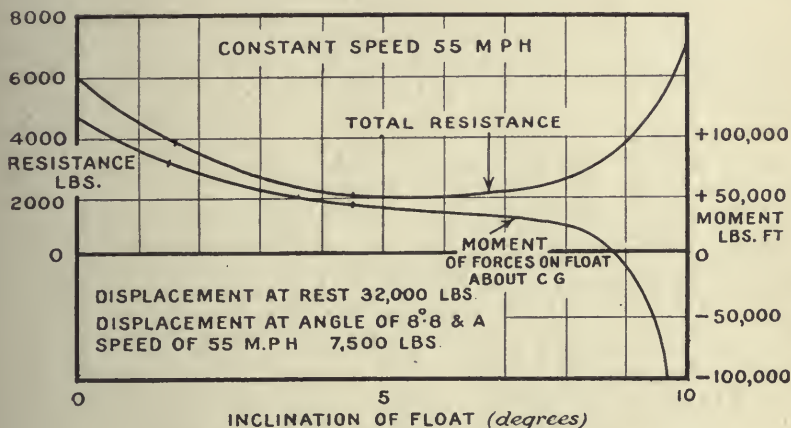
FIG. 37.—Pitching moment on a flying boat hull.

it is added the drag of the float, including its air resistance. To the sum is further added the resistance of the remaining parts of the aircraft. The calculation of the speed and horsepower of the airscrew follows the same fundamental lines as for the aeroplane, and differs from it only in the extension of the airscrew curves to lower forward speeds. The same extension would be needed for a consideration of the taxying of an aeroplane over an aerodrome. The extension of airscrew characteristics is easily obtained experimentally, or may be calculated as shown in a later chapter.

The evidence on longitudinal balance is not wholly satisfactory, but an example of a test is given in Fig. 37, which shows a series of observations at a constant speed, the resistance and the pitching moment being measured for various angles of incidence. In the experiment the height of the model from still water was limited by a stop, and it is improbable that under these circumstances the load on the float would correctly supplement the load on the wings. Treating the diagram, however, as though equilibrium

of vertical load had been attained, it will be noticed that the pitching moment was zero at 8°·8, and that at smaller angles the moment was positive, and thus tended to bring the float, if disturbed, back to 8°·8. For greater angles of incidence the moment changed very rapidly, but for smaller angles the change was very much more gradual, and it is interesting to compare the magnitude with that applicable by suitable elevators on the superstructure. For the present rough illustration the aerodynamic pitching moment due to a full use of the elevators may be taken as $20V^2_{m.p.h.}$ lbs.-feet, and if balanced so that the pilot can use the full angle a couple of 60,000 lbs.-feet at 55 m.p.h. is obtained. A couple of this magnitude is sufficient to change the angle of the float from 9 degrees to 4 degrees, and the pilot has appreciable control over the longitudinal attitude some time before leaving the water.

(iii) Lighter-than-Air Craft

All lighter-than-air craft obtain support for their weight by the utilisation of the differences of the properties of two gases, usually air and hydrogen. In the early days of ballooning the difference in the densities of hot and cold air was used to obtain the lift of the fire balloon, whilst later the enclosed gas was obtained from coal. Very recently, helium has been considered as a possibility, but none of the combinations produce so much lift for a given volume as hydrogen and air, since the former is the lightest gas known. The external gas is not at the choice of the aeronaut. At the same pressure and temperature air is 14·4 times as heavy as pure hydrogen, and the lift on a weightless vessel filled with hydrogen and immersed in air would be $\dfrac{13\cdot4}{14\cdot4}$ of the weight of the air displaced. Helium is twice as dense as hydrogen, whilst coal gas is seven times as dense, and is never used for dirigible aircraft.

Some of the problems relating to the airship bear a great resemblance to problems in meteorology. As in the case of the aeroplane, the stratum of air passed through by the airship is very thick, the limit being about 20,000 feet, where the density has fallen to nearly half that at the surface of the earth. As the lift of an airship depends on the weight of displaced air, it will be seen that the lift must decrease with height unless the volume of displaced air can be increased. It is the limit to which adjustment of volume can take place which fixes the greatest height to which an airship can go. The gas containers inside a rigid airship are only partially inflated at the ground, and under reduced pressure they expand so as to maintain, at least approximately, a lift which is independent of height. The process of adjustment, which is almost automatic in a rigid airship, is achieved by automatic and manual control in the non-rigid type, air from the balloonets being released as the hydrogen expands. In both types, therefore, the apparent definiteness of shape does not apply to internal form.

The first problem in aerostatics which will be considered is the effect, on the volume of a mass of gas enclosed in a flexible bag, of movement from one part of the atmosphere to another. The well-known theorems relating

to the properties of gases will be assumed, and only the applications developed. The gas is supposed to be imprisoned in a partially inflated flexible bag of small size, the later condition being introduced so as to eliminate secondary effects of changes of density from the first example. The gas inside the bag exerts a pressure normal to the surface, whilst other pressures are applied externally by the surrounding air. At B, Fig. 38, the internal pressure will be greater than that at A by the amount necessary to support the column of gas above it. If w be the weight of gas per unit volume, the difference of internal pressure at B and A is wh. Similarly if w' be the weight of air per unit volume, the difference of external pressures is $w'h$, and the vertical component of the internal and external pressures at A and B is $(w' - w)h$. Now for the same gases $(w' - w)$ is constant, and the element of lift is proportional to h and to the horizontal cross-section of the column which stands on B. Adding up all the elements shows that

the total lift is equal to the product of the volume of the bag and the difference of the weights of unit volumes of air and the enclosed gas. At ordinary ground pressure and temperature, 2116 lbs. per sq. foot and 15° C., the value of w' for air is 0·0763 lb. per cubic foot, whilst w for hydrogen would be 0·0053 ; $w' - w$ for air and pure hydrogen would therefore be 0·0710 lb. per cubic foot. In practice pure hydrogen is not obtainable, and under any circumstances becomes contaminated with air after a little use. Instead of the figure 0·071 values ranging from 0·064 to 0·068 are used, depending on the purity of the enclosed gas.
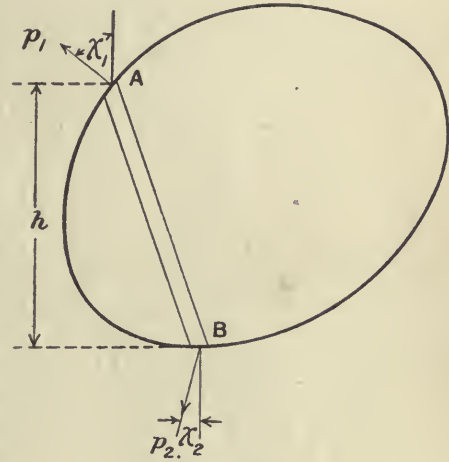
Fig. 38.

If a suitable weight be hung to the bottom of the flexible gas-bag the whole may be made to remain suspended at any particular place in the atmosphere. What will then happen if the whole be raised some thousands of feet and released ? Will the apparatus rise or fall ?

The effect of an increase of height is complex. In the first place, the density of the air falls but with a simultaneous fall of pressure, and the hydrogen expands so long as full inflation has not occurred. For certain conditions not greatly different from those of an ordinary atmosphere the increased volume exactly counterbalances the effect of reduced density, and equilibrium is undisturbed by change of height. The problem involves the use of certain equations for the properties of gases. If p be the pressure, w the weight of unit volume, and t the absolute temperature of a gas, then

$$p = Rwt \quad . \quad . \quad . \quad . \quad . \quad . \quad (8)$$

For air, R = 95·7, and for hydrogen, R = 1375, p being in lbs. per sq. foot,

w in lbs. per cubic foot, and t in Centigrade degrees on the absolute scale of temperature.

When a gas is expanded both its temperature and pressure are changed, and unless heated or cooled by external agency during the process the additional gas relation is

$$\frac{p}{p_0} = \left(\frac{w}{w_0}\right)^\gamma = \left(\frac{t}{t_0}\right)^{\frac{\gamma}{\gamma-1}} \quad . \quad . \quad . \quad . \quad . \quad (9)$$

where γ is a physical constant for the gas and equal to 1·41 for both air and hydrogen. p_0, w_0 and t_0, are the values of p, w and t, which existed at the beginning of the expansion.

Inside the flexible bag gas weighing W lbs. has been enclosed at a pressure p_0 and a density w_0. The volume displaced at any other pressure is $\dfrac{W}{w}$, and as was seen earlier, the lift on the bag when immersed in air is the volume displaced multiplied by the difference of the weights of unit volumes of air and hydrogen. The equation is therefore

$$\text{Lift} = \frac{W}{w}(w' - w)$$

$$= W\left(\frac{w'}{w} - 1\right) \quad . \quad . \quad . \quad . \quad . \quad (10)$$

If the bag be so small that p has sensibly the same value inside and out, equation (8) shows that the weights of unit volumes of the two gases vary inversely as their absolute temperatures, and equation (10) shows that the lift is independent of position in the atmosphere if the temperatures of the two are the same. If the bag be held in any one place equality of temperatures will ultimately be reached, but for rapid changes in position, equation (9) shows the changes of temperature to be determined by the changes of pressure. It is now proposed to investigate the law of variation of pressure with height which will give equilibrium at all heights for rapid changes of position.

Convective Equilibrium

If for the external atmosphere equation (9) is satisfied, the gas inside the bag expands so as to keep the lift constant. Replace the hydrogen by air, and in new surroundings at the reduced pressure reconsider the problem of equilibrium. It will be found that the pressures inside and outside the bag are equal at all points, and the fabric may then be removed without affecting the condition of the air. The conditions are, however, those for equilibrium, and the air would not tend to return to its old position. It is obvious that no tendency to convection currents exists, although the air is colder at greater heights. The quantity which determines the possibility or otherwise of convection is clearly not one of the three used in equations (8) and (9). A quantity called " potential temperature " is employed in this connection, and is the temperature taken by a portion of gas which is compressed adiabatically from its actual state to one in which

its pressure has a standard value. In an atmosphere in convective equilibrium the potential temperature is constant. If the potential temperature rises with height equilibrium is stable, whilst in the converse case up and down currents will be produced.

Applying the conclusions to the motion of an airship with free expansion to the hydrogen containers, it will be seen that in a stable atmosphere the lift decreases with height for rapid changes of position, and hence the airship is stable for height. In an unstable atmosphere the tendency is to fall continuously unless manual control is exerted. Calculations for an atmosphere in convective equilibrium are given below, and are compared with the observations of an average atmosphere.

Law of Variation of Pressure, Density and Temperature in an Atmosphere which is in Convective Equilibrium.—Since the increase of pressure at the base of an elementary column of air is equal to the product of the density and elementary height, the equation of equilibrium is—

$$\frac{dp}{dh} = -w \quad . \qquad . \qquad . \qquad . \qquad . \qquad . \qquad (11)$$

the negative sign indicating decrease of pressure with increase of height. Using equation (9) to substitute for w converts equation (11) into

$$\frac{dp}{dh} = -w_0\left(\frac{p}{p_0}\right)^{\frac{1}{\gamma}} \quad . \qquad . \qquad . \qquad . \qquad . \qquad (12)$$

and the solution of this is

$$h = \frac{\gamma}{\gamma-1} \cdot \frac{p_0}{w_0}\left\{1 - \left(\frac{p}{p_0}\right)^{\frac{\gamma-1}{\gamma}}\right\} \quad . \qquad . \qquad . \qquad . \qquad (13)$$

which clearly gives $h = 0$ when $p = p_0$. For the usual conditions at the foot of a standard atmosphere, $p_0 = 2116$ and $w_0 = 0.0783$, and for these values equation (13) has been used to calculate values of p for given values of h. Values of relative density and temperature follow from equation (9). The corresponding quantities for a standard atmosphere are taken from a table in the chapter on the prediction and analysis of aeroplane performance.

TABLE 20.

Height (ft.).	Atmosphere in convective equilibrium.			Standard atmosphere.			
	Relative pressure.	Relative density.	Temperature Centigrade.	Relative pressure.	Relative density.	Temperature Centigrade.	Potential temperature for standard atmosphere.
0	1·000	1·025	+ 9	1·000	1·025	+ 9	9
5,000	0·827	0·895	− 6	0·829	0·870	+ 1·5	15
10,000	0·676	0·776	−21	0·684	0·740	− 6	25
15,000	0·546	0·668	−37	0·560	0·630	−16	31
20,000	0·435	0·568	−52	0·456	0·535	−26	37
25,000	0·340	0·476	−67	0·369	0·448	−35	45
30,000	0·262	0·395	−82	0·296	0·374	−44	53

It will be seen from Table 20 that the fall of temperature for convective equilibrium is very nearly three degrees Centigrade for each 1000 feet of height.   In the standard atmosphere the fall is less than two degrees for each 1000 ft. of height, *i.e.* the potential temperature rises as the height increases and indicates a considerable degree of stability.

Lift on a Gas Container of Considerable Dimensions.—In the first example the container was kept small, so that the gas density was sensibly the same at all parts.   In a large container the quantity $\dfrac{w'}{w}$ which occurs in equation (10) is not constant, since for the hydrogen in the container and for the air immediately outside the density varies with the height of the point at which it is measured.   To develop the subject further, convective equilibrium inside and outside the gas-bag will be assumed, and equation (13) used to define the relation between pressure and height. The equation in new form is

$$\frac{p}{p_0} = \left(1 - \frac{\gamma - 1}{\gamma} \cdot \frac{w_0}{p_0} h\right)^{\frac{\gamma}{\gamma-1}}$$

and for values of h less than 5000 feet the second term in the bracket is small in comparison with unity.   The expression may then be expanded by the binomial theorem and a limited number of terms retained.   The expansion leads to

$$\frac{p}{p_0} = 1 - \frac{w_0}{p_0} h + \frac{1}{2\gamma}\left(\frac{w_0}{p_0}\right)^2 h^2 \quad . \quad . \quad . \quad . \quad . \quad (14)$$

where w_0 and p_0 are the values of p and w at some chosen point in the gas, say its centre of volume, and h is measured above and below this point. For a difference between ground-level and $h = 5000$ feet the terms of (14) are 1; -0.185 and 0.012, and the terms are seen to converge rapidly.   On the difference of pressure between the two places the accuracy of (14) as given is about 1 per cent.   For any airship yet considered the accuracy of (14) would be much greater than that shown in the illustration, and may therefore be used as a relation between pressure and height in estimating the lift of an airship.

If p_2 be the pressure at B, Fig. 38, due to internal pressure, and χ_2 the angle between the normal to the envelope at B and the vertical, the contribution to the lift is $-p_2 \cos \chi_2 \times$ element of area at B.   If a column be drawn above B, the horizontal cross-section is equal to $\cos \chi_2 \times$ element of area at B, and the value of the latter quantity is equal to an increment of volume, δ (vol.), divided by h, or, what is the same thing, by $h_1 - h_2$.   The total lift is then given by the equation

$$\text{gross lift} = \int \frac{p_1 - p_2}{h_1 - h_2} \delta \,(\text{vol.}) - \int \frac{p_1' - p_2'}{h_1 - h_2} \delta \,(\text{vol.}) \quad . \quad . \quad (15)$$

where the pressures for the air are indicated by dashes.

From equation (14) the necessary values for use in equation (15) can be deduced, since

$$\frac{p_1 - p_2}{h_1 - h_2} = -w_0 \left\{ 1 - \frac{1}{2\gamma} \cdot \frac{w_0}{p_0}(h_1 + h_2) \right\} \quad . \quad . \quad . \quad (16)$$

for hydrogen inside with a similar expression for air outside. Equation (15) becomes

$$\text{gross lift} = (w_0' - w_0)\int\left\{1 - \frac{1}{2\gamma}\cdot\frac{w_0' + w_0}{p_0}(h_1 + h_2)\right\}\delta\,(\text{vol.})$$

$$= (w_0' - w_0)\,\text{vol.} - \frac{1}{\gamma}\cdot\frac{(w_0')^2 - w_0^2}{p_0}\int\frac{h_1 + h_2}{2}\delta\,(\text{vol.}).\quad(17)$$

The term $(w_0' - w_0)$ vol. is that which would be obtained by considering the hydrogen and air of uniform density w_0 and w_0' respectively. The second term depends on the mean height of the points A and B above the centre of volume, and in a symmetrical airship on an even keel the quantity $\frac{h_1 + h_2}{2}$ is zero for all pairs of points and the second integral vanishes. If the axis of the airship is inclined the integral of (17) must be examined further. For a fully inflated form which has a vertical plane of symmetry the average value of $\frac{h_1 + h_2}{2}$ for any section is equal to $x \sin\theta$, x being the distance from the centre of volume along the axis, and the section being normal to the axis. The element of volume is then equal to the area of cross-section multiplied by dx, and

$$\int\frac{h_1 + h_2}{2}\delta\,(\text{vol.}) = \sin\theta\int\text{A}x\,dx\ .\quad.\quad.\quad.\quad.\quad(18)$$

This integral is easily evaluated graphically for any form of envelope, but for the purposes of illustration a cylinder of length $2l$ and diameter d will be used. The first point is easily deduced, and shows that the gross lift of an inclined cylinder is the same as that on an even keel. Generalising from this, it may be said that for an airship the gross lift is not appreciably affected by the inclination of the axis, and the lift may be calculated from the displacement and the difference of densities at the height of the centre of volume.

Pitching Moment due to Inclination of the Axis.—Moments will be taken about the centre of volume of the airship. To do this it is only necessary to multiply the lift of an element by $-x$ before the integration in (17) is performed. The first term will be zero, whilst the second has a value equal, for the cylinder, to

$$\text{Pitching moment} = \frac{1}{\gamma}\cdot\frac{(w_0')^2 - w_0^2}{p_0}\sin\theta\int_{-l}^{l}\text{A}x^2\,dx$$

$$= \frac{2}{3}\cdot\frac{1}{\gamma}\cdot\frac{(w_0')^2 - w_0^2}{p_0}\cdot\text{A}\sin\theta\cdot l^3\ .\quad.\quad(19)$$

To appreciate the significance of (19) consider a numerical case. A height of 15,000 feet in a convective atmosphere has been chosen as corresponding with fully expanded hydrogen containers. The pressure is here 1150 lbs. per square foot, and w_0' is 0·0433. The value of w_0 is of no importance. An airship 70 feet in diameter and of length 650 feet shows for an inclination of 15° a couple of more than 25,000 lbs.-ft., and to

counteract this a force of 90 lbs. on the horizontal fin and elevators would
be needed.   The couple may, however, occur when the airship has no
motion relative to the air, in which case it is balanced by a moment due
to the weight of the airship, which in the illustration would be 100,000
lbs.   A movement of 3 ins. would suffice, whilst the movement caused by
a pitch of 15° would be about 8 feet.   The effect is then equivalent to a
reduction of metacentric height of 3 per cent.

Equation (19) shows that the pitching moment increases rapidly with
the length of the ship, but in these cases the type of construction adopted
reduces the moment to a small amount.   The length of the airship is divided
into compartments separated by bulkheads which can support a consider-
able pressure.   In each compartment is a separate hydrogen container,
and the arrangement is therefore such that the gas cannot flow freely
from end to end of the airship.   This greatly reduces the changes of
density due to inclination of the axis, and so reduces the pitching moment.
The arrangement also effectively intervenes to prevent surging of the
hydrogen, which might increase the pitching moments as a result of the
effects of inertia of the hydrogen.

It may therefore be concluded that the result of displacing air by
hydrogen is a force acting upwards at the centre of the volume of the
displaced air, and with suitable precautions in large airships no other
consequences are of primary importance.

Forces on an Airship due to its Motion through the Air

The aerodynamics of the airship is fundamentally much simpler than
that of the aeroplane.   This follows when once it is appreciated that the
attitude relative to the wind does not depend on the speed of the airship.
The most important forces are the drag, which varies as the square of
the speed, and the airscrew thrust, which also varies as the square of the
speed since it counterbalances the drag.   A secondary consequence of the
variation of thrust as the square of the speed is that at all speeds the
airscrew may be working in the condition of maximum efficiency, a state
which was not possible in the aeroplane for an airscrew of fixed shape.

It is true that dynamic lift may be obtained·from an airship envelope,
but this has not the same significance as in the case of the aeroplane, since
height can be gained apart from the power of the engine.   The number
of experiments from which observations of drag for airships can be deduced
with accuracy is very small, and the figures now quoted are based on full
scale observations and speed attained, together with a certain amount
of analysis based on models of airships both fully rigged and partially
rigged.

The two illustrations chosen correspond with the non-rigid and rigid
airships shown in Figs 7–9, Chapter I.   The N.S. type of non-rigid
airship has a length of 262 feet and a maximum width of 57 feet.
The gross lift is 24,000 lbs., and the result of the analysis of flight tests
shows that the drag in pounds is approximately $0.77V^2_{m.p.h.}$ The drag is
made up in this instance in the proportions of 40 per cent. for the envelope,

35 per cent. for the car and rigging cables, and 25 per cent. for the vertical and horizontal fins, rudder and elevators. The horsepower necessary to propel the airship depends on the efficiency of the airscrew, η, the relation being

$$0.77V^3_{\text{m.p.h.}} = 375 \cdot \eta \cdot \text{B.H.P.} \quad . \quad . \quad . \quad (20)$$

It has already been mentioned that the airscrew if correctly designed would always be working at its maximum efficiency at all speeds and a reasonable value for the efficiency is 0.75. At maximum power the two engines of the N.S. type of airship develop 520 B.H.P., and from equation (20) it is then readily found that the maximum speed of the airship is 57.5 m.p.h. The drag at this speed is 2500 lbs.

For a large rigid airship, 693 feet in length and with an envelope 79 feet in diameter the drag in lbs. was $1.25V^2_{\text{m.p.h.}}$, and the gross lift 150,000 lbs. The drag of the envelope was about 60 per cent. of the total, with cars and rigging accounting for 30 per cent. and fins and control surfaces for 10 per cent. It will be noticed that the envelope of the rigid airship has a greater proportionate resistance than that of the non-rigid, and this is largely accounted for by the smaller relative size of the cars and rigging in the former case.

The relation between horsepower and speed has a similar form to (20), and is

$$1.25V^3_{\text{m.p.h.}} = 375\eta \text{ B.H.P.} \quad . \quad . \quad . \quad . \quad (21)$$

With engines developing 1800 B.H.P. and an airscrew efficiency of 0.75 equation (21) shows a maximum speed of 74 m.p.h. The drag is then 6800 lbs.

A convenient formula which is frequently used to express the resistance of airships is

$$\text{Resistance in lbs.} = C \cdot \rho \cdot V^2 \, (\text{vol.})^{\frac{2}{3}} \quad . \quad . \quad . \quad (22)$$

where C is a constant defining the quality of the airship for drag. The advantage of the formula is that C does not depend on the size of the airship or its velocity or on the density of the air, but is directly affected by changes of external form. In the formula ρ is the weight in pounds of a cubic foot of air divided by g in feet per sec. per sec., V is the velocity of the airship in feet per sec., and "vol." is the volume in cubic feet of the air displaced by the envelope. For the non-rigid airship above, the value of C is 0.03, and for the rigid airship C = 0.016.

Longitudinal Balance of an Airship.—For an airship not in motion, balance is obtained by suitable adjustment of the positions of the weights carried. A certain amount of alteration of "trim" can be obtained by transferring air from one of the balloonets of a non-rigid airship to another. Fig. 9, Chapter I., shows the pipes to the two balloonets which are about 120 feet apart. One pound of air moved from the front to the rear produces a couple of 120 lbs.-ft. If the centre of buoyancy of the hydrogen be taken as 10 feet above the centre of gravity and the weight of the airship is 24,000 lbs., the couple necessary to displace the airship through one degree is 4200 lbs.-feet, and would require a movement of 35 lbs. of air from one balloonet to the other. By this means sufficient adjustment is available

for the trim of the airship when not in motion. In the rigid airship a similar control can be obtained by the movement of water-ballast from place to place.

When in motion the aerodynamic forces introduce a new condition of balance which is maintained by movement of the elevators. The couples due to movements of the elevators are very much greater than those arising from adjustment of the air between the balloonets, a rough figure for the elevators of the N.S. type of airship being $5V^2_{m.p.h.}$ lbs.-feet per degree of movement of the elevator. At a speed of 40 m.p.h. the couple due to one degree change of elevator position is 8000 lbs.-feet, and so would tilt the airship through an angle of about 2°. For a sufficiently large movement of the elevators considerable inclination of the axis of an airship could be maintained at high speeds, and the airship then has an appreciable dynamic lift. For the N.S. type of airship about 200 lbs. of dynamic lift or about 1 per cent. of the gross lift is obtained at 40 m.p.h. for an inclination of the axis of one degree.

The various items briefly touched on in connection with longitudinal balance are more naturally developed in considering the stability of airships, since it is the variation from normal conditions which constitutes the basis of stability, and apart from a tendency to pitch and yaw the control of an airship presents no fundamental difficulties.

EQUILIBRIUM OF KITE BALLOONS

The conditions for the equilibrium of a kite balloon are more complex than those for the airship. The kite balloon has its own buoyancy, which is all important at low wind speeds but unimportant in high winds. The aerodynamic forces of lift and drag and of pitching moment are all of importance, and in addition there is the constraint of a kite wire. It is now proposed to consider in detail the equilibrium of the two types of kite balloon shown in Fig. 10, Chapter I., and to explain why one of them is satisfactory in high winds and the other unsatisfactory.

A diagram of a kite balloon is shown in Fig. 39, on which are marked the quantities used in calculation. Axes of reference are taken to be horizontal and vertical, with the origin at the centre of gravity. If towed, the kite balloon would be moving along the positive direction of the axis of X, whilst in the stationary balloon the wind is blowing along the negative direction of the axis. The axis of Z is vertically downward, and the pitching moment M is positive when it tends to raise the nose of the balloon. The kiting effect results from an inclination, α, of the axis of the kite balloon to the relative wind. The buoyancy due to hydrogen has a resultant F which acts upwards at the centre of volume of the enclosed gas, a point known as the centre of buoyancy (CB of Fig. 39). The kite wire comes to a pulley at D, which runs freely in a bridle attached to the balloon at the points E and H. The point D moves in an ellipse of which E and H are the foci, and for a considerable range of inclination the point of virtual attachment is at A, the centre of curvature of the path of D.

By arranging the rigging differently the point of attachment could be transferred to B. To effect this the pulley at D is removed, the points E and H moved nearer the axis of the balloon, the wires from them meeting the kite wire at B. The details of the calculations follow the same routine for all points of attachment, and the effects illustrated will be those of changing from type Fig. 10a to type Fig. 10c with a fixed attachment and those due to changing the point of attachment of type Fig. 11c from A to B of Fig. 39. The co-ordinates of the point of attachment (or virtual point of attachment) of the kite wire are denoted by a and c respectively for distances along the axis of X and Z. The length of the kite balloons considered in these pages was about 80 feet, and the maximum diameter 27 feet.

Fig. 39.—Equilibrium of a kite balloon.

Kite Balloon with three Fins (Figs. 10a and 10b).—For a particular example of this type the weight of the balloon structure was 1500 lbs., and at a height of 2000 feet the buoyancy force F was 2085 lbs. For various angles of inclination of the balloon the values of the lengths a, c and f were calculated from the known geometry of the balloon. The results of the calculations are given in Table 21 below.

A model of the kite balloon was made and tested in a wind channel, so that for various angles of inclination, a, the values of the lift, drag and aerodynamic pitching moment about the centre of gravity were measured. The observations were converted to the full size by multiplying by the square of the scale for the forces and by the cube of the scale for moments. Extensions of observations to speeds higher than those of the wind channel were made by increasing the forces and moment in proportion to the square of the wind speed.

From Fig. 39 it will be seen that the components of the tension of the kite wire are very simply related to the lift and drag of the kite balloon. The relations are

$$T_1 = \text{drag} \atop T_2 = \text{lift} + F - W \Big\} \quad . \quad . \quad . \quad . \quad . \quad (23)$$

The total pitching moment is obtained by taking moments of the forces about CG and adding to them the couple from aerodynamic causes other than lift and drag. The resultant moment must be zero for any position of equilibrium, and hence

$$M + T_1 c - T_2 a + Ff = 0 \quad . \quad . \quad . \quad . \quad . \quad (24)$$

TABLE 21.

Inclination of the axis of the balloon to horizontal. α	Co-ordinates of the position of the point of attachment of the kite wire.		Horizontal distance between centre of gravity and centre of buoyancy, f (ft.).
	a (ft.).	c (ft.).	
0	26·8	36·2	13·5
5	29·9	33·8	12·0
10	32·7	31·0	10·5
15	35·3	28·1	8·8
20	37·6	24·8	7·1
25	39·6	21·5	5·3

Since F — W is constant and equal to 585 lbs., T_2 differs from the lift by a constant amount, and in tabulating the results of experiment T_1 and T_2 have been used directly instead of drag and lift. The value of the aerodynamic moment about the centre of gravity, *i.e.* M of equation (24), is given in the second column of Table 22 for various wind speeds, whilst the value of the whole of the left-hand side of (24) for various angles of incidence and for a range of speeds is shown in the sixth column of the table. From an examination of the figures in columns (3) and (4) it will be seen that for the same angle of incidence the aerodynamic pitching moment and the drag vary as the square of the wind speed. A similar result will be found for $T_2 - 585$.

Equilibrium occurs when the figures in the last column of Table 22 change sign, and an inspection shows a progressive change of angle of incidence from about 12°·5 for no wind to a little more than 15° at a wind speed of 80 m.p.h. A positive moment tends to put the nose of the balloon up and so increase the angle of incidence, the effect being a tendency towards the position of equilibrium.

The figures for no wind give a measure of the importance of the couples due to reserve buoyancy, and by comparison with those due to a combination of buoyancy and aerodynamic couples and forces at 80 m.p.h. it will be realised that the equilibrium of a kite balloon in a high wind depends almost wholly on the aerodynamic forces and couple. This is an illustration of a law which appears on many occasions, that effects of buoyancy

are only important in determining the attitude of floating bodies at very low relative velocities. The theorem applies to the motion of flying boats over water, and explains a critical speed in the motion of airships.

TABLE 22.

Wind speed (m.p.h.).	a (degrees).	Aerodynamic pitching moment, M (lbs.-ft.)	Drag = T_1 (lbs.).	Lift + 585 = T_2 (lbs.).	Total pitching moment about C.G. (lbs.-ft.).
0	0	—	—	585	12,480
	5	—	—	585	7,520
	10	—	—	585	2,790
	15	—	—	585	− 2,300
	20	—	—	585	− 7,200
	25	—	—	585	− 12,100
20	0	2,030	126	607	18,500
	5	4,650	144	763	11,740
	10	7,340	172	889	5,530
	15	9,470	225	1,027	− 2,170
	20	9,870	309	1,210	− 13,170
	25	10,250	424	1,400	− 25,000
40	0	8,290	506	675	36,700
	5	18,600	578	1,298	24,390
	10	29,400	690	1,801	13,750
	15	37,900	900	2,353	− 1,460
	20	39,450	1,236	3,085	− 31,000
	25	41,000	1,696	3,845	− 63,500
60	0	18,700	1,136	787	66,800
	5	41,900	1,299	2,185	45,500
	10	66,100	1,550	3,320	27,700
	15	85,200	2,025	4,560	− 620
	20	88,800	2,786	6,210	− 60,330
	25	92,300	3,816	7,920	−128,200
80	0	33,200	2,024	945	109,300
	5	74,400	2,312	3,440	75,000
	10	117,500	2,760	5,450	46,900
	15	151,500	3,600	7,660	470
	20	157,800	4.944	10,580	−102,800
	25	164,000	6,784	13,630	−218,500

The tension in the kite wire for each of the positions of equilibrium is obtained from Table 22, since it is equal to the square root of the sum of the squares of T_1 and T_2. The values are given in Table 23 below.

TABLE 23.

Wind speed (m.p.h.).	Tension in kite wire (lbs.).
0	585
20	990
40	2460
60	4960
80	8480

At 80 m.p.h. the tension in the kite cable has been increased to more than 14 times its value for no wind. Had the rigging been so arranged that the angle of incidence for equilibrium was 25°, Table 22 shows that the force would have been 80 per cent. greater than at 15°, and conversely a reduction of tension would have been produced by rigging the kite-balloon so as to be in equilibrium as a smaller angle of incidence. The effect of change of position of the point of attachment of the kite wire will now be discussed.

The aerodynamic pitching moment on the kite balloon is seen from column 3 of Table 22 to tend to raise the nose of the balloon at all angles of incidence. The couple due to buoyancy depends on the point of attachment of the kite wire, and the nose will tend to come down as this point is moved nearer the nose. At high speeds it has been seen that the buoyancy couples are unimportant in their effects on equilibrium, and that the only variations of importance are those which affect the couples due to the tension in the kite wire.

Since $T_1 c - T_2 a$ is greater than M, as may be seen from Table 22, it follows that to obtain equilibrium at a lower angle of incidence the former quantity must be increased. $T_1 c - T_2 a$ is the moment of the kite wire about the centre of gravity, and can be increased by moving the point of attachment forward. Changing the vertical position is much less effective, since the kite wire is more nearly vertical than horizontal.

Before the calculation of equilibrium can be said to be complete, an examination of the resultant figure taken by the rigging will need to be made to ensure that all cords are in tension. In reference to Fig. 39 it will be observed that ED and HD will be in tension if the line of the kite wire produced falls between them. A running block ensures this condition, but a joint at D might produce different results. The virtual point of attachment would move to E or H if HD or ED became slack.

Position of a Kite Balloon relative to the Lower End of the Kite Wire.— When equilibrium has been attained the position in space of the kite balloon is determined by the length of kite wire and its weight and by the forces on the balloon. The equilibrium of the balloon has been dealt with, and its connection to the kite wire is fully determined by the tensions T_1 and T_2. The wind forces on the wire being negligible the curve taken by the wire is a catenary, and the horizontal component of the tension in the wire is constant at all points. Define the co-ordinates of the upper end of the wire relative to the lower end by ξ and ζ, and the weight of the wire rope per unit length by w. The equation of the catenary is then

$$\zeta = \frac{T_1}{w}\left\{\cosh\frac{w}{T_1}(\xi + A) - \cosh\frac{w}{T_1}A\right\} \quad . \quad . \quad . \quad (25)$$

where A is a constant so chosen that $\zeta = 0$ when $\xi = 0$, i.e. the distances are measured from the lower end of the kite wire: the equations for a catenary can be found in text-books on elementary calculus. The length of the kite wire to any point is given by

$$S = \frac{T_1}{w}\left\{\sinh\frac{w}{T_1}(\xi + A) - \sinh\frac{w}{T_1}A\right\} \quad . \quad . \quad . \quad (26)$$

and the vertical component of the tension in the wire is

$$T_2 = T_1 \sinh \frac{w}{T_1}(\xi + A) \quad . \quad . \quad . \quad . \quad . \quad (27)$$

As an example take the equilibrium position at 40 m.p.h. :—

$T_1 = 880$ lbs., $T_2 = 2300$ lbs., $S = 2000$ ft., $w = 0.15$ lb. per ft. run.

From equation (27) and a table of hyperbolic sines the value of $\xi + A$ is deduced as 9920 feet. Using both equations (26) and (27) the value of A is found as 9160 feet, and hence $\xi = 760$ feet.

Using the values of $\xi + A$ and A in equation (25) shows that $\zeta = 1850$ feet.

The kite balloon is then 1850 feet up and 760 feet back from the foot of the cable.

Had the cable been quite straight its inclination to the vertical would have been $\tan^{-1} \frac{T_1}{T_2}$, and the height of the balloon would be $2000 \dfrac{T_2}{\sqrt{T_1{}^2 + T_2{}^2}}$, and its distance back $2000 \dfrac{T_1}{\sqrt{T_1{}^2 + T_2{}^2}}$. For this assumption the height would be 1870 feet and the distance back from the base 715 feet.

From the above example it may be concluded that the wire cable is nearly straight and that a very simple calculation suffices for a moderate wind. Since Table 22 shows that the ratio of T_1 to T_2 does not change much at high speeds, it follows that the kite balloon will be blown back to a definite position as the result of light winds, but will then maintain its position as the wind velocity increases.

Kite Balloon with Large Vertical Fin and Small Horizontal Fins (Fig. 10c). —As the calculations follow the lines already indicated the results will be given with very little explanation. The object of the calculations is to draw a comparison between the two forms of kite balloon and to show the difference due to form of fins and point of attachment of the kite wire.

In the new illustration the balloon will be taken to have the weight, 1500 lbs., and buoyancy, 2085 lbs., used for the calculations on the kite balloon with three fins. In one case the point of attachment will be taken as A and will correspond with the running attachment at D, whilst in a second case an actual attachment at B will be used. The points A and B are marked on Fig. 39, and corresponding with them is the table of dimensions below.

<div align="center">TABLE 24.</div>

a	A. Running attachment of kite wire.		B. Fixed attachment of kite wire.		A and B.
Angle of inclination (degrees).	a (ft.).	c (ft.).	a (ft.).	c (ft.).	f (ft.).
0	19·0	− 4·6	25·6	+ 3·3	12·6
10	17·9	− 7·8	25·8	− 1·1	10·0
20	16·2	−10·8	25·2	− 5·7	7·2
30	14·2	−13·5	23·8	− 9·9	4·4
40	11·5	−15·7	21·7	−14·0	1·1

Only the values of pitching moment and tensions in the wire for a speed of 40 m.p.h. will be given, as they suffice for the present purpose of illustrating the limitation of the type.

TABLE 25.

a Angle of inclination (degrees).	Aerodynamic pitching moment. M (lbs.-ft.).	T_1 (lbs.).	T_2 (lbs.).	Total pitching moment.	
				A. Running attachment.	B. Fixed attachment.
0	5,150	500	585	18,000	18,100
10	29,000	596	1,196	23,700	18,400
20	51,100	885	1,855	26,500	14,400
30	66,000	1,435	2,460	20,800	2,400
40	70,900	2,490	3,375	—4,800	—34,900

An examination of the last two columns of Table 25 will show that with the running attachment of kite wire the angle of equilibrium is 39°, and for the fixed attachment $a = 31°$. Both angles are much greater than those shown in Table 22 for the same wind speed, and at higher speeds the results would be still less favourable to the type. The point of attachment will be seen from Table 24 to have been moved forward more than 6 feet between positions A and B, and is already inconveniently placed without having introduced sufficient correction. It may therefore be concluded that the horizontal fins shown in Fig. 10c are wholly inadequate for the control of a kite balloon in a high wind.

CHAPTER III

*GENERAL DESCRIPTION OF METHODS OF MEASUREMENT IN AERO-
DYNAMICS, AND THE PRINCIPLES UNDERLYING THE USE OF
INSTRUMENTS AND SPECIAL APPARATUS*

AERODYNAMICS as we now know it is almost wholly an experimental
science. It is probably no exaggeration to say that not a single case of
fluid motion round an aircraft or part is within the reach of computation.
The effect of forces acting on rigid bodies forms the subject of dynamics,
and is a highly developed mathematical science with which aeronautics
is intimately concerned. Such mathematical assistance can, however,
only lead to the best results if the forces acting are accurately known, and
it is the determination of these forces which provides the basic data on
which aeronautical knowledge rests. Two main methods of attack are
in common use, one of which deals with measurements on aircraft in flight,
and the other with models of aircraft in an artificial wind under laboratory
conditions. The two lines of investigation are required since the possi-
bilities of experiment in the air are limited to flying craft, and are unsuited
to the analysis of the total resistance into the parts due to wings, body,
undercarriage, etc. On the model side the control over the conditions of
experiment is very great and the accuracy attainable of a high order.
There is, however, an uncertainty arising from the small scale, which
makes the order of accuracy of application to the full scale less than that
of the measurement on the model. The theory of the use of models is
of sufficient importance to warrant a separate chapter, and the general
result there reached is that with reasonable care in making the experiments,
observations on the model scale may be applied to aircraft by increasing
the forces measured in proportion to the square of the speed and the square
of the scale.

The full development of the means of measurement would need many
chapters of a book and will not be attempted. This chapter aims only at
explaining the general use of instruments and apparatus and the precautions
which must be observed in applying quite ordinary instruments to experi-
mental work in aircraft. As an example of the need for care it will be shown
that the common level used on the ground ceases to behave as a level in
the air, although it has a sufficient value as an indicator of sideslipping
for it to be fitted to all aeroplanes.

In very few of the cases dealt with are the instruments shown in
mechanical detail, but an attempt has been made to give sufficient descrip-
tion to enable the theory to be understood and the records of the instruments
appreciated. The particular methods and apparatus described are mostly
British as produced for the service of the Air Ministry, but with minor

variations may be taken as representative of the methods and apparatus of the world's aerodynamic laboratories.

The Measurement of Air Velocity.—A knowledge of the speed at which an aircraft moves through the air is perhaps of greater importance in understanding what is occurring than any other single quantity. Its measurement has therefore received much attention and reached a high degree of accuracy. For complete aircraft the instruments used can be calibrated by flight over measured distances, corrections for wind being found from flights to and fro in rapid succession over the same ground. The reading of the instruments is found to depend on the position of certain parts relative to the aircraft, and in order to avoid the complication thus introduced experiments will first be described under laboratory conditions.

All instruments which are used on aircraft for measuring wind velocity, *i.e.* anemometers, depend on the measurement of a dynamic pressure difference produced in tubes held in the wind. The small windmill type of anemometer used for many other purposes has properties which render it unsuitable for aerodynamic experiments either in flight or in the laboratory. One form of tube anemometer is shown in Fig. 40 so far as its essential working parts are involved. It consists of an inner tube, open at one end and facing the air current ; the other end is connected to one side of a pressure gauge. An outer tube is fixed concentrically over the inner, or Pitot, tube and the annulus is open to the air at a number of small holes ; the annulus is connected to the other end of the pressure gauge, and the reading of the gauge is then a measure of the speed.
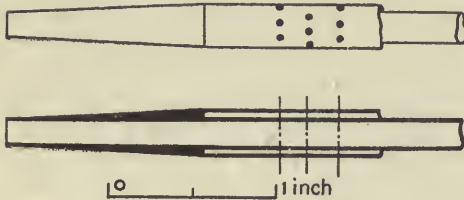
FIG. 40.—Tube anemometer.

For the tube shown the relation between pressure and speed may be given in the form

$$v_{\text{ft.-s.}} = 66 \cdot 2 \sqrt{h} \quad . \quad . \quad . \quad . \quad . \quad . \quad (1)$$

where v is the velocity of air in feet per sec., and h is the head of water in inches which is required to balance the dynamic pressure. The relation shown in (1) applies at a pressure of 760 mm. of water and a temperature of 15°·6 C., this having been chosen as a standard condition for experiments in aerodynamic laboratories. For other pressures and temperatures equation (1) is replaced by

$$v_{\text{ft.-s.}} = 66 \cdot 2 \sqrt{\frac{h}{\sigma}} \quad . \quad . \quad . \quad . \quad . \quad (2)$$

where σ is the density of the air relative to the standard condition.

Except for a very small correction, which will be referred to shortly, the formula given by (2) applies to values of v up to 300 ft.-s.

The tube anemometer illustrated in Fig. 40 has been made the subject of the most accurate determination of the constant of equations

(1) and (2), but the exact shape does not appear to be of very great importance.

As a result of many experiments it may be stated that the pressure in the inner tube is independent of the shape of the opening if the tube has a length of 20 or 30 diameters. The actual size may be varied from the smallest which can be made, say one or two hundredths of an inch in diameter, up to several inches.

The external tube needs greater attention; the tapered nose shown in Fig. 40 may be omitted or various shapes of small curvature substituted. The rings of small holes should come well on the parallel part of the tube and some five or six diameters behind the Pitot tube opening. The diameter of the holes themselves should not exceed three hundredths of an inch in a tube of 0·3 inch diameter, and the number of them is not very important. When dealing with measurements of fluctuating velocities it is occasionally desirable to proportion the number of holes to the size of the opening of the Pitot tube in order that changes of pressure may be transmitted to opposite sides of the gauge with equal rapidity. This can be achieved by covering the whole of the tubes by a flexible bag to which rapid changes of shape are given by the tips of the fingers. By adjustment of the number of holes the effect of these changes on the pressure gauge can be reduced to a very small amount.

The outside tube should have a smooth surface with clearly cut edges to the small holes, but with ordinary skilled workshop labour the tubes can be repeated so accurately that calibration is unnecessary. The instrument is therefore very well adapted for a primary standard.

Initial Determination of the Constant of the Pitot-Static Pressure Head. —The most complete absolute determination yet made is that of Bramwell, Relf and Fage, and is described in detail in Reports and Memoranda, No. 72, 1912, of the Advisory Committee for Aeronautics. The anemometer was mounted on a whirling arm of 30-feet radius rotating inside a building. The speed of the tube over the ground was measured from the radius of the tube from the axis of rotation and the speed of the rotation of the arm. The latter could be maintained constant for long periods, so that timing by stop-watch gave very high percentage accuracy. The air in the building was however appreciably disturbed by the rotation of the whirling arm, and when steady conditions had been reached the velocity of the anemometer through the air was only about 93 per cent. of that over the ground. A special windmill anemometer was made for the evaluation of the movement of air in the room. It consisted of four large vanes set at 30 degrees to the direction of motion, and the rotation of these vanes about a fixed axis was obtained by counting the signals in a telephone receiver due to contact with mercury cups at each rotation. Some such device was essential to success, as the forces on the vanes were so small that ordinary methods of mechanical gearing introduced enough friction to stop the vanes. A velocity of one foot per second could be measured with accuracy. To calibrate this vane anemometer it was mounted on the whirling arm and moved round the building at very low speeds; any error due to motion of air in the room is present in such

calibration, but as it is a 7 per cent. correction on a 7 per cent. difference between air speed and ground speed the residual error if neglected would not exceed 0·5 per cent. As, however, the 7 per cent. is known to exist the actual accuracy is very great if the speed through the air is taken as 93 per cent. of that over the floor of the building. The order of accuracy arrived at was 2 or 3 parts in 1000 on all parts of the measurement.

To determine the air motion in the building due to the rotation of the whirling arm, the tube anemometer was removed, the vane anemometer placed successively at seven points on its path, and the speed measured.

For the main experiment the tube anemometer was replaced at the end of the arm, and the tubes to the pressure gauge led along the arm to its centre and thence through a rotating seal in which leakage was prevented by mercury. As a check on the connecting pipes the experiment was repeated with the tube connections from the gauge to the anemometer reversed at the whirling arm end. The pressure difference was measured on a Chattock tilting gauge described later.

The results of the tests are shown in Table 1 below.

TABLE 1.

Speed over the floor of the building (feet per sec.).	Speed of the air over the floor of the building (feet per sec.).	Speed of tube anemometer through the air (feet per sec.).	$\sqrt{\dfrac{2gh}{v^2}}$
21·8	1·5	20·3	1·006
30·1	2·2	27·9	1·001
33·6	2·4	31·2	1·017 ?
39·8	2·9	36·9	0·994
43·1	3·1	40·0	1·005
48·8	3·6	45·2	1·004
51·1	3·8	47·3	1·001
Connecting tubes reversed.			
21·2	1·5	19·7	0·991
31·2	2·2	29·0	0·991
37·6	2·7	34·9	0·993
45·5	3·4	42·1	1·000
48·8	3·6	45·2	1·000
51·1	3·8	47·3	1·002
53·4	3·9	49·5	1·001

Mean value of $\dfrac{v}{\sqrt{2gh}} = \qquad 1\cdot0005$

or neglecting the doubtful reading $\qquad 0\cdot9997$

The pressure readings on the gauge were converted into " head of air," h, and the value of $\sqrt{\dfrac{2gh}{v^2}}$ is a direct calculation from the observations of pressure and velocity. Its value is seen to be unity within the accuracy of the experiments, the average value being less than $\frac{1}{20}$ per cent. different from unity.

For this form of tube anemometer the relation is

$$v_{\text{ft.-s.}} = \sqrt{2gh_{\text{feet of fluid}}} \quad \cdots \quad \cdots \quad (3)$$

In this equation the relation given is independent of the fluid and would apply equally to water. Most aerodynamic pressure gauges, however, use water as the heavy liquid, and the conversion of (3) to use h in inches of water for an air speed v leads to equation (1).

The determination so far has given the difference of pressure in the two tubes of the anemometer. The pressure in each was compared with the pressure in a sheltered corner of the building, and it was found that in the annular space the effect of motion was negligible. The method of experiment now involves a consideration of the centrifugal effect on the air in the tube along the whirling arm, since there is no longer compensation by a second connecting pipe.

If p be the pressure at any point in the tube on the whirling arm at an angular velocity ω, the equation of equilibrium is

$$dp = \rho\omega^2 r\, dr \quad \cdots \quad \cdots \quad (4)$$

and as the air in the tube is stationary the temperature will be constant, so that

$$p = \frac{p_i}{\rho_i} \cdot \rho \quad \cdots \quad \cdots \quad (5)$$

where p_i and ρ_i are the pressure and density at the inner end of the tube. Equations (4) and (5) are readily combined, and the integration leads to

$$\frac{p_o}{p_i} = e^{\frac{1}{2}\rho_i v_o^2 / p_i} \quad \cdots \quad \cdots \quad (6)$$

where p_o is the pressure at the outer end of the whirling arm tube and v_o the velocity there. The difference of pressure $p_o - p_i$ can be calculated from an expansion of (6) to give

$$p_o - p_i \equiv \delta p = \tfrac{1}{2}\rho_i v_o^2 \Big(1 + \tfrac{1}{4}\frac{\rho_i}{p_i}v_o^2 + \cdots\Big) \quad \cdots \quad (7)$$

or in terms of the velocity of sound, a_i,

$$\delta p = \tfrac{1}{2}\rho_i v_o^2 \Big\{1 + \frac{\gamma}{4}\cdot\Big(\frac{v_o}{a_i}\Big)^2 + \cdots\Big\} \quad \cdots \quad (8)$$

At 300 ft.-s. the second term in the brackets is about 2 per cent. of the first; in the experiments described above it is unimportant.

The expression $\tfrac{1}{2}\rho v^2$ occurs so frequently in aerodynamics that its relation to (3) will be developed in detail. Squaring both sides of (3) gives

$$v^2 = 2gh \quad \cdots \quad \cdots \quad (9)$$

Multiply both sides by $\tfrac{1}{2}\rho$ to get

$$\tfrac{1}{2}\rho v^2 = \rho gh \quad \cdots \quad \cdots \quad (10)$$
$$= \delta p . \quad \cdots \quad \cdots \quad (11)$$

The weight of unit volume of a fluid is ρg, and the value of ρgh is the difference of pressure per unit area between the top and bottom of the column of fluid of height h. If ρ be in slugs per cubic foot and v in feet per sec., the pressure δp is in lbs. per square foot. The equation is, however, applicable in any consistent set of dynamical units.

A comparison of equations (8) and (11) brings out the interesting result that the difference of pressure between the two ends of the tube of the whirling arm is of the same form as to dependence on velocity at flying speeds as the pressure difference in a tube anemometer of the type shown in Fig. 40. The velocity in (11) is relative to the air, whilst in (8) the velocity is related to the floor of the building. Had the air in the building been still so that the two velocities had been equal, the differences of pressures in the anemometer and between the ends of a tube of the whirling arm would have been equal to a high degree of approximation.

One end of the pressure gauge being connected to the air in a sheltered part of the building, equation (8) can be used to estimate the pressure in either of the tubes of the anemometer. The important observation was then made that the air inside the annular space of the tube anemometer at the end of the arm was at the same pressure as the air in a sheltered position in the building. This is a justification for the name " static pressure tube," since the pressure is that of the stationary air through which the tube is moving. The whole pressure difference due to velocity through the air is then due to dynamic pressure in the Pitot tube, which brings the entering air to rest. A mathematical analysis of the pressure in a stream brought to rest is given in the chapter on dynamical similarity, where it is shown that the increment of pressure as calculated is

$$\delta p = \tfrac{1}{2}\rho v^2 \left\{ 1 + \tfrac{1}{4}\left(\frac{v}{a}\right)^2 \cdots \right\} \quad . \quad . \quad . \quad . \quad (13)$$

where a is the velocity of sound in the undisturbed medium, and the second term of (13) is the small correction to equation (2) which was there referred to. At 300 ft.-s, the second term is 1·5 per cent. of the first, and (13) is therefore applicable with great accuracy.

The principles of dynamical similarity (see Chapter VIII.) indicate for the pressure a theoretical relationship of the form

$$\delta p = \tfrac{1}{2}\rho v^2 f\left(\frac{v}{a}, \ \frac{vl}{\nu}\right) \quad . \quad . \quad . \quad . \quad . \quad (14)$$

which contains the kinematic viscosity, ν, not hitherto dealt with, and l, which defies the size of the tubes and is constant for any one anemometer.

The function may in general have any form, but its dependence on $\frac{v}{a}$ in this instance has been shown in equation (13). The experiments on the whirling arm have shown that the dependence of the function on viscosity over the range of speeds possible was negligibly small. The limit of range over which (13) has been experimentally justified in air is limited to 50 ft.-s. It is not however the speed which is of greatest importance in the theory of the instrument, but the quantity $\frac{vl}{\nu}$. If this can be extended by any means the validity of (13) can be checked to a higher stage, and the extension can be achieved by moving the tube anemometer through still water which has a kinematic viscosity 12 or 13 times less than that of air. A velocity of 20 ft.-s. through water gives as much information as a velocity

of 250 ft.-s. through air, and the experiment was made at the William Froude National Tank at Teddington. The anemometer was not of exactly the same pattern as that shown in Fig. 40, but differed from it in minor particulars and has a slightly different constant.

The results of the experiments are shown in Table 2.

TABLE 2.

Speed (ft. per sec.).		Equivalent speed in air (ft. per sec.).	$\sqrt{\dfrac{2gh}{v^2}}$ or $\sqrt{\dfrac{p}{\frac{1}{2}\rho v^2}}$
Air	20	—	1·00
	30	—	0·99
	40	—	0·99
	50	—	0·99
	60	—	0·98
Water	2·88	37	0·98
	3·92	51	1·00
	5·07	65	0·99
	5·78	75	0·99
	6·80	88	0·99
	7·80	101	0·99
	9·69	125	0·97
	9·85	128	0·98
	10·82	140	0·99
	11·04	142	1·00
	11·15	144	0·98
	11·98	154	0·96
	13·10	169	0·97
	14·24	184	0·97
	14·52	187	0·99
	14·76	190	0·99
	16·06	207	0·98
	16·92	218	0·97
	17·59	227	0·99
	18·49	238	0·99
	19·86	256	0·99
	20·10	259	0·98

The values of $\sqrt{\dfrac{2gh}{v^2}}$ shown in the last column vary a little above and below 0·99, and the table may be taken as justification for the use of equation (13) up to 300 ft.-s. The difference between 0·99 and 1·00 may fairly be attributed to changes of form of the tube anemometer from that shown in Fig. 40. In the case of water the velocity of sound is nearly 5000 ft. per sec., and the second term of (13) is completely negligible. From Table 2 it may thus be deduced that the constant of equation (1) is independent of ν up to the highest speeds attained by aircraft.

Effect of Inclination of a Tube Anemometer on its Readings.—It would have been anticipated from the accuracy of calibration attained that the pressure difference between the inner and outer tubes is not extremely sensitive to the setting of the tubes along the wind. At inclinations of 5°, 10° and 15° the errors of the tube anemometer illustrated in Fig. 40 are 1 per cent., 2·5 per cent. and 4·5 per cent. of the velocity, and tend to over-estimation if not allowed for.

Use of Tube Anemometer on an Aeroplane.—Anemometers of the general type described in the preceding pages are used on aeroplanes and airships. In the aeroplane the tubes are fixed on an interplane strut about two-thirds of the way up, and with the opening of the Pitot one foot in front of the strut. The position so chosen is convenient, since it avoids damage during movements of an aeroplane in its shed, but is not sufficiently far ahead of the aeroplane as to be free from the disturbance of the wings. Although the anemometer correctly indicates the velocity of air in its neighbourhood it does not register the motion of the aeroplane relative to undisturbed air. The effect of disturbance is estimated for each aeroplane by flights over a marked ground course, and Fig. 41 illustrates a typical result. The air immediately in front of the aeroplane is pushed forward with a speed varying from 2 per cent. of the aeroplane speed at 100 m.p.h. to 7 per cent. at 40 m.p.h.

How is this correction to be applied? Does it depend on true speed or on the indicator reading? In order to answer these questions it is
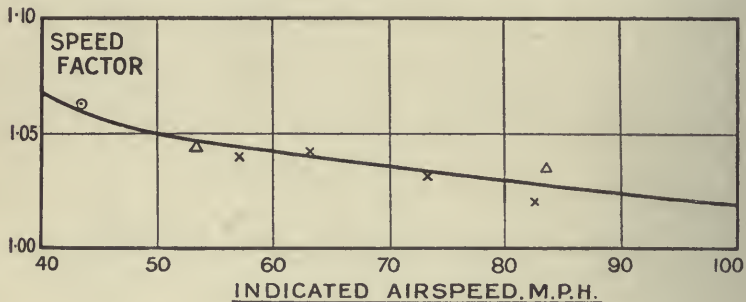
Fig. 41.

necessary to anticipate the result of the analysis in later chapters. The pressure gauge inside the aeroplane cockpit indicates a quantity which may be very different from the true speed, the quantity actually measured being of the type shown in equation (11). Allowing for the interference of the aeroplane, it is found that the reading depends on the density of the air, the speed of the aircraft and its inclination. The inclination of the aeroplane is fixed when $\frac{w}{\sigma v^2}$ is known, w being the loading of the wings in lbs. per square foot, σ the relative density of the air, and v the true velocity. The quantity $\sigma^{\frac{1}{2}}v$ occurs often and is called " indicated air speed " or sometimes " air speed." For aeroplanes designed for a long journey during which the consumption of petrol and oil is an appreciable proportion of the total weight the correction should be applied to $\left(\frac{\sigma}{w}\right)^{\frac{1}{2}}v$. For an aeroplane which flies with its total weight sensibly constant it will be seen that w is constant, and that the inclination of the aeroplane is determined by σv^2, and it is to this quantity therefore that the calibration corrections for position should apply.
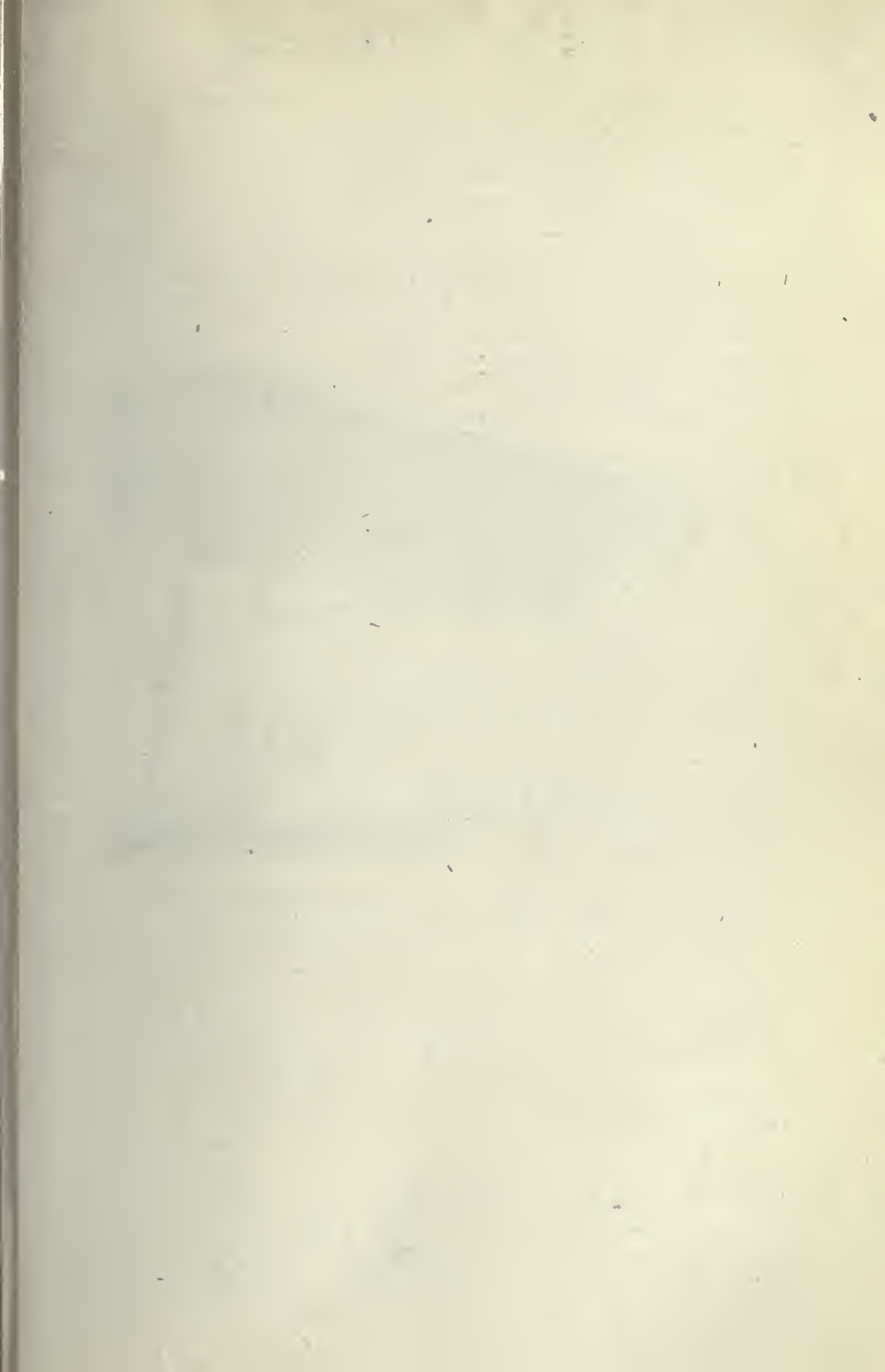
Fig. 42.—Experimental arrangement of tube anemometer on an aeroplane.

For accurate experimental work it is very desirable that the correction for position should be as small as possible, and at the Royal Aircraft Establishment it has been found that projection of the tube anemometer some 6 feet ahead of the wings reduces the correction almost to vanishing point. The arrangement is shown in Fig. 42. To the front strut is attached a wood support projecting forward and braced by wires to the upper and lower wings. The two tubes of the anemometer are separated in the instrument used, the Pitot tube being a short distance below the static pressure tube ; the combination is hinged to the forward end of the wooden support, and is provided with small vanes which set it into the direction of the relative wind. The two tubes to the pressure gauge pass along the wooden support, down the strut and along the leading edge of the wing to the cockpit. The thermometer used in experimental work is shown on the rear strut.

On the aeroplane illustrated the residual error did not exceed 0·5 per cent. at any speed, and there was no sign of variation with inclination of the aeroplane.

Aeroplane "Pressure Gauge" or "Air-speed Indicator."—At 100 m.p.h. the difference of pressure between the two tubes of a tube anemometer is nearly 5 ins. of water, and readings are required to about one-tenth of this amount. The instruments normally used depend on the deflection of an elastic diaphragm, to the two sides of which the tubes from the anemometer are connected. The various masses are balanced so as to be unaffected by inclinations or accelerations of the aeroplane. The instruments are frequently calibrated on the ground against a water-gauge, and have reached a stage at which trouble rarely arises from errors in the instrument.

The scale inscribed on the dial reads true speed only for exceptional conditions. Were the tube anemometer outside the field of influence of the aeroplane the scale would give true speeds when the density was equal to the standard adopted in the aerodynamic laboratories. For the average British atmosphere this standard density occurs at a height of about 800 feet, above which the " indicated air speed " is less than the true speed in proportion to the square root of the relative density. Apart from calibration corrections due to position of the tube anemometer on the aeroplane the indicator reading at 10,000 ft. needs to be multiplied by 1·16 to give true speed. At 20,000 feet and 30,000 feet the corresponding factors are 1·37 and 1·64 respectively, these figures being the reciprocals of the square roots of the relative densities at those heights.

Used in conjunction with a thermometer and an aneroid barometer the speed indicator readings can always be converted into true speeds through the air.

Aneroid Barometer.—The aneroid barometer is a gauge which gives the pressure of the atmosphere in which it is immersed. Its essential part consists of a closed box of which the base and cover are elastic diaphragms, usually with corrugations to admit of greater flexibility. The interior of the box is exhausted of air, and the diaphragms are connected to links and springs for the registration and control of the

motion which takes place owing to changes in the atmospheric pressure. At a height of 30,000 feet the pressure is about one-third of that at the earth's surface, and the aneroid barometer for use on aircraft is required to have a range of 5 lbs. per sq. inch to 15 lbs. per sq. inch. The forces called into operation on small diaphragms are seen to be great, and the supports must be robust. All but the best diaphragms show a lag in following a rapid change of pressure, and the instrument cannot be relied on to give distance from the ground when landing chiefly for this reason.

The aneroid barometer is used in accurate aerodynamic work solely as a pressure gauge. It is divided however into what is nominally a scale of height, in order to give a pilot an indication as to his position above the earth. There is no real connection between pressure at a point and height above the earth's surface, and the scale is therefore an approximation
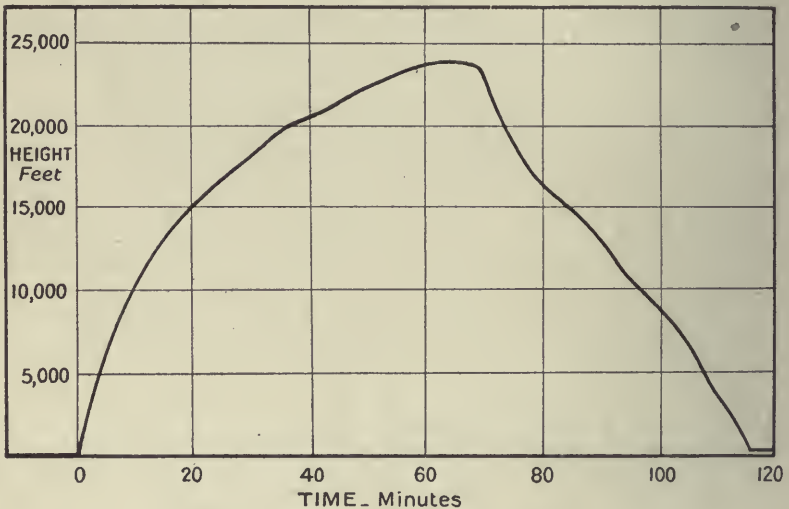
Fig 43.—Barogram taken during a flight.

only and was rather arbitrarily chosen. If h be the height in feet which is marked on the aneroid barometer, and p is the relative pressure, a standard atmosphere being at a pressure of 2116 lbs. per sq. foot, the relation between h and p is

$$h = -62,700 \log_{10} p \quad . \quad . \quad . \quad . \quad . \quad . \quad (15)$$

The relation is shown in tabular form in the chapter on the prediction and analysis of aeroplane performance.

The aneroid barometers used for the more accurate aerodynamic experiments are indicators only, and the readings are taken by the pilot or observer. In some cases recording barometers are used, and Fig. 43 illustrates an example of the type of record obtained during a climb to the ceiling and the subsequent descent. The rapid fall in the rate of climb is clearly shown, for the aeroplane reached a height of 10,000 feet in 10 mins., but to climb an additional 10,000 feet, 27 mins. were required. The return

to earth from this altitude of 24,000 feet occupied three-quarters of an hour. The lag of the barometer is shown at the end of the descent, and corresponds with an error in height of 200 or 300 feet, or about 1 per cent. of the maximum height to which the aeroplane had climbed.

Revolution Indicators and Counters.—Motor-car practice has led to the introduction of revolution indicators, and these have been adopted in the aeroplane. Many instruments depend for their operation on the tendency of a body to fly out under the influence of a centrifugal acceleration, the rotating body being a ring hinged to a shaft so as to have relative motion round a diameter of the ring. The ring is constrained to the shaft by a spring, the amount of distortion of which is a measure of speed of rotation of the shaft. Various methods of calibration of such indicators are in use, and the readings are usually very satisfactory. For the most accurate experimental work the indicator is used to keep the speed of rotation constant, whilst the actual speed is obtained from a revolution counter and a stop-watch.

The air-speed indicator, the aneroid barometer and the revolution indicator are the most important instruments carried in an aeroplane, both from the point of view of general utility and of accurate record of performance. Many other instruments are used for special purposes, and those of importance in aerodynamics will be described.

Accelerometer.—The most satisfactory accelerometer for use on aeroplanes is very simple in its main idea, and is due to Dr. Searle, F.R.S., working at the Royal Aircraft Establishment during the war. The essential part of the instrument is illustrated in Fig. 44, and consists of a quartz fibre bent to a semicircle and rigidly attached to a base block at A and B. If the block be given an acceleration normal to the plane of the quartz fibre the force on the latter causes a deflection of the point C relative to A and
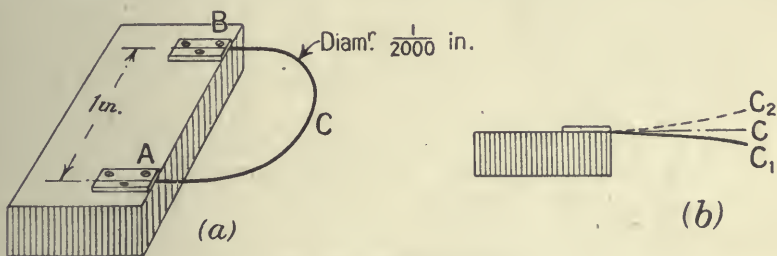
Fig. 44.—Accelerometer.

B, and the deflection is a measure of the magnitude of the acceleration. By the provision of suitable illumination and lenses an image of the point C is thrown on to a photographic film and the instrument becomes recording. The calibration of the instrument is simple : the completed instrument is held with the plane of the fibre vertical, and the vertex then lies at C as shown in Fig. 44 (b). With the plane horizontal the film record shows C_1 for one position and C_2 for the inverted position, the differences CC_1 and CC_2 being due to the weight of the fibre, and therefore equal to the deflections due to an acceleration of g, *i.e.* 32·2 feet per sec. per sec.

The stiffness of the fibre is so great in comparison with its mass that the period of vibration is extremely short, and the air damping is sufficient to make the motion dead beat. As compared with the motions of an aeroplane which are to be registered, the motion of the fibre is so rapid that the instrumental errors due to lag may be ignored. Fig. 45 shows some of the results recorded, the accelerometer having been strapped to the knee of the pilot or passenger during aerial manœuvres in an aeroplane.

In the records reproduced the unit has been taken as g, *i.e.* 32·2 feet per sec. per sec., and in the mock flight between two aeroplanes it may be noticed that four units or nearly 130 ft.-s.^{2} was reached. The interpretation of the records follows readily when once the general principle is appreciated that accelerations are those due to the air forces on the aeroplane. To see this law, consider the fibre as illustrated in Fig. 44 (a) when held in an aeroplane in steady flight, the plane of the fibre being horizontal. A line normal to this plane is known as the accelerometer axis, and in the example is vertical. Since the aeroplane has no acceleration at all, the fibre will bend under the action of its weight only and register g; in the absence of lift the aeroplane would fall with acceleration g, and the record may then be regarded as a measure of the upward acceleration which would be produced by the lift if weight did not exist. If the motion of the aeroplane be changed to that of vertical descent at its terminal velocity, the acceleration is again zero and the weight of the fibre does not produce any deflection. Again it is seen that the acceleration recorded is that due to the air force along the accelerometer axis, and this theorem can be generalised for any motion whatever. The record then gives the ratio of the air force along the accelerometer axis to the mass of the aeroplane.

Consider the pilot as an accelerometer by reason of a spring attachment to the seat. His accelerations are those of the aeroplane, and his apparent weight as estimated from the compression of the spring of the seat will be shown by the record of an accelerometer. When the accelerometer indicates g his apparent weight is equal to his real weight. At four times g his apparent weight is four times his real weight, whilst at zero reading of the accelerometer the apparent weight is nothing. Negative accelerations indicate that the pilot is then held in his seat by his belt.

Examining the records with the above remarks in mind shows that oscillations of the elevator may be made which reduce the pilot's apparent weight to zero, and an error of judgment in a dive might throw a pilot from his seat unless securely strapped in. In a loop the tendency during the greater part of the manœuvre is towards firmer seating. Generally, the first effect occurs in getting into a dive, and the second when getting out. It will be noticed that in three minutes of mock fighting the great preponderance of acceleration tended to firm seating, and on only one occasion did the apparent weight fall to zero.

Levels.—The action of a level as used on the ground depends on the property of fluids to get as low as possible under the action of gravity.
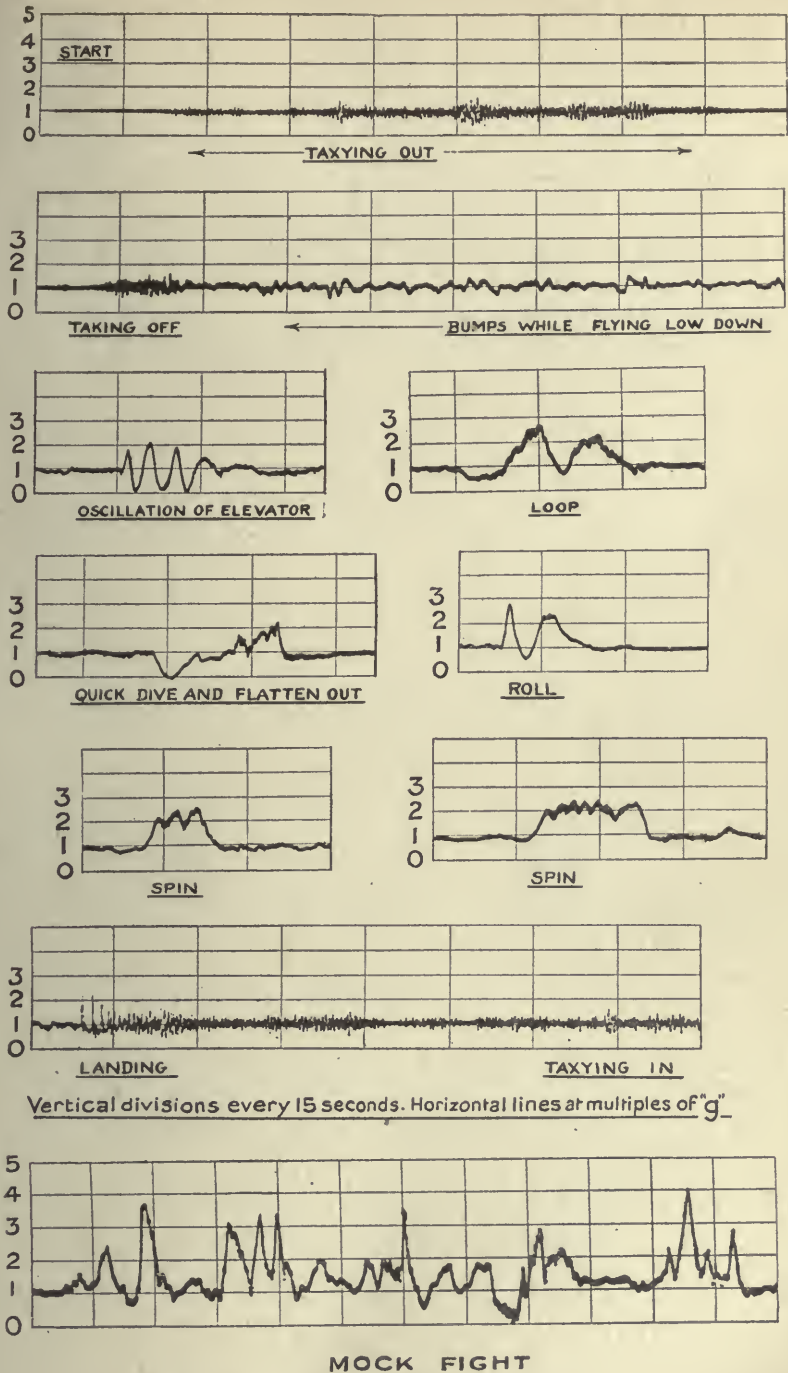
Fig. 45.—Accelerometer records.

In a spirit-level the trapped bubble of gas rises to the top of the curved glass and stays where its motion is horizontal. In this way it is essentially dependent on the direction of gravity and not its magnitude. The principles involved are most easily appreciated from the analogy to a pendulum which hangs vertically when the support is at rest. In an aeroplane the support may be moving, and unless the velocity is steady the inclination is affected. Referring to Fig. 46 (a) a pendulum is supposed to be suspended about an axis along the direction of motion of an aeroplane, and P is the projection of this axis. In steady motion the centre of gravity of the bob B will be vertically below P; if P be given a vertical acceleration a and a horizontal acceleration f, the effect on the inclination can be found by adding a vertical force ma and a horizontal force mf to the bob.
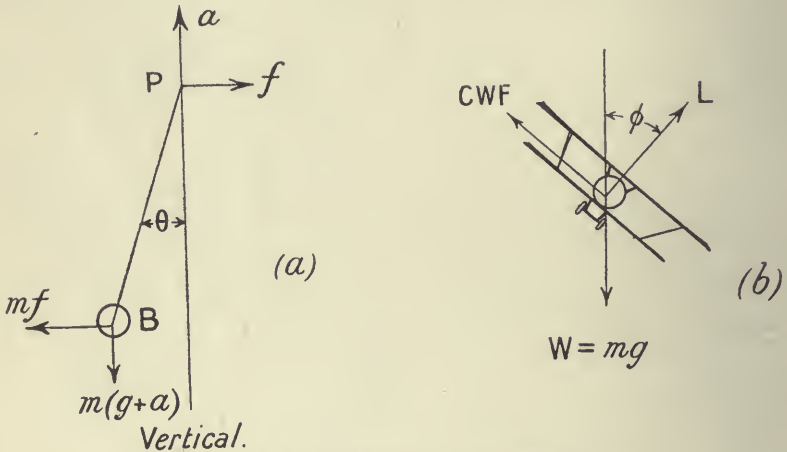
Fig. 46.—The action of a cross-level.

The pendulum will now set itself so that the resultant force passes through P, the inclination θ will be given by the relation

$$\tan \theta = \frac{f}{g + a} \quad . \quad . \quad . \quad . \quad . \quad . \quad (16)$$

and the pendulum will behave in all ways as though the direction of gravity had been changed through an angle θ and had a magnitude equal to $\sqrt{(g + a)^2 + f^2}$.

The accelerations of P are determined by the resultant force on the aeroplane, i.e. as shown by Fig. 46 (b), by the lift, cross-wind force and weight of the aeroplane. The equations of motion for fixed axes are

$$ma = L \cdot \cos \phi + \text{C.W.F.} \sin \phi - mg \quad . \quad . \quad . \quad (17)$$

and

$$mf = L \cdot \sin \phi - \text{C.W.F.} \cos \phi \quad . \quad . \quad . \quad . \quad (18)$$

From equations (17) and (18) it is easy to deduce the further equation

$$-f \cos \phi + (g + a) \sin \phi = \frac{\text{C.W.F.}}{m} \quad . \quad . \quad . \quad (19)$$

where ϕ is the inclination of the plane of symmetry of the aeroplane to the vertical.

From (19) follows a well-known property of the cross-level of an aeroplane, for if the aeroplane is banked so as not to be sideslipping the cross-wind force is zero, and

$$\tan \phi = \frac{f}{g + a} \qquad . \qquad . \qquad . \qquad . \qquad . \qquad . \qquad (20)$$

i.e. the angle of bank of the aeroplane is equal to θ, the inclination of a pendulum to the vertical. To an observer in the aeroplane the final position of the pendulum during a correctly banked turn is the same as if it had originally been fixed to its axis instead of being free to rotate.

The deviation of a cross-level from its zero position is then an indication of sideslipping and not of inclination of the wings of the aeroplane to the horizontal.

There is no instrument in regular use which enables a pilot to maintain an even keel. In clear weather the horizon is used, but special training is necessary in order to fly through thick banks of fog. By a combination of instruments this can be achieved as follows : an aeroplane can only fly straight with its wings level if the cross-level reads zero, and *vice versâ*. The compass is not a very satisfactory instrument when used alone, as it is not sensitive to certain changes of direction and may momentarily give an erroneous indication. It is therefore supplemented by a turn indicator, which may either be a gyroscopic top or any instrument which measures the difference of velocity of the wings through the air. This instrument makes it possible to eliminate serious turning errors and so produce a condition in which the compass is reliable. Straight flying and a cross-level reading zero then ensures an even keel.

Aerodynamic Turn Indicator.—An instrument designed and made by Sir Horace Darwin depends on the measurement of the difference of velocity between the tips of the wings of an aeroplane as the result of turning. The theory is easily developed by an extension of equation (8), where it was shown that the difference of pressure due to centrifugal force on the column of air in a horizontal rotating tube was

$$\delta p = \tfrac{1}{2}\rho v_o{}^2 \qquad . \qquad . \qquad . \qquad . \qquad . \qquad . \qquad (21)$$

where ρ was the air density, v the velocity of the outer end of the pipe of which the inner end was at the centre of rotation. The difference of pressure between points at different radii is then seen to be

$$\delta p = \tfrac{1}{2}\rho(v_o{}^2 - v_i{}^2) \qquad . \qquad . \qquad . \qquad . \qquad . \qquad (22)$$

where v_i is the velocity of the inner end of the tube. If an aeroplane has a tube of length l stretched from wing tip to wing tip, the difference of the velocities of the inner and outer wings is $\omega l \cos \phi$ due to an angular velocity ω, and equation (22) becomes

$$\delta p = \rho v \omega l \cos \phi \qquad . \qquad . \qquad . \qquad . \qquad . \qquad (23)$$

where v is the velocity of the aeroplane and ϕ is the angle of bank. For slow turning $\cos \phi$ is nearly unity, and the pressure difference between

the wing tips is proportional to the rate of turning of the aeroplane. To this difference of pressure would be added the component of the weight of the air in the tube due to banking were this latter not eliminated by the arrangement of the apparatus. The tube is open at its ends to the atmosphere through static pressure tubes on swivelling heads, and the pressure due to banking is then counteracted by the difference of pressures outside the ends of the tube. Turning of the aeroplane would produce a flow of air from the inner to the outer wing, and the prevention of this flow by a delicate pressure gauge gives the movement which indicates turning.

Gravity Controlled Air-speed Indicator.—The great changes of apparent weight which may occur in an aeroplane make it necessary to examine very carefully the action of instruments which depend for their normal properties on the attraction of gravity. In the case of the accelerometer and cross-level the result has been to find very direct and simple uses in an aeroplane, although these were not obviously connected with
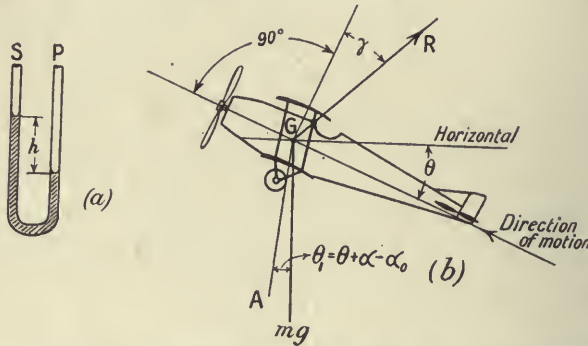
FIG. 47.—The action of a gravity controlled air-speed indicator.

terrestrial uses. A special use can be found for a gravity controlled air-speed indicator, but the ordinary instrument is spring controlled to avoid the special feature now referred to. The complete instrument now under discussion consists of an anemometer of the Pitot and static pressure tubes type with connecting pipes to a U-tube in the pilot's cockpit. The U-tube is shown diagrammatically in Fig. 47, the limbs of the gauge being marked for static pressure and Pitot connections. When the aeroplane is in motion the difference of pressure arising aerodynamically is balanced by a head of fluid, the magnitude of this head h being determined for a given aerodynamic pressure by the apparent weight of the fluid. The two tubes of the gauge may be made concentric so as to avoid errors due to tilt or sideways acceleration, and the calculations now proposed will take advantage of the additional simplicity of principle resulting from the use of concentric tubes.

The relation between the aerodynamic pressure and the head h can be written as

$$k\rho v^2 = h \cdot \rho_w (g \cos \theta_1 + f) \quad . \quad . \quad . \quad . \quad . \quad (24)$$

where k is the constant of the Pitot and static pressure combinations as

affected by inclination of the aeroplane, ρ is the air density, and v the velocity of the aeroplane. On the other side of the equation, h is the head of fluid, ρ_w the weight of unit volume of the fluid as ordinarily obtained, θ_1 the inclination of the gauge to the vertical, and f the upward acceleration of the gauge glass along its own axis. In steady flight f is zero and $\cos \theta_1$ so nearly equal to unity that its variations may be ignored. Equation (24) then shows that h is proportional to the square of the indicated air speed which would be registered by a spring controlled indicator.

The special property of the gravity controlled air-speed indicator is seen by considering unsteady motion. Fig. 47 (b) shows the necessary diagram from which to estimate the value of f. The liquid gauge is fixed to the aeroplane with its axis along the line AG, and its inclination to the vertical will depend on the angle of climb θ, the angle of incidence α, and the angle of setting of the instrument relative to the chord of the wings α_0. The relation may be

$$\theta_1 = \theta + \alpha - \alpha_0 \quad . \quad . \quad . \quad . \quad . \quad (25)$$

The forces on the aeroplane are its weight, mg, and the aerodynamic resultant R acting at an angle $\gamma + 90°$ to the direction of motion. It then follows that

$$mf = \mathrm{R} \cos (\gamma - \alpha + \alpha_0) - mg \cos \theta_1 \quad . \quad . \quad . \quad (26)$$

or

$$g \cos \theta_1 + f = \frac{\mathrm{R}}{m} \cos (\gamma - \alpha + \alpha_0) \quad . \quad . \quad . \quad (27)$$

and combining equations (24) and (27) gives the fundamental equation for h.

$$h = \frac{km\rho v^2}{\rho_w \mathrm{R} \cos (\gamma - \alpha + \alpha_0)} \quad . \quad . \quad . \quad . \quad (28)$$

As the result of experiments on aeroplanes it is known that the lift

$$\mathrm{L} \equiv \mathrm{R} \cos \gamma = k_{\mathrm{L}} \rho v^2 \mathrm{S} \quad . \quad . \quad . \quad . \quad . \quad (29)$$

where k_{L} is known as a lift coefficient and depends only on the angle of incidence of a given wing and not on its area S or speed v. Equation (28) can then be expressed as

$$h = \frac{m}{\rho_w \mathrm{S}} \cdot \frac{k \cos \gamma}{k_{\mathrm{L}} \cos (\gamma - \alpha + \alpha_0)} \quad . \quad . \quad . \quad . \quad (30)$$

The first factor of this expression is constant, whilst the second is a function only of the angle of incidence if the engine and airscrew are stopped. If the engine be running the statement is approximately true, a small error in lift being then due to variation of airscrew thrust unless the airscrew speed be kept in a definite relation to the forward speed.

The result of the analysis is to show that in unsteady flight as well as in steady flight the reading of the gravity controlled air-speed indicator depends on the angle of incidence of the aeroplane and not on the speed. For all wings the quantity k_{L} has a greatest value; $\cos \gamma$ and $\cos (\gamma - \alpha + \alpha_0)$ are nearly unity for a considerable range of angles, and the ratio required by (30) is exactly unity when $\alpha_0 = \alpha$. The value of h then

has a minimum value for an aeroplane in flight, and this minimum gives the lowest speed at which steady level flight can be maintained. The instrument is therefore particularly suited to the measurement of "stalling speed." Although not now used in ordinary flying, the advantages of an instrument which will read angle of incidence on a banked turn or during a loop are obvious for special circumstances. The advantage as an angle of incidence meter is a disadvantage as a speed indicator, for there is no power to indicate speeds after stalling. Given sufficient forward speed the control of attitude is rapid, but the regaining of speed is an operation essentially involving time, and the spring controlled air-speed indicator gives the pilot earliest warning of the need for caution.
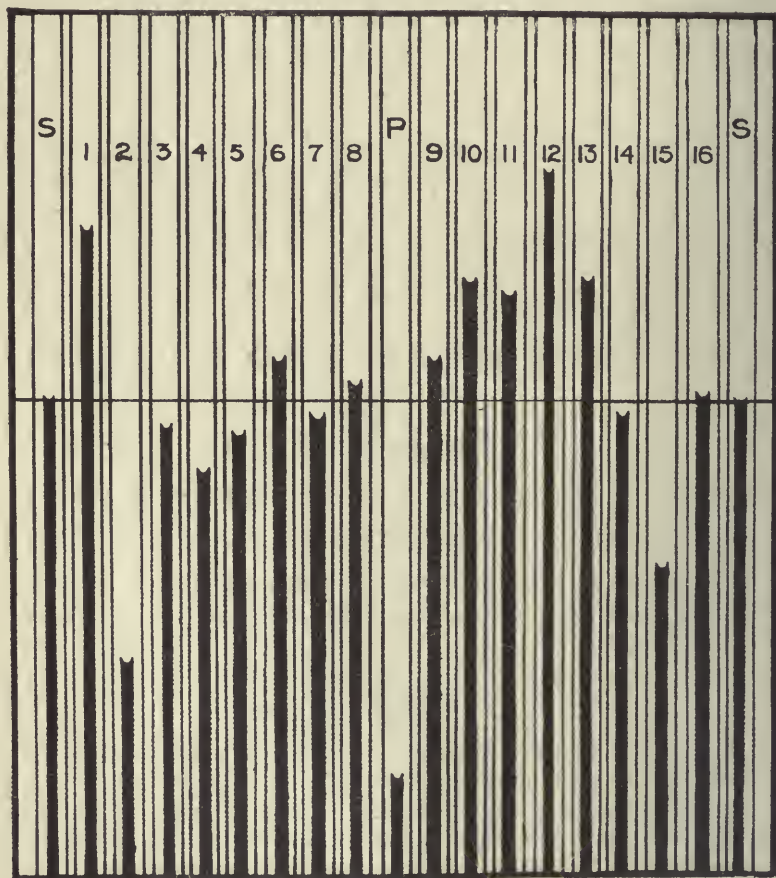
Fig. 48.—Photo-manometer record.

Photo-manometer.—From the discussion just given of the air-speed indicator it will be realised that a **U**-tube containing fluid may be used to measure pressures if the aeroplane is in steady flight, and a convenient apparatus for photographing the height of the fluid has been made and

used at the Royal Aircraft Establishment. A considerable number of tubes is used, each of which communicates with a common reservoir at one end and is connected at the other to the point at which pressure is to be measured. In the latest instrument the tubes are arranged round a half-cylinder and are thirty in number, and the whole is enclosed in a light-tight box. Behind the tubes bromide paper is wound by hand and rests against the pressure gauge tubes ; exposure is made by switching on a small lamp on the axis of the cylinder.

A diagram prepared from one of the records taken in flight is shown in Fig. 48, which shows nineteen tubes in use. The outside tubes are connected to the static pressure tube of the air-speed indicator, and the line joining the tops of the columns of fluid furnishes a datum from which other pressures are measured. The central tube marked P was commonly connected to the Pitot tube of the air-speed indicator, whilst the tubes numbered 1–16 were connected to holes in one of the wing ribs of an aeroplane.

The method of experiment is simple : the bromide paper having been brought into position behind the tubes, the aeroplane is brought to a steady state and maintained there for an appreciable time, during which time the lamp in the camera is switched on and the exposure made. The proportions of the apparatus are sufficient to produce damping, and the records are clear and easily read to the nearest one-hundredth of an inch.

Considerable use has been made of the instrument in determining the pressures on aeroplane wings, on tail planes and in the slip streams of airscrews.

Cinema Camera.—A method of recording movements of aircraft has been developed at the Royal Aircraft Establishment by G. T. R. Hill, by the adaptation of a cinema camera. The camera is carried in the rear seat of an aeroplane, and the film is driven from a small auxiliary windmill. This aeroplane is flown level and straight, and the camera is directed by the operator towards the aeroplane which is carrying out aerial manœuvres. The possible motions of the camera are restricted to a rotation about a vertical and a horizontal axis, and the position relative to the aeroplane is recorded on the film. From the succession of pictures so obtained it is possible to deduce the angular position in space of the pursuing aeroplane. Analytically the process is laborious, but by the use of a globe divided into angles the spherical geometry has been greatly simplified, and the camera is a valuable instrument for aeronautical research.

Camera for the Recording of Aeroplane Oscillations.—A pinhole camera fixed to an aeroplane and pointed to the sun provides a trace of pitching or rolling according to whether the aeroplane is flying to or from the sun or with the sun to one side. A more perfect optical camera for the same purpose has been made and used at Martlesham Heath, the pinhole being replaced by a cylindrical lens and a narrow slit normal to the line image of the sun produced by the lens. The record is taken on a rotating film, and a good sample photograph is reproduced in Fig. 49. The oscillation was that of pitching, the camera being in the rear seat of an aeroplane and the pilot flying away from the sun. At a time called 1 minute on the figure the pilot pushed forward the control column until

the aeroplane was diving at an angle of nearly 20 degrees to the horizontal, and then left the control column free. The aeroplane, being stable, began to dive less steeply, and presently overshot the horizontal and put its nose up to about 11 degrees. The oscillation persisted for three complete periods before being appreciably distorted by the gustiness of the air. The period was about 25 seconds, and such a record is a guarantee of longitudinal stability.
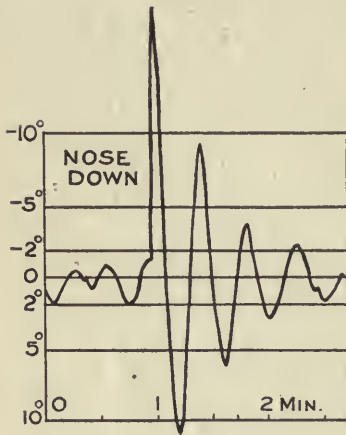
Fig. 50 is a succession of records of the pitching of an aeroplane, the first of which shows the angular movements of the aeroplane when the pilot was keeping the flight as steady as he was able. The extreme deviations from the mean are about a degree. The second record followed with the aeroplane left to control itself, and the fluctuations are not of greatly different amplitude to that for pilot's control. The periodicity is however more clearly marked in the second record, and the period is that natural to the aeroplane. The third record shows the natural period; as the result of putting the nose of the aeroplane up the record shows a well-damped oscillation, which is repeated by the reverse process of putting the nose up.

Fig. 49.—Stability record.

Photographs of lateral oscillations have been taken, but for various reasons the records are difficult to interpret, and much more is necessary
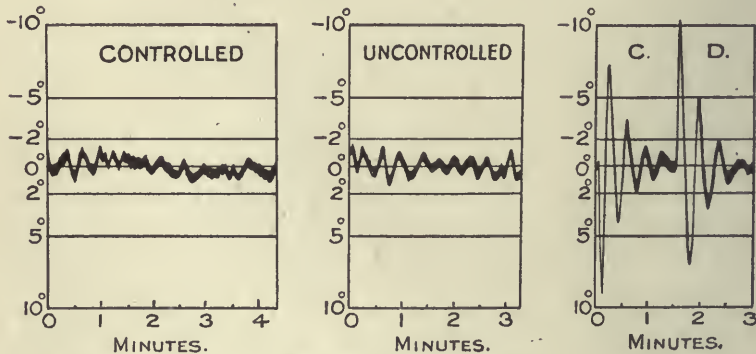
Fig. 50.—Control record.

before the full advantages of the instrument are developed as a means of estimating lateral stability.

Special Modifications of an Aeroplane for Experimental Purposes.— Fig. 51 shows one of the most striking modifications ever carried out on an aeroplane, and is due to the Royal Aircraft Establishment. The body of a BE2 type aeroplane was cut just behind the rear cockpit,

ELECTRIC
CONTACTS
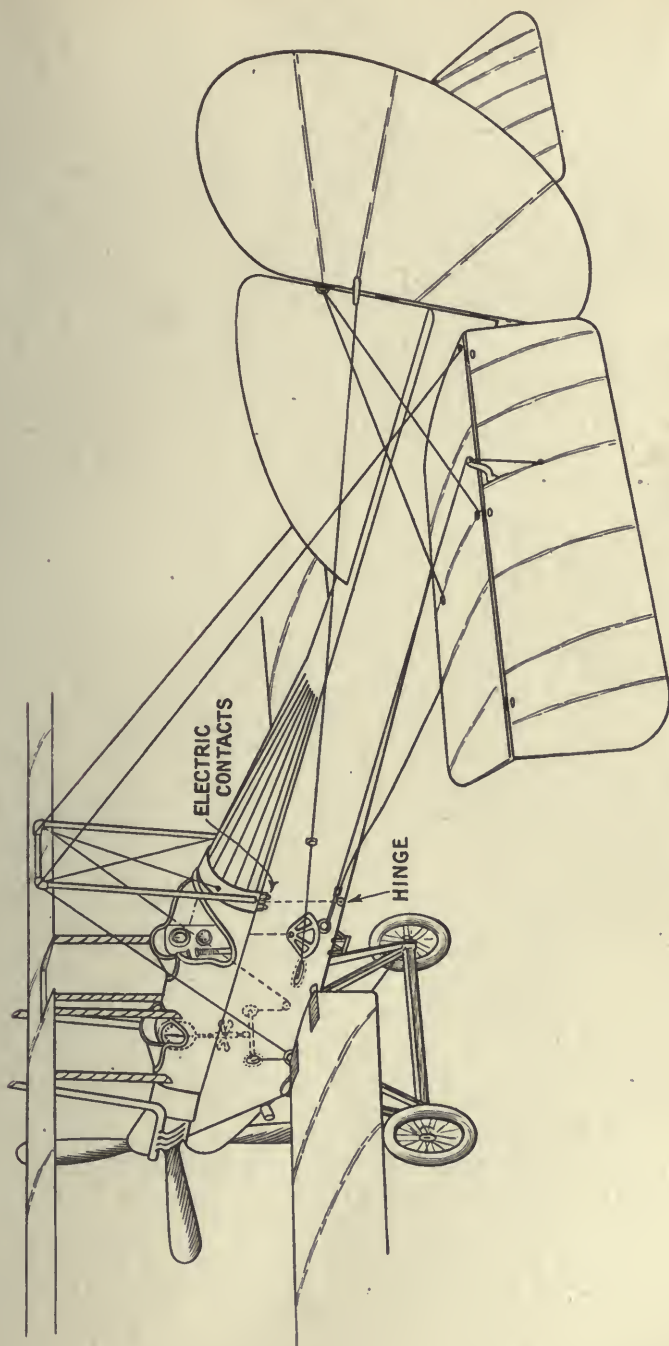
HINGE

FIG. 51.—Specially modified aeroplane.

and the tail portion was then hinged to the front along the underside of the body. At the top of the body a certain amount of freedom of rotation about the hinge was permitted, the conditions " tail up " and " tail down " being indicated by lamps in the cockpit operated by electric contacts at the limits of freedom.

To the rear portion of the body were fixed tubes passing well above the cockpit and braced back to the tail plane by cables. From the top of this tube structure wires passed through the body round pulleys in the front cockpit to a spring balance. The pull in these wires was variable at the wish of an observer in the front seat, and was varied during a flight until contact was made, first tail up and then tail down as indicated by the lamps. The reading of the balance then gave a measure of the moments of the forces on the tail about the hinge. In order to leave the pilot free control over the elevators without affecting the spring balance reading the control cables were arranged to pass through the hinge axis.

The aeroplane has been flown on numerous occasions, and the apparatus is satisfactory in use.

Several attempts have been made to produce a reliable thrust-meter for aerodynamic experiments, but so far no substantial success has been achieved. The direct measurement of thrust would give fundamental information as to the drag of aeroplanes, and the importance of the subject has led to temporary measures of a different kind. It has been found that the airscrews of many aeroplanes can be stopped by stalling the aeroplane, and at the Royal Aircraft Establishment advantage has been taken of this fact to interpose a locking device which prevents restarting during a glide. The airscrew when stopped offers a resistance to motion, but the airflow is such that the conditions can be reproduced in a wind channel for an overall comparison between an aeroplane and a complete model of it. It has already been shown that the angle of glide of an aeroplane is simply related to the ratio of lift to drag, and this furnishes the necessary key to the comparison.

Laboratory Apparatus. The Wind Channel.—The wind channel is one of the most important pieces of apparatus for aerodynamical research, and much of our existing knowledge of the details of the forces on aircraft has been obtained from the tests of models in wind channels. The types used vary between different countries, but all aim at the production of a high-speed current of air of as large a cross-section as possible. The usefulness depends primarily on the product of the speed and diameter of the channel and not on either factor separately, and in this respect the various designs do not differ greatly from country to country. Measuring speeds in feet per sec. and diameters in feet, it appears that the product vD reaches about 1000. The theory of the comparison will be appreciated by a reading of the chapter on dynamical similarity, and except for special purposes the most economical wind channels are of large diameter and moderate speed, the latter being 100 ft.-s. and between the lowest and highest flying speeds of a modern aeroplane.

Fig. 52 shows a photograph of an English type of wind channel as built at the National Physical Laboratory. It is of square section and
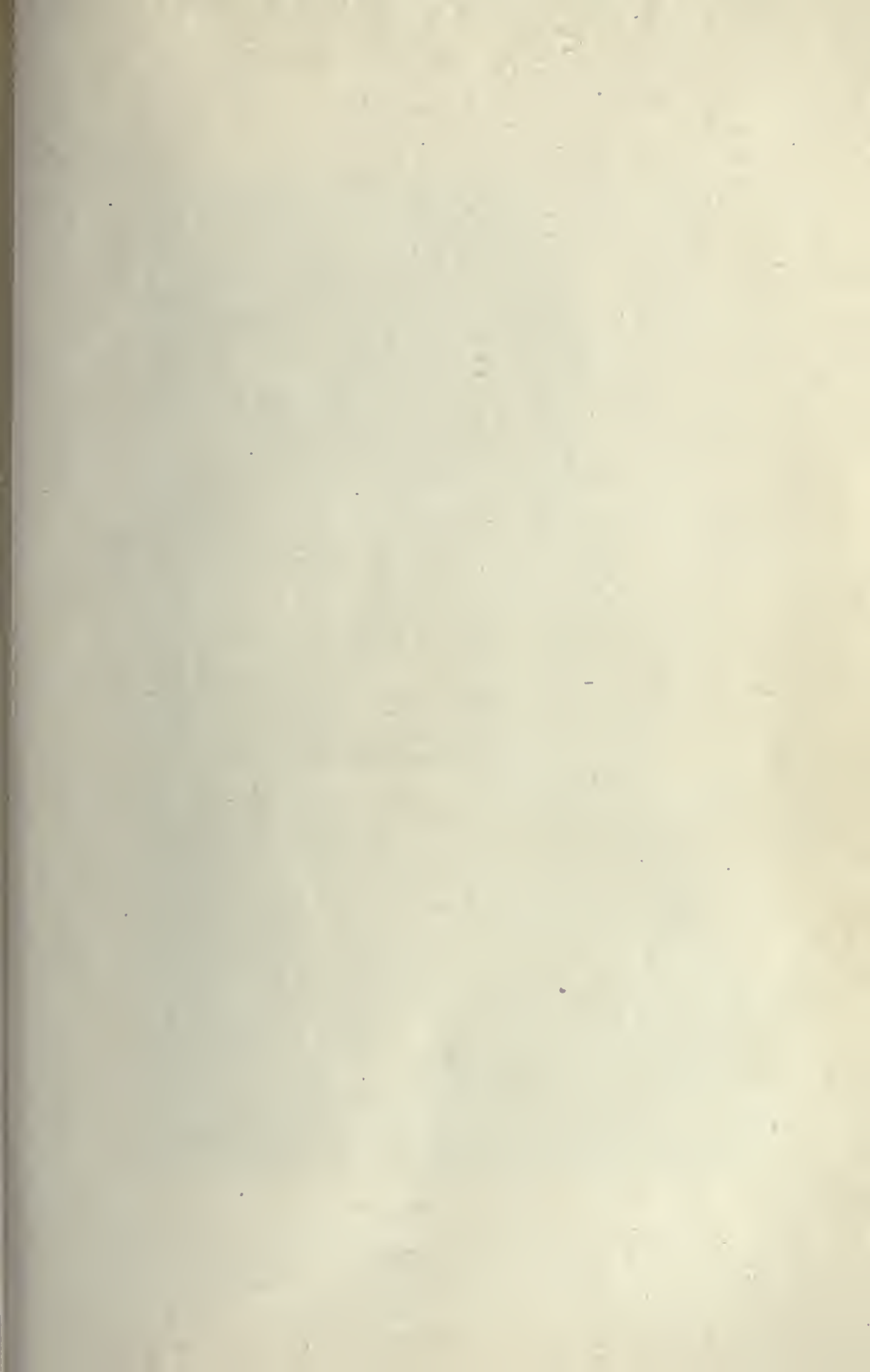
Fig. 52.—Wind channel.

stands in the middle of a large room, being raised from the floor on a light metal framework. The airflow is produced by a four-bladed airscrew driven by electro-motor, and the airscrew is situated in a cone in the centre of the channel, the cone giving a gradual transition from the square forward section to the circular section at the airscrew. The motor is fixed to the far wall of the building and connects by a line of shafting to the airscrew. The airscrew is designed so that air is drawn in to the trumpet mouth shown at the extreme left of Fig. 52, passes through a cell of thin plates to break up small vortices, and thence to the working section near the open door. Just before the end of the square trunk is a second honeycomb to eliminate any small tendency for the twist of the air near the airscrew to spread to the working section. After passing through the airscrew the air is delivered into a distributor, which is a box with sides so perforated that the air is passed into the room at a uniform low velocity. This part

ORDINATE—Percentage change of Velocity. WIND CHANNEL without distributor.

ORDINATE—Percentage change of Velocity. WIND CHANNEL with distributor.
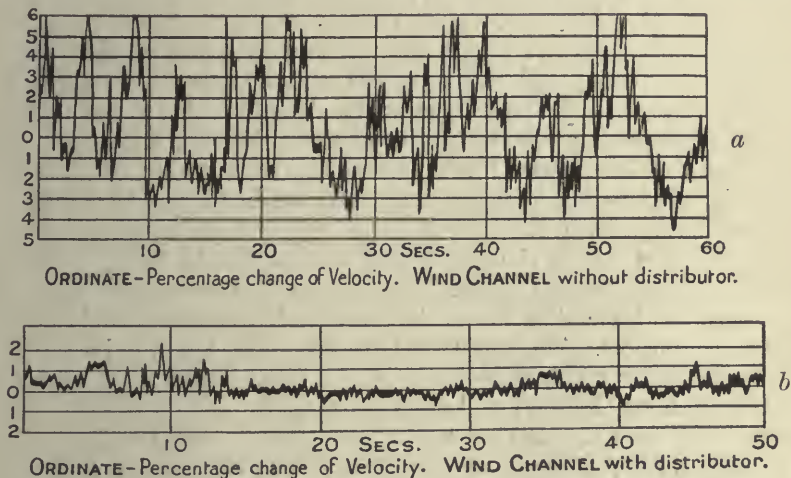
FIG. 53.—The steadiness of the airflow in wind channels.

of the wind channel has an important bearing on the steadiness of the airflow.

The speed of the motor is controlled from a position under the working section, where the apparatus for measuring forces and the wind velocity is also installed.

Over the greater part of the cross-section of the channel the airflow is straight and its velocity uniform within the limits of ± 1 per cent. The rapidity of use depends to a large extent on the magnitude of the fluctuations of speed with time, and Figs. 53 (a) and 53 (b) show the amount of these in a particular case when the channel was tested without a distributor and with a good distributor. Without the distributor the velocity changed by ± 5 per cent. of its mean value at very frequent intervals, and as this would mean changes of force of $\pm 10\%$ on any model held in the stream, it would follow that the balance reading would be sufficiently unsteady to be unsatisfactory. With the distributor the fluctuations of velocity rarely

exceeded ± 0.5 per cent., or one-tenth of the amount in the previous illustration.

A great amount of experimental work has been carried out on the design of wind channels, and the reports of the Advisory Committee for Aeronautics contain the results of these investigations. Although the results of wind-channel experiments form basic material for a book on aerodynamics the details of the apparatus itself are of secondary importance, and the interested reader is referred for further details to the reports mentioned above.

Aerodynamic Balances.—The requirements for a laboratory balance are so varied and numerous that no single piece of apparatus is sufficient to meet them, and special contrivances are continually required to cope with new problems. Some of the arrangements of greatest use will be illustrated diagrammatically, and again for details readers will be referred to the reports of the Advisory Committee for Aeronautics, Eiffel and others.

The first observations of forces and moments which are required are those for steady motion through the air, and in many of the problems, symmetry introduces simplification of the system of forces to be measured. For an airship the important force is the drag, whilst for the aeroplane, lift, drag and pitching moment are measured. For the later problems of control and stability, lateral force, yawing and rolling couples are required when the aircraft is not symmetrically situated in respect to its direction of motion through the air.

At a still later stage the forces and couples due to angular velocities become important, and for lighter-than-air aircraft it is necessary to measure the changes of force due to acceleration and the consequent unsteady nature of the airflow. The problems thus presented can only be dealt with satisfactorily after much experience in the use of laboratory apparatus, but the main lines of attack will now be outlined.

Standard Balance for the Measurement of Three Forces and One Couple for a Body having a Plane of Symmetry.—The diagram in Fig. 54 will illustrate the arrangement. AB, AE and AF are three arms mutually at right angles forming a rigid construction free to rotate in any direction about a point support at A. The arm AB projects upwards through the floor of the wind channel, and at its upper end carries the model the air forces on which are to be measured. Downwards the arm AB is extended to C, and this limb carries a weight Q, which is adjustable so as to balance the weight of any model and give the required degree of sensitivity to the whole by variation of the distance of the centre of gravity below the point of support at A. The arm AB is divided so that the upper part carrying the model can be rotated in the wind and its angle of attack varied ; this rotation takes place outside the channel.

The arms AE and AF are provided with scale pans at the end, and by the variation of the weights in the scale pans the arm AB can be kept vertical for any air forces acting. The system is therefore a " null . method, since the measurements are made without any disturbance of the position of the model.

Moment about the vertical axis AB is measured by a bell-crank lever

GHI, which rests against an extension of the arm AF and is constrained by a knife-edge at H. The moment is balanced by weights in a scale pan hanging from I. It is usually found convenient to make this measurement by itself, and a further constraint is introduced by a support J, which can be raised into contact with the end C of the vertical extension AC. It is not then necessary to have the weights hung from E and F in correct adjustment.

The force along the axis AB can be measured by two steelyards which weigh the whole balance. These are shown as KPN and CMO, the points P and M being knife-edges fixed to a general support from the ground. At C and K the support to the balance is through steel points, and the weight of the balance is taken by counterweights hung from O and N. Variations of vertical force due to wind on the model are measured by changes of weight in the scale pan of the upper steelyard.

Fig. 54.

Suitable damping arrangements are provided for each of the motions, and the part of the arm AB which is in the wind is shielded by a guard fixed to the floor of the channel.

Example of Use on an Aerofoil : Determination of Lift and Drag.—For this purpose the arms KPN and CMO are removed and the arm IH is locked so as to prevent rotation of the balance about a vertical axis. The aerofoil is arranged with its length vertical, and is attached to the arm AB by a spindle screwed into one end. A straight-edge is clamped to the underside of the aerofoil, and by sighting, is made to lie parallel to a fixed line on the floor of the wind channel, this line being along the direction of the wind. The zero indicator on the rotating part of the arm AB is then set, and the weights at Q, E and F are adjusted until balance is obtained with the requisite degree of sensitivity.

In order that this balance position shall not be upset by rotation of the model about the arm AB it is necessary that the centre of gravity of the rotating part shall be in the axis of rotation, and by means of special counterweights this is readily achieved.

The values of the weights in the scale pans at E and F then constitute zero readings of drag and lift. The arms AE and AF are initially set to be along and at right angles to the wind direction within one-twentieth degree, whilst the axis AB is vertical to one part in 5000. The wind is now produced, and at a definite velocity the weights in the scale pans at E and F which are needed for balance are recorded; the difference from the zero values gives the lift and drag at the given angle of incidence. The model is then rotated and the weights at E and F again changed, and so on for a sufficient range of angle of incidence, say $-6°$ to $+24°$.

Centre of Pressure.—For this measurement the lock to the arm IH is removed and the vertical axis constrained by bringing the cup J into contact with C. The weights on the scale pans at E and F are then inoperative, and the weights in the scale pan at I become active. For the angles of incidence used for lift and drag a new series of observations is made of weights in the scale pan at I. From the three readings at each angle of incidence the position of the resultant force relative to the axis AB is calculated. The model being fixed to the arm AB, the axis of rotation relative to the model is found by observing two points which do not move as the model is rotated. This is achieved to the nearest hundredth of an inch, and finally the intersection of the resultant force and the chord of the aerofoil, *i.e.* the centre of pressure, is found by calculation from the observations.

The proportions adopted for the supporting spindle are determined partly by a desire to keep its air resistance very low and partly by an effort to approach rigidity. The form adopted at the National Physical Laboratory is sufficiently flexible for correction to be necessary as a result of the deflection of the aerofoil under air load. Almsot the whole deflection occurs as a result of the bending of the spindle, and as this is round, the plane of deflection contains the resultant force. A little consideration will then show that the moment reading (scale pan at I) is unaffected by deflection, and that the lift and drag are equally affected. The corrections to lift and drag are small and very easily applied, whereas corrections for the aerodynamic effects of a spindle, although small, are very difficult to apply. As a general rule it may be stated that corrections for methods of holding are so difficult to apply satisfactorily when they arise from aerodynamic interference, that the lay-out of an experiment is frequently determined by the method of support which produces least disturbance of the air current. The experience on this point is considerable and is growing, and only in preliminary investigations is it considered sufficient to make the rough obvious corrections for the resistance of the holding spindle.

Example of Use on a Kite Balloon.—For the symmetrical position of a kite balloon the procedure for the determination of lift, drag and moment is exactly as for the aerofoil, the model kite balloon being placed on its side in order to get a plane of symmetry parallel to the plane EAF. Any observer of the kite balloon in the open will have noticed that the craft swings sideways in a wind, slowly and with a regular period. Not only has it an angle of incidence or pitch, but an angle of yaw, and the condition

can be represented in the wind channel by mounting the kite balloon model in its ordinary position and then rotating the arm AB. There is not now a plane of symmetry parallel to EAF, and the procedure is somewhat modified. The model is treated as for the aerofoil so far as the taking of readings on the scale pans E, F and I is concerned, after which the arm IH is locked and the two steelyards brought into operation for the measurement of upward force.

The readings are now repeated with the model upside down in order to allow for the lack of symmetry, and the new weights in the scale pans E and F are observed. With the aid of Fig. 55 the reason for this can be made clear. A' will be taken as a point in the model and also on the axis of AB, and from A' are drawn lines parallel to AE and AF. The complete system of forces and moments on the model can be expressed by a drag along E'A', a cross-wind force along F'A', a lift along A'B', a rolling couple L' about A'E' tending to turn A'F' towards A'B', a pitching couple M' tending to turn A'E' towards A'B', and a yawing couple N' tending to turn A'F' towards A'E'. Now consider the measurements made on the balance. The force A'B' was measured directly on the two steelyards, whilst the couple N' was determined by the weighing at I.

Denoting the weighings at E and F by R_1 and R_2 with distinguishing dashes, it will be seen that

$$R_1' = M' + l \cdot \text{drag} \quad . \quad . \quad . \quad (31)$$
$$\text{and } R_2' = L' + l \cdot \text{cross-wind force} \quad (32)$$

where l is the length AA'. Neither reading leads to a direct measure of drag or cross-wind force. Invert the model

Fig. 55.

about the drag axis A'E' so that A'F' becomes A'F'' and A'B' becomes A'B''. As the rotation has taken place about the wind direction the forces and couples relative to the model have not been changed in any way, and it will follow that the drag and rolling moment are unchanged. The lift, cross-wind force, pitching moment and yawing moment have the same magnitude as before, but their direction is reversed relative to the balance. Instead of equations (31) and (32) there are then two new equations :

$$R_1'' = -M' + l \cdot \text{drag} \quad . \quad . \quad . \quad . \quad . \quad (33)$$
$$R_2'' = L' - l \cdot \text{cross-wind force} \quad . \quad . \quad . \quad (34)$$

It will then be seen from a combination of the two sets of readings that
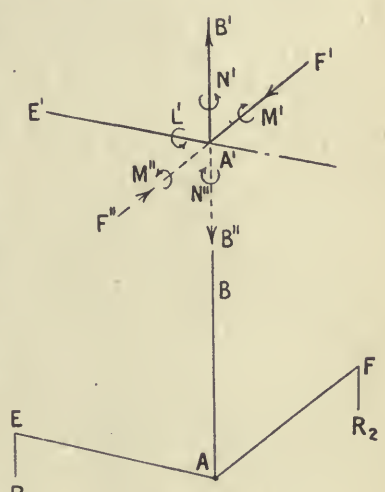
$$\text{drag} = \frac{R_1' + R_1''}{2l} \quad . \quad . \quad . \quad . \quad (35)$$

$$\text{cross-wind force} = \frac{R_2' - R_2''}{2l} \quad . \quad . \quad . \quad . \quad . \quad (36)$$

$$L' = \frac{R_2' + R_2''}{2} \quad . \quad . \quad . \quad . \quad . \quad (37)$$

$$M' = \frac{R_1' - R_1''}{2} \quad . \quad . \quad . \quad . \quad . \quad (38)$$

The result of the experiment is a complete determination of the forces and couples on a model of unsymmetrical attitude, and the generalisation to any model follows at once.

Although the principle of complete determination is correct the method as described is not satisfactory as an experimental method of finding L' and M', although it is completely satisfactory for drag and cross-wind force. The reason for this is that the moment $l \times$ drag is great compared with M', and a small percentage error in it makes a large percentage error in M'. If however l be made zero, equations (31) and (32) show that both L' and M' can be measured directly, and various arrangements have been made to effect this. No universally satisfactory method has been evolved, and the more complex problems are dealt with by specialised methods suitable for each case.

The balance illustrated diagrammatically in Fig. 54 is often used in combination with other devices, such as a roof balance, and various special arrangements will now be described.

Drag of an Airship Envelope.—For a given volume the airship envelope is designed to have a minimum resistance, and for a given cross-section of model the resistance is appreciably less than 2 per cent. of that of a flat plate of the same area put normal to the wind. For sufficient permanence of form and ease of construction models are made solid and of wood, and the resistance of a spindle of great enough strength and stiffness is a very large proportion of the resistance of the model. Further than this, it is found that such a spindle affects the flow over the model envelope to a serious extent and introduces a spurious resistance up to 25 per cent. of that of the envelope. As a consequence of the difficulties experienced at the National Physical Laboratory a method of roof suspension was devised, and is illustrated in Fig. 56. The model is held from the roof of the wind channel by a single wire, the disturbance from which is very small, and the drag is transferred to the balance by a thin rod projecting from the tail and attached by a flexible joint to the vertical arm. The force is measured by weights in the scale pan as in the previous case.

The weight of the model produces a great restoring force in its pendulum action, but this is counteracted by making the balance unstable, so that sufficient sensitivity is obtained. The correction for deflection of the spindle is easily determined and applied. Further, the resistance of the supporting wire can be estimated from standard curves, as its value is a small proportion of the resistance to be measured.

The method has now been in use for a considerable period, and has displaced all others as an ultimate means of estimating the drag of bodies of low resistance.

The model tends to become laterally unstable at high wind speeds, and in that case the single supporting wire to the roof is replaced by two wires meeting at the model and coming to points across the roof of the channel which are some considerable distance apart. The necessary precautions to ensure the safety of a model are easily within the reach of a careful experimenter.
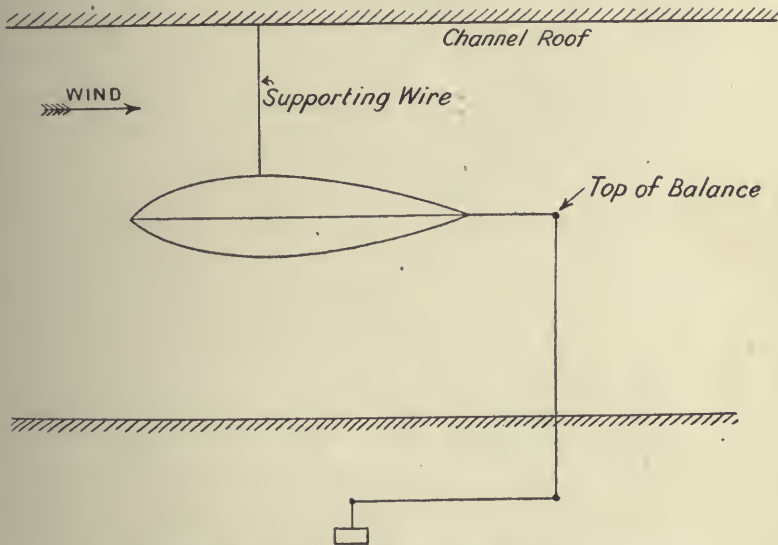
FIG. 56.—Measurement of the drag of an airship envelope model.

Drag, Lift and Pitching Moment of a Complete Model Aeroplane.—The method described for the aerofoil alone becomes unsuitable for the testing of a large complete model aeroplane. The ends of the wings are usually so shaped that the insertion of a spindle along their length is difficult for small models and the size inadequate for large models. Recourse is then made to a suspension on wires, the arrangement being indicated by Fig. 57. The model is inverted for convenience, and from two points, one on each wing, wires are carried to a steelyard outside the wind channel and on the roof. These wires are approximately vertical and take the weight of the model, and any downward load due to the wind. The pull in them is measured by the load in the scale pan hung from the end of the steelyard at U. The knife-edge about which the steelyard turns is supported on stiff beams across the channel.

Another point of support is chosen near the end of the body, and in the illustration is shown at B as situated on the fin. B is attached by a flexible connection to the top of the standard balance, which is arranged as indicated in the diagram to measure the direction and magnitude of the force at B.

The angle of incidence of the wings is altered by a change of length of the supporting wires RS, and although this wire is very long as compared

with the horizontal movements of R, it is necessary to take account of the inclination of the supporting wires. The weight added at E measures the drag, except for a small correction for the inclination of the wires RS ; the weight added at N measures the couple about R, and this point can be chosen reasonably near to the desired place without disturbing the lay-out of the experiment. The weights added at U and N measure the lift, with an error which is usually negligible. The corrections for deflection of
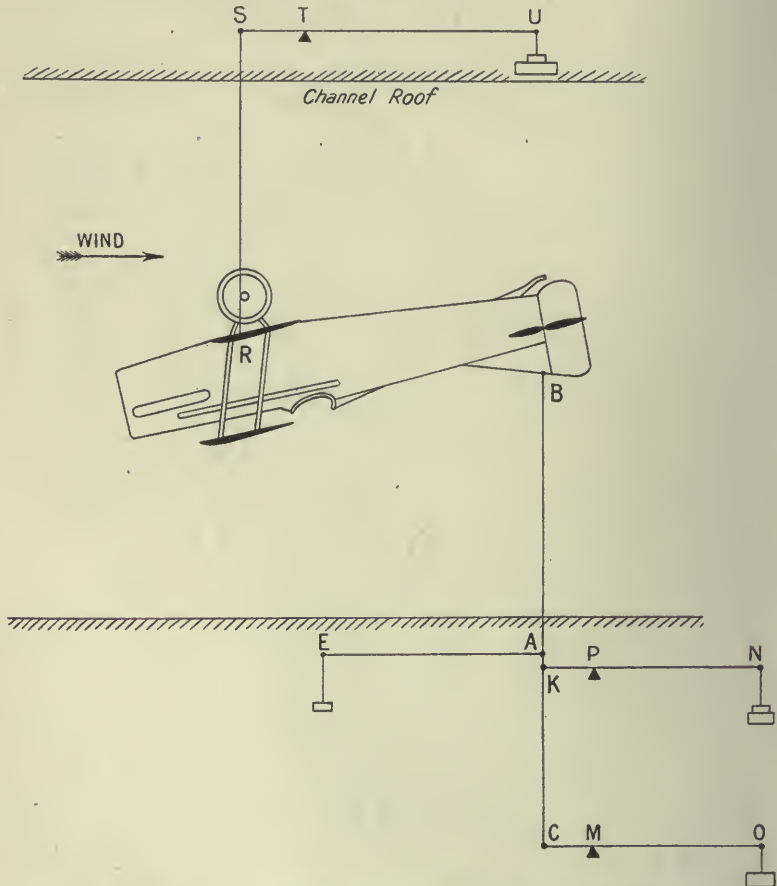
Fig. 57.—Measurements of forces and couple on a complete model aeroplane.

apparatus and inclination of wire involve somewhat lengthy formulæ as compared with the aerofoil method described earlier, but present no fundamental difficulties. As an experimental method the procedure presents enormous advantages over any other, and is being more extensively used as the science of aerodynamics progresses.

Stability Coefficients.—It will be appreciated, once attention is drawn to the fact, that the forces on an oscillating aircraft are different from those on a stationary aeroplane, and that the forces and moment on

an aeroplane during a loop depend appreciably on the angular velocity. The experiment to be described applies more particularly to an aeroplane for a reason given later.

By means of wires or any alternative method, an axis in the wind channel is fixed about which the aeroplane model can rotate, and a rigid arm GFD (Fig. 58) connected to the model is brought through the floor of the channel and ends in a mirror at D. The angular position of the model at any instant is then shown by the position of the image of the lamp H on the scale K, the ray having been reflected from the mirror D. The arm GFD is held to the channel by springs EF and FG, and in the absence of wind in the channel will bring the model and the image on the scale to a definite position. The model if disturbed will oscillate about this position as a mean, and by adjustment of the moment of inertia of the oscillating
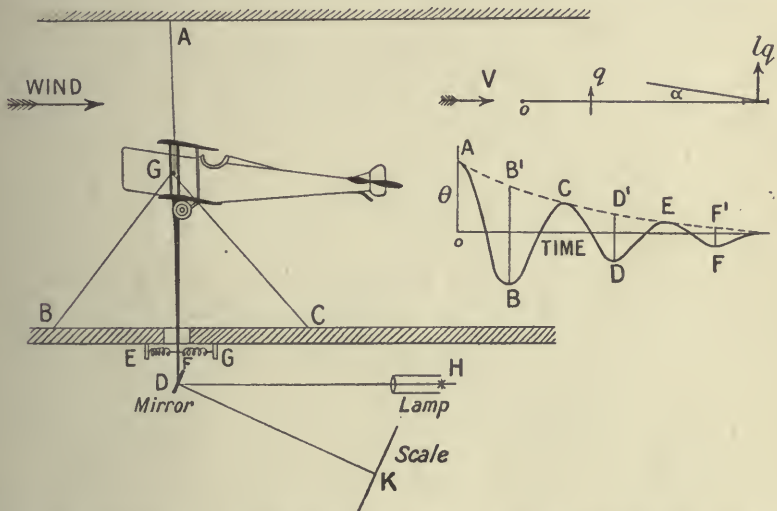
Fɪɢ. 58.—The measurement of resistance derivatives as required for the theory of stability.

system and the stiffness of the spring the period can be made so long that the extremes of successive oscillations can be observed directly on the scale.

The mechanical arrangements are such that the damping of the oscillation in the absence of wind is as small as possible, and considerable success in the elimination of mechanical friction has been attained. When reduced as much as possible the residual damping is measured and used as a correction. In the description to follow the instrument damping will be ignored.

The diagram inset in Fig. 58 will show why the forces and moments on the model depend on the oscillation. A narrow flat plate is presumed to be rotating about a point O, from which it is distant by a distance l. If the angular velocity be q then the velocity of the plate normal to the current will be lq, and the relative wind will be equal to lq and in the opposite direction. Compounding this normal velocity with the wind speed V

shows a wind at an inclination α such that $\tan \alpha = \dfrac{lq}{V}$, and this will produce both a force and a couple opposing the angular elocity. If the angle is small the force on the plate will be proportional to the angle, and also to the square of the speed, and hence proportional to the product of the angular velocity and the forward speed.

The equation of motion of the model in a wind may then be expressed as

$$B\ddot{\theta} + \mu V\dot{\theta} + k\theta = 0 \quad . \quad . \quad . \quad . \quad . \quad (39)$$

where B is the moment of inertia, μ a constant depending on the lengths l and areas of the parts of the model, particularly the tail, k a constant depending on the stiffness of the spring, and θ the angular deflection of the model. The q used earlier is equal to $\dot{\theta}$.

The solution of equation (39) can be found in any treatise on differential equations, and is

$$\frac{\theta}{\theta_0} = e^{-\frac{\mu V}{2B}t} \cdot \frac{\sin\left\{t\sqrt{\frac{k}{B} + \left(\frac{\mu V}{2B}\right)^2} + \epsilon\right\}}{\sin \epsilon} \quad . \quad . \quad . \quad (40)$$

where θ_0 is the value of θ at zero time, and ϵ is a constant giving the phase at zero time. For the present it is sufficient to note that equation (40) represents a damped oscillation of the kind illustrated in Fig. 58. At zero time the value of θ is shown by the point A and is a maximum. The other end of the swing is at B, and the oscillation continues with decreasing amplitude as the time increases. The curve has two well-known characteristics; the time from one maximum to the next is always the same as is the ratio of the amplitudes of successive oscillations. The changes of the logarithms of the maximum ordinates are proportional to the differences of the times at which they occur, and the constant of proportionality is known as the " logarithmic decrement."

In the experiment the measurement of the logarithmic decrement is facilitated by the use of a logarithmic scale at K. The ends of successive swings are observed on this scale, and the observations are plotted against number of swings. The slope of the line so obtained divided by the time of a swing is the logarithmic decrement required, and from equation (40) is equal to $\dfrac{\mu V}{2B}$. This expression shows that the damping is proportional to the wind speed, and the experimental results fully bear out the property indicated.

Before the value of μ can be deduced it is necessary to determine the moment of inertia B, and this is facilitated by the fact that in any practicable apparatus the value of k does not depend appreciably on the wind forces, and that the ratio $\dfrac{k}{B}$ is very much greater than the square of the logarithmic decrement. With these simplifications equation (40) shows that

$$\text{periodic time} = 2\pi\sqrt{\frac{B}{k}} \quad . \quad . \quad . \quad . \quad . \quad (41)$$

k is determined by applying a known force at F and measuring the angular deflections. B is then calculated from the observed periodic time and equation (41). Even were the air forces appreciable the determination of B would present little additional calculation.

The observations have now been reduced to give the value of μ, and consequently the couple $\mu V\dot\theta$ or μVq which is due to oscillation of a model in a wind. Corrections for scale are then applied in accordance with the laws of similar motions.

Some of the quantities which have been determined in this way are very important in their effects on aeroplane motion. The one just described is the chief factor in the damping of the pitching of an aeroplane. Others are factors in the damping of rolling and yawing.

An allied series of measurements to those in a wind channel can be made by tests on a whirling arm. One of the effects is easily appreciated. If an aeroplane model be moved in a circle with its wings in a radial direction the outer wing will move through the air faster than the inner, and if the wings are at constant angle of incidence this will give a greater lift on the outer wing than on the inner. The result is a rolling moment due to turning. In straight flying an airman may roll his aeroplane over by producing a big lift on one side, but this is accompanied by an increased drag and a tendency to yaw. Hence rolling may produce a yawing moment, and in a wind channel the amount may be found by rotating a model about the wind direction and measuring the tendency of one wing to take a position behind the other. The apparatus for the last two factors has not yet been standardised, and few results are available. Further reference to the factors is given in another chapter ; they are generally referred to in aeronautical work as " resistance derivatives."

Airscrews and Aeroplane Bodies behind Airscrews.—The method to be described is applicable particularly simply when the model is of such size that an electromotor for driving the airscrew is small enough to be completely enclosed in the model body. In other cases the power is transmitted by belting or gear, and although the principle used is the same the transmission arrangements introduce troublesome correction in many cases owing to their size and the presence of guards. The diagrammatic arrangement is shown in Fig. 59. The motor is supported by wires, a pair from points on the roof coming to each of the point supports at C and D. This arrangement permits of a parallel motion in the direction CD, together with a rotation about an axis through the points C and D. Movement under the action of thrust and torque is prevented by attaching the rod DM to the aerodynamic balance by a flexible connection. The thrust is measured by weights in the scale pan at E, and the torque by the weights below F.

The body has a similar but independent suspension from the roof, and as shown, rotation about RP and movement along RP is prevented by the wires from L to the floor of the wind channel. By such means the body is fixed in position in the channel irrespective of any forces due to thrust or torque.

The speed of the airscrew is measured by revolution counter

and stopwatch, the counter being arranged to transmit signals to a convenient point outside the channel. In order to keep the speed steady it is usual to employ some form of electric indicator under the control of the operator of the electromotor regulating switches. Torque and thrust are rarely measured simultaneously, one or other of the beams AF or AE being locked as required. To make a measurement of thrust the scale pan at E is loaded by an arbitrary amount, and the wind in the channel turned on and set at its required value. The airscrew motor is
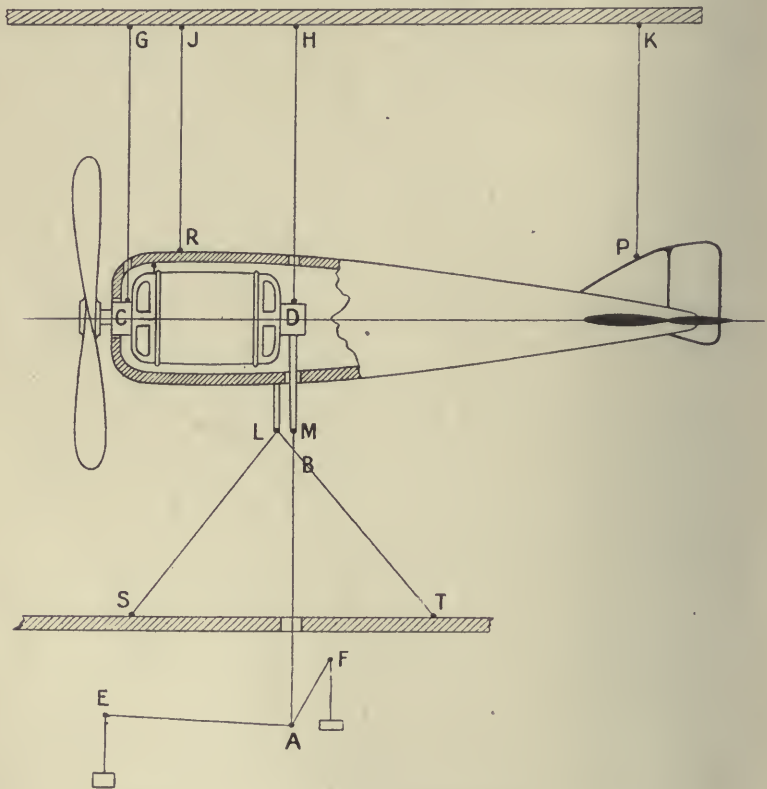
Fig. 59.—The measurement of airscrew thrust and torque.

then started, and its revolutions increased until the thrust balances the weight in the scale pan; the revolutions are kept constant for a sufficient time to enable readings to be taken on a stopwatch. The readings are repeated for the same wind speed but other loads in the scale pan, and finally the scale-pan reading for no wind and no airscrew rotation is recorded.

After a sufficient number of observations at one wind speed the range may be extended by tests at other wind speeds, including zero, before the beam AE is locked and the torque measured on AF. Torque readings are obtained in an analogous manner to those of thrust.

It will be noticed that in this experiment the influence of the body on thrust and torque is correctly represented. In one instance wings and undercarriage were held in place in the same way as the body.

The resistance of the body in the airscrew slip stream is measured by releasing the tie wires SL and TL and connecting L to the top of the balance. M is disconnected from the balance and tied to the floor of the channel so as to fix the motor. For a given wind speed and a number of speeds of rotation of the airscrew the body resistance is measured by weights in the scale pan at E. It is found that the increase in the body resistance is proportional to the thrust on the airscrew and may be very considerable. The effect of the body on the thrust and torque of the airscrew is relatively small ; both effects are dealt with more fully in later chapters.

The apparatus is convenient and accurate in use, and when it can be used has superseded other types in the experiments of the National Physical Laboratory. For smaller models finality has not been reached, and all methods so far proposed offer appreciable difficulties. In this connection the provision of a large wind channel opens up a new field of accurate experiment on complete models in that the airscrew, hitherto omitted, can be represented in its correct running condition.

Measurement of Wind Velocity and Local Pressure.—The pressure tube illustrated in Fig. 40 is used as a primary standard anemometer, and during calibration of a secondary anemometer is placed in the wind channel in the place normally occupied by a model. This secondary anemometer consists of a hole in the side of the channel, and the difference between the pressure at this hole and the general pressure in the wind channel building is proportional to the square of the speed. The special advantage of this secondary standard is that it allows for the determination of the wind speed without obstructing the flow in the channel, and only a personal contact with the subject can impress a full realisation of the effect of the wind shadows from such a piece of apparatus as an anemometer tube. A very marked wind shadow can be observed 100 diameters of the tube away.

For laboratory purposes the pressure differences produced by both the primary and secondary anemometers are measured on a sensitive gauge of the special type illustrated in Fig. 60. Designed by Professor Chattock and Mr. Fry of Bristol the details have been improved at the National Physical Laboratory until the gauge is not only accurate but also convenient in use. The usual arrangement is capable of responding to a difference of pressure of one ten-thousandth of an inch of water, and has a total range of about an inch. For larger ranges of pressure a gauge of different proportions is used, or the water of the normal gauge is replaced by mercury. The instrument does not need calibration, its indications of pressure being calculable from the dimensions of the parts.

In principle the gauge consists of a U-tube held in a frame which may be tilted, and the tilt is so arranged as to prevent any movement of the fluid in the U-tube under the influence of pressure applied at the open ends. The base frame is provided with three levelling screws which support it from the observation table. The frame has, projecting upwards, two

spindles ending in steel points and a third point which is adjustable in height by a screw and wheel, and the three points form a support for the upper frame. A steel spring at one end and a guide at the other are sufficient with the weight of the frame to completely fix the tilting part in position. Rigidly attached to this upper frame is the glasswork which essentially forms a U-tube; to facilitate observation the usual horizontal limb is divided, one part ending inside a concentric vessel which is connected to the other part of the horizontal limb. Above the central vessel is a further attachment for the filling of the gauge. Were the central vessel completely filled with water, flow from one end of the gauge to the other would be possible without visible effect in the observing microscope shown as attached to the tilting frame. Incipient flow is made apparent by the introduction of castor oil in the central vessel for a distance sufficient to cover the otherwise open end of the inner tube. The surface of separation of the water and castor oil is very sharply defined and any tendency to distortion is shown by a departure from the cross wire of the microscope, and is corrected by a tilting of the frame. In this way the effects of viscosity and the wetting of the surfaces of the glass vessels are reduced to a minimum. The film is locked by the closing of a tap in the horizontal limb, and the gauge then becomes portable.
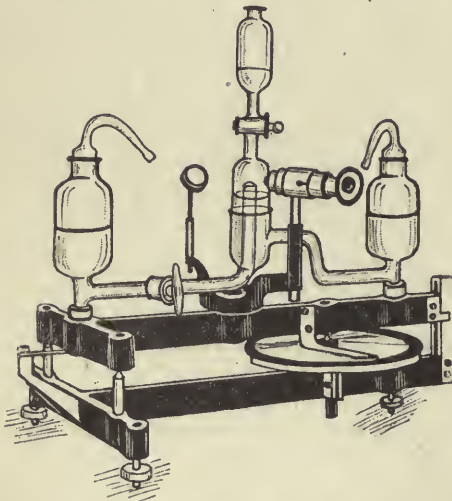
Fig. 60.—Tilting pressure gauge.

A point of practical convenience is the use of a salt-water solution of relative density 1·07 instead of distilled water, as the castor oil in the central vessel then remains clear for long periods. A gauge of this construction carefully filled will last for twelve months without cleaning or refilling. A fracture of the castor oil water surface is followed by a temporarily disturbed zero, but full accuracy is rapidly recovered. The zero can be reset by the levelling screws after such break, and ultimately by transference of salt water from one limb of the U-tube to the other.

As used in the wind channels of the National Physical Laboratory a reading of about 600 divisions is obtained at a wind speed of 40 ft.-s., and the accuracy of reading is one or two divisions determined wholly by the fluctuations of pressure. Speeds from 20 ft.-s. to 60 ft.-s. are read with all desirable accuracy on the same gauge; lower speeds are rarely used, and gauges of the same type but larger range are used up to the highest channel speeds reached.

Chattock tilting gauges have also been used extensively for the measurement of local pressures on models of aircraft and parts of aircraft. If

the wing section be metal, holes are drilled into it at suitable points, each of which is then cross-connected to a common conduit tube. The whole system is arranged to have an unbroken surface in the neighbourhood of the surface holes, and the conduit pipe is led to some relatively distant point before a gauge connection is provided. Before beginning an experiment all the surface openings are closed with soft wax or " plasticene," and the whole system of tubing tested for airtightness. Until this has been attained no observations are taken, and in the case of a complex system it is often difficult to secure the desired freedom from leakage. Once satisfactory, the surface holes are opened one at a time and the pressure at this point measured for variations of the various quantities, such as wind speed, angle of incidence, angle of yaw, etc.

The connection made as above determines the pressure on one limb of the tilting gauge, but it is clear that the readings of the gauge will also depend on the pressure applied at the other limb. This pressure, usually through a secondary standard, is almost invariably taken as the pressure in the static pressure tube of the standard anemometer when in the position of the model. This static pressure differs little from the pressure at the hole in the side of the wind channel, which is the point usually connected to the other limb of the tilting gauge. A standard table of corrections brings the pressure to that of the static-pressure tube of the standard anemometer.

For large wood models the tube system used in pressure distribution is made by inserting a soft lead composition tube below the surface and making good by wax and varnish. Holes at desired points are made with a needle and closed with soft wax when not in use. This method is applied to airship models in most cases, but a variant of value is the use of a hollow metal model, the inside of which is connected to the tilting gauge, and through the shell of which holes can be drilled as required.

The determination of local pressures in this way is one of the simplest precise measurements possible in a wind channel. If the number of observations is large the work may become lengthy, but errors of importance are not easily overlooked. Any errors arise from accidental leakage, and general experience provides a check on this since the greatest positive pressure on a body is calculable, and the position at which it occurs is known with some precision. Measurements have been made over the whole surface of a model wing for a number of angles of incidence, over an airship envelope for angles of yaw, over a cylinder and over a model tail plane. The latter experiment covered the variations of pressure due to inclination of the elevators. An example will be given later showing the accuracy with which the method of pressure distribution can be used to measure the lift and drag of an aerofoil. It will be understood that skin friction is ignored by the method, and that the pressure measured is that normal to the surface. A series of experiments by Fuhrmann at Göttingen University showed that for small holes the reading of pressure was independent of the size of the hole, and the conclusion is supported by experiments at the National Physical Laboratory.

The Water Resistance of Flying-Boat Hulls.—Experiments on the resistance of surface craft are made by towing a model over still water. The general arrangement of the tank consists of a trough some 500 to 600 feet long, 30 feet wide and 12 feet deep. Along the sides are carefully laid rails which support and guide a travelling carriage, the speed of which is regulated by the supply to the electromotors mounted above the wheels. The first 100 to 150 feet of the run are required to accelerate to the final speed, and a rather larger amount for stopping the carriage at the end of the run. Speeds up to 20 feet per sec. can be reached, and the time available for observation is then limited to fifteen seconds, so that all the measurements are most conveniently taken automatically. At lower speeds the time is longer, and direct observation of some quantities comes easily within the limits of possibility.

The water resistance of a flying-boat hull is associated intimately with the production of waves, and the law followed in the tests is known as Froude's law, and states that the speed of towing a model should be less than that of the full-size craft in the proportion of the square root of the relative linear dimensions. This rule is dealt with in greater detail in the chapter on dynamical similarity, where it is shown that once the law is satisfied the forces on the full scale are deduced from those on the model by multiplying by the cube of the relative linear dimensions.

The flying boat at rest is supported wholly by the reaction of the water, and the displacement is then equal to the weight of the boat. As the air speed increases, part of the weight is taken by the wings until ultimately the whole weight comes on to the wings and the flying boat takes to the air. The testing arrangements are shown diagrammatically in Fig. 61. Points of attachment of the apparatus to the tank carriage are indicated by shaded areas. The model of the flying-boat hull is constrained to move only in a vertical plane, but is otherwise free to take up any angle of incidence and change of height under the action of the forces due to motion. The measuring apparatus is attached at A by free joints, the resistance being balanced by a pull in the rod AB, and the air lift from the wings being represented by an upward pull in the rod AD. The trim of the boat can be changed by the addition of weight at P, and the angle for each trim is read on the graduated bar N, which moves with the float.

The upper end of the rod AD moves in a vertical guide, and a wire cord passing over pulleys to a weight O gives the freedom of vertical adjustment mentioned, together with the means of representing the air lift. The pull in the rod AB is transmitted to a vertical steelyard EFG and is balanced in part by a weight hung from G, and for the remainder by the pull in the spring HJ. From J there is a rod JK operating a pen on a rotating drum, whilst other pens at L and M record time and distance moved through the water. The record taken automatically is sufficient for the determination of speed and resistance.

Since the model is free to rotate about an axis through A, the observations of pull in AB and of lift in AB are sufficient, in addition to the observation of inclination, to completely define the forces of the model at any speed. The conditions of experiment can be varied by changes in the weights
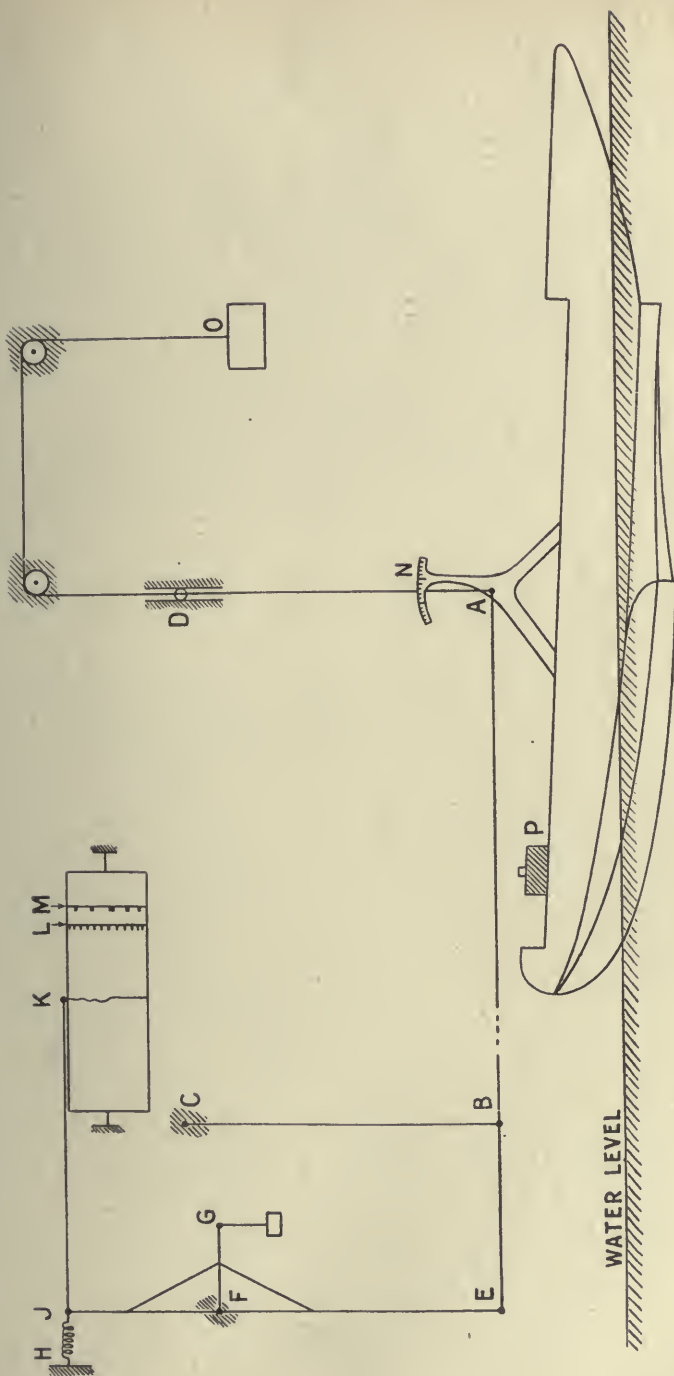
Fig. 61.—The measurement of float resistance.

at O and P, and the whole of the possibilities of motion for the particular float can be investigated.

The observations include a general record of the shape of the waves formed, the tendency to throw up spray or green water, or to submerge the bow. Occasionally more elaborate measurements of wave form have been made. Flying boats of certain types bounce on the water from point to point in a motion known as "porpoising," and by means of suitable arrangements this motion can be reproduced in a model.

Forces due to Accelerated Fluid Motion.—In aviation it is usual to assume that the forces on parts of aeroplanes depend only on the velocities of the aeroplane, linear and angular, and are not affected appreciably by any accelerations which may occur. A little thought will show that this assumption can only be justified as an approximation, for acceleration of the aircraft means acceleration of fluid in its neighbourhood, with a consequent change of pressure distribution and total force on the model. In recent years the examination of the effects of acceleration on aerodynamic forces has become prominent in the consideration of the stability of airships. To estimate its importance recourse is had to experiments on the oscillations of a body about a state of steady motion, and the principle may be illustrated for a sphere. Fig. 62 shows an arrangement which can be used to differentiate between effects due to steady and to unsteady motion. The sphere is mounted on a pendulum swinging about the point A, the sphere itself being in some liquid such as water. On an extension of the pendulum at D is a counterweight which brings the centre of mass of the pendulum to A, so that the whole restoring couple is due to the springs at EF and FG and the eccentric counterweight C.

FIG. 62.—Forces due to acceleration of fluid motion.

The moment of inertia about A will be denoted by I, and the oscillations will be such that θ is always a small angle and within the limits $\sin \theta = \theta$ and $\cos \theta = 1$. The equation of motion may be written as

$$I\ddot{\theta} = b\mathrm{W}_1 - k\theta - f(v + l\dot{\theta}, \ddot{\theta}) \quad . \quad . \quad . \quad . \quad (42)$$

where $b\mathrm{W}_1$ is the couple due to the counterbalance weight at C, $k\theta$ is the restoring couple arising from the springs at EF and FG, and $f(v + l\dot{\theta}, \ddot{\theta})$ is the hydrodynamic couple. The linear velocity of the centre of the sphere is

$v + l\theta$, whilst the linear acceleration is proportional to $\ddot{\theta}$. A somewhat similar equation to (42) could be written down in which θ was not restricted to be small, but the general solution is unknown until f is completely specified. With the special assumption f can be expanded in powers of $\dot{\theta}$ and $\ddot{\theta}$ and powers higher than the first neglected, leading to

$$f(v + l\dot{\theta}, \ddot{\theta}) = f(v, o) + l\dot{\theta}\frac{\partial f}{\partial v} + \ddot{\theta}\frac{\partial f}{\partial \ddot{\theta}} \quad . \quad . \quad . \quad . \quad (43)$$

where $f(v, o)$ is the hydrodynamic couple when the motion is steady. The counterbalancing couple bW_1 will be taken equal to $f(v, o)$ as a condition of the experiment, and equation (42) becomes

$$\left(I + \frac{\partial f}{\partial \ddot{\theta}}\right)\ddot{\theta} + l\dot{\theta}\frac{\partial f}{\partial v} + k\theta = 0 \quad . \quad . \quad . \quad . \quad (44)$$

The resulting motion indicated is a damped oscillation of the type already dealt with in equation (39). The logarithmic decrement and the periodic time are

$$\log \text{dec.} = \frac{l\frac{\partial f}{\partial v}}{2\left(I + \frac{\partial f}{\partial \ddot{\theta}}\right)}, \quad \text{and} \quad T = 2\pi \bigg/ \sqrt{\frac{k}{I + \frac{\partial f}{\partial \ddot{\theta}}} + (\log \text{dec.})^2} \quad (45)$$

and from the observation of the logarithmic decrement and the periodic time the value of $\frac{\partial f}{\partial \ddot{\theta}}$ can be deduced from (45). I may be determined by an experiment in air (or *vacuo* if greater refinement is attempted), whilst k is measured as explained in connection with equation (39). It will be noticed that the acceleration coefficient $\frac{\partial f}{\partial \ddot{\theta}}$ occurs as an addition to the moment of inertia, and might be described as a " virtual moment of inertia." In translational motion it would appear as a " virtual mass." The idea of virtual mass is only possible in those cases for which f can be expanded as a linear function of acceleration. The case of small oscillations is one important instance of the possibility of this type of expansion.

In the case of the sphere the virtual mass appears to be about 80 per cent. of the displaced fluid ; for an airship moving along its axis the proportion is about 25 per cent., and for motion at right angles over 100 per cent. The accelerations of an airship along and at right angles to its axis are therefore reduced to three-quarters and half their values as estimated by a calculation which ignores virtual mass. On the other hand no appreciable correction for heavier-than-air craft is suspected, and a few experiments on flat plates show that the effect of accelerations of the fluid motion on the aerodynamic forces is not greater than the accidental error of observation.

Model Tests on the Rigging of an Airship Envelope.—Calculations relating to the rigging of the car of a non-rigid airship to the envelope become very complex when they are intended to cover flight both on an

even keel and when inclined as the result of pitching. Advantage is taken of a theorem first propounded in 1911 by Harris Booth in England and by Crocco in Italy. A model of the envelope is made with rigging wires attached, and is held in an inverted position by the wires, which pass over pulleys and carry weights at their free ends. The model is filled with water, and a sufficient pressure applied to the interior of the envelope by connection to a head of water.

The arrangement is shown diagrammatically in Fig. 63, the number of wires having been chosen only for illustration and not as representing any real rigging. A beam NO carries a number of pulleys F, E, D, which can be adjusted in position along the beam so as to vary the inclinations
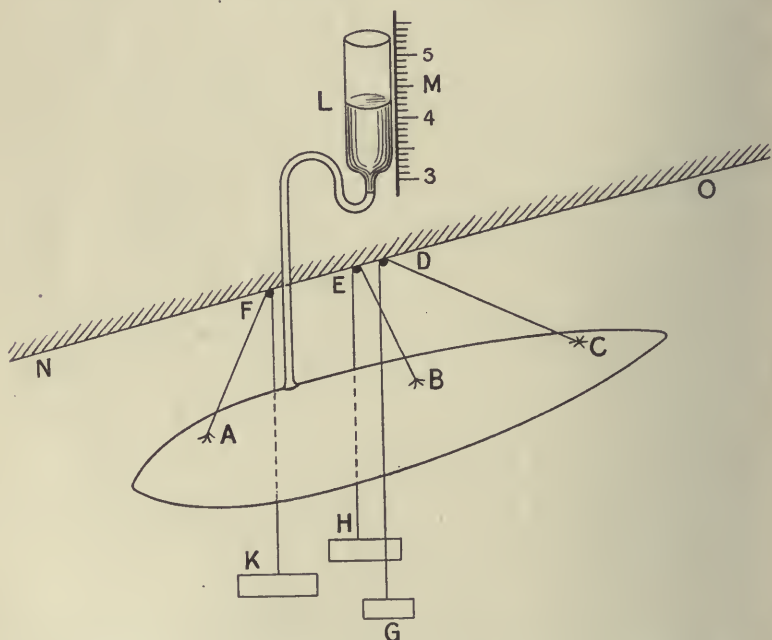
Fig. 63.—Experiment to determine the necessary gas pressure in a non-rigid airship.

of the rigging wires AF, BE and CD. The tensions in these rigging wires are produced by weights K, H and G. The model being inflated with water, the pressure can be varied by a movement of the reservoir L, and can be measured on the scale M. The points F, E and D will be on the car of an airship, and the geometry of the rigging and the loads in the wires will be known approximately from calculation or general experience. Once this point has been reached an experiment consists of the gradual lowering of the reservoir L until puckering of the fabric takes place at some point or other. By carefully adjusting the positions of the rigging wires and the loads to be taken by them it may be possible to reduce the head of water before puckering again takes place, and by a process of trial and error the best disposition of rigging is obtained.

The relation of the experiment to the full scale is found by the principles of similarity. The shape of the envelope is fixed by the difference between the pressures due to hydrogen and those due to air. The internal pressure can be represented by the effect of the head in a tube below the envelope, the length of the hydrogen column produced being an exactly analogous quantity to the length of the column of water in the model experiment. In the model the shape of the envelope depends on the difference between water and air, and the pressures for a given head are 900 times as great as that for hydrogen and air at ground-level, or 1050 times as great as at 10,000 feet. The law of comparison states that the stresses in the fabric of the model envelope will be equal to those in the airship if the scale is $\sqrt{900}$, *i.e.* 30, for ground-level, or $\sqrt{1050}$, *i.e.* 32·4, for 10,000 ft. The necessary internal pressure to prevent puckering of the airship envelope fabric is calculated from the head of hydrogen obtained by scaling up the head of water.

The method neglects the weight of the fabric, but the errors on this account do not appear to be important.

CHAPTER IV

DESIGN DATA FROM THE AERODYNAMICS LABORATORIES

PART I.—STRAIGHT FLYING

THE mass of data relating to design, particularly that collected under the auspices of the Advisory Committee for Aeronautics, is very considerable and will be the ultimate resort when new information is required. The reports and memoranda have been collected over a period of ten years, part of which was occupied by the Great War. To this valuable material it is now becoming essential to have a summary and guide, which in itself would be a serious compilation not to be compressed into even a large chapter of a general treatise. Some general line of procedure was necessary therefore in preparing this chapter in order to bring it within reasonable compass, and in making extracts it was thought desirable in the first place to give detailed descriptive matter covering the whole subject in outline. In scarcely any instance has a report been used to its full extent, and readers will find that extension in specific cases can be obtained by reference to original reports. Although detailed reference is not given, the identity of the original work will almost always be readily found in the published records of the Advisory Committee for Aeronautics.

A second main aim of the chapter has been the provision of enough data to cover all the various problems which ordinarily arise in the aerodynamic design of aircraft, so that as a text-book for students the volume as a whole is as complete as possible in itself.

The chapter is divided into two parts, which correspond with a natural physical division. In the first, " Straight Flying," the measurements involved are drag, lift and pitching moment, and have only passing reference to axes of inertia. " Non-rectilinear flight " is, however, most suitably approached from the point of view of forces and moments relative to the moving body, and the second part of the chapter opens with a definition of body axes and the nomenclature used in relation to motion about them. The first part of the chapter is not repeated in new form in the second, as the transformations are particularly simple and it is only in the case of complete models that they are required. In its second part this chapter, in addition to dealing with the data of circling flight, gives some of the fundamental data to which the mathematical theory of stability is applied.

Wing Forms.—The wings of an aeroplane are designed to support its weight, and their quality is measured chiefly by the smallness of the resistance which accompanies the lift. The best wings have a resistance which is little more than 4 per cent. of the supporting force. Almost the

whole of our knowledge of the properties of wing forms as dependent on shape and the combinations of more than one pair of wings is derived from tests on models and is very extensive. The most that can ever be expected from flight tests is the determination of wing characteristics in a limited number of instances, and it is fortunate for the development of aeronautics that the use of models leads to results applicable to the full scale with little uncertainty. The theory of model tests and a comparison with full scale is given in the chapter on Dynamical Similarity, and in the present chapter typical examples are selected to show how form affects the characteristics of aeroplane wings without special reference to the changes from model to full scale.

Wing forms, owing to their importance, are described by a number of terms which have been standardised by the Royal Aeronautical Society, Some of these are reproduced below, and are accompanied by explanatory sketches in Figs. 64 and 65. Wing forms may be so complex that simple definition is impossible, but in all cases the geometry can be fixed by sufficiently detailed drawings. The complex definitions are less important than, and follow so naturally from, the simple ones that they will be ignored in the definitions now put forward, and readers are referred to the Glossary of the Royal Aeronautical Society for them.

Geometry of Wings : Definitions.—The simplest form of wing is that illustrated in Fig. 64 (a) by the full lines. In plan the projection is a rectangle of width c and length $\frac{s}{2}$. Two wings together make a plane of " span " s and " chord " c. In the standard model s is

Fig. 64.

made equal to six times c, and the ratio is known as the " aspect ratio." A section of the wings parallel to the short edges is made the same as every other and is called the " wing section." The area of the projection, *i.e.* $s \times c$, is the " area of the plane " and has the symbol S.

Departures from this simple standard occur in all aeroplanes, the commonest change being the rounding of the wing tips. A convenient way of accurately recording the shape is illustrated in Fig. 80, where contours have been drawn. The leading edges of the wings may be inclined in the pair which go to form a plane, and the inclinations are
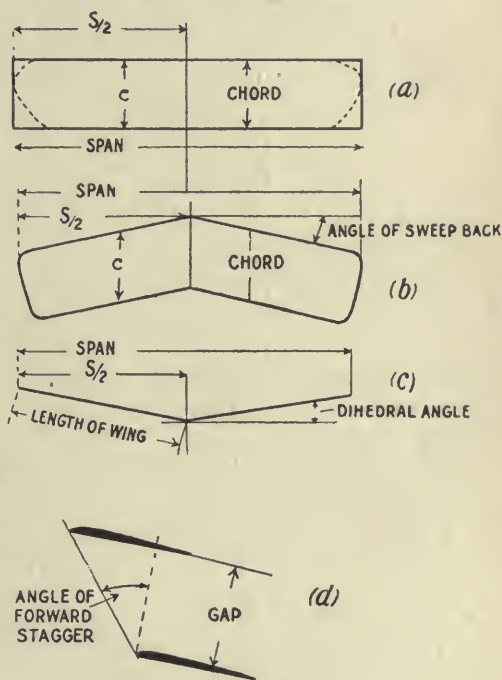
called the angle of sweepback if in plan, Fig. 64 (b), and dihedral angle if in elevation, Fig. 64 (c).

When two planes of equal chord are combined the perpendicular distance between the chords is called the "gap," whilst the distance of the upper wing ahead of the lower is defined by the "angle of stagger," Fig. 64 (d). Similar definitions apply to a triplane.

For tail planes, struts, etc., the chord is taken as the median line of a section, and in general the chord of an aerofoil is the longest line in a section, and the area its maximum projected area.

With these definitions it is possible to proceed with the description of the forces on a wing in motion through the air, and an account of the tables and diagrams in which the results of observation are presented.

Aerodynamics of Wings : Definitions (Fig. 65).—In the standard model wing the attitude relative to the wind is fixed by the inclination of the chord of a section to the direction of the relative wind. The angle α is known as the "angle of incidence." The forces on the wing in the standard atmosphere of a wind channel are fixed by the angle α, the wind speed V, and the area of the model. No matter what the relation between the angle, velocity and forces, the latter can always be completely represented by a force of magnitude R, Fig. 65, in a definite position AB. Various alternative methods of expressing this possibility have current use. The resultant R
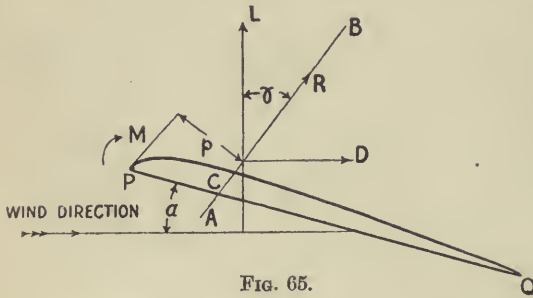
FIG. 65.

may be resolved into a lift component L normal to the wind direction and a drag component D along the wind. If γ be the angle between AB and the normal to the wind direction, it will be seen that the relation between L and D and R and γ is

$$L = R \cos \gamma, \qquad D = R \sin \gamma \quad . \quad . \quad . \quad . \quad . \quad (1)$$

The position of AB is often determined by the location of the point C, which shows the intersection with the chord of the section. It is equally well defined by a couple M about a point P at the nose of the wing, M being due to the resultant force R acting at a leverage p. The sign is chosen for convenience in later work. The point P may be chosen arbitrarily; in single planes it is usually the extreme forward end of the chord, in biplanes the point midway between the forward ends of the chords, and in triplanes the forward end of the chord of the middle plane.

The next step in representation arises from the result of experiments. It is found that for all sizes of model and for all wind speeds, the angle γ is nearly constant so long as α is not changed, and that the ratio CP to PQ is also little affected. On the other hand, the magnitude of R is nearly proportional to the plane area and to the square of the speed. On theoretical

grounds it is found that the magnitude is also proportional to the density of the air. Putting these quantities into mathematical form shows that

$$\frac{CP}{PQ}, \gamma, \text{ and } \frac{R}{\rho S V^2} \quad \cdot \quad \cdot \quad \cdot \quad \cdot \quad \cdot \quad \cdot \quad (2)$$

are all nearly independent of the size of the model or the wind speed during the test. The quantities are therefore peculiarly well suited for a comparison of wing forms and the variation of their characteristics with angle of incidence. The first quantity is clearly the same whether C P and PQ are measured in feet or in metres, and is therefore international. Similarly, the radian as a measure of angle and the degree are in use all over the civilised world. The third quantity can be made international by the use of a consistent dynamical system of units.*

Quantities which have no dimensions in mass, length and time are denoted by the common letter k, are particularised by suffixes and referred to as coefficients. The following are important particular cases as applied to wings, and are derived from the three already mentioned (2), by the ordinary process of resolution of forces and moments :—

$$\left.\begin{aligned}
\text{Centre of pressure coefficient} &\equiv k_{\text{CP}} = \frac{CP}{PQ} \text{ of Fig. 65}\\[2mm]
\text{Lift coefficient} &\equiv k_{\text{L}} = \frac{L}{\rho V^2 S}\\[2mm]
\text{Drag coefficient} &\equiv k_{\text{D}} = \frac{D}{\rho V^2 S}\\[2mm]
\text{Moment coefficient} &\equiv k_{\text{M}} = \frac{M}{\rho V^2 S c}
\end{aligned}\right\} \quad \cdot \quad (3)$$

* The choice of units inside the limits of dynamical consistency leads to difficulties between the pure scientist and the engineer. Whilst both agree to the fundamental character of mass as differentiated from weight, usage of the word " pound " as a unit for both mass and weight or force is common. To the author it appears that any system in which such confusion can occur is defective, and in England part of the defect lies in the absence of a legal definition of force which has any simple relation to the workaday problems of engineering. Thus, in aeronautics, the English-speaking races invariably speak of the thrust of an airscrew in pounds and of pressures in pounds per square inch or per square foot. The whole of the difficulty does not lie here, for the metric system has separate names for force and mass, and yet the French aeronautical engineer expresses air pressure in kilogrammes per square metre instead of the roughly equal quantity megadynes per square metre, which is consistent with his system of units. It would appear that the conception of weight as a unit of force is so much simpler than that of mass acceleration that only students will systematically use the latter. If we were now to make the weight of the present standard of mass into a standard of force by specifying g at the place of measurement as some number near to 32·2 and introduce a new unit of mass 32·2 times as great as our present unit, it appears to the author that the divergence of language between science and engineering would disappear. In this belief, the standard indicated above has been adopted throughout this book from amongst those in current use at teaching institutions as being the best of three alternatives. The rather ugly name of " slug " was given to this unit of mass by some one unknown. The standard density of air in aeronautical experiments is 0·00237 slug per cubic foot, and not 0·0765 lb. per cubic foot. To meet objections as far as possible full use has been made of non-dimensional coefficients, so that in many cases readers may use their own pet system without difficulty in applying the tables of standard results.

All results obtained in aerodynamic laboratories apply also to a non-standard atmosphere if the expressions (3) are used, but the speed of test usually quoted applies only to air at 760 mm. Hg and a temperature of 15°·6 C.

Fig. 66 shows how the various quantities of (3) are arranged in presenting results. The independent variable of greatest occurrence is " angle of
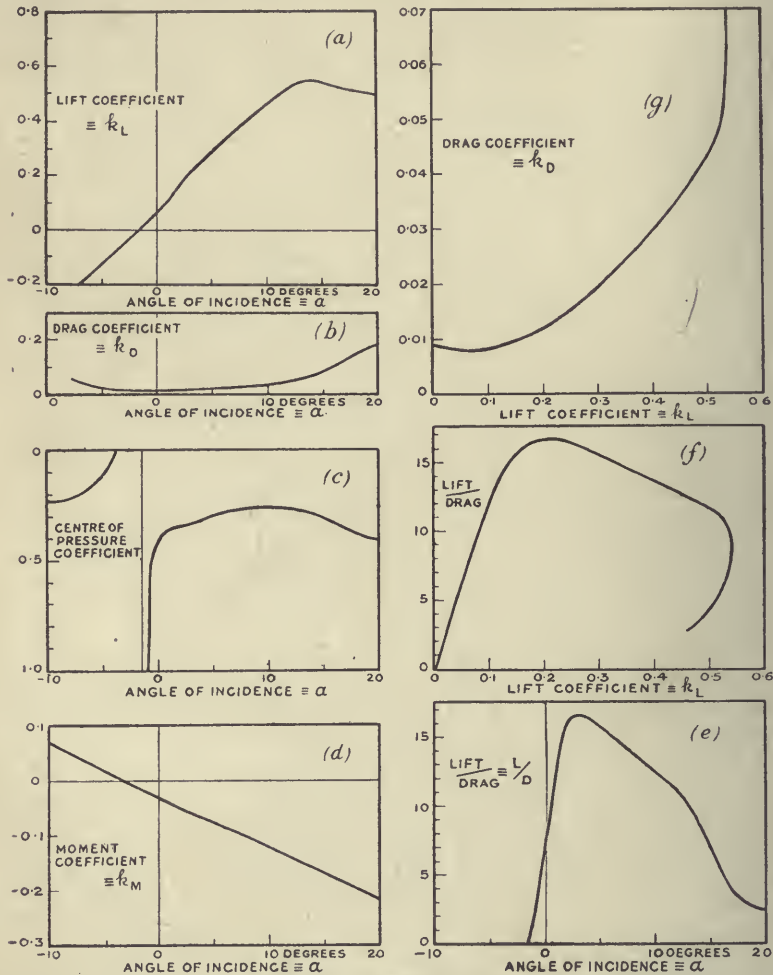
Fig. 66.—Methods of illustrating wing characteristics.

incidence," but for many purposes the lift coefficient k_L is used as an independent variable. The reasons for this will appear after a study of the chapter on the Prediction and Analysis of Aeroplane Performance.

The useful range of angle of incidence in the flight of an aeroplane is from $-1°$ to $+15°$, and model experiments usually exceed this range at both ends. An example is given a little later in which observations were taken for all possible angles of incidence, but this case is exceptional.

Fig. 66 (a). **Lift Coefficient and Angle of Incidence.**—For angles of incidence which give rise to positive lift the curve of lift coefficient against angle of incidence has an initial straight part, the slope of which varies little from one wing to another. At some angle, usually between 10 and 20 degrees, the lift coefficient reaches a maximum value, and this varies appreciably ; the fall of the curve after the maximum may be small or great, and the condition appears to correspond with an instability of the fluid motion over the wing. The maximum lift coefficient is very important in its effect on the size of an aeroplane, since it fixes the area for a given weight and landing speed. By rearrangement of (3) it will be seen that

$$S = \frac{L}{\rho V^2 k_L} \quad . \quad . \quad . \quad . \quad . \quad . \quad . \quad (4)$$

and in level flight L is equal to the weight of the aeroplane. Near the ground, the air density ρ does not vary greatly, and for a chosen landing speed the area required is inversely proportional to the lift coefficient k_L. The ratio of total weight to total area is often spoken of as loading and is denoted by w, and equation (4) shows that the permissible loading is proportional to the lift coefficient.

TABLE 1.

LIFT COEFFICIENT, LOADING AND LANDING SPEED.

Landing speed.		Loading (lbs. per sq. ft.).		
ft.-s.	m.p.h.	$k_L = 0\cdot4$	$k_L = 0\cdot6$	$k_L = 0\cdot8$
20	13·6	0·38	0·57	0·76
40	27·3	1·52	2·28	3·03
60	40·9	3·4	5·1	6·8
80	54·5	6·1	9·1	12·2
100	68·2	9·5	14·2	19·0

Table 1 shows, for a possible range of lift coefficients, the values of wing loading which may be used for chosen landing speeds. It will be noticed that the size of an aeroplane is primarily fixed by the weight and landing speed, and only to a secondary extent by possible changes of lift coefficient. For an aeroplane weighing 2000 lbs., using wings having a maximum lift coefficient of 0·6, the areas required are 3,500, 390 and 141 sq. ft. for landing speeds of 20, 60 and 100 ft. per sec. In normal practice the area varies from 250 to 350 sq. feet for an aeroplane weighing 2000 lbs., but in earlier designs an area of 700 or 800 sq. feet would have been considered appropriate. The difficulties of landing are much increased by heavy wing loading, and at speeds of 50 m.p.h. and upwards prepared grounds with a smooth surface are required for safety.

It is important to bear in mind the above restriction on the choice of wing area, for efficiency calls for loadings which are prohibited on this score.

Fig. 66 (*b*).   **Drag Coefficient and Angle of Incidence.**—The curve is shown to the same scale as lift coefficient, but is rarely used in this form although the numbers are given in tables for all wing forms tested under standard conditions.   The smallness of the ordinates over the flying range for any reasonable scale of drag at the critical angle of lift is the chief reason for a limited use of this type of diagram.

Fig. 66 (*c*).   **Centre of Pressure Coefficient and Angle of Incidence.**—Considerable variation in curves of centre of pressure occur in wing forms, but that illustrated is typical of the present day high-speed wing.   The curve has two infinite branches occurring near to the angle of zero lift, and the changes in this region are great.   For larger angles of incidence the changes are smaller in amount, and the curve has an average position about one-third of the chord behind the leading edge of the wings.   The exact position of infinite centre of pressure coefficient is defined by the angle at which the resultant force (R of Fig. 65) becomes parallel to the chord, and therefore depends to some extent on the definition of the chord.   If the centre of pressure moves forward with increase of angle of incidence, the tendency of the wing is to further increase the angle and is therefore towards instability.   Turning up the trailing edge of a wing may reverse the tendency, as will appear in one of the illustrations to be given.

Fig. 66 (*d*).   **Moment Coefficient and Angle of Incidence.**—The infinite value of centre of pressure coefficient near zero lift has no special significance in flight, and it is often more convenient to use a moment coefficient. The curve has no marked peculiarities over the flying range, but may be very variable at the critical angle of lift.

Fig. 66 (*e*).   **Lift/Drag and Angle of Incidence.**—The ratio of lift to drag is one of the most important items connected with the behaviour of aeroplane wings, and in level steady flight is the ratio of the weight of an aeroplane to the resistance of its wings.   The curve starts from zero when the lift coefficient is zero, and rapidly reaches a maximum which may be as great as 20 to 25, and then falls more slowly to less than half that value at maximum lift coefficient.   It is obvious that every effort is made to use a wing at its best, *i.e.* where $\dfrac{\text{L}}{\text{D}}$ is a maximum, but the limitation of landing speed can be seen to affect the choice as below.   Denoting the speed of flight by V and the landing speed by V_l, it will be seen that the condition of constant loading requires that

$$\rho_l \text{V}_l{}^2 (k_\text{L})_{\max.} = \rho \text{V}^2 k_\text{L} \qquad . \quad . \quad . \quad . \quad . \quad (5)$$

Equation (5) can be arranged in a more convenient form as

$$\sigma^{\frac{1}{2}}\text{V} = \sqrt{\frac{(k_\text{L})_{\max.}}{k_\text{L}}} \cdot \text{V}_l \quad . \quad . \quad . \quad . \quad . \quad (6)$$

where σ is the relative density of the atmosphere at the place of flight, and $\sigma^{\frac{1}{2}}\text{V}$ will be recognised as indicated airspeed.   The whole of the right-hand side of (6) is fixed by the landing speed and the wing form if k_L be chosen as the lift coefficient for maximum lift/drag, and hence the indicated air speed for greatest efficiency is fixed.

Referring to Figs. 66 (a) and 66 (e) it will be found that k_L has a maximum value of 0·54 and a value of 0·21 for maximum $\dfrac{L}{D}$. This shows an indicated air speed of 1·6 times the landing speed. As applied to an aeroplane the theorem would use the lift/drag of the complete structure and not of the wings alone, and the number 1·6 is much reduced. Near the ground the speed of most efficient flight is well below that of possible flight, but the difference becomes less at great heights. For high-speed fighting scouts the ratio of lift to drag for the wings may be only 10 instead of the best value of 20, and it becomes important to produce a wing which has a high value of lift to drag at low lift coefficients. This is the distinguishing characteristic of a good high-speed. wing, and appears to be unattainable at the same time as a high lift coefficient.

Fig. 66 (f). **Lift/Drag and Lift Coefficient.**—The remarks on Fig. 66(e) have indicated the importance of the present curve, and particular attention has been paid to the development of wing forms having a high speed value of $\dfrac{L}{D}$ at a lift coefficient of 0·1 and as high a value as possible at a lift coefficient 0·9 times as great as the maximum, the latter being important in the climbing of an aeroplane. It will thus be seen that in modern practice the maximum lift/drag of a wing is not the most important property of its form as an intrinsic merit, but only as it is associated with other properties. Equation (6) suggests that the quantity under the root sign is important as an independent variable, and this is recognised in certain reports on wing form.

Fig. 66 (g). **Drag Coefficient and Lift Coefficient.**—The diagram is convenient in its relation to a complete aeroplane, for the change from the curve for wings alone is almost solely one of position of the zero ordinate. A tangent from the new origin shows the value of the maximum lift/drag of the aeroplane and the lift coefficient at which it occurs. The diagram shows more clearly than any other that the useful range of flying positions lies within the limits 0·01 and 0·05 for drag coefficient, and that small changes of lift coefficient and therefore of indicated air speed produce large changes of drag near the critical angle. The indicated air speed at the critical angle of lift is known as the " stalling speed," and has been used in these notes as identical with " landing speed." The latter is, however, always greater than the former for reasons of control over the motion of the aeroplane at the moment of alighting.

Particular Cases of Wing Form

Effect of Change of Section (Fig. 67 and Tables 2–5).—The shape of the section of the standard model aerofoil is conveniently given by a table of the co-ordinates of points in it, the chord being taken as a standard from which to measure and the front end as origin. For two wings, R.A.F. 15 for high speed and R.A.F. 19 for high maximum lift coefficient, the co-ordinates which define their shapes are given in Table 2 below. The length of the chord is taken as unity, and all other linear measurements are given

in terms of it. It will be seen that R.A.F. 15 has a maximum height above the chord of 0·068, and this number is often called the upper surface camber
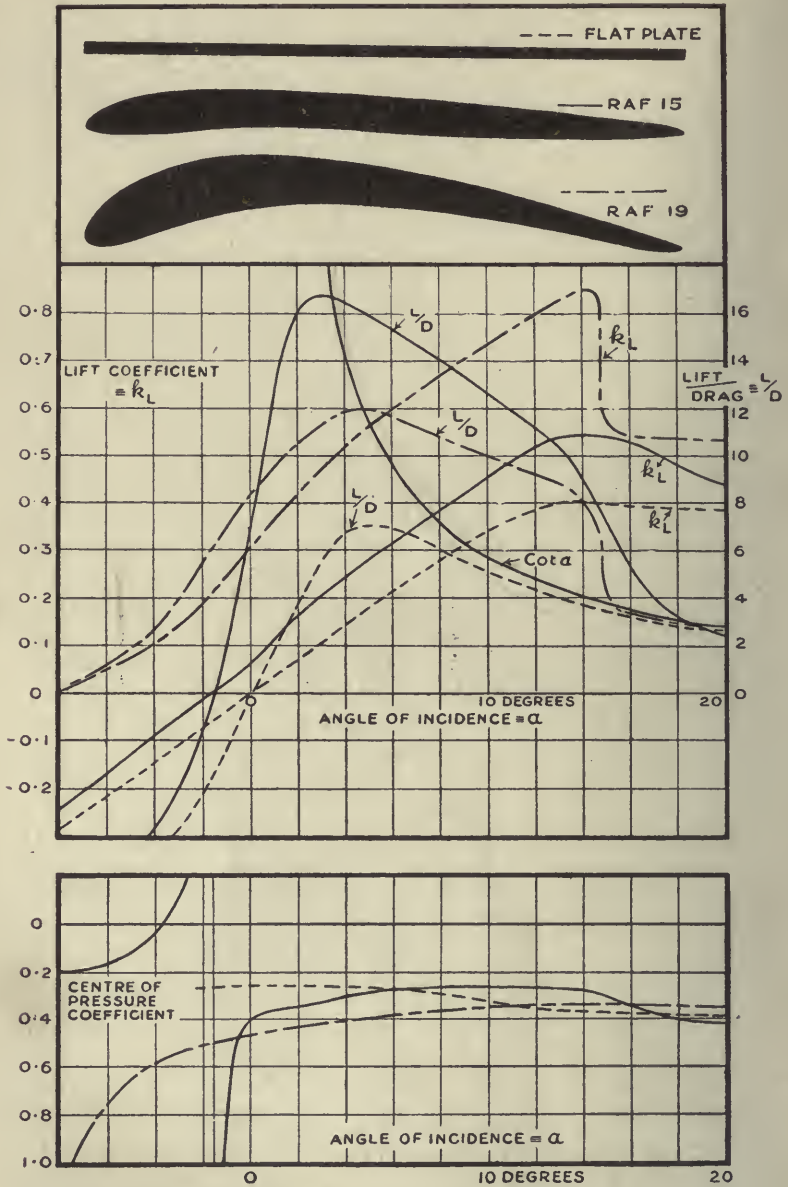
FIG. 67.—Effect of change of wing section.

for the wing section. The other wing of the table, R.A.F. 19 has an upper surface camber of 0·152, or more than twice that of R.A.F. 15, and this

difference is characteristic of the difference between high speed and high lift wings.

TABLE 2.

SHAPES OF WING SECTIONS.

Distance from leading edge.	R.A.F. 15.		R.A.F. 19.	
	Height of upper surface.	Height of lower surface.	Height of upper surface.	Height of lower surface.
0	0·013	0·013	0·012	0·012
0·01	0·027	0·008	0·034	0·003
0·02	0·035	0·005	0·051	0·001
0·03	0·041	0·003	0·065	0·000
0·04	0·045	0·002	0·076	0·000
0·05	0·047	0·001	0·085	0·001
0·06	0·052	0·001	0·093	0·003
0·08	0·057	0·000	0·107	0·008
0·12	0·063	0·001	0·127	0·021
0·16	0·066	0·003	0·140	0·034
0·22	0·068	0·006	0·150	0·054
0·30	0·067	0·008	0·152	0·069
0·40	0·065	0·008	0·147	0·075
0·50	0·062	0·006	0·134	0·072
0·60	0·056	0·002	0·117	0·062
0·70	0·048	0·000	0·095	0·050
0·80	0·040	0·001	0·071	0·034
0·90	0·029	0·003	0·043	0·017
0·95	0·023	0·005	0·026	0·008
0·98	0·017	0·006	0·015	0·002
0·99	0·015	0·007	0·011	0·000
1·00	0·010	0·010	0·006	0·006

The aerodynamic properties of these wings are compared with those of a plane which is defined by a rectangular section of which the width is one-fiftieth of the length. A less precise but more obvious definition of the shapes of the sections is given in Fig. 67 above the diagrams showing their aerodynamic properties. Tables 3–5 show data for the sections in the form in which they appear in the reports of test from an aerodynamic laboratory.

Table 3 is compiled from results given by Eiffel in his book "La Resistance de l'air et l'Aviation," and is sufficient to show variations of lift, drag and centre of pressure at all angles of incidence. The lift coefficient has a first maximum of 0·400 at 15° and a second of the same magnitude at about 30°. The drag steadily increases from a minimum at 0° angle of incidence to a maximum of 0·590 when perpendicular to the wind. It is interesting to notice that the lift at 15° is two-thirds of the maximum possible force on the plate. The lift/drag ratio of 7·0 is very small and occurs at a lift coefficient of 0·18, where it is not of the greatest use. One feature of the table is of interest as showing that the centre of pressure moves back as the angle of incidence increases, and it is this property which makes it possible to fly small mica plates. With the centre of gravity adjusted to lie at one-third of the chord by attaching lead shot to the

leading edge, thin mica sheets can be made to fly steadily across a room.

TABLE 3.

FORCES AND MOMENTS ON A FLAT PLATE.

Angle of incidence (degrees).	Lift coefficient.	Drag coefficient.	Lift/Drag	Centre of pressure coefficient.	Moment coefficient about the leading edge.
0	0·000	0·019	0·0	0·26	0·00
5	0·177	0·025	7·0	0·27	—0·05
10	0·340	0·067	5·1	0·33	—0·11
15	0·400	0·114	3·5	0·33	—0·14
20	0·388	0·144	2·7	0·39	—0·16
30	0·400	0·235	1·7	0·41	—0·19
40	0·380	0·320	1·2	0·43	—0·21
50	0·335	0·400	0·85	0·45	—0·23
60	0·275	0·475	0·58	0·47	—0·26
70	0·190	0·540	0·35	0·48	—0·28
80	0·100	0·580	0·17	0·49	—0·29
90	0·000	0·590	0·00	0·50	—0·30

Tables 4 and 5 are representative tables of wing characteristics in their best form. The intervals in angle of incidence are usually 2°, with interpolated values at small angles of incidence where the ratio of lift to drag is varying most rapidly. All the terms which occur have been defined, and the characteristics of the wings are most easily seen from the curves of Fig. 67, which was produced from the numbers in Tables 2–5.

TABLE 4.

R.A.F. 15 AEROFOIL.

Size of plane, 3″ × 18″.   Wind speed, 40 ft.-s.

Angle of incidence (degrees).	Lift coefficient.	Drag coefficient.	Lift/Drag	Centre of pressure coefficient.	Moment coefficient about leading edge.
—6	—0·170	0·0310	—5·50	0·167	+0·028
—4	—0·087	0·0156	—5·61	0·034	+0·003
—2	—0·0163	0·0099	—1·66	—0·725	—0·011
—1	+0·0173	0·0085	2·03	0·822	—0·014
0	0·057	0·0082	6·96	0·404	—0·023
1	0·107	0·0084	12·7	0·362	—0·038
2	0·164	0·0104	16·0	0·350	—0·057
3	0·203	0·0123	16·6	0·327	—0·067
4	0·242	0·0148	16·4	0·307	—0·075
6	0·312	0·0205	15·2	0·278	—0·087
8	0·387	0·0277	14·0	0·268	—0·104
10	0·454	0·0363	12·5	0·274	—0·124
12	0·519	0·0460	11·2	0·280	—0·145
14	0·538	0·0630	8·9	0·280	—0·160
16	0·530	0·100	5·3	0·341	—0·183
18	0·476	0·148	3·2	0·394	—0·197

The first noticeable feature of the lift coefficient curves is, that whilst the plate only begins to lift at a positive angle of incidence, the high speed wing R.A.F. 15 lifts at angles above $-1.5°$ and the high lift wing at $-8°$. This feature is common to all 'similar changes of upper surface camber. The surprising fact is well established that an aeroplane wing may lift with the wind directed towards the upper surface.

TABLE 5.

R.A.F. 19 AEROFOIL.

Size of plane, $3'' \times 18''$. Wind speed, 40 ft.-s.

Angle of incidence (degrees).	Lift coefficient.	Drag coefficient.	Lift / Drag	Centre of pressure coefficient.	Moment coefficient about leading edge.
-12	-0.063	0.0750	-0.83	$+0.218$	$+0.017$
-10	-0.038	0.0648	-0.59	$+0.130$	$+0.006$
$- 8$	$+0.006$	0.0541	$+0.11$	-21.04	-0.021
$- 6$	0.050	0.0550	1.11	$+0.758$	-0.034
$- 4$	0.103	0.0390	2.64	0.588	-0.059
$- 2$	0.189	0.0351	5.4	0.512	-0.096
$- 1$	0.246	0.0359	6.8	0.487	-0.120
0	0.302	0.0371	8.1	0.472	-0.142
$+ 1$	0.358	0.0381	9.4	0.449	-0.161
2	0.413	0.0396	10.4	0.434	-0.180
4	0.516	0.0438	11.8	0.412	-0.214
6	0.591	0.0506	11.7	0.387	-0.230
8	0.662	0.0617	10.7	0.369	-0.245
10	0.737	0.0740	10.0	0.355	-0.262
12	0.797	0.0865	9.2	0.348	-0.278
14	0.845	0.1012	8.3	0.341	-0.288
15	0.531	0.1420	3.74	0.339	-0.184
16	0.531	0.1515	3.52	0.339	-0.187
18	0.529	0.1715	3.08	0.343	-0.191
20	0.531	0.189	2.81	0.344	-0.194

All the lift coefficient curves show a maximum at $14°$, but the values are very different, being 0.40 for the plate, 0.54 for R.A.F. 15 and 0.84 for R.A.F. 19. This is partly due to a progressive increase in the average slope of the curves, the values being 0.035, 0.040 and 0.045, but much more to the increase of range of angle between zero lift and maximum lift coefficient. The very high lift coefficient of 0.84 given by R.A.F. 19 appears to be highly critical, and the maximum is followed by a rapid fall, so that at an angle of incidence of 20 degrees the difference between the wings is greatly reduced. At still greater angles the effects of differences of wing form tend to disappear.

The curves giving the ratio of lift to drag show a different order to the curves for lift coefficient, for the plate gives a maximum of 7, R.A.F. 15 of 16.6, and R.A.F. 19 of 12.0. It is therefore clear that there is some section which has a maximum lift to drag ratio. R.A.F. 15 is the outcome of many experiments on variation of wing section, none of which has given a higher ratio under standard conditions. As is usual in the case of variations near a maximum condition, it is possible to change the section

within moderately wide limits without producing great changes in wing characteristics.

On the same diagram as the lift to drag curves has been plotted the cotangent of the angle of incidence, as it brings out an interesting property of cambered wings. For a value of lift to drag given by a point on this curve the resultant force on the wing is normal to the chord, and both R.A.F. 14 and R.A.F. 19 have two such points. For values of lift to drag which lie below the cotangent curve the resultant force lies behind the normal to the chord, whilst the converse holds for points above the curve. It will be seen that the resultant force on the plate is always behind the normal, whereas for R.A.F. 15 an extreme value of 7°·5 ahead of the chord is shown. When a description of the pressure distribution round a wing is given, it will be seen that this forward resultant is associated with an intense suction over the forward part of the upper surface. The resultant is of course always behind the normal to the wind direction, but in R.A.F. 14 its value has a minimum of 3°·5. The value of γ shown in Fig. 65 is then very small, and it will be understood that errors of appreciable magnitude would follow from any want of knowledge of the direction of the wind relative to the wind channel balance arms. One degree of deviation would introduce an error of 28 per cent. into the drag reading, and even with great care it is difficult to make absolute measurements of minimum drag coefficient to within 5 per cent. Comparative experiments made on the same model and with the same apparatus have an accuracy much greater than this and more nearly equal to 1 per cent. Within the limits indicated wind channel observations are remarkably consistent.

The centre of pressure coefficient curves show that the wing forms R.A.F. 14 and R.A.F. 19 have unstable movements, that is, the centre of pressure moves forward as the angle of incidence increases. The plate on the other hand has the stable condition previously referred to.

Wing Characteristics for Angles of Incidence outside the Ordinary Flying Range.—In discussing some of the more complicated conditions of motion of an aeroplane knowledge is required of the properties of wings in extraordinary attitudes. Not only is steady upside-down flying possible, but backward motion occurs for short periods in the tail slide which is sometimes included in a pilot's training.

For a flat plate observations are recorded in Table 3 for a range of angles from 0° to 90°, and from the symmetry of the aerofoil these observations are sufficient for angles from 0° to 360°. The values of the lift coefficient, lift to drag ratio and centre of pressure coefficient are shown in Fig. 68 in comparison with similar curves for R.A.F. 6 wing section. The shape of the latter is shown in the figure and the detailed description in the height of contours is given in Table 6 below. The numbers apply only to the upper surface ; the small camber of the under surface is of little importance in the present connection. A modification known as R.A.F. 6a has been used on many occasions, and differs from R.A.F. 6 only in the fact that in the former the under surface is flat.

The dissymmetry of the section made it necessary to test the aerofoil

at angles of incidence over the whole range 0° to 360°, with the results
shown in Table 7 and in Fig. 68.

TABLE 6.

SHAPE OF WING SECTION R.A.F. 6A.

Height above chord.	Distance from leading edge.	Distance from trailing edge.
0·000	0·007	0·004
0·003	0·001	0·000
0·007	0·000	0·003
0·010	0·001	0·009
0·013	0·003	0·021
0·017	0·006	0·037
0·020	0·010	0·054
0·023	0·013	0·072
0·027	0·018	0·091
0·030	0·023	0·110
0·033	0·028	0·129
0·037	0·033	0·149
0·040	0·039	0·170
0·043	0·045	0·191
0·047	0·053	0·215
0·050	0·061	0·238
0·053	0·070	0·265
0·057	0·080	0·292
0·060	0·092	0·322
0·063	0·106	0·353
0·067	0·123	0·391
0·070	0·146	0·436
0·073	0·181	0·493
0·077	0·250	0·583
0·0776	0·320 max.	0·680 max.
0·0785	—	—

Above figures are expressed as fractions of chord.

Fig. 68 shows that the lift coefficient of the cambered wing section is
numerically greater than that of the plate so long as the thicker end or
normal front part is facing the wind, but the plate gives the greater lift
coefficients with the tail into the wind. The effect of camber at ordinary
flying angles is seen to be greater than elsewhere, and this is emphasized
in the lift to drag curves, where the greatest value is 16 for the wing section
and 7 for the plate. At the other peaks of the lift to drag curve the
difference is much less marked, and with the tail first the wing section is
again seen to be inferior to the plate.

For the centre of pressure coefficient both wing section and plate have
a stable movement of the centre of pressure with angle over the greater
part of the range. The unstable movement associated with cambered wings
is confined to the region of common flying angles and is a disadvantageous
property. Judging from current practice it appears that the high ratio
of lift to drag is far more important than the type of curve for centre of
pressure, as this latter can always be corrected for by the use of a tail, an
organ which would exist for control under any circumstances.

The comparison between the plate and wing section shows a very considerable degree of similarity of form for the various curves, and indicates the special character of the differences at ordinary flying angles which have been developed as the result of systematic study of the effect of variation of aerofoil section on its aerodynamic properties.

TABLE 7.

FORCES AND MOMENTS ON R.A.F. 6..

Size 2″·5 × 15″.   Wind speed, 40 ft.-s.

Angle of incidence (degrees).	Lift coefficient.	Drag coefficient.	Lift / Drag	Centre of pressure coefficient.	Moment coefficient about leading edge.
0	+0·090	0·0152	+ 5·9	0·523	−0·0472
5	+0·325	0·0210	+15·5	0·346	−0·1128
10	+0·498	0·0415	+12·0	0·305	−0·1515
15	+0·613	0·0721	+ 8·5	0·279	−0·1707
20	+0·528	0·1712	+ 3·1	0·368	−0·2025
30	+0·472	0·273	+ 1·73	0·389	−0·2117
40	+0·453	0·395	+ 1·15	0·408	−0·2450
50	+0·398	0·465	+ 0·86	0·422	−0·2550
60	+0·327	0·557	+ 0·59	0·434	−0·2707
70	+0·232	0·632	+ 0·37	0·458	−0·3055
80	+0·117	0·679	+ 0·17	0·469	−0 3265
90	+0·000	0·701	0·0	—	—
100	−0·119	0·674	− 0·18	0·500	−0·3375
110	−0·268	0·625	− 0·43	0·513	−0·3460
120	−0·318	0·556	− 0·57	0·526	−0·3380
130	−0·388	0·466	− 0·83	0·545	−0·3300
140	−0·469	0·397	− 1·19	0·552	−0·3370
150	−0·479	0·278	− 1·73	0·567	−0·3130
160	−0·478	0·1700	− 2·80	0·575	−0·2920
170	−0·425	0·0505	− 8·4	0·649	−0·2760
180	−0·055	0·0172	− 3·1	0·089	−0·0049
190	+0·311	0·0812	+3·83	0·702	+0·2185
200	+0·320	0·1588	+2·04	0·662	+0·2185
210	+0·351	0·260	+1·35	0·654	+0·2840
220	+0·349	0·360	+0·97	0·638	+0·3180
230	+0·290	0·426	+0·68	0·615	+0·3140
240	+0·228	0·497	+0·46	0·598	+0·3255
250	+0·154	0·557	+0·28	0·579	+0·3290
260	+0·067	0·608	+0·11	0·545	+0·3310
270	−0·028	0·618	−0·05	0·528	+0·3145
280	−0·128	0·610	−0·21	0·478	+0·3035
290	−0·211	0·598	−0·35	0·445	+0·2715
300	−0·273	0·497	−0·55	0·428	+0·2414
310	−0·318	0·409	−0·78	0·397	+0·2047
320	−0·369	0·343	−1·08	0·377	+0·1890
330	−0·336	0·243	−1·39	0·378	+0·1555
340	−0·274	0·1395	−1·98	0·340	+0·1033
345	−0·245	0·1005	−2·44	0·330	+0·0866
350	−0·219	0·0649	−3·38	0·298	+0·0673
355	−0·111	0·0308	−3·60	0·080	+0·0091
360	+0·090	0·0152	+5·9	0·522	−0·0472

Wing Characteristics as dependent on Upper Surface Camber.—In the early days of aeronautics at the National Physical Laboratory a series of
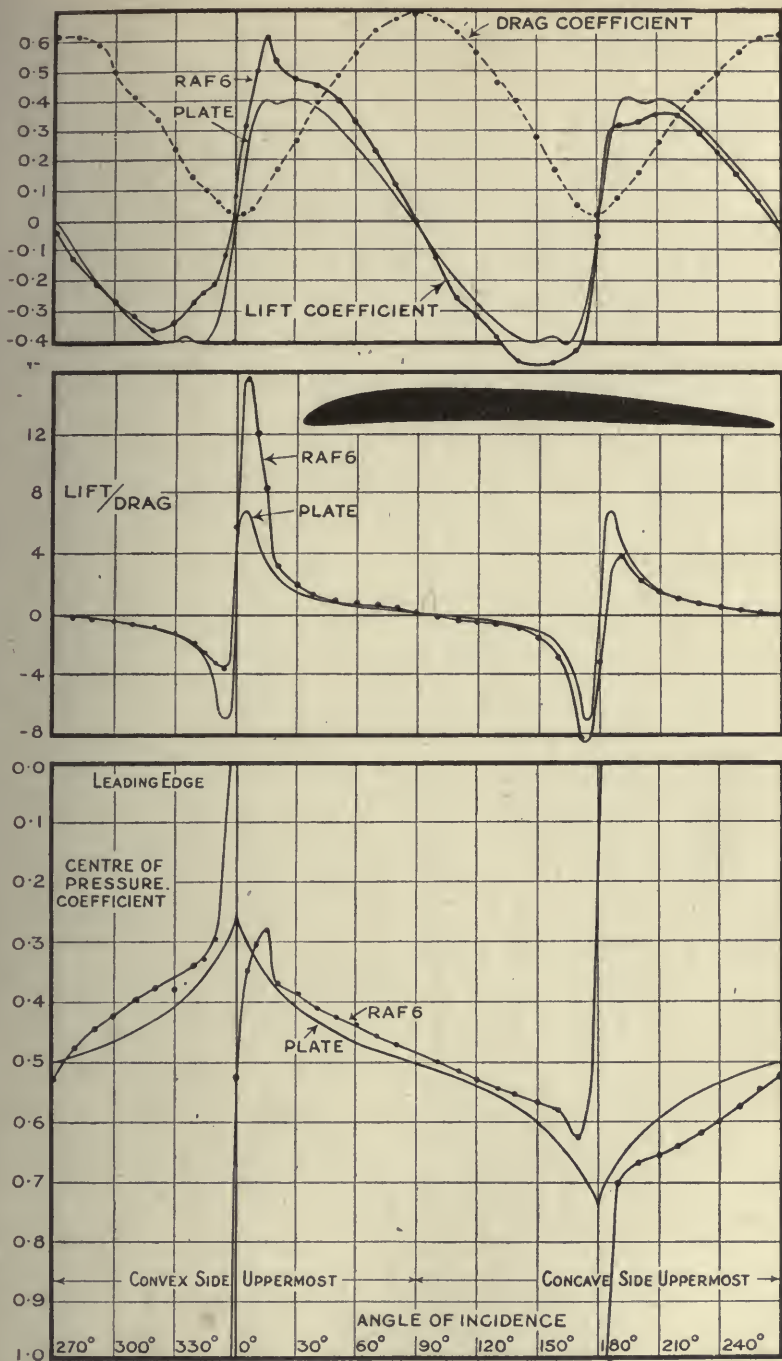
Fig. 68.—Wing characteristics at all possible angles of incidence.

experiments on the variation of upper surface camber and upper surface shape was carried out and laid the foundation for a reasoned choice of wing section. Knowledge of methods of tests and particularly the discovery of an effect on wing characteristics of size and wind speed have reduced their value, and other examples are now chosen from various somewhat unconnected sources. No up-to-date equivalent of these early experiments exists, but it is to be hoped that our National Institution will ultimately undertake such experiments with all the refinements of modern methods. Until this series appears the results deduced from the early experiments may be accepted as qualitatively correct, and, although not quoted directly, have been used to guide the choice of examples and to give weight to the deductions drawn from the study of special cases.

Aerofoils having large upper surface camber are used only in the design of airscrews, and on pages 304 and 305 will be found details of the shapes of a number of sections and the corresponding tables of the aerodynamic properties. In most of these sections the under surface was flat. The general conclusion may be drawn that a fall in the value of the maximum lift to drag ratio is produced by thickening a wing to more than 7 or 8 per cent. of its chord, and that the fall is great when the thickness reaches 20 per cent. of the chord. The exact shape of the upper surface does not appear to be very important, but a series of experiments at a camber ratio of 0·10 indicated an advantage in having the maximum ordinate of the section in the neighbourhood of one-third of the chord from the leading edge. The position of the maximum ordinate was found to have a marked effect on the breakdown of flow at the critical angle of lift, but in the light of modern experimental information it appears that these differences may be largely reduced in a larger model tested at a higher speed. A very similar series of changes to those now under review occurred in the test of an airscrew section at different speeds and is illustrated and described in the chapter on Dynamical Similarity. Further reference to the effect of size of model and the speed of the wind during the test is given later in this chapter.

Changes of Lower Surface Camber of an Aerofoil.—It has been the general experience that changes of lower surface camber of an aerofoil are of less importance in their effect on wing characteristics than are those of the upper surface. Wings rarely have a convex lower surface, but for sections of airscrews a convex under surface is not unusual. In Table 8 and Fig. 69 are shown the effects of variation of R.A.F. 6A by adding a convex lower surface, the ordinates of which were proportional to those of the upper surface. The range from R.A.F. 6A to a strut form was covered in three steps in which the ordinates of the under side were one-third, two-thirds and equal to those of the upper surface. Inset in Fig. 69 are illustrations of the aerofoil form.

In this series the chord was taken in all cases as the under side of the original wing, and the table shows the gradual elimination of the lift at negative angles of incidence as the under-surface camber grows to that of the upper surface. A distinct fall in maximum lift coefficient is observable without corresponding change of angle of incidence at which it occurs.

The minimum drag coefficient is seen to occur with a convex lower surface, but not with the symmetrical section. Incidentally it may be noted that a strut may have a lift-to-drag ratio of 13.
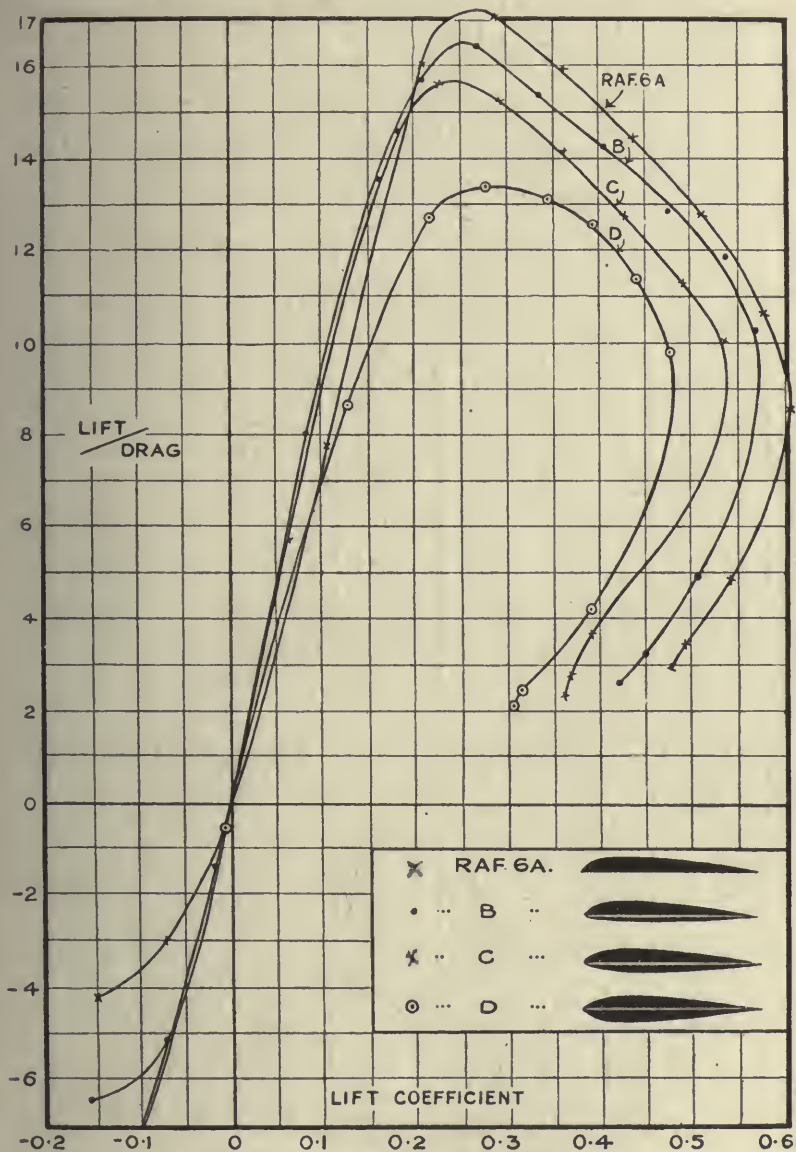
FIG. 69.—Variation of lower surface camber.

The important deductions from Table 8 are more readily obtained from Fig. 69, which shows the ratio of lift to drag as dependent on lift coefficient. A lower surface camber of one-third of that of the upper surface is very large for a wing, but on a high-speed aeroplane the gain

of 20 per cent. in lift to drag at a lift coefficient of 0·1 might more than compensate for the smaller proportionate loss at larger values of the lift coefficient. It may be observed that there is a limit to the amount of under-surface camber which could be used with advantage, and reference to the wing form of R.A.F. 15 suggests that the advantages can be attained by a slight convexity at the leading edge only.

TABLE 8.

EFFECT OF VARIATION OF BOTTOM CAMBER OF AEROFOIL, R.A.F. 6A.

Aerofoil, 3″ × 18″.   Wind speed, 40 ft.-s.

Angle (degrees).	Lift coefficient.				Drag coefficient.			
	A	B	C	D	A	B	C	D
−6	−0·149	−0·160	−0·216	−0·283	0·0348	0·0248	0·0178	0·0221
−4	−0·068	−0·101	−0·151	−0·218	0·0224	0·0170	0·0142	0·0184
−2	+0·0126	−0·017	−0·072	−0·131	0·0164	0·0131	0·0117	0·0153
0	+0·106	+0·083	+0·064	−0·006	0·0137	0·0106	0·0110	0·0133
2	+0·210	+0·183	+0·162	+0·127	0·0131	0·0126	0·0119	0·0146
4	+0·288	+0·258	+0·228	+0·218	0·0168	0·0158	0·0145	0·0172
6	+0·362	+0·333	+0·295	+0·280	0·0226	0·0216	0·0193	0·0208
8	+0·437	+0·406	+0·363	+0·346	0·0301	0·0284	0·0255	0·0264
10	+0·508	+0·477	+0·428	+0·395	0·0396	0·0370	0·0335	0·0314
12	+0·575	+0·536	+0·489	+0·441	0·0536	0·0450	0·0432	0·0388
14	+0·604	+0·565	+0·536	+0·476	0·0630	0·0553	0·0528	0·0485
16	+0·542	+0·511	+0·392	+0·392	0·110	0·1032	0·1044	0·0923
18	+0·491	+0·450	+0·367	+0·317	0·141	0·1386	0·130	0·129
20	+0·479	+0·422	+0·361	+0·306	0·164	0·1598	0·152	0·147

Angle (degrees).	$\frac{\text{Lift}}{\text{Drag}}$				Moment coefficient about leading edge.			
	A	B	C	D	A	B	C	D
−6	−4·28	− 6·47	−12·1	−12·8	+0·020	+0·022	+0·049	+0·081
−4	−3·02	− 5·9	−10·6	−11·9	+0·008	+0·010	+0·036	+0·067
−2	+0·77	− 1·3	− 5·1	− 8·6	−0·029	−0·011	+0·016	+0·043
0	7·77	+ 8·0	+ 5·8	− 0·49	−0·055	−0·043	−0·031	−0·007
2	16·0	14·6	13·6	+ 8·7	−0·084	−0·069	−0·068	−0·044
4	17·1	16·4	15·7	12·7	−0·102	−0·086	−0·072	−0·068
6	16·0	15·4	15·3	13·4	−0·118	−0·102	−0·085	−0·081
8	14·5	14·3	14·2	13·1	−0·136	−0·120	−0·101	−0·094
10	12·8	12·9	12·8	12·6	−0·154	−0·135	−0·115	−0·100
12	10·7	11·9	11·3	11·4	−0·171	−0·147	−0·130	−0·107
14	8·70	10·3	10·1	9·8	−0·184	−0·153	−0·139	−0·112
16	4·9	4·9	3·7	4·3	−0·159	−0·164	−0·128	−0·104
18	3·5	3·3	2·8	2·5	−0·129	−0·170	−0·133	−0·111
20	2·9	2·6	2·4	2·1	−0·122	−0·167	−0·138	−0·114

Camber of upper surfaces of A, B, C and D was that of R.A.F. 6A.
Ordinates of lower surface of A = 0, i.e. flat lower surface.
  ,,   ,,   ,,   B = ½ × ordinates of upper surface of R.A.F. 6A. convex.
  ,,   ,,   ,,   C = ⅔ ×   ,,   ,,   ,,   ,,   ,,
  ,,   ,,   ,,   D = 1 ×   ,,   ,,   ,,   ,,   ,

Changes of Section arising from the Sag of the Fabric Covering of an Aeroplane Wing.—The shape of an aeroplane wing is determined primarily by a number of ribs made carefully to template, but spaced some 12 to 15 ins. apart on a small aeroplane.   These ribs are fixed to the main spars, and over them is stretched a linen fabric in which a considerable tension is produced by doping with a varnish which contracts on drying.   On the upper surface the wing shape is affected by light former ribs from the leading edge to the front spar.   Fig. 1, Chapter I., shows the appearance of a finished wing, whilst Fig. 70 shows the contours measured in a particular instance.   From the measurements on a wing a model was made with the full variations of section represented, and was tested in a wind channel.
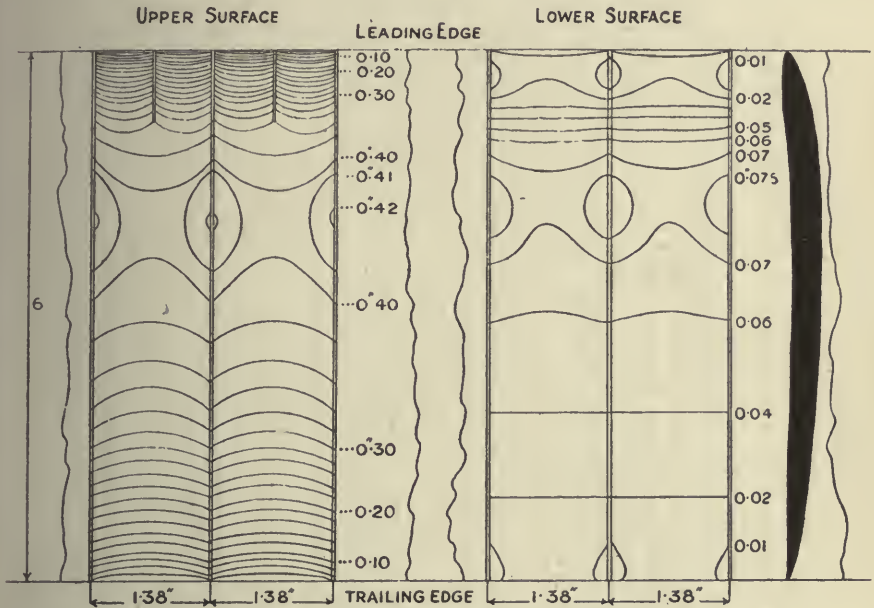
FIG. 70.—Contours of a fabric-covered wing.

After the first test the depressions were filled with wax, and a standard plane of uniform section resulted on which duplicate tests were made. Table 9 gives the results of both tests.

It is not necessary to plot the results in order to be able to see that the effect of sag in the fabric of a wing in modifying the aerodynamic characteristics of this wing is small at all angles of incidence.   The high ratio of lift to drag is partly due to the large model, which is twice that previously used in illustration.

Aspect Ratio, and its Effect on Lift and Drag.—The aerodynamic characteristics of an aerofoil are affected by aspect ratio to an appreciable extent, but the number of experiments is small owing to the fact that the length of a wing is fixed by other considerations than wing efficiency.   One of the more complete series of experiments has been used to prepare

Fig. 71 ; in the upper diagram, lift coefficient is shown as dependent on angle of incidence, and both the slope and the maximum are increased by an increase of aspect ratio. These changes get more marked at smaller aspect ratios and less marked at higher values, although an effect can still be found when the wing is 15 times as long as its chord. The changes resulting from change of aspect ratio are most strikingly shown in the ratio of lift to drag, the maximum value of which rises from 10 at an aspect ratio of 3 to 15 for an aspect ratio of 7 and probably 20 for an aspect ratio of 15. The effect at low lift coefficients is small, and aspect ratio has no appreciable influence on the choice of section for a high-speed wing.

TABLE 9.

COMPARISON BETWEEN THE LIFT AND DRAG OF AN AEROFOIL OF UNIFORM SECTION (R.A.F. 14), AND OF AN AEROFOIL SUITABLY GROOVED TO REPRESENT THE SAG OF THE FABRIC OF AN ACTUAL WING.

Aerofoil, 6″ × 36″. Wind speed, 40 ft.-s.

Angle of incidence (degrees).	R.A.F. 14 section.			R.A.F. 14 modified.			Distance of C.P. from nose as a fraction of the chord.
	Lift coefficient (abs.).	Drag coefficient (abs.).	$\frac{L}{D}$	Lift coefficient (abs.).	Drag coefficient (abs.).	$\frac{L}{D}$	
− 6	−0·162	0·0363	−4·45	−0·163	0·0354	−4·62	+0·178
− 4	−0·066	0·0230	−2·89	−0·0682	0·0225	−3·04	−0·144
− 2	+0·037	0·0133	+2·77	+0·0388	0·0125	+3·10	1·15
0	0·137	0·0096	14·30	0·134	0·0094	14·3	0·52
+ 2	0·214	0·0104	20·55	0·215	0·0102	21·1	0·413
3	0·249	0·0122	20·40	0·249	0·0120	20·7	—
4	0·284	0·0144	19·8	0·284	0·0143	19·8	0·37
6	0·356	0·0200	17·8	0·356	0·0199	17·8	0·33
8	0·423	0·0270	15·7	0·419	0·0270	15·5	0·316
10	0·485	0·0354	13·7	0·474	0·0360	13·1	0·297
12	0·521	0·0462	11·3	0·510	0·0484	10·54	0·288
14	0·534	0·0617	8·65	0·536	0·0753	7·12	0·290
15	0·544	0·0857	6·35	0·545	0·0957	5·68	—
16	0·542	0·1104	4·90	0·544	0·1140	4·76	0·324
18	0·535	0·1420	3·76	0·535	0·1475	3·63	0·365
20	0·504	0·1655	3·04	0·503	0·1720	2·92	—

Changes of Wing Form which have Little Effect on the Aerodynamic Properties.—The wings of aeroplanes are always rounded to some extent, and it does not appear that the exact form matters. The difference between any reasonable rounding and a square tip accounts for an increase of 2 to 5 per cent. on the maximum value of the lift to drag ratio and an inappreciable change of lift coefficient at any angle.

A dihedral angle less than 10° appears to have no measurable effect on lift, drag or centre of pressure. Its importance arises in a totally different connection, a dihedral angle being effective in producing a corrective rolling moment when an aeroplane is overbanked.

A similar conclusion as to absence of effect is reached for variations of sweepback up to 20°. This type of wing modification is not very common,

but may be resorted to in order to bring the centre of gravity of the aeroplane into correct relation to the wings. The requirements of balance and stability do not here conflict with those of performance.
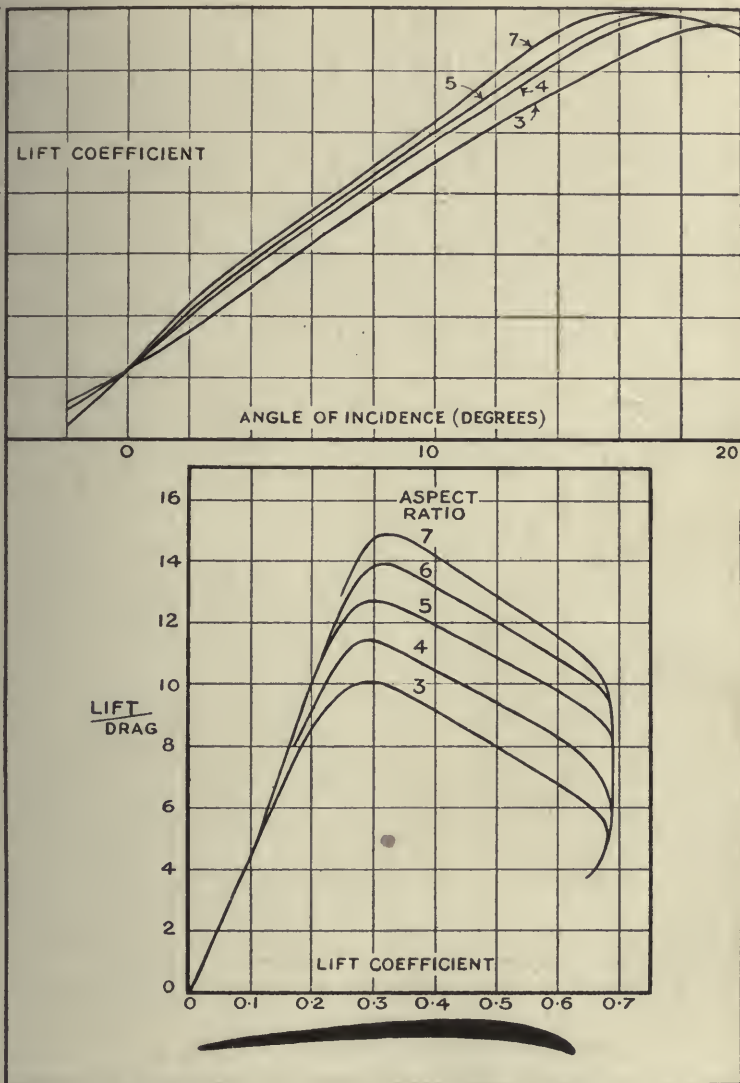
Fig. 71.—Effect of aspect ratio.

Effect of the Speed of Test on the Lift and Drag of an Aerofoil.—Fig. 72 shows the lift coefficient as a function of angle of incidence and speed, and the lift to drag ratio as dependent on lift coefficient and speed, for an aerofoil of section R.A.F. 6a. The model had a chord of 6 inches, and was tested at speeds of 20, 40 and 60 ft.-s., with the results illustrated. Over

a range of angle of incidence of 2° to 10° the effect of speed on lift coefficient
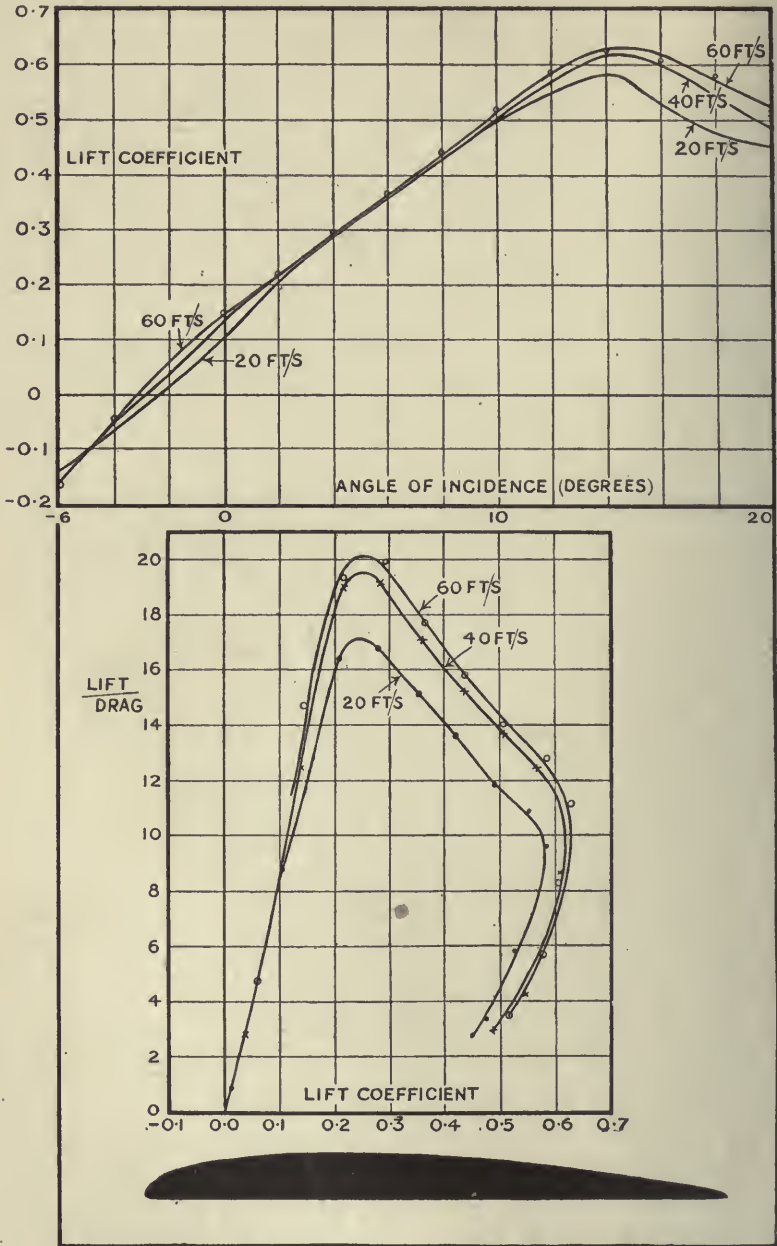
FIG. 72.—Effect of speed of test.

is not important, but appreciable changes occur at both smaller and larger angles. There is a tendency towards an asymptotic value at high speeds,

A series of five models shows for envelope forms how the drag coefficients vary with the fineness ratio, or length to diameter ratio. A similar series of tests for strut forms has already been given in which the drag coefficient on projected area was roughly 0·042. On the envelope forms the coefficient is appreciably less and may fall to half the value just quoted. The forms tested were solids of revolution of which the front part was ellipsoidal; in all cases the maximum diameter was made to occur at one-third of the total length from the nose. The shapes of the longitudinal sections are shown in Fig. 100, and have numbers attached to them which are equal to their fineness ratio. The observations made are recorded in Table 41 and need a little explanation. It is pointed out in the chapter on dynamical similarity that neither the size of the model nor the speed of the wind has a fundamental character in the specification of resistance coefficients, but that the product of the two is the determining variable. In accordance with that chapter, therefore, the first column of Table 41 shows the product of the wind speed in feet per second and the diameter of the model in feet. Further, two drag coefficients denoted respectively by k_D and C have been used for each model, the former giving a direct comparison with other data on the basis of projected area, and the latter a coefficient of special utility in airship design which is closely related to the gross lift.

TABLE 41.

RESISTANCE COEFFICIENTS OF AIRSHIP ENVELOPE FORMS.

Vd (ft.²-s.).	No. 6.		No. 4·5.		No. 4.		No. 3·5.		No. 3.	
	k_D	C	k_D	C	k_D	C	k_D	C	k_D	C
8·7	0·0351	0·0142	0·0313	0·0149	0·0319	0·0166	0·0318	0·0182	0·0323	0·0207
9·8	0·0334	0·0135	0·0305	0·0145	0·0298	0·0155	0·0298	0·0170	0·0301	0·0192
11·7	0·0327	0·0132	0·0290	0·0138	0·0282	0·0147	0·0292	0·0167	0·0287	0·0184
13·7	0·0323	0·0130	0·0287	0·0136	0·0272	0·0142	0·0276	0·0155	0·0263	0·0168
15·7	0·0322	0·0130	0·0280	0·0133	0·0262	0·0136	0·0262	0·0149	0·0253	0·0161
17·7	0·0320	0·0129	0·0269	0·0128	0·0252	0·0131	0·0252	0·0143	0·0238	0·0152
19·7	0·0330	0·0133	0·0269	0·0128	0·0254	0·0132	0·0249	0·0142	0·0238	0·0152
21·5	0·0331	0·0133	0·0265	0·0126	0·0250	0·0130	0·0242	0·0138	0·0232	0·0148
23·6	0·0337	0·0136	0·0272	0·0129	0·0247	0·0129	0·0246	0·0140	0·0230	0·0147
25·4	0·0342	0·0138	0·0270	0·0128	0·0255	0·0132	0·0244	0·0139	0·0228	0·0145
27·5	0·0344	0·0139	0·0271	0·0129	0·0251	0·0131	0·0245	0·0139	0·0228	0·0146
29·3	0·0346	0·0139	0·0277	0·0132	0·0249	0·0130	0·0245	0·0139	0·0224	0·0143
31·3	0·0348	0·0142	0·0279	0·0132	0·0251	0·0130	0·0245	0·0140	0·0224	0·0143

The coefficients k_D and C are defined by the equations

$$\text{Drag} = k_D \rho V^2 . \frac{\pi d^2}{4} \qquad . \qquad . \qquad . \qquad . \qquad . \quad (20)$$

and

$$\text{drag} = C \rho V^2 \, (\text{volume})^{\frac{2}{3}} \qquad . \qquad . \qquad . \qquad . \quad (21)$$

where d is the maximum diameter of the envelope.

An examination of the columns of Table 41 shows some curious changes of coefficient which are perhaps more readily appreciated from Fig. 101, where the values of k_D are plotted on a base of Vd. For the longest model the curve first shows a fall to a minimum, followed by a rise to its initial value. For the model of fineness ratio 4·5 the minimum occurs later, and it is possible that the three short models all have minima outside the range of the diagram. It is clearly impossible to produce these curves with any degree of certainty. In Chapter II. it was deduced that for a rigid airship the full-scale trials give to C a value of 0·016, and for a non-rigid, 0·03.
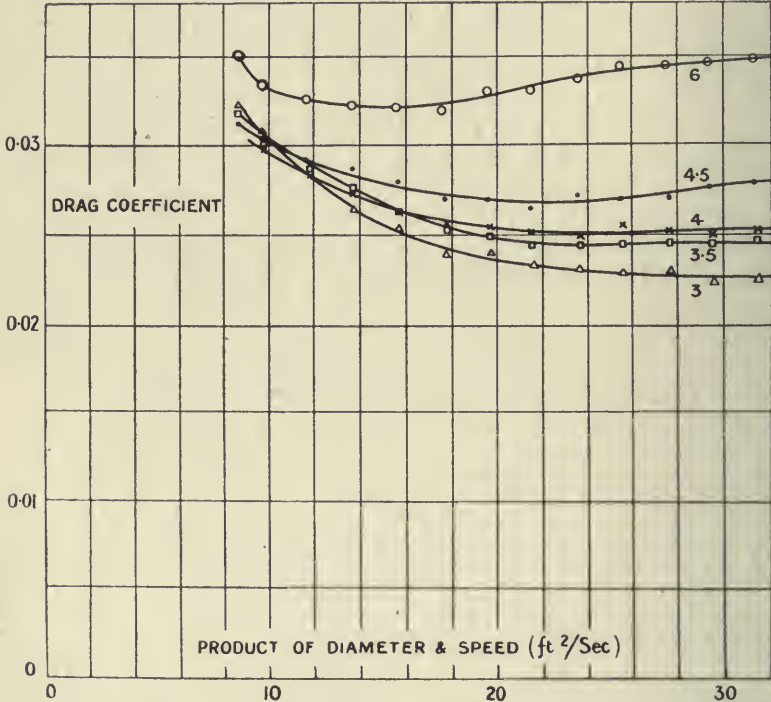
Fig. 101.—Resistance of airship envelope models.

These figures contain the allowance for cars and rigging, and do not indicate any marked departure from the figure of 0·013 given above for the envelope alone. The comparison is very rough, but accurate full-scale experiments of a nature similar to those on models have yet to be made.

It will be noticed from Table 41 that whilst the drag coefficient calculated on maximum projected area falls with decrease of fineness ratio, the coefficient C which compares the forms on unit gross lift is less variable and has its least values for the longer models. The importance of the second drag coefficient " C " is then seen to be considerable as an aid to the choice of envelope form.

Complete Model of a Non-rigid Airship.—A complete model, illustrated

in Fig. 102, was made of one of the smaller British non-rigid airships, and the

ELEVATOR PLANE

RUDDER PLANE

ELEVATOR PLANE
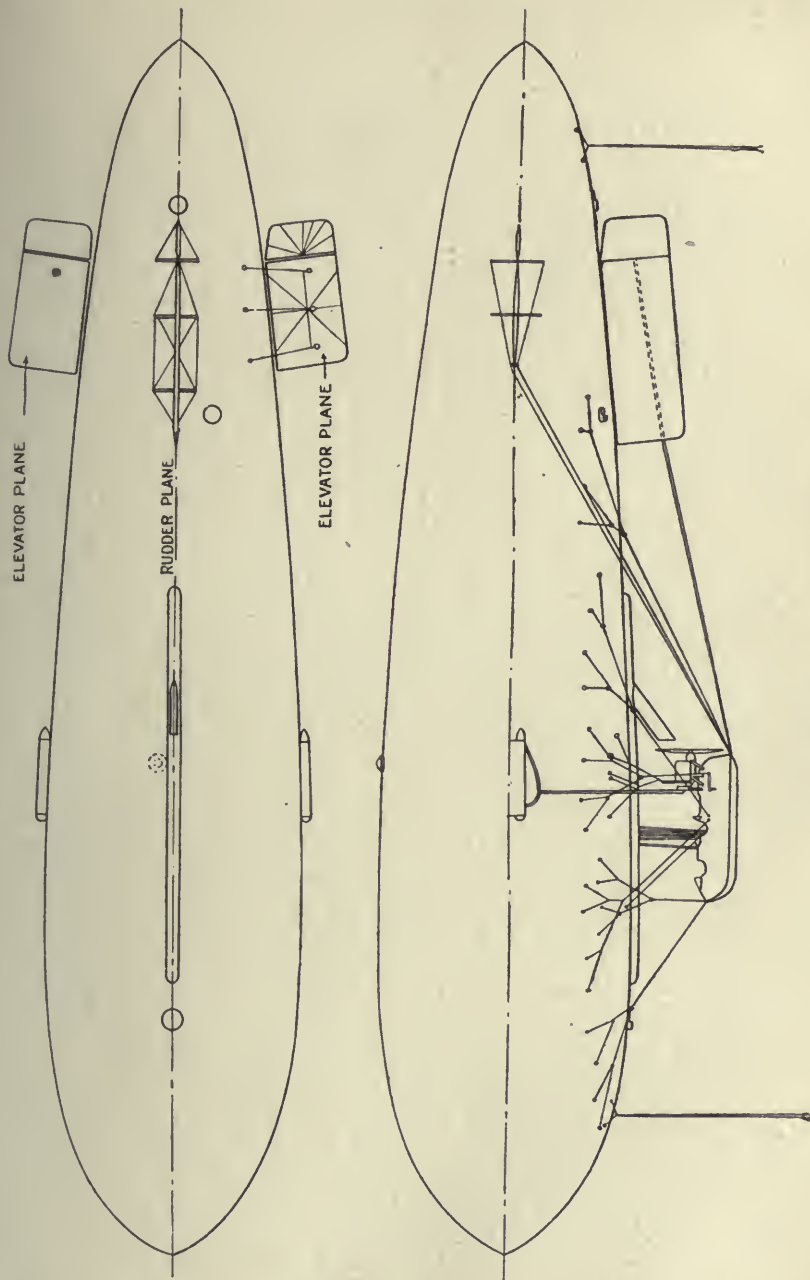
FIG. 102.—Model of a non-rigid airship.

analysis of the total drag to show its dependence on main parts was carried out.   The results of the observation are shown in Table 42.

TABLE 42.

RESISTANCE OF NON-RIGID AIRSHIP.

Drag (lbs.).   Diameter of envelope, 6·65 ins.   Wind speed, 40 ft.-s.

	Description of Model.	Angle of incidence (degrees).					
		0°	4°	8°	12°	16°	20°
a	Complete airship	0·102	0·109	0·132	0·170	0·225	0·300
b	Rigging cables removed . .	0·081	—	—	—	—	—
c	Without car or rigging cables	0·066	0·073	0·092	0·127	0·187	0·258
d	Without car, rigging cables or rudder plane . . .	0·052	0·058	0·078	0·115	0·171	0·234
e	Without car, rigging cables or elevator planes . . .	0·051	0·054	0·061	0·077	0·099	0·129
f	Envelope alone	0·035	0·036	0·041	0·054	0·074	0·101
g	Main rigging cables . . .	0·021	0·021	0·021	0·021	0·021	0·021
h	Car alone	0·016	0·016	0·016	0·016	0·016	0·016
i	Rudder plane alone . . .	0·012	0·012	0·011	0·011	0·012	0·012
j	Elevator planes alone . .	0·017	0·017	0·022	0·032	0·048	0·070
k	Airship drag by addition of parts	0·101	0·102	0·111	0·134	0·171	0·220

Each column of the table shows the drag on the model and its parts in lbs. at a wind speed of 40 ft.-s., the maximum diameter of the model being 6·65 inches. The rows a—f give the result of removing parts successively from the complete model, whilst rows f—j refer to the resistances of the parts separately. At an angle of incidence of 0°, that is with the airship travelling along the axis of symmetry of its envelope, the total resistance is nearly three times that of the envelope alone. From the further figures in the column it will be seen that the difference is almost equally distributed between the rigging cables (g), the car (h), the rudder plane (i) and the elevator plane (j). The resistance of the whole model is very closely equal to that estimated by the addition of parts, the figures being 0·102 as measured and 0·101 as found by addition. The agreement between direct observation and computation from parts is less satisfactory at large angles of incidence, an observed figure of 0·300 comparing with the much lower figure of 0·220. The difference is probably connected with the influence of the rudder and elevator fins in producing a more marked deviation from streamline form than the inclined envelope alone.

Drag, Lift and Pitching Moment on a Rigid Airship.—The form of the airship is shown in Fig. 103, and the model to $\frac{1}{20}$th scale had a maximum diameter of 7·87 inches. Forces are given in lbs. on the model at 40 ft.-s., whilst moments are given in lbs.-ft. Apart from any scale effect, application to full scale is made by increasing the forces in proportion to the square of the product of the scale and speed, whilst for moments the square of the speed still remains, but the third power of the scale is required. At a value of Vd equal to 50, V being the velocity in feet per second and d the diameter in feet, the partition of the resistance was measured as in Table 43.

It was noticeable that the variation of resistance coefficient " C " for the complete model with speed of test was much less marked than that of the envelope alone, the coefficient ranging from 0·0195 to 0·0210 for a range of Vd of 15 to 50, whilst for the envelope the change was 0·0096 to 0·0131.

TABLE 43. Value of the drag coefficient " C."

Complete model	.	.	.	.	0·0207
Envelope alone	.	.	.	.	0·0131
Fins and controls	.	.	.	.	0·0014
Four cars	.	.	.	.	0·0038
Airscrew structure	.	.	.	.	0·0024

In Table 44 are collected the results of observations on the model airship for a range of angle of incidence −20° to +20°, the lift and pitching moment as well as the drag being measured. For comparison, the value of the pitching moment on the envelope alone has been added. A further table shows the variation of pitching moment due to the use of the elevators, and the salient features of the two tables are illustrated in Fig. 104 (a) and (b).

Angle of incidence has the usual conventional meaning, a positive value indicating that the nose of the airship is up whilst the motion is horizontal. A positive inclination of the elevators increases their local angle of incidence and clearly tends to put the nose of the airship down.

Table 44 indicates a marked increase of resistance due to an inclination of 10° of the axis of the airship to the relative wind, but a somewhat more remarkable fact is the magnitude of the lift, which may be 2·5 times as great as the drag at the same angle of incidence.

The column of pitching moment shows a feature common to all types of airship in the absence of a righting moment at small angles of incidence. It does not follow that the airship is therefore unstable, since there is a
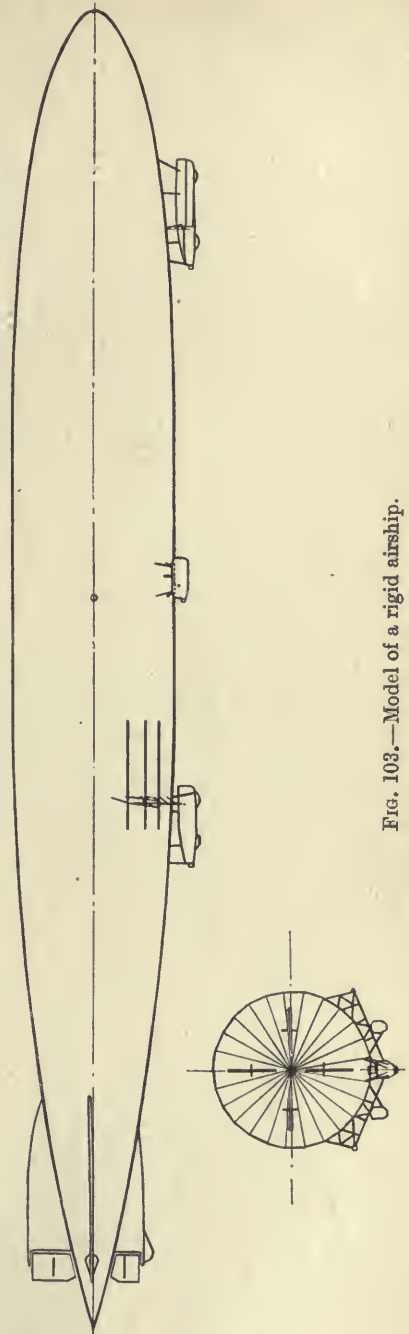
FIG. 103.—Model of a rigid airship.

further pitching moment due to the distribution of weight ; moreover, it will be found that the criterion of longitudinal stability of an airship differs appreciably from that of the existence or otherwise of a righting moment.

TABLE 44.

DRAG, LIFT AND PITCHING MOMENT ON A MODEL OF A RIGID AIRSHIP.

Maximum diameter, 7·87 ins.   Wind speed, 40 ft.-s.

Angle of incidence (degrees).	Drag (lbs.).	Lift (lbs.).	Pitching moment (lbs.-ft.).	Pitching moment envelope alone (lbs.-ft.).
−20	0·267	−0·647	−0·180	−1·055
−16	0·173	−0·459	−0·238	−0·868
−12	0·119	−0·291	−0·274	−0·698
− 8	0·087	−0·159	−0·256	−0·490
− 4	0·079	−0·051	−0·178	−0·256
0	0·083	+0·019	−0·008	0
4	0·098	0·112	+0·146	0·256
8	0·130	0·240	0·220	0·490
12	0·196	0·418	0·216	0·698
16	0·301	0·621	0·180	0·868
20	0·459	0·861	0·102	1·055

At small angles of incidence the indication of Table 44 is that the elevator fins and elevators neutralise only one-third of the couple on the envelope alone, but at greater angles, where the fin is in less disturbed air, more than 85 per cent. is neutralised.   A position of equilibrium which is stable would exist at an inclination of about 35° to the relative wind.

TABLE 45.

PITCHING MOMENT ON A RIGID AIRSHIP MODEL DUE TO THE ELEVATORS.

(Lbs.-ft. at 40 ft.-s.).

Angle of incidence (deg.).	Angle of elevator (degrees).								
	−20	−15	−10	−5	0	5	10	15	20
−15	+0·004	−0·033	−0·095	−0·154	−0·250	−0·315	−0·396	−0·462	−0·505
−10	−0·020	−0·055	−0·134	−0·178	−0·270	−0·328	−0·421	−0·459	−0·520
− 8	−0·009	−0·046	−0·119	−0·174	−0·257	−0·315	−0·378	−0·439	−0·486
− 6	+0·013	−0 029	−0·102	−0·146	−0·226	−0·282	−0·341	−0·390	−0·445
− 4	0·037	+0·002	−0·066	−0·106	−0·178	−0·227	−0·289	−0·333	−0·372
− 2	0·078	0·048	−0·013	−0·044	−0·104	−0·152	−0·202	−0·247	−0·280
0	0·154	0·122	+0·076	+0·039	−0·008	−0·060	−0·123	−0·156	−0·185
2	0·243	0·218	0·164	0·130	+0·097	+0·027	−0·020	−0·083	−0·103
4	0·312	0·278	0·227	0·194	0·146	0·093	+0·040	−0·015	−0·044
6	0·370	0·338	0·270	0·240	0·190	0·133	0·070	+0·009	−0·020
8	0·405	0·364	0·314	0·270	0·220	0·165	0·096	0·028	+0·024
10	0·432	0·392	0·334	0·281	0·225	0·163	0·085	0·027	+0·011
15	0·442	0·381	0·329	0·268	0·192	0·119	0·052	0·009	−0·038
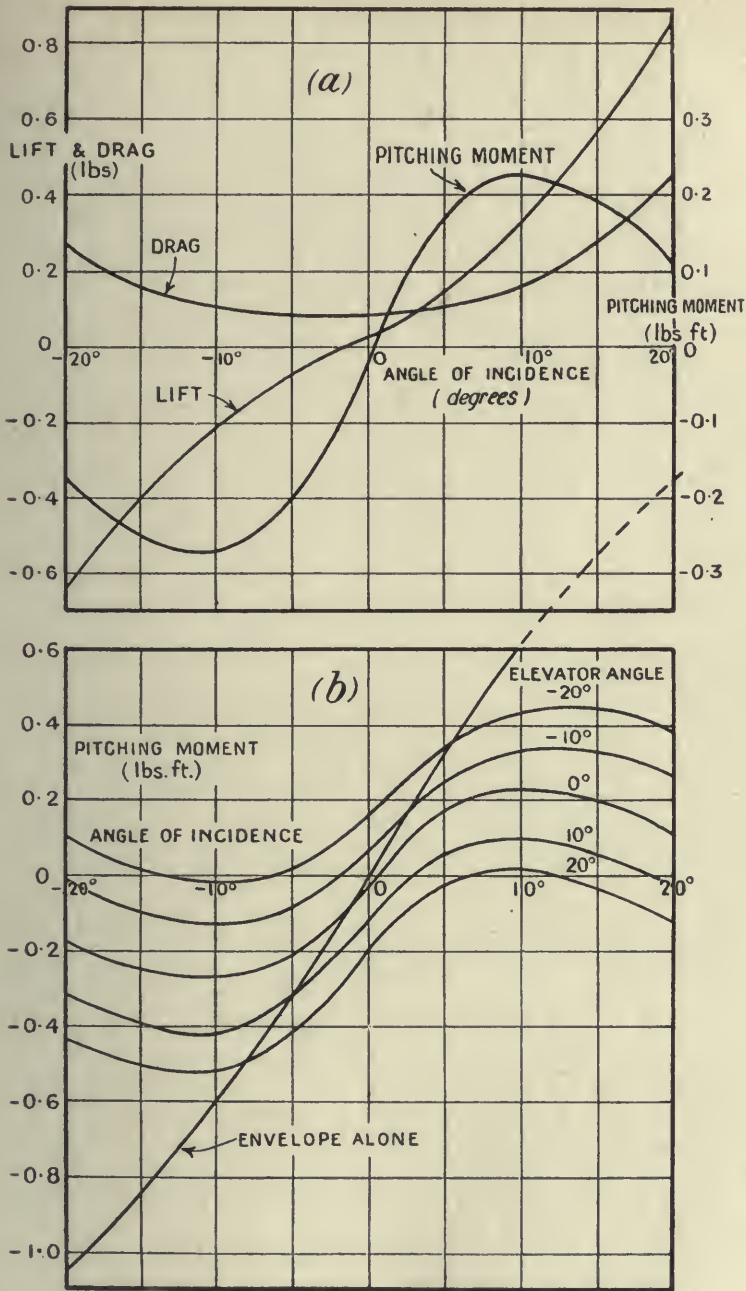
FIG. 104.—Forces and moments on a model of a rigid airship.

Fig. 104 (*a*) shows the pitching moment on the complete model as dependent on angle of incidence The rapid change at small angles of incidence is followed by a falling off to a maximum at 10° and a further fall at 20°. The lower diagram, Fig. 104 (*b*), shows how the couple which can be applied by the elevators compares with that on the airship. It appears that at an angle of 20° the maximum moment can just be overcome by the elevators, and that a gust which lifts the nose to 10° will require an elevator angle of that amount to neutralise its effect. It is quite possible that most airships are unstable to some slight degree but are all controllable, at low speeds with ease and at high speeds with some difficulty. The attachment of fins of area requisite to produce a righting moment at small angles of incidence is seen to present a problem of a serious engineering character, and the tendency is therefore to some sacrifice of aerodynamic advantage.

Pressure Distribution round an Airship Envelope.—A drawing of the

PRESSURE DISTRIBUTION
ON MODEL AIRSHIP.
Axis along the Wind

$\frac{p}{\frac{1}{2}\rho V^2}$
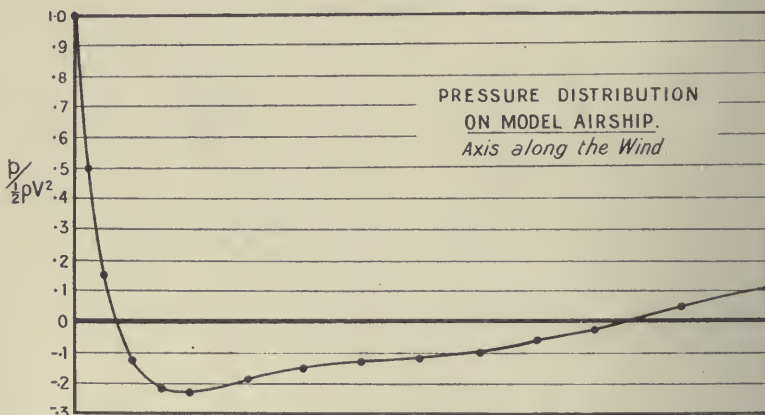
Fig. 105a.

model is given in Fig. 105B, on which are marked the positions of the points at which pressures were measured Somewhat greater precision is given by Table 46, the last column of which shows the pressures for the condition in which the axis of the envelope was along the wind. Other figures and diagrams show the pressure distribution when the axis of the airship is inclined to the relative wind at angles of 10° and 30°. The product of the wind speed in feet per second and the diameter in feet was 15, whilst the pressures have been divided by ρV^2 to provide a suitable pressure coefficient.

With the axis along the wind, Fig. 105A shows a pressure coefficient of half at the nose, which falls very rapidly to a negative value a short distance further back. The pressure coefficient does not rise to a positive value till the tail region is almost completely traversed, and its greatest value at the tail is only 10 per cent. of that at the nose. It is of some interest and importance to know that the region of high pressure at the nose can be investigated on the hypothesis of an inviscid fluid which there

gives satisfactory results as to pressure distribution. The stiffening of the nose mentioned in an earlier chapter can therefore be proved on *à priori* reasoning.

When the axis of the envelope is inclined to the wind, lack of symmetry introduces complexity into the observations and representations. By rolling the model about its axis each of the pressure holes is brought into positions representative of the whole circumference ; with the hole on the windward side the angle has been denoted by —90°, and the symmetry of the model shows that observations at 0° and 180° would be the same. The results are shown in Table 46 and in Fig. 105B. From the latter it will be
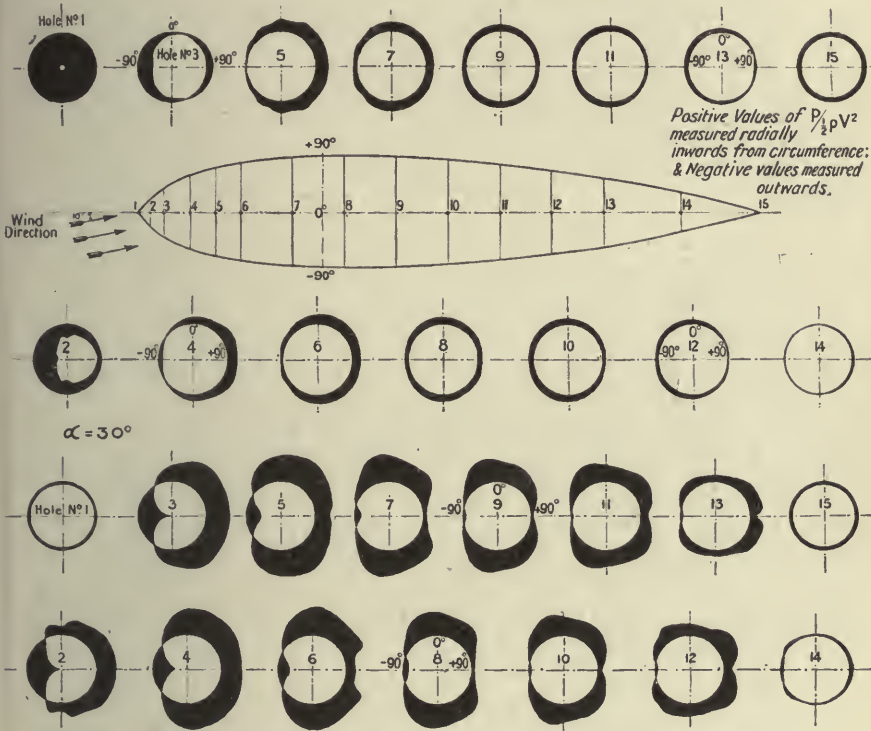
Fig. 105B.—Pressure distribution on an inclined airship model.

seen that the pressure round the envelope at any section normal to the axis is very variable, a positive pressure on the windward side of the nose giving place to a large negative pressure at the back. The diagrams for an inclination of 30° show the effects in most striking form owing to their magnitude.

Kite Balloons.—For typical observations on kite balloons the reader is referred to the section in Chapter II., where in the course of discussion of the conditions of equilibrium a complete account was given of the observations on a model.

TABLE 46.

PRESSURE ON A MODEL AIRSHIP.

Inclination, 0°.

Hole.	Diameter at hole as fraction of maximum diameter.	Axial position of hole as fraction of maximum diameter.	$\frac{P/\rho V^2}{Vd} = 15.$
1	0·000	0·000	+0·500
2	0·269	0·117	+0·241
3	0·436	0·237	+0·073
4	0·670	0·474	−0·064
5	0·805	0·710	−0·112
6	0·890	0·948	−0·112
7	0·979	1·420	−0·100
8	1·000	1·895	−0·078
9	0·990	2·37	−0·068
10	0·938	2·85	−0·063
11	0·855	3·32	−0·055
12	0·755	3·79	−0·032
13	0·618	4·26	−0·015
14	0·347	4·98	+0·030
15	0·000	5·69	+0·057

Values of pressure as a fraction of ρV^2.   Inclination, 10°.

Angle of roll (deg.).	Hole No. 1	2	3	4	5	6	7	8
+90	+0·475	+0·060	−0·091	−0·165	−0·170	−0·132	−0·096	−0·069
+75	+0·475	+0·086	−0·086	−0·169	−0·168	−0·134	−0·100	−0·073
+60	+0·475	+0·091	−0·066	−0·186	−0·171	−0·144	−0·108	−0·095
+45	+0·475	+0·129	−0·050	−0·156	−0·143	−0·110	−0·088
+30	+0·475	+0·149	−0·028	−0·122	−0·210	−0·160	−0·123	−0·094
+15	+0·475	+0·145	+0·021	−0·124	−0·155	−0·143	−0·126	−0·100
0	+0·475	+0·200	+0·045	−0·100	−0·168	−0·134	−0·130	−0·107
−15	+0·475	+0·179	+0·069	−0·077	−0·122	−0·115	−0·124	−0·105
−30	+0·475	+0·257	+0·114	−0·025	−0·120	−0·111	−0·110	−0·102
−45	+0·475	+0·300	+0·147	−0·013	−0·069	−0·074	−0·085	−0·087
−60	+0·475	+0·319	+0·170	+0·017	−0·050	−0·067	−0·077	−0·073
−75	+0·475	+0·354	+0·203	+0·050	−0·016	−0·038	−0·059	−0·055
−90	+0·475	+0·368	+0·218	+0·062	−0·015	−0·020	−0·048	−0·057

Angle of roll (deg.).	Hole No. 9	10	11	12	13	14	15
+90	−0·045	−0·037	−0·017	+0·005	+0·007	+0·023	+0·052
+75	−0·055	−0·032	−0·023	−0·005	+0·006	+0·023	+0·052
+60	−0·066	−0·037	−0·026	−0·024	−0·005	+0·016	+0·052
+45	−0·081	−0·060	−0·048	−0·020	−0·011	+0·010	+0·052
+30	−0·082	−0·073	−0·060	−0·034	−0·020	+0·013	+0·052
+15	−0·091	−0·081	−0·073	−0·053	−0·038	+0·005	+0·052
0	−0·096	−0·086	−0·080	−0·060	−0·041	+0·005	+0·052
−15	−0·105	−0·089	−0·088	−0·064	−0·048	+0·003	+0·052
−30	−0·100	−0·088	−0·094	−0·073	−0·053	+0·000	+0·052
−45	−0·087	−0·078	−0·091	−0·068	−0·054	+0·005	+0·052
−60	−0·073	−0·074	−0·075	−0·070	−0·053	+0·005	+0·052
−75	−0·069	−0·068	−0·070	−0·058	−0·045	+0·005	+0·052
−90	−0·056	−0·065	−0·062	−0·050	−0·045	0·000	+0·052

TABLE 46—*continued.*

Values of pressure as a fraction of ρV^2.   Inclination, 30°.

Angle of roll (deg.).	Hole No. 1	2	3	4	5	6	7	8
+90	+0·034	−0·285	−0·340	−0·290	−0·210	−0·121	−0·048	−0·033
+75	+0·034	−0·275	−0·355	−0·310	−0·261	−0·135	−0·081	−0·048
+60	+0·034	−0·296	−0·359	−0·337	−0·300	−0·315	−0·200	−0·136
+45	+0·034	−0·270	−0·370	−0·368	−0·368	−0·303	−0·312	−0·272
+30	+0·034	−0·233	−0·376	−0·380	−0·413	−0·328	−0·302	−0·292
+15	+0·034	−0·221	−0·290	−0·383	−0·390	−0·373	−0·332	−0·301
0	+0·034	−0·122	−0·232	−0·348	−0·372	−0·380	−0·378	−0·341
−15	+0·034	−0·146	−0·151	−0·275	−0·314	−0·330	−0·370	−0·336
−30	+0·034	+0·056	0·000	−0·148	−0·241	−0·224	−0·281	−0·275
−45	+0·034	+0·208	+0·139	−0·010	−0·062	−0·098	−0·150	−0·156
−60	+0·034	+0·306	+0·267	+0·133	+0·050	0·000	−0·062	−0·056
−75	+0·034	+0·428	+0·390	+0·261	+0·175	+0·123	+0·044	+0·045
−90	+0·034	+0·492	+0·450	+0·324	+0·226	+0·182	+0·120	+0·078

Angle of roll (deg.).	Hole No. 9	10	11	12	13	14	15	
+90	−0·015	−0·051	−0·081	−0·100	−0·081	−0·046	+0·043	
+75	−0·076	−0·121	−0·160	−0·191	−0·195	−0·031	+0·043	
+60	−0·168	−0·191	−0·240	−0·256	−0·186	−0·017	+0·043	
+45	−0·223	−0·238	−0·266	−0·253	−0·175	−0·019	+0·043	
+30	−0·272	−0·253	−0·223	−0·169	−0·116	−0·012	+0·043	
+15	−0·281	−0·252	−0·220	−0·155	−0·094	0·000	+0·043	
0	−0·298	−0·261	−0·226	−0·158	−0·088	0·000	+0·043	
−15	−0·331	−0·310	−0·266	−0·181	−0·102	0·000	+0·043	
−30	−0·263	−0·256	−0·259	−0·208	−0·122	0·000	+0·043	
−45	−0·156	−0·172	−0·200	−0·158	−0·128	−0·039	+0·043	
−60	−0·061	−0·086	−0·100	−0·113	−0·087	−0·014	+0·043	
−75	+0·012	−0·010	−0·028	−0·024	−0·018	+0·015	+0·043	
−90	+0·065	+0·031	+0·021	+0·021	+0·013	+0·032	+0·043	

CHAPTER IV

DESIGN DATA FROM THE AERODYNAMICS LABORATORIES

PART II.—Body Axes and Non-rectilinear Flight

In collecting the more complex data of flight it is advisable for ease of comparison and use that results be referred to some standard system of axes. The choice is not easily made owing to the necessity for compromise, but recently the Royal Aeronautical Society has recommended a complete system of notation and symbols for general adoption. The details are given in " A Glossary of Aeronautical terms," and will be followed in the chapters of this book. The axes proposed differ from others on which aeronautical data has been based, and some little care is necessary in attaching the correct signs to the various forces and moments. It happens that very simple changes only are required for the great bulk of the available data.

Axes (Fig. 106).—The origin of the axes of a complete aircraft is commonly taken at its centre of gravity and denoted by G. The reason for this arises from the dynamical theorem that the motion of the centre of gravity of a body is determined by the resultant force, whilst the rotation of a body depends only on the resultant couple about an axis through the centre of gravity. This theorem is not true for any other possible origin.

From G, the longitudinal axis GX goes forward, and for many purposes may be roughly identified with the airscrew axis. The normal axis GZ lies in the plane of symmetry and is downwards, whilst the lateral axis GY is normal to the other two axes and towards the pilot's right hand.

The axes are considered to be fixed in the aeroplane and to move with it, so that the position of any given part such as a wing tip always has the same co-ordinates throughout a motion. This would not be true if wind axes were chosen, and difficulties would then occur in the calculation of such a motion as spinning. For many purposes the axis GX may be chosen arbitrarily, whilst in other instances it is conveniently taken as one of the principal axes of inertia.

In dealing with parts of aircraft it is not always possible to relate the results initially to axes suitable for the aircraft, since the latter may not then be defined. It is consequently necessary to consider the conversion of results from one set of body axes to another. So far as is possible, the axes of separate parts are taken to conform with those of the complete aircraft.

Angles relative to the Wind.—Any possible position of a body relative to the wind can be defined by means of the angular positions of the axes. Two angles, those of pitch and yaw, are required, and are denoted respectively by the symbols α and β. They are specified as follows : first, place

the axis of X along the wind; second, rotate the body about the axis of Z through an angle β and, finally rotate the body about the new position of the axis of Y through an angle α. The positive sign is attached to an angle if the rotation of the body is from GX to GY, GY to GZ or GZ to GX. This is a convenient convention which is also applied to elevator angles, flap settings and rudder movements. With such a convention it is found that confusion of signs is easily avoided.

Angles are given the names roll, pitch or yaw for rotations about the axes of X, Y and Z respectively. It should be noticed that an angular displacement about the original position of the axis of X does not change the attitude of the body relative to the wind.

Forces along the Axes.—The resultant force on a body is completely specified by its components along the three body axes. Counted positive when acting from G towards X, Y and Z (Fig. 106), they are denoted by mX, mY and mZ, and spoken of as longitudinal force, lateral force and
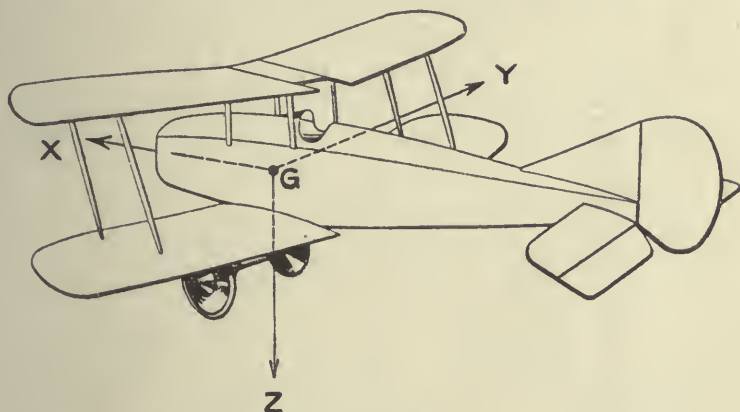
FIG. 106.—Standard axes.

normal force. "m" represents the mass of an aircraft, and may not be known when the aerodynamical data is being obtained; the form is convenient when applying the equations of motion.

Moments about the Axes.—The resultant couple on a body is completely specified by its components about the three body axes. Counted positive where they tend to turn the body from GY to GZ, from GZ to GX and from GX to GY, they are denoted by the symbols L, M and N and are known as rolling moment, pitching moment and yawing moment.

Angular Velocities about the Axes.—The component angular velocities known as rolling, pitching and yawing are denoted by the symbols p, q and r, and are positive when they tend to move the body so as to increase the corresponding angles.

The forces and couples on a body depend on the magnitude of the relative wind, V, the inclinations α and β and the angular velocities p, q and r. In a wind channel where the model is stationary relative to the channel walls, p, q and r are each zero, and most of the observations hitherto

resolution into lift, drag and pitching moment ; A may be chosen at any place, and through it the resolved components normal to and along the wind are drawn and are independent of the position of A.   The moment of the resultant force ab about A gives the couple M, which clearly depends on the perpendicular distance of A from the line of action of the resultant.

Body Axes in a Wing Section.—Keeping the point A as in Fig. 107 (*b*), the axis of X has been drawn in Fig. 107 (*c*) as making an angle α_0 with the chord of the aerofoil.   The angle of pitch is then equal to $\alpha + \alpha_0$, and the double use of α for angle of incidence and angle of pitch should be noted together with the fact that they differ only by a constant.   The components of force are now mX and mZ in the directions shown by the arrows, whilst M has
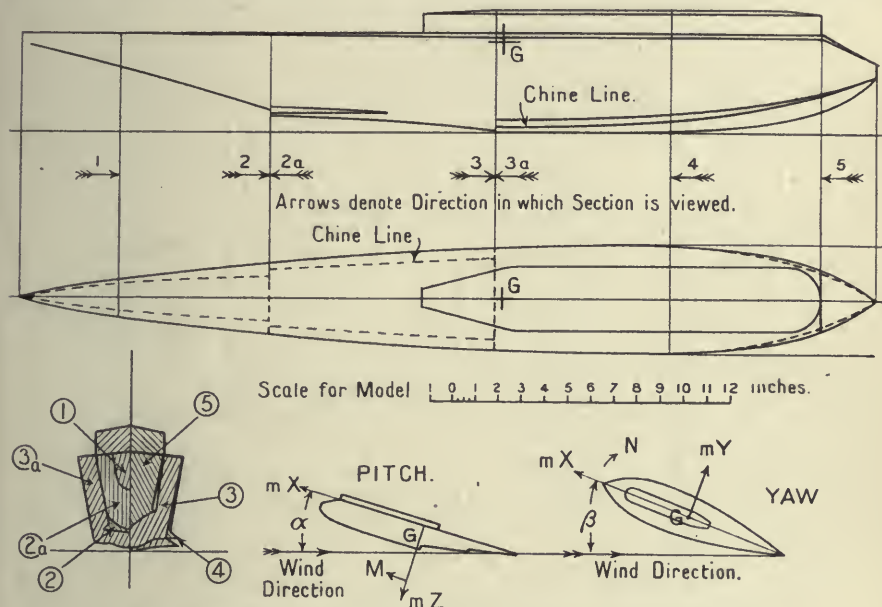
Fig. 108.—Model of a flying-boat hull; shape and position of axes.

identically the same value as for Fig. 107 (*b*).   To move the point A to B without changing the inclination of the axes it is only necessary to make use of Fig. 107 (*d*), where x and z are the co-ordinates of B relative to the old axes.   It then follows that

$$M_B = M_A - zm\text{X} + xm\text{Z} \quad . \quad . \quad . \quad . \quad (1)$$

whilst mX and mZ are unchanged.   In general it appears to be preferable to take the most general case of change of origin and orientation in two stages as shown, *i.e.* first change the orientation at the old origin, and then change the origin.

It is worthy of remark here, that although drag cannot be other than positive, longitudinal force may be either negative or positive, and usually bears no obvious relation to drag.

Longitudinal Force, Lateral Force, Normal Force, Pitching Moment and Yawing Moment on a Model of a Flying Boat Hull.—A drawing of the model is shown in Fig. 108, together with two small inset diagrams of the positions of the axes. Experiments were made to determine the longitudinal and normal forces and the pitching moment for various angles of pitch α but with the angle of yaw zero, and also to determine the longitudinal and lateral forces and the yawing moment for various angles of yaw β but with the angle of pitch zero. The readings are given in Tables 1 and 2, and curves from them are shown in Fig. 109.

TABLE I.

FORCES AND MOMENTS ON A FLYING BOAT HULL (PITCH).

Wind speed, 40 ft.-s.

Angle of pitch α (degrees).	Longitudinal force mX (lbs.).	Normal force mZ (lbs.).	Pitching moment M (lbs.-ft.).
+20	−0·067	−0·407	+0·291
15	−0·065	−0·281	+0·217
10	−0·057	−0·166	+0·153
8	−0·054	−0·122	+0·130
6	−0·050	−0·084	+0·100
4	−0·047	−0·051	+0·077
2	−0·044	−0·022	+0·049
0	−0·041	+0·007	+0·024
− 2	−0·040	+0·020	+0·002
− 4	−0·041	+0·043	−0·019
− 6	−0·040	+0·069	−0·036
− 8	−0·040	+0·102	−0·056
−10	−0·041	+0·142	−0·072
−15	−0·041	+0·273	−0·108
−20	−0·038	+0·446	−0·148

TABLE 2.

FORCES AND MOMENTS ON A FLYING BOAT HULL (YAW).

Wind speed, 40 ft.-s.

Angle of yaw β (degrees).	Longitudinal force mX (lbs.).	Lateral force mY (lbs.).	Yawing moment N (lbs.-ft.).
0	−0·041	0	0
5	−0·042	0·078	+0·063
10	−0·037	0·179	+0·120
15	−0·032	0·296	+0·190
20	−0·028	0·419	+0·249
25	−0·019	0·597	+0·294
30	−0·005	0·767	+0·342
35	+0·011	0·952	+0·381

Fig. 109 shows that the normal force mZ and the pitching moment M change by much greater proportionate amounts than the longitudinal force mX when the angle of pitch is changed, and that the lateral force mY and yawing moment N show a similar feature as the angle of yaw is changed.
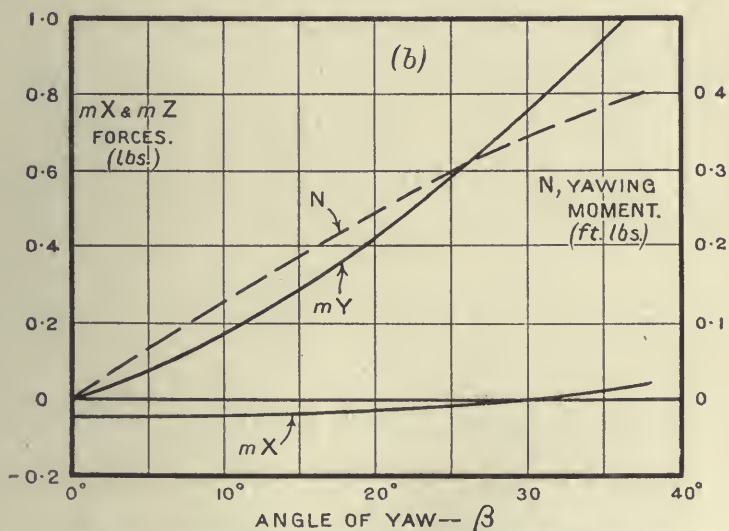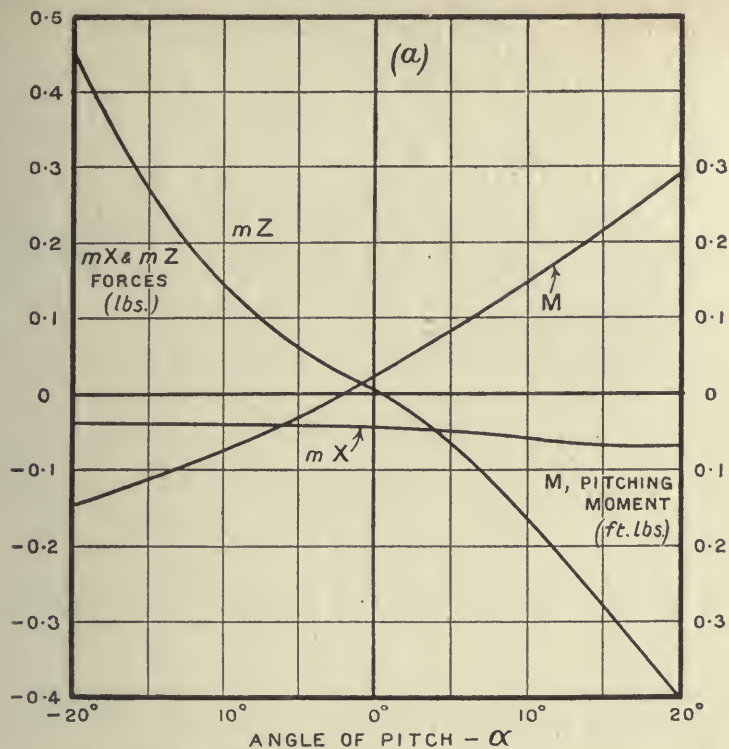
FIG. 109.—Forces and moments on a model of a flying-boat hull.

In the latter case, Fig. 109 (b), it may be noticed that the longitudinal force mX becomes zero at an angle of yaw of 30°. The rolling moment was considered to be too small to be worthy of measurement.

For each angle of pitch it is obvious that there will be a diagram in which the angle of yaw is varied. The number of instances in which measurements have been made for large variations of both α and β is very small and partial results have therefore been used even where the more complete observations would have been directly applicable. It only needs to be pointed out that the six quantities X, Y, Z, L, M, N are needed for all angles α, β, for all angular velocities p, q, r, and for all settings of the elevators, rudder and ailerons for it to be realised that it is not possible to cover the whole field of aeronautical research in general form. For this reason it is expected that specific tests on aircraft will ultimately be made by constructing firms, and that the aerodynamics laboratories will develop the new tests required and give the lead to development.

TABLE 3.

FORCES AND MOMENTS ON AN AEROPLANE BODY (YAW).

Wind speed, 40 ft.-s.

Angle of yaw (degrees).	Body without fin and rudder.			Body with fin and rudder (rudder at 0°).		
	Longitudinal force (lbs.).	Lateral force (lbs.).	Yawing moment (lbs.-ft.).	Longitudinal force (lbs.).	Lateral force (lbs.).	Yawing moment (lbs.-ft.).
0	−0·0697	0	0	−0·0753	0	0
5	−0·0740	0·0676	0·049	−0·0780	0·1353	−0·056
10	−0·0780	0·1437	0·095	−0·0806	0·3158	−0·186
15	−0·0827	0·2481	0·131	−0·0811	0·5347	−0·330
20	−0·087	0·390	0·153	−0·081	0·768	−0·472
25	−0·089	0·560	0·153	−0·080	1·027	−0·631
30	−0·085	0·754	0·140	−0·080	1·307	−0·815

TABLE 4.

EFFECT OF RUDDER (YAW).

Wind speed, 40 ft.-s.

Angle of yaw (degrees).	Body with fin and rudder (rudder at +10°).			Body with fin and rudder (rudder at +20°).		
	Longitudinal force.	Lateral force.	Yawing moment.	Longitudinal force.	Lateral force.	Yawing moment.
−30	−0·071	−1·132	+0·466	−0·091	−0·942	+0·153
−25	−0·080	−0·845	0·293	−0·104	−0·674	0
−20	−0·084	−0·602	0·181	−0·108	−0·4668	−0·083
−15	−0·087	−0·376	+0·066	−0·1132	−0·2270	−0·177
−10	−0·089	−0·1691	−0·058	−0·1224	−0·0236	−0·313
− 5	−0·092	−0·0021	−0·169	−0·1270	+0·1364	−0·429
0	−0·089	+0·1330	−0·227	−0·1333	0·283	−0·487
+ 5	−0·099	0·2976	−0·330	−0·1547	0·460	−0·631
10	−0·107	0·4921	−0·483	−0·1678	0·644	−0·771
15	−0·115	0·708	−0·639	−0·1785	0·852	−0·912
20	−0·122	0·959	−0·804	−0·196	1·110	−1·113
25	−0·129	1·219	−0·995	−0·212	1·380	−1·320
30	−0·133	1·497	−1·160	−0·217	1·562	−1·434

Forces and Moments due to the Yaw of an Aeroplane Body fitted with Fin and Rudder.—The experiment on the model shown in Fig. 110 was made
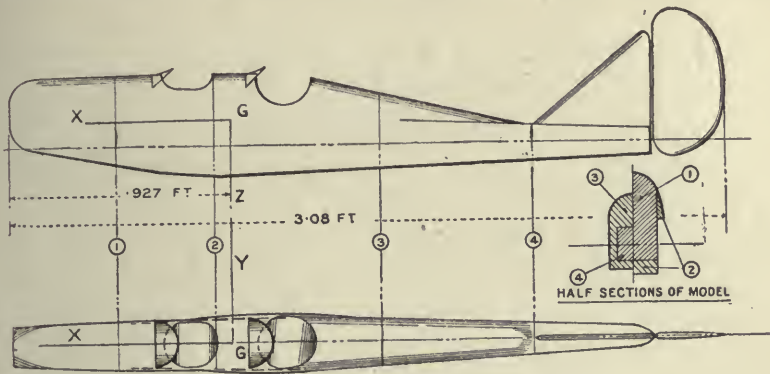
FIG. 110.—Aeroplane body with fin and rudder.

with the angle of pitch zero. For various angles of yaw the longitudinal and lateral forces and the yawing moment were measured without fin and rudder ; also with the fin in place and the rudder set over at various angles. The results are given in Tables 3 and 4 and illustrated in Fig. 111.

The body alone, shows a zero yawing moment with its axis along the wind and positive values for all angles of yaw up to 30°. Regarded as a weathercock with its spindle along the axis of Z, the body alone would tend to turn round to present a large angle to the wind. With the fin and rudder shown in Fig. 110, however, a comparatively large couple is introduced which would bring the weathercock into the wind. Setting the rudder over to 10° and 20° is seen to be equivalent to an additional yawing moment which is roughly constant for all
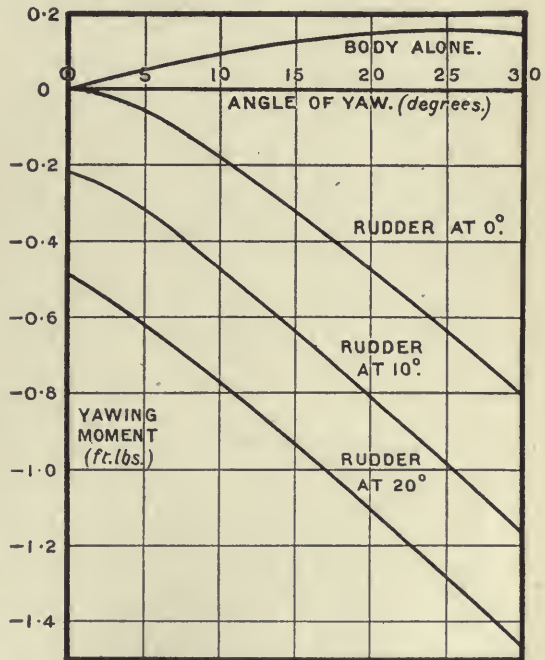
FIG 111.—Yawing moments due to fin and rudder on a model aeroplane body.

angles of yaw within the range of the test. The amount of the couple due to 10° of rudder is about twice as great as that due to an inclination

of the body of 30°, and hence the positions of equilibrium shown by
Table 4 at −12° for a rudder angle of 10° and at −25° for a rudder angle
of 20° must be due to the counteracting effect of the fixed fin.   It will
thus be seen that the lightness of the rudder of an aeroplane depends on
the area of the fixed fin.   The best result will clearly be obtained if the
fin just counteracts the effect of the body.   The experiment to find this
condition could be performed by measuring the yawing moment on the
body and fin with rudder in place but not attached at the hinge.   It
would not be sufficient to merely remove the rudder, since the forces on
the fin would thereby be affected.   The possibilities of this line of inquiry
have not been seriously investigated.

   **The Effect of the Presence of the Body and Tail Plane and of Shape of
Fin and Rudder on the Effectiveness of the Latter.**—For this experiment the
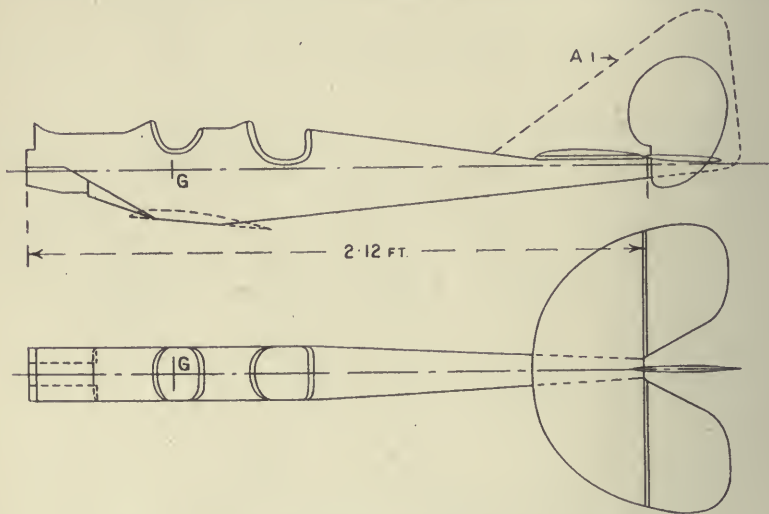
Fig. 112.—Model aeroplane body with complete tail unit.

rudder was set at zero angle, and cannot therefore be differentiated from
the fin.   The basis of comparison has been made the lateral force per unit
area divided by the square of the wind speed.   It is found that the coefficient
so defined depends not only on the shape of the vertical surface, but also
on the presence of the body and the tail plane and elevators.   The drawing
of the model used is shown in Figs. 112 and 113, the latter giving to an
enlarged scale the shapes of the fins attached in the second series of ex-
periments.

   The experiments recorded in Table 5 apply to the model as illustrated
by the full lines of Fig. 112, that is without the fin marked A1.   The test
leading to the second column of Table 5 was made with rudder alone held
in the wind, and will be found to show greater values of the lateral force
coefficient than when in position as part of the model.   A range of angle
of pitch of 10 degrees is not uncommon in steady straight flying, and the
body was tested with the axis of X upwards (+5°), with it along the wind

and with it pitched downwards ($-5°$), both with and without the elevators in position.

TABLE   5.

EFFECT OF BODY AND ELEVATORS ON THE RUDDER.

Lateral forces on the rudder of Fig. 112 in lbs. divided by area in sq. ft. and by square of wind speed in feet per sec.

Angle of yaw (deg.).	Rudder alone (free from interference effects).	Rudder when attached to body pitched $+5$ degrees.		Rudder when attached to body in normal flying position.		Rudder when attached to body pitched -5 degrees.	
		Without tail plane and elevators.	With ditto.	Without tail plane and elevators.	With ditto.	Without tail plane and elevators.	With ditto.
2	0·000104	0·000057	0·000050	0·000071	0·000063	0·000083	0·000065
4	0·000205	0·000114	0·000104	0·000155	0·000133	0·000183	0·000143
6	0·000315	0·000186	0·000170	0·000247	0·000216	0·000274	0·000226
8	0·000421	0·000265	0·000249	0·000337	0·000303	0·000370	0·000306
10	0·000528	0·000350	0·000330	0·000433	0·000402	0·000482	0·000397

Considering first the coefficients for the model with tail plane and elevators.   In all cases the value is markedly less than that for the free
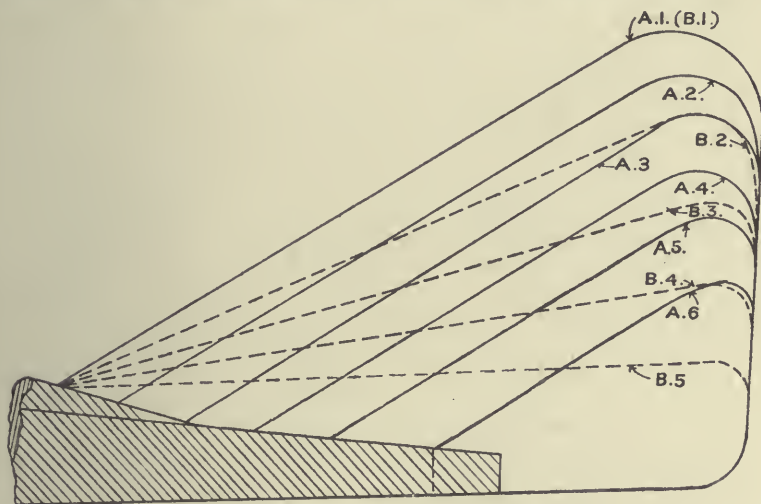
FIG. 113.—Variations of fin and rudder area.

rudder, and there is some indication of a greater shielding by the body when the nose is up than when it is either level or down.   This feature is more readily seen from Fig. 114 (a), where the curves for $0°$ and $-5°$ pitch are seen to lie below those of the rudder alone, but above the curve for an angle of pitch of $+5°$.   Fig. 114 (b) shows, in this instance, the effect of the presence of the elevators ;   as ordinate, is plotted the lateral force coefficient with tail plane, on an abscissa of the similar coefficient without tail plane.   The points are seen to group themselves about a straight line which shows a

loss of 14 per cent. due to the presence of the tail plane. A further reduction may be expected from the introduction of the main planes in a complete aircraft due to the slowing up of the air when gliding. On the other hand, the influence of the airscrew slipstream may be to increase the value materially until the final resultant effect is greater than that on the free rudder.

The tests on the effect of shape were carried out on the same body, but without tail plane and elevators, and the results are given in Table 6.

The fins were divided into two groups, A 1 to A 6, and B 1 to B 5, of
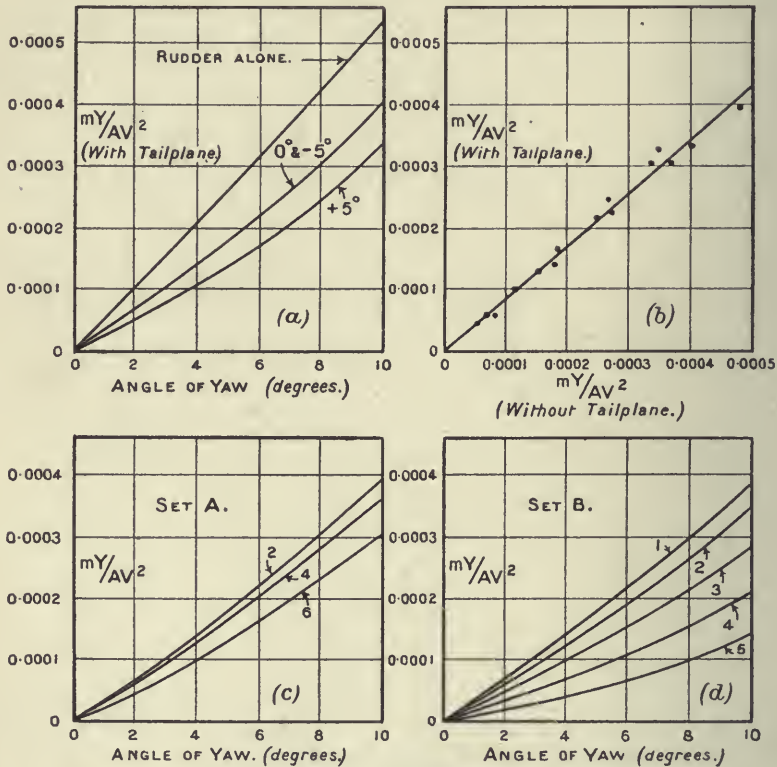
FIG. 114.—Effect of variations of fin and rudder area.

which A 1 and B 1 were identical in size and shape. In the A series the forms of the vertical surface were roughly similar, the main change being one of size. Fig. 114 (c) indicates little change in the lateral force coefficient until the area has been much reduced. Series B, on the other hand, shows a marked loss of efficiency due to reduction of the height of the fin (Fig. 114 (d)), and both results are consistent with and are probably explained by a reduction in the speed of the air in the immediate neighbourhood of the body. Experiments on the flow of fluid round streamline forms have shown that this slowing of the air may be marked over a layer of air of appreciable thickness.

TABLE 6.

Fin Shape as affecting Usefulness.

Forces on the fins of Set A.

| Angle of yaw (degrees). | Lateral force in lbs. per sq. ft. of fin area divided by square of wind speed (40 ft. per sec.). | | | | | |
	A 1.	A 2.	A 3.	A 4.	A 5.	A 6.
2	0·000063	0·000065	0·000062	0·000058	0·000046	0·000042
4	0·000131	0·000133	0·000128	0·000124	0·000105	0·000099
6	0·000214	0·000216	0·000214	0·000198	0·000177	0·000164
8	0·000297	0·000298	0·000295	0·000273	0·000260	0·000219
10	0·000383	0·000386	0·000385	0·000357	0·000333	0·000302

Forces on the fins of Set B.

| Angle of yaw (degrees). | Lateral force in lbs. per sq. ft. of fin area divided by square of wind speed (40 ft. per sec.). | | | | |
	B 1 or A 1.	B 2.	B 3.	B 4.	B 5.
2	0·000063	0·000054	0·000041	0·000031	0·000018
4	0·000131	0·000114	0·000091	0·000064	0·000037
6	0·000214	0·000192	0·000156	0·000109	0·000066
8	0·000297	0·000270	0·000216	0·000150	0·000098
10	0·000383	0·000347	0·000281	0·000210	0·000145

TABLE 7.

Yawing Moments due to the Rudders of a Rigid Airship.

Wind speed, 40 ft.-s.   Model illustrated in Fig. 103.

Yawing Moments on Airship (lbs.-ft. at 40 ft.-s.).

| Angle of yaw (degrees). | Angle of rudders (degrees). | | | | | | | | |
	−20	−15	−10	−5	0	5	10	15	20
0	0·118	0·105	0·066	0·032	0	−0·032	−0·066	−0·105	−0·118
2	0·230	0·210	0·171	0·140	0·107	+0·062	+0·031	−0·013	−0·035
4	0·333	0·309	0·271	0·227	0·196	0·144	0·105	+0·052	+0·027
6	0·421	0·385	0·338	0·304	0·260	0·206	0·157	0·102	0·073
8	0·478	0·448	0·395	0·360	0·309	0·245	0·202	0·137	0·105
10	0·529	0·495	0·438	0·401	0·348	0·282	0·226	0·168	0·138
15	0·591	0·544	0·495	0·440	0·394	0·308	0·250	0·202	0·168

Airship Rudders.—Owing to the considerable degree of similarity between the airship about vertical and horizontal planes, the rudders behave for variations of angle of yaw very much in the same way as the elevators for angles of pitch.   For the airship dealt with in Part I. of this chapter, Fig. 103, the yawing moments on the model were measured and are given in Table 7.   The type of result is sufficiently represented by the

Q

elevators and does not need a separate figure. It should be noted that the yawing moment is positive, and therefore tends to increase a deviation from the symmetrical position. The effect of the lateral force which appears when an airship is yawed tends on the other hand to a reduction of the angle, and it is necessary to formulate a theory of motion before a satisfactory balance between the two tendencies is obtained.

Ailerons and Wing Flaps.—The first illustration here given of the determination of the three component forces and component moments in which α and β are both varied relates to a simple model aerofoil. A later table which is an extension shows the effect of wing flaps. The model was an aerofoil 18 ins. long and 3 ins. chord with square ends; for the experiments with flaps two rectangular portions 4·5 ins. long and 1·16 ins. wide were attached by hinges so that their angles could be adjusted independently of that of the main surface.

TABLE 8.

AEROFOIL R.A.F. 6, 3 INCHES × 18 INCHES, WITH FLAPS EQUAL TO $\frac{1}{4}$ SPAN. FORCES AND MOMENTS ON MODEL AT A WIND-SPEED OF 40 FEET PER SEC.

Both flaps at 0°.

	Angle of pitch (deg.).	Longi- tudinal force mX (lbs.).	Lateral force mY (lbs.).	Normal force mZ (lbs.).	Rolling moment L (lbs.-ft.).	Pitching moment M (lbs.-ft.).	Yawing moment N (lbs.-ft.).
Angle of yaw 0°	− 8	−0·0222	0	+0·107	0	−0·0151	0
	− 4	−0·0322	0	−0·148	0	−0·0032	0
	0	−0·0257	0	−0·411	0	+0·0089	0
	+ 4	−0·0030	0	−0·619	0	0·0198	0
	8	+0·0404	0	−0·812	0	0·0288	0
	12	+0·073	0	−0·873	0	0·0314	0
	16	−0·027	0	−0·753	0	+0·0129	0
Angle of yaw 10°	− 8	−0·0218	0·0043	+0·107	−0·0014	−0·0146	−0·0001
	− 4	−0·0316	0·0050	−0·141	+0·0010	−0·0033	−0·0004
	0	−0·0248	0·0053	−0·404	0·0028	+0·0085	−0·0008
	+ 4	−0·0037	0·0062	−0·603	0·0044	0·0190	−0·0014
	8	+0·0270	+0·0069	−0·782	0·0075	0·0272	−0·0025
	12	+0·076	−0·0011	−0·860	0·0318	0·0309	+0·0029
	16	−0·023	−0·0029	−0·762	+0·0572	+0·0129	+0·0037
Angle of yaw 20°	− 8	−0·0208	0·0090	+0·100	+0·0002	−0·0140	−0·0005
	− 4	−0·0291	0·0091	−0·125	0·0016	−0·0029	−0·0009
	0	−0·0242	0·0094	−0·370	0·0039	+0·0073	−0·0016
	+ 4	−0·0036	0·0099	−0·556	0·0059	0·0166	−0·0029
	8	+0·0338	+0·0132	−0·722	0·0102	0·0243	−0·0046
	12	+0·072	−0·0022	−0·810	0·0496	0·0296	+0·0048
	16	−0·013	−0·0028	−0·775	+0·0906	+0·0141	+0·0074

Table 8 shows that, the angle of yaw having been set at the values 0°, 10° and 20° in each series of measurements, the angle of pitch was varied during the experiment by steps of 4° from −8° to +16°. The origin of the axes was a point in the plane of symmetry 0·06 in. above the chord and 1·33 ins. behind the leading edge. With the axis of X in the direction of the wind the aerofoil made an angle of incidence of 4° when the angle of yaw was zero: *i.e.* the angle α_0 of Fig. 107 *c* was −4°. With the

angle of yaw zero it follows from symmetry that the lateral force and the rolling and yawing moments are all zero no matter what the angle of pitch. The longitudinal force on an aerofoil appears for the first time, and a consideration of the table shows that from a negative value at an angle of pitch of $-8°$ it rises to a greater positive value at $+8°$, and then again becomes negative as the critical angle of attack is exceeded. The normal force $-mZ$ has the general characteristics of lift, whilst the pitching moment differs from the quantities previously given only by being referred to a new axis.

TABLE 9.

AEROFOIL WITH WING FLAPS.

Flaps at $\pm 10°$ (right-hand flap down, and left-hand flap up).

	Angle of pitch (deg.).	Longi-tudinal force mX (lbs.).	Lateral force mY (lbs.).	Normal force mZ (lbs.).	Rolling moment L (lbs.-ft.).	Pitching moment M (lbs.-ft.).	Yawing moment N (lbs.-ft.).
Angle of yaw $-20°$	-8	$-0·0312$	$-0·0080$	$+0·059$	$-0·0600$	$-0·0140$	$+0·0069$
	-4	$-0·0329$	$-0·0069$	$-0·162$	$-0·0641$	$-0·0027$	$0·0085$
	0	$-0·0327$	$-0·0094$	$-0·385$	$-0·0685$	$+0·0068$	$0·0088$
	$+4$	$-0·0131$	$-0·0107$	$-0·580$	$-0·0684$	$0·0165$	$0·0093$
	8	$+0·0302$	$-0·0118$	$-0·755$	$-0·0698$	$0·0244$	$0·0106$
	12	$+0·0324$	$-0·0027$	$-0·804$	$-0·0955$	$0·0197$	$0·0049$
	16	$-0·0193$	$-0·0054$	$-0·778$	$-0·1043$	$+0·0152$	$+0·0127$
Angle of yaw $-10°$	-8	$-0·0330$	$-0·0039$	$+0·069$	$-0·0629$	$-0·0152$	$+0·0080$
	-4	$-0·0357$	$-0·0036$	$-0·173$	$-0·0664$	$-0·0030$	$0·0086$
	0	$-0·0341$	$-0·0052$	$-0·418$	$-0·0724$	$+0·0076$	$0·0086$
	$+4$	$-0·0104$	$-0·0054$	$-0·629$	$-0·0730$	$0·0180$	$0·0084$
	8	$+0·0341$	$-0·0052$	$-0·814$	$-0·0732$	$0·0266$	$0·0086$
	12	$+0·0401$	$-0·0005$	$-0·852$	$-0·0767$	$0·0209$	$0·0085$
	16	$-0·0430$	$+0·0018$	$-0·748$	$-0·0723$	$+0·0097$	$+0·0148$
Angle of yaw $0°$	-8	$-0·0329$	$-0·0002$	$+0·079$	$-0·0654$	$-0·0146$	$+0·0076$
	-4	$-0·0412$	0	$-0·168$	$-0·0660$	$-0·0036$	$0·0080$
	0	$-0·0343$	$+0·0005$	$-0·422$	$-0·0724$	$+0·0076$	$0·0075$
	$+4$	$-0·0102$	$0·0012$	$-0·629$	$-0·0713$	$0·0182$	$0·0067$
	8	$+0·0342$	$0·0018$	$-0·814$	$-0·0654$	$0·0268$	$0·0058$
	12	$+0·0431$	$0·0010$	$-0·852$	$-0·0415$	$0·0267$	$0·0112$
	16	$-0·0350$	$0·0025$	$-0·748$	$-0·0134$	$+0·0111$	$+0·0163$
Angle of yaw $10°$	-8	$-0·0316$	$+0·0049$	$+0·093$	$-0·0654$	$-0·0125$	$+0·0068$
	-4	$-0·0405$	$0·0049$	$-0·153$	$-0·0632$	$-0·0040$	$0·0075$
	0	$-0·0338$	$0·0058$	$-0·401$	$-0·0671$	$+0·0072$	$0·0064$
	$+4$	$-0·0098$	$0·0074$	$-0·603$	$-0·0632$	$0·0175$	$0·0048$
	8	$-0·0356$	$0·0080$	$-0·802$	$-0·0552$	$0·0260$	$0·0031$
	12	$+0·0411$	$0·0055$	$-0·827$	$-0·0094$	$0·0233$	$0·0149$
	16	$-0·0252$	$0·0044$	$-0·756$	$+0·0335$	$+0·0132$	$+0·0196$
Angle of yaw $20°$	-8	$-0·0299$	$+0·0075$	$+0·096$	$-0·0628$	$-0·0118$	$+0·0051$
	-4	$-0·0369$	$0·0087$	$-0·131$	$-0·0603$	$-0·0038$	$0·0058$
	0	$-0·0319$	$0·0088$	$-0·363$	$-0·0621$	$+0·0060$	$0·0054$
	$+4$	$-0·0103$	$0·0099$	$-0·553$	$-0·0531$	$0·0154$	$0·0032$
	8	$+0·0310$	$0·0120$	$-0·733$	$-0·0464$	$0·0233$	$0·0009$
	12	$+0·0415$	$0·0064$	$-0·794$	$+0·0038$	$0·0222$	$0·0115$
	16	$-0·0118$	$0·0083$	$-0·770$	$+0·0550$	$+0·0151$	$+0·0200$

At an angle of yaw of $10°$ all the forces and couples have value, but not all are large. The lateral force mY is not important as compared with longitudinal force, whilst the yawing moment N is small compared with the pitching moment. On the other hand, the rolling moment L

becomes very important at large angles of incidence. This may be ascribed
to the critical flow occurring more readily on the wing which is down wind
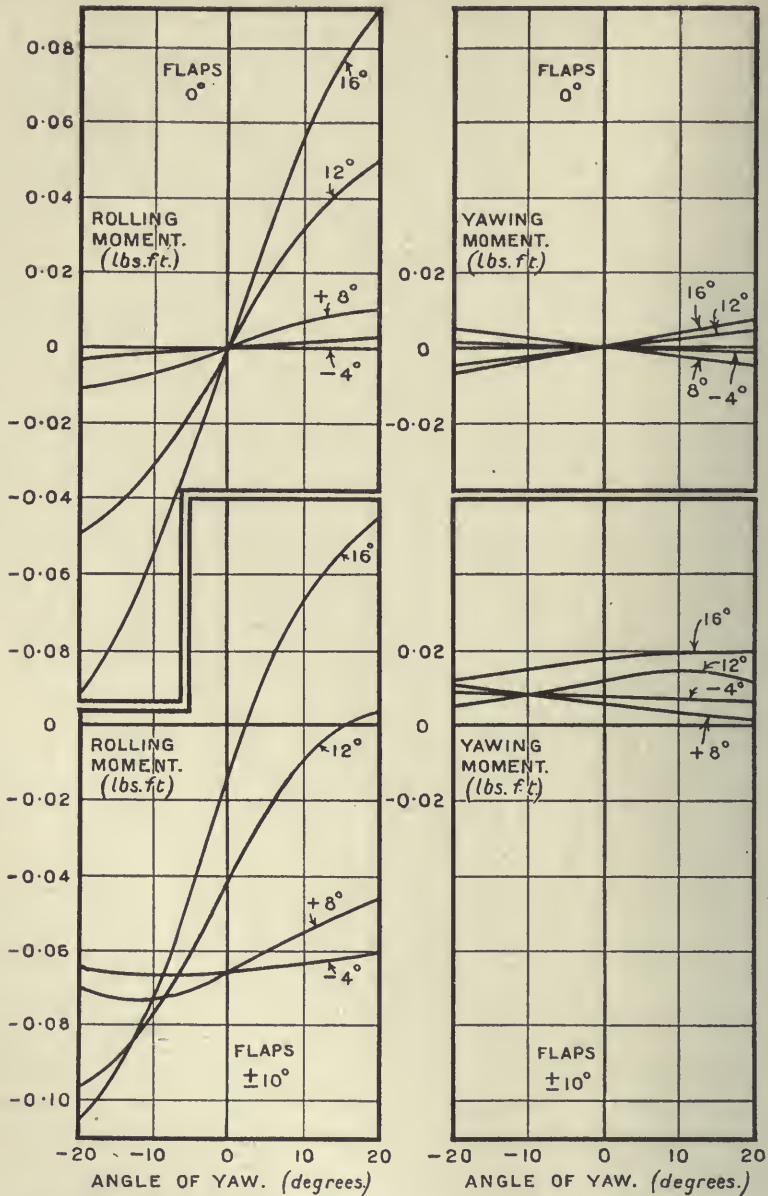
Fig. 115.—Rolling and yawing moments due to the use of ailerons.

due to the yaw than to that facing into the wind. The remarks apply
with a little less force when the angle of yaw is 20°. The results show that

side slipping to the left (+ve yaw) tends to raise the left wing (+ve roll), and that aileron control would be necessary to counterbalance this rolling couple. It will be found from Table 9 that the amount of control required is considerable at an angle of yaw of 20°; and calls for large angles of flap.

Only the quantities dealing with rolling moment and yawing moment have been selected for illustration by diagram. Much further information is given in Report No. 152 of the Advisory Committee for Aeronautics. Referring to Fig. 115, it will be found that with the flaps at 0° neither the rolling moment nor the yawing moment have large values until the angle of pitch exceeds 8° (i.e. angle of incidence exceeds 12°). At larger angles of pitch the rolling moment is large for angles of yaw of 10° and upwards, i.e. for a not improbable degree of side slipping during flight. The best idea of the importance of the rolling couple is obtained by comparing the curves with those of the figure below, which correspond with flaps put over to angles of ± 10°. The curves readily suggest an additional rolling moment due to the flaps which is roughly independent of angle of yaw, but very variable with angle of pitch. At values of the latter of −4° to +8° the addition to rolling moment is rather more than −0·06 lb.-ft. At an angle of pitch of 12° the effect of the flaps has fallen to two-thirds of the above value, whilst at 16° it is only one-fifth of it. Quite a small degree of side slipping on a stalled aerofoil introduces rolling couples greater than those which can be applied by the wing flaps. The danger of attempting to turn a stalled aeroplane has a partial explanation in this fact.

It will be noticed that the yawing moments are relatively small, but the rudder is also a small organ of control, and appreciable angles may be required to balance the yawing couple which accompanies the use of wing flaps.

The Balancing of Wing Flaps.—The arrangement of the model is shown in Fig. 116, the end of the wings only being shown. Measurements were made on both upper and lower flaps, but Fig. 117 refers only to the upper at a speed of 40 ft.-sec. The model was made so that the strips marked 1, 2 and 3 could be attached either to the main part of the aerofoil or to the flaps. The moments about the hinge were measured at zero angle of yaw for various angles of pitch and of flap. In view of the indications given in the last example that the flow at the wing tips breaks down at different angles of incidence on the two sides, it is probable that the balance is seriously disturbed by yaw and further experiments are needed on the point. Other systems of balance are being used which may in this respect prove superior to the use of a horn.

The results are shown in Fig. 117, where the ordinate is the hinge moment of the flap. The abscissa is the angle of flap, whilst the different diagrams are for angles of incidence of 0°, 4° and 12°. In each diagram are four curves, one for each of the conditions of distribution of the balance area.

Since in no case can an interpolated curve fall along the line of zero ordinates, it follows that accurate balance is not attainable. In all cases, however, an area between that of 1 and 2 leads to a moment which is nearly independent of the angle of flap, and which is not very great. As each

angle of incidence corresponds with a steady flight speed, large angles being associated with low speeds, it will be seen that some improvement could
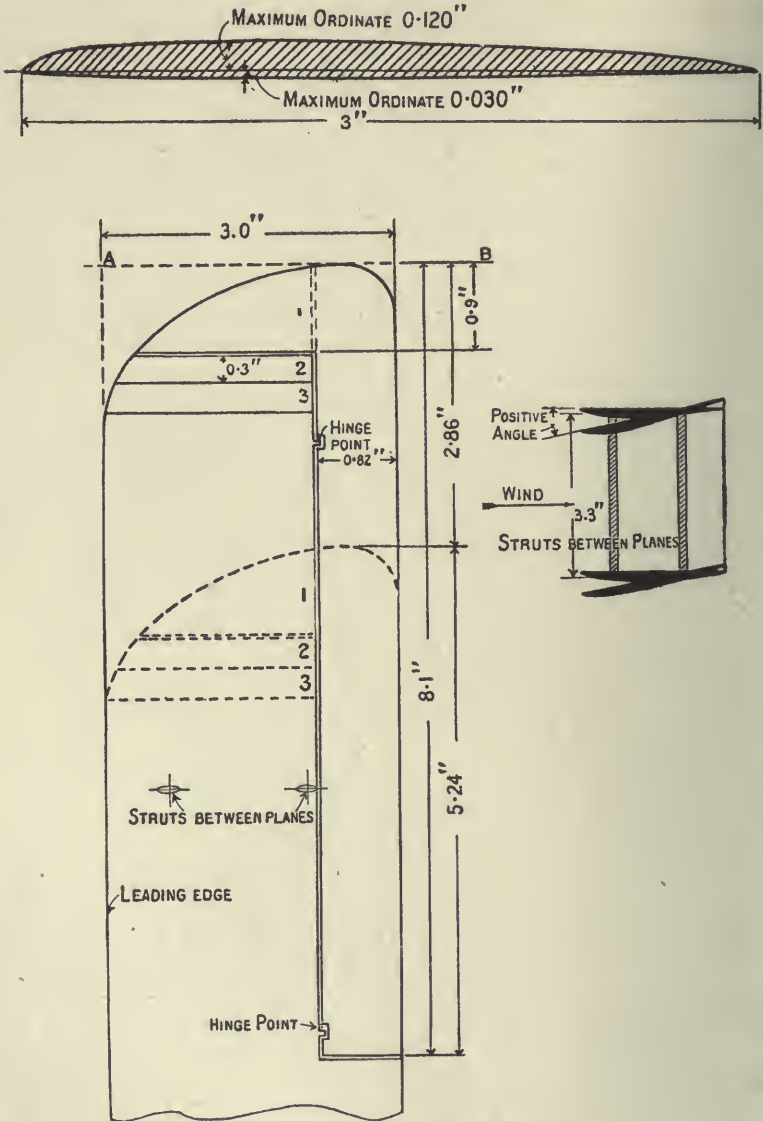
FIG. 116.—The balancing of ailerons.

be obtained over the range 4° to 12° by the use of a spring with a constant pull acting on the aileron lever.

There is, of course, no reason why this type of balance should not be applied to elevators and rudders as well as to ailerons, and many instances of such use exist. Owing to lack of opportunity for making measurements

of scientific accuracy, little is known as to the value of the degrees of balance obtained. The clearest indication given is that pilots dislike a close approximation to balance in ordinary flight.
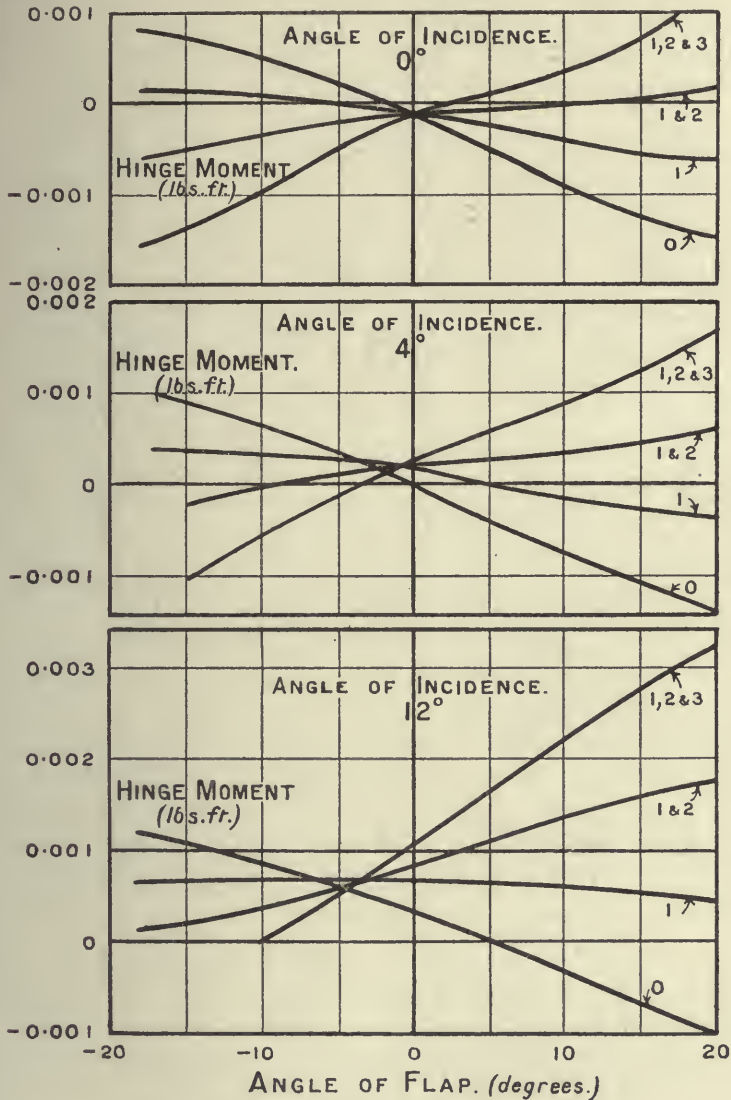
Fig. 117.—Moments on balanced ailerons.

Forces and Moments on a Complete Model Aeroplane.—The experiments refer to a smaller model of the BE 2 than that described in Part I., but the results have been increased in the proportion of the square of the linear dimensions, etc., so as to be more directly comparable. The wings had no dihedral angle, nor was there any fin. Photographs of the model are

shown in Report No. 111, Advisory Committee for Aeronautics. The axis of X was taken to lie along the wind at an angle of incidence of 6° and an angle of yaw of 0°. Experiments were made for large variations of angle of yaw and small variations of angle of pitch. Although limited in scope, the results are the only ones available on the subject of flight at large angles of yaw and represent one of the limits of knowledge. Application is still further from completeness.

TABLE 10.

Forces and Moments on a Complete Model Aeroplane.

Complete Model BE 2 Aeroplane.

$\frac{1}{10}$th scale.   40 ft.-s.   Angle of incidence=angle of pitch+60.

Angle of pitch a (deg.).	Angle of yaw β (deg.).	Longitudinal force mX (lbs.).	Lateral force mY (lbs.).	Normal force mZ (lbs.).	Rolling moment L (lbs.-ft.).	Pitching moment M (lbs.-ft.).	Yawing moment N (lbs.-ft.).
	0	−0·610	0	−3·23	0	+0·222	0
	5	−0·620	0·138	−3·17	−0·005	0·220	−0·034
	10	−0·631	0·281	−3·09	+0·002	0·209	−0·083
−2°	15	−0·618	0·454	−2·94	+0·014	0·197	−0·150
	20	−0·606	0·635	−2·74	+0·028	0·194	−0·217
	25	−0·589	0·823	−2·60	+0·019	0·126	−0·280
	30	−0·564	1·020	−2·38	−0·003	+0·039	−0·354
	35	−0·535	1·175	−2·15	+0·002	−0·051	−0·360
	0	−0·586	0	−4·13	0	0·158	0
	5	−0·598	0·140	−4·08	−0·003	0·146	−0·041
	10	−0·593	0·285	−3·99	+0·011	0·154	−0·092
0°	15	−0·590	0·460	−3·81	0·031	0·157	−0·157
	20	−0·564	0·633	−3·57	0·052	0·157	−0·223
	25	−0·556	0·830	−3·33	0·035	0·073	−0·293
	30	−0·538	1·025	−3·03	0·023	+0·002	−0·363
	35	−0·497	1·190	−2·74	0·036	−0·096	−0·385
	0	−0·506	0	−5·10	0	+0·085	0
	5	−0·506	0·133	−5·06	−0·005	0·096	−0·038
	10	−0·515	0·280	−4·96	+0·020	0·093	−0·091
+2°	15	−0·523	0·452	−4·70	0·043	0·092	−0·159
	20	−0·520	0·621	−4·44	0·071	0·093	−0·226
	25	−0·506	0·828	−4·14	0·062	+0·030	−0·298
	30	−0·489	1·020	−3·70	0·035	−0·063	−0·367
	35	−0·464	1·200	−3·41	0·051	−0·156	−0·392

The results of the observations are given in Table 10, and are shown graphically for zero angle of pitch in Fig. 118. The six curves, three for forces and three for moments, are rapidly divided into two groups according to whether they are symmetrical or assymetrical with respect to the vertical at zero yaw. In the symmetrical group are longitudinal force, normal force and pitching moment, whilst in the asymmetrical group are lateral force, rolling moment and pitching moment. It is for this reason that certain motions are spoken of as longitudinal or symmetrical, and others as lateral or asymmetrical, and corresponding with the distinction is the separation of two main types of stability.

Up to angles of yaw of ±20° it appears that longitudinal force and

pitching moment are little changed, whilst there is a drop in the numerical value of the normal force which indicates the necessity for increased speed to obtain the support necessary for steady asymmetrical flight.   Both lateral force and yawing moment are roughly proportional to angle of yaw, but the rolling moment is more variable in character.   From the figures of

Fig. 118.—Forces and moments on complete model aeroplane referred to body axes.

Table 10 it is possible to extract a great many of the fundamental derivatives required for the estimation of stability of non-symmetrical, but still rectilinear, flight.   Before developing the formulæ, however, one more example will be given dealing with the important properties of an aerofoil which are associated with a dihedral angle.

Forces and Moments due to a Dihedral Angle.—The aerofoil was of 3 ins. chord and 18 ins. span, with elliptical ends, the section being that of

R.A.F. 6. It was bent about two lines near the centre, the details being shown in Fig. 119. The origin of axes was taken as 0·07 in. above the chord and 1·40 ins. behind the leading edge, whilst the axis of X was parallel to the chord. In this case, therefore, angle of pitch and angle of incidence
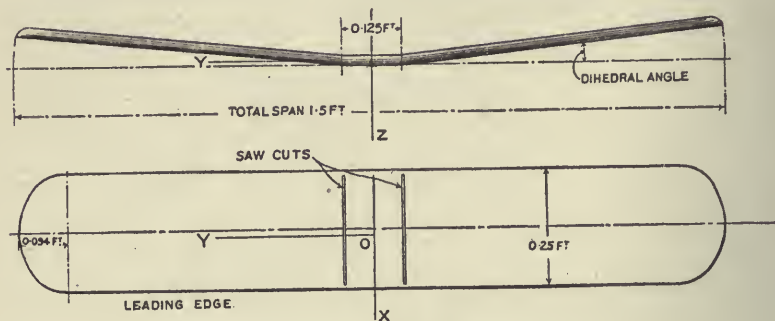
Fɪɢ. 119.—Model aerofoil with dihedral angle.

have the same meaning. Many observations were made, and from them has been extracted Table 11, which gives for one dihedral angle and several angles of pitch and yaw the three component forces and moments. Fig. 120, on the other hand, shows rolling moment only for variations of yaw, pitch and dihedral angle.

TABLE 11.

FORCES AND MOMENTS ON AN AEROFOIL HAVING A DIHEDRAL ANGLE OF 4°.

Angle of pitch, 0°.　Wind-speed, 40 feet per sec.

β (degrees).	mX (lbs.).	mY (lbs.).	mZ (lbs.).	L (lbs.-ft.).	M (lbs.-ft.).	N (lbs.-ft.).
0	−0·0161	0	−0·149	0	−0·0002	0
5	−0·0160	0·0023	−0·148	+0·0054	−0·0001	+0·0003
10	−0·0159	0·0044	−0·141	0·0096	0·0000	0·0005
15	−0·0153	0·0061	−0·134	0·0142	+0·0001	0·0007
20	−0·0150	0·0080	−0·125	0·0187	0·0004	0·0008
25	−0·0139	0·0098	−0·113	0·0224	0·0005	0·0008
30	−0·0131	0·0119	−0·098	0·0250	0·0007	0·0009
35	−0·0120	0·0128	−0·084	+0·0276	+0·0008	+0·0008

Angle of pitch, 5°.

0	+0·0133	0	−0·440	0	+0·0136	0
5	0·0131	0·0021	−0·438	+0·0045	0·0137	+0·0003
10	0·0126	0·0040	−0·429	0·0087	0·0131	0·0007
15	0·0111	0·0055	−0·406	0·0133	0·0128	0·0010
20	0·0103	0·0075	−0·385	0·0171	0·0120	0·0013
25	0·0092	0·0093	−0·357	0·0205	0·0113	0·0014
30	0·0079	0·0101	−0·327	0·0235	0·0101	0·0017
35	0·0059	0·0115	−0·287	+0·0262	+0·0088	+0·0018

TABLE 11—*continued*.

Angle of pitch, 10°.

0	+0·0667	0	−0·683	0	+0·0245	0
5	0·0666	0·0026	−0·679	+0·0052	0·0244	+0·0004
10	0·0647	0·0048	−0·664	0·0106	0·0239	0·0009
15	0·0613	0·0067	−0·633	0·0155	0·0229	0·0012
20	0·0575	0·0083	−0·601	0·0201	0·0214	0·0017
25	0·0528	0·0096	−0·560	0·0239	0·0200	0·0019
30	0·0464	0·0111	−0·505	0·0279	0·0178	0·0024
35	0·0404	0·0128	−0·454	+0·0306	+0·0157	+0·0027

Angle of pitch, 15°.

0	+0·1336	0	−0·821	0	+0·0329	0
5	0·1345	0·0019	−0·811	+0·0089	0·0331	+0·0003
10	0·1319	0·0035	−0·795	0·0172	0·0324	0·0009
15	0·1264	0·0050	−0·769	0·0258	0·0308	0·0011
20	0·1203	0·0057	−0·741	0·0338	0·0284	0·0015
25	0·1084	0·0068	−0·700	0·0408	0·0263	0·0022
30	0·0945	0·0075	−0·646	0·0480	0·0236	0·0029
35	0·0827	0·0081	−0·592	+0·0520	+0·0208	+0·0039

Angle of pitch, 20°.

0	+0·0395	0	−0·754	0	+0·0173	0
5	0·0415	0·0017	−0·754	+0·0194	0·0176	+0·0003
10	0·0424	0·0034	−0·755	0·0388	0·0177	0·0015
15	0·0456	0·0047	−0·757	0·0565	0·0180	0·0029
20	0·0503	0·0064	−0·750	0·0728	0·0172	0·0043
25	0·0542	0·0077	−0·736	0·0855	0·0186	0·0078
30	0·0573	0·0093	−0·715	0·0931	0·0187	0·0099
35	0·0599	0·0109	−0·687	+0·0958	+0·0188	+0·0126

The variation of longitudinal force with dihedral angle presents no point of importance except at high angles of incidence, where as usual the flow shows erratic features. Lateral force is, however, more regular and is roughly proportional both to the dihedral angle and the angle of yaw, and independent of the angle of incidence up to 20°. Its value is never so great as to give mY any marked importance in considering the motions of an aeroplane. Normal force shows no changes of importance even at large angles of incidence, whilst pitching moment is not strikingly affected by the dihedral angle except at the critical angle of incidence.

The most interesting property of the dihedral angle is the production of a rolling moment nearly proportional to itself and nearly independent of angle of incidence until the critical value is approached. This is most readily appreciated from Fig. 120, ordinates of which show the rolling moment in lbs.-feet on the model at a wind speed of 40 ft.-s. There is a small rolling couple for no dihedral angle at angles of incidence up to 10° and a considerable couple at 15° and 20°. At very large angles the effect of the dihedral angle has become reversed and is not the
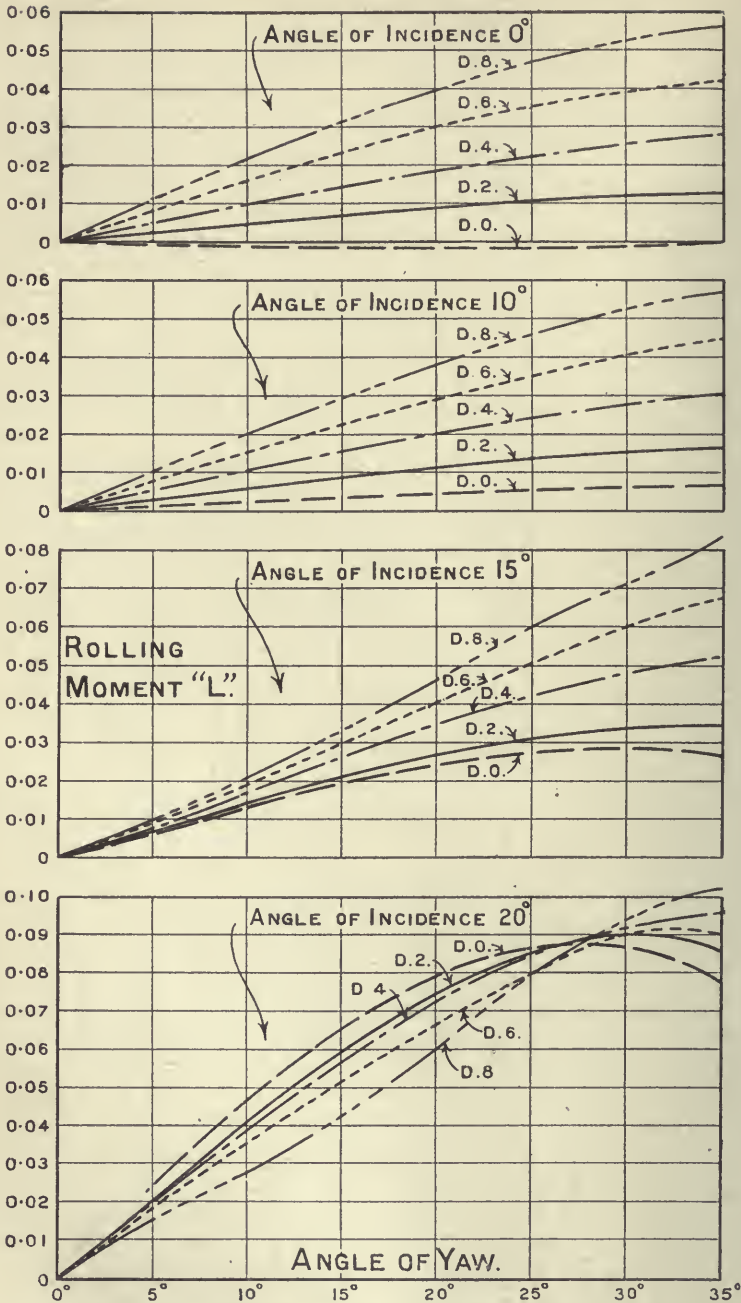
Fig. 120.—Rolling moments due to a dihedral angle on an aerofoil.

predominant effect. The general character of the curves will be found on inspection to be indicated by an element theory when it is realised that positive dihedral angle increases the angle of incidence on the forward wing.

Accompanying the rolling moment is a yawing moment of somewhat variable character, but in all cases appreciably dependent on the value of the dihedral angle. Much additional information will be found in Report No. 152 of the Advisory Committee for Aeronautics.

Changes of Axes and the Resolution of Forces and Moments.

(a) **Change of Direction without Change of Origin.**—Referring to Fig. 121, the axes to which the forces and moments were referred originally are denoted by GX_0, GY_0 and GZ_0, and it is desired to find the corresponding quantities for the axes GX, GY and GZ, which are related to them by the
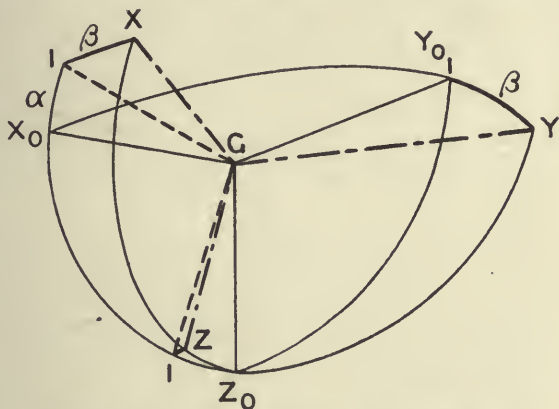
Fig. 121.—Change of direction of body axes.

rotation α about the axis GY_0 and β about GZ_0. These angles correspond exactly with those of pitch and yaw, the order being unimportant with the definitions given. The problem of resolution resolves itself into that of finding the cosines of the inclinations of the two sets of axes to each other, and the latter is a direct application of spherical trigonometry. The results are

$$\left. \begin{aligned} l_1 &\equiv \cos XGX_0 = \cos \alpha \cos \beta \\ m_1 &\equiv \cos XGY_0 = \cos \alpha \sin \beta \\ n_1 &\equiv \cos XGZ_0 = -\sin \alpha \end{aligned} \right\} \quad . \quad . \quad . \quad (2)$$

$$\left. \begin{aligned} l_2 &\equiv \cos YGX_0 = -\sin \beta \\ m_2 &\equiv \cos YGY_0 = \cos \beta \\ n_2 &\equiv \cos YGZ_0 = 0 \end{aligned} \right\} \quad . \quad . \quad . \quad (3)$$

$$\left. \begin{aligned} l_3 &\equiv \cos ZGX_0 = \sin \alpha \cos \beta \\ m_3 &\equiv \cos ZGY_0 = \sin \alpha \sin \beta \\ n_3 &\equiv \cos ZGZ_0 = \cos \alpha \end{aligned} \right\} \quad . \quad . \quad . \quad (4)$$

The formulae given in (2), (3) and (4) suffice to convert forces measured along wind axes to those along body axes. In converting from one set of body axes to another it will usually happen that β is zero, and the conversion is thereby simplified.

With the values given, the expressions for X, Y, Z, L, M, and N in terms of X_0, Y_0, Z_0, L_0, M_0 and N_0 are

$$\left.\begin{array}{l} X = l_1X_0 + m_1Y_0 + n_1Z_0 \\ Y = l_2X_0 + m_2Y_0 + n_2Z_0 \\ Z = l_3X_0 + m_3Y_0 + n_3Z_0 \end{array}\right\} \quad . \quad . \quad . \quad . \quad (5)$$

$$\left.\begin{array}{l} L = l_1L_0 + m_1M_0 + n_1N_0 \\ M = l_2L_0 + m_2M_0 + n_2N_0 \\ N = l_3L_0 + m_3M_0 + n_3N_0 \end{array}\right\} \quad . \quad . \quad . \quad . \quad (6)$$

(b) **Change of Origin without Change of Direction.**—If the original axes be X_0G_0, Y_0G_0 and Z_0G_0 of Fig. 122, and the origin is to be transferred
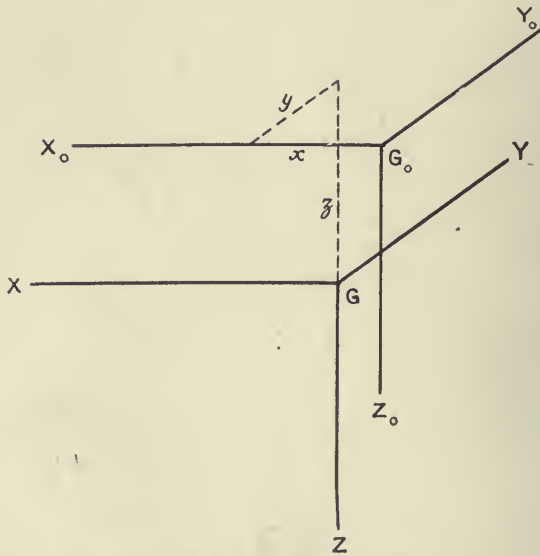
Fig. 122.—Change of origin of body axes.

from G_0 to G, the co-ordinates of the latter relative to the original axes being x, y and z, then

$$\left.\begin{array}{l} L = L_0 + mY_0 \cdot z - mZ_0 \cdot y \\ M = M_0 + mZ_0 \cdot x - mX_0 \cdot z \\ N = N_0 + mX_0 \cdot y - mY_0 \cdot x \end{array}\right\} \quad . \quad . \quad . \quad . \quad (7)$$

The forces are not affected by the change of origin. For changes both of direction and origin the processes are performed in two parts.

Formulae for Special Use with the Equations of Motion and Stability.

The equations of motion in general form do not contain the angles α and β explicitly, but obtain the equivalents from the components of velocity along the co-ordinate axes. The resultant velocity being denoted by V and the components along the axes of X, Y and Z by u, v and w, it will be seen from (2), (3) and (4) that

$$u = \mathrm{V} \cos \alpha \cos \beta, \quad v = -\mathrm{V} \sin \beta, \quad w = \mathrm{V} \sin \alpha \cos \beta \quad . \quad (8)$$

and the reciprocal relations are

$$\alpha = \tan^{-1} \cdot \frac{w}{u}, \quad \beta = -\sin^{-1} \frac{v}{\mathrm{V}}, \quad \mathrm{V} = \sqrt{u^2 + v^2 + w^2}. \quad . \quad (9)$$

By means of (8) and (9) it is not difficult to pass from the use of the variables V, α and β to u, v and w.

Stability as covered by the theory of small oscillations approximates to the value of forces and couples in the neighbourhood of a condition of equilibrium by using a linear law of variation with each of the variables. Mathematically the position is that any one of the quantities X . . . N is assumed to be of the form

$$\mathrm{X} = f_{\mathrm{X}}(u, \, v, \, w, \, p, \, q \, . \, r). \quad . \quad . \quad . \quad . \quad . \quad (10)$$

and certain values of u . . . r which will be denoted by the suffix zero give a condition of equilibrium. For the usual conditions applying to heavier-than-air craft it is assumed that X can be expanded in the form

$$\mathrm{X} = f_{\mathrm{X}}(u_0, \, v_0, \, w_0, \, p_0, \, q_0, \, r_0)$$
$$+ \delta u \frac{\partial f}{\partial u} + \delta v \frac{\partial f}{\partial v} + \delta w \frac{\partial f}{\partial w} + \delta p \frac{\partial f}{\partial p} + \delta q \frac{\partial f}{\partial q} + \delta r \frac{\partial f}{\partial r} \quad . \quad . \quad (11)$$

The quantities $\frac{\partial f}{\partial u}$, etc., are called resistance derivatives and denoted by X_u, etc. As the aerodynamic data usually appear in terms of V, α and β, it is convenient to deduce the derivatives from the original curves, and this is possible (for the cases in which p, q and r are zero) by means of the standard formulae below :—

$$
\left.
\begin{aligned}
\frac{\partial \alpha}{\partial u} &= -\frac{1}{\mathrm{V}} \frac{\sin \alpha}{\cos \beta} \\
\frac{\partial \beta}{\partial u} &= -\frac{1}{\mathrm{V}} \cos \alpha \sin \beta \\
\frac{\partial \mathrm{V}}{\partial u} &= \cos \alpha \cos \beta
\end{aligned}
\right\} v \text{ and } w \text{ constant } . \quad (12)
$$

$$\frac{\partial \alpha}{\partial v} = 0$$

$$\frac{\partial \beta}{\partial v} = -\frac{1}{V} \cos \beta \left. \right\} u \text{ and } w \text{ constant} \quad . \quad (13)$$

$$\frac{\partial V}{\partial v} = -\sin \beta$$

$$\frac{\partial \alpha}{\partial w} = \frac{1}{V} \cdot \frac{\cos \alpha}{\cos \beta}$$

$$\frac{\partial \beta}{\partial w} = -\frac{1}{V} \sin \alpha \sin \beta \left. \right\} u \text{ and } v \text{ constant} \quad . \quad (14)$$

$$\frac{\partial V}{\partial w} = \sin \alpha \cos \beta$$

From the experimental side it is known that

$$X = V^2 F_x(\alpha \cdot \beta) \quad . \quad . \quad . \quad . \quad . \quad . \quad (15)$$

and by differentiation

$$X_u \equiv \frac{\partial X}{\partial u} = 2V \frac{\partial V}{\partial u} F_x + V^2 \frac{\partial F_x}{\partial \alpha} \cdot \frac{\partial \alpha}{\partial u} + V^2 \frac{\partial F_x}{\partial \beta} \cdot \frac{\partial \beta}{\partial u}$$

$$= 2V \cos \alpha \cos \beta \cdot F_x - V \frac{\sin \alpha}{\cos \beta} \cdot \frac{\partial F_x}{\partial \alpha} - V \cos \alpha \sin \beta \frac{\delta F_x}{\partial \beta} \quad . \quad (16)$$

with similar relations for the other quantities, so that

$$\frac{1}{V} X_u = 2 \cos \alpha \cos \beta \frac{X}{V^2} - \frac{\sin \alpha}{\cos \beta} \cdot \frac{\partial F_x}{\partial \alpha} - \cos \alpha \sin \beta \frac{\partial F_x}{\partial \beta}$$

$$\frac{1}{V} Y_u = \quad ,, \quad \frac{Y}{V^2} \quad ,, \quad \frac{\partial F_Y}{\partial \alpha} \quad ,, \quad \frac{\partial F_Y}{\partial \beta}$$

$$\frac{1}{V} Z_u = \quad ,, \quad \frac{Z}{V^2} \quad ,, \quad \frac{\partial F_Z}{\partial \alpha} \quad ,, \quad \frac{\partial F_Z}{\partial \beta}$$

$$\frac{1}{V} L_u = \quad ,, \quad \frac{L}{V^2} \quad ,, \quad \frac{\partial F_L}{\partial \alpha} \quad ,, \quad \frac{\partial F_L}{\partial \beta}$$

$$\frac{1}{V} M_u = \quad ,, \quad \frac{M}{V^2} \quad ,, \quad \frac{\partial F_M}{\partial \alpha} \quad ,, \quad \frac{\partial F_M}{\partial \beta} \left. \right\} \quad . \quad (17)$$

$$\frac{1}{V} N_u = \quad ,, \quad \frac{N}{V^2} \quad ,, \quad \frac{\partial F_N}{\partial \alpha} \quad ,, \quad \frac{\partial F_N}{\partial \beta}$$

$$\frac{1}{V} X_v = -2 \sin \beta \frac{X}{V^2} - \cos \beta \frac{\partial F_x}{\partial \beta}$$

$$. \quad . \quad . \quad . \quad . \quad . \quad . \quad . \quad . \quad . \quad . \quad . \quad .$$

$$\frac{1}{V} X_w = 2 \sin \alpha \cos \beta \frac{X}{V^2} + \frac{\cos \alpha}{\cos \beta} \cdot \frac{\partial F_x}{\partial \alpha} - \sin \alpha \sin \beta \frac{\partial F_x}{\partial \beta}$$

$$. \quad . \quad . \quad . \quad . \quad . \quad . \quad . \quad . \quad . \quad . \quad . \quad .$$

From the formula given in (17) it is possible to use aerodynamic data in the form in which they are usually presented. An alternative method is to use equations (8) to replot the observations with u, v and w as variables, but this is not convenient except when $\beta = 0$.

For airships and lighter-than-air craft in general, the quantities have a more complex form; for stability it is necessary to assume that

$$X = f_x(u,\ v,\ w,\ p,\ q,\ r,\ \dot{u},\ \dot{v},\ \dot{w},\ \dot{p},\ \dot{q},\ \dot{r}) \quad . \quad . \quad . \quad (18)$$

and a new series of derivatives are introduced which depend on the accelerations of the craft. Some little work has been carried out in the determination of these derivatives, but the experimental work is still in its infancy.

Examples of derivatives both for linear and angular velocities will be found in the chapter on stability, whilst a theory of elements which goes far towards providing certain of the quantities is developed in Chapter V.

CHAPTER V

AERIAL MANOEUVRES AND THE EQUATIONS OF MOTION

The conditions of steady flight of aircraft have been dealt with in considerable detail in Chapter II., where the equations used were simple because of the simplicity of the problem. When motions such as looping, spinning and turning are being investigated, or even the disturbances of steady motion, a change of method is found to be desirable. The equations of motion now introduced are applicable to the simplest or the most complex problems yet proposed. Evidence of an experimental character has been accumulated, and apparatus now exists which enables an analysis of aerial movements to be made. The number of records taken is not yet great, but is sufficiently important to introduce the subject of the calculation of the motion of an aeroplane during aerial manoeuvres. After a brief description of these records the chapter proceeds to formulate the equations of motion and to apply them to an investigation of some of the observed motions of aeroplanes in flight.

Looping.—In making a loop, the first operation is to dive the aeroplane in order to gain speed. An indicated airspeed of 80–100 m.p.h. is usually sufficient, but at considerable heights it should be remembered that the real speed is greater than the airspeed. Since the air forces depend on indicated airspeed and the kinetic energy on real speed through the air, it will be obvious that the rule which fixes the airspeed is favourable to looping at considerable heights. Having reached a sufficient speed in the dive the control column is pulled steadily back as far as it will go, and this would be sufficient for the completion of a loop. The pilot, however, switches off his engine when upside down, and makes use of his elevator to come out of the dive gently. Not until the airspeed is that suitable for climbing is the engine restarted.

In looping aeroplanes which have a rotary engine it may be necessary to use considerable rudder to counteract gyroscopic couples. The effect of the airscrew is felt in all aeroplanes, and unless the rudder is used the loop is imperfect in the sense that the wings do not keep level.

The operation of looping is subject to many minor variations, and until the pilot's use of the elevator and engine during the motion is known it is not possible to apply the methods of calculation in strictly comparative form. A full account of the calculation is given a little later in the chapter, and from it have been extracted the particulars which would be expected from instruments used in flight. The instruments were supposed to consist of a recording speed meter and a recording accelerometer. Both have

been referred to in Chapter III., but it may perhaps be recalled here that the latter gives a measure of the air forces on the aeroplane. The accelerometer is a small piece of apparatus which moves with the aeroplane; the moving part of it, which gives the record, has acting on it the force of gravity and any forces due to the accelerations of its support. It is therefore a mass which takes all the forces on the aeroplane proportionally except those due to the air. The differential movement of this small mass and the large mass of the aeroplane depends only on the air force along its axis. For complete readings three accelerometers would be required with their axes mutually perpendicular. In practice only one has been used, with its axis approximately in the direction of lift in steady flight, and the acceleration measured in units of g has been taken as a measure of the increase of wing loading.

Speed and Loading Records in a Loop.—Fig. 123 shows a record of the true speed of an aeroplane during a loop, with a corresponding diagram
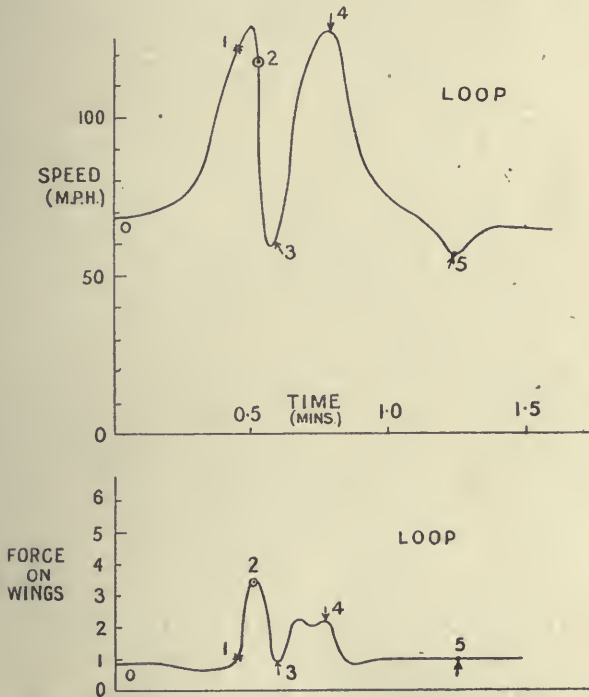
FIG. 123.—Speed and force on wings during a loop (observed).

for the force on the wings. The time scale for the two curves is the same and corresponding points on the diagrams have been marked for ease of reference. The preliminary dive from 0 to 1 takes nearly half a minute, during which time the force on the wings was reduced because of the inclination of the path. At 1 the pilot began to pull back the stick, with an increase in the force on the wings to $3\frac{1}{2}$ times its usual value within 5

or 6 secs. Whilst this force was being developed the speed had scarcely changed. Between 2 and 3 the aeroplane was climbing to the top of the loop with a rapid fall of force on the wings. From 3 to 4 the recovering dive was taking place with a small increase of force on the wings, after which, 4 to 5, the aeroplane was flattened out and level flight resumed. The two depressions, just before 4 on the force diagram and at 5 in the speed diagram, probably correspond with switching the engine off and on.

The calculated speed and loading during a loop are shown in Fig. 124, the
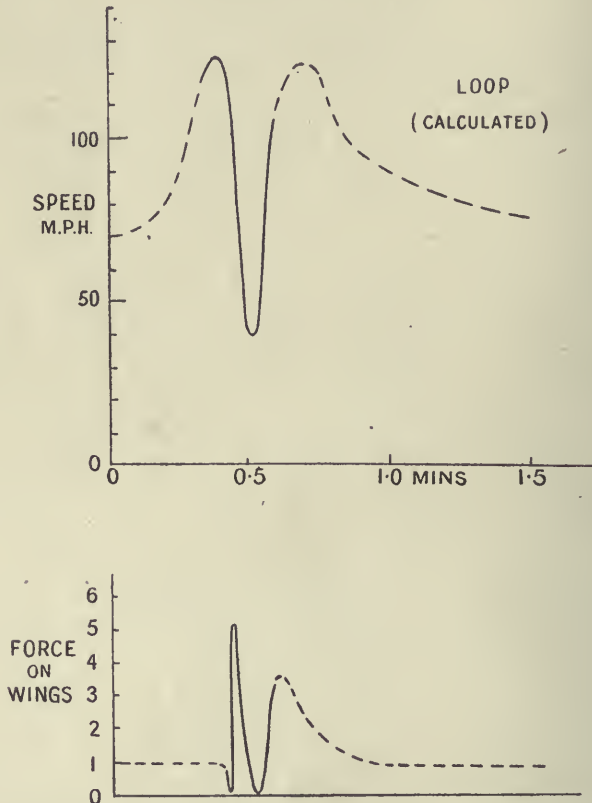
Fig. 124.—Speed and force on wings during a loop (calculated).

important period of ten seconds being shown by the full lines. The dotted extensions depend very greatly on what the pilot does with the controls, and are of little importance in the comparison. The main features of the observed records are seen to be repeated, the general differences indicating the advantage of an intelligent use of the elevator in reducing the peaks of stress over that of the rigid manoeuvre assumed in the calculations. It will be found when considering the calculation that any use of the elevator can be readily included and the corresponding effects on the loop and stresses investigated in detail.

The conclusion that looping is a calculable motion within the reach of existing methods is important, and when it has been shown that spinning is also a calculable motion of a similar nature the statement appears to be justified that no movement of an aeroplane is so extreme that the main features cannot be predicted beforehand by scientific care in collecting aerodynamic data and sufficient mathematical knowledge to solve a number of simultaneous differential equations.

Dive.—Fig. 125 shows a dive on the same machine from which the loop record was obtained. At a time on the record of about 10 secs. a perceptible fall in force on the wings was registered due to the movement of the elevator which put the nose of the aeroplane down. The change of angular velocity
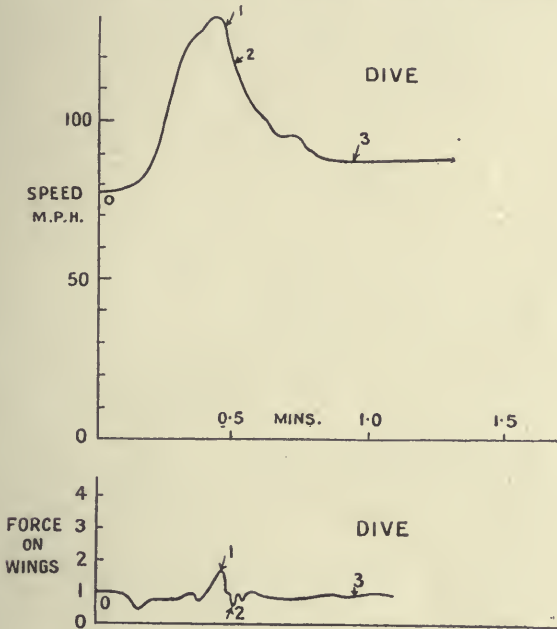
FIG. 125.—Speed and force on wings during a dive.

near 1 was less rapid than in the loop, and the force on the wings was correspondingly reduced. The stresses in flattening out were quite small, and the worst of the manoeuvre only lasted for two or three seconds. The record shows quite clearly the possibility of considerable changes of speed with inconsiderable stresses, and indicates the value of " light hands " when flying. The pilot is a natural accelerometer and uses the pressure on his seat as an indicator of the stresses he is putting on the aeroplane. An increase of weight to four times normal value produces sensations which cannot be missed in the absence of excitement due to fighting in the air. On the other hand, incautious recovery from a steep dive introduces the most dangerous stresses known in aerial manoeuvres.

Spinning.—To spin an aeroplane the control column is pulled fully back

with the engine off. As flying speed is lost the rudder is put hard over in the direction in which the pilot wishes to spin. So long as the controls are held, particularly so long as the column is back, the aeroplane will continue to spin. To recover, the rudder is put central and the elevator either central or slightly forward, the spinning ceases and leaves the aeroplane in a nose dive from which it is flattened out.

Spinning has been studied carefully both experimentally and theoretically. It provides a simple means of vertical descent to a pilot who is not apt to become giddy. There is evidence to show that the manoeuvre is not universally considered as comfortable, in sharp contrast to looping which has far less effect on the feelings of the average pilot.

Force and Speed Records in a Spin.—At " 0," Fig. 126, the aeroplane was flying at 70 m.p.h. and the stick being pulled back. The speed fell
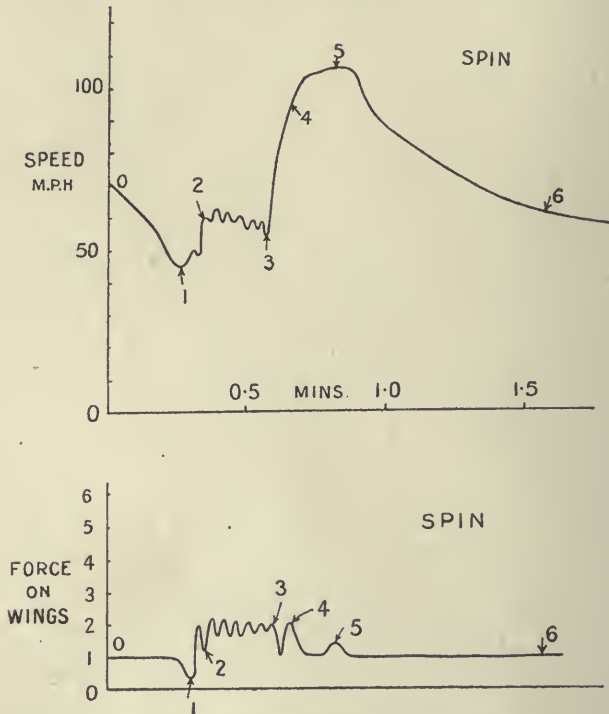
Fig. 126.—Speed and force on wings during spinning.

rapidly, and at 1 the aeroplane had stalled and was putting its nose down rapidly. This latter point is shown by the reduction of air force on the wings. The angle of incidence continued to increase although the speed was rising, and at 2 the spin was fully developed. The body is then usually inclined at an angle of 70°-80° to the horizontal, and is rotating about the vertical once in every 2 or 2½ secs. The rotation is not quite regular, as will be seen from both the velocity and force diagrams, but has a

nutation superposed on the average speed. There is no reason to suppose that the period of nutation is the period of spin.

At 3 the rudder was centralised and the stick put slightly forward, and almost immediately flattening out began as shown by the increased force at 4. The remainder of the history is that of a dive, the flattening out having been accelerated somewhat at 5.

It has been shown by experiments on models that stalling of an aeroplane automatically leads to spinning, and that the main feature of the phenomenon is calculable quite simply.

Roll (Fig. 127).—The record of position of an aeroplane shown in Fig. 127 was taken by cinema camera from a second aeroplane. Mounted in the rear cockpit, the camera was pointed over the tail of the camera aeroplane towards that photographed. The camera aeroplane was flown carefully in a straight line, but the camera was free to pitch and to rotate about a vertical axis. For this reason the pictures are not always in the centre of the film. In discussing the photographs, which were taken at intervals of about $\frac{1}{4}$ sec., it is illuminating to use at the same time a velocity and force record (Fig. 128), although it does not apply to the same aeroplane.

Fig. 127.—Photographic records of rolling.

Photograph 1 shows the aeroplane flying steadily and on an even keel some distance above the camera. The speed would be about 90 m.p.h., *i.e.* just before 1 on the speed chart. The second photograph shows the beginning of the roll, which is accompanied by an increase in the angle of incidence. The latter point is shown by the increased length of projection of the body as well as by peak 1 in the force diagram. Both roll and pitch are increased in the next interval, with a corresponding fall of speed. At four the bank is nearly 90° and the pitch is slightly reduced. The vertical bank is therefore reached in a little more than a second.

Once over the vertical the angle of incidence (or pitch) is rapidly reduced, and as the speed is falling rapidly the total air force on the wings falls until the aeroplane is upside down after rather more than $1\frac{1}{2}$ secs. At about this period the force diagram shows a negative air force on the wings, and unless strapped in the pilot would have left his seat. This negative air force does not always occur during a roll, and is avoided by maintaining the angle of incidence at a high value for a longer time. The pilot tends to fall with an acceleration equal to g, but if a downward air force occurs on the wings of the aeroplane it tends to fall faster than the pilot, and therefore maintains the pressure on his seat. This more usual condition in a roll involves as a consequence a very rapid fall when the aeroplane is upside

down. The most noticeable feature of the remaining photographs is the fact that the pilot is holding up the nose of the aeroplane by the rudder, a manoeuvre accompanied by vigorous side slipping. As the angle of incidence is now normal, the speed picks up again during the recovery of an even keel. The manoeuvres after 3, Fig. 128, are those connected with flattening out, and occur subsequently to the roll. The complete roll takes rather less than four seconds for completion.

The roll may be carried out either with or without the engine, and except for speed the manoeuvres are the same as for a spin, *i.e.* the stick is pulled back and the rudder put hard over. The angle is never reduced to that for stalling, and this is the essential aerodynamic difference from spinning.
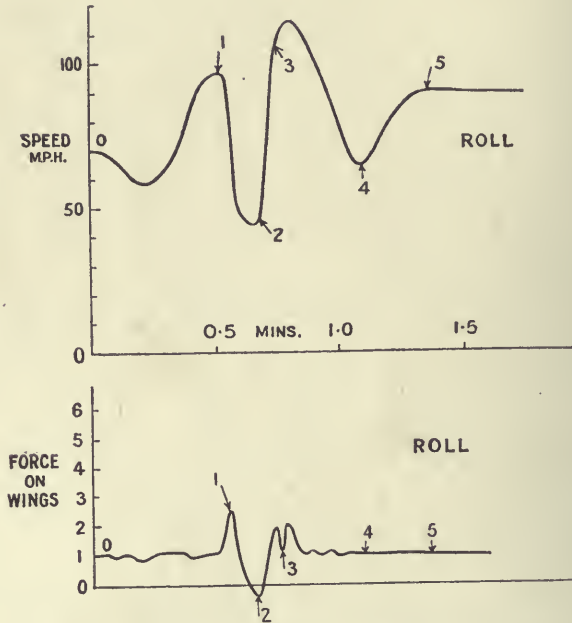
Fig. 128.—Speed and force on wings during a roll.

The photographs show that these simple instructions are supplemented by others at the pilot's discretion, and that the aerodynamics of the motion is very complex.

Equations of Motion.—In dealing with the more complex motions of aircraft it is found to be advantageous to follow some definite and comprehensive scheme which will cover the greater part of the problems likely to occur. Systems of axes and the corresponding equations of motion are to be found in advanced books on dynamics, and from these are selected the particular forms relating to rigid bodies.

An aeroplane can move freely in more directions than any other vehicle; it can move upwards, forwards and sideways as well as roll, pitch and turn. The generality of the possible motions brings into prominence the value to

the aeronautical engineer of the study of three-dimensional dynamics, and furnishes him with an unlimited series of real problems.

The first impression received on looking at the systems of axes and equations is their artificial character. A body is acted on by a resultant force and a resultant couple, and to express this physical fact with precision six quantities are used as equivalents. Attempts have been made to produce a mathematical system more directly related to physical conceptions, but co-ordinate axes have survived as the most convenient form known to us of representing the magnitudes and directions of forces and couples and more generally the quantities concerned with motion.

Of the various types of co-ordinate axes of value, reference in this book is made only to rectilinear orthogonal axes. Some use of them has been made in the last chapter, where it was shown that experimental results are equally conveniently expressed in any arbitrarily chosen form of such axes. If, therefore, it appears from a study of the motion of aircraft that some particular form is more advantageous than another, there is no serious objection on other grounds to its use.

It happens that for symmetrical steady flight, the only point of importance in the choice of the axes required, is that the origin should be at the centre of gravity in order to separate the motions of translation and rotation. For circling flight, in which the motion is not steady, it saves labour in the calculation of moments of inertia and the variations of them if the axes are fixed in the aircraft and rotate with it. A further simplification occurs if the body axes are made to coincide with the principal axes of inertia. Some of these points will be enlarged upon in connection with the symbolical notation, but for the moment it is desired to draw attention to the different sets of axes required in aeronautics and allied subjects.

Choice of Co-ordinate Axes.—The first point to be borne clearly in mind is the relative character of motion. Two bodies can have motion relative to each other which is readily appreciated, but the motion of a single body has no meaning. In general, therefore, the simplest problems of motion involve the idea of two sets of co-ordinate axes, one fixed in each of the two bodies under consideration. The introduction of a third body brings with it another set of axes. In the case of tests on a model in a wind channel it has been seen that one set of axes was fixed to the channel and another to the model. The relation of the two sets was defined by the angles of pitch and yaw α and β, whilst the forces and couples were referred to either set of axes without loss of generality. Instead of the angles of pitch and yaw the relative positions of the axes could, as already indicated in Chapter IV., have been defined by the direction cosines of the members of one set relative to the other, and for many purposes of resolution of forces and couples this latter form has great advantages over the former. Both are sufficiently useful for retention and a table of equivalents was given in the treatment of the subject of the preparation of design data.

The relation between the positions of the axes of two bodies is affected and changed by forces and couples acting between them or between them and some third body, and only when the whole of the forces concerned in the motion of a particular system of bodies have been included and related

to their respective axes is the statement of the problem complete. As an example consider the flight of an aeroplane : the forces and couples on it depend on the velocities, linear and angular, through the air, and hence two sets of axes are here required, one in the aeroplane and the other in the air. The weight of the aeroplane brings in forces due to the earth, and hence earth axes. In the rare cases in which the rotation of the earth is considered, a fourth set of axes fixed relative to the stellar system would be introduced, and so on.

The statement of a problem prior to the application of mathematical analysis requires a knowledge of the forces and couples acting on a body for all positions, velocities, accelerations, etc., relative to every other body concerned. This data is usually experimental and has some degree of approximation which is roughly known. By accepting a lower degree of precision one or more sets of axes may be eliminated from the problem, with a corresponding simplification of the mathematics. This step is the justification for ignoring the effect of the earth's rotation in the usual estimation of the motion of aircraft.

A further simplification is introduced by the neglect of the variations of gravitational attraction with height and with position on the earth's surface, the consequence of which is that the co-ordinates of the centre of gravity of an aeroplane do not appear in the equations of motion of aircraft in still air. The angular co-ordinates appear on account of the varying components of the weight along the axes as the aircraft rolls, pitches and turns. In considering gusts and their effects it will be found necessary to introduce linear co-ordinates either explicitly or implicitly.

The forces on aircraft due to motion relative to the air depend markedly on the height above the earth, and of recent years considerable importance has attached to the fact. The vertical co-ordinate, however, rarely appears directly, the effect of height being represented by a change in the density ρ, and here again the approximation often suffices that ρ is constant during the motions considered. Apart from this reservation the air forces on an aircraft depend only on the relative motion, and advantage is taken of this fact to use a special system of axes. At the instant at which the motion is being considered the body axes of the aircraft have a certain position relative to the air, and the air axes are taken to momentarily coincide with them. The rate of separation of the two sets of axes then provides the necessary particulars of the relative motion.

The equations of motion which cover the majority of the known problems require the use of three sets of axes as follows :—

(1) Axes fixed in the aircraft. " Body axes." For convenience the origin of these is taken at the centre of gravity, and the directions are made to coincide with the principal axes of inertia. The latter point is far less important than the former.

(2) Axes fixed in the air. " Air axes." Instantaneously coincident with the body axes. In most cases the air is supposed still relative to the earth.

(3) Axes fixed in the earth. " Earth axes."

The angular relations between the axes defined in (1) and (2) have

already been referred to (Chapter IV., page 237), as angles of pitch and yaw; also by means of direction cosines and the component velocities u, v and w. The corresponding relations between (1) and (3) are required; the angles being denoted by θ, ϕ and ψ the aeroplane is put into the position defined by these angles by first placing the body and earth axes into coincidence, and then

(a)   rotating the aircraft through an angle ψ about the Z axis of the aircraft;

(b) then   ,,   ,,   ,,   ,, θ about the new position of the Y axis of the aircraft;

and (c) finally   ,,   ,,   ,,   ,, ϕ about the new position of the X axis of the aircraft.

The angles ψ, θ and ϕ are spoken of as angles of yaw, pitch and roll respectively, and the double use of the expressions " angle of yaw " and " angle of pitch " should be noted. Confusion of use is not seriously incurred since the angles α and β do not occur in the equations of motion, but are represented by the component velocities of the resultant relative wind. That is, the quantities V, α and β of the aerodynamic measurements are converted into u, v and w before mathematical analysis is applied.

With these explanations the equations of motion of a rigid body as applied to aircraft are written down and described in detail :—

$$\left.\begin{array}{l} m\{\dot{u} + wq - vr\} = m\mathrm{X}' \quad \ldots \quad 1u \\ m\{\dot{v} + ur - wp\} = m\mathrm{Y}' \quad \ldots \quad 1v \\ m\{\dot{w} + vp - uq\} = m\mathrm{Z}' \quad \ldots \quad 1w \\ \dot{h}_1 - rh_2 + qh_3 = \mathrm{L}' \quad \ldots \ldots \quad 1p \\ \dot{h}_2 - ph_3 + rh_1 = \mathrm{M}' \quad \ldots \ldots \quad 1q \\ \dot{h}_3 - qh_1 + ph_2 = \mathrm{N}' \quad \ldots \ldots \quad 1r \end{array}\right\} \quad \ldots \quad \ldots \quad (1)$$

where

$$\left.\begin{array}{l} h_1 = p\mathrm{A} - q\mathrm{F} - r\mathrm{E} \\ h_2 = q\mathrm{B} - r\mathrm{D} - p\mathrm{F} \\ h_3 = r\mathrm{C} - p\mathrm{E} - q\mathrm{D} \end{array}\right\} \quad \ldots \quad \ldots \quad (2)$$

In these equations m is the mass of the aircraft, whilst A, B, C, D, E and F are the moments and products of inertia. All are experimental and depend on a knowledge of the distribution of matter throughout the aircraft. The quantities $m\mathrm{X}'$, $m\mathrm{Y}'$, $m\mathrm{Z}'$, L', M' and N' are the forces and couples on the aircraft from all sources, and one of the first operations is to divide them into the parts which depend on the earth and those which arise from motion relative to the air. The remaining quantities, u, v, w, p, q, and r define the motion of the body axes relative to the air axes. The equations are the general series applicable to a rigid body, and only the description is limited to aircraft.

The quantities m. A . . . F are familiar in dynamics and do not

need further attention except to note that D and F are zero from symmetry. It has already been shown how the parts of $X'-N'$ which depend on motion relative to the air are measured in a wind channel in terms of u, v and w, p, q and r.[1]

It now remains to determine the components of gravitational attraction. A little thought will show that the component parts of the weight along the body axes are readily expressed in terms of the direction cosines of the downwardly directed vertical relative to the axes. Rotation about a vertical axis through an angle ψ has no effect on these direction cosines, and the only angles which need be considered are θ and ϕ as illustrated in Fig. 129. The earth axes are GX_0, GY_0 and GZ_0, and before rotation the body axes GX, GY and GZ are supposed to coincide with the former.
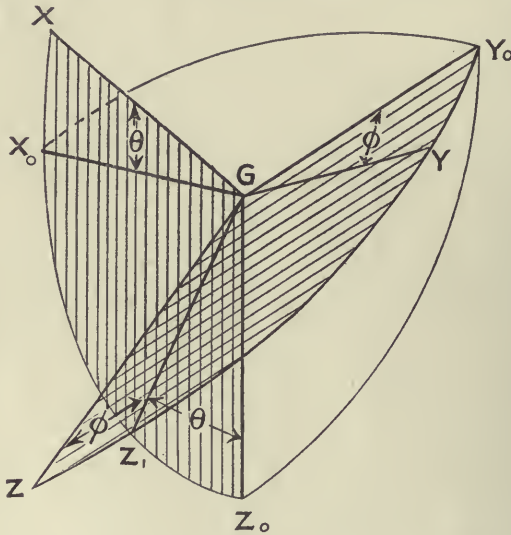
Fig. 129.—Inclinations of an aeroplane to the earth.

Rotation through an angle θ about GY_0 brings X_0 to X and Z_0 to Z_1, whilst a subsequent rotation through an angle ϕ about GX brings Y_0 to Y and Z_1 to Z, and the body axes are now in the position defined by θ and ϕ. The direction cosines of GZ_0 relative to the body axes are

$$\left.\begin{aligned} n_1 &\equiv \cos XGZ_0 = -\sin\theta \\ n_2 &\equiv \cos YGZ_0 = \cos\theta\sin\phi \\ n_3 &\equiv \cos ZGZ_0 = \cos\theta\cos\phi \end{aligned}\right\} \quad . \quad . \quad . \quad (3)$$

and the components of the weight are mg times the corresponding direction cosines. The symbols n_1, n_2 and n_3 have often been used to denote the longer expressions given in (3). The first example of calculation from the equations of motion will be that of the looping of an aeroplane, and con-

[1] The experimental knowledge of the dependence of $X'-N'$ on angular velocities relative to the air is not yet sufficient to cover a wide range of calculation.

siderable simplification occurs as a result of symmetry about a vertical plane.

The Looping of an Aeroplane.—The motion being in the plane of symmetry leads to the mathematical conditions

$$v = 0 \qquad r = 0 \qquad p = 0 \qquad \phi = 0 \quad . \quad . \quad . \quad (4)$$
$$Y' = 0 \qquad L' = 0 \qquad N' = 0 \quad . \quad . \quad . \quad . \quad . \quad (5)$$

and equations (1) and (2) become

$$\left. \begin{aligned} \dot{u} + wq &= X' \\ \dot{w} - uq &= Z' \\ \dot{q}B &= M' \end{aligned} \right\} \quad . \quad . \quad . \quad . \quad . \quad . \quad (6)$$

Making use of equations (3) to separate the parts of X' which depend on gravity from those due to motion through the air converts (6) to

$$\left. \begin{aligned} \dot{u} + wq &= -g \sin\theta + X \\ \dot{w} - uq &= g \cos\theta + Z \\ \dot{q}B &= M \end{aligned} \right\} \quad . \quad . \quad . \quad . \quad (7)$$

where X, Z and M now refer only to air forces. X depends on the airscrew thrust as well as on the aeroplane, and the variation for the aeroplane with u and w is found in a wind channel in the ordinary way. The dependence of X on q is so small as to be negligible. If the further assumption be made that the airscrew thrust always acts along the axis of X, a simple form is given to Z which then depends on the aeroplane only. The component of Z due to q is appreciable and arises from the force on the tail due to pitching. The pitching moment M also depends appreciably on u, w and q, and the assumption is made that the effects due to q are proportional to that quantity, and that the parts dependent on u and w are not affected by pitching. Looping is not a definite manoeuvre until the motion of the elevator and the condition of the engine control are specified, and more detailed experimental data can always be obtained as the requirements of calculation become more precise. The general method of calculation is unaffected by the data, and those given below may be taken as representative of the main forces and couples acting on an aeroplane during a loop.

Fig. 130 shows the longitudinal force on an aeroplane without airscrew, the value of the force in pounds having been divided by the square of the speed in feet per second before plotting the curves. The abscissa is $\dfrac{w}{V}$, i.e. the ratio of the normal to the resultant velocity. This ratio is equal to $\sin \alpha$, where α is the angle of pitch as used in a wind channel, and no difficulty will be experienced in producing similar figures from aerodynamical data as usually given. The aeroplane to which the data refers may be taken as similar to that illustrated in Fig. 94, Chapter IV. Details of weight and moments of inertia are given later.

The corresponding values of normal force are shown in Fig. 131. The separate curves show that aeroplane characteristics appreciably depend on the position of the elevators. The thrust of the airscrew is given in

Fig. 132 and is shown as dependent only on the resultant velocity of the

$$\frac{m X_1}{V^2} \equiv \frac{\text{LONGITUDINAL FORCE } \textit{in lbs.}}{\textit{Square of Speed in ft/sec}}$$

ELEVATOR ANGLE
0° -10° & -15°
+10°
-30°
+30°

w/V
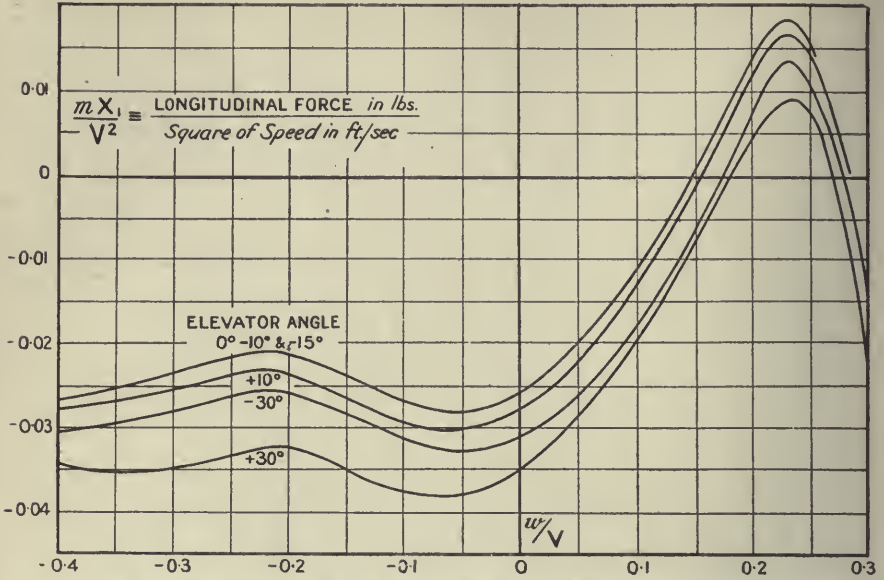
FIG. 130.—Longitudinal force on an aeroplane without airscrew due to inclination to the relative wind.

$$\frac{m Z_1}{V^2} \equiv \frac{\text{NORMAL FORCE } \textit{in lbs.}}{\textit{Square of speed in ft./sec.}}$$

-30°
-10°
0°
+10°
+30°

w/V
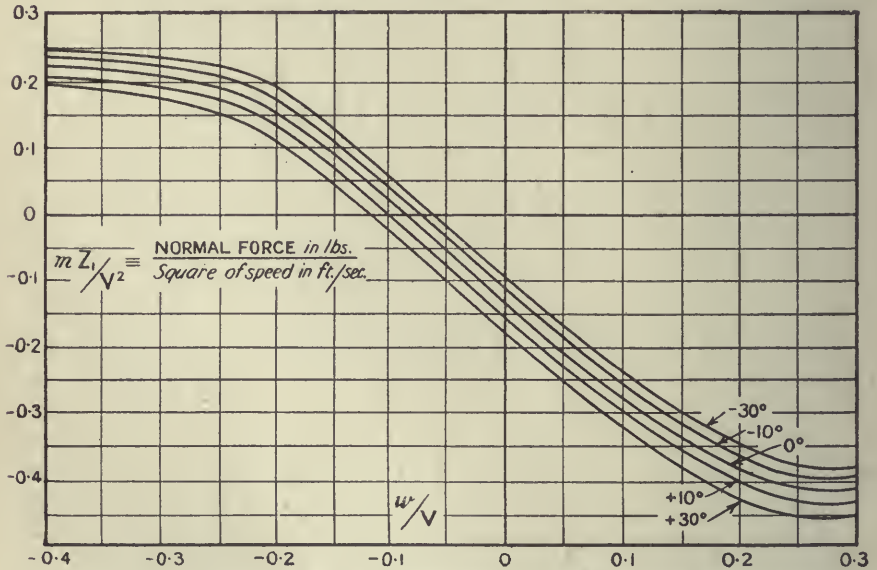
FIG 131 —Normal force on an aeroplane due to inclination to the relative wind.

aeroplane, and here a careful student will see that the representation can only be justified as a good approximation in the special circumstances

The chief items in pitching moment are illustrated by the curves of Figs. 133 and 134, of which the former relates to variation with angle of incidence, and the latter to variation with the angular velocity of pitching. Since the couple due to pitching arises almost wholly from the tail, a simple approximation allows for the change of force due to pitching. If l be
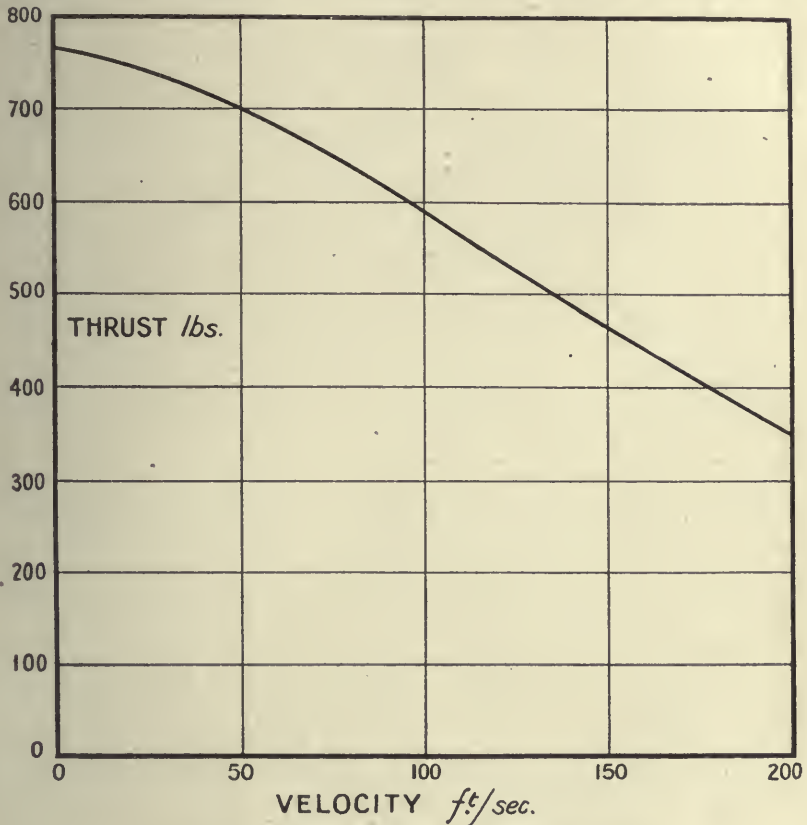
FIG. 132.—Airscrew thrust and aeroplane velocity.

the distance from the centre of gravity of the aeroplane to the centre of pressure of the tail, the equation

$$m \cdot l \cdot Z_q = M_q \quad . \quad . \quad . \quad . \quad . \quad . \quad (8)$$

can be seen to express the above idea that the tail is the only part of the aeroplane which is effective in producing changes due to pitching.

With the aerodynamic data in the form given, equations (7) are conveniently rewritten as

$$\dot{} = -wq - g \sin \theta + \frac{mX_1}{V^2} \cdot \frac{V^2}{m} + \frac{T}{m} \cdot \quad . \quad . \quad . \quad . \quad (9)$$

$$\dot{w} = uq + g \cos \theta + \frac{mZ_1}{V^2} \cdot \frac{V^2}{m} + \frac{M_q}{V} \cdot \frac{qV}{ml} \quad . \quad . \quad (10)$$

$$\dot{q} = \frac{M_1}{V^2} \cdot \frac{V^2}{B} + \frac{M_q}{V} \cdot \frac{qV}{B} \quad . \quad . \quad . \quad . \quad . \quad (11)$$

These equations show the changes of u, w and q with time for any given conditions of motion, and enable the loop to be calculated from the initial conditions by a step to step process. The initial conditions

$$\frac{M_1}{V^2} \equiv \frac{\text{PITCHING MOMENT } in\ lbs.ft}{\text{Square of speed } in\ ft/sec}$$
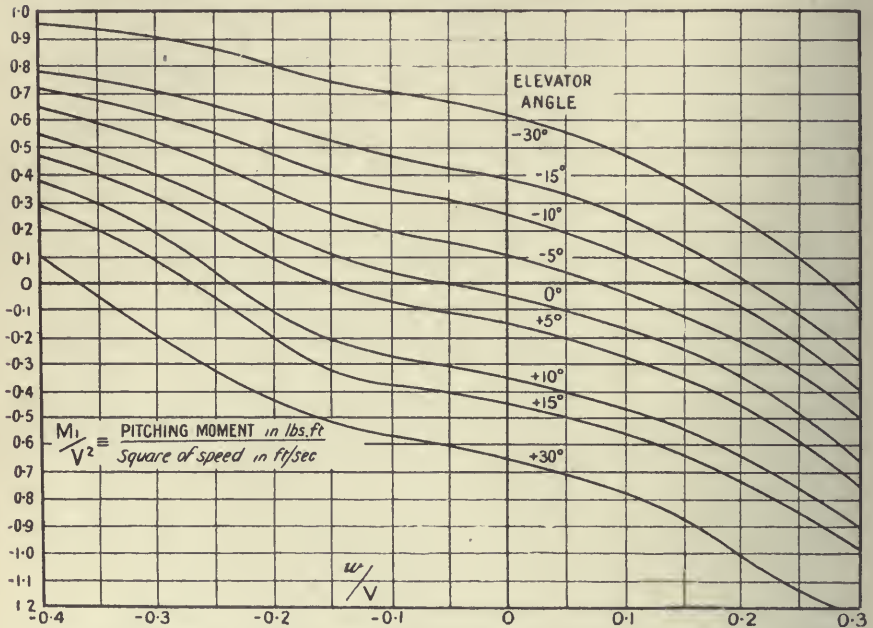
Fig. 133.—Pitching moment due to inclination of an aeroplane to the relative wind.

$$\frac{Mq}{V} \equiv \frac{\text{PITCHING MOMENT } due\ to\ pitching,\ lbs.ft.}{\text{Angular velocity} \times \text{Linear velocity},\ in\ ft.sec.}$$
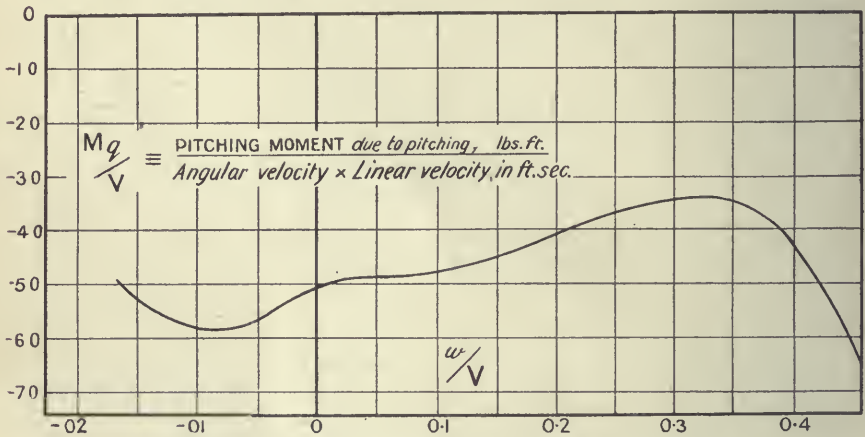
Fig. 134.—Pitching moment due to pitching of an aeroplane.

must be chosen such as to give a loop, and some further experience or trial and error is necessary before this can be done satisfactorily. Usually, looping takes place only at some considerable altitude, but the calculations now given assume an atmosphere of standard density.

The weight of the aeroplane was assumed to be 1932 lbs., and other data relating to its dimensions and masses are

$$m = 60, \quad B = 1500, \quad l = 15 \quad . \quad . \quad . \quad . \quad (12)$$

At the particular instant for which the calculation was started the motion is specified by

$$\theta = -20° \qquad V = 180 \text{ ft.-s.} \qquad \frac{w}{V} = -0.06 \Bigg\} \quad . \quad . \quad (13)$$
$$q = 0 \qquad \text{Elevator angle } -15°$$

The processes now become wholly mathematical, and the chief remaining difficulty is that of making a beginning; a little experience shows that for the first 0·1 or 0·2 seconds certain approximations hold which simplify the calculation. It may be assumed that in the early stages

$$\begin{aligned} &V = \text{constant.} \qquad \cos\theta = \text{constant} \\ &\frac{M_1}{V^2} \text{ and } \frac{M_q}{V} \text{ const.} \qquad \frac{mZ_1}{V^2} \text{ a linear function of } \frac{w}{V} \end{aligned} \Bigg\} \quad . \quad . \quad (14)$$

The limitation of time to which (14) applies is indicated in the course of the subsequent work.

Equation (11) becomes for this early period

$$\dot{q} - \frac{M_q}{B}q = \frac{M_1}{B} \quad . \quad . \quad . \quad . \quad . \quad (15)$$

and a solution consistent with the assumptions as to constancy of M_q and M_1 is

$$q = -\frac{M_1}{M_q}\left(1 - e^{\frac{M_q}{B}t}\right) \quad . \quad . \quad . \quad . \quad (16)$$

and

$$\theta = \theta_0 - \frac{M_1}{M_q}t + \frac{B}{M_q}q \quad . \quad . \quad . \quad . \quad (17)$$

These equations for q and θ are easily deduced and verified. From the initial data and the curves in Figs. 130–134, it will be found that for $\frac{w}{V} = -0.06$

$$\frac{M_1}{V^2} = 0.43, \quad \frac{M_q}{V} = -58, \quad V = 180 \text{ and } \theta_0 = -0.349 \text{ radian} \Bigg\}$$

and by deduction from these   (18)

$$\frac{M_1}{M_q} = -1.33 \text{ and } \frac{M_q}{B} = -6.96$$

Equations (16) and (17) now become

$$\begin{aligned} q &= 1.33(1 - e^{-6.96t}) \\ \theta &= -0.349 + 1.33t - \frac{q}{6.96} \end{aligned} \Bigg\} \quad . \quad . \quad . \quad . \quad (19)$$

and from them can be calculated the various values of q and θ which are given in Table 1.

s

A similar process will now be followed in the evaluation of w for small values of t. Equation (10) may be written as

$$\dot{w} = Z_1 + \left(u + \frac{M_q}{ml}\right)q + g \cos \theta \quad . \quad . \quad . \quad . \quad (20)$$

and from Fig. 131 it is found that in the neighbourhood of $\dfrac{w}{V} = -0\cdot06$, and for elevators at $-15°$ the value of Z_1 is given by

$$\frac{mZ_1}{V^2} = -1\cdot59\left(\frac{w}{V} + 0\cdot07\right)$$

or

$$Z_1 = -4\cdot77w - 60 \quad \text{when} \quad V = 180 \Bigg\} \quad . \quad . \quad . \quad (21)$$

Inserting numerical values, equation (20) becomes

$$\dot{w} = -4\cdot77w + 168\cdot4q - 29\cdot7 \quad . \quad . \quad . \quad . \quad (22)$$

The value of q previously obtained, equation (19), may be used and an integral of (22) is

$$w = Ae^{-4\cdot77t} + 40\cdot8 + 102\cdot2e^{-6\cdot96t} \quad . \quad . \quad . \quad . \quad (23)$$

Since $\dfrac{w}{V} = -0\cdot06$ and $V = 180$ at the time $t = 0$, it follows that the initial value of w is $-10\cdot8$, and the value of A in (23) is then found to be $-153\cdot8$, so that

$$w = -153\cdot8e^{-4\cdot77t} + 40\cdot8 + 102\cdot2e^{-6\cdot96t} \quad . \quad . \quad (24)$$

and

$$\dot{w} = 733e^{-4\cdot77t} - 711e^{-6\cdot96t} \quad . \quad . \quad . \quad . \quad . \quad (25)$$

Values of w and $\dot{w}$ are shown in Table 1.

TABLE 1.

INITIAL STAGES OF A LOOP.

$t_{\text{sec.}}$	$e^{-6\cdot96t}$	q	$\dot{q}$	θ	$\cos \theta$	$e^{-4\cdot77t}$	w	$\dot{w}$
0	1·000	0	9·26	−0·349	0·940	1·000	−10·8	22
0·05	0·707	0·390	6·55	−0·339	0·942	0·790	− 8·2	76
0·10	0·500	0·665	4·63	−0·312	0·952	0·621	− 3·5	99
0·15	0·352	0·862	3·26	−0·274	0·962	0·489	+ 1·6	108
0·20	0·249	0·999	2·31	−0·226	0·975	0·385	7·1	105
0·30	0·124	1·165	1·15	−0·117	0·992	0·239	16·7	87
0·40	0·062	1·249	0·57	+0·006	1·000	0·149	24·2	65

Of the various limitations imposed by (14) the one of greatest importance is that relating to the constancy of $\dfrac{M_1}{V^2}$, and reference to Fig. 133 will indicate that this should not be pushed further than the value for $\dfrac{w}{V} = -0\cdot02$. Table 1 then shows a limit of time of 0·10 sec. before the step-to-step method is started. The work may be arranged as in Table 2 for convenience. Across the head of the table are intervals of time arbitrarily

chosen ; as the calculation proceeds and the trend of the results is seen it is usually possible to use intervals of time of much greater magnitude than those shown in Table 2. For $t = 0$ a number of quantities such as V, w, q, θ are given as the initial data of the problem, whilst others like $\frac{mX_1}{V^2}$, $\frac{T}{m}$, etc., are deduced from the curves of Figs. 130–134. A comparison between the expressions in the table and those in equations (9), (10), and (11) will indicate the method followed. The additional equation for finding $\dot{V}$ comes from

$$V^2 = u^2 + w^2 \quad . \quad . \quad . \quad . \quad . \quad . \quad . \quad (26)$$

by simple differentiation and arrangement of terms.

TABLE 2.
BEGINNING OF STEP-TO-STEP CALCULATION.

$t_{secs.}$	0	0·05	0·10	0·15	$t_{secs.}$	0	0·05	0·10
V	180	180	180·1	180·2	uq	0	70·0	115·3
u	179·6	179·8	180·1	180·2	$g\cos\theta$	30·25	30·31	30·6
w	−10·8	− 8·2	− 3·1	+ 1·2	$\frac{mZ_1}{V^2}\cdot\frac{V^2}{m}$	− 8·64	−18·9	− 46·0
q	0	0·390	0·640	0·854	$\frac{1}{15}\cdot\frac{M_q}{V}\cdot\frac{qV}{m}$	0	− 4·4	− 6·4
$q\delta t$	—	0·039	0·064	0·085				
θ	− 0·349	− 0·339	− 0·310	− 0·275	$\dot{w}$	—	77·0	93·5
$\cos\theta$	0·940	0·942	0·952	—	$\dot{w}\delta t$	—	7·7	9·4
$\sin\theta$	− 0·342	− 0·332	− 0·305	—	$\frac{1}{1500}\cdot\frac{M_1}{V^2}\cdot V^2$	9·29	9·07	8·64
$\frac{w}{V}$	− 0·060	− 0·046	− 0·017	—	$\frac{1}{1500}\cdot\frac{M_q}{V}\cdot qV$	0	− 2·67	− 4·00
$\frac{V^2}{m}$	540	540	541	—	$\dot{q}$	—	6·40	4·64
$-wq$	0	3·20	1·98	—	$\dot{q}\delta t$	—	0·64	0·46
$-g\sin\theta$	11·0	10·6	9·82	—				
$\frac{mX_1}{V^2}\cdot\frac{V^2}{m}$	−15·39	−15·39	−14·53	—	$\frac{u}{V}\dot{u}$	—	5·00	3·83
$\frac{T}{m}$	6·58	6·58	6·56	—	$\frac{w}{V}\dot{w}$	—	− 3·51	− 1·61
$\dot{u}$	—	5·00	3·83	—	$\dot{V}$	—	1·49	2·22
$\dot{u}\delta t$	—	0·50	0·38	—	$\dot{V}\delta t$	—	0·15	0·22
					—	—	—	—
					—	—	—	—

The fundamental figures for $t = 0·05$ are taken from Table 1, and using them the necessary calculations indicated by equations (9), (10), and (11) are made to give the instantaneous values of $\dot{u}$, $\dot{w}$, $\dot{q}$. The necessary basis for step-to-step calculation is then complete, and many differences of detail

would probably be made to suit the habits of an individual calculator. The assumption which was made in proceeding to the next column was that the values of $\dot{u}$, $\dot{w}$, $\dot{q}$, q at $t=0.5$ were equal to the average values over the interval of time 0 to 0.10 secs. As an example consider the value of w; at $t=0$, $w=-10.8$. At $t=0.05$, $\dot{w}=77.0$, and in the interval of 0.10 sec. the change of w is taken as 7.7. Adding this to the value of w at $t=0$ gives -3.1 as the value of w at $t=0.10$ as tabulated. A comparison of the values of w, $\dot{w}$, q, $\dot{q}$ and θ as calculated in this way with those of Table 1 will show that the mathematical approximations of (14) had not led to large errors. The preliminary stages of calculation for $t=0.15$ are shown, and the procedure followed will now be clear.

TABLE 3.

DETAILS OF LOOP.

Time (secs.).	$V_{ft.-s.}$	$w_{ft.-s.}$	$u_{ft.-s.}$	q (rads.-s.).	θ (degrees).	Angle of incidence (degrees).	$\dfrac{mZ_1}{1932}$
0	180	−10·8	179·8	0	−20·0	− 0·4	0·2
0·5	177·8	+24·0	176·3	0·835	+ 4·0	10·7	5·2
1·0	167·5	21·8	166·2	0·658	24·3	10·5	4·6
1·5	154·8	20·2	153·5	0·624	42·1	10·5	3·9
2·0	139·4	17·8	135·7	0·560	61·8	10·5	3·2
2·5	123·3	15·6	122·3	0·518	74·7	10·3	2·4
3·0	107·1	12·9	106·4	0·478	89·0	9·9·	1·8
3·5	92·5	10·0	92·0	0·451	102·3	9·2	1·2
4·0	79·6	6·9	79·3	0·435	115·0	8·0	0·8
5·0	61·7	0·5	61·7	0·450	140·1	+ 3·5	0·3
6·0	58·5	− 5·8	58·3	0·450	165·7	− 2·7	0·0
6·5	62·8	− 7·0	62·4	0·488	179·0	− 3·3	−0·1
7·0	70·7	− 5·9	70·5	0·526	193·5	− 1·8	0·0
8·0	94·8	+ 2·7	94·7	0·639	226·5	+ 4·5	0·8
9·0	125·1	11·8	124·5	0·642	263·6	8·4	2·2
10·0	151·6	17·6	150·5	0·666	300·1	9·7	3·5

The calculations were carried out for a complete loop, and Table 3 shows the variation of the quantities concerned at chosen times. At the beginning of the loop the angle of incidence is shown as -0.4 degree, whilst less than half a second later it has risen to 11.0 degrees. The loading on the wings can be calculated at any time from the value of mZ corresponding with the tabulated numbers for V and w and Fig. 131. The maximum is 5.2 times the weight of the aeroplane, but owing to the fact that the load on the tail is downward this does not represent the load on the wings, which is then about 10 per cent. greater.

The shape of the loop can be obtained by integration at the end of the calculations since the horizontal co-ordinate is

$$x = \int (u \cos \theta + w \sin \theta)dt \quad . \quad . \quad . \quad . \quad (27)$$

whilst the vertical co-ordinate is

$$z = \int (u \sin \theta - w \cos \theta)dt . \quad . \quad . \quad . \quad (28)$$

The integrals may be obtained in any of the well-known ways, and the results for the above example are shown in Fig. 135. It will be seen that the closed curve is appreciably different to a circle, has a height of nearly 300 feet and a width of 230 feet. A diagram of the aeroplane inset to scale shows the relative proportions of aircraft and loop. The time
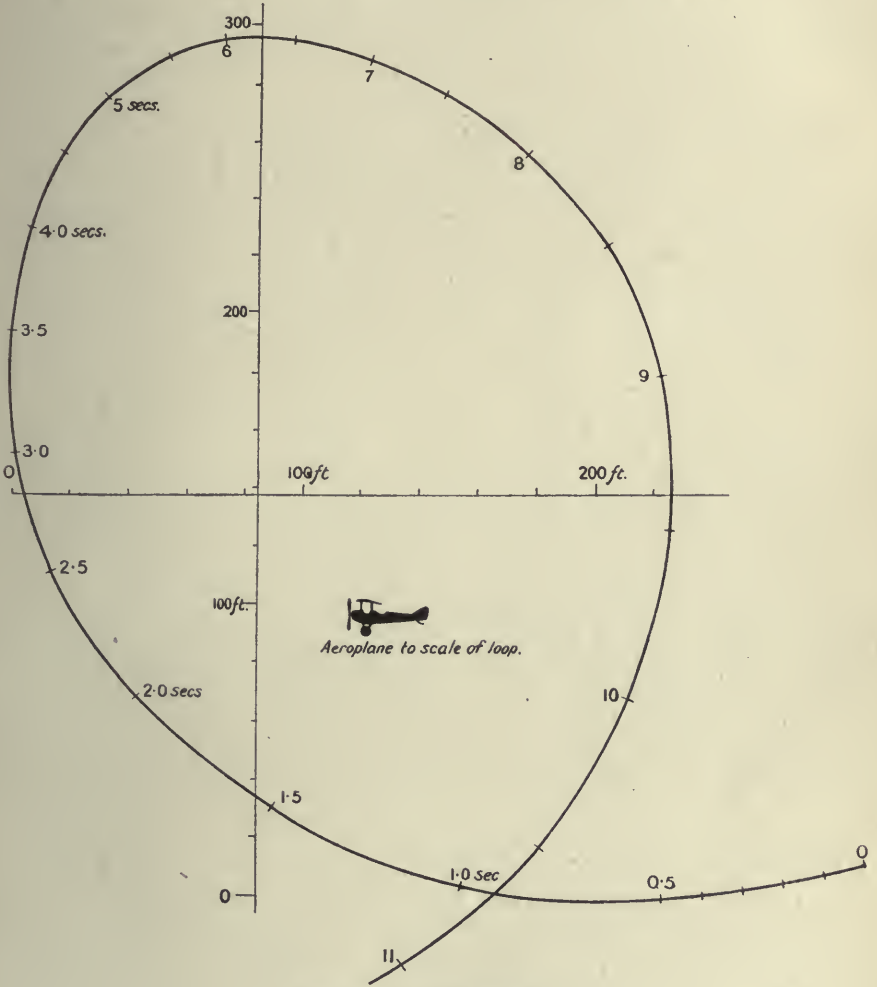
Fig. 135.—A calculated loop.

taken is 10 or 11 seconds, and a pilot frequently feels the bump when passing the air which he previously disturbed.

In the calculations as made, the engine has been assumed to be working at full power and the elevator held in a fixed position. In many cases the engine is cut off after the top of the loop has been passed, and the elevator is probably never held still. In addition to the longitudinal controls, it is

found necessary to apply rudder to counteract the gyroscopic effect of the airscrew and so maintain an even keel.

Failure to complete a Loop.—The calculations just made assumed an initial speed of 180 ft.-s. in a dive at 20°, and indicated some small reserve of energy at the top of the loop. A reduction of the speed to 140 ft.-s. and level flight before pulling over the control column leads, with the same assumptions as to the aeroplane, to a failure to complete the loop.

<div align="center">

TABLE 4.

FAILURE TO LOOP.

</div>

Time (secs.).	Resultant velocity V (ft.-s.).	Inclination of airscrew axis to horizontal θ (degrees).	Angle of incidence (degrees).
0	140	− 1·7	4·4
0·5	138	+14·7	10·7
1·0	131	29·8	11·5
1·5	121	42·4	11·5
2·0	110	54·3	11·6
2·5	97	65·2	11·6
3·0	85	74·7	11·6
3·5	73	83·2	11·5
4·0	60	90·2	11·1
4·5	49	97·8	10·1
5·0	38	104·0	8·0
5·5	28	110·2	3·4
5·7	23	112·7	− 0·2
5·9	19	115·0	− 5·8
6·1	15	117·3	−16·5

The figures in Table 4 are of considerable interest as showing one of the ways in which an aeroplane may temporarily become uncontrollable owing to loss of flying speed. Up to the end of four seconds the course of the motion presents little material for comment ; the aeroplane is then moving vertically upwards at the low speed of 60 ft.-s. and is turning over backwards. The energy is insufficient to carry the aeroplane much further, but at 5 seconds the aeroplane is 20 degrees over the vertical with a small positive angle of incidence, but a speed of only 28 ft.-s. In the next half-second the aeroplane begins to fall, and at the end of 6·1 secs. is still losing speed and has a large negative angle of attack, *i.e.* is flying on its back, with the pilot supported from his belt. Owing to the low speed the controls are practically inoperative, and the pilot must perforce wait until the aeroplane recovers speed before he can resume normal flight. If the aeroplane is unstable in normal straight flight some difficulty may be experienced in passing from a steady state of upside-down flying to one in a normal attitude.

The detailed calculations from which Tables 3 and 4 have been compiled were made by Miss B. M. Cave-Browne-Cave, to whom the author is indebted for assistance on this and other occasions.

Steady Motions, including Turning and the Spiral Glide.—The equations of motion given in (1) and (2) take special forms if the motion is steady.

Not only are the quantities $\dot{u}$, $\dot{v}$, $\dot{w}$, $\dot{p}$, $\dot{q}$ and $\dot{r}$ equal to zero, but there is a relation between the quantities p, q and r. As the forces on an aeroplane along its axes depend on the inclinations of the aeroplane relative to the vertical, it will be evident that they can only remain constant if the resultant rotation is also about the vertical. This rotation is denoted by Ω, and looking down on the aircraft the positive direction is clockwise.

The direction cosines of the body axes relative to the vertical were found and recorded in (3), and from them the component angular velocities about the body axes are

$$
\left.\begin{array}{l}
p = -\Omega \sin \theta \\
q = \quad \Omega \cos \theta \sin \phi \\
r = \quad \Omega \cos \theta \cos \phi
\end{array}\right\} \quad . \quad . \quad . \quad . \quad . \quad (30)
$$

With the products of inertia D and F equal to zero the equations of steady motion are

$$
\left.\begin{array}{rll}
wq - vr = X - g \sin \theta & . & . & . & (31u) \\
ur - wp = Y + g \cos \theta \sin \phi & . & . & (31v) \\
vp - uq = Z + g \cos \theta \cos \phi & . & . & (31w) \\
rq(C - B) - pqE = L & . & . & . & . & . & (31p) \\
pr(A - C) + (p^2 - r^2)E = M & . & . & . & . & . & (31q) \\
qp(B - A) + qrE = N & . & . & . & . & . & (31r)
\end{array}\right\} \quad . \quad (31)
$$

In equations (31), X, Y, Z, L, M, and N refer only to forces and couples due to relative motion through the air. If the values of p, q and r given by (30) are used in (31), the somewhat different forms below are obtained:—

$$
\left.\begin{array}{rl}
\Omega \cos \theta (w \sin \phi - v \cos \phi) = X - g \sin \theta & . \quad . \quad (32u) \\
\Omega (u \cos \theta \cos \phi + w \sin \theta) = Y + g \cos \theta \sin \phi & (32v) \\
\Omega (-v \sin \theta - u \cos \theta \sin \phi) = Z + g \cos \theta \cos \phi & (32w) \\
\Omega^2 \cos \theta \sin \phi \{ (C - B) \cos \theta \cos \phi + E \sin \theta \} = L & . \quad (32p) \\
\Omega^2 \{ -(A - C) \sin \theta \cos \theta \cos \phi + E(\sin^2 \theta - \cos^2 \theta \cos^2 \phi) \} = M & (32q) \\
\Omega^2 \cos \theta \sin \phi \{ -(B - A) \sin \theta + E \cos \theta \cos \phi \} = N & (32r)
\end{array}\right\} \quad (32)
$$

The equations for steady rectilinear symmetrical motion are obtained from (32) by putting $\Omega = 0$, $\phi = 0$; they then become

$$
\left.\begin{array}{c}
X = \quad g \sin \theta \\
Z = - g \cos \theta \\
Y = 0 \quad L = 0 \quad M = 0 \quad \text{and} \quad N = 0
\end{array}\right\} \quad . \quad . \quad (33)
$$

and the great simplicity of form is very noticeable. The solutions of (33) formed the subject-matter of Chapter II, and cover many of the most important problems in flying. Some discussion of the more general equations (32) will now be given; the process followed will be the deduction of the particular from the general case. This method is not always advantageous, but is not unsuitable for the discussion of asymmetrical motions.

Equations (32) contain six relations between the twelve quantities u, v, w, θ, ϕ, Ω, X, Y, Z, L, M, N and certain constants of the aircraft. There are only four controls to an aeroplane and three to an airship, consisting of the engine, elevator, rudder and ailerons for the former and the

first three of these for the latter. In the best of circumstances, therefore, only four of the quantities X, Y, Z, L, M, and N are independently variable, but all are functions of u, v, w, θ, ϕ and Ω which are determinable in a wind channel or by other methods of obtaining aerodynamic data. Equations (32) may then be looked on as six equations between the quantities u, v, w, θ, ϕ, Ω, of which four are independently variable in an aeroplane and three in an airship.

It has already been shown in the case of symmetrical straight flight that the elevator determines the angle of incidence, whilst the engine control affects the angle of descent. The aeroplane then determines by its accelerations the speed of flight. For the lateral motions the new considerations show that the rate of turning and angle of bank can be varied at will, but that the rate of side slipping is then determined by the proportions of the aeroplane.

It follows from the equations of motion that, within the limits of his controls, a pilot may choose the speed of flight, the rate of climb, the rate of turning and the angle of bank, but the angle of incidence and rate of side slipping are then fixed for him. A very usual condition observed during a turn is that side slipping shall be zero, and the angle of bank cannot be simultaneously considered as an independent variable.

A number of cases of lateral motion will now be considered in relation to equations (32).

Turning in a Horizontal Circle without Side Slipping.—The condition that no side slipping is occurring is shortly stated as

$$v = 0 \qquad \qquad \qquad (34)$$

but that of horizontal flight is less direct. If h be the height above the ground, the resolution of velocities leads to the equation

$$\dot{h} = u \sin \theta - v \cos \theta \sin \phi - w \cos \theta \cos \phi . \quad . \quad (35)$$

and for the conditions imposed (35) becomes

$$u \sin \theta = w \cos \theta \cos \phi \qquad . \quad . \quad . \quad . \quad (36)$$

Simplification of the various expressions can be obtained by a careful choice of the position of the body axes. The axis of X will be taken as horizontal, and therefore along the direction of flight; this is equivalent to $\theta = 0$, $w = 0$, $u = \mathrm{V}$, $p = 0$, whilst $-m\mathrm{Z}$ becomes equal to the lift. $m\mathrm{X}$ differs from the drag by the airscrew thrust, and will be found to be zero. The six equations of motion now become

$$
\left.
\begin{aligned}
\mathrm{X} &= 0 . \qquad . \qquad . \qquad . \qquad & (37u) \\
\mathrm{V}\Omega \cos \phi &= \mathrm{Y} + g \sin \phi \quad . \qquad & (37v) \\
-\mathrm{V}\Omega \sin \phi &= \mathrm{Z} + g \cos \phi . \quad . \qquad & (37w) \\
\Omega^2(\mathrm{C} - \mathrm{B}) \sin \phi \cos \phi &= \mathrm{L} \quad . \qquad . \qquad . \qquad & (37p) \\
\Omega^2 \mathrm{E} \cos^2 \phi &= \mathrm{M} \quad . \qquad . \qquad . \qquad & (37q) \\
\Omega^2 \mathrm{E} . \sin \phi \cos \phi &= \mathrm{N} \quad . \qquad . \qquad . \qquad & (37r)
\end{aligned}
\right\} \quad . \quad . \quad (37)
$$

Owing to the slight want of symmetry of the aeroplane which arises from the use of ailerons and rudder, the lateral force $m\mathrm{Y}$ will not be strictly

zero. It is, however, unimportant and will be ignored; equation ($37v$) with $Y = 0$ shows that

$$\tan \phi = \frac{V\Omega}{g} \qquad \qquad \qquad (38)$$

The angle ϕ given by (38) is often spoken of as the angle of natural bank, and is seen to be determined by the flight speed and angular velocity. As an example, consider a bank of $45°$, i.e. $\tan \phi = 1$ and a speed of 120 feet per second. Equation (38) shows that Ω is then 0·268 radian per second, or one complete turn in 23·4 secs. A vertical bank, which gives an infinite value to $\tan \phi$, is not within the limits of steady motion and can only be one phase of a changing motion.

If (38) be used to eliminate $V\Omega$ from ($37w$) the equation becomes

$$\text{Lift} = -mZ = mg \sec \phi \qquad \qquad (39)$$

and the lift is seen to be greater during a banked turn than in level flight by the factor $\sec \phi$. For a banked turn at $45°$ this increase of loading is 41 per cent.

It will be noticed that the couples, L, M and N all have values which may be written alternatively as

$$L = \frac{(C - B)V\Omega^3 g}{g^2 + V^2\Omega^2}, \quad M = \frac{E\Omega^2 g^2}{g^2 + V^2\Omega^2} \text{ and } N = \frac{EV\Omega^3 g}{g^2 + V^2\Omega^2} \cdot \quad (40)$$

and an estimate of their magnitude depends on the moments and products of inertia. For an aeroplane of about 2000 lbs. total weight the value of C—B would be about 700. E is more uncertain and probably not greater than 200. With $V = 120$ and $\Omega = 0·268$, the values of L, M and N in lbs.-feet would be 25, 7 and 7 respectively, and therefore insignificant. It must not be inferred, however, that the couple exerted by the rudder is insignificant, but that it is almost wholly used in overcoming the resistance to turning of the rest of the aeroplane. This part of the analysis, which is of great importance, can only come from a study of the aerodynamics of the aeroplane, and not from its motion as a whole. The difference here pointed out is analogous to the mechanical distinction between external forces and stresses.

Spiral Descent.—The conditions of steady motion differ from those for horizontal turning only in the fact that equation (35) is used to evaluate $\dot{h}$ and not to determine a relation between w and θ. It is still permissible to choose the axis of X in such a position that w is zero, and the conditions of equilibrium of forces are in the absence of side slipping

$$\left. \begin{array}{l} X = g \sin \theta \\ V\Omega \cos \theta \cos \phi = Y + g \cos \theta \sin \phi \\ -V\Omega \cos \theta \sin \phi = Z + g \cos \theta \cos \phi \end{array} \right\} \qquad \qquad (41)$$

As for rectilinear flight, the inclination of the axis of X to the horizontal and, since $w = 0$, the inclination of the flight path, is changed by the variation of longitudinal force, or in practice, change of airscrew thrust.

The angle of bank for Y=0 is identical with that given by (38) for horizontal turning without side slipping, whilst the normal air force is

$$-mZ = mg \cos \theta \sec \phi \quad . \quad . \quad . \quad . \quad . \quad (42)$$

It appears that the angle of the spiral with $Y = 0$ may become greater and greater until the axis of X is inclined to the horizontal at 80° or more, and the radius of the circle of turning is only a few feet. The following table indicates some of the possibilities of steady spiral flight :—

<div align="center">

TABLE 5.

SPIRALS AND SPINS.

</div>

Angle of descent θ (degrees).	Angle of bank ϕ (degrees).	Resultant angular velocity Ω (rads.-s.).	Resultant velocity V (ft.-s.).	Radius of plan of spiral R (ft.).
40	42·7	0·37	80	164
50	58·8	0·61	87	92
60	69·1	0·91	92·5	51
70	77·0	1·44	96·5	23
80	83·7	2·95	99	6

Table 5 applies to an aeroplane at an angle of incidence of 30°, *i.e.* an angle well above the critical, and is deduced from observations in flight. The motion of wings at large angles of incidence produces remarkable effects, and it will be seen from an experiment on a model that the rotation about the axis of descent is necessary in order to produce a steady motion which is stable.

Approximate Methods of deducing the Aerodynamic Forces and Couples on an Aeroplane during Complex Manoeuvres.—A complete model aeroplane mounted in a wind channel as shown in Fig. 136 was found to rotate about an axis along the wind with a definite speed of rotation for each angle of incidence and wind speed. The analysis of the experiment is of very great importance, as it shows the possibility of building up the total force or couple from a consideration of the parts.

If the axis of X be identified with the axis of rotation, the various constraints introduced by the apparatus reduce the six equations of motion to one, (31p). Since q is zero, this equation takes the very simple form $L = 0$, and one of the solutions for equilibrium is that for which the model is not rotating. At small angles of incidence this condition is stable, and rotation is rapidly stopped should it be produced by any means. Above the critical angle of incidence the condition of no rotation is unstable, and an accidental disturbance in either direction produces an accelerating couple until a steady state is reached with the model in continuous rotation.

Figs. 137 and 138 relate to the model with its rudder and ailerons in the symmetrical position, the direction of rotation being determined by accidental disturbance. The speed of rotation was taken by stop-watch, and the first experiment consisted of a measurement of the speed of rotation at various wind speeds. As was to be expected on theoretical grounds, the

Fig. 136.—Model aeroplane arranged to show autorotation.

speed of rotation was found to be proportional to the wind speed (Fig. 138). The second experiment covered the variation of rotational speed with
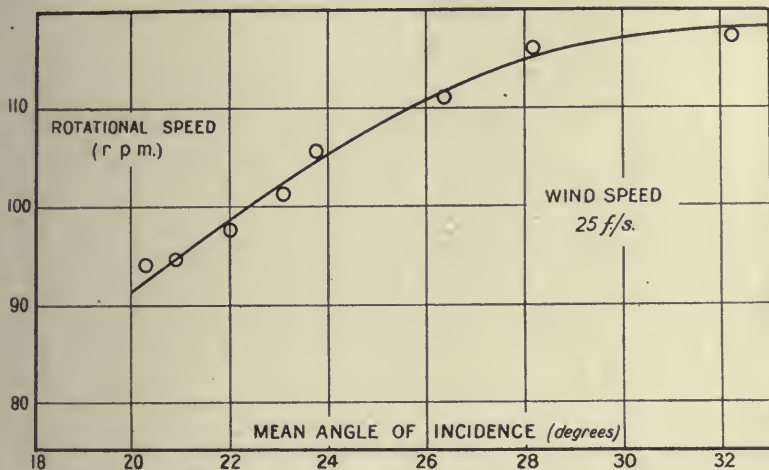
FIG. 137.—Autorotation of a model aeroplane as dependent on angle of incidence.
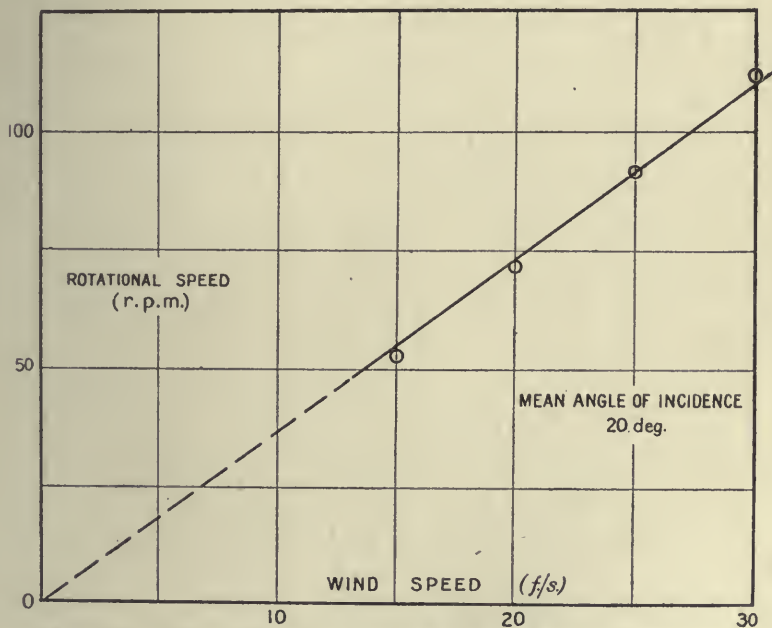
FIG. 138.—Autorotation of model aeroplane as dependent on wind speed.

change of angle of incidence, and it will be noticed that increase of the latter leads to faster spinning, at least up to angles of 33°. The analytical process now to be described, if carried out over the whole range of possible angles of incidence, shows that the spinning is confined to a limited range.

Over part of this range, the spinning will not occur unless the disturbance is great, but when started will maintain itself.

Simpler Experiment which can be compared with Calculation.—Instead of the complete model aeroplane a simple aerofoil was mounted on the same apparatus; a first approximation to a wing element theory was used as a
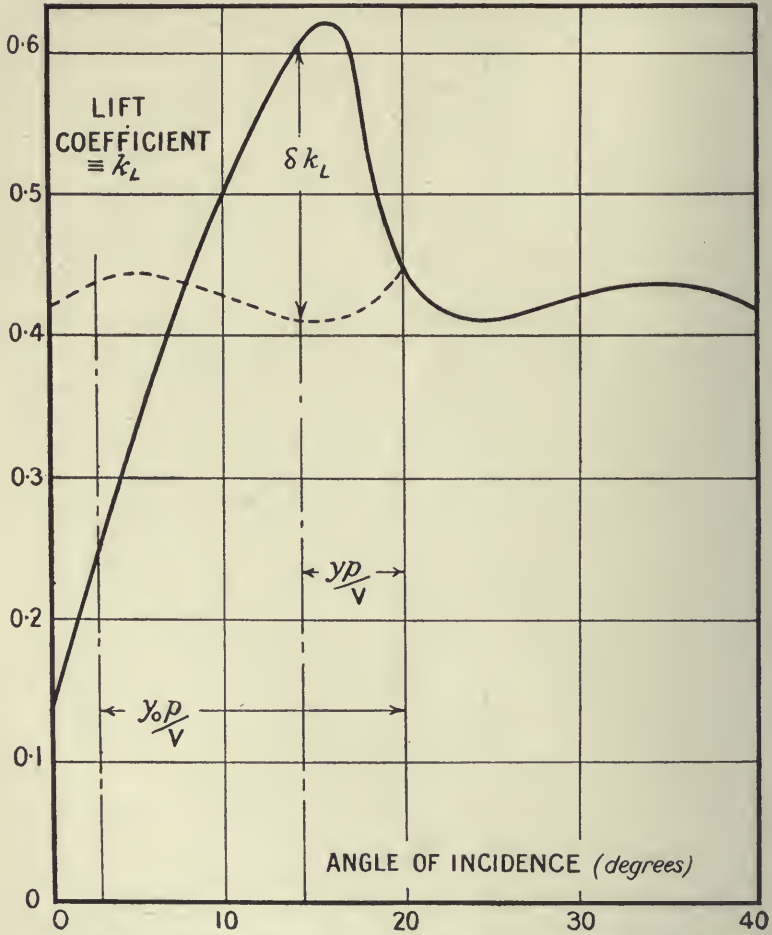
FIG. 139.—Lift-coefficient curve for aerofoil as used in calculating the speed of autorotation.

basis for calculation. In this illustration the difference between lift and $-mZ$ is ignored, and the curve shown in Fig. 139 is the ordinary lift coefficient curve for an aerofoil on a base of angle of incidence which has been extended to 40°. An angle of incidence of 20° at the centre of the aerofoil was chosen for the calculation, and is indicated by an ordinate of Fig. 139. As a result of uniform rotation the angle of incidence at points away from the centre is changed, being increased on one wing and decreased on the other. The

distance from the axis of rotation to an element being y, the change of angle of incidence due to an angular velocity p is roughly equal to $\frac{yp}{V}$. Since $\frac{p}{V}$ is constant along the wings it may be left as indefinite temporarily; the lift coefficient on the element of one wing at 14° say, will be shown by the ordinate of the full curve.   Reflecting the lift coefficient curve as shown in Fig. 139 brings the corresponding ordinate at 26° into a convenient
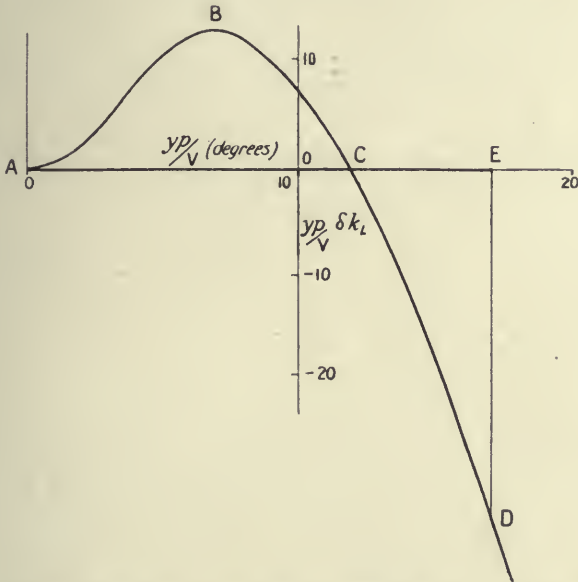
Fɪɢ. 140.—Calculation of the speed of autorotation of an aerofoil.

position for the estimation of the difference δk_{L}, and the couple due to the pair of elements is

$$\rho \mathrm{V}^2 c \delta k_{\mathrm{L}} y dy \quad . \quad . \quad . \quad . \quad . \quad . \quad (42a)$$

The couple on the complete aerofoil of half span y_0, is then

$$\mathrm{L} = \rho \mathrm{V}^2 c \int_0^{y_0} y \delta k_{\mathrm{L}} dy \quad . \quad . \quad . \quad . \quad . \quad (43)$$

The form of (43) can be changed to one more suitable for integration by the use of the variable $\frac{yp}{V}$ instead of y, and it then becomes

$$\mathrm{L} = \frac{\rho \mathrm{V}^4 c}{p^2} \int_0^{\frac{y_0 p}{V}} \frac{yp}{V} \cdot \delta k_{\mathrm{L}} \cdot d\left(\frac{yp}{V}\right) \quad . \quad . \quad . \quad . \quad (44)$$

Since δk_{L} is a known function of $\frac{yp}{V}$, the value of $\frac{\mathrm{L}p^2}{\rho \mathrm{V}^4 c}$ can be found by the plotting shown in Fig. 140.   For steady notion it has been seen that $\mathrm{L} = 0$,

and the curve ABCD is continued until the area between it and AE is zero. This occurs at the ordinate ED, which then represents the value of $\frac{y_0 p}{V}$; both y_0 and V are known, and hence p is deduced from the ratio so determined.

A more accurate method of calculation will be given later, but the errors admitted above are thought to be justified by the simplicity of the calculations and the consequent ease with which the physical ideas can be traced in the ultimate motion. On one wing the angle of incidence is seen to be increased to about 37° at the tip, whilst on the other it is reduced to 3°, Fig. 139, before steady rotation is reached. Further, the spinning
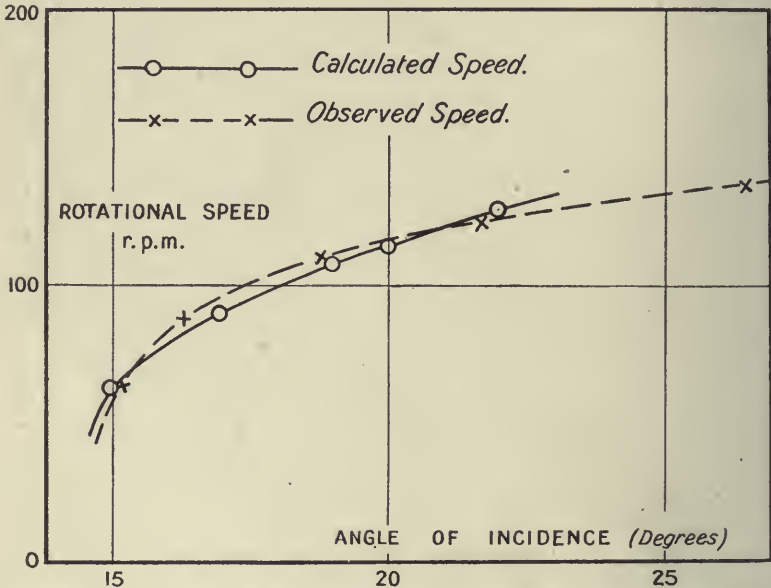
FIG. 141.—Comparison of the observed and calculated speeds of autorotation of an aerofoil.

is seen to depend on the evidence of an intersection of the lift curve and its image, a condition which would not have occurred had the angle of incidence been chosen as 10°.

Qualitatively, therefore, the theory of addition of elements agrees with observation. The quantitative comparison can be made since the aerofoil to which the lift curve of Fig. 139 applies was tested in a wind channel, and the observed and calculated curves of rotational speed are reproduced in Fig. 141. The aerofoil was 18 ins. long with a chord of 3 ins., and the speed of test 30 feet per sec.

The agreement between the calculated and observed values of the speed of rotation is close, perhaps closer than would be expected in view of the approximations in the calculation, and may be taken as strong support for the element theory. The extra power given in the calculation of aero-

plane motion is extremely great, and will enable future investigators to proceed to analyse in detail the motions of spinning, rolling and rapid turning without reference to complex experiments.

Further observations in the wind channel were made on the effect of changes of wind speed and of aspect ratio. As in the case of the complete model aeroplane, the speed of rotation was found to be proportional to the wind speed. Reference to (44) will show that the integral depends only on the value of $\frac{y_0 p}{V}$, and hence for aerofoils of greater length it would be expected that the rate of the steady spin would be proportionately less. The observed and calculated results are given in Table 6.

TABLE 6.

	Aspect ratio.	Observed rate of spin (r.p.m.).	Calculated rate of spin (r.p.m.).
Angle of incidence, 17° . .	4	125	142
	6	95	95
	8	74	71
Angle of incidence, 22° . . .	4	155	182
	6	121	121
	8	100	91

It will be noticed that the agreement is far less complete than was the case for variation of angle of incidence. It is possible that the tip effects which have been ignored are producing measurable changes in this case, and for a higher degree of accuracy resort should be had to observations of pressure distribution on an aerofoil. It is to be expected that future experiments will throw further light on the possibilities of the element theory, and probably lead to greater accuracy of calculation.

More Accurate Development of the Mathematics of the Aerofoil Element Theory.—Any element theory can only be an approximation to the truth, and for this reason somewhat different expressions may be equally justifiable. On the other hand all such theories assume that the forces on an element are determined by the local relative wind, and are sensibly independent of changes of velocity round neighbouring elements. Further, it is not usual to make any applications to small areas of a body, but only to strips of aerofoils parallel to a plane of symmetry, and to take the x co-ordinate of this strip as that of its centre of pressure. The last assumption may be regarded as a convenient method of taking a weighted mean of the variations over a strip, and not intrinsically more sound than the taking of areas small in both directions and summing the results.

Usually, the aerofoils to which calculation is applied lie either in the plane of symmetry or nearly normal to it, and consist of the fin and rudder, tail plane and elevator, and main planes. Of these, the last provides the more complex problem on account of the dihedral angle, and since the treatment covers the subject a pair of wings has been chosen for illustration of the method of calculation.

The relations written down will have sufficient generality to cover variations of angle of incidence and dihedral angle from centre to wing tip, and such dissymmetry as arises from the use of the lateral controls. The method of presentation followed is adopted as it shows with some precision the assumptions made in applying the element theory. Axes of reference are indicated in Fig. 106, but the first operation in the theory uses a new set of axes obtained by rotating the standard axes GX, GY and GZ to new positions specifically related to the orientation of one of the elements. Referring to Fig. 142 (a), which represents one wing of an aeroplane of which the element at P is being considered, the axes marked GX_1, GY_1 and GZ_1 have been obtained from the standard axes by rotation through an angle α_x about GY * and through a dihedral angle $-\Gamma$ about GX_1. The plane X_1GY_1 is then parallel to the plane containing the chord of the element and the tangent to the curve joining the centres of pressure of elements in a direction normal to the chord.
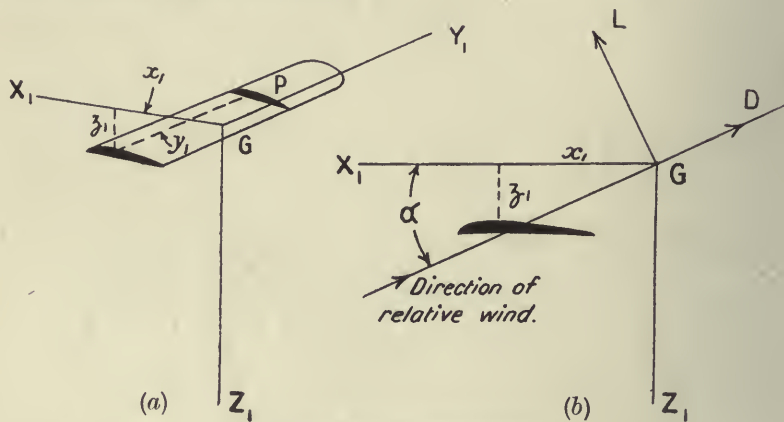
FIG. 142.—Aerofoil element theory.

With the axes in their new position the aerodynamics of the problem takes simple form. If u_1, v_1 and w_1 be the component velocities of P, whilst u_1', v_1', and w_1' are the corresponding velocities of G along these axes and p_1, q_1 and r_1 the angular velocities about them, then

$$
\left.
\begin{aligned}
u_1 &= u_1' + q_1 z_1 - r_1 y_1 \\
v_1 &= v_1' + r_1 x_1 - p_1 z_1 \\
w_1 &= w_1' + p_1 y_1 - q_1 x_1
\end{aligned}
\right\} \quad . \quad . \quad . \quad . \quad . \quad (45)
$$

and the angle of incidence and resultant velocity at P are defined by

$$
\tan \alpha_1 = \frac{w_1}{u_1} \quad . \quad . \quad . \quad . \quad . \quad . \quad . \quad (46)
$$

$$
V^2 = u_1^2 + v_1^2 + w_1^2 \quad . \quad . \quad . \quad . \quad . \quad (47)
$$

---

* The angle of pitch, *i.e.* the inclination of the chord of an element to the axis of X as here defined is denoted by a_x. a is used generally for angle of incidence, *i.e.* the inclination of the chord of an element to the direction of the relative wind as defined in (46), whilst a_0 is the angle of incidence in the absence of rotations. If the axis of X coincides with the direction of the relative wind in the absence of rotations, $a_x = a_0$.

The two quantities α and V suffice to determine the lift and drag on an element from a standard test, preferably one in which the pressure distribution over a similar aerofoil was determined.

Using Fig. 142 (b) as representing the assumed resolution of forces, leads to the force and moment equations

$$\left.\begin{aligned}
md\mathrm{X}_1 &= \quad (k_\mathrm{L}\sin\alpha - k_\mathrm{D}\cos\alpha)\rho\mathrm{V}^2 cdy_1 \\
md\mathrm{Y}_1 &= \quad 0 \\
md\mathrm{Z}_1 &= -(k_\mathrm{L}\cos\alpha + k_\mathrm{D}\sin\alpha)\rho\mathrm{V}^2 cdy_1 \\
d\mathrm{L}_1 &= \quad y_1 md\mathrm{Z}_1 \\
d\mathrm{M}_1 &= -x_1 md\mathrm{Z}_1 + z_1 md\mathrm{X}_1 \\
d\mathrm{N}_1 &= -y_1 md\mathrm{X}_1
\end{aligned}\right\} \quad . \quad . \ (48)$$

Equations (48) complete the statement of the element theory, and will be seen to assume that the resultant force lies in a plane parallel to $\mathrm{X}_1\mathrm{G}\mathrm{Z}_1$.

In certain problems, equations (45)—(48) may be the most convenient form of application, but in general it will be necessary to resolve the components about the original axes before integration can be effected. The necessary relations for this purpose are given.

Forces and Moments related to Standard Axes.—It may be noticed that the angles of rotation α_x and Γ correspond closely with those of θ and ϕ, as illustrated in Fig. 129. A positive dihedral angle on the right-hand wing, however, corresponds with a negative ϕ. The direction cosines of the displaced axes relative to the original are

$$\left.\begin{aligned}
l_1 &\equiv \cos \mathrm{XGX}_1 = \cos \alpha_x \\
m_1 &\equiv \cos \mathrm{YGX}_1 = 0 \\
n_1 &\equiv \cos \mathrm{ZGX}_1 = -\sin \alpha_x \\
l_2 &\equiv \cos \mathrm{XGY}_1 = -\sin \alpha_x \sin \Gamma \\
m_2 &\equiv \cos \mathrm{YGY}_1 = \cos \Gamma \\
n_2 &\equiv \cos \mathrm{ZGY}_1 = -\cos \alpha_x \sin \Gamma \\
l_3 &\equiv \cos \mathrm{XGZ}_1 = \sin \alpha_x \cos \Gamma \\
m_3 &\equiv \cos \mathrm{YGZ}_1 = \sin \Gamma \\
n_3 &\equiv \cos \mathrm{ZGZ}_1 = \cos \alpha_x \cos \Gamma
\end{aligned}\right\} \quad . \quad . \quad . \ (49)$$

for the right-hand wing and similar expressions with the sign of Γ changed for the left-hand wing.

If x, y and z be the co-ordinates of P relative to the standard axes,

$$\left.\begin{aligned}
x_1 &= l_1 x + m_1 y + n_1 z \\
y_1 &= l_2 x + m_2 y + n_2 z \\
z_1 &= l_3 x + m_3 y + n_3 z
\end{aligned}\right\} \quad . \quad . \quad . \quad . \ (50)$$

In a similar way

$$\left.\begin{aligned}
u_1' &= l_1 u + m_1 v + n_1 w \\
v_1' &= l_2 u + m_2 v + n_2 w \\
w_1' &= l_3 u + m_3 v + n_3 w \\
p_1 &= l_1 p + m_1 q + n_1 r \\
q_1 &= l_2 p + m_2 q + n_2 r \\
r_1 &= l_3 p + m_3 q + n_3 r
\end{aligned}\right\} \quad . \quad . \quad . \quad . \ (51)$$

T

The relations given by (49), (50) and (51) suffice for the determination of $\tan \alpha_1$ and V as given by equations (45), (46) and (47), and thence the elementary forces and couples from experiment and equations (48). The final step is the resolution from the displaced to the standard axes, which is covered by the following equations :—

$$
\left.
\begin{aligned}
dX &= l_1 dX_1 + l_2 dY_1 + l_3 dZ_1 \\
dY &= m_1 dX_1 + m_2 dY_1 + m_3 dZ_1 \\
dZ &= n_1 dX_1 + n_2 dY_1 + n_3 dZ_1 \\
dL &= l_1 dL_1 + l_2 dM_1 + l_3 dN_1 \\
dM &= m_1 dL_1 + m_2 dM_1 + m_3 dN_1 \\
dN &= n_1 dL_1 + n_2 dM_1 + n_3 dN_1
\end{aligned}
\right\} \quad . \quad . \quad . \quad (52)
$$

As the expressions in (52) now all apply to the same axes the elements may be summed by integration, the element of length being

$$
dy_1 = l_2 dx + m_2 dy + n_2 dz \quad . \quad . \quad . \quad . \quad (52a)
$$

where l_2, m_2 and n_2 are the disection cosines of the line joining successive centres of pressure.

Examples of the Use of the General Equations.—Two examples will be given, one dealing with the problem of autorotation discussed earlier, and the other with the properties connected with a dihedral angle.

1. Autorotation.—In the experiment described earlier in the chapter it was arranged that the quantities x, z, Γ, v, w, q and r were all zero. The only possible motion was a rotation about the axis of X, and the couple L was therefore the only one of importance. Denoting the wind velocity by u_0 and using equations (45) to (52) leads to $\alpha_x = \alpha_0$, and

$$
\left.
\begin{aligned}
& l_1 = \cos \alpha_0 && m_1 = 0 && n_1 = -\sin \alpha_0 \\
& l_2 = 0 && m_2 = 1 && n_2 = 0 \\
& l_3 = \sin \alpha_0 && m_3 = 0 && n_3 = \cos \alpha_0 \\
& x_1 = 0 && y_1 = y && z_1 = 0 \\
& u_1' = u_0 \cos \alpha_0 && v_1' = 0 && w_1' = u_0 \sin \alpha_0 \\
& p_1 = p \cos \alpha_0 && q_1 = 0 && r_1 = p \sin \alpha_0 \\
& u_1 = u_0 \cos \alpha_0 - py \sin \alpha_0 \\
& w_1 = u_0 \sin \alpha_0 + py \cos \alpha_0
\end{aligned}
\right\} \quad . \quad . \quad (53)
$$

Therefore $\qquad \alpha_1 = \alpha_0 + \mu$, where $\mu = \tan^{-1} \dfrac{py}{u_0} \quad . \quad . \quad . \quad (54)$

and $\qquad\qquad V^2 = u_0{}^2 + p^2 y^2 = u_0{}^2 \sec^2 \mu \quad . \quad . \quad . \quad (55)$

Finally from (52) and the values of dL_1 and dN_1 is obtained the relation

$$
dL = -(k_L \cos \mu + k_D \sin \mu) \frac{\rho c u_0{}^4}{2p^2} \sec^2 \mu \; d(\sec^2 \mu) \quad . \quad (56)
$$

Equation (56) reduces to an element of equation (44) if μ be considered as a small quantity, *i.e.* if the linear velocity of the wing tip due to rotation

is small compared with the translational velocity. The value of L is obtained by integration as

$$L = +\frac{\rho c u_0^4}{2p^2} \int_1^{1 + \frac{p^2 y_0^2}{u_0^2}} \delta(k_L \cos \mu + k_D \sin \mu) \sec^2\mu \, d \,(\sec^2 \mu) \quad . \quad (57)$$

δ signifies the difference of the values of $k_L \cos \mu + k_D \sin \mu$ on the two elements of the wings of the aerofoil where μ has the same numerical value, but opposite sign.

2. **The Effect of a Dihedral Angle during Side Slipping.**—The simplest case will be taken and the origin chosen on the central chord at the centre of pressure. The wings will be assumed to be straight and of uniform chord, and to be bent about the central chord. The mathematical conditions are

$$\left.\begin{array}{ccc} u'_1 = u_0 & v'_1 = v_0 & w'_1 = 0 \\ p_1 = 0 & q_1 = 0 & r_1 = 0 \\ x_1 = 0 & y_1 = y_1 & z_1 = 0 \end{array}\right\} \quad . \quad . \quad . \quad . \quad (58)$$

It should be noticed that the co-ordinates are in this case taken with respect to displaced axes, as this is convenient in the present illustration. The direction cosines $l_1 \ldots n_3$ are given by (49), α_0 and Γ are independent of y_1, and the following further relations are obtained :—

$$\left.\begin{array}{l} u_1 = u_1' = u_0 \cos \alpha_0 \\ v_1 = v_1' = -u_0 \sin \alpha_0 \sin \Gamma + v_0 \cos \Gamma \\ w_1 = w_1' = u_0 \sin \alpha_0 \cos \Gamma + v_0 \sin \Gamma \\ p_1 = 0 \qquad q_1 = 0 \qquad r_1 = 0 \end{array}\right\} \quad . \quad . \quad . \quad (59)$$

$$\tan \alpha_1 = \frac{u_0 \sin \alpha_0 \cos \Gamma + v_0 \sin \Gamma}{u_0 \cos \alpha_0} \quad . \quad . \quad . \quad . \quad (60)$$

$$V^2 = (u_0 \cos \alpha_0)^2 + (-u_0 \sin \alpha_0 \sin \Gamma + v_0 \cos \Gamma) + (u_0 \sin \alpha_0 \cos \Gamma + v_0 \sin \Gamma)^2 \quad . \quad . \quad . \quad . \quad (61)$$

Both α and V are seen from (60) and (61) to be independent of y_1. From (48) it then follows that

$$\left.\begin{array}{l} m d Z_1 = \dfrac{d L_1}{y_1} = -(k_L \cos \alpha_1 + k_D \sin \alpha_1)\rho c V^2 dy_1 \\[2mm] m d X_1 = -\dfrac{d N_1}{y_1} = (k_L \sin \alpha_1 - k_D \cos \alpha_1)\rho c V^2 dy_1 \end{array}\right\} \quad . \quad . \quad (62)$$

and in these expressions k and k_D may be functions of y_1, owing to variation along the wings. Since

$$dL = \cos \alpha_0 \, dL_1 + \sin \alpha_0 \cos\Gamma \, dN_1 \quad . \quad . \quad . \quad . \quad (63)$$

the value can be obtained from (62) for the right-hand wing. A similar expression holds for the left-hand wing if the sign of Γ be changed. The important quantities v_0 and Γ only appear explicitly in $\tan \alpha$ and V^2, and V represents the quantity usually measured in a wind channel.

Instead of attempting to evaluate (63) in the general case, the problem will be limited to the case of greatest importance in aeroplane stability by assuming that both $\dfrac{v_0}{u_0}$ and Γ are small quantities of which the squares can be neglected. Equation (60) then becomes

$$\tan \alpha_1 = \tan \alpha_0 + \frac{v_0}{u_0} \cdot \frac{\Gamma}{\cos \alpha_0} \quad . \quad . \quad . \quad . \quad (64)$$

or after trigonometrical changes

$$\alpha_1 - \alpha_0 = \frac{v_0}{u_0} \Gamma \cos \alpha_0 . \quad . \quad . \quad . \quad . \quad (65)$$

The second term on the right-hand side of (63) becomes negligible with respect to the first, and for the right-hand wing dL becomes

$$dL = -\rho c V^2 \{ k_L \cos (\alpha_1 - \alpha_0) + k_D \sin (\alpha_1 - \alpha_0) \} y_1 dy_1 \quad . \quad (66)$$

From (65) the term in k_D is seen to be small compared with that in k_L, whilst $\cos (\alpha - \alpha_0)$ can be replaced by unity. Hence—

$$dL = -\rho c V^2 k_L y_1 dy_1 . \quad . \quad . \quad . \quad . \quad (67)$$

If k_L' represent the value of k_L when $\alpha = \alpha_0$, it follows that

$$k_L = k_L' + \frac{v_0}{u_0} \Gamma \cos \alpha_0 \frac{\partial k_L}{\partial \alpha} \quad . \quad . \quad . \quad . \quad (68)$$

for the right-hand wing, and

$$k_L = k_L' - \frac{v_0}{u_0} \Gamma \cos \alpha_0 \frac{\partial k_L}{\partial \alpha} \quad . \quad . \quad . \quad . \quad (69)$$

for the left-hand wing. The value of L then is

$$L = -2\rho V v_0 \Gamma \cos \alpha_0 \int_0^l c \frac{\partial k_L}{\partial \alpha} y_1 dy_1 \quad . \quad . \quad . \quad (70)$$

Making the further approximation that c and $\dfrac{\partial k_L}{\partial \alpha}$ are independent of y_1 reduces (70) to

$$L = -\rho c l^2 V v_0 \cos \alpha_0 . \Gamma \frac{\partial k_L}{\partial \alpha} . \quad . \quad . \quad . \quad (71)$$

For comparison with tests on an aerofoil (71) may be used for a numerical example. Since the angle of yaw β is equal to $-\sin^{-1} \dfrac{v_0}{V}$, an angle of yaw of 10° and a velocity of 150 ft. per sec. gives

$$v_0 = -26 \cdot 1 \qquad V = 150$$

For a chord of 6 feet and a length of wing of 20 feet the value of L in a standard atmosphere for $\Gamma = 6°$ is 5600 lbs.-ft. when α_0 has any small value. From a test the couple would have been found as about 4000 lbs.-ft., but this includes end effects not represented in the present calculation.

Calculation of Rotary Derivatives.—It has been seen in Chapter IV. that the rates of variation of forces and couples with variations of u, w and v are easily determined in a wind channel, whilst variations with p, q and r are less simply obtained. The number of observations in the latter case is somewhat small, and as a consequence the element theory has been freely used in calculating the rotary derivatives required for aeroplane stability. It is usual to consider v, p, q and r as small quantities, and to neglect squares, the derivatives then being functions of u_0 and w_0 or of V and α_0.

It is now convenient to express the values of α and V in terms of u', v', w', p, q and r instead of the corresponding variables for the displaced axes. From the equations developed earlier it will be seen that

$$u_1 = l_1(u' + qz - ry) + m_1(v' + rx - pz) + n_1(w' + py - qx) \quad (72)$$

with two similar equations for v_1 and w_1. Using a shorter notation, the values of u_1, v_1, and w_1 are

$$\left.\begin{aligned}
u_1 &= a_0(1 + a_1p + a_2q + a_3r)\\
v_1 &= b_0(1 + b_1p + b_2q + b_3r)\\
w_1 &= c_0(1 + c_1p + c_2q + c_3r)
\end{aligned}\right\} \quad . \quad . \quad . \quad . \quad (73)$$

where
$$\left.\begin{aligned}
a_0 &= l_1u' + m_1v' + n_1w'\\
b_0 &= l_2u' + m_2v' + n_2w'\\
c_0 &= l_3u' + m_3v' + n_3w'\\[4pt]
a_1a_0 = n_1y - m_1z \quad & a_2a_0 = l_1z - n_1x \quad a_3a_0 = m_1x - l_1y\\
b_1b_0 = n_2y - m_2z \quad & b_2b_0 = l_2z - n_2x \quad b_3b_0 = m_2x - l_2y\\
c_1c_0 = n_3y - m_3z \quad & c_2c_0 = l_3z - n_3x \quad c_3c_0 = m_3x - l_3y
\end{aligned}\right\} \quad (74)$$

With this notation

$$\tan \alpha_1 \equiv \frac{w_1}{u_1} = \frac{c_0}{a_0}\{1 + (c_1 - a_1)p + (c_2 - a_2)q + (c_3 - a_3)r\}$$

or $\quad \alpha_1 - \alpha_0 = \sin \alpha_0 \cos \alpha_0\{(c_1 - a_1)p + (c_2 - a_2)q + (c_3 - a_3)r\}$. (75)

and $\quad V^2 = V_0^2 + 2p(a_1a_0^2 + b_1b_0^2 + c_1c_0^2)$
$$+ 2q(a_2a_0^2 + b_2b_0^2 + c_2c_0^2) + 2r(a_3a_0^2 + b_3b_0^2 + c_3c_0^2) \quad . \quad (76)$$

If ω be used to represent generally one of the quantities p. q or r,

$$\frac{\partial}{\partial \omega}(mdX_1) = \rho V_0 cdy_1\left[\sin \alpha_0\left\{2k_L{'}\frac{\partial V}{\partial \omega} + \left(k_D{'} + \frac{\partial k_L}{\partial \alpha}\right)V_0\frac{\partial \alpha}{\partial \omega}\right\}\right.$$
$$\left. + \cos \alpha_0\left\{-2k_D{'}\frac{\partial V}{\partial \omega} + \left(k_L{'} - \frac{\partial k_D}{\partial \alpha}\right)V_0\frac{\partial \alpha}{\partial \omega}\right\}\right] \quad . \quad . \quad (77)$$

and $\dfrac{\partial}{\partial \omega}(mdZ_1) = \rho V_0 cdy_1\left[\sin \alpha_0\left\{-2k_D{'}\dfrac{\partial V}{\partial \omega} + \left(k_L{'} - \dfrac{\partial k_D}{\partial \alpha}\right)V_0\dfrac{\partial \alpha}{\partial \omega}\right\}\right.$
$$\left. - \cos \alpha_0\left\{2k_L{'}\frac{\partial V}{\partial \omega} + \left(k_D{'} + \frac{\partial k_L}{\partial \alpha}\right)V_0\frac{\partial \alpha}{\partial \omega}\right\}\right] \quad . \quad . \quad (78)$$

and the remaining equations are given in (48) to (50).

Denote by μ_ω the expression $2k_L'\dfrac{\partial V}{\partial \omega} + \left(k_D' + \dfrac{\partial k_L}{\partial \alpha}\right)V_0\dfrac{\partial \alpha}{\partial \omega}$

and by ν_ω the expression $-2k_D'\dfrac{\partial V}{\partial \omega} + \left(k_L' - \dfrac{\partial k_0}{\partial \alpha}\right)V_0\dfrac{\partial \alpha}{\partial \omega}$ . . (79)

to reduce equations (77) and (78) to

$$\frac{\partial}{\partial \omega}(mdX_1) = \rho V_0 cdy_1(\mu_\omega \sin \alpha_0 + \nu_\omega \cos \alpha_0) \quad . \quad . \ (80)$$

$$. \ \frac{\partial}{\partial \omega}(mdZ_1) = \rho V_0 cdy_1(\nu_\omega \sin \alpha_0 - \mu_\omega \cos \alpha_0) \quad . \quad . \ (81)$$

Application to L_p, L_r, N_p, and N_r for a pair of Straight Wings.

Assumed conditions :—

$$\begin{array}{ccc} u' = u_0 & v' = 0 & w' = w_0 \\ x = 0 & y_1 = y & z = 0 \\ & q = 0 \quad \Gamma = 0 & \end{array} \quad . \quad . \quad . \quad . \ (82)$$

From (49) it then follows that

$$\begin{array}{ccc} l_1 = \cos \alpha_x & m_1 = 0 & n_1 = -\sin \alpha_x \\ l_2 = 0 & m_2 = 1 & n_2 = 0 \\ l_3 = \sin \alpha_x & m_3 = 0 & n_3 = \cos \alpha_x \end{array} \quad . \quad . \quad . \ (83)$$

From (74) and the above

$$\left.\begin{array}{l} a_0 = u_0 \cos \alpha_x - w_0 \sin \alpha_x = V_0 \cos \alpha_0 \\ b_0 = 0 \\ c_0 = u_0 \sin \alpha_x + w_0 \sin \alpha_x = V_0 \sin \alpha_0 \\ \end{array}\right\} \quad . \quad . \quad . \ (84)$$

since $\qquad \alpha_0 = \alpha_x + \tan^{-1}\dfrac{w_0}{u_0}$

$$\begin{array}{ccc} a_1 a_0 = -y \sin \alpha_x & a_2 a_0 = 0 & a_3 a_0 = -y \cos \alpha_x \\ b_1 b_0 = 0 & b_2 b_0 = 0 & b_3 b_0 = 0 \\ c_1 c_0 = y \cos \alpha & c_2 c_0 = 0 & c_3 c_0 = -y \sin \alpha_x \end{array}$$

$c_1 = \dfrac{y \cos \alpha_x}{V_0 \sin \alpha_0} \qquad a_1 = -\dfrac{y \sin \alpha_x}{V_0 \cos \alpha_0} \qquad$ and $\therefore \quad c_1 - a_1 = \dfrac{yu_0}{V_0^2 \sin \alpha_0 \cos \alpha_0}$

$c_3 = -\dfrac{y \sin \alpha_x}{V_0 \sin \alpha_0} \qquad a_3 = -\dfrac{y \cos \alpha_x}{V_0 \cos \alpha_0} \qquad$ and $\therefore \quad c_3 - a_3 = \dfrac{yw_0}{V_0^2 \sin \alpha_0 \cos \alpha_0}$

Using these expressions and equations (75) and (76)

$$\left.\begin{array}{l} \dfrac{\partial \alpha}{\partial p} = (c_1 - a_1) \sin \alpha_0 \cos \alpha_0 = \dfrac{yu_0}{V_0^2} \\[2mm] \dfrac{\partial \alpha}{\partial r} = (c_3 - a_3) \sin \alpha_0 \cos \alpha_0 = \dfrac{yw_0}{V_0^2} \\[2mm] \dfrac{\partial V}{\partial p} = \dfrac{a_1 a_0^2 + b_1 b_0^2 + c_1 c_0^2}{V_0} = \dfrac{yw_0}{V_0} \\[2mm] \dfrac{\partial V}{\partial r} = \dfrac{a_3 a_0^2 + b_3 b_0^2 + c_3 c_0^2}{V_0} = -\dfrac{yu_0}{V_0} \end{array}\right\} \quad . \quad . \ (85)$$

Since $l_2=0$, the formulæ for dL_ω and dN_ω given by (52), (80), and (81) take the forms

$$\left.\begin{aligned}
dL_{\dot\omega} &\equiv \frac{\partial}{\partial\omega}(dL) = -\mu_\omega\rho V_0 cy\,dy \\
dN_{\dot\omega} &\equiv \frac{\partial}{\partial\omega}(dN) = -\nu_\omega\rho V_0 cy\,dy
\end{aligned}\right\} \quad . \quad . \quad . \quad (86)$$

and from (79) and (85)—

$$\left.\begin{aligned}
\mu_p &= \frac{y}{V_0}\left\{2k_L'w_0 + \left(k_D' + \frac{\partial k_L}{\partial\alpha}\right)u_0\right\} \\
\mu_r &= \frac{y}{V_0}\left\{-2k_L'u_0 + \left(k_D' + \frac{\partial k_L}{\alpha}\right)w_0\right\} \\
\nu_p &= \frac{y}{V_0}\left\{-2k_D'w_0 + \left(k_L' - \frac{\partial k_D}{\partial\alpha}\right)u_0\right\} \\
\nu_r &= \frac{y}{V_0}\left\{2k_D'u_0 + \left(k_L' - \frac{\partial k_D}{\partial\alpha}\right)w_0\right\}
\end{aligned}\right\} \quad . \quad . \quad (87)$$

If the variations of lift and drag towards the wing tips be ignored the integrals take simple form. Calling the length of each wing l, the values are, for constant chord,

$$L_p = -\tfrac{2}{3}l^3\rho c\left\{2k_L'w_0 + \left(k_D' + \frac{\partial k_L}{\partial\alpha}\right)u_0\right\} \quad . \quad . \quad . \quad (88)$$

$$L_r = -\tfrac{2}{3}l^3\rho c\left\{-2k_L'u_0 + \left(k_D' + \frac{\partial k_L}{\partial\alpha}\right)w_0\right\} \quad . \quad . \quad (89)$$

$$N_p = -\tfrac{2}{3}l^3\rho c\left\{-2k_D'w_0 + \left(k_L' - \frac{\partial k_D}{\partial\alpha}\right)u_0\right\} \quad . \quad . \quad (90)$$

$$N_r = -\tfrac{2}{3}l^3\rho c\left\{2k_D'u_0 + \left(k_L' - \frac{\partial k_D}{\partial\alpha}\right)w_0\right\} \quad . \quad . \quad . \quad (91)$$

Numerical values can be obtained for the condition of maximum lift of the wings in illustration of (88) to (91). The wings being assumed of chord 6 ft. and length 20 ft., the velocity of 150 feet per sec. will be taken as along the axis of X. Approximate values for the aerodynamic quantities involved are

$$\frac{\delta k_L}{\partial\alpha} = 2\cdot3 \quad \frac{\delta k_D}{\partial\alpha} = 0\cdot1 \quad k_L' = 0\cdot2 \quad \text{and} \quad k_D' = 0\cdot01$$

and lead to $\quad L_p=-26,000 \quad L_r=4500 \quad N_p=-1100$ and $N_r=-200$ (92)

It was seen in connection with rapid turning that values of p in excess of 0·5 were obtained, and it now appears that a rolling couple of more than 10,000 lbs.-ft. would need to be overcome by the ailerons if the conditions of (92) applied. The angle of incidence in flight is, however, much larger and the speed lower, both of which lead to lower values of the total couple.

In the case of the tail plane of an aeroplane the effect of downwash should be included. It is the values of the air velocities at the aerofoil

which enter into the equations, and these are only the same as the velocity of the centre of gravity of the aeroplane in the absence of downwash.   The difference between the two quantities introduces little further complication into the formulæ developed.

The reader who reaches this fringe of the subject will find the limits of accuracy much wider than those admitted in dealing with steady motion. It should be remembered that less precision is required in the treatment of unsteady motions, and that more can always be obtained in a particular instance of sufficient importance.   It will be some time yet before the fundamental soundness of the blade element theory is established by the experiments of the aerodynamics laboratories to a higher degree of accuracy than at present.

CHAPTER VI

AIRSCREWS

I. General Theory

The theory of the operation of airscrews has been made the subject of many special experiments, and in its broad outlines is well established. Calculation of the fluid motion from first principles is far beyond our present powers, and the hypotheses used are justifiable only on experimental grounds. Whilst frankly empirical, the main principles follow lines indicated by somewhat simple theories of fluid motion, and in this connection the calculated motion of an inviscid fluid most nearly approaches that of a real fluid. The discontinuous motion indicated by a jet of fluid resembles the motion in the stream of air from an airscrew, and W. E. Froude has formulated a theory of propulsion on the analogy. In this theory the thrust on an airscrew is estimated from the momentum generated per second in the slip stream.

Another theory, not necessarily unconnected with the former, was also proposed by Froude and developed by Drzewiecki and others. The blades of the airscrew are regarded as aerofoils, the forces on which depend on their motion relative to the air in the same way as the forces on the wings of an aeroplane. It is assumed that the elementary lengths behave as though unaffected by the dissimilarity of the neighbouring elements, and the forces acting on them are deduced from wind-channel experiments on the lift and drag of aerofoils.

The most successful theory of airscrew design combines the two main ideas indicated above.

In spite of imperfections, the study of the motion of an inviscid incompressible fluid forms a good introduction to experimental work, as it draws attention to some salient features not otherwise easily appreciated. In connection with the estimation of thrust by the momentum generated, W. E. Froude introduced into airscrew theory the idea of an actuator. No mechanism is postulated, but at a certain disc, ABC, Fig. 143, it is presumed that a pressure difference may be given to fluid passing through it.

The fluid at an infinite distance, both before and behind the disc, has a uniform velocity in the direction of the axis of the actuator. At infinity, except in the slip stream, where the velocity is $V_{-\infty}$, the fluid has the velocity V_∞. The only external forces acting on the fluid occur at the actuator disc, and the simple form of Bernoulli's equation developed in the chapter on fluid motion may be applied separately to the two parts of streamlines which are separated by the actuator disc.

When dealing with the motion of an inviscid fluid in a later chapter, it is shown that pressure in parallel streams is uniform, and if this theorem be applied to the hypothetical flow illustrated in Fig. 143 it will be seen that the pressure over the boundary DEGF tends to become uniform when the boundary is very large. The continuous pressure at the boundary of the slip stream is associated with discontinuous velocity.

The total force on the block DEFG is due partly to pressure and partly to momentum, and the first part becomes zero when the pressure becomes uniform over the surface. The excess momentum per sec. leaving the block is the increase of velocity in the slip stream over that well in front of the actuator, multiplied by the area of the slip stream, its velocity and the density of the fluid. If the thrust T applied by the actuator
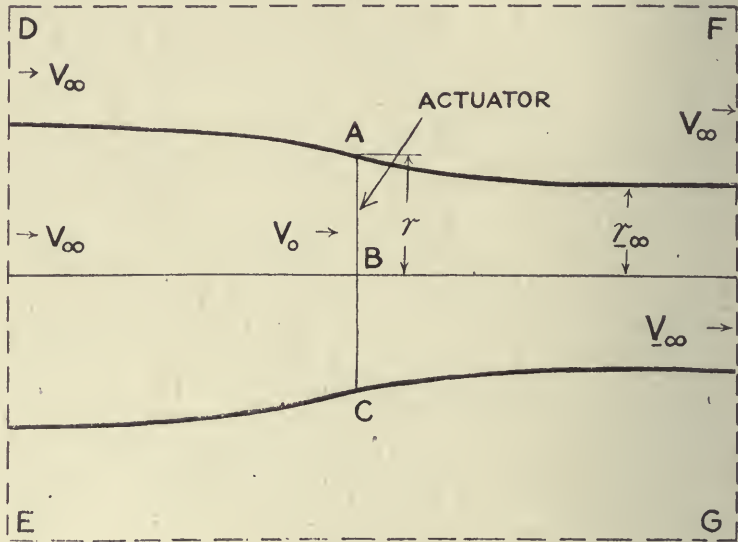
Fig. 143.

is balanced by a force between the disc and the block DEFG and the latter is to be in equilibrium, the following equation for momentum :

$$\mathrm{T} = \rho \cdot \pi r_{-\infty}^2 \mathrm{V}_{-\infty}(\mathrm{V}_{-\infty} - \mathrm{V}_\infty) \quad . \quad . \quad . \quad . \quad (1a)$$

must be satisfied.

Making use of Bernoulli's equation, another expression may be obtained for T which by comparison with (1a) leads to the ideas mentioned in the opening paragraphs of this chapter.

For any streamline not passing through the actuator disc Bernoulli's equation gives

$$p_1 + \tfrac{1}{2}\rho \mathrm{V}_1{}^2 = p_\infty + \tfrac{1}{2}\rho \mathrm{V}_\infty^2 \quad . \quad . \quad . \quad . \quad . \quad (2a)$$

where p_1 and V_1 are the pressure and velocity of the fluid at any point of a streamline. This equation applies to the whole region in front of the actuator and to the fluid behind outside the slip stream. Inside the

slip stream, the pressure being p_2 and the velocity V_2, the equation corresponding to $(2a)$ is

$$p_2 + \tfrac{1}{2}\rho V_2{}^2 = p_\infty + \tfrac{1}{2}\rho V_{-\infty}^2 \quad . \quad . \quad . \quad . \quad . \quad (3a)$$

If p_∞ be eliminated between $(2a)$ and $(3a)$ an important expression for the pressure difference on the two sides of the actuator is obtained, as

$$(p_2 - p_1) + \tfrac{1}{2}\rho(V_2{}^2 - V_1{}^2) = \tfrac{1}{2}\rho(V_{-\infty}^2 - V_\infty^2) \quad . \quad . \quad (4a)$$

Continuity of area of the stream in passing through the actuator disc being presumed, the value of V_2 will gradually approach that of V_1 as the points 1 and 2 on the streamline approach the disc. On the disc both velocities will be the same and equal to V_0, and equation $(4a)$ becomes

$$(p_2 - p_1)_0 = \tfrac{1}{2}\rho(V_{-\infty}^2 - V_\infty^2) \quad . \quad . \quad . \quad . \quad . \quad (5a)$$

The right-hand side of $(5a)$ is constant for all streamlines inside the slip stream, and hence the pressure difference on the two sides of the actuator is uniform over the whole disc.

A second equation for the thrust T obtained from this uniform pressure is

$$T = \tfrac{1}{2}\rho\pi r_0{}^2(V_{-\infty}^2 - V_\infty^2) \quad . \quad . \quad . \quad . \quad . \quad (6a)$$

The quantity of fluid passing through the actuator disc being the same as that in the slip stream, it follows that $r_0{}^2 V_0$ is equal to $r_{-\infty}^2 V_{-\infty}$, and using this relation with $(1a)$ and $(6a)$ shows that

$$V_0 = \tfrac{1}{2}(V_{-\infty} + V_\infty) \quad . \quad . \quad . \quad . \quad . \quad . \quad (7a)$$

The value of V_0 over the actuator disc is seen from $(7a)$ to be a mean of the velocity of the undisturbed stream, and the velocity in the slip stream after it has reached a uniform value.

For the purposes of experimental check it is clear that no measurements far from the airscrew will be satisfactory owing to the breaking up of the slip stream due to viscosity, and the position of least diameter of slip stream is usually taken as sufficiently representative of parallel streamlines. By a modification of equations $(4a)$ and $(6a)$ difficulty in an experimental check can be avoided. A rearrangement of terms in $(4a)$ and $(6a)$ leads to the equation

$$\frac{T}{\pi r_0{}^2} = \overline{p_2 + \tfrac{1}{2}\rho V_2{}^2} - \overline{p_1 + \tfrac{1}{2}\rho V_1{}^2} \quad . \quad . \quad . \quad (8a)$$

and the quantity $p + \tfrac{1}{2}\rho V^2$ happens to be very easily measured. It is therefore possible to choose the points 1 and 2 in any convenient place, one in front and one behind the airscrew.

Equation $(8a)$ is given as applied to the whole airscrew as though p_1, p_2, V_1, V_2 were constant over the whole disc. More rigorously the equation should be developed to apply to an elementary annulus, and the expression $\dfrac{T}{\pi r_0{}^2}$ becomes $\dfrac{dT}{2\pi r dr}$; T is then obtained by integration. With this modification $(8a)$ applies with considerable accuracy to the real flow of air through an airscrew.

Had the actuator given to the fluid a pressure increment which was

inclined to the disc, a flow resulting in torque might have been simulated. The result would have been a twisting of the slip stream, and the angular momentum of the air when the streams had become parallel would have been a measure of the torque. The pressure on the streams when parallel would not have been uniform, but would have varied in such a way as to counteract centrifugal effects.

The air near an airscrew does not, in all probability, move in stream-lines of the kind assumed above, and only an average effect is observable. There is, however, this connection with the simple theory, that not only is equation (8a) nearly satisfied, but a relation similar to that given in equation (7a) is required to explain observed results. The constant which in (7a) is equal to $\frac{1}{2}$ appears to be replaced by a number more nearly equal to $\frac{1}{3}$.

Experimental Evidence for the Applicability of Equation (8a).—A pitot tube, *i.e.* an open-ended tube facing a current, measures the value of $p+\frac{1}{2}\rho V^2$. Within a moderate range of angle of inclination to the stream the reading is constant, and so a pitot tube is a suitable piece of apparatus with which to test the applicability of equation (8a) to airscrews. A considerable number of experiments made in a wind channel showed that for distances of the pitot tube up to 3 or 4 diameters of the airscrew in front of its disc no failure was observed sufficiently large to throw doubt on equation (8a). Except for points of a streamline which lie on opposite sides of the airscrew disc, T of equation (8a) is zero, and hence $p_2 + \frac{1}{2}\rho V_2{}^2 = p_1 + \frac{1}{2}\rho V_1{}^2$ when the two pitot tubes are both in front of the disc or both behind it.

A typical result is given : Denoting the speed well away from the airscrew by V, the flow was $1 \cdot 22$V at a chosen radius near the airscrew disc. The change of pressure necessary to increase the velocity from V to $1 \cdot 22$V is $0 \cdot 240\rho V^2$, whilst the difference between $p_1 + \frac{1}{2}\rho V_1{}^2$ and $p_2 + \frac{1}{2}\rho V_2{}^2$ was $0 \cdot 008\rho V^2$, or little more than 3 per cent. of the change in either p or $\frac{1}{2}\rho V^2$. A similar observation was made for the airscrew running as in a "static" test, and equation (8a) was again found to hold with con-siderable accuracy.

In the above experiments two pitot tubes ahead of the airscrew were used. For a continuation of the experiment one of the pitot tubes was moved into the slip stream, and the difference between $p_1 + \frac{1}{2}\rho V_1{}^2$ in front of the airscrew and $p_2 + \frac{1}{2}\rho V_2{}^2$ behind was observed. Since in front of the airscrew the value of $p_1 + \frac{1}{2}\rho V_1{}^2$ was everywhere the same, it was not necessary to ensure that points 1 and 2 were on the same streamline. In producing the results from which Fig. 144 was prepared, one pitot tube was placed about $0 \cdot 1$D in front of the airscrew disc and the other $0 \cdot 05$D behind, D being the diameter of the airscrew. It was found that with the second pitot tube just behind the airscrew disc the difference in total head became very small at the radius of the tip of the airscrew, and this showed the outer limit of the slip stream.

The speed, V, of the air past the screws and the revolutions of the screw, n, were changed so that the ratio $\dfrac{V}{nD}$ varied from $0 \cdot 562$ to $0 \cdot 922$. The value of the thrust on an element as calculated from the difference of the
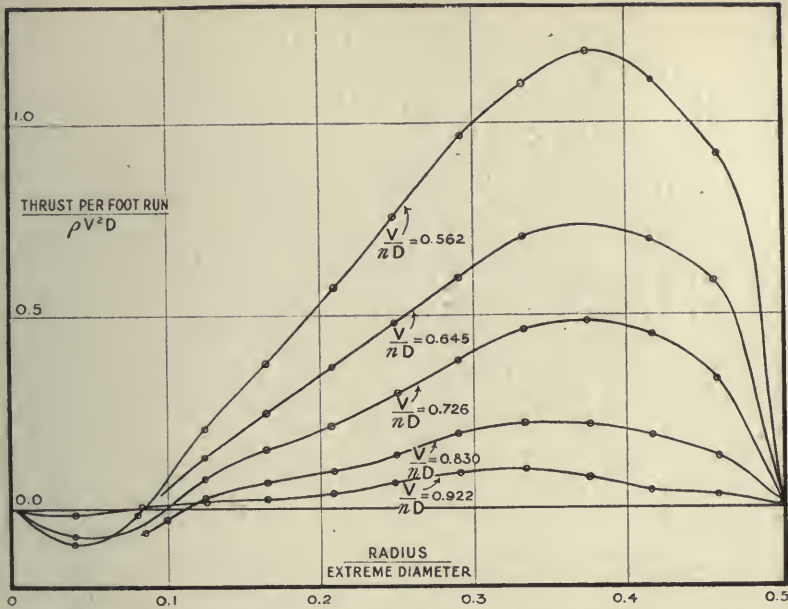
FIG. 144.—Thrust variation along an airscrew blade (experimental).
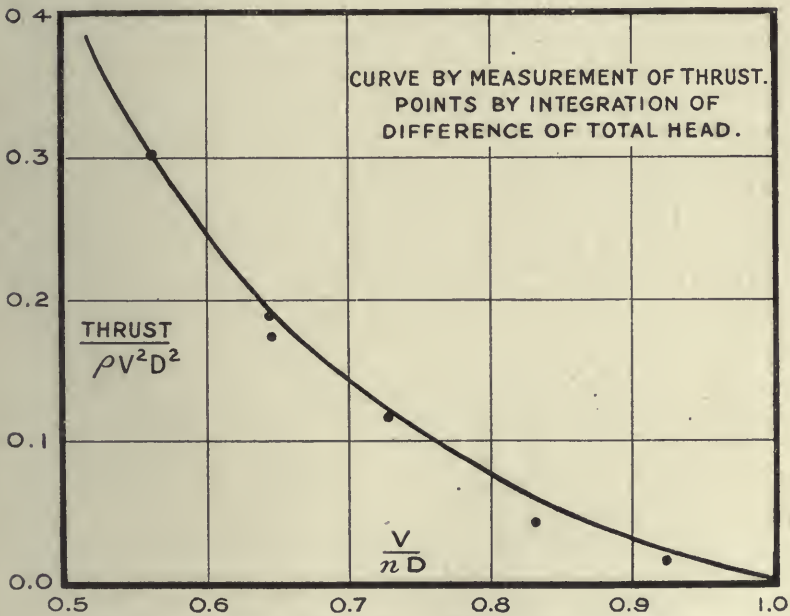
FIG. 145.—Comparison between two methods of thrust measurement.

total heads has been divided by $\rho V^2 D$ before plotting. The reason for this choice of variables is not of importance here and will be dealt with at a later stage. The curves of Fig. 144 show the variation of thrust along

the airscrew on the basis of equation (8a), whilst the area completed by the line of zero ordinate is proportional to the total thrust. It will be noticed that the inner part of the airscrew opposes a resistance to the airflow, and that by far the greater proportion of the thrust is developed on the outer half of the blade. The total thrust as shown by the area of the curves decreases as $\dfrac{V}{nD}$ increases, and would become zero for $\dfrac{V}{nD}$ equal to nearly unity.

For comparison with the total thrust as calculated from equation (8a) and Fig. 144 a measurement of the total thrust was made by a direct method and led to the curve of Fig. 145. The points marked in the figure are the result of the experiments just described. It will be noticed that the agreement between the two methods is good, with a tendency for the points to lie a little below the curve. The agreement is almost as great as the accuracy of observation, and the conclusion may be drawn that in applications of fluid theory to airscrews a reasonable application of Bernoulli's theorem will lead to good results. Later in the chapter it will be shown that this theorem carried through in detail enables a designer to calculate such curves as those of Fig. 144, and that the agreement with the observations is again satisfactory.

Having shown that the total head gives much information on the airflow round an airscrew, it is proposed to extend the consideration of the flow to the different problem of the distribution of velocity before and behind an airscrew disc. Replacing the pitot tube by an anemometer, repetition o the previous experiments provides an adequate means of measuring the velocity and direction of the air near the airscrew.

Measurements of the Velocity and Direction of the Airflow near an Airscrew.—Experiments on the flow of air near an airscrew have been carried out at the N.P.L., and from a consideration of the results obtained Figs. 146 and 147 have been produced. Whilst they give the general idea of flow to which it is now desired to draw attention, it should be mentioned that the curves shown are faired and therefore, for the purposes of developing or checking a new theory of airscrews, less reliable than the original observations.

It will readily be understood that measurements of velocity and direction of the airflow cannot be made in the immediate neighbourhood of the airscrew disc, and any values given in the figures as relating to the airscrew disc are the result of interpolation and are correspondingly uncertain. Qualitatively, however, the figures may be taken as correct representations of observation, whilst quantitatively they are roughly correct.

Each figure has been subdivided into Figs. (a), (b) and (c), which have the following features :—

(a) The diagram shows the "streamlines" in the immediate neighbourhood of the airscrew, the linear scale being expressed in terms of the diameter of the airscrew. On each of the "streamlines" are numbers representing the velocity of the air at several points, whilst at a few of these points the angle of the spiral followed by

the air is indicated by further numbers. The velocity is denoted by V, and the angle of the spiral by ϕ.

(b) The distribution of velocity at various radii is shown in these diagrams. Each of the curves corresponds with a section of (a) parallel to the airscrew disc, and the position of the section is indicated by the number attached to the curve. The radii are expressed as fractions of the diameter of the airscrew. If the airscrew be not moving relative to air at infinity the velocity scale is arbitrary, as it depends on the revolutions of the airscrew only. Where the airscrew is moving with velocity V relative to the distant air this is a convenient measure for other velocities connected with the motion of the air through the airscrew.

(c) Each of the " streamlines " of (a) is a spiral, with the angle of the spiral variable from point to point. The relation between the angle of the spiral and the radius is shown in (c), each curve as before corresponding with a different section of (a).

The Difference of Condition between Fig. 146 and Fig. 147.—Within the limits of accuracy attained the figures give a complete account of the motion of the air over the most important region, and the two groups of figures have been chosen to represent widely different conditions of running. In Fig. 146 the airscrew was stationary relative to distant air, and its efficiency therefore zero. In Fig. 147 the condition was that of maximum efficiency, and was obtained by suitably choosing the ratio of the forward speed to the revolutions.

The figures are strikingly different ; for the stationary airscrew the streamlines converge rapidly in front of the airscrew disc, and for some little distance behind. They are nearly parallel at a distance behind the disc equal to half the airscrew diameter. For the moving airscrew the most noticeable feature is the bulging of the streamlines just behind the airscrew disc and near the axis. Outside the central region the streamlines are nearly parallel to the airscrew axis but show a slight convergence towards the rear.

Had the value of $\frac{V}{nD}$ been increased from 0·75 to 2·0 the airscrew would have been running as a windmill. The corresponding streamlines are more closely related to the moving airscrew than to the stationary one, the only simple change from Fig. 147 being a slight divergence of the streams behind the airscrew. The bulge on the inner streamlines tends to persist.

Stationary Airscrew, Fig. 146.—

(b) The curves of velocity show a very rapid change at radii in the neighbourhood of 0·3 to 0·5D. These rapid changes define the edge of the slip stream, so far as it can be defined. When the streamlines have become roughly parallel at 0·5D (Fig. 146 a) it will be noticed that the greater part of the flow occurs within a radius of 0·4D, and this represents a very considerable reduction of area below that of the airscrew disc and a consequent considerable increase of average velocity between the airscrew disc and the minimum section. The figure shows the velocity at the disc to be roughly 70 per cent. of

that 0·5D behind the disc. The curve marked 4·0D in (b) indicates that at four times the airscrew diameter behind the airscrew disc the mean velocity at small radii has fallen greatly, and the slip streams must therefore have begun to widen again.
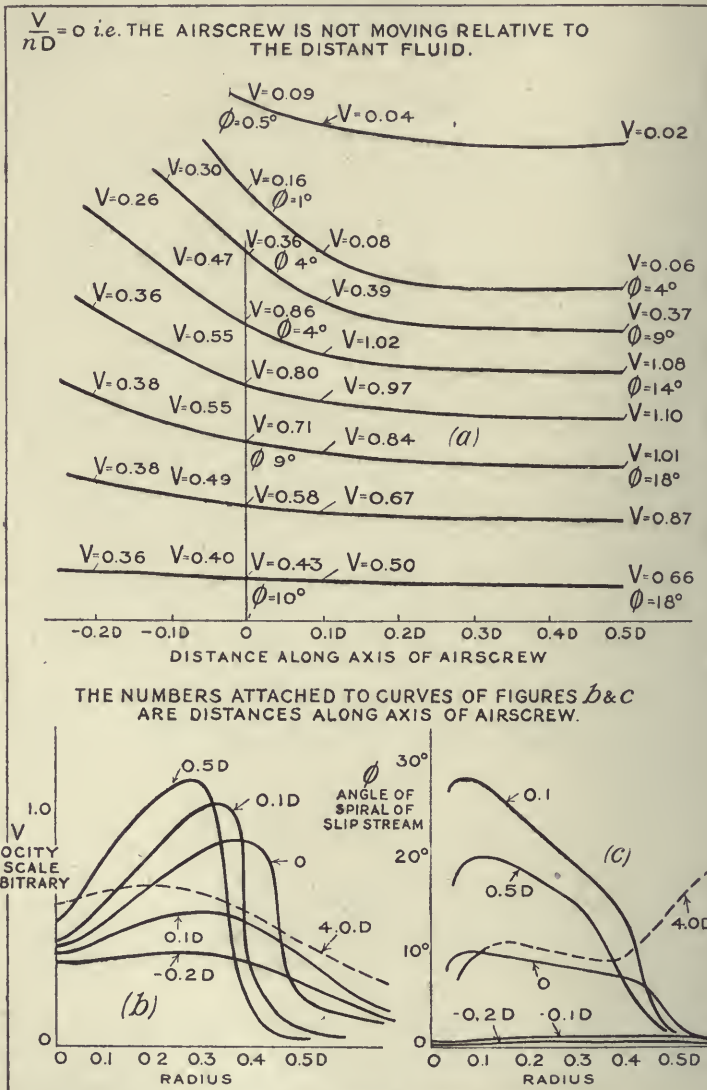
FIG. 146.—Flow of air near a stationary airscrew.

(c) The angle of the spiral of the streamlines varies as markedly as the velocity. In front of the airscrew disc the observed angles never exceeded one degree. Behind it and near the centre, angles of 25° and over were observed. On the edge of the slip stream the

values are of the order of 10° or 15°. At the airscrew disc the interpolated curve shows angles of 10° at the centre, falling to 3° or 4° just inside the blade tip.

If the deductions from the figure be compared with those from the
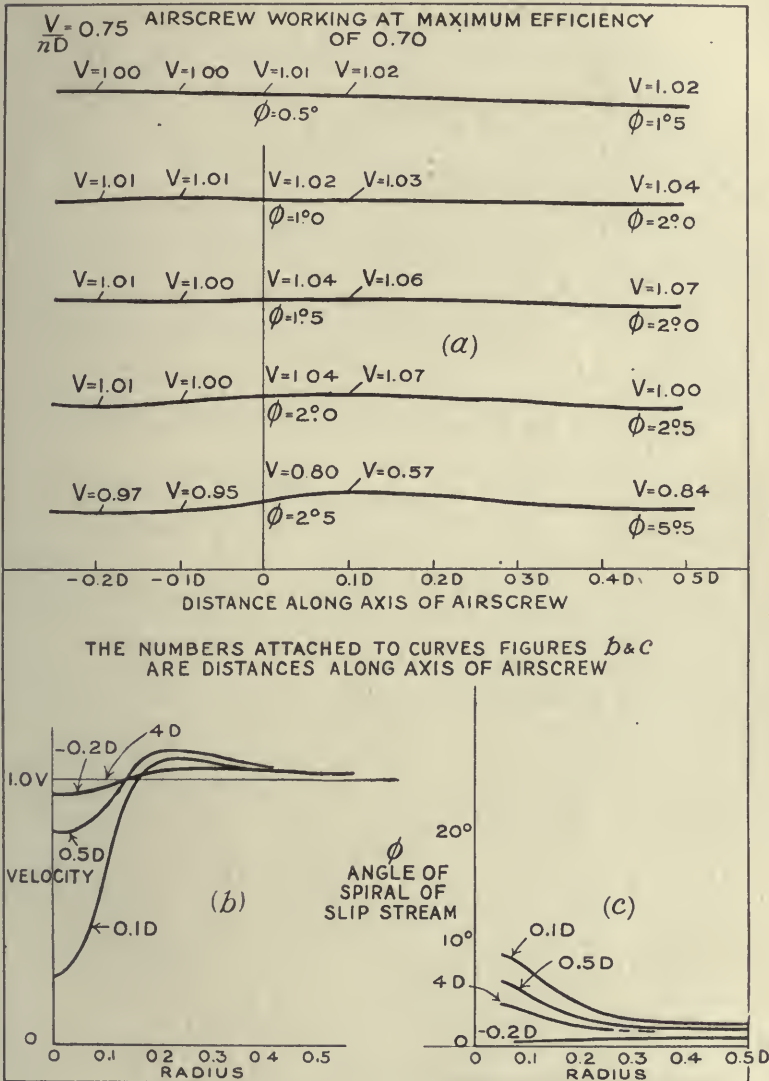
Fig. 147.—Flow of air near a moving airscrew.

theoretical analysis given earlier, it will be seen that the ideas of translational and rotational inflow are applicable to the average motion of air round an airscrew. Further, there is a region of roughly parallel motion at some moderate distance behind the airscrew in which it may be

supposed that the pressure distribution adds nothing to the thrust a calculated from pressure and momentum by the use of (8a).

Moving Airscrew (Fig. 147).

(b) The velocity does not change rapidly with the radius at large radii, and the edge of the slip stream is not clearly defined. The most marked changes of velocity occur at the centre and just behind the airscrew boss. The drop of speed is there very marked. This part of an airscrew adds very little to the total thrust or torque, and is relatively unimportant. The velocity is unity well ahead of the airscrew, and has added to it an amount never exceeding 7 per cent. Along each streamline, roughly half the increment of speed is shown as having occurred before the air crosses the airscrew disc. This condition of the working of an airscrew is of great practical importance, and the accuracy of direct observation is better than for the stationary airscrew. The contraction of the stream is small, but the increment of momentum is not inconsiderable.

(c) In front of the airscrew the twist is shown by the observations to be small. Even behind the airscrew disc the angles are very much smaller than for the stationary airscrew, and do not anywhere exceed 10°.

II. Mathematical Theory of the Airscrew

The experimental work just described was necessary in order to outline clearly the basic assumptions on which a theory of the airscrew should rest. In the theory itself appeal is made to experiment only for the determination of one number, which is the ratio of the velocity added at the airscrew disc to that added between the parallel part of the slip stream and the parallel streams in front. The assumption is usually made that this number is constant, *i.e.* does not depend on the radius, an assumption which is only justified by the utility of the resulting equations.[1] In the earlier stages, in order to bring into prominence its actual character, this assumption will not be made.

The airscrew stream is illustrated in Fig. 148 to show the nomenclature used. The half diameter of the airscrew is denoted by r_0, whilst the half diameter of the slip stream at its minimum section is r_{10}. Radii measured at the airscrew disc are denoted by r and at the minimum section by r_1. The axial velocity of the air at the airscrew disc is $V(1+a_1)$ and at the minimum section $V(1+b_1)$, V being the velocity in front of the airscrew at an infinite distance; a_1 and b_1 are the "inflow" and "outflow" factors of translational velocity.

The rotational velocity is better seen from the next diagram, which also introduces the idea of the application of the aerofoil and its known characteristics. Each element is considered as though independent of its neighbour, and this involves some assumption as to the aspect ratio of

---

[1] Later experiments are providing data for a more general assumption, but application is as yet undeveloped.

the aerofoil on which the basic data were obtained and the shape of the airscrew blade. The value taken is rather arbitrarily chosen, since real knowledge is not yet reached.
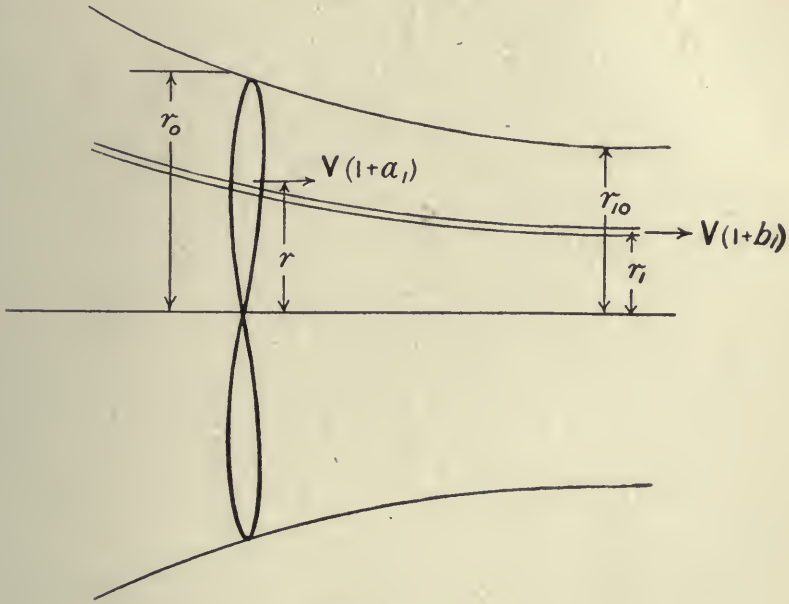
FIG. 148.

Fig. 149 represents an element of an airscrew blade at a radius r. The translational velocity relative to air a considerable distance away is V, and the rotational velocity ωr, ω being the angular velocity of the air-
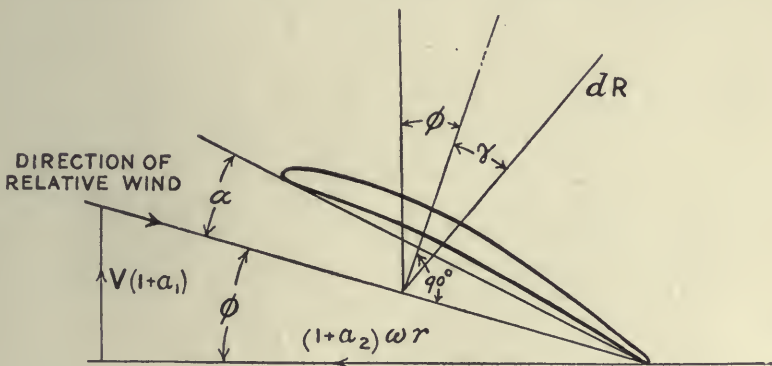
FIG. 149.

screw. Relative to the air at the airscrew disc the velocities are $V(1+a_1)$ and $\omega r(1+a_2)$, a_2 being the rotational inflow factor. These two velocities define the angle ϕ, i.e. the direction of the relative wind, and since the chord of the element makes a known angle with the airscrew disc the

angle of incidence, α, of the element is known when ϕ has been evaluated.

The element is considered as though in a wind channel at angle α and velocity $\sqrt{V^2(1+a_1)^2+\omega^2 r^2(1+a_2)^2}$, and observations of lift and drag determine the resultant force dR and the angle γ. It is clearly necessary to know something more about a_1 and a_2 before the above calculation can lead to definite results, but in order to develop the theory expressions for elements of thrust and torque are first obtained in general terms.

Resolving parallel to the axis of the airscrew leads to

$$dT = dR \cos (\phi + \gamma) \quad . \quad . \quad . \quad . \quad . \quad (1)$$

for the element of thrust, whilst the element of torque is found by taking moments about the airscrew axis, and gives the equation

$$dQ = dR \cdot r \cdot \sin (\phi + \gamma) \quad . \quad . \quad . \quad . \quad . \quad (2)$$

Expressions for Thrust and Torque in Terms of Momentum at the Minimum Section of the Slip Stream.—An alternative to the aerofoil expressions (1) and (2) can be obtained in terms of quantities other than a_1 and a_2, etc., by considering the momentum in the elements of the slip stream at its minimum section, and it is the assumptions connecting the two points of view which are of present importance.

The elementary annulus of radius r at the airscrew disc is replaced by an annulus of decreased radius r_1 at the minimum section of the slip stream. The quantity of air flowing through each annulus being the same, the relation between radii is expressed as

$$(1 + a_1)r\,dr = (1 + b_1)r_1\,dr_1 \quad . \quad . \quad . \quad . \quad (3)$$

At this point is made the important assumption on which the practicability of the inflow theory of airscrew design depends. It is supposed that

$$a_1 = \lambda_1 b_1 \quad . \quad . \quad . \quad . \quad . \quad . \quad (4)$$

where λ_1 is constant for all airscrews and for all the variations of condition under which an airscrew may operate. The method of finding λ_1 will be described later, but the assumption finds some rough justification in the measurements made and described in Figs. 146 and 147.

However arbitrary the theorem may seem to be, it leads to results far better than any other yet known to us, and at the present moment the theory may be accepted as good.

Equation (3) becomes

$$(1 + a_1)r\,dr = \left(1 + \frac{a_1}{\lambda_1}\right)r_1\,dr_1 \quad . \quad . \quad . \quad . \quad (5)$$

or in its integral form

$$r_1{}^2 = \int \frac{1 + a_1}{1 + \dfrac{a_1}{\lambda_1}}\,dr^2 \quad . \quad . \quad . \quad . \quad . \quad (6)$$

and expresses the radius of the slip stream in terms of r, a_1 and λ_1.

The elements of thrust and torque can now be written down. The mass of air flowing through the annulus of the slip stream is $2\pi\rho V(1+b_1)r_1 dr_1$, the velocity added from rest is $b_1 V$, and therefore the thrust is

$$dT = 2\pi\rho(1+b_1)b_1 V^2 r_1 dr_1 \quad . \quad . \quad . \quad . \quad . \quad (7)$$

Using equations (4) and (5) to transform (7) leads to

$$dT = 2\pi\rho(1+a_1)\frac{a_1}{\lambda_1}V^2 r dr \quad . \quad . \quad . \quad . \quad . \quad (8)$$

and if the momentum and aerofoil theories are to lead to identical estimates this thrust should be the same as that given by (1). Hence

$$dR \cos(\phi+\gamma) = 2\pi\rho(1+a_1)\frac{a_1}{\lambda_1}V^2 r dr \quad . \quad . \quad . \quad (9)$$

In this equation every term is, by hypothesis, known in terms of a_1 and a_2 and equation (9) is therefore one relation between a_1 and a_2. A second relation may be obtained from the equality of the expressions for torque.

The element of torque is readily seen to be

$$dQ = 2\pi\rho(1+b_2)b_2 V\omega r_1^3 dr_1 \quad . \quad . \quad . \quad . \quad (10)$$

and making the corresponding assumption to (4) that

$$a_2 = \lambda_2 b_2 \quad . \quad . \quad . \quad . \quad . \quad . \quad . \quad (11)$$

(11) and (5) may be used to transform (10) to

$$dQ = 2\pi\rho(1+a_1)\frac{a_2}{\lambda_2}V\omega r_1^2 . r dr \quad . \quad . \quad . \quad (12)$$

Unlike equation (9) for the elementary thrust, which contains r only, equation (2), for elementary torque, involves both r and r_1, and the relation which is given by (6) does not lend itself to simple substitution in (12).

Equating (12) and (2) gives a second relation between a_1 and a_2 as

$$dR \sin(\phi+\gamma) = 2\pi\rho(1+a_1)\frac{a_2}{\lambda_2}V\omega r_1^2 dr \quad . \quad . \quad (13)$$

λ_1 and λ_2 being known constants, equations (9) and (13) are sufficient to determine both a_1 and a_2 in terms of aerofoil characteristics.

Transformation of Equations (9) and (13) to more Convenient Form for Calculation.—From the geometry of the airflow it follows that

$$\tan\phi = \frac{(1+a_1)}{(1+a_2)} . \frac{V}{\omega r} \quad . \quad . \quad . \quad . \quad . \quad (14)$$

and that the resultant velocity is

$$(1+a_2)\omega r \sec\phi \quad . \quad . \quad . \quad . \quad . \quad (15)$$

The element of force, dR, is known from general wind-channel experiments to have the form

$$dR = \rho c dr (1+a_2)^2 \omega^2 r^2 \sec^2\phi . f(a) \quad . \quad . \quad . \quad (16)$$

where c is the sum of the chords of the aerofoil elements at radius r, and $f(a)$ is the absolute coefficient of resultant force. In the same way it is known that

$$\tan \gamma = \frac{\text{drag}}{\text{lift}} = \mathrm{F}(a) \quad . \quad . \quad . \quad . \quad . \quad (17)$$

The algebraic work in transforming (9) by use of (14), (16), and (17) is simple, and leads to

$$\frac{a_1}{1 + a_1} = \frac{\lambda_1}{2\pi} \cdot \frac{c}{r} \cdot f(a) \operatorname{cosec}^2 \phi \cos(\phi + \gamma) \quad . \quad . \quad . \quad (18)$$

whilst (13) becomes

$$\frac{a_2}{1 + a_2} = \frac{\lambda_2}{2\pi} \left(\frac{r}{r_1}\right)^2 \cdot \frac{c}{r} \cdot f(a) \operatorname{cosec} \phi \sec \phi \sin(\phi + \gamma) . \quad . \quad (19)$$

To solve in any particular case, it is most convenient to assume successive values for a. Since $\phi + a$ is known from the geometry of the airscrew this fixes ϕ, and equations (18) and (19) then determine a_1 and a_2. Finally, equation (14) gives the correct value of $\dfrac{\mathrm{V}}{\omega r}$ for the values of ϕ assumed.

Example of the Calculation of a_1.—The forces on an aerofoil as taken from wind-channel experiments are most commonly given as lift and drag coefficients k_{L} and k_{D}. In the present notation

$$\left. \begin{aligned} k_{\mathrm{L}} &= f(a) \cos \gamma \\ k_{\mathrm{D}} &= f(a) \sin \gamma \end{aligned} \right\} \quad . \quad . \quad . \quad . \quad . \quad (20)$$

$$\left. \begin{aligned} f(a) \cos(\phi + \gamma) &= k_{\mathrm{L}} \cos \phi - k_{\mathrm{D}} \sin \phi \\ f(a) \sin(\phi + \gamma) &= k_{\mathrm{L}} \sin \phi + k_{\mathrm{D}} \cos \phi \end{aligned} \right\} \quad . \quad . \quad (21)$$

Take $r = 33 \cdot 6$ ins., $c = 2 \times 9 \cdot 65$ ins., *i.e.* $\dfrac{c}{r} = 0 \cdot 575$, $a + \phi = 22° \cdot 1$, $\lambda_1 = 0 \cdot 35$,

and proceed to fill in the table below from known data.

The tabulation starts from column (1) with arbitrarily chosen values of a, and in this illustration a very wide range of a has been taken. Since $a + \phi = 22° \cdot 1$ column (2) follows immediately. The lift coefficient k_{L} is taken from wind-channel observations on a suitable aerofoil for the given values of a, the $\dfrac{\text{lift}}{\text{drag}}$ ratio of column (4) is similarly obtained, and by the use of trigonometrical tables leads to column (5). The remaining columns follow as arithmetical processes from the first four columns and equation (18).

The values found for a_1 show very great variations, but discussion of the results is deferred until a_2 has been evaluated.

Assumptions as to λ_2 and a_2.—The assumption which has received most attention hitherto has been that $\lambda_2 = 0$, and equation (19) then shows that a_2 is zero. This is equivalent to assuming no rotational inflow and other assumptions now appear to be better.

λ_2 plays the same part in relation to torque that λ_1 does to the thrust,

and it would be possible to carry empiricism one stage further and choose λ_1 and λ_2 so that both the thrust and torque agreed with experiment at some particular value of $\dfrac{V}{nD}$. This would lead to more difficult calculations, but not to fundamentally different ideas. A more obvious and equally probable assumption is that the air at the airscrew disc is given an added velocity in the direction opposite to dR, in which case

$$\frac{a_2 \omega r}{a_1 V} = -\tan(\phi + \gamma) \quad . \quad . \quad . \quad . \quad . \quad . \quad (22)$$

TABLE 1.

1	2	3	4	5	6	7	8	9	10
a (deg.)	ϕ (deg.)	k_L	$\dfrac{L}{D}$	γ (deg.)	Cos ϕ	Sin ϕ	$k_L \cos\phi - k_D \sin\phi$	(7) multiplied by $\dfrac{\lambda_1}{2\pi}\cdot\dfrac{c}{r}\cdot\mathrm{cosec}^2\phi$ i.e. $\dfrac{a_1}{1+a_1}$	a_1
-10	32·1	$-0\cdot170$	$-3\cdot1$	$-17\cdot2$	0·847	$+0\cdot532$	$\left\{\begin{matrix}-0\cdot144\\-0\cdot029\end{matrix}\right\}=-0\cdot173$	$-0\cdot0196$	$-0\cdot020$
-5	27·1	$+0\cdot010$	$+0\cdot3$	73·0	0·890	$+0\cdot455$	$\left\{\begin{matrix}+0\cdot009\\-0\cdot015\end{matrix}\right\}=-0\cdot006$	$-0\cdot0009$	$-0\cdot001$
0	22·1	0·195	17·5	3·3	0·926	$+0\cdot376$	$\left\{\begin{matrix}+0\cdot180\\-0\cdot004\end{matrix}\right\}=+0\cdot176$	$+0\cdot0399$	$+0\cdot0415$
2	20·1	0·275	19·5	2·9	0·939	0·343	$\left\{\begin{matrix}+0\cdot258\\-0\cdot005\end{matrix}\right\}=+0\cdot253$	$+0\cdot0691$	$+0\cdot0740$
4	18·1	0·350	18·2	3·1	0·950	0·311	$\left\{\begin{matrix}+0\cdot332\\-0\cdot006\end{matrix}\right\}=+0\cdot326$	$+0\cdot108$	$+0\cdot121$
6	16·1	0·425	16·5	3·5	0·961	0·277	$\left\{\begin{matrix}+0\cdot408\\-0\cdot007\end{matrix}\right\}=+0\cdot401$	$+0\cdot167$	$+0\cdot200$
8	14·1	0·495	15·0	3·8	0·970	0·244	$\left\{\begin{matrix}+0\cdot480\\-0\cdot008\end{matrix}\right\}=+0\cdot472$	$+0\cdot254$	$+0\cdot339$
10	12·1	0·560	13·5	4·2	0·974	0·210	$\left\{\begin{matrix}+0\cdot545\\-0\cdot009\end{matrix}\right\}=+0\cdot536$	$+0\cdot390$	$+0\cdot640$
15	7·1	0·595	8·0	7·2	0·992	0·124	$\left\{\begin{matrix}+0\cdot590\\-0\cdot009\end{matrix}\right\}=+0\cdot581$	$+1\cdot21$	$-5\cdot8$
20	2·1	0·545	4·3	13·0	0·999	0·036	$\left\{\begin{matrix}+0\cdot545\\-0\cdot005\end{matrix}\right\}=+0\cdot540$	$+10\cdot60$	$-1\cdot10$

The accuracy of this assumption is not less than that relating to a_1. The radial velocity is still ignored, and the assumption is made that a_1 and a_2 are constant across the blade, which will probably be more correct for narrow than for wide blades. Equation (18) remains as before, but equation (14) becomes

$$\tan\phi = \frac{1+a_1}{1 - a_1 \tan(\phi+\gamma)\dfrac{V}{\omega r}} \cdot \frac{V}{\omega r} \quad . \quad . \quad . \quad . \quad (23)$$

$$= \frac{1+a_1}{\dfrac{\omega r}{V} - a_1 \tan(\phi+\gamma)} \quad . \quad . \quad . \quad . \quad . \quad (24)$$

As applied to the element considered above the calculation proceeds to determine $\dfrac{V}{\omega r}$ from the figures in Table 1 and equation (24), which is more conveniently written as

$$\frac{\omega r}{V} = \frac{1 + a_1}{\tan \phi} + a_1 \tan (\phi + \gamma) \quad . \quad . \quad . \quad . \quad (25)$$

TABLE 2.

a (degrees).	ϕ (degrees).	$\dfrac{V}{\omega r}$	a_1.	a_2.
—10	32·1	0·633	—0·020	0·011
— 5	27·1	0·508	—0·001	0·003
0	22·1	0·389	+0·041	—0·008
2	20·1	0·337	0·074	—0·011
4	18·1	0·288	0·121	—0·014
6	16·1	0·236	0·200	—0·017
8	14·1	0·184	0·339	—0·020
10	12·1	0·128	0·640	—0·024
15	7·1	—0·025	—5·8	—0·037
20	2·1	—0·360	—1·1	—0·010

This table repays careful examination in conjunction with Table 1. Equation (8) shows that the thrust on the element is zero when a_1 is zero, and Table 1 shows that a_1 changes sign at about —5°. The thrust is then seen to change sign at an angle of incidence rather greater than that at which the lift changes sign; the value of $\dfrac{V}{\omega r}$ is roughly 0·51. The section considered occurred in the airscrew blade at 0·7D, where D is the diameter of the airscrew, and the more familiar expression $\dfrac{V}{nD}$ has the value 1·12 when the thrust on the element vanishes. With $a = -10°$ the airscrew is acting as a windmill, i.e. is opposing a resistance to motion and is delivering power.

Continuing the examination, using Table 2, it will be noticed that $\dfrac{V}{\omega r}$ changes sign at an angle of incidence of about 14°, and the aerofoil reaches its critical angle of incidence at about 12°. The further cases in Table 2 correspond with backward movement of the airscrew along its axis. From an angle of incidence of 14° onwards a_1 is negative, but $\dfrac{a_1}{1 + a_1}$ is still positive and passes through the value ∞ when ϕ is zero, as may be seen either from Table 1 by interpolation or more readily from equation (18). There is no special change in the physical conditions at this value of ϕ, as may be seen from the continuity of a_1, which is —1 when $\dfrac{a_1}{1 + a_1} = \infty$. The history of further changes of $\dfrac{V}{\omega r}$, if continued, shows continuously increasing angle

of incidence up to $90° + 22°·1$ as a limit, as the airscrew moves backwards more and more rapidly.

Efficiency of the Element.—The useful work done, being measured relative to air at infinity, is VdT, whilst the power expended is ωdQ. The efficiency is then

$$\eta = \frac{V}{\omega} \cdot \frac{dT}{dQ} \quad \cdots \cdots \quad (26)$$

Substituting from equations (1) and (2) converts (26) to

$$\eta = \frac{\dfrac{V}{\omega r}}{\tan(\phi + \gamma)} \quad \cdots \cdots \quad (27)$$

and combining this with (14) leads to

$$\eta = \frac{1 + a_2}{1 + a_1} \cdot \frac{\tan \phi}{\tan(\phi + \gamma)} \quad \cdots \cdots \quad (28)$$

TABLE 3.

		a (degrees).	$\dfrac{V}{\omega r}$.	Efficiency, η
Windmill {	No torque ... No lift	-10	$0·633$	$+2·38$
		-5	$0·508$	$-0·090$
Airscrew {	No thrust			
		0	$0·389$	$0·820$
	Maximum efficiency	2	$0·337$	$0·793$
		4	$0·288$	$0·744$
		6	$0·236$	$0·669$
		8	$0·184$	$0·570$
		10	$0·128$	$0·439$
No translational velocity, i.e. static test condition				
		15	$-0·025$	$-0·098$
		20	$-9·360$	$-1·33$

A word might here be said as to the meaning of efficiency and the reason for choosing VdT as a measure of work done. Efficiency is a relative term, as may be seen from the following example: Imagine an aeroplane flying through the air against a wind having a speed equal to its own. Relative to the ground the aeroplane is stationary, but the petrol consumption is just as great as if there were no wind. As a means of transport over the ground the aeroplane has no efficiency in the above instance. On the other hand, if it turns round and flies with the wind the aeroplane would be said to be an efficient means of transport, and yet in neither case does the aeroplane do any useful work in the sense of storing energy unless it has happened to climb. It is obvious that no useful definition of efficiency can depend on the strength of the wind, and what

is usually meant by the efficiency of the airscrew is its value as an instrument for the purpose of moving the rest of the aeroplane through the air. The conception of efficiency is not simple and well repays special attention during a study of aerodynamics.

From equation (28) may be calculated the values of efficiency η corresponding with Tables 1 and 2. The values are given in Table 3.

In interpreting Table 3 it is convenient to refer to Fig. 150, which shows the airscrew characteristics of the element in comparison with those
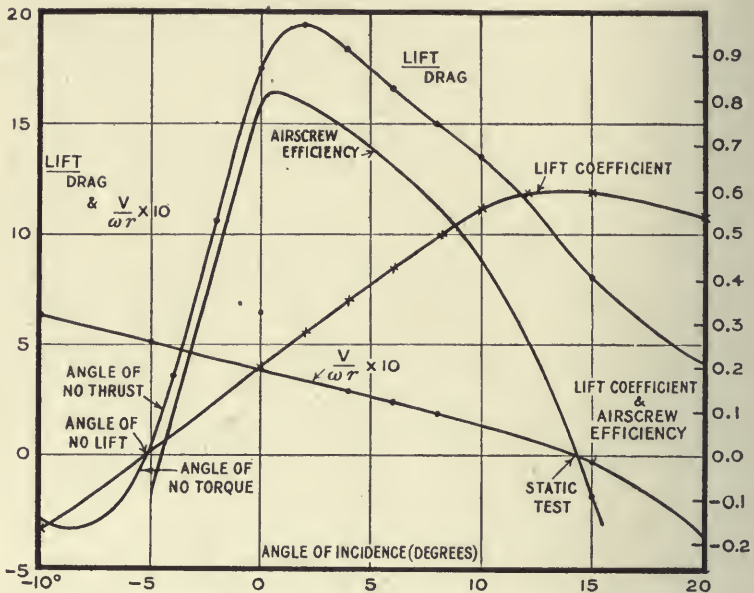
FIG. 150.—Comparison of characteristics of elements of aerofoil and airscrew.

of the elementary aerofoil. The characteristics are shown as dependent on angle of incidence of the aerofoil, and the curves show $\dfrac{V}{\omega r}$ and efficiency for the airscrew and lift coefficient and $\dfrac{\text{lift}}{\text{drag}}$ for the aerofoil.

At an angle of incidence of $-10°$ the thrust and torque are both negative, and Table 3 shows the efficiency to be positive. The airscrew is working as a windmill, the work output is ωdQ and not VdT, and (26) represents the reciprocal of the efficiency of the windmill; the value $\eta = 2·38$ of Table 3 represents a real efficiency of 42 per cent. At an angle of incidence of $-5°·5$ the point of zero torque occurs, and the efficiency as a windmill is zero corresponding with an infinite value in Table 3. As the angle of incidence increases the torque becomes positive, whilst the thrust remains negative and the efficiency is negative. At $-4·4°$ the thrust becomes positive and the airscrew begins its normal functions as a propelling agent, the efficiency being zero at this point,

but rising rapidly to 0·83 at an angle of incidence of about 0°·5.   At greater angles of incidence the efficiency falls to zero when the airscrew is not moving relative to distant air.   If the airscrew be moved backwards $V d T$ is negative and the efficiency is negative, but this condition is unimportant and no detailed study of it is given.

The general similarity of the efficiency and $\dfrac{\text{lift}}{\text{drag}}$ curves may be noticed and suggests the importance of high $\dfrac{\text{lift}}{\text{drag}}$ ratio.   This is seen to be a general property of airscrew elements by reference to equation (28). Other things being equal, equation (28) shows maximum efficiency when γ is least, i.e. when $\dfrac{L}{D}$ is greatest.

Relative Importance of Inflow Factors.—It is now possible to make a quantitative examination of the importance of the inflow factors a_1 and a_2, and for this purpose Table 4 has been prepared.   The first column contains the angle of incidence of the blade element, whilst the remaining columns show the values of $\dfrac{V}{\omega r}$ and η on the separate hypotheses that (1) both a_1 and a_2 are used ; (2) that neither is used, and (3) that only a_1 is used.   The general conclusion is reached that a_1 is very important, but that a_2 may be ignored in many calculations without serious error.

TABLE 4.—Effect of Inflow Factors on the Calculated Advance per Revolution and Efficiency of a Blade Element.

1	2	3	4	5	6	7
α (degrees).	$\dfrac{V}{\omega r}$	$\dfrac{V}{\omega r}$ a_1 and a_2 zero.	$\dfrac{V}{\omega r}$ a_2 zero.	η	η a_1 and a_2 zero.	η a_2 zero.
−10	0·633	0·627	0·642	+2·38	+2·36	+2·42
− 5	0·508	0·512	0·511	−0·090	−0·091	−0·091
0	0·389	0·406	0·390	0·820	0·855	0·821
2	0·337	0·366	0·340	0·793	0·862	0·800
4	0·288	0·327	0·292	0·743	0·845	0·753
6	0·236	0·289	0·240	0·669	0·820	0·680
8	0·184	0·251	0·188	0·570	0·777	0·582
10	0·128	0·214	0·131	0·438	0·733	0·448
15	−0·025	0·125	−0·026	−0·098	0·490	−0·102
20	−0·360	0·037	−0·360	−1·34	0·137	−1·34

At the angle of no thrust, −5°·5, the three hypotheses differ by very small and unimportant amounts, but at an angle of incidence of 6°, which would correspond with the best climbing rate of an aeroplane, the difference of $\dfrac{V}{\omega r}$ for the assumption of no inflow and that for full inflow is more than 20 per cent.   If V be fixed by the conditions of flight the theory of no inflow would indicate a lower speed of rotation for a given thrust than does

the theory of full inflow. This means that a design on the former basis would lead to an airscrew which at the speed of rotation used in the design would not be developing the thrust expected. The effect of inflow factors on efficiency for $a = 6°$ is equally strongly marked, for in one case an efficiency of 0·820 is estimated, whilst in the more complete theory only 0·669 is found.

General experience of airscrew design shows that the "inflow" theory leads to better results than the older "no inflow" theory.

Although the effect of inflow factors is great, it appears that almost the whole is to be ascribed to the effect of a_1. The differences between columns 2 and 4 and columns 5 and 7 are due to the assumption that a_2 has a value in one and is zero in the other. In no case are the differences great, and this is a justification for the fact that a great amount of airscrew design and experimental analysis has been carried out on the basis that a_2 is zero.

It appears that a_2 is never very great, and that calculation leads to agreement with Pannell and Jones in their observation that the rotational inflow to an airscrew is very small.

$\dfrac{V}{\omega r}$ and a.—Since $\phi + a$ is constant (22°·1 in our illustration) equation (14) may be written as

$$\begin{array}{c} \text{constant} - a = \tan^{-1}\dfrac{(1+a_1)}{1+a_2}\cdot\dfrac{V}{\omega r} \quad . \quad . \quad . \quad (26) \\ (22°·1) \end{array}$$

If a_1 and a_2 be small $\dfrac{V}{\omega r}$ is sensibly a function of a only, and hence its general importance as a fundamental variable in airscrew design. Fig. 150 shows that when inflow is taken into account the relation between $\dfrac{V}{\omega r}$ and a is linear for a large range of a. The constant in this linear relation is 15°·5 instead of the 22°·1 of (26), and this is due partly to the inflow factor a_1 and partly to the fact that the tangent is not proportional to the angle over the range in question.

Approximation to the Value of a_1 for Efficient Airscrews.—An examination of column 8, Table 1, will show that the part of a_1 which depends on the drag coefficient is very small, and that

$$f(a)\cos(\phi + \gamma) \text{ is nearly equal to } k_L\cos\phi \quad . \quad . \quad (29)$$

over the whole range of the example. This agreement is partly accidental, but the expression can be examined in order to lay down the conditions necessary for the approximation to hold.

An expansion for $f(a)\cos(\phi + \gamma)$ is given in (21), which may be rewritten as

$$f(a)\cos(\phi + \gamma) = k_L\cos\phi\left(1 - \dfrac{k_D}{k_L}\tan\phi\right) - \quad . \quad . \quad (30)$$

and the second term inside the bracket on the right-hand side of (30) is

seen to be small in comparison with unity if $\frac{k_L}{k_D}$, *i.e.* $\frac{L}{D}$ is large and tan ϕ small. $\frac{k_L}{k_D}$ may be as great as 20 and tan $\phi = 0.5$ in the parts of an efficient aeroplane or airship airscrew which are important. Hence for the circumstances of greatest practical importance we may use (29) as indicating a good approximation; over the working range a_1 does not exceed 0.3, and an error of 5 per cent. in a_1 makes an error of 1 per cent. in the estimated efficiency. At maximum efficiency the approximation is very much closer. Instead of (18) a new approximate expression for a_1 for the ordinary design of airscrews is

$$\frac{a_1}{1+a_1} = \frac{\lambda_1}{2\pi} \cdot \frac{c}{r} \cdot k_L \cos \phi \operatorname{cosec}^2 \phi \quad . \quad . \quad . \quad . \quad (31)$$

Points of no Torque, no Thrust, and no Lift.—From equation (2) it will be seen that the torque of the element will be zero if $d\mathrm{R} \sin (\phi + \gamma) = 0$, and if the value of $d\mathrm{R}$ from (16) be used, the condition of no torque reduces to

$$d\mathrm{Q} = 0 \text{ when } f(a) \sin (\phi + \gamma) = 0$$

$$\textit{i.e. when } k_L \sin \phi + k_D \cos \phi = 0$$

$$\textit{i.e. when } \frac{k_L}{k_D} = - \cot \phi \quad . \quad . \quad . \quad . \quad . \quad (32)$$

In a similar way it may be found that

$$d\mathrm{T} = 0 \text{ when } \frac{k_L}{k_D} = \tan \phi \quad . \quad . \quad . \quad . \quad (33)$$

The point of no lift occurs, of course, when $\frac{k_L}{k_D} = 0$.

In ordinary practice ϕ is positive at the angle of no lift, and the positions found from (32) and (33) are not far removed from the no-lift position. For the element of the previous example $\frac{k_L}{k_D} = -\frac{1}{2}$ for (32) and $+2$ for (33) when the solution is obtained, the angles of incidence being

$$
\left.
\begin{array}{ll}
\text{no torque} & - 5°.4 \\
\text{no lift} & - 5°.1 \\
\text{no thrust} & - 4°.4
\end{array}
\right\} \quad . \quad . \quad . \quad . \quad (34)
$$

This result may be taken as typical of the important sections of airscrew blades.

Integration for a Number of Elements to obtain Thrust and Torque for an Airscrew.—The process carried out in detail for an element can be repeated for other radii and the total thrust and torque obtained. The expressions may be collected as

$$\mathrm{T} = \int_0^{D/2} \rho c (1 + a_2)^2 \omega^2 r^2 \sec^2 \phi (k_L \cos \phi - k_D \sin \phi) dr . \quad . \quad (35)$$

$$\mathrm{Q} = \int_0^{D/2} \rho c (1 + a_2)^2 \omega^2 r^3 \sec^2 \phi (k_L \sin \phi + k_D \cos \phi) dr . \quad . \quad (36)$$

and
$$\eta = \frac{V}{\omega r} \cdot \frac{T}{Q} . \quad . \quad . \quad . \quad . \quad . \quad . \quad (37)$$

from the aerofoil side, and

$$T = \int_0^{D/2} 2\pi\rho(1 + a_1)\frac{a_1}{\lambda_1} V^2 r dr . \quad . \quad . \quad . \quad (38)$$

and
$$Q = \int_0^{D/2} 2\pi\rho(1 + a_1)\frac{a_2}{\lambda_2} V\omega r_1{}^2 . r dr \quad . \quad . \quad (39)$$

from considerations of momentum,

where
$$\int (1 + a_1) r dr = \int \left(1 + \frac{a_1}{\lambda_1}\right) r_1 dr_1 \quad . \quad . \quad . \quad . \quad . \quad . \quad (40)$$

defines the r_1 of (39).

In considering a single element it has been shown that a_2 may be taken as zero, but that $\frac{a_2}{\lambda_2}$ is finite. It has been shown that (35) and (38) can be made to agree by suitable choice of a_1, and (38) may most suitably be used during integration to find T. As λ_2 may be unknown, equation (36) is used to calculate Q.
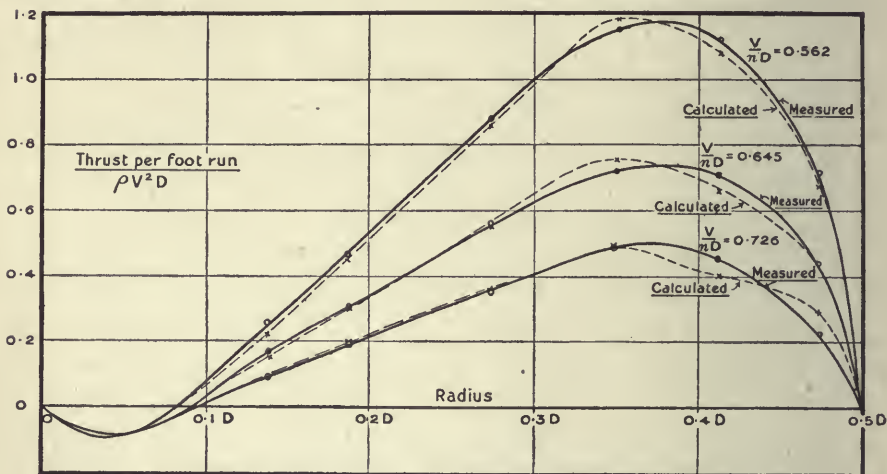
Fig. 151.—Comparison between observed and calculated variations of thrust along an airscrew blade.

Determination of λ_1.—If various values of λ_1 be chosen it is obvious that for some particular one the calculated thrust at a given advance per revolution will agree with the observed thrust on the airscrew. It may be supposed that this has been done in a particular case (see Fig. 151), and that for a value of $\frac{V}{nD}$ of 0·645 the best value of λ_1 has been found to be 0·35. Using this value of λ_1 for $\frac{V}{nD} = 0·562$ and $\frac{V}{nD} = 0·726$ further values

of total thrust are calculable and may be compared with observation. Curves for the blade elements may be compared by the method used by Dr. Stanton and Miss Marshall in measuring the thrust on the elements of an airscrew blade (see page 284), and the result of the comparison is shown in Fig. 151. This is the most complete check of the inflow theory which has yet been made. Generally, the agreement between calculation and observation is very good in view of the numerous assumptions in the theory.

It will be realized that in the check as applied above, any errors in our knowledge of the $\dfrac{\text{lift}}{\text{drag}}$ of the sections will appear as attributed to inflow and will affect the value of λ_1 ; any loss of efficiency at the tip will appear in the same way. Fage has shown, however, that for a moderate range of airscrew design and for such values of $\dfrac{V}{nD}$ as are used in practice λ_1 is roughly constant. The best value is yet to be determined, but is apparently in the neighbourhood of 0·35. The comparison given in Fig. 151 showed the presence of an appreciable " end loss," the thrust observed near the tip being less than that calculated until a reduction of lift co-efficient had been made. At a little over 95 per cent. of the radius the lift coefficient was apparently reduced to half the value it would have had if far from the tip.

It will be seen that on present assumptions the value of the torque is completely determined when λ_1 is known. When compared with experiment the calculated values of the torque are in good agreement with observation, the average difference being of the order of 2 or 3 per cent.

Summary of Conclusions on the Mathematical Theory.—As a result of a combined theoretical and experimental examination of airscrew performance it is concluded that rotational inflow may be neglected, and that an average value of 0·35 may be used for the translational inflow factor λ_1. There is a tip loss which is taken to be inappreciable at 85 per cent. of the radius, 100 per cent. at the tip and 40 per cent. at 0·95 of the maximum radius. The values of these losses, although admittedly not of high percentage accuracy, are of the nature of corrections, and the final calculations of thrust and torque are in good agreement with practice.

III. Applications of the Mathematical Theory

Example of the Calculation of the Thrust, Torque and Efficiency of an Airscrew.—In developing the method of calculation for the performance of an airscrew opportunity will be taken to collect the formulæ and necessary data. Following the previous part of this chapter it will be unnecessary to prove any of the formulæ in use, as they may be obtained from equations (14), (18), (38), (36) and (37) by simple transformations where they differ from the forms there shown.

The first step will be to collect a representative set of aerofoil sections suitable for airscrew design, together with tables of their characteristics. The results chosen were obtained in a wind channel at a high value of vl, and may be used without scale correction. The shapes of six aerofoil

sections are shown in Fig. 152, and numerical data defining them more precisely are tabulated below.

TABLE 5.—CONTOURS OF SIX AEROFOILS SUITABLE FOR AIRSCREW DESIGN (ASPECT RATIO 6).

Distance of ordinate from leading edge, expressed as a fraction of chord.	Length of ordinate above chord, expressed as a fraction of chord.						
	No. 1.	No. 2.	No. 3.	No. 4.	No. 5.	No. 6. Top.	No. 6. Bottom.
0.05	0·0510	0·0465	0·0528	0·0794	0·1167	0·1033	−0·0300
0·10	0·0651	0·0625	0·0758	0·1020	0·1505	0·1433	−0·0383
0·20	0·0775	0·0785	0·0976	0·1218	0·1810	0·1866	−0·0475
0·30	0·0817	0·0816	0·1014	0·1270	0·1880	0·2000	−0·0500
0·40	0·0806	0·0790	0·0985	0·1244	0·1816	0·1933	−0·0492
0·50	0·0761	0·0711	0·0925	0·1151	0·1665	0·1758	−0·0475
0·60	0·0694	0·0631	0·0836	0·1020	0·1455	0·1525	−0·0425
0·70	0·0593	0·0531	0·0705	0·0860	0·1210	0·1233	−0·0367
0·80	0·0451	0·0410	0·0533	0·0668	0·0925	0·0883	−0·0317
0·90	0·0273	0·0265	0·0325	0·0423	0·0587	0·0500	−0·0233

AEROFOILS SUITABLE

FOR AIRSCREW DESIGN

Aerofoil No 1. CAMBER RATIO 0·0817

Aerofoil No 2. 0·0815

Aerofoil No 3. 0·1015

Aerofoil No 4. 0·127

Aerofoil No 5. 0·188

Aerofoil No 6. 0·25
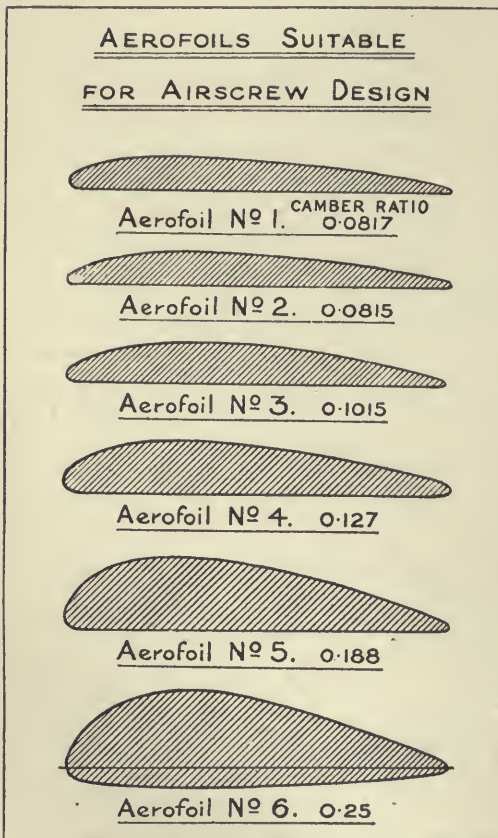
FIG. 152.

The aerofoils Nos. 1–5 have flat undersurfaces, whilst No. 6 has a convex undersurface. The shape of any of the aerofoils is easily reproduced from the figures of Table 5, where all the dimensions are expressed as fractions of the chord. The table is not an exhaustive collection of the best aerofoils for airscrew design, but may be taken as fully representative.

Corresponding with the numbers in Table 5 are values in Table 6 of the lift coefficient, k_L, and of the ratio of lift to drag. In using the figures for calculation it is almost always most convenient to convert them into curves on a fairly open scale, as the readings required rarely occur at the definite angles for which the results are tabulated. Interpolation, especially on $\dfrac{\text{lift}}{\text{drag}}$, is most easily carried out from plotted curves.

The aerofoil characteristics have been expressed wholly in non-dimne-

TABLE 6.—AEROFOILS SUITABLE FOR AIRSCREW DESIGN.

Angle of incidence, (degrees).	Absolute lift coefficient.					
	No. 1.	No. 2.	No. 3.	No. 4.	No. 5.	No. 6.
−20	—	—	—	—	—	−0·0390
−18	—	—	—	—	—	−0·0134
−16	—	—	—	—	−0·0406	+0·0193
−14	—	—	−0·192	−0·142	−0·0054	+0·0423
−12	—	—	−0·188	−0·134	+0·0257	+0·0440
−10	—	—	−0·179	−0·120	0·0389	+0·0012
− 8	—	—	−0·131	−0·0695	0·0498	−0·0005
− 6	−0·0865	−0·1210	−0·036	+0·0099	0·0985	+0·0545
− 4	+0·0125	−0·0271	+0·047	+0·0890	0·174	+0·115
− 2	0·0935	+0·0562	0·124	+0·163	0·245	0·178
0	0·167	0·1270	0·196	0·234	0·314	0·242
2	0·242	0·202	0·274	0·308	0·391	0·320
4	0·314	0·276	0·351	0·382	0·460	0·420
6	0·384	0·353	0·425	0·453	0·536	0·484
8	0·457	0·430	0·490	0·518	0·599	0·548
10	0·530	0·500	0·562	0·586	0·661	0·599
12	0·585	0·565	0·614	0·643	0·718	0·287
14	0·618	0·603	0·610	0·700	0·765	0·277
16	0·486	0·602	0·581	0·746	0·795	0·283
18	0·448	0·538	0·558	0·774	0·382	0·306
20	0·444	0·465	0·543	0·774	0·389	0·326
22	0·434	—	0·494	0·434	—	0·340
24	0·431	—	0·449	0·425	—	0·355

Angle of incidence, (degrees).	$\dfrac{\text{Lift}}{\text{Drag}}$					
	No. 1.	No. 2.	No. 3.	No. 4.	No. 5.	No. 6.
−20	—	—	—	—	—	− 0·32
−18	—	—	—	—	—	− 0·13
−16	—	—	—	—	− 0·45	+ 0·21
−14	—	—	− 2·4	− 1·78	− 0·07	+ 0·52
−12	—	—	− 2·7	− 1·95	+ 0·40	+ 0·68
−10	—	—	− 3·2	− 2·14	0·71	+ 0·03
− 8	—	—	− 3·3	− 1·69	1·14	− 0·03
− 6	− 3·79	− 4·12	− 1·5	+ 0·38	2·73	+ 3·86
− 4	+ 1·08	− 1·62	+ 3·2	5·12	7·45	8·20
− 2	10·90	+ 5·45	11·8	12·0	12·25	11·60
0	18·80	14·00	17·6	16·6	14·40	13·40
2	22·00	18·80	19·7	17·5	14·70	14·30
4	19·80	20·40	18·3	17·0	13·90	13·30
6	17·10	18·10	16·5	15·5	13·0	12·60
8	15·30	16·10	14·8	14·1	12·0	12·00
10	13·30	14·50	13·4	12·6	11·1	11·10
12	12·00	12·80	11·8	11·3	10·2	2·85
14	10·40	11·10	8·9	10·4	9·5	2·40
16	4·07	8·45	6·9	9·4	8·75	2·15
18	3·01	4·35	5·45	8·5	2·40	2·12
20	2·70	3·04	4·38	7·3	2·20	2·00
22	2·40	—	2·76	2·4	—	1·97
24	2·22	—	2·20	2·17	—	1·88

sional or " absolute " units, and a similar procedure will be followed for the airscrew. The typical length of an airscrew is almost always taken

as its diameter, and the width of the chord of any section will be expressed as a fraction of D. Similarly the radius of the section will be given as a fraction of the extreme radius, i.e. of $\dfrac{D}{2}$.

An application of the principles of dynamical similarity suggests the following variables as suitable for airscrews : $\dfrac{V}{nD}$, or the advance of the airscrew per revolution as a fraction of its diameter; a thrust coefficient, k_T, such that

$$T = k_T \rho n^2 D^4 \quad . \quad . \quad . \quad . \quad . \quad . \quad (41)$$

a torque coefficient, k_Q, defined by

$$Q = k_Q \rho n^2 D^5 \quad . \quad . \quad . \quad . \quad . \quad . \quad (42)$$

and the efficiency, η.

The equations already developed are easily converted to a form suitable for the calculation of k_T and k_Q in terms of the generalised variables, and the five equations required are

$$a_2 = -\frac{a_1}{\pi} \cdot \frac{V}{nD} \cdot \frac{D}{2r} \cdot \tan(\phi + \gamma) \quad . \quad . \quad . \quad . \quad . \quad (43)$$

$$\tan \phi = \frac{1}{\pi} \cdot \frac{1 + a_1}{1 + a_2} \cdot \frac{V}{nD} \cdot \frac{D}{2r} \quad . \quad . \quad . \quad . \quad . \quad (44)$$

$$\frac{a_1}{1 + a_1} = \frac{\lambda_1}{\pi} \cdot \frac{c}{D} \cdot \frac{D}{2r} \cdot \frac{k_L}{\sin \phi} \left(\cot \phi - \frac{D}{L} \right) \quad . \quad . \quad . \quad (45)$$

$$k_T = \frac{\pi}{4\lambda_1} \cdot \left(\frac{V}{nD} \right)^2 \int_0^1 a_1 (1 + a_1) d\left(\frac{2r}{D} \right)^2 \quad . \quad . \quad . \quad (46)$$

$$k_Q = \frac{\pi}{12\lambda_1} \cdot \left(\frac{V}{nD} \right)^2 \int_0^1 a_1 (1 \times a_1) \tan(\phi + \gamma) d\left(\frac{2r}{D} \right)^3 \quad . \quad (47)$$

The value of λ_1 will be taken to be 0·35.

TABLE 7.

Aerofoil number.	$\dfrac{2r}{D}$	$\dfrac{c}{D}$ *	Angle of incidence for maximum $\dfrac{L}{D}$ (degrees).
2	0·96	0·036	3
2	0·88	0·098	3
3	0·76	0·137	2
4	0·602	0·163	2
5	0·412	0·164	2
6	0·324	0·147	2

The plan form of the blades of the airscrew is defined by Table 7, $\dfrac{c}{D}$ giving the sum of the widths of the two blades for various values of $\dfrac{2r}{D}$.

* In this example c is the sum of the chords of two blades.

Since D is not specifically defined, the shape applies to all similar airscrews. In addition to the blade widths, the particulars of the sections at various values of $\frac{2r}{D}$ are given in the first column, the aerofoil Nos. being the same as those of Fig. 152. The last column of the table shows the angle of incidence of each section for which the $\frac{\text{lift}}{\text{drag}}$ is a maximum.

The shape of the blade is not completely defined until the inclination of the chord of each section to the screw disc has been given. This angle, denoted by ϕ_0, depends on the duties for which the airscrew is to be designed. In general the maximum forward speed of an aircraft, the speed of rotation of the engine, and the airscrew diameter are fixed by independent considerations; if the diameter is open to choice, a suitable value can be fixed from general knowledge by the use of a chart such as that on page 319. The value of $\frac{V}{nD}$ fixed in this way is not sufficient to define ϕ in terms of $\frac{D}{2r}$, as may be seen from (43), as the values of a_1 and a_2 are not known and the most convenient method of procedure is to make a first set of calculations with approximate values and to repeat the calculations if greater accuracy is desired. Instead of the value of $\frac{V}{nD}$, which is assumed known at some speed of flight, it is convenient to guess a value for $\frac{1+a_1}{\pi} \cdot \frac{V}{nD}$ in the first approximation, and in the illustration now given it is supposed that the design requires that at maximum efficiency

$$\frac{1+a_1}{\pi} \cdot \frac{V}{nD} = 0\cdot241 \quad . \quad . \quad . \quad . \quad . \quad . \quad (48)$$

The preliminary calculations may be made with $a_2 = 0$ and neglecting $\frac{D}{L}$ in equation (45). With these conditions the calculation for the section at $\frac{2r}{D} = 0\cdot88$ proceeds as in Table 8.

The first column of Table 8 contains arbitrarily chosen values of $\frac{1+a_1}{\pi} \cdot \frac{V}{nD}$, and since $\frac{2r}{D} = 0\cdot88$, this leads rapidly by use of (44) to the value of $\tan \phi$ in column 2. ϕ is obtained from $\tan \phi$ by the use of tables of trigonometrical functions, and the angle a is chosen as 3° when $\frac{1+a_1}{\pi} \cdot \frac{V}{nD} = 0\cdot241$. This is in accordance with the earlier analysis which showed that the maximum efficiency of a section occurred when the $\frac{\text{lift}}{\text{drag}}$ ratio of the aerofoil was a maximum. The choice of a as 3° when $\phi = 15°\cdot3$ fixes the value of ϕ_0, i.e. of the blade angle to the airscrew disc; the remaining values of a are obtained from the expression $a = \phi_0 - \phi$.

From the angles of incidence and Table 6 the values of the lift coefficient k_L are obtained. Using equation (45) and the values of ϕ, a and k_L of Table 8, $\dfrac{a_1}{1+a_1}$ was calculated, thence a_1, and finally the value of $\dfrac{V}{nD}$.

At this stage would be introduced the second approximation if the full accuracy were desired. From equation (43) it is possible to calculate values of a_2 corresponding with the values of a_1 in Table 8, and as a_1 and a_2 then become known with considerable accuracy the table can be repeated using equations (43), (44) and (45) with their full meaning. The calculation is not made in these notes, as the first approximation is sufficient for the purposes of illustration.

TABLE 8.

1	2	3	4	5	6	7	8
$\dfrac{1+a_1}{\pi} \cdot \dfrac{V}{nD}$ chosen arbitrarily.	$\tan\phi$ from equation (4) with $a_2 = 0$	ϕ (degrees).	a, angle of incidence (degrees).	k_L, lift coefficient from Table 2.	$\dfrac{a_1}{1+a_1}$ from equation (5).	a_1.	$\dfrac{V}{nD}$ from columns 1 and 7.
0·319	0·332	19·9	−1·6	0·070	0·0070	0·0070	0·995
0·287	0·299	18·0	+0·3	0·135	0·0166	0·0178	0·885
0·256	0·267	16·2	2·1	0·205	0·0312	0·0322	0·779
0·241	0·251	15·3	$\left\{\begin{array}{c}3\cdot0\\ \phi_0 = 18\cdot3\end{array}\right\}$	0·240	0·0410	0·0428	0·725
0·223	0·232	14·2	4·1	0·280	0·0558	0·0591	0·661
0·191	0·199	12·2	6·1	0·355	0·0955	0·1056	0·541
0·160	0·167	10·3	8·0	0·430	0·1635	0·1955	0·420
0·128	0·133	8·3	10·0	0·505	0·2980	0·4250	0·282

Thrust.—A table similar to 8 was calculated for each of the other five blade sections of the airscrew, and the various terms give the data from which k_T is calculated. Equation (46) implies integration for a constant value of $\dfrac{V}{nD}$, and the tables do not provide values of $a_1(1+a_1)$ directly suitable for the purpose. Values of $a_1(1+a_1)$ were therefore plotted for each section as ordinates on a base of $\dfrac{V}{nD}$, and from these curves the following table was prepared :—

TABLE 9.

$\dfrac{V}{nD}$	$a_1(1+a_1)$					
	$\dfrac{2r}{D} = 0\cdot96$	$\dfrac{2r}{D} = 0\cdot88$	$\dfrac{2r}{D} = 0\cdot76$	$\dfrac{2r}{D} = 0\cdot602$	$\dfrac{2r}{D} = 0\cdot412$	$\dfrac{2r}{D} = 0\cdot324$
1·0	0·0030	0·0070	0·0080	0·0090	0·0100	0·0110
0·9	0·0064	0 0160	0·0204	0·0230	0·0225	0·0112
0·8	0·0122	0·0290	0·0389	0·0438	0·0416	0·0256
0·7	0·0215	0·0510	0·0692	0·0750	0·0704	0·0492
0·6	0·0360	0·0900	0·1160	0·1300	0·1185	0·0875
0·5	0·0620	0·1450	0·1950	0·2100	0·1990	0·1160
0·4	0·1100	0·2600	0·3250	0·3650	0·3490	0·0980

Numbers can be deduced from Table 9 for comparison with Fig. 151. The value of

$$\frac{\text{thrust per foot run}}{\rho V^2 D} = \frac{\pi}{\lambda_1} . a_1 (1 + a_1) \frac{2r}{D} \qquad . \qquad . \qquad . \quad (49)$$

and values calculated by means of (49) and plotted against $\frac{r}{D}$ give curves very similar to those of Fig. 151. The central part of the airscrew has been ignored as of little importance.

Using equation (46) in the form shown, the value of $a_1(1 + a_1)$ was plotted on a base of $\left(\frac{2r}{D}\right)^2$ and the value of the integral obtained graphically, the results being set out in the table below.

TABLE 10.

$\dfrac{V}{nD}$	$\displaystyle\int_0^1 a_1(1+a_1)d\left(\frac{2r}{D}\right)^2$	Thrust coefficient, k_T
1·0	0·0069	0·0155
0·9	0·0168	0·0305
0·8	0·0309	0·0443
0·7	0·0544	0·0596
0·6	0·0904	0·0728
0·5	0·1504	0·0842
0·4	0·2561	0·0918

If the values of k_T are plotted on a basis of $\frac{V}{nD}$ and the curve produced, it will be found that k_T becomes zero when $\frac{V}{nD} = 1\cdot1$, and this number is the ratio of pitch to diameter for the airscrew in question. The pitch here defined is called the "experimental mean pitch," and is the advance per revolution of the airscrew when the thrust is zero.

Torque.—The calculation of torque follows from equation (47) as below.

TABLE 11.

1	2	3	4	5	6
$\dfrac{V}{nD}$ from Table 8.	$a_1(1 + a_1)$ calculated from column 7, Table 8.	$\dfrac{L}{D}$ corresponding with the values of a in Table 8.	$\gamma = \tan^{-1}\dfrac{L}{D}$ (degrees).	$\tan(\phi + \gamma)$ ϕ from Table 8.	$a_1(1+a_1)\tan(\phi+\gamma)$ from columns 2 and 5.
0·995	0·0071	7·0	8·13	0·533	0·0038
0·885	0·0181	14·8	3·87	0·402	0·0073
0·779	0·0333	19·0	3·02	0·349	0·0116
0·725	0·0446	21·0	2·71	0·326	0·0142
0·661	0·0625	20·4	2·80	0·306	0·0191
0·541	0·1170	18·1	3·17	0·276	0·0322
0·420	0·2340	16·4	3·42	0·246	0·0574
0·286	0·6050	14·6	3·92	0·216	0·1310

The numbers in Table 11 correspond with those in Table 8, and apply to a value of $\frac{2r}{D}$ of 0·88. The table was repeated for other values of $\frac{2r}{D}$, and the results of calculations such as are shown in column 6 of Table 11 were plotted against $\frac{V}{nD}$. From the curves so plotted Table 12 was prepared by reading off values of $a_1(1 + a_1) \tan (\phi + \gamma)$ at chosen values of $\frac{V}{nD}$.

TABLE 12.

$\frac{V}{nD}$	$a_1(1 + a_1) \tan (\phi + \gamma).$					
	$\frac{2r}{D} = 0\cdot96$	$\frac{2r}{D} = 0\cdot88$	$\frac{2r}{D} = 0\cdot76$	$\frac{2r}{D} = 0\cdot602$	$\frac{2r}{D} = 0\cdot412$	$\frac{2r}{D} = 0\cdot324$
1·0	0·0012	0·0038	0·0052	0·0075	0·0145	0·0160
0·9	0·0025	0·0060	0·0100	0·0142	0·0200	0·0130
0·8	0·0040	0·0100	0·0160	0·0230	0·0300	0·2240
0·7	0·0060	0·0160	0·0250	0·0350	0·0465	0·0395
0·6	0·0095	0·0248	0·0380	0·0520	0·0710	0·0630
0·5	0·0150	0·0390	0·0600	0·0820	0·1100	0·0900
0·4	0·0240	0·0630	0·0940	0·1320	0·1740	0·0900

The numbers in Table 12 were plotted as ordinates with $\left(\frac{2r}{D}\right)^3$ as abscissa, and curves for each value of $\frac{V}{nD}$ drawn through the points. The areas of the curves obtained by planimeter gave the values of the integral of equation (47), and from them the calculation for k_Q was easily completed (see Table 13).

TABLE 13.

$\frac{V}{nD}$	$\int_0^1 a_1(1 + a_1) \tan (\phi + \gamma) d\left(\frac{2r}{D}\right)^1$	Torque coefficient, k_Q	Efficiency, η
1·0	0·00570	0·00426	0·580
0·9	0·00897	0·00543	0·806
0·8	0·01431	0·00685	0·825
0·7	0·02228	0·00817	0·814
0·6	0·03377	0·00908	0·765
0·5	0·05311	0·00992	0·676
0·4	0·0826	0·00987	0·591

The efficiency of the whole airscrew is

$$\eta = \frac{TV}{2\pi nQ} = \frac{1}{2\pi} \cdot \frac{V}{nD} \cdot \frac{k_T}{k_Q}. \qquad . \quad . \quad . \quad . \quad . \quad (50)$$

and the values of η are obtained from Tables 10 and 13 and equation (50). It will be seen that a high efficiency of 0·825 is found, and this is partly

due to the fact that all elements have been chosen to give their maximum efficiency at the same value of $\dfrac{V}{nD}$.

Effect of Variations of the Pitch Diameter Ratio of an Airscrew.— By choosing different values of $\dfrac{V}{nD}$ for the state of maximum efficiency and repeating the calculations, the effect of variation of pitch could have been obtained. Instead of repeating the calculations, an experiment described in a report of the American Advisory Committee on Aeronautics will be used to illustrate the effect of variation of pitch-diameter ratio. The report, by Dr. Durand, contains a systematic series of tests on 48 air-
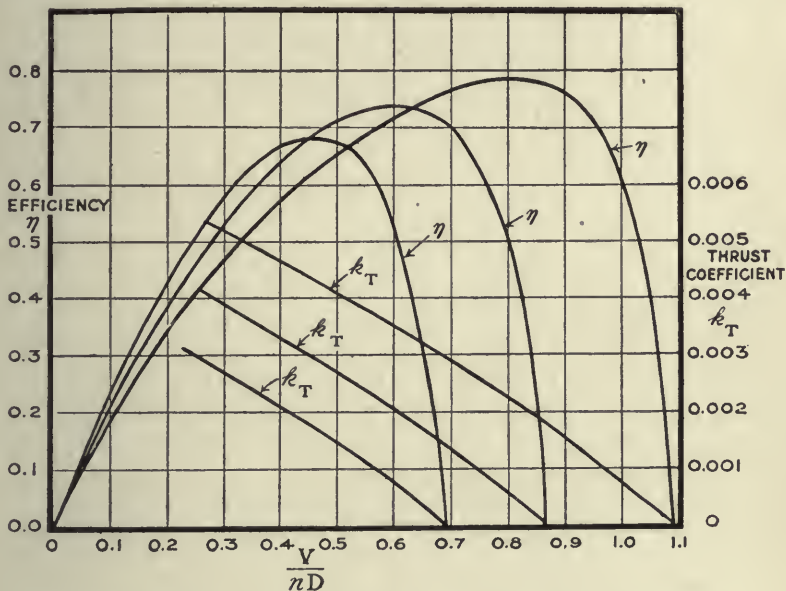
Fig. 153.—Effect of variations of pitch diameter ratio of an airscrew.

screws of various plan forms and pitches, and the results shown are typical of the whole. For details the original work should be consulted.

The three screws used in the particular experiment referred to, were of the same diameter, and had the same aerofoil sections at the same radii. The general shapes of the sections were not greatly different from those just referred to in the calculation of the performance of an airscrew and illustrated in Fig. 152, the lower surfaces being flat except near the centre of the airscrew. The chords of the sections were inclined at 3° to the surface of a helix, and the pitch of this helix was 0·5D, 0·7D and 0·9D in the three airscrews used in producing the results plotted in Fig. 153. The experimental mean pitches, *i.e.* the values of $\dfrac{V}{n}$ when the thrust is zero, were 0·69D, 0·87D and 1·09D, and do not bear any simple relation to the helical pitches.

The most interesting feature of the curves of Fig. 153 is the increase of maximum efficiency as the pitch diameter ratio increases, an effect which would be continued to higher values than 1·1. It is easily shown that the greatest efficiency is obtained for any element when $\phi + \frac{1}{2}\gamma = 45°$, and as γ is small for an efficient airscrew the pitch diameter ratio would need to be π before the maximum efficiency was reached. It is not usually possible to rotate the screw at a low enough speed to ensure the absolute maximum efficiency, and in addition the whole of the effective area of the blade cannot be given the best angle on account of stresses in the material of which the airscrew is built.

Fig. 153 can be used to illustrate the advantages of a variable pitch airscrew, although the comparison is not exact since the screws cannot be converted from one to another by a rotation about a fixed axis. This latter condition is almost always present in any variable pitch airscrew, and the details of performance may be worked out by the methods already detailed except that in successive calculations a constant addition to ϕ_0 is made for all sections.

Consider the medium airscrew of Fig. 153 as designed to give maximum efficiency to the aeroplane when flying " all out " on the level, the value of $\frac{V}{nD}$ being then 0·6. For the condition of maximum rate of climb $\frac{V}{nD}$ may be 0·4, and changing to the lower pitch increases the efficiency by about 4 per cent. During a dive or glide at $\frac{V}{nD} = 1·0$ the change to the larger pitch converts a resistance of the airscrew into a thrust, and a higher speed is possible. Usually a dive can be made sufficiently fast without airscrew adjustment, and for a non-supercharged engine the advantages of a variable pitch airscrew are not very great.

For a supercharged engine the conditions are very different. The limiting case usually presupposed is the maintenance at all heights of the power of the engine at its ground-level value, so that at a given number of revolutions per minute the horsepower available is independent of the atmospheric density. For the same conditions of running, the horse-power absorbed by an airscrew of fixed pitch is proportional to the density, and any attempt to " open out " the engine at a considerable altitude would lead to excessive revolutions. With a variable pitch airscrew this excessive speed could be avoided by an increase of pitch, and Fig. 153 shows that a gain of efficiency would result. From the curves of Fig. 153 it is possible to work out the performance of the airscrew at constant velocity and revolutions, but in the flight of an aeroplane with sufficient supercharge the value of V would change, and hence the complete problem can only be dealt with by some such means as those given in the chapter on the Prediction of Aeroplane Performance.

Tandem Airscrews.—In some of the larger aeroplanes in which four engines have been fitted, the latter have been arranged on the wings in pairs, a rear engine driving an airscrew in the slip stream from the airscrew of the forward engine. It is not usual for the rear screw to be much greater than one diameter behind the front one, and the slip stream is

still unbroken and of practically its minimum diameter. The velocity of the air, both translational and rotational, at the rear airscrew can be approximately calculated by the use of equations (45) and (47), and an example of the method which may be followed will now be given.

The forward airscrew will be taken to be that worked out in this chapter on pages 306 to 310, and of which details are given in Tables 8–13.

The first operation peculiar to tandem airscrews is the calculation of the details of the slip stream from the forward airscrew. From the values of $a_1(1 + a_1)$ given in Table 9 the value of $(1 + a_1)$ is calculated without difficulty, since

$$(1 + a_1) = 0.50 + \sqrt{0.25 + a_1(1 + a_1)} \quad . \quad . \quad . \quad (51)$$

Taking $\dfrac{V}{nD} = 0.6$ as example, the following table shows the required steps in the calculation of the radius of the slip stream :—

TABLE 14.

$\dfrac{2r}{D}$	0.960	0.880	0.760	0.602	0.412	0.324
$1 + a_1$	1.035	1.083	1.105	1.116	1.107	1.080
$1 + \dfrac{a_1}{\lambda_1}$	1.100	1.242	1.300	1.331	1.305	1.228
$\dfrac{1 + a_1}{1 + \dfrac{a_1}{\lambda_1}}$	0.941	0.872	0.850	0.838	0.848	0.880
$\dfrac{2r_1}{D}$	0.892	0.814	0.705	0.567	0.400	0.306

The first two rows of Table 14 are obtained from Table 9, and the third row is easily obtained from the second since $\lambda_1 = 0.35$. The figures in row four are plotted in Fig. 154 on a base of $\left(\dfrac{2r}{D}\right)^2$, a form suggested by equation (46). The integral required was obtained by the mid-ordinate method of finding the area of a diagram, and the result is shown in the lower part of Fig. 154. The extreme value of the square of the radius of the slip stream is seen to be 0.87 times that of the airscrew, and the radius of the slip stream 0.93 times as great as the tip radius. This value may be compared with the direct observations illustrated in Fig. 147.

Rotational Velocity in Slip Stream.—From equation (47) the relation

$$\frac{dk_Q}{d\left(\dfrac{2r}{D}\right)} = \frac{\pi}{4\lambda_1} \cdot \left(\frac{V}{nD}\right)^2 a_1(1 + a_1) \tan(\phi + \gamma) \left(\frac{2r}{D}\right)^2 \quad . \quad . \quad (52)$$

is obtained by differentiation.

From equation (12) a second relation for the same quantity is obtained in terms of the outflow factor b_2. This latter expression is

$$\frac{dk_Q}{d\left(\dfrac{2r}{D}\right)} = -\frac{\pi^2}{4}(1 + a_1)b_2\left(\frac{2r_1}{D}\right)^2 \cdot \frac{2r}{D} \quad . \quad . \quad . \quad (53)$$

and a combination of (52) and (53) leads to

$$b_2 = -\frac{1}{\pi\lambda_1} \cdot \frac{V}{nD} \cdot \frac{\left(\frac{2r}{D}\right)}{\left(\frac{2r_1}{D}\right)^2} \overline{\frac{a_1(1+a_1)\tan(\phi+\gamma)}{(1+a_1)}} \qquad . \quad . \quad (54)$$

and all the quantities required for the calculation of b_2 have already been tabulated.

The rotational air velocity is $b_2\pi \cdot \dfrac{nD}{V} \cdot \dfrac{2r_1}{D} \cdot V$, or

$$\frac{a_1}{\lambda_1}V \cdot \frac{\dfrac{2r}{D}}{\dfrac{2r_1}{D}} \tan(\phi+\gamma) \quad . \quad . \quad . \quad . \quad . \quad . \quad (55)$$
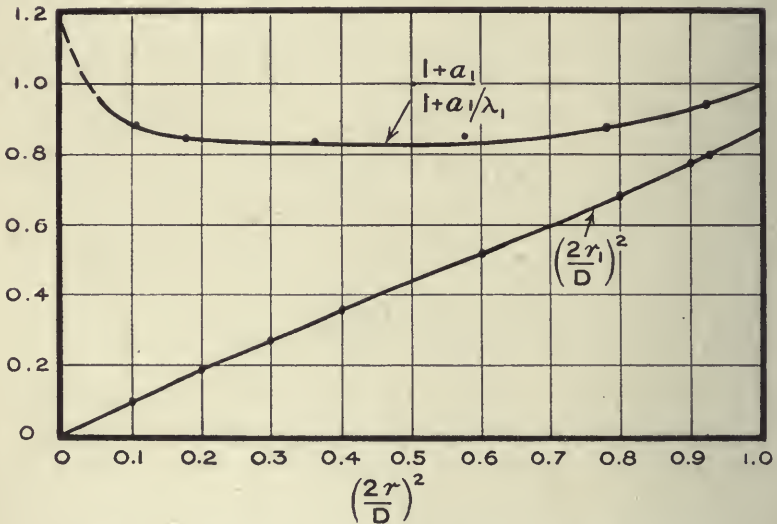
FIG. 154.—Calculation of the size of the slip stream of an airscrew.

In this expression $\dfrac{a_1}{\lambda_1}V$ will be recognized as the added translational velocity between undisturbed air and the slip stream, and the factor $\dfrac{a_1}{\lambda_1}V \tan(\phi+\gamma)$ is the component rotational velocity which would follow from the assumption that the direction of the resultant force at the blade is also the direction of added velocity. The remaining factor is due to the change from airscrew diameter to slip stream diameter.

The following table shows the values of b_2 and the angle of the spiral in the slip stream calculated from (54) and (55), and the latter can be compared directly with Fig. 147 for observations on an airscrew :—

TABLE 15.

$\dfrac{2r}{D}$	0·96	0·88	0·76	0·602	0·412	0·324
b_2	−0·0060	−0·0166	−0·0297	−0·0476	−0·0903	−0·1095
Angle of spiral (degrees)	1·5	3·2	4·6	6·0	8·5	8·1

The calculations for a second airscrew working in the slip stream of the first can now be proceeded with almost as before. If a_1' and a_2' apply to the second airscrew whilst V has the same meaning as before, then the whole of the previous equations can be used with the following substitutions :—

$$\text{Instead of } a_1 \text{ use } \left.\frac{a_1}{\lambda_1} + a_1'\right\} \qquad \cdots \qquad \cdots \qquad (56)$$
$$\text{and instead of } a_2 \text{ use } \pm b_2 + a_2'$$

the values of a_1 and b_2 being taken with the corresponding values of r_1 as obtained from Table 14. The ambiguity of sign corresponds with rotations in the same and in opposite directions respectively.

If the rear airscrew runs in the opposite direction to the front one, the existence of b_2 tends to increase the efficiency, since (28) now becomes

$$\eta = \frac{1 \pm b_2 + a_2'}{1 + \dfrac{a_1}{\lambda_1} + a_1'} \cdot \frac{\tan \phi}{\tan (\phi + \gamma)} \qquad \cdots \qquad \cdots \qquad (57)$$

and as b_2 is negative the numerator of (57) is increased.

The translational inflow reduces the efficiency by the introduction of the factor $\dfrac{a_1}{\lambda_1}$ into the denominator, but as the speed of the rear airscrew relative to the air is now higher the value of $\dfrac{\tan \phi}{\tan (\phi + \gamma)}$ is increased owing to the larger values of ϕ.

In general it appears that some loss of efficiency occurs in the use of tandem airscrews. The subject has been examined experimentally, and one of the experiments is quoted below because of its bearings on the present calculations.

The airscrews were used on a large aeroplane, and each absorbed 350 horsepower at about 1100 r.p.m., rotation being in opposite directions. The diameter of the front airscrew was 13 feet, and that of the rear airscrew 12 feet. The maximum speed of the aeroplane in level flight was about 100 m.p.h. Models of the airscrews were made and tested in a wind channel, and from the results obtained Fig. 155 has been prepared.

Curves for thrust coefficient and efficiency are shown for both airscrews. In the case of the front airscrew the curves were not appreciably altered by the running of that at the rear. An examination of the figure will show that the ratio of pitch to diameter of the rear screw is 0·86, whilst

that of the forward screw is 0·80. In accordance with the experiments on the effect of variation of pitch it would have been expected that the maximum efficiency of the rear airscrew running alone would be higher than that of the forward airscrew. The experiment showed an increase of efficiency from 0·74 to 0·78 on this account.

The efficiency of the rear airscrew when working in tandem is shown by one of the two dotted curves, and its maximum value is seen to be 0·70. In this diagram V is the velocity of the aeroplane through the air, and hence $\dfrac{V}{nD}$ has a different meaning to the similar quantity for the forward airscrew. In the latter case the velocity of the airscrew through
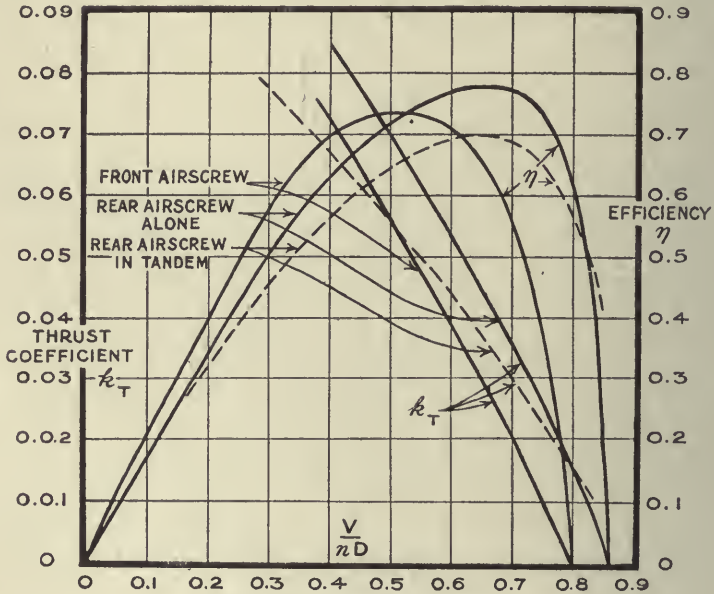
Fig. 155.—Tandem airscrews.

the air is equal to that of the aeroplane, whilst in the former the velocity of the airscrew through the air is appreciably greater than that of the aeroplane. A general idea of the increased velocity in the slip stream is given below.

TABLE 16.

Airspeed of aeroplane (ft.-s.).	Velocity of air at rear airscrew (ft.-s.).	Ratio of speeds.
70	102	1·46
80	110	1·38
100	125	1·25
120	139	1·16
140	154	1·10
160	172	1·07

The velocity in the slip stream of the front airscrew is not uniform, and the value as given in Table 16 is obtained by making the assumption that the thrust coefficient of the rear airscrew when working in tandem has the same value as when working alone, if the value of $\dfrac{V'}{nD}$ is the same in the two cases, V' being the average velocity of the airscrew relative to the air. The calculation involves the variation of engine power with speed, and details of the methods employable are given in the chapter on Prediction. In the present instance the object aimed at is satisfied when the detailed theory of tandem airscrews has been developed and the result illustrated. It will be noticed from Fig. 155 that for values of $\dfrac{V}{nD}$ in excess of 0·62 the efficiency of the combination is greater than that of two independent airscrews like the forward one. At the maximum speed of an aeroplane the loss of efficiency on the tandem arrangement of airscrews is not very great, since $\dfrac{V}{nD}$ is usually chosen a little larger than the value giving maximum efficiency. At climbing, say at $\dfrac{V}{nD} = 0\cdot4$, the efficiency of the rear airscrew is 82 per cent. of the forward airscrew, and the combination has an efficiency 91 per cent. of that of the front airscrew alone, which was designed without restriction as to diameter. It may be concluded, therefore, that the losses in a tandem arrangement of airscrews may be very small at the maximum speed of flight, and that they will become greater and greater as the maximum rate of climb and the reserve horsepower for climbing increase. It will, however, be the usual case that tandem airscrews are only needed on the aeroplanes which have least reserve horsepower, *i.e.* where the losses are least.

The Effect of the Presence of the Aeroplane on the Performance of an Airscrew

The number of tests which relate to the effect of the presence of an aeroplane on its airscrew are not very numerous. Partial experiments on a combination of model airscrew and body are more numerous chiefly because the effect of the airscrew slip stream in increasing the body resistance is very great. This increase of resistance is dealt with elsewhere in discussing the estimation of resistance for the aeroplane as a whole and in detail. All the available experiments show a consistent effect of body on airscrew, which is roughly equivalent to a small increase of efficiency and an increase of experimental mean pitch. One example has been chosen, and the results are illustrated in Fig. 156. This example is typical of such effects as arise from a nacelle closely surrounding the engine, and apply particularly to a tractor airscrew. Where the front of the body of a tractor aeroplane is designed to take a water-cooled engine the results would also apply, but it might be anticipated that the large body required for a rotary or radial engine would have more appreciable effects.

The effects of the nacelle of a pusher aeroplane are of the same general character as for a tractor ; both the thrust and torque coefficients are increased by the presence of the nacelle, and the efficiency and pitch are increased. The amounts are on the whole rather greater than those shown in Fig. 156.

Fig. 156 shows the thrust coefficient and efficiency of a four-bladed tractor airscrew when tested alone, when tested in front of a body, and when tested in front of a complete aeroplane. The observations were taken on a model in a wind channel. The cross-section of the body a short distance behind the airscrew had an area of 7 per cent. of that of the airscrew disc. The thrust coefficient is increased by the body over the whole range of $\dfrac{V}{nD}$ by an amount which increases as $\dfrac{V}{nD}$ increases. The maximum efficiency is little affected, but the experimental mean pitch
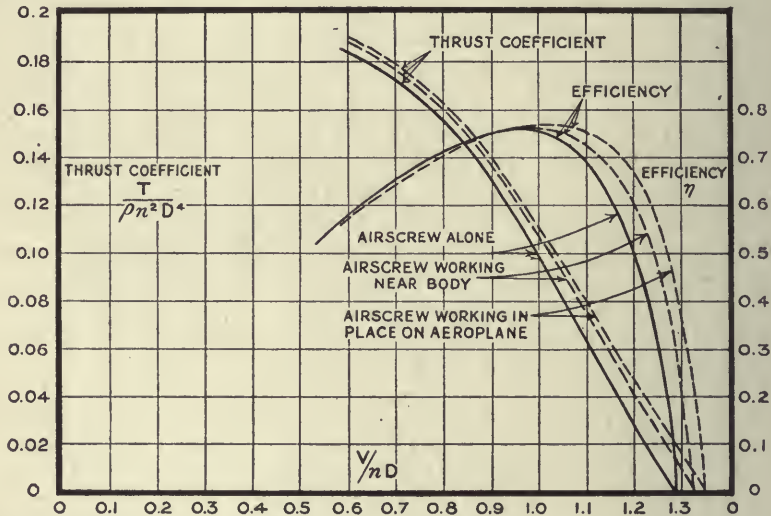
FIG. 156.—Effect of the body and wings of an aeroplane on the thrust of an airscrew.

is increased by nearly 3 per cent. The addition of the wings and general structure of the aeroplane brings the total effect on the airscrew to an increase of 1 per cent. on efficiency and 5 per cent. on pitch.

On a particular pusher nacelle of greater relative body area the maximum efficiency was raised by 3 per cent., and the experimental mean pitch by 9 per cent.

In the present state of knowledge it will probably be sufficient to assume that calculations made on an airscrew alone can be applied to the airscrew in place on an aeroplane by changing the scale of $\dfrac{V}{nD}$ by 5 per cent.

and increasing the ordinates of the thrust coefficient and efficiency curves by 2 per cent. These changes are small, and great accuracy is therefore not required in the practical applications of airscrew design.

Approximations to Airscrew Characteristics

Before proceeding to the detailed design of an airscrew it is necessary to know the general proportions of the blades, and the sections to be used. These are at the choice of any designer, who will adopt standards of his own, but the choice for good design is so limited that rough generaliza-
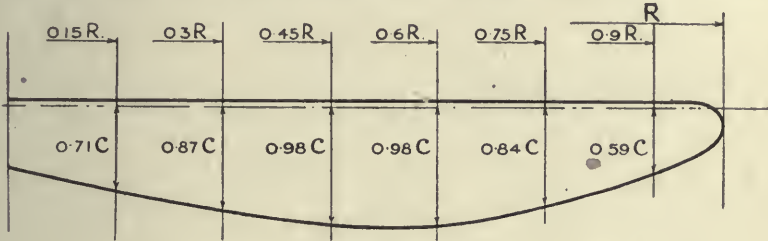
Fig. 157.

tions can be made for all airscrews. The plan form of the blades is perhaps the quantity which varies most in any design, and in connection with the approximate formulæ and curves is given a drawing of the plan form to which they more particularly refer (see Fig. 157).
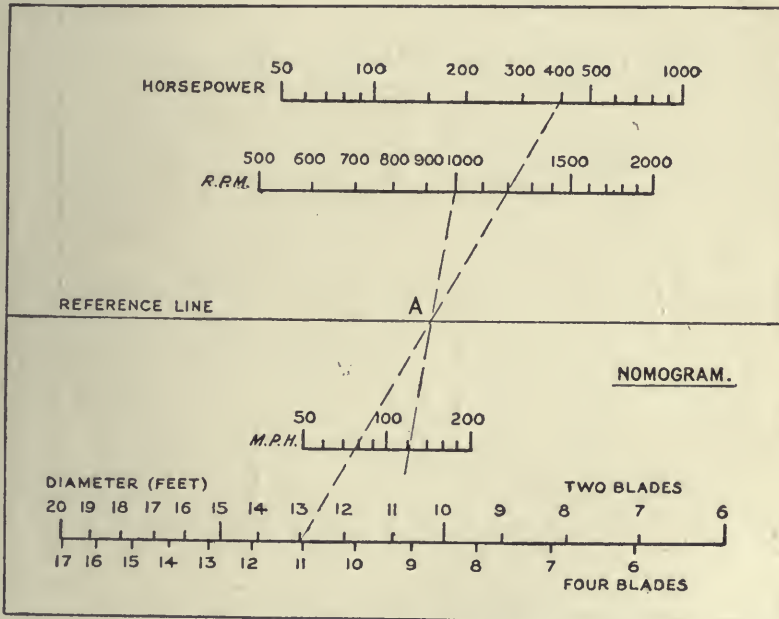
Fig. 158.—Nomogram for the calculation of airscrew diameter.

For this shape of blade H. C. Watts has given a nomogram connecting the airscrew diameter of the most efficient airscrews with the horsepower, speed of translation and rate of rotation.

Diameter.—Example of the use of the nomogram (Fig. 158).

" What is the approximate diameter of an airscrew for an aeroplane which will travel 120 m.p.h. at ground-level with an engine developing 400 horsepower at 1000 r.p.m. ? "

On the scales for translational and rotational speeds the numbers 120 and 1000 are found and joined by a straight line cutting the reference line at A of Fig. 158. The position of the 400 horsepower mark is then joined to A by a straight line which is produced to cut the scale of diameters. In this case the diameter of a two-bladed airscrew is given as 13 feet, and of a four-blader as 11 feet.

In air of reduced density the ground horsepower should still be used in the above calculation.

The nomogram may be taken as a convenient expression of current practice.

Maximum Efficiency.—The results of a number of calculations are given in Table 17 to show how the efficiency of an airscrew may be expected to depend on the horsepower, speed of translation, and diameter. As before, the ground horsepower should be taken in all cases, and not the actual horsepower developed for the conditions of reduced density. The table covers the ordinary useful range of the variables. For the example just given the table shows an efficiency of about 0·80. Interpolation is necessary, but for rough purposes this can be carried out by inspection.

TABLE 17.—Efficiencies of Airscrews (Approximate Values).

		Aeroplane speed, m.p.h.	800 r.p.m.			1200 r.p.m.		1600 r.p.m.
			8 ft. diam.	12 ft. diam.	16 ft. diam.	8 ft. diam.	12 ft. diam.	8 ft. diam.
200 B.H.P.	Level flight	100	0·80	—	—	0·78	—	0·74
		120	0·84	—	—	0·82	—	0·79
		140	0·86	—	—	0·84	—	0·81
	Climb	60	0·60	—	—	0·55	—	0·51
		80	0·68	—	—	0·64	—	0·61
400 B.H.P.	Level flight	100	0·74	0·78	—	0·72	0·73	0·69
		120	0·79	0·82	—	0·77	0·77	0·75
		140	0·83	0·84	—	0·81	0·81	0·79
	Climb	60	0·54	0·56	—	0·50	0·50	0·46
		80	0·63	0·66	—	0·60	0·61	0·56
600 B.H.P.	Level flight	100	—	0·75	0·75	—	0·71	—
		120	—	0·80	0·80	—	0·76	—
		140	—	0·83	0·83	—	0·79	—
	Climb	60	—	0·53	0·52	—	0·46	—
		80	—	0·63	0·63	—	0·57	—

Further Particulars of the Airscrew.—For many purposes it is desirable to know more about the airscrew without proceeding to full detail, and Fig. 159 is a generalization which enables the characteristics of an airscrew to be given approximately if four constants are determined. These constants are the experimental mean pitch, P, the pitch diameter ratio,

$\dfrac{P}{D}$, and two others denoted by T_o and Q_o. T_o is a number such that $T_o k_T = 1$

when $\dfrac{V}{nP} = 0.5$, and similarly $Q_o k_q = 1$ for the same value of $\dfrac{V}{nP}$. k_T and

k_Q are the usual absolute thrust and torque coefficients as defined on p. 306.

To apply the curves to the example a further note is required; it can
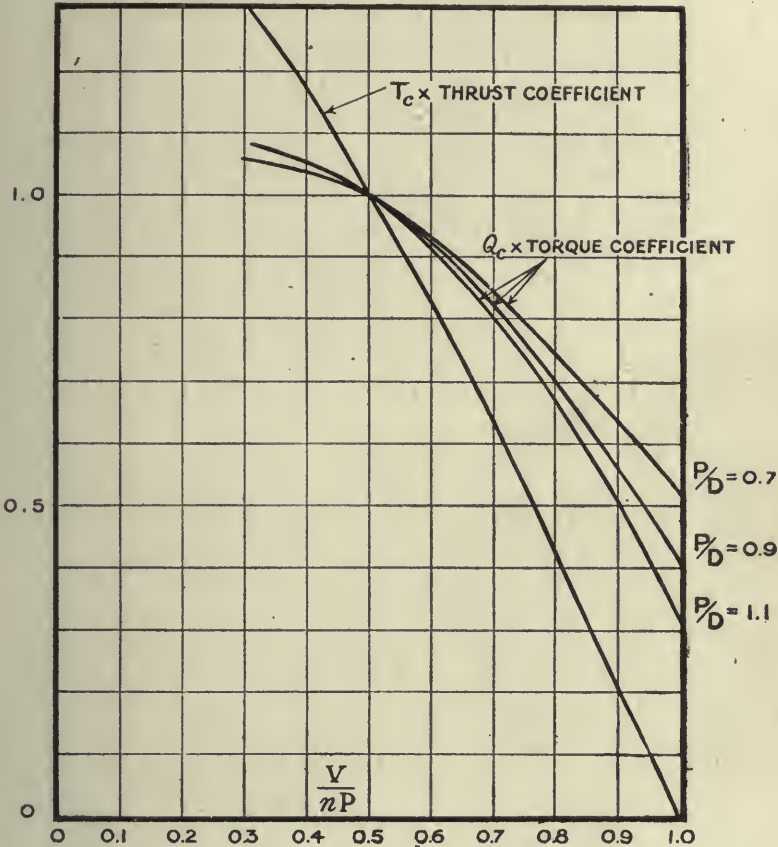
FIG. 159.—Standard airscrew characteristics.

be deduced from Fig. 159 by calculating the efficiency. For a pitch diameter

ratio of 0·7 the maximum efficiency occurs at about $\dfrac{V}{nP} = 0.6$, whilst for

$\dfrac{P}{D} = 1.1$ the value of $\dfrac{V}{nP}$ is about 0·65. In order to keep the average

efficiency of an aeroplane airscrew as high as possible the maximum speed

is made to occur at a value of $\dfrac{V}{nP}$ somewhat greater than that giving

maximum efficiency. $\dfrac{V}{nP}$ will often be 0·7 or even 0·75 at maximum speed.

Y

Continuing the example, it is then found that

$$\frac{V}{nP} = \frac{10 \cdot 5}{P} = 0 \cdot 7, \text{ say}$$

and therefore P = 15 feet and $\frac{P}{D} = \frac{15}{13} = 1 \cdot 15$.

Calculation of T_C and Q_C.—The efficiency having been found to be 0·80, the thrust is found from the horsepower available. Since

$$\text{thrust} = \frac{400 \times 0 \cdot 80 \times 33,000}{120 \times 88} = 1000 \text{ lbs.}$$

The thrust coefficient $k_T = \dfrac{1000}{0 \cdot 00237 \times 176^2 \times 13^2} = 0 \cdot 0808$

These figures will depend on the air density, both T and k_T being affected. The horsepower available for a given throttle position, etc., varies rather more rapidly than density, and hence the thrust varies rapidly with density. k_T involves the ratio of horsepower to density, and is not therefore greatly altered. Ground conditions of density and horsepower may therefore always be used in the approximate expressions for T_C and Q^C.

From Fig. 159 the value of $T_C k_T$ at $\dfrac{V}{nP} = 0 \cdot 7$ is seen to be 0·635, and hence $T_C = \dfrac{0 \cdot 635}{0 \cdot 0808} = 7 \cdot 95$.

Similarly
$$\text{torque} = \frac{400 \times 33,000}{6 \cdot 28 \times 1000} = 2100 \text{ lbs.-ft.}$$

$$k_Q = \frac{2100}{0 \cdot 00237 \times 176^2 \times 13^3} = 0 \cdot 0131$$

From Fig. 159 the value of $Q_C k_Q$ at $\dfrac{V}{nP} = 0 \cdot 7$ and $\dfrac{P}{D} = 1 \cdot 15$, is read off as 0·805. Hence $Q_C = \dfrac{0 \cdot 805}{0 \cdot 0131} = 61 \cdot 5$.

Having determined P, $\dfrac{P}{D}$, T_C, and Q_C in this way, the characteristics of the airscrew at all values of $\dfrac{V}{nD}$ are readily deduced from Fig. 159. Use is made of these approximations in analysing the performance of aeroplanes.

IV. Forces on an Airscrew which is not moving Axially through the Air

Modifications of formulae already developed will be considered in order to cover non-axial motion of the airscrew relative to the air undisturbed by its presence. It is necessary to introduce a system of axes as below.

The axis of X will be taken along the airscrew axis, and in relation to Fig. 160 is directed into the paper. The velocity of the airscrew perpen-

dicular to the X axis is v, and the axis of Y is chosen so as to include this motion.

The only new assumption to be made is that the component of v along the airscrew blade is without appreciable effect on the force on it.

The velocity of the element AB due to rotation and lateral motion is made up of the constant part ωr and a variable part $-v \cos \theta$, and comparison with Fig. 149 suggests the writing of the resultant velocity normal to the X axis in the form

$$\omega r\left(1 - \frac{v}{\omega r} \cos \theta\right). \quad . \quad . \quad . \quad . \quad (58)$$

$-\dfrac{v}{\omega r} \cos \theta$ now takes the place of a_2. The further procedure is the same as in the case for which $v=0$ up to the point at which it was necessary to make an assumption as to the value of a_2, i.e. until the completion of
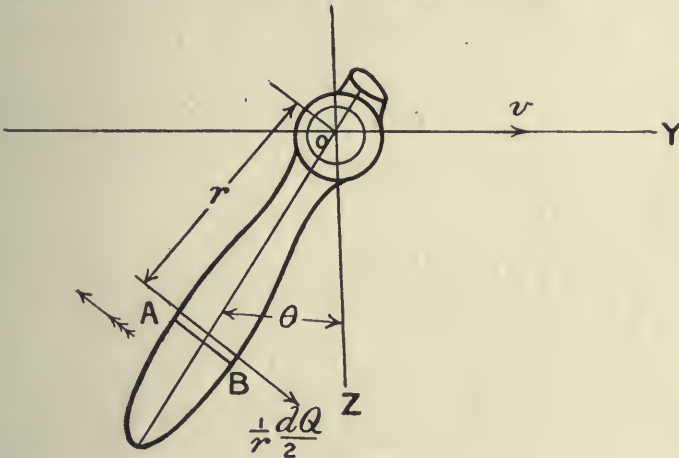
Fig. 160.

Table 1. (The rotational inflow previously included will be ignored here as unimportant in the present connection.)

Equation (14) becomes

$$\tan \phi_v = \frac{1+a_1}{1 - \dfrac{v}{\omega r}\cos \theta} \cdot \frac{V}{\omega r} \quad . \quad . \quad . \quad . \quad (59)$$

This equation may be written as

$$\frac{\tan \phi_v}{1+a_1} = \frac{1}{\dfrac{\omega r}{V} - \dfrac{v}{V}\cos \theta} \quad . \quad . \quad . \quad . \quad (60)$$

For given values of ϕ the corresponding values of a_1 have been calculated and are given in Table 1.

For the purposes of illustration, $\dfrac{V}{\omega r}$ is taken as 0·340, so that results may be compared with those for which $a=2°$ in the axial motion. The

calculations of angle of incidence, for the element to which Table 1 refers, are now extended to cover variations of θ during one revolution of the airscrew. $\dfrac{v}{V}$ is taken as 0·174, i.e. motion at 10° to the airscrew axis.

TABLE 18

θ (degrees).	$\dfrac{v}{V}\cos\theta.$	$\dfrac{\omega r}{V}-\dfrac{v}{V}\cos\theta.$	$\tan\phi_v$ $a_1=0.074.$	ϕ_v (degrees).	$\phi_v+a_v=22°\!\cdot\!1$ a_v (degrees)
0 and 360	0·174	2·766	0·3880	21·20	0·90
20 ,, 340	0·164	2·776	0·3875	21·15	0·95
40 ,, 320	0·134	2·806	0·3830	20·95	1·15
60 ,, 300	0·087	2·853	0·3770	20·65	1·45
80 ,, 280	0·030	2·910	0·3695	20·29	1·81
100 ,, 260	−0·030	2·970	0·3620	19·90	2·20
120 ,, 240	−0·087	3·027	0·3555	19·57	2·53
140 ,, 220	−0·134	3·074	0·3500	19·28	2·82
160 ,, 200	−0·164	3·104	0·3460	19·08	3·02
180	−0·174	3·114	0·3450	19·05	3·05

Columns 2 and 3 need no explanation since they are calculated values corresponding with the assumed values of θ, $\dfrac{v}{V}$ and $\dfrac{\omega r}{V}$. The fourth column comes from equation (60) and the previous column. ϕ_v is obtained from column 4. The last column follows from the relation that ϕ_v+a_v is constant and in our example equal to 22°·1. The value of a given in Table 2 was 2°, and by interpolation will be seen to occur in the above table when $\theta=90°$ and 270°.

The first noticeable feature of Table 18 is the variation of angle of incidence during a revolution of the airscrew. With $\theta=$ zero, the angle of incidence is reduced by 1°·10 due to sideslipping, and with θ equal to 180° the angle of incidence is increased by 1°·05. With the blade vertically downwards it may then be expected that the thrust on the element is decreased as compared with the axial motion, when horizontal there is no change, whilst with the blade upwards the thrust is increased. The calculation of the elementary thrust and torque is carried out below.

TABLE 19.

θ (degrees).	Table 18. a_v (degrees).	k_L	k_D	$\cos\phi_v$	$\sin\phi_v$	$\dfrac{1}{\rho V^2 c}\cdot\dfrac{dT}{dr}$	$\dfrac{1}{\rho V^2 cr}\cdot\dfrac{dQ}{dr}$
0 and 360	0·90	0·229	0·0120	0·934	0·359	1·81	0·828
20 ,, 340	0·95	0·230	0·0122	0·934	0·358	1·83	0·833
40 ,, 320	1·15	0·237	0·0125	0·935	0·355	1·95	0·885
60 ,, 300	1·45	0·250	0·0130	0·936	0·352	2·12	0·940
80 ,, 280	1·81	0·268	0·0137	0·938	0·347	2·36	1·02
100 ,, 260	2·20	0·280	0·0143	0·940	0·342	2·57	1·09
120 ,, 240	2·53	0·295	0·0151	0·941	0·335	2·81	1·17
140 ,, 220	2·82	0·306	0·0157	0·942	0·328	3·00	1·23
160 ,, 200	3·02	0·314	0·0161	0·943	0·326	3·15	1·27
180	3·05	0·315	0·0162	0·944	0·325	3·17	1·29

Columns 1 and 2 are taken from Table 18, and the 3rd and 4th columns are then read from Fig. 161. This figure shows k_L and k_D as dependent on angle of incidence and agrees with the values of Table 1.

From equations (46) and (47) are deduced the expressions

$$\frac{1}{\rho V^2 c} \cdot \frac{dT}{dr} = \left(1 - \frac{v}{V}\cos\theta \cdot \frac{V}{\omega r}\right)^2 \left(\frac{\omega r}{V}\right)^2 \sec^2\phi_v\{k_L\cos\phi_v - k_D\sin\phi_v\} \quad (61)$$

and

$$\frac{1}{\rho V^2 cr} \cdot \frac{dQ}{dr} = \left(1 - \frac{v}{V}\cos\theta \cdot \frac{V}{\omega r}\right)^2 \left(\frac{\omega r}{V}\right)^2 \sec^2\phi_v\{k_L\sin\phi_v + k_D\cos\phi_v\} \quad (62)$$

and from the values in Tables (18) and (19) the right-hand sides of these
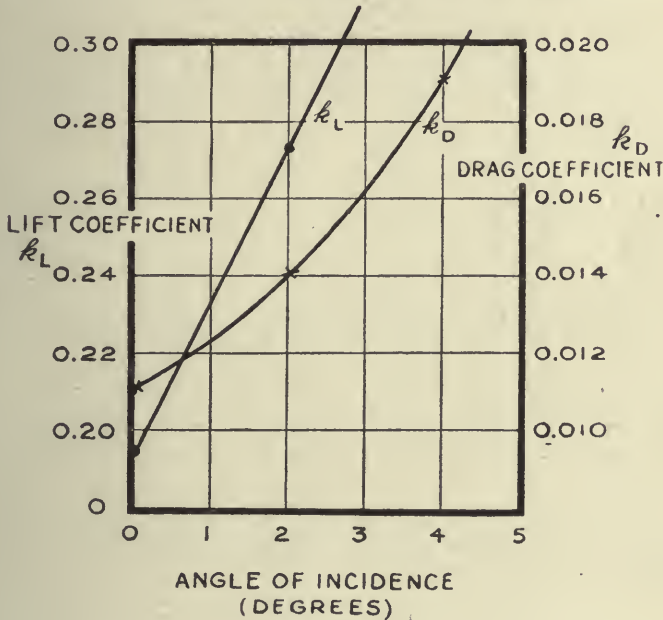
FIG. 161.

expressions are evaluated to form the last columns of Table 19. The comparative values of $\frac{1}{\rho V^2 c}\cdot\frac{dT}{dr}$ and $\frac{1}{\rho V^2 cr}\cdot\frac{dQ}{dr}$ for the axial motion are 2·46 and 1·05 respectively.

The table shows that, due to an inclination of 10°, the thrust on the blade element varies from 74 per cent. to 126 per cent. of its value when moving axially. The elementary torque ranges between 79 per cent. and 123 per cent. of its axial value.

There are seen to be appreciable fluctuations of thrust and torque on each blade during a revolution of the airscrew which need to be examined further. $\frac{1}{r}\cdot\frac{dQ}{2}$ represents an elementary force acting on each blade of a

two-bladed airscrew normal to the direction of motion. On the blade at the bottom this elementary force is $0 \cdot 828 \rho V^2 \frac{c}{2} dr$, whilst on the opposing blade at the top it is $1 \cdot 290 \rho V^2 \frac{c}{2} dr$. The torque on the two blades is then $1 \cdot 06 \rho V^2 c dr$ as against the value $1 \cdot 05 \rho V^2 c dr$ for axial motion. Similar results follow for other positions, and for airscrews with two or four blades the variation of torque with θ is seen to be very small.

On the lower blade the force $0 \cdot 828 \rho V^2 \frac{c}{2} dr$ acts in the direction of the axis of Y, whilst on the upper blade the force is $1 \cdot 290 \rho V^2 \frac{c}{2} dr$ in the opposite direction. There is therefore a force $dY = -0 \cdot 23 \rho V^2 c dr$ on the pair of blades; this is the same effect as would be produced by a fin in the place of the airscrew and lying along the axis of X and Z. Such a fin would oppose a resistance to the non-axial motion.

The thrust on the lower blade element is $1 \cdot 81 \rho V^2 \frac{c}{2} dr$, and on the upper blade is $3 \cdot 17 \rho V^2 \frac{c}{2} dr$, the resultant thrust on the two blades being $2 \cdot 49 \rho V^2 c dr$ as compared with $2 \cdot 46 \rho V^2 c dr$ in the axial motion. As for torque, it appears that the effect of lateral motion on thrust at any instant is very small for two and four bladed airscrews.

On the lower blade the thrust gives a couple about the axis of Y of $1 \cdot 81 \rho V^2 \frac{c}{2} r dr$, whilst on the upper blade the couple is $-3 \cdot 17 \rho V^2 \frac{c}{2} r dr$. The resultant couple is then $-0 \cdot 68 \rho V^2 c r dr$. The lower blade, as illustrated in Fig. 160, would then tend to enter the paper at a greater rate than the centre.

The values of the differences between axial and non-axial motion for the element of a single blade are given below as the result of calculation from the following formulae :—

$$\delta Y = \frac{1}{r} \left(\frac{\delta Q}{2} - 0 \cdot 525 \rho V^2 c r dr \right) \cos \theta \quad . \quad . \quad . \quad (63)$$

$$\delta Z = \frac{1}{r} \left(\frac{\delta Q}{2} - 0 \cdot 525 \rho V^2 c r dr \right) \sin \theta \quad . \quad . \quad . \quad (64)$$

$$\delta M = -r \left(\frac{\delta T}{2} - 1 \cdot 23 \rho V^2 c dr \right) \cos \theta \quad . \quad . \quad . \quad (65)$$

$$\delta N = -r \left(\frac{\delta T}{2} - 1 \cdot 23 \rho V^2 c dr \right) \sin \theta \quad . \quad . \quad . \quad (66)$$

These formulae assume two blades for the airscrew, and the differences from axial motion are used instead of the actual forces during lateral motion; $0 \cdot 525 \rho V^2 c r dr$ and $1 \cdot 23 \rho V^2 c dr$ are the elementary torque and thrust on each blade during axial motion.

The mean values given at the foot of Table 20 show that the average variations of δT, δQ, δZ and δN as a result of non-axial motion are very small as compared with the average thrust and torque on the element. The lateral force δY is about 4 per cent. of the thrust in this example, whilst the pitching couple δM is about 32 per cent. of the torque. These mean figures apply to any number of blades. For variations on two blades during rotation the last six columns of Table (20) should be inverted and the figures added to those there given. For thrust and torque the effect is to leave small differences at all angles. The same applies to the normal force δZ and the yawing couple δN. For the lateral force δY and the pitching moment δM the effect is to double the figures approximately, and these then compare with double thrust and torque.

TABLE 20.

θ degrees.	Cos θ	Sin θ	$\dfrac{\delta T}{\rho V^2 cdr} - 1\cdot23$	$\dfrac{\delta Q}{\rho V^2 crdr} - 0\cdot525$	$\dfrac{\delta Y}{\rho V^2 cdr}$	$\dfrac{\delta Z}{\rho V^2 cdr}$	$\dfrac{\delta M}{\rho V^2 crdr}$	$\dfrac{\delta N}{\rho V^2 crdr}$
0 and 360	1·000	0	−0·33	−0·11	−0·11	0	0·33	0
20 ,, 340	0·940	0·342	−0·32	−0·11	−0·10	−0·03	0·30	−0·09
40 ,, 320	0·766	0·643	−0·25	−0·08	−0·06	−0·05	0·19	−0·16
60 ,, 300	0·500	0·866	−0·17	−0·05	−0·02	−0·04	0·08	−0·15
80 ,, 280	0·174	0·985	−0·05	−0·01	−0·00	−0·01	0·01	−0·05
100 ,, 260	−0·174	0·985	+0·05	+0·02	0·00	+0·02	0·01	+0·05
120 ,, 240	−0·500	0·866	+0·17	0·06	−0·03	+0·05	0·08	+0·15
140 ,, 220	−0·766	0·643	+0·27	0·09	−0·06	0·05	0·20	+0·17
160 ,, 200	−0·940	0·342	+0·34	0·11	−0·09	0·03	0·32	0·11
180	−1·000	0	+0·35	0·12	−0·12	0	0·35	0
			Mean 0·01 or less than 1% of 1·23	Mean 0·003 or about ½% of 0·525	Mean −0·05 or about 4% of 1·23	Mean 0·002 or about 0·2% of 1·23	Mean 0·17 or about 32% of 0·525	Mean 0·002 or about 0·4% of 0·525

For a four-bladed airscrew the averaging of δY and δM would be appreciably better, since four columns displaced by 90° in θ would then be added to provide the resultant.

An angle of 10° as here used may easily occur in the normal range of horizontal flight of an aeroplane, the displacement of velocity being then in the vertical plane. The necessary changes of notation between Y and Z, M and N can readily be made. For lateral stability the present notation is most convenient.

Integration from Element to Airscrew.—The repetition of the preceding calculations for a number of elements and values of $\dfrac{V}{\omega r}$ provides all the data necessary for determination of the torque, thrust, lateral force, etc., on an airscrew.

It has been seen that for an element most of the effects of non-axial motion are unimportant and attention will be directed to the evaluation of Y and M. The symmetry of the figures of Table 20 and their general appearance suggests the applicability of simple formulae, so long as the angle of yaw does not exceed 10°.

Consider equation (61) when $\dfrac{v}{V}\cos\theta\left(\dfrac{V}{\omega r}\right)$ is small enough for expansion of the factor containing it with squares and higher powers neglected. As ϕ depends on this quantity, it is necessary to expand (59) to get

$$\tan\phi_v = (1 + a_1)\frac{V}{\omega r}\left\{1 + \frac{v}{\omega r}\cos\theta\right\}$$

$$= \tan\phi_0\left(1 + \frac{V}{\omega r}\cdot\frac{v}{V}\cos\theta\right) \quad . \quad . \quad . \quad (67)$$

Since as a general trigonometrical theorem

$$\tan(\phi_v - \phi_0) = \frac{\tan\phi_v - \tan\phi_0}{1 + \tan\phi_v\tan\phi_0}$$

and since the numerator is seen from (67) to be of first order in $\dfrac{v}{V}$ the expression becomes

$$\tan(\phi_v - \phi_0) = (\phi_v - \phi_0)_{\text{approx.}} = \frac{\dfrac{v}{V}\cos\theta\,.\,\tan\phi_0\,.\,\dfrac{V}{\omega r}}{\sec^2\phi_0} \quad . \quad (68)$$

and (68) gives an expression for $\delta\phi$ due to change $v\cos\theta$.

To obtain the variations of T differentiate (61) with respect to ϕ, retaining only terms of first order in $\dfrac{v}{V}$. Substitute for $\delta\phi$, i.e. $(\phi_v - \phi_0)$ from (68).

$$\frac{1}{\rho V^2 c}\cdot\delta\frac{d\mathrm{T}}{dr} = -2\frac{v}{V}\cos\theta\sec^2\phi_0(k_L\cos\phi_0 - k_D\sin\phi_0)\cdot\frac{\omega r}{V}$$

$$+\left(\frac{\omega r}{V}\right)^2\cdot\frac{\dfrac{v}{V}\cos\theta\,.\,\tan\phi_0\,.\,\dfrac{V}{\omega r}}{\sec^2\phi_0}\left\{2\sec^2\phi_0\tan\phi_0(k_L\cos\phi_0 - k_D\sin\phi_0)\right.$$

$$\left. + \sec^2\phi_0\left(-k_L\sin\phi_0 - k_D\cos\phi_0 - \frac{dk_L}{da}\cos\phi_0 + \frac{dk_D}{da}\sin\phi_0\right)\right\}$$

$$= \frac{\omega r}{V}\cdot\frac{v}{V}\cos\theta\left\{-k_L\left(\cos\phi_0 + \frac{1}{\cos\phi_0}\right) + k_D\sin\phi_0 - \frac{dk_L}{da}\sin\phi_0\right.$$

$$\left. + \frac{dk_D}{da}\cdot\frac{\sin^2\phi_0}{\cos\phi_0}\right\} \quad . \quad . \quad (69)$$

The formula above may be applied to the previous example where for the element

$$\left.\begin{array}{ll} \phi_0 = 20°\cdot 1 & a = 2° \\[4pt] \dfrac{V}{\omega r} = 0\cdot 340 & \dfrac{v}{V} = 0\cdot 174 \\[8pt] k_L = 0\cdot 275 & k_D = 0\cdot 0141 \\[8pt] \dfrac{dk_L}{da} = 2\cdot 26 & \dfrac{dk_D}{da} = 0\cdot 115 \end{array}\right\} \quad . \quad . \quad . \quad (70)$$

With these values equation (69) leads to

$$\frac{1}{\rho V^2 c} \cdot \delta \frac{dT}{dr} = -0.67 \cos \theta \quad . \quad . \quad . \quad (71)$$

For each blade the numerical factor should be halved before comparison with column 4, Table 20. The simple expression, (71), gives results in good agreement with those of Table 20.

From (69) and (65) the expression for M for the airscrew may be written as

$$\frac{M}{\rho V^2} = \frac{v}{V} \cos^2 \theta \int_0^{\frac{D}{2}} \frac{\omega r}{V} \cdot cr \Big\{ -k_L \Big(\cos \phi_0 + \frac{1}{\cos \phi_0} \Big) + k_D \sin \phi_0 - \frac{dk_L}{da} \sin \phi_0$$

$$+ \frac{dk_D}{da} \cdot \frac{\sin^2 \phi_0}{\cos \phi_0} \Big\} dr \quad . \quad . \quad . \quad (72)$$

The average value of M is half the maximum. The value of $\frac{M}{v \rho V}$ depends on the advance per revolution, chiefly because of the variation of k_L with $\frac{V}{\omega r}$. The relation is not so simple as to be obviously deducible from (72), since the important terms change in opposite directions.

Treating the torque equation (63) in a similar way to that followed for thrust will give the lateral force

$$\frac{1}{\rho V^2 cr} \cdot \delta \frac{dQ}{dr} = -2 \frac{v}{V} \cos \theta \cdot \frac{\omega r}{V} \cdot \sec^2 \phi_0 \ (k_L \sin \phi_0 + k_D \cos \phi_0)$$

$$+ \frac{v}{V} \cos \theta \cdot \frac{\omega r}{V} \cdot \frac{\tan \phi_0}{\sec^2 \phi_0} \Big\{ 2 \sec^2 \phi_0 \tan \phi_0 (k_L \sin \phi_0 + k_D \cos \phi_0)$$

$$+ \sec^2 \phi_0 \Big(-\frac{dk_L}{da} \sin \phi_0 - \frac{dk_D}{da} \cos \phi_0 + k_L \cos \phi_0 - k_D \sin \phi_0 \Big) \Big\}$$

$$= \frac{\omega r}{V} \cdot \frac{v}{V} \cos \theta \Big\{ -k_L \sin \phi_0 - k_D \Big(\frac{1}{\cos \phi_0} + \cos \phi_0 \Big) - \frac{dk_L}{da} \cdot \frac{\sin^2 \phi_0}{\cos \phi_0}$$

$$- \frac{dk_D}{da} \sin \phi_0 \Big\} \quad . \quad . \quad (73)$$

With the values given in connection with pitching moment, equation (73) leads to

$$\frac{1}{\rho V^2 cr} \cdot \delta \frac{dQ}{dr} = -0.22 \cos \theta \quad . \quad . \quad . \quad (74)$$

and for a single blade the numerical factor should be halved. Compared with column 5 of Table 20 the results will again be found to be in good agreement.

The value of the lateral force Y on the whole airscrew is

$$\frac{Y}{\rho V^2} = \frac{v}{V} \cos^2 \theta \int_0^{\frac{D}{2}} \frac{\omega r}{V} \cdot c \Big\{ -k_L \sin \phi_0 - k_D \Big(\frac{1}{\cos \phi_0} + \cos \phi_0 \Big) - \frac{dk_L}{da} \cdot \frac{\sin^2 \phi_0}{\cos \phi_0}$$

$$- \frac{dk_D}{da} \sin \phi_0 \Big\} dr \quad . \quad . \quad (75)$$

and the average value is again half the maximum.

Experimental Determination of Lateral Force on an Inclined Airscrew.
—The experiments which led to the curves of Fig. 162 were obtained on
a special balance in one of the wind channels of the National Physical
Laboratory. The airscrew was 2 feet in diameter, but the results have
been expressed in a form which is independent of the size of the airscrew
in accordance with the principles of dynamical similarity.

The ordinates of the curves of Fig. 162 are the values of the lateral force
on the airscrew divided by $\rho V^2 D^2$ except for one curve which shows the
thrust divided by $\rho V^2 D^2$ to one-tenth its true scale. The number of degrees
shown to the left of each of the curves indicates the angle at which the
airscrew axis was inclined to the direction of relative motion.
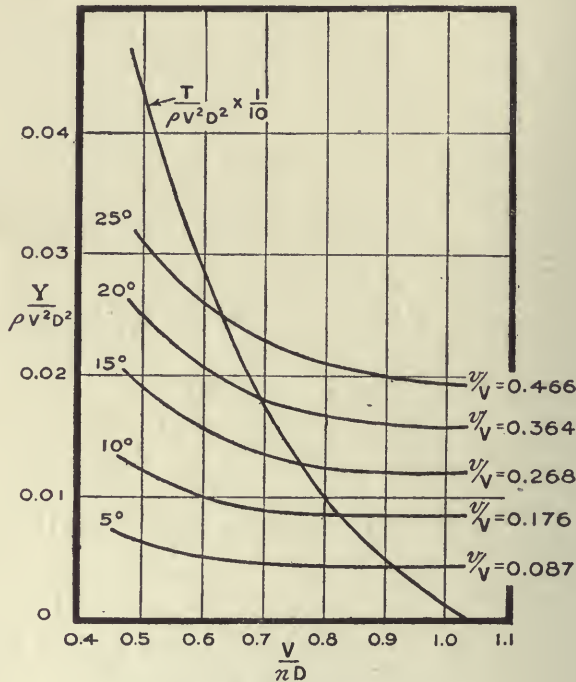
Fig. 162.—Lateral force on inclined airscrew.

The values of the ordinates for the different angles of yaw will be
found to be nearly proportional to the ratio of lateral velocity to axial
velocity, *i.e.* to $\dfrac{v}{V}$. The change of lateral force coefficient with $\dfrac{V}{nD}$ is small
at high values of $\dfrac{V}{nD}$, and in all cases the ratio of lateral force to thrust
increases greatly as $\dfrac{V}{nD}$ increases.

As an example of the magnitude of the lateral force for flying speeds
take at maximum speed

$D = 9$ ft., $V = 160$ ft.-s. (109 m.p.h.), $\dfrac{V}{nD} = 0\cdot75$ and angle of yaw $= 10°$

The lateral force is 43 lbs., and the thrust 655 lbs.
At the speed of climbing

$$V = 100 \text{ ft.-s. (68 m.p.h.), } \frac{V}{nD} = 0\cdot50$$

The lateral force is 23 lbs., and the thrust 815 lbs.

V. The Stresses in Airscrew Blades

The more important stresses in an airscrew blade are due to bending under the combined action of air forces and centrifugal forces and the direct effects of centrifugal force in producing tension. Both types of stress are dealt with by straightforward applications of the engineer's theory of the strength of beams. Recently, attention has been paid to torsional stresses and to the twisting of the blades, but the calculations require more elaborate theories of stress. The progress made, although considerable, has not yet had any appreciable effect on design, and the importance of torsional stresses is not yet accurately estimated. A further series of calculations deals with the resonance of the natural periods of an airscrew blade with periods of disturbance, and one general theorem of importance has been deduced. It states that the natural frequency of vibration of an airscrew blade must be higher than its period of rotation, and that as a consequence resonance can only occur from causes not connected with its own rotation.

The calculation of stresses due to bending and centrifugal force will be dealt with in some detail, but torsion and resonance will not be further treated. As a general rule, it may be said that the evidence in relation to airscrews of normal design is that the twisting is not definitely discernible in the aerodynamics, but appears occasionally in the splitting of the blades. The flexure of the blade under the influence of thrust is sufficient to introduce an appreciable couple as the result of the deflection and centrifugal force.

Bending Moments due to Air Forces.—The blade of an airscrew is twisted, and the air forces acting on it at various radii have resultants lying in different planes. As each section is chosen of aerofoil form one of the moments of inertia of the section is small as compared with the other, and it is sufficient to consider the bending which occurs about an axis of inertia through the centre of area of a section and parallel to the chord. The resolution of the air forces presents no particular difficulty and the details are given below. All the air forces on elements between the tip of a blade and the section chosen for calculation enter into the bending moment, and it is necessary to have a distinguishing notation for different sections. For this purpose dashes have been added to letters to signify use in connection with the base element for which the moment is being calculated.

The formulae required follow in most convenient form from the expressions for thrust and torque, as these admit of ready addition for the

various sections. The thrust element is a force always normal to the airscrew disc, whilst the torque element lies in a plane parallel to the airscrew disc.

If ϕ_0' be the inclination of the chord of the base element to the airscrew disc at radius r', then the elementary addition to the moment due to the forces at radius r is

$$dM = \left(dT \cos \phi_0' + \frac{dQ}{r} \sin \phi_0'\right)(r - r') \quad . \quad . \quad . \quad (76)$$

and using the expressions for dT and $\dfrac{dQ}{r}$ which are given in equations (1) and (2), (76) becomes

$$dM = \frac{dT}{\cos (\phi + \gamma)}\{\cos \phi_0' \cos (\phi - \gamma) + \sin \phi_0' \sin (\phi + \gamma)\}(r - r')$$

or

$$\frac{dM}{d\left(\dfrac{2r}{D}\right)} = \frac{dT}{d\left(\dfrac{2r}{D}\right)} \cdot \frac{D}{2} \cdot \left(\frac{2r}{D} - \frac{2r'}{D}\right) \frac{\cos (\phi + \gamma - \phi_0')}{\cos (\phi + \gamma)} \quad . \quad . \quad . \quad . \quad (77)$$

The value of $\dfrac{dT}{d\left(\dfrac{2r}{D}\right)}$ can be obtained by differentiation of equation (46), and using the value so obtained, equation (77) becomes

$$\frac{1}{\rho V^2 D^3} \cdot \frac{dM}{d\left(\dfrac{2r}{D}\right)} = \frac{\pi}{8\lambda_1} \cdot \left(\frac{2r}{D} - \frac{2r'}{D}\right)a_1(1 + a_1)\frac{\cos (\phi + \gamma - \phi_0')}{\cos (\phi + \gamma)} \quad (78)$$

and M is obtained by integration between the proper limits as

$$\frac{M}{\rho V^2 D^3} = \frac{\pi}{8\lambda_1}\int_{\frac{2r_1}{D}}^{1} a_1(1 + a_1)\left(\frac{2r}{D} - \frac{2r'}{D}\right) \cdot \frac{\cos (\phi + \gamma - \phi_0)}{\cos (\phi + \gamma)}d\left(\frac{2r}{D}\right) \quad (79)$$

In the form shown in (79) the expressions inside the integral are easily evaluated from the earlier work on the aerodynamics of the airscrew, and the important quantities for one value of $\dfrac{V}{nD}$ are collected in Table 21 below.

TABLE 21.—$\dfrac{V}{nD} = 0\cdot60$.

$\dfrac{2r}{D}$	$a_1(1 + a_1)$ from Table 9.	ϕ_0	ϕ	$\phi + \gamma$	Cos $(\phi + \gamma)$
0·960	0·0360	17·1	11·6	14·7	0·967
0·880	0·0900	18·3 [1]	13·2 [2]	15·2 [3]	0·965
0·760	0·1160	19·6	15·6	18·7	0·947
0·602	0·1300	23·8	19·5	22·9	0·921
0·412	0·1185	32·3	27·1	31·4	0·854
0·324	0·0875	38·6	32·4	37·0	0·799

[1] From Table 8.   [2] By interpolation in Table 8.   [3] γ from Table 11.

For the particular values of $\frac{2r}{D}$ chosen, the whole of column 2 will be found reproduced from Table 9. The value of ϕ_0 for $\frac{2r}{D} = 0.880$ is given in Table 8 as 18·3 degrees, and the other values were taken from the similar tables not reproduced. Similar remarks apply to ϕ and $\phi + \gamma$ as shown at the foot of the table, and the last column of Table 21 is obtained from trigonometrical tables.

TABLE 22.

1	2	3	4	5	6
$\frac{2r}{D}$	$a_1(1 + a_1)$	$\frac{2r}{D} - \frac{2r'}{D}$	$\phi + \gamma - \phi_0'$ (degrees).	$\cos(\phi + \gamma - \phi_0')$	$2 \times 3 \times 5$ to give element of integral equation (79).
	0·0360	0·636	−23·9	0·907	0·0208
	0·0900	0·556	−23·4	0·911	0·0456
0·324	0·1160	0·436	−19·9	0·940	0·0475
	0·1300	0·278	−15·7	0·963	0·0348
	0·1185	0·088	− 7·2	0·992	0·0103
	0·0875	0·000	− 1·6	1·000	0
	0·0360	0·548	−17·6	0·953	0·0188
	0·0900	0·468	−17·1	0·956	0·0402
0·412	0·1160	0·348	−13·6	0·972	0·0392
	0·1300	0·190	− 9·4	0·987	0·0244
	0·1185	0·000	− 0·9	1·000	0
	0·0360	0·358	− 9·1	0·987	0·0127
0·602	0·0900	0·278	− 8·6	0·989	0·0247
	0·1160	0·158	− 5·1	0·996	0·0182
	0·1300	0·000	− 0·9	1·000	0
	0·0360	0·200	− 4·9	0·997	0·0071
0·760	0·0900	0·120	− 4·4	0·997	0·0108
	0·1160	0·000	− 0·9	1·000	0
0·880	0·0360	0·080	− 3·6	0·997	0·0029
	0·0900	0·000	− 3·1	0·998	0

The elements of the integral of (79) are calculated as in Table 22 from values extracted from Table 21. The processes are simple and call for no special comment. The values in column 6 of Table 22 are plotted as ordinates in Fig. 163, with $\frac{2r}{D}$ as abscissae. The areas of these curves give the values of the integral at the various values of $\frac{2r'}{D}$, and were obtained by the mid-ordinate method. The values, which represent $\frac{8\lambda_1}{\pi} \cdot \frac{M}{\rho D^3 V^2}$, are shown in the curve marked "moment factor" in Fig. 163. Since the air forces on the blade near the centre are small the curve tends to become straight as the radius decreases and for practical purposes may be extrapolated in accordance with this observation. The values of the integral, denoted by $F\left(\frac{2r}{D}\right)$ are shown in Table 24, but before

use can be made of them to calculate stresses it is necessary to estimate the area, moment of inertia and distance to outside fibres for each of the
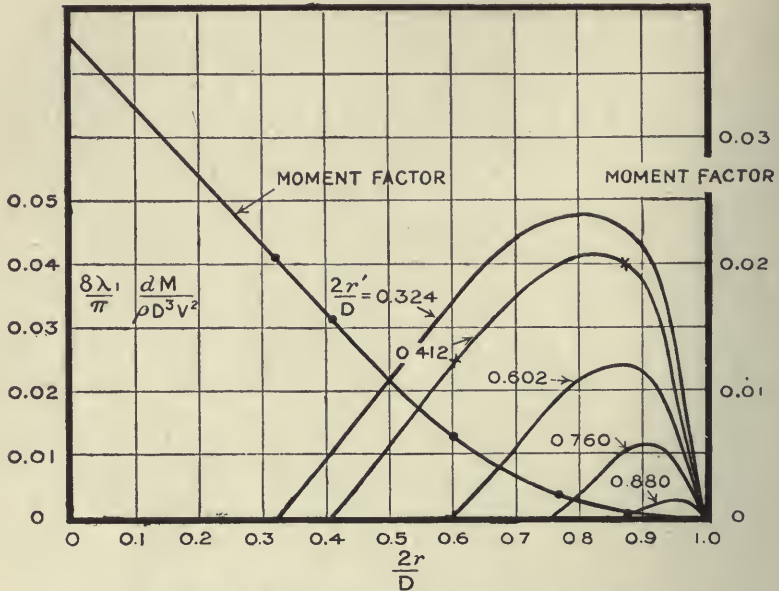
FIG. 163.—Calculation of bending stresses due to thrust.

aerofoil sections used. The values are given in Table 23 in terms of the chord so as to be applicable to airscrews of different blade widths.

TABLE 23.

1	2	3	4
Number of aerofoil.	$k_A c_1^2$ Area of section.	$k_I c_1^4$ Minimum moment of inertia (axis assumed parallel to chord).	$k_e c_1$ Distance of extreme fibre from axis.
1	$0 \cdot 059 c_1^2$	$0 \cdot 000027 c_1^4$	$0 \cdot 049 c_1$
2	$0 \cdot 059 c_1^2$	$0 \cdot 000027 c_1^4$	$0 \cdot 049 c_1$
3	$0 \cdot 073 c_1^2$	$0 \cdot 000051 c_1^4$	$0 \cdot 061 c_1$
4	$0 \cdot 091 c_1^2$	$0 \cdot 000100 c_1^4$	$0 \cdot 076 c_1$
5	$0 \cdot 135 c_1^2$	$0 \cdot 000325 c_1^4$	$0 \cdot 113 c_1$
6	$0 \cdot 180 c_1^2$	$0 \cdot 000765 c_1^4$	$0 \cdot 150 c_1$

In Table 23, c_1 is used to denote the chord to distinguish it from c, which is the sum of the chords of all the blades. If the number of blades is two, the value of M given by (79) should be halved, whilst for four blades one quarter of the value should be taken. Using the ordinary engineer's expression, the maximum stress due to bending is

$$f = \frac{M}{I} y \quad . \quad . \quad . \quad . \quad . \quad . \quad . \quad (80)$$

where I is the moment of inertia and y is the distance to the extreme fibre. Using (80) in conjunction with (79) and denoting the integral of (79) by $\mathrm{F}\!\left(\dfrac{2r}{\mathrm{D}}\right)$, leads to

$$f = \frac{\pi}{2\lambda_1} \cdot \rho \mathrm{V}^2\!\left(\frac{\mathrm{D}}{c}\right)^{3}\!\mathrm{F}\!\left(\frac{2r}{\mathrm{D}}\right) \cdot \frac{k_e}{k_\mathrm{I}} \quad . \quad . \quad . \quad . \quad (81)$$

k_e being the coefficient of c_1 in column 4 of Table 23, and k_I the coefficient of $c_1{}^4$ in column 3. The c of equation (81) has its usual meaning as the sum of the chords of the blades. Evaluation of (81) leads to Table 24.

TABLE 24.

1	2	3	4	5	6	7
$\dfrac{2r}{\mathrm{D}}$	$\dfrac{c}{\mathrm{D}}$	$\mathrm{F}\!\left(\dfrac{2r}{\mathrm{D}}\right)$	$\dfrac{k_e}{k_\mathrm{I}}$	f lbs. per sq. ft. $\dfrac{\pi}{2\lambda_1}\rho\mathrm{V}^2$	Compressive stress, lbs. per sq. in.	Tensile stress, lbs. per sq. in.
0·960	0·036	0·0000	1800	0	0	0
0·880	0·098	0·0002	1800	380	600	400
0·760	0·137	0·0016	1180	730	1150	760
0·602	0·163	0·0060	760	1050	1660	1100
0·412	0·164	0·0154	288	1000	1580	1050
0·324	0·147	0·0204	196	1260	2000	1330

The values of $\dfrac{2r}{\mathrm{D}}$ and $\dfrac{c}{\mathrm{D}}$ of Table 24 are taken directly from Table 7. $\mathrm{F}\!\left(\dfrac{2r}{\mathrm{D}}\right)$ is the ordinate of the curve in Fig. 163 at the proper value of $\dfrac{2r}{\mathrm{D}}$ and $\dfrac{k_e}{k_\mathrm{I}}$ is deduced from Table 23. The fifth column of Table 24 follows from the figures in the previous column and equation (81). Before the results can be interpreted numerically it is further necessary to know $\rho\mathrm{V}^2$ and columns 6 and 7 are calculated for $\rho = 0\cdot00237$ and $\mathrm{V}=147$ ft.-s. (100 m.p.h.). For the proportions of section chosen the tensile stress due to bending is two-thirds of the compressive stress.

The stresses increase rapidly from the tip inwards for the first quarter of the blade, and then more slowly, the highest value shown being 2000 lbs. per square inch for the section nearest the centre for which calculations have been made.

It is important to note that the stress in the airscrew has been calculated without fixing its diameter. Since, in the calculations shown, $\dfrac{\mathrm{V}}{n\mathrm{D}}$ is fixed by hypothesis, the choice of V is equivalent to a choice of $n\mathrm{D}$, and the stress depends on either V or $n\mathrm{D}$. The latter quantity for airscrews of different diameters is proportional to the tip speed, and hence the conclusion is reached that for the same tip speed and value of $\dfrac{\mathrm{V}}{n\mathrm{D}}$ the stress

in similar airscrews is constant. This theorem will be shown to apply in a wider sense than its present application to bending stresses due to air forces.

Centrifugal Stresses.—The stress due to centrifugal force depends on the mass of material outside the section considered, on the distance to its centre of gravity, and on the angular velocity. As most airscrews are solid it is convenient to use the weight of unit volume, and this will be denoted by w. For a solid airscrew the weight of the part external to the section at radius r' is

$$\mathrm{W} = w \int_{r'}^{r_0} k_{\mathrm{A}} c_1{}^2 dr$$

$$= \frac{w \mathrm{D}^3}{8} \int_{\frac{2r'}{\mathrm{D}}}^{1} k_{\mathrm{A}} \left(\frac{c}{\mathrm{D}}\right)^2 d\left(\frac{2r}{\mathrm{D}}\right). \quad \cdot \quad \cdot \quad \cdot \quad \cdot \quad (82)$$

k_{A} is defined as the coefficient of $c_1{}^2$ in column 2 of Table 23.

The centrifugal force on an element at radius r is

$$\frac{w}{g} \cdot k_{\mathrm{A}} c_1{}^2 dr \cdot (2\pi n)^2 r \quad \cdot \quad \cdot \quad \cdot \quad \cdot \quad \cdot \quad (83)$$

and the total force at the section r' is

$$\mathrm{C.F.} = (2\pi)^2 \frac{w}{g} \int_{r'}^{r_0} k_{\mathrm{A}} c_1{}^2 n^2 r \, dr \quad \cdot \quad \cdot \quad \cdot \quad \cdot \quad (84)$$

The stress on the section is

$$\frac{(2\pi)^2}{k_{\mathrm{A}}'(c_1')^2} \cdot \frac{w}{g} \int_{r'}^{r_0} k_{\mathrm{A}} c_1{}^2 n^2 r \, dr . \quad \cdot \quad \cdot \quad \cdot \quad \cdot \quad (85)$$

This stress can be expressed in terms of the generalised variables found convenient in the previous calculations, and (85) leads to

Stress due to centrifugal force (lbs. per sq. ft.)

$$= \frac{\pi^2}{2k_{\mathrm{A}}'\left(\frac{c'}{\mathrm{D}}\right)^2} \cdot \frac{w}{g} \mathrm{V}^2 \cdot \left(\frac{n\mathrm{D}}{\mathrm{V}}\right)^2 \int_{\frac{2r'}{\mathrm{D}}}^{1} k_{\mathrm{A}} \left(\frac{c}{\mathrm{D}}\right)^2 d\left(\frac{2r}{\mathrm{D}}\right)^2 \quad \cdot \quad \cdot \quad (86)$$

The note already made in regard to bending stresses, that the stress depends only on the tip speed for similar airscrews working at the same value of $\frac{\mathrm{V}}{n\mathrm{D}}$, is seen to apply equally to the direct stress arising from centrifugal force.

The value of the integral of (86) is obtained as shown in Table 25 and Fig. 164.

$\frac{2r}{\mathrm{D}}$ and $\frac{c}{\mathrm{D}}$ are taken from Table 24 and k_{A} from Table 23. Columns 4 and 5 then follow by calculation, and $k_{\mathrm{A}}\left(\frac{c}{\mathrm{D}}\right)^2$ is plotted as ordinate with

$\left(\dfrac{2r}{D}\right)^2$ as abscissa. The integral was obtained by the mid-ordinate method of finding areas, the value of the integral being zero at the tip of the blades
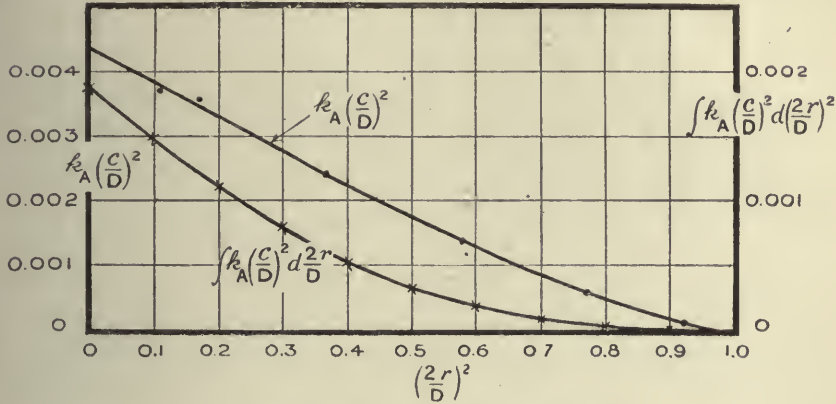
Fig. 164.—Calculation of centrifugal stresses.

where $\dfrac{2r}{D} = 1$. From the curve for the integral the values in column 6 of Table 25 were read off.

TABLE 25.

1	2	3	4	5	6	7
$\dfrac{2r}{D}$	$\dfrac{c}{D}$	k_A	$k_A\left(\dfrac{c}{D}\right)^2$	$\left(\dfrac{2r}{D}\right)^2$	Value of integral of equation (86).	Stress (lbs. per sq. in.).
0·960	0·036	0·059	0·000072	0·920	0·000004	15
0·880	0·098	0·059	0·000537	0·774	0·000050	250
0·760	0·137	0·073	0·00137	0·577	0·000220	430
0·602	0·163	0·091	0·00241	0·362	0·000630	700
0·412	0·164	0·135	0·00363	0·170	0·00122	900
0·324	0·147	0·180	0·00389	0·105	0·00145	1000

With $\qquad\qquad$ $V = 147$ ft.-s.

$$\frac{V}{nD} = 0{\cdot}60$$

and $\qquad\qquad$ $w = 42$ lbs. per cubic foot (walnut).

the direct stress due to centrifugal force can be calculated from equation (86) and the figures of Table 25. The stress is of course tensile, and is additive to the stress calculated and shown in column 7 of Table 24. The combined stress is 2300 lbs. per sq. in., and 3000 lbs. per sq. in. is not regarded as an excessive value for walnut. This value would be reached for a somewhat higher value of nD.

Bending Moments due to Eccentricity of Blade Sections and Centrifugal Force.—It will be seen shortly that as a result of centrifugal force the bending moments arising from small eccentricity of the airscrew sections from the airscrew disc are of appreciable magnitude. The eccentricities considered will be of comparable size with those produced by the deflection of the blade under the action of thrust. The calculations are somewhat complex, and will be illustrated by a direct example which assumes the values of the eccentricities. The more practical problem involves processes of trial and error for complete success.

As the area of the section of a blade at radius r' is $\frac{1}{4}k_A'(c')^2$ the centrifugal force obtained from equation (86) is

$$\text{C.F.} = \frac{\pi^2}{8} \cdot \frac{w}{g} V^2 D^2 \Big(\frac{nD}{V}\Big)^2 \int_{\frac{2r'}{D}}^{1} k_A \Big(\frac{c}{D}\Big)^2 d\Big(\frac{2r}{D}\Big)^2 \quad . \quad . \quad . \quad (87)$$

Consider now the couples acting due to centrifugal force; if from some pair of fixed axes the co-ordinates of the centres of area of each section be given as x and y, the perpendicular distance, p, from any one of these centres of area on to the axis of least inertia of another is

$$p = (x - x') \cos \phi_0' + (y - y') \sin \phi_0' \quad . \quad . \quad . \quad (88)$$

and the resultant moment at the section denoted by dashes is

$$\frac{M_{CF}}{\rho V^2 D^3} = \frac{\pi^2}{8} \cdot \frac{1}{\rho} \cdot \frac{w}{g} \cdot \Big(\frac{nD}{V}\Big)^2 \int_{\frac{2r'}{D}}^{1} k_A \Big(\frac{c}{D}\Big)^2 \frac{(x - x') \cos \phi_0' + (y - y') \sin \phi_0'}{D} d\Big(\frac{2r}{D}\Big)^2 \quad (89)$$

The form of (89) has been chosen for convenience of comparison with equation (79).

Given x and y as functions of $\Big(\frac{2r}{D}\Big)^2$, the value of M_{CF} can be calculated from (89) and data previously given.

TABLE 26.

1	2	3	4	5
$\Big(\frac{2r}{D}\Big)^2$	$k_A\Big(\frac{c}{D}\Big)^2$	Cos ϕ_0.	$\frac{x}{D}$	$\frac{y}{D}$
0·920	0·000072	0·956	0.00920	0
0·774	0·000537	0·949	0·00774	0
0·577	0·00137	0·943	0·00577	0
0·362	0·00241	0·915	0·00362	0
0·170	0·00363	0·845	0·00170	0
0·105	0·00389	0·782	0·00105	0

As an example the values of $\frac{x}{D}$ have been taken as the one-hundredth part of $\Big(\frac{2r}{D}\Big)^2$. On a 12 ft. 6 ins. diameter airscrew the eccentricity due to

design and deflection under load would be 1·5 ins. at the tip of the blades. Eccentricities of greater amount may easily occur in practice. The value of y has been taken as zero everywhere. Table 26 shows the data necessary for the calculation of moments from equation (89). The details are given below in Table 27.

TABLE 27.

1	2	3	4	5	6
$\left(\dfrac{2r}{D}\right)^2$	$\left(\dfrac{2r'}{D}\right)^2$	$k_A\left(\dfrac{c}{D}\right)^2$	$\cos\phi_0'$	$\dfrac{x-x'}{D}$	Element of integral of (89).
0·920	0·105	0·000072	0·782	−0·00815	−0·46 × 10⁻⁶
0·774	,,	0·000537	,,	−0·00669	−2·80 ,,
0·577	,,	0·00137	,,	−0·00472	−5·05 ,,
0·362	,,	0·00241	,,	−0·00257	−4·85 ,,
0·170	,,	0·00363	,,	−0·00065	−1·84 ,,
0·105	,,	0·00389	,,	0	0
0·920	0·170	0·000072	0·845	−0·00750	−0·45 × 10⁻⁶
0·774	,,	0·000537	,,	−0·00604	−2·74 ,,
0·557	,,	0·00137	,,	−0·00407	−4·70 ,,
0·362	,,	0·00241	,,	−0·00192	−3·90 ,,
0·170	,,	0·00363	,,	0	0
0·920	0·362	0·000072	0·915	−0·00558	−0·37 × 10⁻⁶
0·774	,,	0·000537	,,	−0·00412	−2·03 ,,
0·577	,,	0·00137	,,	−0·00215	−2·70 ,,
0·362	,,	0·00241	,,	0	0
0·920	0·577	0·000072	0·943	−0·00343	−0·23 × 10⁻⁶
0·774	,,	0·000537	,,	−0·00197	−1·00 ,,
0·577	,,	0·00137	,,	0	0
0·920	0·774	0·000072	0·949	−0·00146	−0·10 × 10⁻⁶
0·774	,,	0·000537	,,	0	0

The values given in column 6 of Table 27 are plotted as ordinates in Fig. 165 with $\left(\dfrac{2r}{D}\right)^2$ as abscissa. For each value of $\left(\dfrac{2r'}{D}\right)^2$ there is a separate curve, the area of which is required. Found in the usual way these areas are plotted to give the "integral" curve of Fig. 165.

To show the results in comparison with those for bending due to thrust as shown in Table 24 the value of $\dfrac{8\lambda_1}{\pi}\cdot\dfrac{M_{CF}}{\rho V^2 D^3}$ has been calculated and tabulated in Table 28.

TABLE 28.

$\dfrac{2r}{D}$	$\dfrac{8\lambda_1}{\pi}\cdot\dfrac{M_T}{\rho V^2 D^3}$	$\dfrac{8\lambda_1}{\pi}\cdot\dfrac{M_{CF}}{\rho V^2 D^3}$
0·960	0·0000	−0·0000
0·880	0·0002	−0·00005
0·760	0·0016	−0·0005
0·602	0·0060	−0·0018
0·412	0·0154	−0·0041
0·324	0·0204	−0·0049

The first two columns of Table 28 are taken from the first and third columns of Table 24. The third column of Table 28 is calculated from equation (89) and the integral curve of Fig. 165.

The example chosen had the tip of the airscrew forward of the boss, and the bending moment is opposed to that due to the thrust. Roughly speaking, the effect of the centrifugal force is one quarter that of the thrust, and had all the values of x been increased four times, the residual bending moment due to thrust and centrifugal force would have been very small at all points. Appropriate variation of x would lead to complete elimination, but trial and error might make the operation rather long. It is
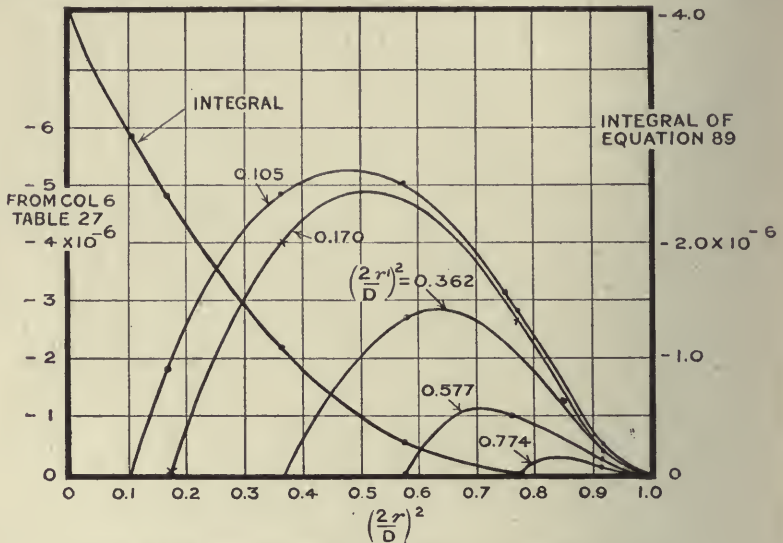
Fig. 165.—Calculation of bending moments due to centrifugal force.

only possible to get complete balance for moments and so eliminate flexural distortion for one value of $\dfrac{V}{nD}$, and in practice a compromise would be necessary. It is not, however, quite clear that the possibility of eliminating moments is a useful one in practice, since airscrews are built up of various laminae with glued joints. In order to keep these joints in compression deviations from the condition of no flexural distortion are admitted. All that can be done in a treatise of this description is to point out the methods of estimating the consequences of any such compromise as is made in the engineering practice of airscrew design.

It may be noticed here that the effect of distortion under thrust is to reduce the stress below that calculated on the assumption of a rigid blade.

The problems connected with the calculation of the deflection and twisting of airscrew blades are more complex than those given, and have not received enough attention for the results to be applicable to general practice. In this direction there are opportunities for both experimental and mathematical research.

FORMULAE FOR AIRSCREWS SUGGESTED BY CONSIDERATIONS OF DYNAMICAL
SIMILARITY

In the course of the detailed treatment of airscrew theory it has been found that $\dfrac{V}{nD}$ is a convenient variable. It has also been seen that the density of the air and of the material of the airscrew are important. In discussing the forces on aerofoils it was shown that both the viscosity and elasticity of the air are possible variables, whilst consideration of the elasticity of the timber occurs as an item in the calculation of deflections and stresses.

It may then be considered, in summary, that the variables worth consideration are—

$V \equiv$ the forward velocity of the airscrew.
$n \equiv$ the rotational speed.
$D \equiv$ the diameter.
$\rho \equiv$ the air density.
$\dfrac{w}{g} \equiv$ the density of the material of the airscrew.
$a \equiv$ the velocity of sound in air as representing its elasticity.
$E \equiv$ Young's modulus for the material of the airscrew.

All the quantities, thrust, torque, efficiency, stress and strain then depend on a function of five variables, of which

$$F\left(\frac{V}{nD},\ \frac{VD}{\nu},\ \frac{V}{a},\ \frac{1}{\rho}\cdot\frac{w}{g},\ \frac{E}{\rho V^2}\right) \quad . \quad . \quad . \quad . \quad . \quad (90)$$

may be taken as typical. The first argument, $\dfrac{V}{nD}$, is of great importance and is the most characteristic variable of airscrew performance. If care is taken in choosing a sufficiently large model aerofoil and wind speed the variable $\dfrac{VD}{\nu}$ may be ignored. $\dfrac{V}{a}$ becomes important only at tip speeds exceeding 600 or 700 ft.-s., but complete failure occurs at 1100 ft.-s. if this variable is ignored. The argument $\dfrac{1}{\rho}\cdot\dfrac{w}{g}$ simply states that the ratio of the density of the material of the airscrew to that of the air affects the performance. Since thrust depends primarily on ρ and centrifugal force on $\dfrac{w}{g}$, it is obvious that moments and forces from the two causes can only be simply related if $\dfrac{1}{\rho}\cdot\dfrac{w}{g}$ be constant. A similar conclusion is reached in regard to $\dfrac{E}{\rho V^2}$.

The density and elasticity of the materials of which airscrews are made are rarely introduced into the formulae of practice. Where the material

is wood the choice has been between walnut and mahogany, and neither the density nor elasticity are appreciably at the choice of the designer. Some progress has been made with metal airscrews, and the stresses causing greatest difficulty are those leading to buckling of the thin sheets used. In order to reduce the weight of a metal airscrew to a reasonable amount it is obvious that hollow construction must be used and that similarity of design cannot cover both wood and metal airscrews. Some very special materials such as " micarta " have been used in a few cases, and since the blades are solid and homogeneous, the arguments from similarity might be applied with terms depending on density and elasticity. (" Micarta " is a preparation of cotton fabric treated with cementing material.)

The common forms of expression used are

$$\text{Thrust} = \rho n^2 D^4 F_1\left(\frac{V}{nD}\right) \quad . \quad . \quad . \quad . \quad . \quad (91)$$

$$\text{Torque} = \rho n^2 D^5 F_2\left(\frac{V}{nD}\right) \quad . \quad . \quad . \quad . \quad . \quad (92)$$

$$\text{Efficiency} = \qquad F_3\left(\frac{V}{nD}\right) \quad . \quad . \quad . \quad . \quad . \quad (93)$$

$$\text{Stress} = \rho n^2 D^2 F_4\left(\frac{V}{nD}\right) \quad . \quad . \quad . \quad . \quad . \quad (94)$$

From (94) follows the statement that for similar airscrews working at the same value of $\frac{V}{nD}$ the stress depends on the tip speed of the airscrew, and is otherwise independent of the diameter. The numerical values of F_1 and F_2 are usually given under the description of absolute thrust and torque coefficients respectively.

CHAPTER VII

FLUID MOTION

Experimental Illustrations of Fluid Motion ; Remarks on Mathematical Theories of Aerodynamics and Hydrodynamics

Forces on aeroplanes and parts of aeroplanes are consequences of motion through a viscous fluid, the air, and if our mathematical knowledge were sufficiently advanced it would be possible to calculate from first principles the lift and drag of a new wing form. No success has yet been attained in the analysis of such a problem from the simplest assumptions, and recourse is at present made to direct experiments. The viscosity of air is always important in its effect on motion, and as the effect depends on the size of the object it will be necessary to discuss the conditions under which aircraft may be represented by models. The relation between fluid motions round similar objects is so important that a separate chapter is devoted to it under the head "Dynamical Similarity." It will be found that for most aerodynamics connected with aeroplane and airship motion air may be regarded as an incompressible fluid.

The present chapter contains material on fluid motion which throws some light on the resistance of bodies. It also covers, in brief *résumé*, the existing mathematical theories, indicating their uses and limitations, but no attempt is made to develop the theories of fluid motion beyond the earliest stages, as they can be found in the standard works on hydrodynamics. For experimental reasons the photographs shown will refer to water. It will be found that a simple law will enable us to pass from motion in one fluid to motion in any other, and the analogy between water and air is illustrated by a striking example under the treatment of similar motions.

Whilst it is true that the fluid motions with which aeronautics is directly concerned are unknown in detail there are nevertheless some others which can be calculated with great accuracy, the discussion of which leads to the ideas which explain failure to calculate in the general case. Fig. 166 represents a calculable motion, and when the mathematical theory is developed later in the chapter it is carried to the stage at which Fig. 166 is substantially reproduced. The photograph was produced by a method due to Professor Hele-Shaw who kindly proffered the loan of his apparatus for the purpose of taking the original photographs of which Figs. 166, 171, 176–178, are reproductions.

The apparatus consists of two substantial plates of glass separated from each other by cardboard one or two hundredths of an inch thick. In Fig.

166 the shape of the cardboard is shown by the black parts, the centre being a circular disc, whilst at the sides are curved boundaries. The space between the boundaries is filled with water, the motion of which is caused by applying pressure at one end. To follow the motion when once started small jets of colour are introduced well in front of the disc and before the fluid is sensibly deflected.

Steady Motion.—After a little time the bands of clear and coloured water take up the definite position shown in Fig. 166, and the picture remains unaltered, so far as the eye can judge, although the fluid continues to flow. When such a condition can be reached the final fluid motion is described as "steady." The point of immediate interest is that the shape of all the bands can be calculated (see p. 355). The mathematical analysis of the problem of flow in these layers was first given by Sir George Stokes, and an account of the theory will be found in Lamb's "Hydrodynamics." Except for a region in the neighbourhood of the disc and boundaries the accuracy of calculation would exceed that of an experiment. Near the solid boundaries, for a distance comparable with the thickness of the film, the theory has not been fully applied.

It is, of course, perfectly clear that there is nothing in the neighbourhood of the wheel axle of an aeroplane, say, which corresponds with the two plates of glass, and Fig. 166 cannot be expected to apply. It is difficult to mark air in such a way that motion can be observed, but it is possible to make a further experiment with water by removing the constraint of the glass plates. Even at very low velocities the flow is " eddying " or " unsteady," and a long exposure would lead to a blurred picture. To avoid confusion a cinema camera has been used, and the life-history of an eddy traced in some detail in Figs. 167–170. The colouring matter in Fig. 167 is Nestlé's milk, and the flow does not at any stage even faintly resemble that shown in Fig. 167. With eddying motion the colour is rapidly swept out of the greater part of the field of view, and only remains dense behind the cylinder where the velocity of the fluid is very low. The eddying motion depicted in Fig. 167 is yet far beyond our powers of mathematical analysis, but a considerable amount of experimental analysis has been made, and to this reference will be made almost immediately.

The water flows from right to left, and the cylinder is shown as a circle at the extreme right of each photograph. The numbers at the side represent the order in which the film was exposed, and an examination shows a progressive change running through the series of photographs. Starting from the first, it will be seen that a small hook on the upper side grows in size and travels to the left until it reaches the limit of the photograph in the sixteenth member of the series. By this time a second small hook has made its appearance and has about the same size as that in 1. Some of the more perfect photographs occur under the numbers 18–24, and show clearly the simultaneous existence of four hooks or " eddies " in various stages of development and decay. The eddies leave the cylinder alternately on one side and then on the other, growing in size as they recede from the model.
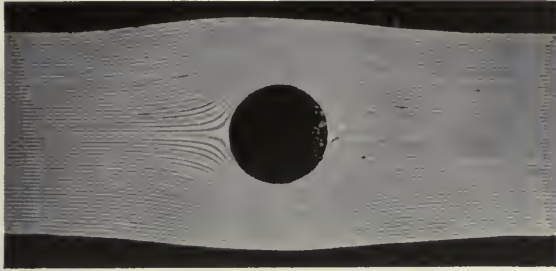
Fig. 166.—Viscous flow round disc (Hele-Shaw).
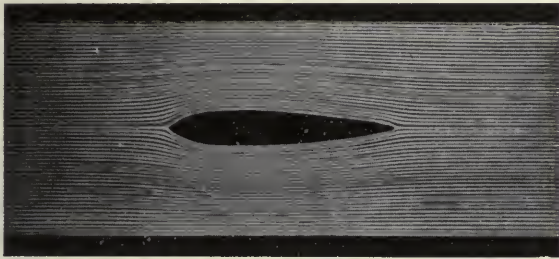
Fig. 171.—Viscous flow round strut section (Hele-Shaw).

Fig. 172.—Viscous flow round strut section (free fluid).
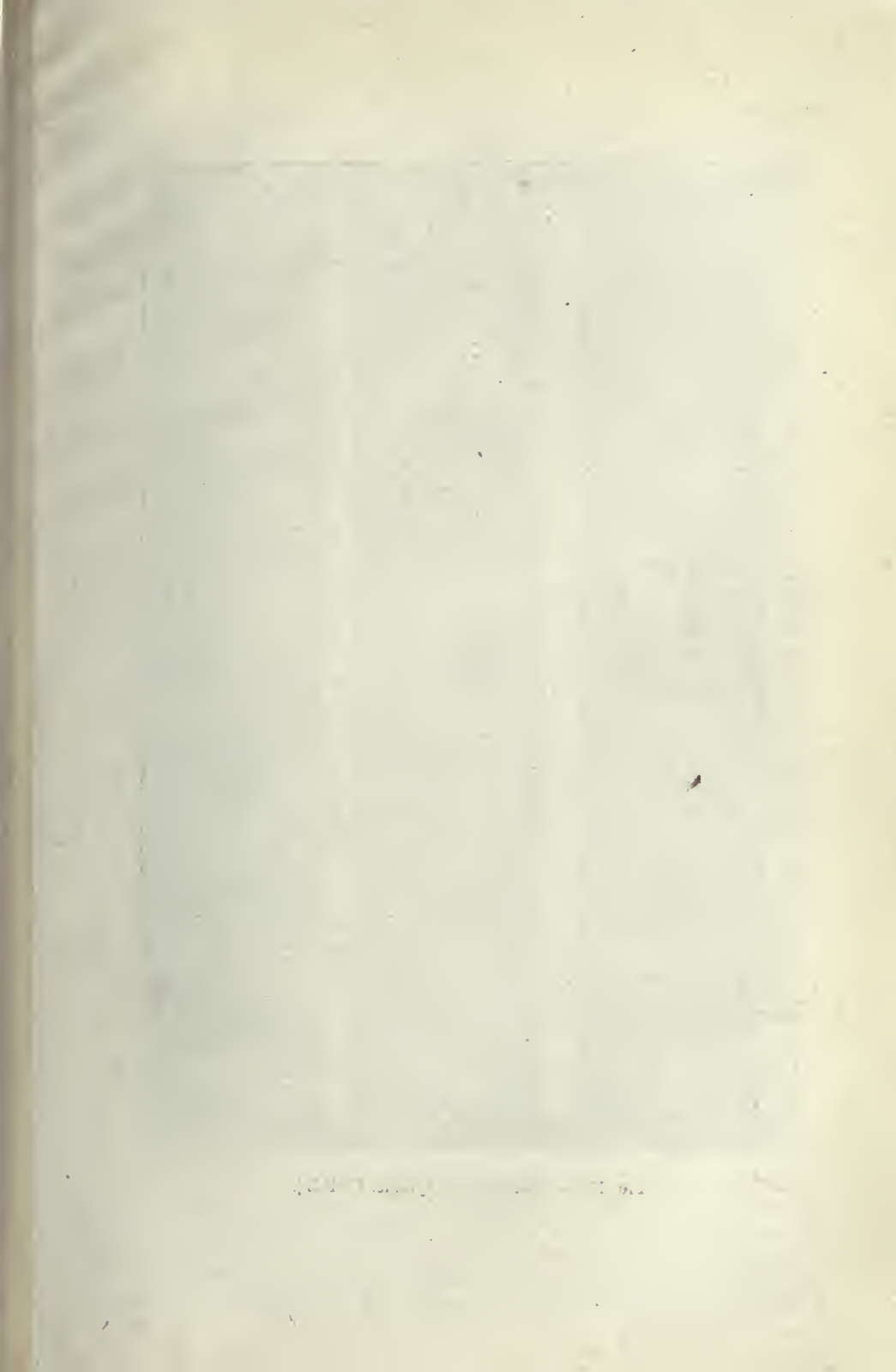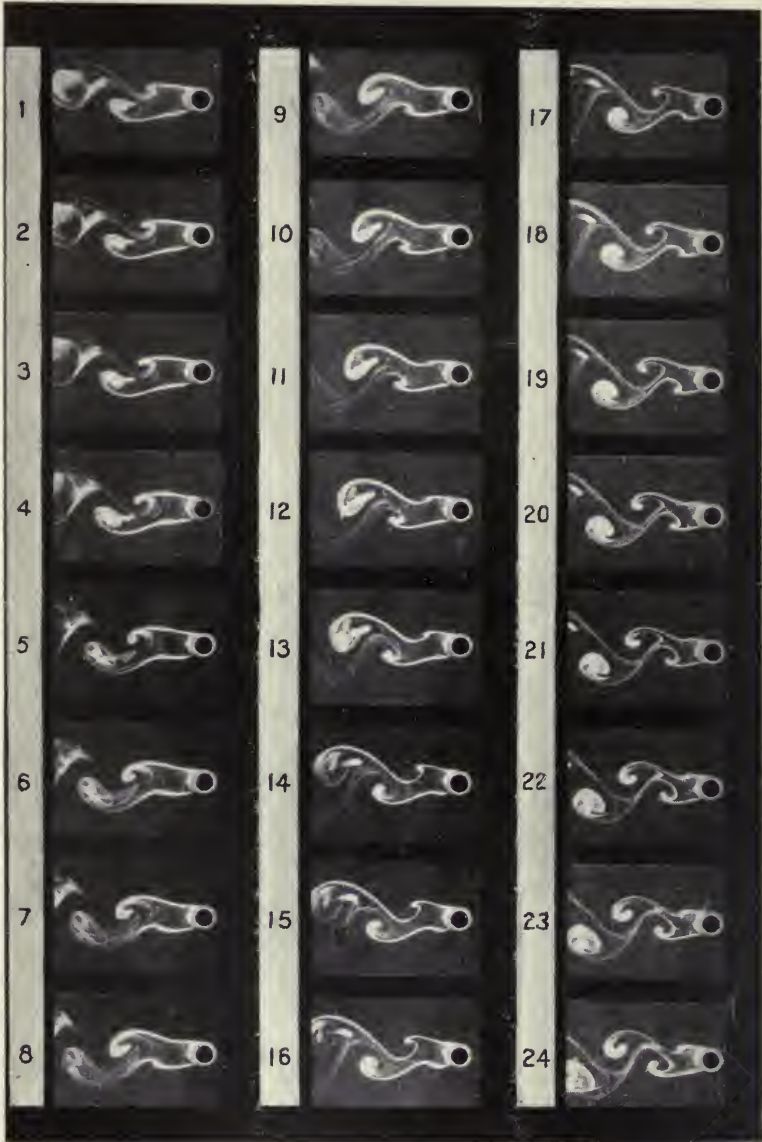
FIG. 167.—Eddies behind cylinder (N.P.L.).

Unsteady Motion.—The root ideas underlying the unsteady motion of a fluid are far less simple than those for steady motion. Figs. 167–170 all refer to the same motion, and yet there is little evident connection between the figures. An attempt will now be made to trace a connection, and we start with the definitions suggested by the illustrations.

Stream Lines.—In an unsteady motion the position of each stream line depends on the time. In all cases with which we are concerned in aerodynamics the position of the stream lines in the region of disturbed flow repeats at definite intervals, *i.e.* the flow is periodic. The period in Fig. 167 can be seen to extend over 13 or 14 pictures. In producing Fig. 168 the flow was recorded by the motion of small oil drops, and no less than eighty periods were observed. The cinematograph picture for the beginning of each period was selected and projected on a screen whilst the lines of flow
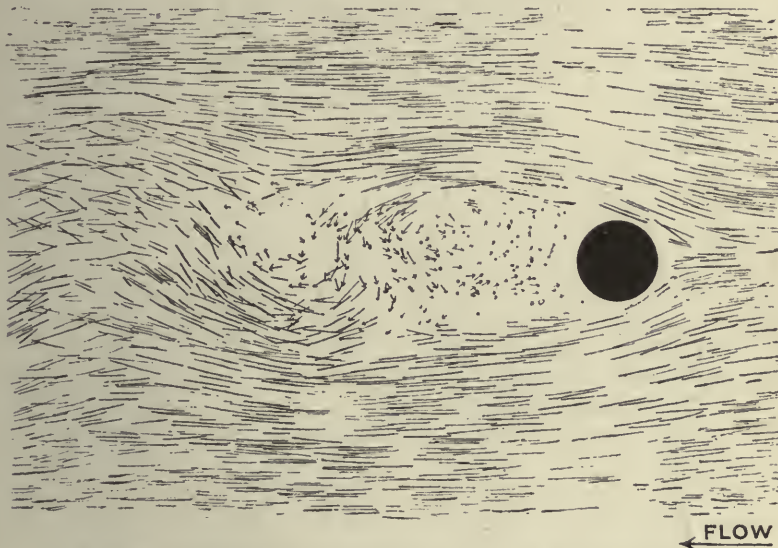
FIG. 168.—Instantaneous distribution of velocity in an eddy (N.P.L.).

were marked, and Fig. 168 is the result of the superposition of 80 pictures. Had the accuracy of the experiment been perfect none of the lines so plotted would have crossed each other. As it is, the crossings do not confuse the figure until the eddies have broken up appreciably.

If now one proceeds to join up the lines so that they become continuous across the picture, the result is the production of stream lines. Stream lines have the property that at the instant considered the fluid is everywhere moving along them.

Fig. 169 shows the general run of the stream lines at intervals of one-tenth of a complete period. Only five diagrams are shown, since the remaining five are obtained by reversing the others about the direction of motion; Fig. 169 (*f*) would be like Fig. 169 (*a*) turned upside down, and so on. Most of the stream lines follow a sinuous path across the field, but occasionally bend back upon themselves (Fig. 169 (*a*)). Two parts may then approach

each other and coalesce so as to make a closed stream line. The bend of Fig. 169 (b) is seen in Fig. 169 (c) to have become divided into a small
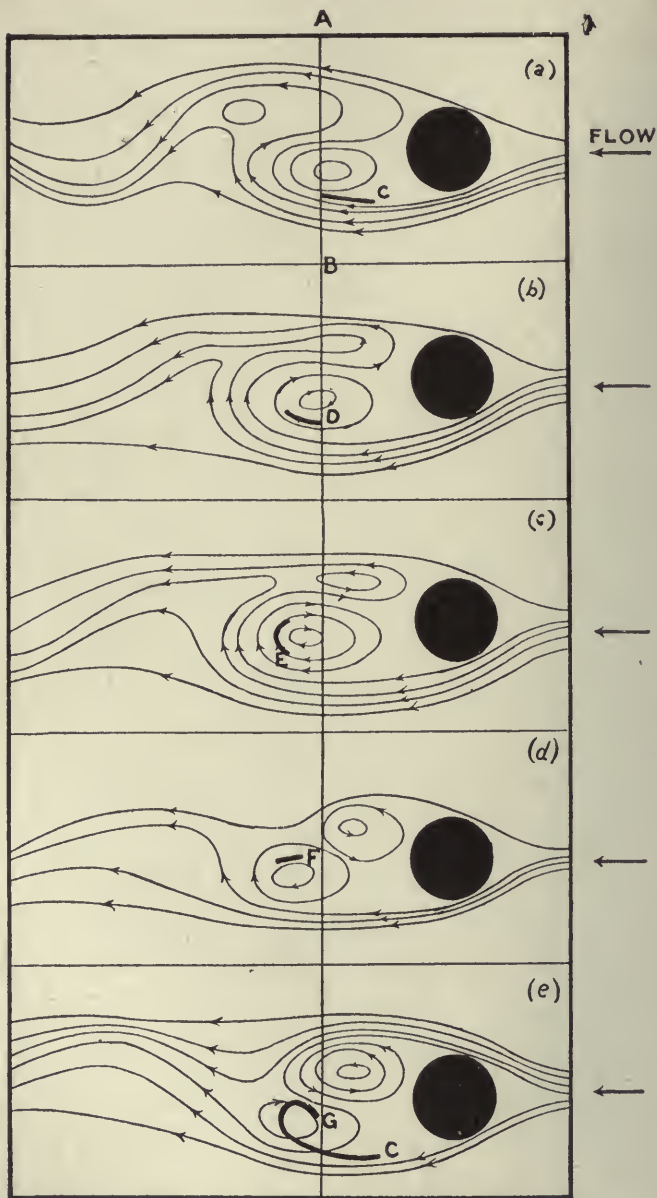
FIG. 169.—Stream lines in an eddy at different periods of its life (N.P.L.).

closed stream line and a sinuous line through the field. The process is continued between Figs. 169 (d) and 169 (e), where two closed streams are

shown, and so on. These closed streams represent vortex motion, and as the vortices travel down-stream they are somewhat rapidly dissipated.

Fig. 168 shows that the velocity inside the vortex is small compared with that of the free stream.

Paths of Particles.—Fig. 170 shows the paths followed by individual particles across the field of view. Unlike " stream lines " " paths of particles " cross frequently. Some of the particles were not picked up by the camera until well in the field of view. In one case (the lowest of Fig. 170) a particle had entered a vortex and for four complete turns travelled slowly against the main stream, which it then joined. The upper part of Fig. 170 shows a series of paths varying from a loop to a cusp, for particles all of which had passed close to the cylinder.
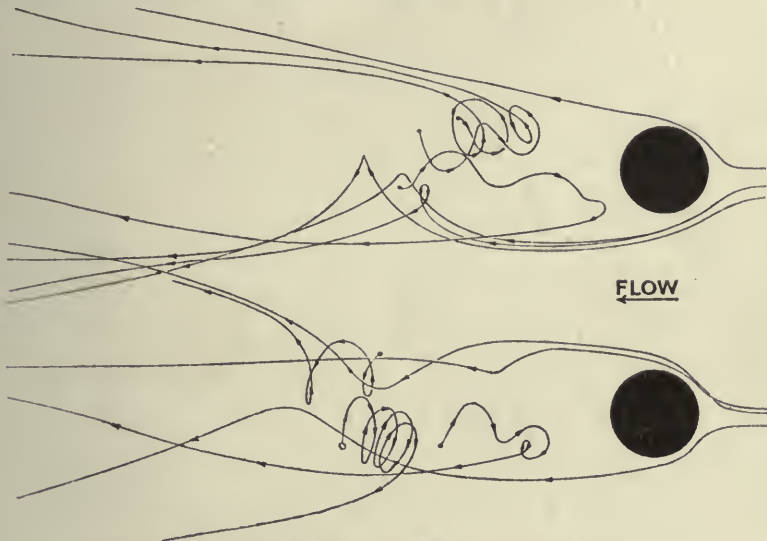
FIG. 170.—Motion of particles of fluid in an eddy (N.P.L.).

To produce these curves it was only necessary to expose the plate in a camera during the passage of a strongly illuminated oil drop across the field. Since observation of all oil drops across the field gives both stream lines and paths of particles, one set of pictures must be deducible from the other. Before paths of particles can be obtained by calculation from the stream lines of Fig. 169 the velocity at each point of the stream lines must be deduced. Draw a line AB across Fig. 169 as indicated; the quantity of fluid flowing between each of the stream lines being known, the number representing this quantity can be plotted against distances of the stream lines from A. The slope of the curve so obtained is the velocity at right angles to AB. Since the resultant velocity is along the stream line the component then leads to the calculation of the resultant velocity. The calculation is simple, but may need to be repeated so many times as to be laborious in any specified instance of fluid motion. For the present we only need to see that Fig. 169 gives not only the stream lines but the velocities along them.

From Fig. 169 we can now calculate the path of a particle. Starting at C, for instance, in Fig. 169 (a), a short line has been drawn parallel to the nearest stream line. This line represents the movement of the particle in the time interval between successive pictures. In the next picture the point D has been chosen as the end of the first and another short line drawn, and so on, the whole leading to the line CG of Fig. 169 (e). Further application of the process would complete the loop. The line CG is illustrative only, since the velocity along each of the stream lines was not calculated; it is sufficient to show the connection between the lines of Fig. 169 obtained experimentally and those of Fig. 170, also deduced from the same experiment.

There are two standard mathematical methods of presenting fluid motion which correspond with the differences between " stream lines " and " paths of particles."

Filament Lines.—Filament lines have been so called since they are the instantaneous form taken by a filament of fluid which crosses the field of disturbed flow. They are the lines shown in Fig. 167. The colouring matter of Fig. 167 was introduced through small holes in the side of the cylinder. The white lines therefore represent the form taken by the line joining all particles which have at any time passed by the surface of the cylinder. They could be deduced from the paths of particles by isolating all the paths passing through one point, marking on each path the point corresponding with a given time and joining the points.

In experimental investigations of fluid motion it is important to bear in mind the properties of filament lines when general colouring matter is used. The use of oil drops presents a far more suitable line of experimental research where attempt is made to relate experimental and mathematical methods.

Although eddying motion is very common in fluids, it is not the universal condition in a large mass. Two examples will be given of a comparison between steady free flow and the flow illustrated by Prof. Hele-Shaw's experiments. The question will arise, does the method of flow between plate glass surfaces indicate the only type of steady flow? There is, of course, no obvious reason why it should. As a further example of Prof. Hele-Shaw's method of illustrating fluid motion, the case of a strut section will be considered (Fig. 171 opposite p. 344). It will be noticed that the streams were quite gently disturbed by the presence of the obstruction. If we consider the fluid moving between the stream lines and the side of the model, it will be noticed that the streams, which are widest ahead of the model, gradually narrow to the centre of the strut and then again expand. The fact that the coloured bands keep their position at all times means that the same amount of fluid passing between any point of a stream line and the strut must also pass inside all other points on the same stream line, and because of the constriction the velocity will be greatest where the stream is narrowest and *vice versâ*.

It is interesting to compare Fig. 171 with another figure illustrating the flow of water round a strut of the section used for Fig. 171, the flow not being confined by parallel glass plates. The stream lines in Fig. 172 are shown as
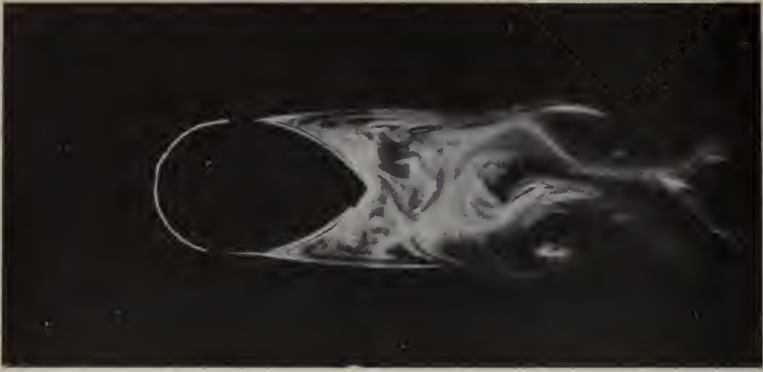
Fig. 173.—Eddying motion behind short strut (N.P.L.).
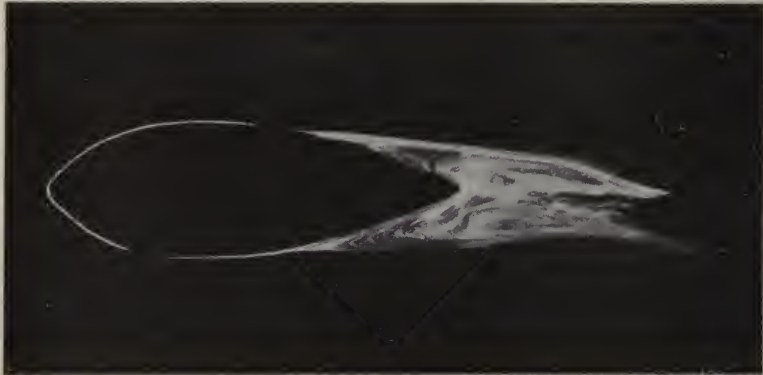
Fig. 174.—Eddying motion behind medium strut (N.P.L.).

Fig. 175.—Eddying motion behind long strut (N.P.L.).

broken lines, the lengths of which represent the velocity of the fluid. The flow will be seen to consist of streams with the narrowest part near the nose, and from that point a steadily increasing width until the tail is reached. The gaps in the stream lines are produced at equal intervals of time, and their shortening near the strut shows the effect of the viscous drag of the surface.

The general resemblance between Figs. 171 and 172, which relate [to struts, is in marked contrast with the difference between Figs. 166 and 167 for cylinders. When measurements are made in a wind channel of the forces acting on struts and on cylinders, it is found that to this difference in the flow corresponds a very wide difference in resistance. A cylinder will have 10 to 15 times the resistance of a good strut of the same cross-sectional area. On examining the photographs given in Fig. 167 a region will be found immediately behind the cylinder which is not greatly affected in width during the cycle of the eddies. Just behind the body the water is almost stationary and is often spoken of as " dead water." In the case of the cylinder illustrated, the dead water is seen to be somewhat wider than the diameter of the cylinder itself. Figs. 173–175 show further photographs of motion round struts in free water; in Fig. 173 the " dead water " is shown to be as great as for a cylinder, the strut being very short. The longer strut of Fig. 174 is distinctly less liable to produce the dead water, whilst a further reduction is evident on passing to the still longer strut, Fig. 175. The photographs were taken in water, and it does not necessarily follow that they will apply to air without a discussion which is to come later, but it is of immediate interest to compare between themselves the resistances of a cylinder and three struts under conditions closely approaching those of use in an aeroplane. The relative resistances are given in Table 1.

TABLE 1.—THE RESISTANCE OF CYLINDERS AND STRUTS.

Model.	Relative resistance.
Cylinder, Fig. 167 .	6
Strut, Fig. 173 . .	3·5
,, Fig. 174 . .	1·2
,, Fig. 175 . .	1·0

The general connection between the size of the " dead-water " region and the air resistance is too obvious to need more than passing comment. The more aerodynamic experiments are made, the more is it clear that high resistance corresponds with a large dead-water region, and perhaps the most satisfactory definition of a " stream-line body " is that which describes it as " least liable to produce dead water."

If, now, a return be made to Fig. 166—Prof. Hele-Shaw's photograph of flow round a cylinder—it will be seen that there is neither " dead water " nor " turbulence," and the mathematical analysis leads to the conclusion that if the plates be near enough together no body would be sufficiently

blunt and far removed from " stream line " to produce eddying motion. The influence at work to produce this result is the viscous drag of the water over the surface of the two sheets of plate glass. It is obvious without proof that this viscous drag will be greater the closer the surfaces are to each other, and that on moving them far from each other this essential constraint is reduced. It is not equally obvious that an increase of velocity of the fluid between the plates has the effect of reducing the constraint, but on the principles of dynamical similarity the law is definite, and advantage is taken of this fact in producing Figs. 176 and 177, which show different motions for the same obstacle.

The photographs, taken by Professor Hele-Shaw's method, show the flow round a narrow rectangle placed across the stream in a parallel-sided channel. The thickness of the water film was made such that at low velocities it was only just possible to produce Fig. 176, which shows streams behind the rectangle which are symmetrical with those in front. Without changing the apparatus in any way the velocity of the fluid was very greatly increased and Fig. 177 produced. In front of the obstacle careful examination of the figures is necessary in order to detect differences between Figs. 176 and 177, but at the back the change is obvious. The first points at which the difference is clearly marked are the front corners of the rectangle. The fluid is moving past the corners with such high velocity that the constraint of the glass plates is insufficient to suppress the effects of inertia. The fluid does not now close in behind the obstacle as before, and an approach to " dead water " is evident. There is a want of definition in the streams to the rear which seems to indicate some mixing of the clear and coloured fluids, but there is no evidence of eddying. We are thus led to consider three distinct stages of fluid motion.

(1) Steady motion where the forces due to viscosity are so great that those due to inertia are inappreciable.

(2) Steady motion when the forces due to viscosity and inertia are both appreciable ; and

(3) Unsteady motion, and possibly steady motion, when the inertia forces are large compared with those due to viscosity.

The extreme case of (3) is represented by the conventional inviscid fluid of mathematical theory where the forces due to viscosity are zero. It is not a little surprising to find that the calculated stream lines for the steady motion of an inviscid fluid are so nearly like those obtained in Professor Hele-Shaw's experiments as to be scarcely distinguishable from them. It needed a mathematical analysis by Sir George Stokes to show that the very different physical conditions should lead to the same calculation. The common calculation illustrates the important idea that mathematical methods developed for one purpose may have applications in a totally different physical sense, and the student of advanced mathematical physics finds himself in the possession of an important tool applicable in many directions. This is, perhaps, the chief advantage to be obtained from the study of the motion of a conventional inviscid fluid. Before considering the theory, one further illustration from experiment will be given.
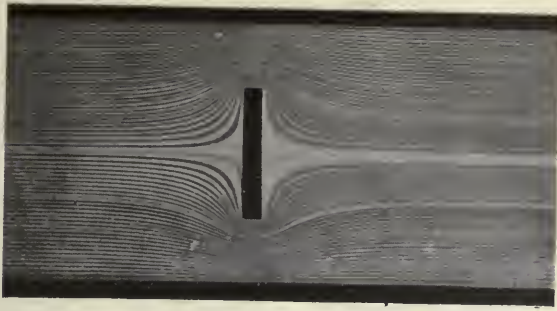
Fɪɢ. 176.—Viscous flow round section of flat plate (Hele-Shaw). Low speed.
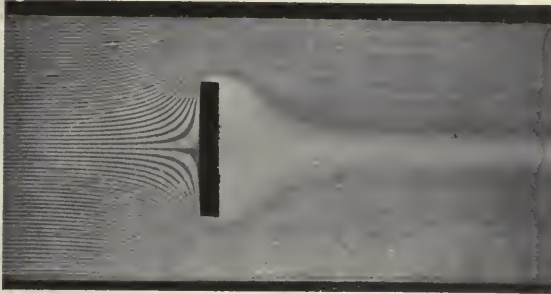
Fɪɢ. 177.—Viscous flow round section of flat plate (Hele-Shaw). High speed.

Fɪɢ. 178.—Viscous flow round wing section (Hele-Shaw).

Fɪɢ. 179.—Viscous flow round wing section (free fluid).

Wing Forms.—The motion round the wing of an aeroplane probably only becomes eddying when the angle of incidence is large, and the resistance is then so great as to render flight difficult. At the usual flying angles, there is some reason to believe that the motion is " steady." Two further photographs, Figs. 178 and 179, one by Prof. Hele-Shaw's method and the other by the use of oil drops, show for a wing section two steady motions which differ more than appeared for the struts.

If Fig. 178 be examined near the trailing edge of the aeroplane wing, it will be noticed that the streams close in very rapidly. At a bigger angle of attack it would be obvious that on the back there is a dividing point in one of the streams. At this dividing point the velocity of the fluid is zero, and such a point is sometimes called a " stagnation point." A second " stagnation point " is present on the extreme forward end of the wing shape.

In the freer motion of a fluid, such as that of air round a wing, the forward " stagnation " point can always be found, but the second or rear " stagnation point " is never recognisable. The effect of removing the constraint of the glass plates will be seen by reference to Fig. 179, although this does not accurately represent the flow at high speed on a large wing. The slowing up of the stream by the solid surface, which was noticed for the strut, is again seen in the case of the wing model.

Elementary Mathematical Theory of Fluid Motion

Frictionless Incompressible Fluid.—In spite of the fact that other and more powerful methods exist, it is probably most instructive to start the study of fluid motion from the calculations relating to " sources and sinks." In his text-book on Hydrodynamics, Lamb has shown that the more complex problems can all be reduced to problems in sources and sinks. The combinations may become very complex, but methods relating to complex sources and sinks are developed in a paper by D. W. Taylor, Inst. Naval Architects, to which reference should be made for details.

A " source " may be defined as a place from which fluid issues, and a " sink " a place at which fluid is removed ; either may have a simple or complex form.

Consider Fig. 180 (a) as an illustration of a simple source, the fluid from which spreads itself out over a surface parallel to that of the paper. The thickness of this fluid may be conveniently taken as unity, the assumption being that it forms part of a stream of very great thickness.

If m be the total quantity of fluid coming from the source, the "strength" is said to be m. A corresponding sink would emit fluid of amount $-m$.

Since the fluid is equally free in all directions, symmetry indicates a continuous sheet of fluid issuing from the centre, and ultimately passing through the circular section CPG. Whether on account of instability the flow would break into jets or not we have no means of saying at present, but it should be remembered that the " continuity " of the fluid throughout the region of fluid motion is definitely an assumption. Such a physical phenomenon as " cavitation " in the neighbourhood of

propeller blades in water would be a violation of this assumption. As cavitation arises from the presence of points of very low pressure, it is clear that even in a hypothetical fluid no solution can be accepted for which the pressure at any point is required to be enormous and negative. An instance of this occurs in relation to one of the so'utions for the motion of an inviscid fluid round a plane surface.

Assuming continuity and incompressibility for the fluid, it is obvious
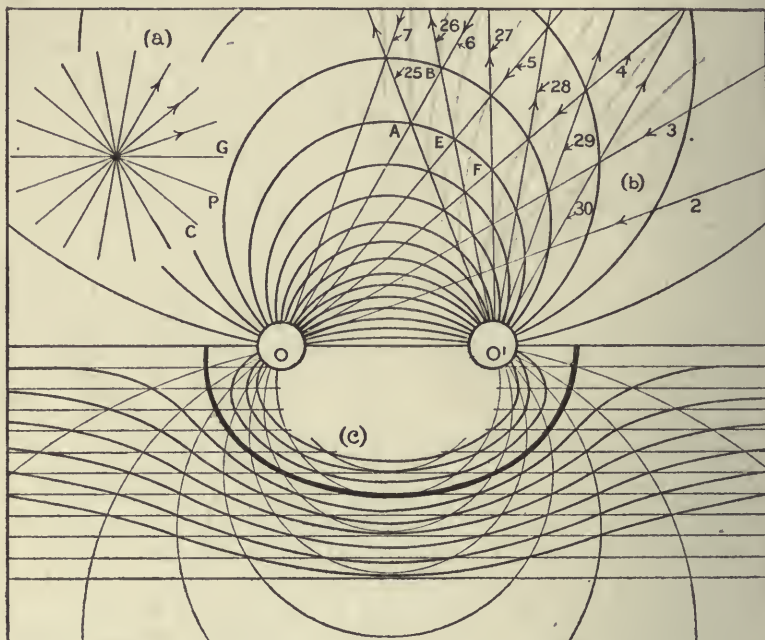
Fig. 180.—Fluid motions developed from sources and sinks in an inviscid fluid.

that the velocity of outflow across the circle CPG will be uniform, and calling the velocity v we have

$$2\pi r v = m \quad . \quad . \quad . \quad . \quad . \quad . \quad . \quad (1)$$

or

$$v = \frac{m}{2\pi r} \quad . \quad . \quad . \quad . \quad . \quad . \quad (1a)$$

so that the velocity becomes smaller and smaller as the distance from the source increases.

For the motion of any inviscid incompressible fluid whatever, there is a relation between the pressure and velocity at any point of a stream line. The equation, proved later, is extremely useful in practical hydrodynamics, and is one particular form of Bernoulli's equation. It states that

$$p + \tfrac{1}{2}\rho v^2 = \text{const.} \quad . \quad . \quad . \quad . \quad . \quad (2)$$

where ρ is equal to the mass of unit volume of the fluid. We have seen that the stream lines in Fig. 180 (a) are radial lines, and from (1a) it appears that

v ultimately becomes zero when r becomes very great ; this is true for all the stream lines impartially. If in (2) the value of v be put equal to zero when r is very great, it will be seen that the " const." on the right-hand side is the pressure of the stream a long way from the source, and since this is the same for all stream lines it follows that (2) gives a relation between p and v for any point whatever in the fluid. The same proposition is true for all motions of frictionless incompressible fluids if the " const." does not vary from one stream to the next. Most problems come within this definition. Equation (2) is only true for an inviscid incompressible fluid, and cannot be applied with complete accuracy to any fluid having viscosity.

Stream Function.—It has been shown that the total quantity of fluid moving across the circle CPG is m. The same quantity obviously flows across any boundary which encloses the source. It is convenient to have an expression for the quantity of fluid which goes across part of a boundary. The " stream function " which gives this is usually represented by ψ. It is clear that the same quantity of fluid flows across any line joining two stream lines, and the change of ψ from one stream line to another is therefore always the same, no matter what the path taken. It follows from this that along a stream line $\psi = $ const.

In arriving at this conclusion, it will be remarked that the only assumptions made are that the fluid fills the whole space and is incompressible. It need not be inviscid.

In the particular case of the source of Fig. 180 (a) it is immediately obvious that the amount of fluid flowing across the line CP is equal to $\dfrac{\theta}{2\pi} m$, and it is usual to write

$$\psi = -\frac{m}{2\pi}\theta. \quad . \quad . \quad . \quad . \quad . \quad . \quad (3)$$

for the value of ψ which corresponds with a source of strength m, the negative sign being conventional. If m be suitably chosen, the diagram of Fig. 180 (a) may be divided up by equal angles such that $\psi = 0$ along OG, $\psi = 1$ along OP, $\psi = 2$ along OC, and so on. Any line might have been called that of zero ψ, as in all calculations it is only the differences between the values of ψ which are of importance.

Fig. 180 (b) shows the drawing of stream lines for a combination of simple source and sink. Two sets of radial lines, similar to Fig. 180 (a), are drawn, and these produce a series of intersections. For the case shown, equal angles represent equal quantities of flow for both source and sink. If the strengths had been unequal, the angles would have been proportioned so as to give equal flow, *i.e.* the lines are lines of constant ψ differing by equal amount from one line to its successor.

If lines be drawn from O to O_1 through the points of intersection of the stream lines in the way OAO$_1$ and OBO$_1$ are drawn, the lines so obtained are the stream lines for a source and sink of equal strength. Lines drawn through the points of intersection along the other diagonals of the elementary quadrilaterals would give the stream lines for two equal sources.

The assumption has here been made that the effect of a sink on the motion is independent of the existence of the source, and *vice versâ*. The assumption is legitimate for an inviscid fluid, but does not always hold for the viscous motions of fluids; it is proved without difficulty that any number of separate possible inviscid fluid motions may be added together to make a more complex possible motion.

Addition of Two Values of ψ.—The construction given in Fig. 180 (*b*) can be seen to follow from the statement that two separate systems may be added together to produce a resultant new system. The group of radial lines round O is numbered in accordance with the scheme of Fig. 180 (*a*), and represents values of ψ for a source. For the sink a set of numbers are arranged round O_1, the sink being indicated by the fact that the numbers increase when travelling round the circle in the opposite way to that for increasing numbers round the source. If we call ψ_1 the value for the source and ψ_2 the value for the sink, the addition gives $\psi_1 + \psi_2$ for the combination, or

$$\psi = \psi_1 + \psi_2 \quad . \quad . \quad . \quad . \quad . \quad . \quad (5)$$

As a stream line is indicated by ψ being constant, we may write

$$\psi_1 + \psi_2 = \text{const.} \quad . \quad . \quad . \quad . \quad . \quad (5a)$$

and by giving the "const." various values the new stream lines can be drawn. As an example, take "const." $= 31$, and consider the point A of Fig. 180 (*b*); the line from the source through this point is $\psi_1 = 25$, and from the sink $\psi_2 = 6$, or $\psi_1 + \psi_2 = 31$. At E, $\psi_1 = 26$, $\psi_2 = 5$, $\psi_1 + \psi_2 = 31$. Hence both A and E are on a stream line of the new system. The advantage of the method lies in the ease with which it can be extended, and to one such extension it is proposed to call immediate attention.

A steady stream of fluid will be superposed on the source and sink of Fig. 180 (*b*). The stream lines for this are equidistant straight lines, and they will be taken parallel to OO_1. It can easily be shown that the curves of Fig. 180 (*b*) are circles, but this would only be true for a simple source and sink, and not for a case presently to be discussed. The method of procedure is not confined to such a simple source and sink. If parallel lines be drawn on a sheet of tracing paper which is then placed over the lines from source to sink, a set of intersecting lines will again be formed of which the diagonals may be drawn to form the new system; the result is indicated in Fig. 180 (*c*).

The result is interesting; an oval-shaped stream in the middle of the figure separates it into two parts. Inside there are stream lines passing from source to sink, and outside streams passing from a great distance on one side to a great distance on the other. As the fluid is frictionless, the oval may be replaced by a solid obstruction without disturbing the stream lines, and the method of sources and sinks may then be used to develop forms of obstacles and the corresponding flow of an inviscid fluid round them.

By the addition of the velocities of the fluid due to source, sink and translation separately by the parallelogram of velocities, the resultant velocity of the fluid at any point round the oval can be obtained. The

direction of this resultant must be tangential to the oval at the point because it is a stream line. Once the magnitude of the resultant velocity has been obtained, equation (2) will give the pressure at the point. From the symmetry of Fig. 180 (c), back and front, it is clear that the pressures will be symmetrically distributed, and there will be no resultant force on the oval obstacle. The theorem is true that no body in an inviscid fluid can experience a resistance due to a steady rectilinear flow of the fluid past it, unless a discontinuity is produced.

Flow of an Inviscid Fluid round a Cylinder.—It has already been remarked that the stream lines in Professor Hele-Shaw's method can be calculated, and it is proposed to make one calculation (graphically). The method of sources and sinks is used, not because the fluid is inviscid

Fig. 181.—Calculated flow round circular disc for comparison with Fig. 166.

but because the equation of motion in Professor Hele-Shaw's experiment happens to agree with that for an inviscid fluid.

If the source and sink of Fig. 180 (b) be brought nearer and nearer together, the circles showing the stream lines will become more and more like the larger ones there shown, and ultimately when the source and sink almost coincide the circles will be tangential to the line joining them. They then take the form shown in the lower half of Fig. 181, the radii being inversely proportional to the value of ψ.

On to these stream lines superpose those for a uniform stream and draw the diagonals. Instead of the oval of Fig. 180 (c) the closed curve obtained is now a circle, and three of the stream lines have been drawn on the lower half of the figure. The upper half of the figure was completed in this way with a larger number of stream lines, and alternative streams

were filled in so that the figure might bear as much resemblance as possible to the photographs shown by Professor Hele-Shaw. The result is somewhat striking.

The Equations of Motion of an Inviscid Fluid.—Readers are referred to the text-books on Hydrodynamics for a full treatment of the subject as applied to compressible fluids and the effects of gravity, and attention will be limited to the cases outlined in the previous notes.

Suppose that Fig. 182 represents a steady motion in the plane of the paper. Isolate a small element between two stream lines and consider the forces acting on it, which are to be such that it will not change its position with time although filled with new fluid. The force on the elementary block is due to pressures over its four faces and the difference between
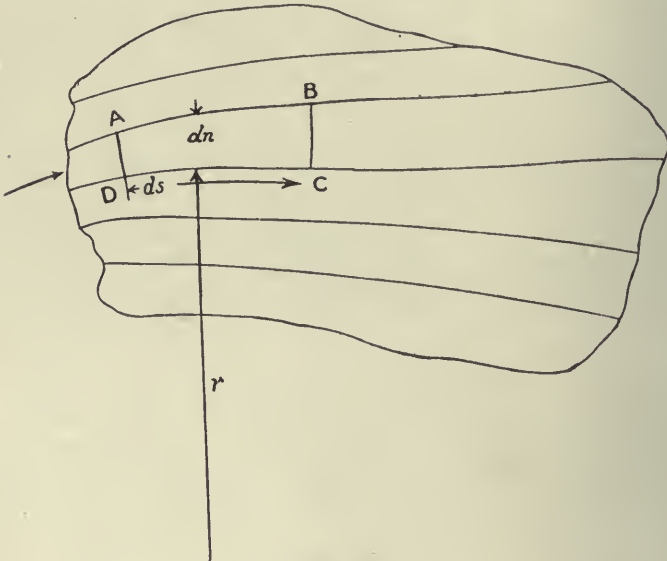

Fig. 182.

the momentum entering by the face AD and that leaving by BC. If the block is not to move the resultant of these two must be zero.

Forces in the Direction of Motion.—If p be the pressure on AD. that on BC will be $p + \dfrac{\partial p}{\partial s} ds$, and along the faces AB and DC the pressure will be variable. The resultant of the uniform pressure p over all the faces is zero, and the total force against the arrow is therefore

$$\frac{\partial p}{\partial s} . ds . dn \quad . \quad . \quad . \quad . \quad . \quad . \quad . \quad (4)$$

if we neglect quantities of relatively higher order. The mass of fluid passing AD and BC per unit time is the same and is equal to $\rho v dn$, where ρ is the density of the fluid and v its velocity. The momentum entering is then $\rho v^2 dn$, and that leaving is $\rho v dn \left(v + \dfrac{\partial v}{\partial s} ds \right)$, and the difference is

$$\rho v \frac{\partial v}{\partial s} . \, dsdn \quad . \quad . \quad . \quad . \quad . \quad . \quad . \quad . \quad (5)$$

in the direction of the arrow, and therefore exerting a force in the opposite direction on the element. The force equation is made up of (4) and (5), and is

$$\frac{\partial p}{\partial s} + \rho v \frac{\partial v}{\partial s} = 0 \quad . \quad . \quad . \quad . \quad . \quad . \quad . \quad (6)$$

Equation (6) is easily integrated and gives

$$p + \tfrac{1}{2}\rho v^2 = \text{const.} \quad . \quad . \quad . \quad . \quad . \quad . \quad . \quad (7)$$

Equation (7) is very important, and often applies approximately to the motion of real fluids.

Forces Normal to the Direction of Motion.—If r be the radius of the path, the centrifugal force necessary to keep the block from moving outwards is $\rho \dfrac{v^2}{r} . \, dnds$, whilst the difference of pressure producing this force is $\dfrac{\partial p}{\partial r} . \, dnds$, and hence the equation of motion at right angles to the direction of motion of the fluid is

$$\rho \frac{v^2}{r} = \frac{\partial p}{\partial n} . \quad . \quad . \quad . \quad . \quad . \quad . \quad (8)$$

Substitute from (7) for $\dfrac{\partial p}{\partial n}$, and (8) becomes

$$\frac{v}{r} + \frac{\partial v}{\partial n} = 0 \quad . \quad . \quad . \quad . \quad . \quad . \quad (9)$$

In dealing with sources and sinks equation (9) was assumed to hold, and it is now seen that the assumption was justified, since r is infinite and $\dfrac{\partial v}{\partial n}$ is zero along each of the stream lines.

If the radius of stream lines be infinite, equation (9) shows that $\dfrac{\partial v}{\partial n}$ must be zero, *i.e.* the velocity must be uniform from stream to stream. Equation (7) then shows that p is constant. The converse is of course true, that uniform pressure means uniform velocity and straight stream lines.

Comparison of Pressures in a Source and Sink System with those on a Model in Air.—The calculations and experiments to which reference will now be made are due to G. Fuhrmann working in the Göttingen University Laboratory. The general lines of the calculations follow those outlined, but the source and sink system is not simple. The models, instead of being long cylinders as in the cases worked out in previous pages, were solids of revolutions, but the transformations on this account are extremely simple. The complex sources and sinks are obtained by

integration from a number of elementary simple sources and simple sinks
and present little difficulty. For details, reference should be made to the
original report or to the paper by Taylor already mentioned.

The original paper by Fuhrmann contains the analysis and experi-
mental work relating to six models of the shape taken by airship envelopes.
Some of these shapes had pointed tails, whilst one of them had both pointed
head and tail. The investigation was carried out in relation to the
development of the well-known Parseval airship, and the model most
like the envelope of that type of dirigible is chosen for the purpose of
illustration. Starting with various sources and sinks the flow was calcu-
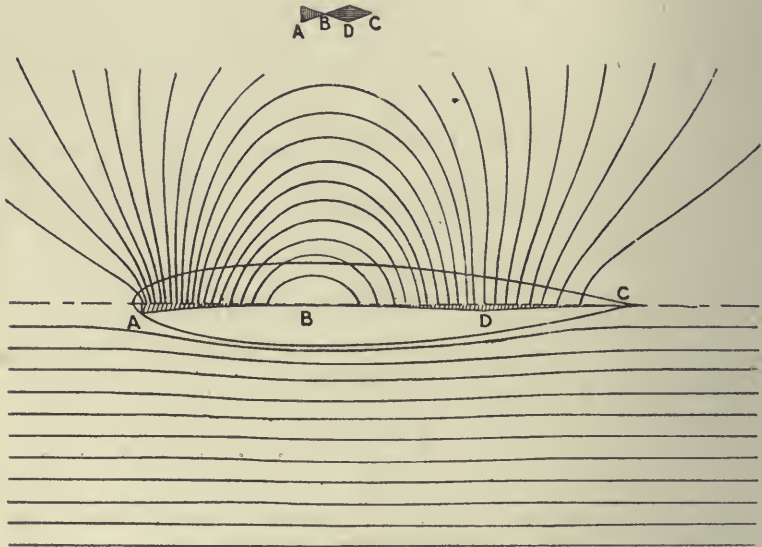lated by methods similar to those leading to Fig. 180, but needing the

Fig. 183.—Calculated flow of inviscid fluid round an airship envelope.

application of the integral calculus for their simplest expression. The
type of source chosen for the model in question is illustrated by the sketch
above Fig. 183. The sink begins at C, gets stronger gradually to D and
then weaker to B; at this latter point the source begins and grows in
strength to A, when it ceases abruptly.

The complex source and sink so defined are reproduced in Fig. 183, the
upper half of which shows the stream lines due to the system. The resem-
blance to circular arcs is slight. Superposing on these streams the
appropriate translational velocity Fuhrmann found the balloon-shaped
body indicated, together with the stream lines past it. These stream lines
are shown in the lower half of Fig. 183. The model has a rounded head
a little distance in front of the source head A and a pointed tail, the tip
of which coincides with the tip C of the sink.

Having obtained a body of a desired character, Fuhrmann proceeded

to calculate the pressures round the model in the way indicated in relation to Fig. 180 (c), using the formula $p + \frac{1}{2}\rho v^2 =$ const. ; the results are shown plotted in Fig. 184, and are there indicated by the dotted curve. The pressure is highest at the extreme nose and tail, and has the value $\frac{1}{2}\rho v^2$, where v is the free velocity of the fluid stream far from the model. Near the nose the pressure falls off very rapidly and becomes negative long before the maximum section is reached, and does not again become positive until within a third of the length of the model from the tail. The calculated resistance of the balloon model is zero.

For comparison with the calculations, experiments were made. Models were constructed by depositing copper electrolytically on a plaster of Paris mould, the shape being accurately obtained by turning in a lathe to carefully prepared templates. The models were made in two or three sections, these being joined together after the removal of the plaster of Paris. As a result a light hollow model was obtained suitable for test in a wind tunnel. To measure the pressures, small holes were drilled through the copper, and the pressure at each hole measured by connecting the interior of the model to a sensitive manometer. Finally, the total force on the model was measured directly on an aerodynamic balance. For the elaborate precautions taken to ensure accuracy the original paper should be studied; some recent researches suggest a source

FIG. 184.—Comparison of calculated and observed pressure on a model of an airship envelope.

of error not then appreciated, but the error is of secondary importance, and the results may be accepted as substantially accurate.

The observed pressures are plotted in Fig. 184 in full lines, the black dots indicating observations. The first point to be noticed is that at the extreme nose the maximum pressure is $\frac{1}{2}\rho v^2$ as indicated by the calculation, and that good agreement with the calculation holds until the pressure becomes negative. From this point the observed negative pressures are appreciably greater than those calculated, whilst at the tail the positive pressure is not so great as one-tenth of that calculated. The total force due to pressure now has a distinct value, which Fuhrmann calls "form resistance." The method of pressure observation does not, of course, include the tangential drag of the air over the model. The total resistance, including tangential drag or "skin friction" and "form resistance," was found by direct measurement, and it was found that "skin friction" accounted for some 40 per cent. of the whole, and "form resistance" for the remainder.

The effect of friction in the real fluid is therefore twofold : in the first place the flow is so modified that the pressure distribution is altered, and in the second the force at any point has a component along the surface

of the model ; both are of considerable importance in the measured total resistance. From the analogy with flat boards towed with the surfaces in the direction of motion, so that the normal pressures cannot exert a retarding influence, the tangential drag is generally referred to as "skin friction." It will be seen that appreciable error, 50 per cent. or 60 per cent., would result if the pressure distribution were taken to be that of an inviscid fluid.

Six models in all were tested in the air-channel at Göttingen, and the results are summarised in the following table :—

TABLE 2.—The Form Resistance and Skin Friction of Airship Envelopes.

Number of model.	Fraction of resistance caused by the change of pressure distribution arising from the viscosity of the fluid (form resistance).	Fraction of resistance caused by the tangential forces arising from the viscosity of the fluid (skin friction).	Relative total resistances.
1	0·57	0·43	1
2	0·53	0·47	1·22
3	0·53	0·47	1·20
4	0·63	0·37	0·79
5	0·59	0·41	0·87
6	0·69	0·31	0·81

The general conclusion which might have been drawn is that for forms of revolution of airship shape the resistances are more dependent on form resistance than on skin friction. This conclusion should be accepted with reserve in the light of more recent experiments.

The experiments referred to above were all carried out at one speed. Measurements were made of the total resistance at many speeds, but there are no corresponding records of pressure measurements. A series of tests on a model of an airship envelope has been carried out at the N.P.L. at a number of speeds with the following results :—

TABLE 3.—Variation of Form Resistance and Skin Friction with Speed

Speed (ft.-s.)	.	.	20	30	40	50	60
Form resistance	.	.	1	0·90	0·61	0·59	0·56
Skin friction	.	.	1	0·89	0·89	0·84	0·84
Form resistance / Total resistance	.	.	0·23	0·23	0·17	0·17	0·16

From the last row of Table 3, it will be seen that the form resistances are far smaller fractions of the total at all speeds than those given in Table 2. Further examination of the original figures shows that the measurements of total resistance at the N.P.L. are very much the same in magnitude as those at Göttingen. No suggestion is here put forward to account for the difference, the experiments at various speeds having an interest apart from this. It will be noticed that both the

" form resistance " and the " skin friction " vary with speed, and in the particular illustration the variation of the pressure is the greater. This evidence is directly against an assumption sometimes made that the pressure on a body varies as the square of the speed whilst the skin friction increases as some power of the speed appreciably less than two. There is certainly no theoretical justification for such an assumption, as will be seen later, and many practical resu'ts could be produced to show that experimental evidence is against such assumption.

One other illustration of the variation of pressure distribution with speed, may be mentioned here. A six-inch sphere in a wind of 40 ft.-s. has a resistance dependent almost wholly on the pressure over its surface, but this resistance is extremely sensitive to changes of speed ; the curious result is obtained that for certain conditions a reduced resistance accompanies an increase of speed. A corresponding effect is produced by covering with sand the smooth surface formed by varnish on wood. At about the speed mentioned the resistance may be decreased to less than half by such roughening. The general aspects of the subject are dealt with under the heading of Dynamical Similarity. For the present it is only desired to draw attention to the fact that the law of resistance proportional to square of speed is not accurately true for either the pressure distribution on a body in a fluid or for the skin friction on it. The departures are not usually so great that the v^2 law is seriously at fault if care is taken in application. A fuller explanation of this statement will appear shortly, when the conditions under which the v^2 law may be taken to apply with sufficient accuracy for general purposes will be discussed.

Cyclic Motion in an Inviscid Fluid.—In the fluid motions already discussed, the flow has been obtained from a combination of a motion of translation and the efflux and influx from a source and sink system. The initial assumptions involve as consequences—

(a) Finite slipping of the fluid over the boundary walls ;

(b) No resultant force on the body in any direction ;

(c) A liability to produce negative fluid pressures.

No theory has yet been proposed, and from the nature of an inviscid fluid it would appear that no theory could exist which avoids the finite slipping over the boundary. It appears to be fundamentally impossible to represent the motion of a real fluid accurately by any theory relating to an inviscid fluid. It is not, however, immediately obvious that such theories cannot give a good approximation to the truth, and as claims in this direction have often been made, further study is necessary before any opinion can be formed as to the merits of any particular solution.

The difficulties (b) and (c) can be avoided by introducing special assumptions ; two standard methods are developed, one involving " cyclic " motion and the other " discontinuous " motion.

Leaving the second of these for the moment, attention will be directed to the case of " cyclic " motion of an inviscid fluid. A simple cyclic motion can perhaps best be described in reference to a simple source. In the simple source the stream lines were radial and the velocity outwards varied inversely as the radius. In a simple cyclic motion the stream lines

are concentric circles, the velocity in each circle being inversely proportional to the radius.

From the connection between pressure and velocity it will be seen that the surfaces of uniform pressure in a cyclic motion and in motion due to a simple source are the same.

As in the case of sources and sinks, complex cyclic motions could be produced by adding together any number of simple cyclic motions. Cyclic and non-cyclic motions may also be added.

Consider the effect of superposing a cyclic motion on to the flow of an inviscid fluid round a body, say a cylinder placed across the stream ; before the cyclic motion is added the stream lines are those indicated in Fig. 166 ; add the cyclic motion as in Fig. 185.

The angles AOP, DOP, BOQ and COQ having been chosen equal, the symmetry of Fig. 166 shows that the velocities there will be equal for the upper and lower parts of the cylinder. These velocities are indicated by short lines on t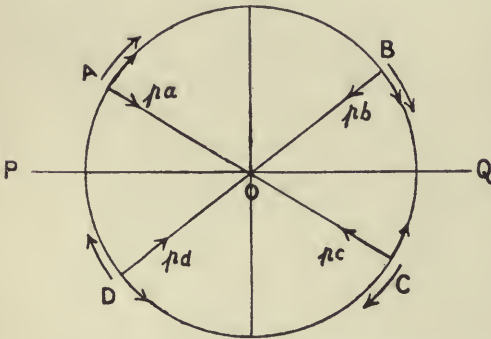he circle, the arrow-head indicating the direction of flow. Since the pressure in an inviscid fluid is perpendicular to the surface it can easily be seen that the pressures, all being equal and symmetrically disposed, have no resultant. Superpose a cyclic motion which has its centre at O, and which adds a velocity at the surface represented by the lines just outside the circle ABCD. On the upper half of the cylinder, the cyclic motion adds to the velocity and adds equally at A and B. Below, the velocity is reduced or possibly reversed, but the resultant has the same value at C and D. From the relation between pressure and velocity given in equation (2) the deduction is immediately made that p_a and p_b are less than p_d and p_c, and a simple application of the parallelogram of forces then shows that a resultant force acts on the cylinder upwards. The result is somewhat curious, and may be summarized as follows : if a cylinder is moved in a straight line through an inviscid fluid which has imposed upon it a cyclic motion concentric with the cylinder, there will be a force acting on the cylinder at right angles to the path, but no resistance to the motion.

Fig. 185.—Cyclic flow round cylinder.

If the body had been a wing form, it appears that the resultant force would not then have been at right angles to the line of motion, and there would have been a resistance component.

Kutta in Germany and Joukowsky in Russia have developed the mathematics of cyclic motion in relation to aerofoils to a great extent. Starting from a circular arc, Kutta calculates the lift and drag for various angles of incidence, and compares the results with those obtained in a wind tunnel. Before giving the figures it is desirable to outline the basis of

the calculation a little more closely. If by the source and sink method the flow round the circular arc ABC (Fig. 186) is investigated when the stream comes in the direction PQ, it is found that one stream line (shown dotted) coming from P strikes the model at D where the velocity is zero and there divides, one part bending back to A and then round the upper surface to F, whilst the other part takes the path DCF round the aerofoil. The point F where the two parts reunite is a second place of zero velocity, and from F to Q the speed increases, ultimately reaching the original value. The
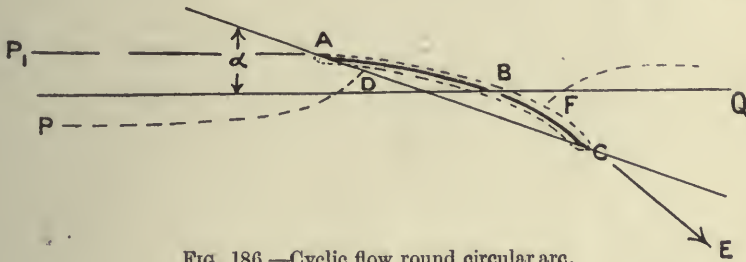

Fig. 186.—Cyclic flow round circular arc.

points D and F have been referred to previously as " stagnation points." The velocity of the fluid at A and C is found to be enormous, and so to require negative fluid pressure. This violates one of the conditions imposed by any real fluid.

By adding a cyclic motion it would appear to be possible to move the stagnation points D and F towards A and C, and if this could be done completely the fluid would come from P_1, strike the arc tangentially at A, and there divide finally leaving the arc tangentially at C. All very great velocities would then be avoided.

Kutta showed that it is always possible to find a cyclic motion which will make F coincide with C, no matter what the inclination of the chord
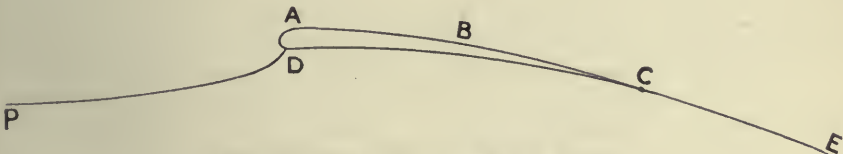
Fig. 187.—Cyclic flow round wing section.

of the arc might be. He did not, however, succeed in making D coincide with A as well as F with C except when α was equal to zero. In that particular case the aerofoil, according to calculation, gave lift without drag just as we have seen was the case for a cylinder. To meet the difficulty as to enormous velocity of fluid at A, Kutta introduced a rounded nosepiece ; Joukowsky by a particular piece of analysis showed how to obtain a section having a rounded nose and pointed tail which solved the mathematical difficulties and made it possible to find the cyclic flow round a body of the form shown in Fig. 187, such that the stream leaves C tangentially. There is then no difficulty in satisfying the requirements as to absence

of negative pressure at any angle of incidence whatever for a limited range of velocity.

TABLE 4.—Kutta's Table a Comparison of Calculated and Measured Forces.

Inclination of chord α.	Measured lift per unit area. Lilienthal (kg/m²).	Calculated lift per unit area. Kutta (kg/m²).	Drag per unit area. Lilienthal (kg/m²).	Excess of drag per unit area over that at 0°. Lilienthal (kg/m²).	Calculated drag per unit area. Kutta (kg/m²).
− 9°	0·20	0·72	0·90	0·60	0·78
− 6°	1·74	2·45	0·54	0·24	0·36
− 3°	3·25	4·30	0·36	0·06	0·09
0	4·96	6·23	0·30	0·00	0·00
+ 3°	7·27	8·21	0·37	0·07	0·10
+ 6°	9·08	10·20	0·70	0·40	0·39
+ 9°	10·43	12·16	1·12	0·82	0·88
+12°	11·08	14·06	1·51	1·21	1·56
+15°	11·52	15·86	1·95	1·65	2·44

The table of figures by Kutta is given above. The experiments referred to were probably not very accurate, and the disagreement of the calculated and observed values of lift and drag is not so great as to discredit the theory. It may be noticed that the calculated drag has been compared with the excess of the observed drag above its minimum value, and so throws no light on the economical form of a wing. The theory cannot in its existing form indicate even the possibility of the well-known critical angle of an aeroplane wing. It is not possible to justify the assumptions made, and the result is a somewhat complex and not very accurate empirical formula.

Discontinuous Fluid Motion.—The simplest illustration of the meaning of discontinuous motion is that presented by a jet issuing into air from an orifice in the side of a tank of water. If the orifice is round and has a sharp edge the water forms a smooth glass-like surface for some distance after issuing. After a little time the column breaks into drops, and Lord Rayleigh has shown that this is due to surface tension; further, if the jet issues horizontally the centre line is curved due to the action of gravity, whilst if vertical an increase of velocity takes place which reduces the section of the column.

Neglecting the effects of gravity and surface tension, a horizontal jet would continue through the air with a free surface along which the pressure was constant and equal to that of the atmosphere. The method of discontinuous motion is essentially identified with the mathematical analysis relating to constant pressure, free surfaces. The examples actually worked out apply to an inviscid fluid and almost exclusively to two-dimensional flow. Lamb states that the first example was due to Helmholtz, and it appears that the method of calculation was made regular and very general by Kirchhoff and Lord Rayleigh. The main results have been collected in Report No. 19 of the Advisory Committee for Aeronautics by Sir George Greenhill, and since that time extensions have been made to curved barriers.

It is not proposed to attempt any description of the special methods of solution, but to discuss some of the results. The first problem examined by Sir George Greenhill is the motion of the fluid in a jet before and after impinging on an inclined flat surface. The jet coming from I, Fig. 188, impinges on the plate AA′ and splits into two jets, the separate horns of which are continued to J and J′. One stream line IB comes up to the barrier at a stagnation point B, and then travels along the barrier A′A in the two directions towards J and J′. Finite slipping is here involved, and the analysis must therefore be looked on as an approximation to reality only. In the case of jets it appears to be justifiable to assume that the effect of viscosity on the fluid motion and pressures is very small compared with that arising from the usual resolutions of momentum, and so far as experimental evidence exists, it suggests that the motion of jets worked out in this way is a satisfactory indication of the motion of a real fluid such as water, when issuing into another much less dense fluid such as air.
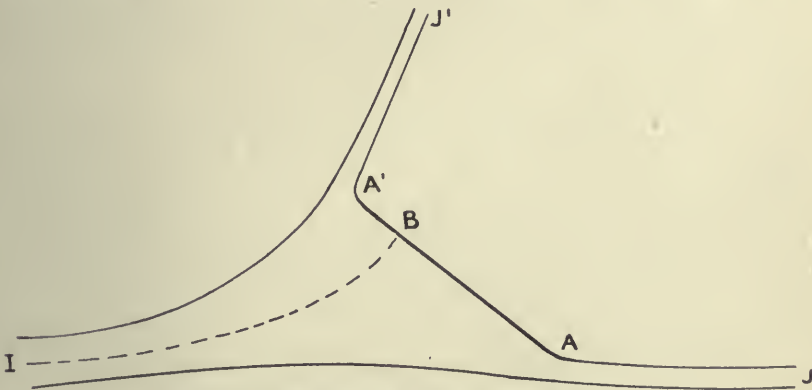

Fig. 188.—Discontinuous motion of a jet of fluid.

From I to J, from I to J′, and from A′ to J′, A to J the fluid is bounded by free surfaces along which the pressure is constant. From equation (2) this will be seen to imply the condition that the velocity is constant; further, if the free surface extends to great distances from the barrier, the velocity all along it must be that of the fluid at such great distances. Solutions of discontinuous motions almost always involve the assumption that the velocity along the free surfaces is that of the stream before disturbance by the barrier.

Fig. 168, already referred to, shows behind a cylinder a region of almost stagnant fluid the limits of which in the direction of the stream are very sharply defined, and it is clear that in real fluids, in addition to the periodicity, there is indication of the existence of a free surface. Direct experiments show that inside such a region the pressure is often very uniform, but appreciably below that of the fluid far from the model.

Assuming a free surface enclosing stagnant fluid extending far back from the model the whole details of the pressure, position of centre of pressure, and shape of stream lines for an inclined plate have been worked

out. In addition to finite slipping at the model, there is now also finite slipping over the boundary of the stagnant fluid and objections on the score of stability have been raised, notably by Lord Kelvin. The following summary of the position is given by Lamb :—

"As to the practical value of this theory opinions have differed. One obvious criticism is that the unlimited mass of ' dead-water ' following the disk implies an infinite kinetic energy ; but this only means that the type of motion in question could not be completely established in a finite time from rest, although it might (conceivably) be approximated to asymptotically. Another objection is that surfaces of discontinuity between fluids of comparable density are as a rule highly unstable. It has been urged, however, by Lord Rayleigh that this instability may not seriously affect the character of the motion for some distance from the place of origin of the surfaces in question.

"Lord Kelvin, on the other hand, maintains that the types of motion here contemplated, with surfaces of discontinuity, have no resemblance to anything which occurs in actual fluids ; and that the only legitimate application of the methods of von Helmholtz and Kirchhoff is to the case of free surfaces, as of a jet."

With the advance of experimental hydrodynamics, and since the advent of aviation particularly, the position taken by Lord Kelvin has received considerable experimental support ; one instance of the difference between the pressure of air on a flat plate and the pressure as calculated is given below. It is clearly impossible to make an experiment on a flat surface of no thickness, and for that reason the experimental results are not strictly comparable with the calculations : in addition, the conditions were not such as to fully justify the assumption of two-dimensional flow. Nevertheless the discrepancies of importance between experiment and calculation are not to be explained by errors on the experimental side, but to the initial assumptions made as the basis of the calculations.

The experiments were carried out in an air channel at the National Physical Laboratory, and are described in one of the Reports of the Advisory Committee for Aeronautics. The abscissae, representing points at which pressures were observed, are measured from the leading edge of the plane as fractions of its width. The scale of pressures is such that the excess pressure at B over that at infinity would just produce the velocity v in the absence of friction. It appears to be very closely true, whether the fluid be viscous or inviscid, that the drop of pressure in the stream line which comes to a stagnation point is $\frac{1}{2}\rho v^2$. There are other reasons, which will appear in the discussion of similar motions, for choosing ρv^2 as a basis for a pressure scale.

In the experiment the pressure of $+\frac{1}{2}\rho v^2$ is found on the underside of the inclined plane, very near to the leading edge ; this is shown at B in Fig. 189. Travelling on the lower surface towards the trailing edge, the pressure at first falls rapidly and then more slowly until it changes sign just before reaching the trailing edge. The whole of the upper surface is under reduced pressure, the variation from the trailing edge to the leading edge being indicated by the curve EFGHKA.
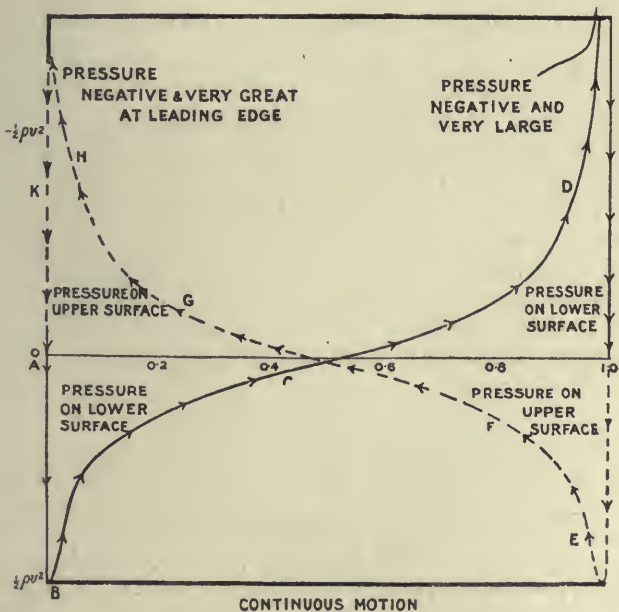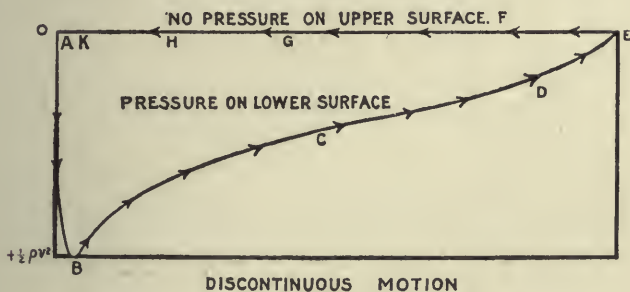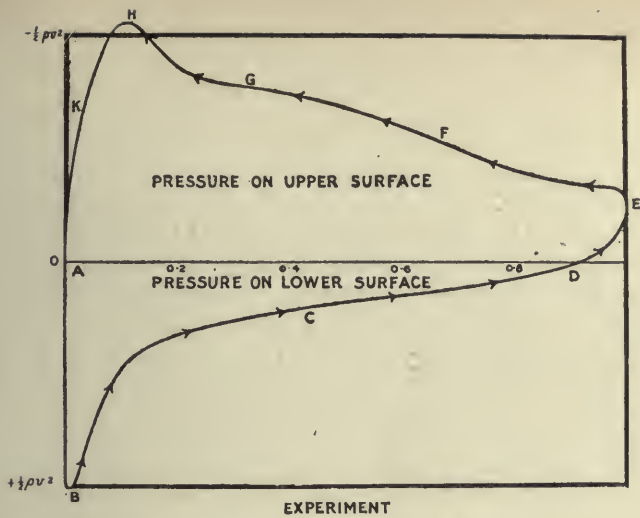
FIG. 189.—Observation and calculation of the pressure distribution on a flat plate inclined at 10° to the current.

The area inside the curve ABC . . . HKA gives a measure of the force on the plate due to fluid pressures. At an inclination of 10° it appears that more than two-thirds of the force due to pressure is negative and is due to the upper surface. The same holds for aeroplane wing sections to perhaps a greater degree, the negative pressure at H sometimes exceeding three times that shown in Fig. 189.

Fig. 189 shows for the same position of a plane the pressures calculated as due to the discontinuous motion of a fluid. On the under surface the value of $\frac{1}{2}\rho v^2$ at B is reached very much in the same place as the experimental value. Travelling backwards on the under surface the pressures fall to zero at the trailing edge, but are appreciably greater than those of the experimental results. On the upper surface there is no negative pressure at any point. The total force is again proportional to the area inside the curve ABC . . . HKA, and is clearly much less than the area of the corresponding curve for the experimental determination. The degree of approximation is obviously very unsatisfactory in several respects, the only agreement being at the $\frac{1}{2}\rho v^2$ point.

For the sake of comparison, the pressure distribution corresponding with the source and sink hypothesis is illustrated in Fig. 189. As before, starting at the leading edge A and travelling on the under side, the $\frac{1}{2}\rho v^2$ point at B occurs in much the same place as before, but from this point the pressure falls rapidly and becomes negative just behind the centre of the plane; proceeding further, the pressure continues to fall more and more rapidly until it becomes infinitely great at the trailing edge. Exactly the same variations of pressure are observed on returning from the trailing edge to the leading edge *via* the upper surface as have been described in passing in the reverse direction on the lower surface.

The total area is now zero, the convention in the graphical construction being that when travelling round the curve ABCD . . . EFGHKA areas to the left hand shall be counted positive and areas to the right hand negative. It is clear, however, that the moment on the aerofoil is not zero, and the centre of pressure is therefore an infinite distance away; the couple tends to increase the angle of incidence, and further analysis shows that the couple does not vanish until the plate is broadside on to the stream.

It will be noticed that the edges of the plate are positions of intense negative pressure, such as we have seen no real fluid is able to withstand.

This brief summary covers in essentials all the conventional mathematical theories of the motion of inviscid incompressible fluids, and will, it is hoped, have shown how far the theories fall short of being satisfactory substitutes for experiment in most of the problems relating to aeronautics.

MOTIONS IN VISCOUS FLUIDS

Definition of Viscosity.—OO_1, Fig. 190, is a flat surface over which a very viscous fluid, such as glycerine, is flowing as the result of pressure applied across the fluid at AB . . . F. By direct observation the velocity is known to be zero all along OO_1, and to gradually increase as the distance from the flat surface increases. If the velocity is proportional

to y the definition of viscosity states that the force on the surface OO_1 is given by the equation

$$F = \text{Area} \times \mu \times \frac{v}{y} \quad . \quad . \quad . \quad . \quad . \quad . \quad (7)$$

In this equation v is the velocity of the fluid at a distance y from the surface, and " Area " represents the extent of the surface of OO_1 on which the force is measured ; μ is the coefficient of viscosity.

If the fluid velocity is not proportional to y but has a form such as that shown by the dotted line of Fig. 190, the force on the surface is Area $\times \mu \times \left(\dfrac{\partial v}{\partial y}\right)_{\text{surface}}$. In exactly the same way the force acting on a fluid surface such as DD_1 is Area $\times \mu \times \left(\dfrac{\partial v}{\partial y}\right)_{DD_1}$. The definition is equivalent to the statement that the forces due to viscosity are pro-
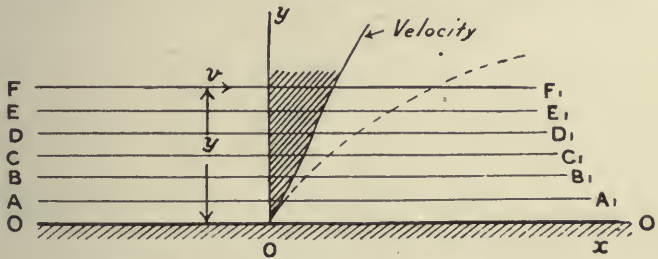
Fig. 190.—Laminar motion of a viscous fluid.

portional to the rate at which neighbouring parts of the fluid are moving past each other.

Experimental Determination of μ.—If the motion of a viscous fluid as defined above be examined in the case of a circular pipe, pressure being applied at the two ends, it is found that under certain circumstances the motion can be calculated in detail from theoretical considerations. Moreover, the predictions of theory are accurately borne out by direct experiment. Only the result of the mathematical calculation will be given, as it is desired to draw attention to the results rather than to the method of calculation.

The quantity of fluid flowing per second through a pipe of length l is found theoretically to be

$$\text{vol. per sec.} = \frac{\pi d^4}{128\mu} \cdot \frac{p_1 - p_2}{l} \quad . \quad . \quad . \quad . \quad (8)$$

where d is the diameter and p_1 and p_2 the pressures at the ends of the length l. The calculation assumes that μ is constant and that the motion satisfies the condition of no slipping at the sides of the tube.

When the corresponding experiment is carried out in capillary tubes of different diameters and different lengths, it is found that the law of variation given by (8) is satisfied very accurately. Lamb states that Poiseuille's experiments showed that " the time of efflux of a given volume of water is

2 B.

directly as the length of the tube, inversely as the difference of pressure at the two ends, and inversely as the fourth power of the diameter. Formula (8) then gives a practical means of determining μ which is in fact that almost always adopted in determining standard values for any fluid.

As indicated by (8) it is easily seen that the skin friction on the pipe is equal to $(p_1 - p_2) \cdot \dfrac{\pi d^2}{4}$, or the product of the pressure drop and the area of the cross-section. Also the average velocity is $\dfrac{\text{vol. per sec.}}{\pi d^2/4}$. If F is the total force and v the velocity, we then have

$$\left. \begin{aligned} \mathrm{F} &= (p_1 - p_2)\frac{\pi d^2}{4} \\[2mm] \text{vol. per sec.} &= v\,\frac{\pi d^2}{4} \end{aligned} \right\} \quad . \quad . \quad . \quad . \quad . \quad (11)$$

Substituting for $p_1 - p_2$ and vol. per sec. in (8) the values given by (11), we have

$$v\,\frac{\pi d^2}{4} = \frac{d^2}{32}\cdot\frac{\mathrm{F}}{\mu l}$$

or

$$\mathrm{F} = \frac{1}{8\pi}\mu \cdot v \cdot l \quad . \quad . \quad . \quad . \quad . \quad (12)$$

trom which it appears that the force is proportional to the coefficient of viscosity μ, the velocity v, and to the length of the tube l. The variation of force as the first power of v appears to be characteristic of the motion of very viscous fluids.

If the experiment is attempted in a large tube at high speeds the resistance is found to vary approximately as the square of the speed, and it is then clear that equation (8) does not hold. The explanation of the difference of high-speed and low-speed motions was first given by Professor Osborne Reynolds, who illustrated his results by experiments in glass tubes. Water from a tank was allowed to flow slowly through the tube, into which was also admitted a streak of colour ; so long as the speed was kept below a certain value, the colour band was clear and distinct in the centre of the tube. As the speed was raised gradually, there came a time at which, more or less suddenly, the colour broke up into a confused mass and became mixed with the general body of the water. This indicated the production of eddies, and Professor Osborne Reynolds had shown why the law of motion as calculated had failed.

Carrying the experiment further, it was shown that the law of breakdown could be formulated, that is, having observed the breakdown in one case, breakdown could be predicted for other tubes and for other fluids, or for the same fluid at different temperatures. Denoting the mass of unit volume of the fluid by ρ, Osborne Reynolds found that breakdown of the steady flow always occurred when

$$\frac{\rho v d}{\mu} \quad . \quad . \quad . \quad . \quad . \quad . \quad . \quad (13)$$

reached a certain fixed value. This result indicates some very remarkable conclusions. It has been shown that μ is usually determined by an experiment in a capillary tube where d is very small. (13) indicates that if v be very small the result might be true for a large pipe, or that if μ is very large both v and d might be moderately large and yet the motion would be steady. As an illustration of the truth of these deductions, it is interesting to find that the flow in a four-inch pipe of heavy oils suitable for fuel is steady at velocities used in transmission from the store to the place of use.

The expressions ρ and μ both express properties of the fluid, and it is only the ratio with which we are concerned in (13) ; as the quantity occurs repeatedly a separate symbol is convenient, and it is usual to write ν for $\dfrac{\mu}{\rho}$. The quantity $\dfrac{vl}{\nu}$, which now expresses (13), is of considerable importance in aeronautics. Before proceeding to the discussion of similar motions to which this quantity relates, the reference to calculable viscous motions will be completed.

The motions shown experimentally by Professor Hele-Shaw comprise perhaps the greatest number of cases of calculable motions and these have already been dealt with at some length. The experiments of Professor Osborne Reynolds indicate that the flow will become unstable as the viscosity is reduced, and it seems to be natural to assume that the inviscid fluid motion having the same stream lines would be unstable. If this should be the case, then the function of viscosity in such mobile fluids as water is obvious.

Very few other calculable motions are known ; the case of small spheres falling slowly is known, the first analysis being due to Stokes, and is applicable to minute rain-drops as they probably exist in clouds. Another motion is that of the water in a rotating vessel, the free surface of which is parabolic, and which can only be generated through the agency of viscosity.

Although the number of cases of value which can be deduced from theory are so few, there are some far-reaching consequences relating to viscosity which must be dealt with somewhat fully. Up to the present it has only been shown that for steady motion μ is sufficient to define the viscous properties of a fluid. It will be shown in the next chapter that μ is still sufficient in the case of eddying motion, and that results of apparent complexity can often be shown in simple form by a judicious use of the function $\dfrac{vl}{\nu}$.

CHAPTER VIII

DYNAMICAL SIMILARITY AND SCALE EFFECTS

Geometrical Similarity.—The idea of similarity as applied to solid objects is familiar. The actual size of a body is determined by its scale, but if by such a reduction as occurs in taking a photograph it is possible to make two bodies appear alike the originals are said to be similar. If one of the bodies is an aircraft or a steamship and the other a small-scale reproduction of it, the smaller body is described as a model.

Dynamical Similarity extends the above simple idea to cover the motion of similarly shaped bodies. Not only does the theory cover similar motions of aeroplanes and other aircraft, but also the similar motions of fluids. It may appear to be useless to attempt to define similarity of fluid motions in those cases where the motion is incalculable, but this is not the case. It is, in fact, possible to predict similarity of motion, to lay down the laws with considerable precision and to verify them by direct observation. The present chapter deals with the theory, its application and some of the more striking and important experimental verifications.

A convenient arbitrary example, the motion of the links of Peaucellier cells, leads to a ready appreciation of the fundamental ideas relating to similar motions. A Peaucellier cell consists of the system of links illustrated in Fig. 191. The four links CD, DP, PE and EC are equal and freely jointed to each other. AD and AE are equal and are hinged to CDEP at D and E and to a fixed base at A. The link BC is hinged to CDEP at C and to the same fixed base at B. The only possible motion of P is perpendicular to ABF. The important point for present purposes is that for any given position of P the positions of D, C and E are fixed by the links of the mechanism.

Consider now the motion of a second cell which is L times greater than that of Fig. 191, and denote the new points of the link work by the same letters with dashes. The length AN will become A'N'=L×AN. Put P' in such a position that P'N'=L×PN, and the shape of the link work will be similar to that of Fig. 191. A limited class of similar motions may now be defined for the cells, as being such that at all times the two cells have similar shapes.

An extension of the idea of similar motions is obtained by considering the similar positions to occur at different times. Imagine two cinema cameras to be employed to photograph the motions of the cells, the images being reduced so as to give the same size of picture. Make one motion twice as fast as the other and move the corresponding cinema camera twice as fast. The pictures taken will be exactly the same for both cells, and the motions will again be called similar motions. We are thus led to

consider a scale of time, T, as well as a scale of length, L. All similar motions are reducible to a standard motion by changes of the scales of length and time.

If the links be given mass it will be necessary to apply force at the point P in order to maintain motion of any predetermined character, and this force, depending as it does on the mass of each link, may be different for similar motions. The study of the forces producing motion is known as " dynamics," and " dynamical similarity " is the discussion of the conditions under which the external forces acting can produce similar motions.

Still retaining the cell as example, an external force can be produced by a spring stretched between the points P and F. The force in this spring depends on the position of P, and therefore on the motion of the cell. It may be imagined that a spring can be produced having any law of force
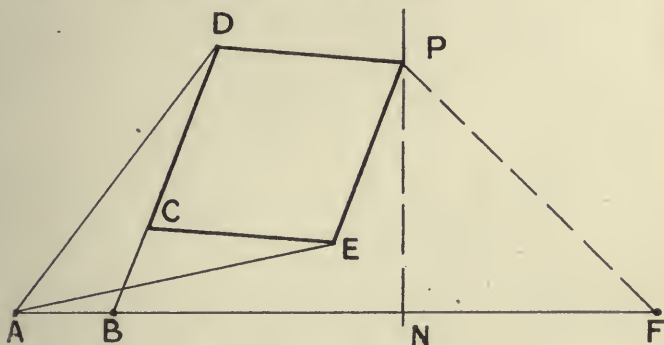
FIG. 191.—Peaucellier cell.

as a function of extension, and if two suitable springs were used in the similar cells it would then follow that similar free motions could be produced, no matter what the distribution of mass in the two cases.

Particular Class of Similar Motions

At this point the general theorem, which is intractable, is left for an important particular class of motions exemplified as below. In the cell of Fig. 191 the distribution of mass may still be supposed to be quite arbitrary, but in the similar mechanism a restriction is made which requires that at each of the similar points the mass shall be M times as great as that for the cell of Fig. 191.

For similar motions of cell any particular element of the second cell moves in the same direction as the corresponding element of the first. It moves L times as far in a time T times as great. Its velocity is therefore $\frac{L}{T}$ times as great, and its acceleration $\frac{L}{T^2}$ times as great. Since the force producing motion is equal to the product " mass × acceleration," the ratio of the forces on the corresponding elements is $\frac{ML}{T^2}$. This ratio, for the

limited assumption as to distribution of mass, is constant for all elements and must also apply to the whole mechanism. The force applied at P′ will therefore be $\dfrac{ML}{T^2}$ times that at P if the resulting motions are similar.

The constraints in a fluid are different from those due to the links of the Peaucellier cell, but they nevertheless arise from the state of motion. The motion of each element must be considered instead of the motion of any one point, and the force on it due to pressure, viscosity, gravity, etc., must be estimated. If the fluid be incompressible, the mass of corresponding elements will be proportional to the density and volume. Consider as an example the motion of similar cylinders through water, an account of which was given in a previous chapter.
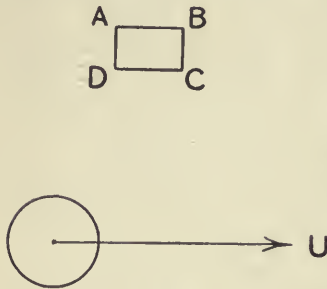

Fig. 192.

The cylinders being very long, it may be assumed that the flow in all sections is the same, and the equations of motion for the block ABCD, Fig. 192, confined to two dimensions. The fluid being incompressible and without a free surface, gravity will have no influence on the motion, and the forces on ABCD will be due to effects on the faces of the block. These may be divided into normal and tangential pressures due to the action of inertia and shear of the viscous fluid.

From any text-book on Hydrodynamics it will be found that the appropriate equations of motion of the block are

$$
\left.
\begin{aligned}
\rho\frac{Du}{Dt} &= -\frac{\partial p}{\partial x} + \mu\left(\frac{\partial^2 u}{\partial x^2} + \frac{\partial^2 u}{\partial y^2}\right) \\[2mm]
\rho\frac{Dv}{Dt} &= -\frac{\partial p}{\partial y} + \mu\left(\frac{\partial^2 v}{\partial x^2} + \frac{\partial^2 v}{\partial y^2}\right) \\[2mm]
\frac{\partial u}{\partial x} &+ \frac{\partial v}{\partial y} = 0
\end{aligned}
\right\} \quad . \quad . \quad . \quad . \quad (1)
$$

and

It is the solution of these equations for the correct conditions on the boundary of the cylinder which would give the details of the eddies shown in a previous chapter. With such a solution the present discussion is not concerned, and it is only the general bearing of equations (1) which is of interest. Equations (1) are three relations from which to find the quantities u, v and p at all points defined by x and y. If by any special hypothesis u and v be known, then p is determined by either the first or the second equation of (1). Consideration of the first equation is all that is required in discussing similar motions.

Define a second motion by dashes to obtain

$$
\rho'\frac{Du'}{Dt'} = -\frac{\partial p'}{\partial x'} + \mu'\left(\frac{\partial^2 u'}{(\partial x')^2} + \frac{\partial^2 u'}{(\partial y')^2}\right) \quad . \quad . \quad . \quad (2)
$$

As applied to a similar and similarly situated block there will be certain

relations between some of the quantities in (2) and some of those in (1). The elementary length $\partial x'$ will be equal to $L\partial x$, where L is the ratio of the diameters of the two cylinders. Similarly $\partial y' = L\partial y$. The element of time Dt' will be equal to $T \cdot Dt$, and $u' = \dfrac{L}{T}u$. Make the suggested substitutions in (2) to get

$$\rho' \frac{L}{T^2} \cdot \frac{Du}{Dt} = -\frac{1}{L} \cdot \frac{\partial p'}{\partial x} + \frac{\mu'}{LT}\left(\frac{\partial^2 u}{\partial x^2} + \frac{\partial^2 u}{\partial y^2}\right). \quad \text{. . . . (3)}$$

and now compare equation (3) item by item with the first equation of (1). The terms on the left-hand sides differ by a constant factor $\dfrac{\rho'}{\rho} \cdot \dfrac{L}{T^2}$, whilst the second terms on the right-hand sides differ by a second constant factor $\dfrac{\mu'}{\mu} \cdot \dfrac{1}{LT}$. In general, if L and T are chosen arbitrarily it is not probable that the equation

$$\frac{\rho'}{\rho} \cdot \frac{L}{T^2} = \frac{\mu'}{\mu} \cdot \frac{1}{LT} \quad \text{. . . . . . . (4)}$$

will be satisfied.

Law of Corresponding Speeds.—Since L is a common scale of length applying to all parts of the fluid, it must also apply to those parts in contact with the cylinder, and L is therefore at choice by selecting a cylinder of appropriate diameter. Similarly T is at choice by changing the velocity with which the cylinder is moved. For any pair of fluids equation (4) can always be satisfied by a correct relation between L and U, that is, by a law of corresponding speeds.

To find the law, rearrange (4) as

$$\frac{\rho'}{\mu'} \cdot \frac{L^2}{T} = \frac{\rho}{\mu} \quad \text{. . . . . . . (5)}$$

and multiply both sides by DU, the product of the diameter of the standard cylinder and its velocity. Equation (5) becomes

$$\frac{\rho'}{\mu'} \cdot D'U' = \frac{\rho}{\mu}DU . \quad \text{. . . . . . (6)}$$

Since $\dfrac{\mu}{\rho} = \nu$, the kinematic viscosity of the fluid, equation (6) shows that the multipliers of the terms in equations (1) and (3) not involving p become the same if $\dfrac{D'U'}{\nu'}$ is equal to $\dfrac{DU}{\nu}$.

With the above relation for $\dfrac{DU}{\nu}$, equations (1) and (3) give the connection between the pressures at similar points. They can be combined to give

$$\frac{1}{L}dp' = \frac{\rho'}{\rho} \cdot \frac{L}{T^2}dp \quad \text{. . . . . . . (7)}$$

or

$$\frac{dp'}{dp} = \frac{\rho'}{\rho} \cdot \frac{L^2}{T^2} = \frac{\rho'(U')^2}{\rho U^2} \quad \text{. . . . . . (8)}$$

and between corresponding points in similar motions the increments of pressure dp vary as ρU^2.

This case has been developed at some length, although, as will be shown, the law of corresponding speeds can be found very rapidly without specific reference to the equations of motion. It has been shown on a fundamental basis why a law of corresponding speeds is required in the case of cylinders in a viscous fluid, and that the pressures then calculated as acting in similar motions obey a certain definite law of connection. The result may be expressed in words as follows : " Two motions of viscous
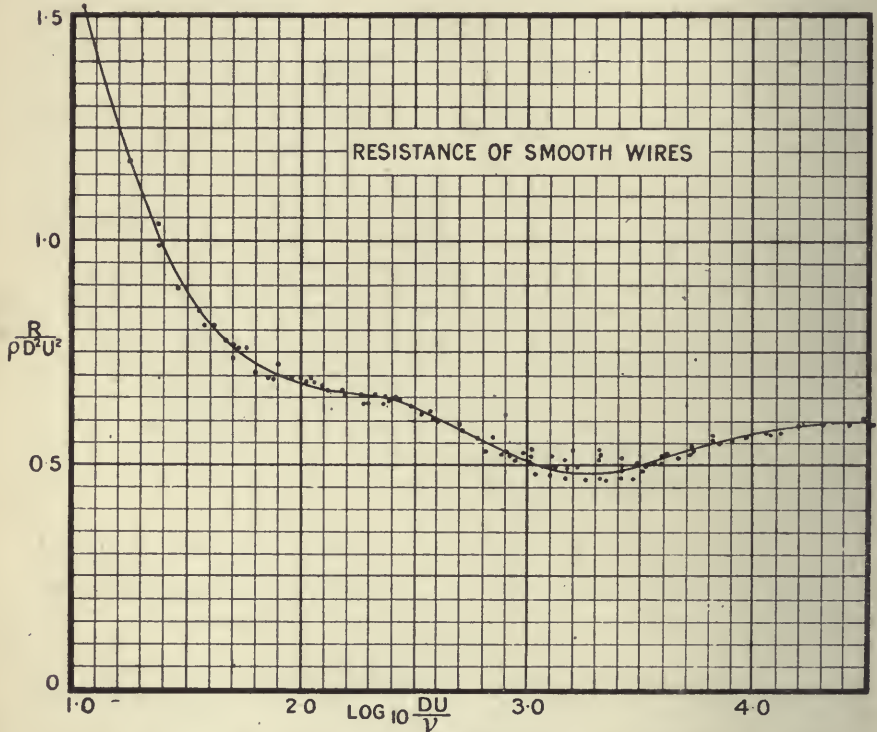
Fig. 193.—Application of the laws of similarity to the resistance of cylinders.

fluids will be similar if the size of the obstacle and its velocity are so related to the viscosity that $\dfrac{UD}{\nu}$ is constant. The pressures at all similar points of the two fluids will then vary as ρU^2."

Since the pressures vary as ρU^2 at all points of the fluid, including those on the cylinder, the total resistance will vary as $\rho U^2 D^2$, and it follows that $\dfrac{R}{\rho U^2 D^2}$ varies only when $\dfrac{UD}{\nu}$ varies.

The law is now stated in a form in which it can very readily be submitted to experimental check. Smooth wires provide a range of cylinders

of different diameters, and they can be tested in a wind channel over a considerable range of speed. Two out of the three quantities in $\dfrac{UD}{\nu}$ are then independently variable, and the resistance of a wire 0·1 in. in diameter tested at a speed of 50 ft.-s. can be compared with that of a wire 0·5 in. in diameter at 10 ft.-s.

The experiment has been made, the diameter of the cylinders varying from 0·002 in. to 1·25 ins., and the wind speeds from 10 to 50 ft.-s. The number of observations was roughly 100, and the result is shown in Fig. 193. Instead of $\dfrac{UD}{\nu}$ as a variable, the value of $\log \dfrac{UD}{\nu}$ has been used, as the resulting curve is then more easily read. The result of plotting $\dfrac{R}{\rho U^2 D^2}$ as ordinate with $\log \dfrac{UD}{\nu}$ as abscissa is to give a narrow band of points which includes all observations * for wires of thirteen different diameters.

The rather surprising result of the consideration of similar motions is that it is possible to say that the resistance of one body is calculable from that of a similar body if due precautions are taken in experiment, although neither resistance is calculable from first principles. The importance of the principle as applied to aircraft and their models will be appreciated.

Further Illustrations of the Law of Corresponding Speeds for Incompressible Viscous Fluids

A parallel set of experiments to those on cylinders is given in the *Philosophical Transactions of the Royal Society,* in a paper by Stanton and Pannell. These experiments constitute perhaps the most convincing evidence yet available of the sufficiency of the assumption that in many applications of the principles of dynamical similarity to fluid motion, even when turbulent, ν and ρ are the only physical constants of importance.

The pipes were made of smooth drawn brass, and varied from 0·12 in. to 4 inches. Both water and air were used as fluids, and the speed range was exceptionally great, covering from 1 ft.-s. to 200 ft.-s. at ordinary atmospheric temperature and pressure. The value of ν for air is approximately 12 times that for water.

The curve connecting friction on the walls of the pipes with $\dfrac{DU}{\nu}$ or $\dfrac{vl}{\nu}$ was plotted as for Fig. 193, with a result of a very similar character as to the spreading of the points about a mean line. The experiments covered not only the frictional resistance but also the distribution of velocity across the pipe, and showed that the flow at all points is a function of $\dfrac{vl}{\nu}$. The original paper should be consulted by those especially interested in the theory of similar motions.

In the course of experimental work a striking optical illustration of similarity of fluid motion has been found. Working with water, E. G. Eden

* Further particulars are given in R. & M. No. 102, Advisory Committee for Aeronautics.

observed that the flow round a small inclined plate changed its type as the speed of flow increased.

In one case the motion illustrated in Fig. 194 was produced ; the coloured fluid formed a continuous spiral sheath, and the motion was apparently steady. In the other case the motion led to the production of Fig. 195, and the flow was periodic. The flow, Fig. 194, is from left to right, the plate being at the extreme left of the picture. The stream was rendered visible by using a solution of Nestlé's milk in water, and the white streak shows the way in which this colouring material entered the region under observation. At the plate the colouring matter spread and left the corners in two continuous sheets winding inwards. The form of these sheaths can be realised from the photograph.

For Fig. 195 the flow is in the same direction as before, and the plate more readily visible. Instead of the fluid leaving in a corkscrew sheath, the motion became periodic, and loops were formed at intervals and succeeded each other down-stream. The observation of this change of type of flow seemed to form a convenient means of testing the suitability of the law of similarity thought to be proper to the experiment. To test for this a small air channel was made, and in it the flow of air was made visible by tobacco smoke, carefully cooled before use. The effects of the heat from the electric arc necessary to produce enough light for photography was found to be greater than for water, and equal steadiness of flow was difficult to maintain.

In spite of these difficulties it was immediately found that the same types of flow could be produced in air as have been depicted in Figs. 194 and 195. Variations of the size of plate were tried and involved changes of speed to produce the same types of flow. Two photographs for air are shown in Figs. 196 and 197, and should be compared with Figs. 194 and 195 for water. The flow is in the same direction as before, and the smoke jet and plate are easily seen. The sheath of Fig. 196 is not so perfectly defined as in water, but its character is unmistakably the same as that of Fig. 194. Fig. 197 follows the high-speed type of motion found in water and photographed in Fig. 195.

To make the check on similarity still more complete, measurements were taken of the air and water velocities at which the flow changed its type for all the sizes of plate tested. Taking three plates, $\frac{1}{4}$ in., $\frac{1}{2}$ in. and $\frac{3}{4}$ in. square, all in water, it was found that the speeds at which the flow changed were roughly in the ratios $3 : 2 : 1$ respectively. Using a plate $1\frac{1}{2}$ ins. square in the air channel, the speed of the air when the flow changed type was found to be 6 or 7 times that of water with a $\frac{3}{4}$–in. plate.

This is in accordance with the law of similarity which states that $\dfrac{vl}{\nu}$ should be constant ; if for instance the fluid is not changed, ν remains constant and v should vary inversely as l. If both l and ν are changed by doubling the scale of the model and increasing ν 12 or 14 times, clearly v must be 6 or 7 times as great. The experiments were not so exactly carried out that great accuracy could be obtained, but it is clear that great accuracy was not needed to establish the general law of similarity.

Fig. 194.—Flow of water past an inclined plate.   Low speed.

Fig. 195.—Flow of water past an inclined plate.   High speed.

Fig. 196.—Flow of air past an inclined plate.   Low speed.
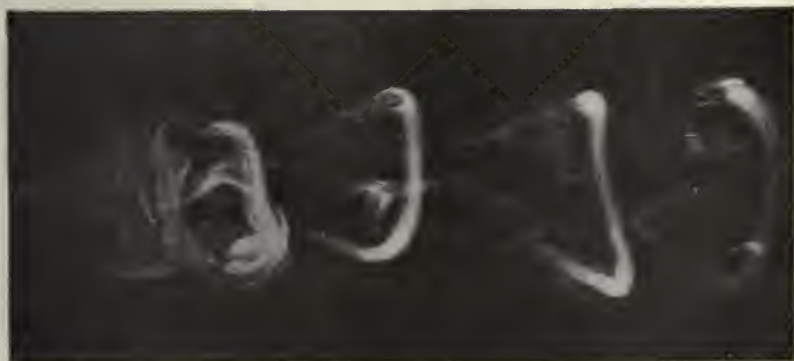
Fig. 197.—Flow of air past an inclined plate.   High speed.

The Principle of Dimensions as applied to Similar Motions.—All dynamical equations are made up of terms depending on mass M, length L and time T, and are such that all terms separated by the sign of addition or of subtraction have the same "dimensions" in M, L and T.

As examples of some familiar terms of importance in aeronautics reference may be made to the table below.

TABLE 1.

Quantity.	Dimensions.
Angular velocity	$\dfrac{1}{T}$
Linear velocity	$\dfrac{L}{T}$
Angular acceleration . . .	$\dfrac{1}{T^2}$
Linear acceleration . . .	$\dfrac{L}{T^2}$
Force	$\dfrac{ML}{T^2}$
Pressure	$\dfrac{M}{LT^2}$
Density	$\dfrac{M}{L^3}$
Kinematic viscosity . . .	$\dfrac{L^2}{T}$

In order to be able to apply the principle of dimensions, it is necessary to know on experimental grounds what quantities are involved in producing a given motion. Using the cylinder in an incompressible viscous fluid as an example, we say that as a result of experiment—

The resistance of the cylinder depends on its size, the velocity relative to distant fluid, on the density of the fluid and on its viscosity, and so far as is known on nothing else. The last proviso is important, as a failure in application of the principles of dynamical similarity may lead to the discovery of another variable of importance.

Expressed mathematically the statement is equivalent to

$$R = f(\rho, l, \nu, v) \quad . \quad . \quad . \quad . \quad . \quad . \quad (9)$$

As the dimensions of R and f must be the same, a little consideration will show that the form of f is subject to certain restrictions. For instance, examine the expression

$$R = \frac{\rho^2 l^3 v}{\nu^2} \quad . \quad . \quad . \quad . \quad . \quad (10)$$

which is consistent with an unrestricted interpretation of (9). The dimensions of R are $\dfrac{ML}{T^2}$, whilst those of $\dfrac{\rho^2 l^3 v}{\nu}$ are $\dfrac{M^2}{L^6} . L^3 . \dfrac{L}{T} . \dfrac{T}{L^2}$, i.e. $\dfrac{M^2}{L^4}$, and the dimensions of the two sides of (10) are inconsistent.

It is not, however, sufficient that the dimensions of the terms of an equation be the same ; the equation

$$R = \rho l^2 v^2 \quad . \qquad . \quad . \quad . \quad . \quad . \quad . \quad (11)$$

has the correct dimensions, but clearly makes no use of the condition that the fluid is viscous, and the form is too restricted for valid application. It will now be appreciated that the correct form of (9) is that which has the correct dimensions and is also the least restricted combination of the quantities which matter.

The required form may be found as follows :—

Assume as a particular case of (9) that

$$R = \rho^a l^b \nu^c v^d \quad . \qquad . \quad . \quad . \quad . \quad . \quad . \quad (12)$$

and, to form a new equation, substitute for R, ρ, l, ν, and v quantities expressing their dimensions :

$$\frac{ML}{T^2} = \left(\frac{M}{L^3}\right)^a L^b \left(\frac{L^2}{T}\right)^c \left(\frac{L}{T}\right)^d \quad . \quad . \quad . \quad . \quad . \quad (13)$$

Equate the dimensions separately. For M we have

$$M = M^a \quad . \qquad . \quad . \quad . \quad . \quad . \quad (14)$$

and therefore $a = 1$. For L the equation is

$$L = L^{(-3a + b + 2c + d)} \quad . \quad . \quad . \quad . \quad . \quad (15)$$

and with $a = 1$ this leads to

$$b + 2c + d = 4 \quad . \qquad . \quad . \quad . \quad . \quad . \quad (16)$$

The equation for T is

$$T^{-2} = T^{-c - d}$$

or

$$c + d = 2 \quad . \qquad . \quad . \quad . \quad . \quad . \quad (17)$$

From equations (16) and (17) are then obtained the relations

$$\left.\begin{array}{l} c = 2 - d \\ b = d \end{array}\right\} . \quad . \quad . \quad . \quad . \quad . \quad (18)$$

and

and with $a = 1$ equation (12) becomes

$$R = \rho l^d \nu^{2-d} v^d$$

$$= \rho v^2 \left(\frac{vl}{\nu}\right)^d \quad . \quad . \quad . \quad . \quad . \quad . \quad (19)$$

The value of d is undetermined, and the reason for this will be seen if the dimensions of $\dfrac{vl}{\nu}$ are examined, for they will be found to be zero. It is also clear that any number of terms of the same form but with different values of d might be added and the sum would still satisfy the principle of dimensions. All possible combinations are included in the expression

$$R = \rho v^2 F\left(\frac{vl}{\nu}\right) . \quad . \quad . \quad . \quad . \quad (20)*$$

where F is an undetermined function.

Equation (20) may be written in many alternative forms which are exact equivalents, but it often happens that some one form is more convenient than any of the others. In the case of cylinders the resistance varies approximately as the square of the speed, and $\left(\dfrac{vl}{\nu}\right)^2 F_1\left(\dfrac{vl}{\nu}\right)$ is written instead of $F\left(\dfrac{vl}{\nu}\right)$ to obtain

$$R = \rho l^2 v^2 F_1\left(\frac{vl}{\nu}\right) \quad . \quad . \quad . \quad . \quad . \quad . \quad (21)$$

or

$$\frac{R}{\rho l^2 v^2} = F_1\left(\frac{vl}{\nu}\right) \quad . \quad . \quad . \quad . \quad . \quad . \quad . \quad (21a)$$

A reference to Fig. 193 shows that the ordinate and abscissa there used are indicated by (21 a). An equally correct result would have been obtained by the use as ordinate of $\dfrac{R}{\rho v^2}$ as indicated by (20), but the ordinate would then have varied much more with variation of $\dfrac{vl}{\nu}$, and the result would have been of less practical value.

After a little experience in the use of the method outlined in equations (12) to (19) it is possible to discard it and write down the answer without serious effort.

Compressibility.—If a fluid be compressible the density changes from point to point as an effect of the variations of pressure. It is found experimentally that changes of density are proportional to changes of pressure, and a convenient method of expressing this fact is to introduce a coefficient of elasticity E such that

$$E = \frac{\delta p}{\dfrac{\delta \rho}{\rho}} \quad . \quad . \quad . \quad . \quad . \quad . \quad . \quad (22)$$

where E is a constant for the particular physical state of the fluid. E has the dimensions of pressure and therefore of ρv^2, and hence the quantity $\dfrac{\rho v^2}{E}$ is of no dimensions.

If the viscosity of the fluid does not matter, the correct form for the resistance is

$$R = \rho l^2 v^2 F_2\left(\frac{\rho v^2}{E}\right). \quad . \quad . \quad . \quad . \quad . \quad (23)$$

where F_2 is an arbitrary function. It is shown in text-books on physics that $\sqrt{\dfrac{E}{\rho}}$ is the velocity of sound in the medium, and denoting this quantity by " a," equation (23) becomes

$$R = \rho l^2 v^2 F_3\left(\frac{v}{a}\right). \quad . \quad . \quad . \quad . \quad . \quad (24)$$

Whilst equation (24) shows that the effect of compressibility depends on the velocity of the body through the fluid as a fraction of the velocity

of sound in the undisturbed fluid, it does not give any indication of how resistance varies with velocity.

The knowledge of this latter point is of some importance in aeronautics, and a solution of the equation of motion for an inviscid compressible fluid will be given in order to indicate the limits within which air may safely be regarded as incompressible.

In developing Bernoulli's equation when dealing with inviscid fluid motion the equation

$$dp + \rho v dv = 0 \quad . \quad . \quad . \quad . \quad . \quad . \quad (25)$$

between pressure, density and velocity was obtained and integrated on the assumption that ρ was a constant. The fluid now considered being compressible, there is a relation between ρ and p, which depends on the law of expansion. Assuming adiabatic flow the relation is

$$p = \frac{p_0}{\rho_0^\gamma} \rho^\gamma . \quad . \quad . \quad . \quad . \quad . \quad . \quad (26)$$

where p_0 and ρ_0 refer to some standard point in the stream where v is uniform and equal to v_0 and γ is a constant for the gas. Differentiating in (26) and substituting for dp in (25) leads to

$$\frac{\gamma}{\gamma - 1} \cdot \frac{p_0}{\rho_0} \cdot \left(\frac{\rho}{\rho_0}\right)^{\gamma - 1} = -\tfrac{1}{2}v^2 + \text{constant} \quad . \quad . \quad . \quad (27)$$

and the constant is evaluated by putting $v = v_0$ when $\rho = \rho_0$. The value of $\dfrac{\gamma p_0}{\rho_0} = \dfrac{E}{\rho_0}$ and is equal to the square of the velocity of sound in the undisturbed fluid. Equation (27) becomes

$$\frac{\rho}{\rho_0} = \left(1 + \frac{\gamma - 1}{2} \cdot \frac{v_0^2 - v^2}{a^2}\right)^{\frac{1}{\gamma - 1}} . \quad . \quad . \quad . \quad (28)$$

and since $\dfrac{p}{p_0} = \left(\dfrac{\rho}{\rho_0}\right)^\gamma$ a new relation from (28) is

$$\frac{p}{p_0} = \left(1 + \frac{\gamma - 1}{2} \cdot \frac{v_0^2 - v^2}{a^2}\right)^{\frac{\gamma}{\gamma - 1}} . \quad . \quad . \quad . \quad (29)$$

The greatest positive pressure difference on a moving body occurs at a "stagnation point," i.e. where $v = 0$. Making $v = 0$ in (29) and expanding by the binomial theorem

$$\frac{p}{p_0} = 1 + \frac{\gamma}{2} \cdot \frac{v_0^2}{a^2} + \frac{\gamma}{8} \cdot \frac{v_0^4}{a^4} + \quad . \quad . \quad . \quad . \quad (30)$$

Denoting the increase of pressure $p - p_0$ by δp leads to the equation

$$\delta p = \frac{\gamma p_0}{a^2} \cdot \tfrac{1}{2}v_0^2 \left(1 + \frac{1}{4} \cdot \frac{v_0^2}{a^2} + \ldots\right) \quad . \quad . \quad . \quad (31)$$

or since $\dfrac{\gamma p_0}{a^2} = \rho_0$

$$\delta p = \tfrac{1}{2}\rho_0 v_0^2 \left(1 + \frac{1}{4} \cdot \frac{v_0^2}{a^2} + \ldots\right) \quad . \quad . \quad . \quad (32)$$

If $\frac{v_0}{a}$ be small the increase of pressure at a stagnation point over that
of the uniformly moving stream is $\frac{1}{2}\rho_0 v_0^2$, and this value is usually found
in wind-channel experiments. For air at ordinary temperatures the
velocity of sound is about 1080 ft.-s., and the velocity of the fastest
aeroplane is less than one quarter of this. The second term of (32) is
then not more than 1·5 per cent. of the first. As the greatest suction on
an aeroplane wing is numerically three or four times that of the greatest
positive increment the effect of compressibility may locally be a little
more marked, but to the order of accuracy yet reached air is substantially
incompressible for the motion round wings.

The same equation shows that for airscrews, the tips of the blades
of which may reach speeds of 700 or 800 ft.-s., the effect of compressi-
bility may be expected to be important. At still higher velocities it appears
that a radical change of type of flow occurs, and when the tip speed
exceeds that of half the velocity of sound normal methods of design
need to be supplemented by terms depending on compressibility.

Similar Motions as affected by Gravitation.—An aeroplane is supported
against the action of gravity, and hence g is a factor on which motion
depends. Ignoring viscosity and compressibility temporarily, the motion
will be seen to depend on the attitude of the aeroplane, its size, its velocity,
on the density of the fluid and on the value of g. The principle of dimen-
sions then leads to the equation

$$R = \rho l^2 v^2 F_4\left(\frac{v^2}{lg}\right). \quad . \quad . \quad . \quad . \quad . \quad (33)$$

For two similar aeroplanes to have the same motions when not flying
steadily the initial values of $\frac{v^2}{lg}$ must be the same. For terrestrial purposes
g is very nearly constant, and the law of corresponding speeds says that
the speed of the larger aeroplane must be greater than that of the smaller
in the proportion of the square roots of their scales. This may be recognised
as the Froude's law which is applied in connection with Naval Architecture.
The influence of gravity is there felt in the pressures produced at the base
of waves owing to the weight of the water.

Combined Effects of Viscosity, Compressibility and Gravity.—The
principle of dimensions now leads to the equation

$$R = \rho l^2 v^2 F_5\left(\frac{vl}{\nu}, \frac{v}{a}, \frac{v^2}{lg}\right) \quad . \quad . \quad . \quad . \quad . \quad (34)$$

and a law of corresponding speeds is no longer applicable. It is clearly
not possible in one fluid and with terrestrial conditions to make $\frac{vl}{\nu}$, $\frac{v}{a}$ and $\frac{v^2}{lg}$
each constant for two similar bodies. It is only in those cases for which
only one or two of the arguments are greatly predominant that the prin-
ciples of dynamical similarity lead to equations of practical importance.

Static Problems and Similarity of Structures.—The rules developed for
dynamical similarity can be applied to statical problems and one or two

cases are of interest in aeronautics. Some idea of the relation between the strengths of similar structures can be obtained quite readily.

Consider first the stresses in similar structures when they are due to the weight of the structure itself. The parts may either be made of the same or of different materials, but to the same drawings. If of different materials the densities of corresponding parts will be assumed to retain a constant proportion throughout the structure. Since the density appears separately, the weight can be represented by $\rho l^3 g$, and if the structure be not redundant it is known that the stress depends only on ρ, l and g. If f_s represent stress, the equation of correct dimensions and form is

$$f_s = \rho g l \quad . \quad . \quad . \quad . \quad . \quad . \quad . \quad (35)$$

This equation shows that for the same materials, stress is proportional to the scale of structure, and for this condition of loading large structures are weaker than small ones. It is in accordance with (35) that it is found to be more and more difficult to build bridges as the span increases.

The other extreme condition of loading is that in which the weight of the structure is unimportant, and the stresses are almost wholly due to a loading not dependent on the size of the structure. If w be the symbol representing an external applied load factor between similar structures, the principle of dimensions shows that

$$f_s = \frac{w}{l^2} \quad . \quad . \quad . \quad . \quad . \quad . \quad . \quad (36)$$

If the external loads increase as l^2, i.e. as the cross-sections of the similar members, equation (36) shows that the stress is independent of the size, The weight of the structure, however, increases as l^3 if the same materials are used.

In an aeroplane the conditions of loading are nearly those required by (36). If the loading of the wings in pounds per square foot is constant, the total weight to be carried varies as the square of the linear dimensions. Of this total weight it appears that the proportion due to structure varies from about 26 per cent. for the smallest aeroplane to 33 per cent. for the largest present-day aeroplane. The change of linear dimensions corresponding with these figures is 1 to 4, but it should not be forgotten that the principles of similarity are appreciably departed from. In building a large aeroplane it is possible to give more attention to details because of their relatively larger size, and because the scantlings are then not so frequently determined by the limitations of manufacturing processes.

Since small aeroplanes have been used for fighting purposes where they are subjected to higher stresses than larger aeroplanes, a lower factor of safety has been allowed for the latter. The margin of safety for small present-day aeroplanes would be almost twice as great as for the larger ones if both were used on similar duties.

In the case of engines the power is frequently increased by the multiplication of units and not by an increase of the dimensions of each part. The number of cylinders may be two for 30 to 60 horsepower, 12 for 300 horsepower to 500 horsepower, and for still higher powers the whole engine

may be duplicated.   For 1500 horsepower there will be say 4 engines with 48 cylinders, each of the latter having the same strength as a cylinder giving 30 horsepower.   The process of subdivision which is carried to great lengths in the engine is being applied to the whole aeroplane as the number of complete engines is increased, and this tends to keep the structure weight from increasing as the cube of the linear dimensions of the aeroplane as would be required in the case of strict similarity.   In the extreme case two aeroplanes may be assumed to fly independently side by side, and some connecting link used to bind them into one larger aeroplane.   In principle this is carried out in the design of big aeroplanes.   The weight of the connecting mechanism appears to be of appreciable magnitude, since with advantages of manufacture and factors of safety the structure weight as a fraction of the whole shows a distinct tendency to increase.   There is, however, no clear limitation in sight to the size of possible aeroplanes. The position with regard to airships is of a very similar character, and the structure weight will tend to become a greater proportion of the whole as the size of airship increases, but the rate is so slow that again no clear limitation on size can be seen.

Aeronautical Applications of Dynamical Similarity.—Fig. 193 may be used to illustrate an application to aeronautical purposes of curves based on similarity.   As an example suppose that a tube containing engine control leads is required in the wind, and that it is desired to know how much resistance will be added to the aeroplane if the tube is circular and unfaired. The diameter of the tube will be taken as $0\cdot5$ in. ($0\cdot0417$ ft.), and its length 6 ft. or 144 diameters.   At or near ground-level the density ($0\cdot00237$) and the kinematic viscosity ($0\cdot000159$) may be found from a table of physical constants.*   At a speed of 100 ft.-s. the value of $\log \dfrac{vl}{\nu}$ will

---

* **Kinematic Viscosity, ν.**—If μ is the coefficient of fluid friction, $\nu = \mu/\rho$.

<div align="center">AIR.</div>

<div align="center">Ft.-lb.-sec. units.</div>

Temp.	$\sigma\nu$ in sq. ft. per sec. where $0\cdot00237\sigma = \rho$.
$0°$ C.	$0\cdot000152$
$15°$	$0\cdot000159$
$100°$	$0\cdot000194$

<div align="center">WATER.</div>

<div align="center">Ft.-lb.-sec. units.</div>

Temp.	ν in sq. ft. per sec.
$6°$ C	$0\cdot0000159$
$8°$	$0\cdot0000150$
$10°$	$0\cdot0000141$
$15°$	$0\cdot0000123$
$20°$	$0\cdot0000108$

easily be found from the above figures to be 4·42, and Fig. 193 then shows that

$$\frac{R}{\rho l^2 v^2} = 0·595$$

R being the resistance of a piece of tube of length equal to its diameter. The resistance of the whole tube is then

$$144 \times 0·595 \times 0·00237 \times (0·0417)^2 \times 100^2 = 3·54 \text{ lbs.}$$

At 10,000 ft. the resistance will be different. The density is there equal to 0·00175, and the kinematic viscosity to 0·000201. The value of $\log \frac{vl}{\nu}$ is 4·32, and that of $\frac{R}{\rho l^2 v^2}$ is 0·592. Finally the resistance is 2·60 lbs.

In this calculation no assumption has been made that resistance varies as the square of the speed, and the fact that $\frac{R}{\rho l^2 v^2}$ has changed is an indication of departure from the square law and strict similarity. The value of $\frac{R}{\rho l^2 v^2}$ has only changed from 0·595 to 0·592 as a result of changing the height from 1000 ft. to 10,000 ft. Most of the change in resistance is due to change in air density. It might have happened that the curve of Fig. 193 had been a horizontal straight line, and in that case the resistance coefficient $\frac{R}{\rho l^2 v^2}$ would not have changed at all, and motions at all values of $\frac{vl}{\nu}$ would have been similar. We may then regard the variations of the ordinates of Fig. 193 as measures of departure from similarity. It does not follow that similar flow necessarily occurs when $\frac{R}{\rho l^2 v^2}$ has the same value, the correct condition being that $\frac{vl}{\nu}$ is constant.

If such curves as that of Fig. 193 do not vary greatly with $\frac{vl}{\nu}$ the fluid motions might be described as nearly similar, and with a certain loss of precision we may say that the resistance of the cylinders does not depend appreciably on $\frac{vl}{\nu}$. In many cases our lack of knowledge is such that much use must be made of the ideas of nearly similar motions, and this applies particularly to the relations between models of aircraft and the aircraft themselves. Fortunately for aeronautics, most of the forces for a given attitude of the aircraft or part vary nearly as the square of the speed, and $\frac{vl}{\nu}$ is only of importance as a correction. The law of resistance given by (21), i.e.

$$R = \rho l^2 v^2 F_1\left(\frac{vl}{\nu}\right) \quad . \quad . \quad . \quad . \quad . \quad . \quad (37)$$

is worth special attention in its bearing on the present point. Both model

and aircraft move in the same medium, and therefore ν is constant. If $\dfrac{vl}{\nu}$ is also to be constant it follows that vl is constant, and equation (37) then shows that R is constant. This means that similarity of flow can only be expected on theoretical grounds if the force on the model is as great as that on the aircraft. Stated in this way, it is obvious that the law of corresponding speeds as applied to aerodynamics is useless for complete aircraft. For parts, it may be possible to double the size for wind channel tests, and so get the exact equivalent of a double wind speed. This is the case for wires and struts, and the law of corresponding speeds is wholly satisfied.

For aircraft as a whole and for wings in particular it is necessary to investigate the nature of F_1 over the whole range of $\dfrac{vl}{\nu}$ between model and full scale if certainty is to exist, and, if the changes are great, the assistance which models give in design is correspondingly reduced, since results are subject to a scale correction.

Aeroplane Wings.—The scale effect on aeroplane wings has received more attention than that of any other part of aircraft for which the range of $\dfrac{vl}{\nu}$ cannot be covered without flight tests. It has been found possible in flight to measure the pressure distribution round a wing over a wide range of speeds. For the purposes of comparison a complete model structure was set up in a wind channel and the pressure distribution observed at corresponding points. The full-scale experiments are more difficult to carry out than those on the model, and the accuracy is relatively less. It is, however, great enough to warrant a direct comparison such as is given in Fig. 198. The abscissae of the diagrams represent the positions of the points at which the pressures were measured, whilst the values of the latter divided by ρv^2 are the ordinates in each case. The points located on the upper surface will be clear from the marking on each diagram. The curves represent the extreme observed angles of incidence for the lower and upper wings of a biplane, the continuous curves being obtained on the full scale and the dots on the model.

The general similarity of the curves is so marked that no hesitation will be felt in saying that the flow of air round a model wing is nearly similar to that round an aeroplane wing.

A close examination of the diagrams discloses a difference on the lower surface of the upper wing which is systematic and greater than the accidental errors of observation. It is difficult to imagine any reason why this difference should appear on one wing and not on the other, and no satisfactory explanation of the difference has been given. It must be concluded from the evidence available that the model represents the full scale with an accuracy as great as that of the experiments, since it is not possible to give any quantitative value to the difference. It follows from this that until a higher degree of accuracy is reached on the full scale the characteristics of aeroplane wings can be determined completely by experiments on models.

It is not possible from diagrams of pressure distribution alone to determine the lift and drag of a wing. An independent measurement is necessary before resolution of forces can be effected, and on the full scale
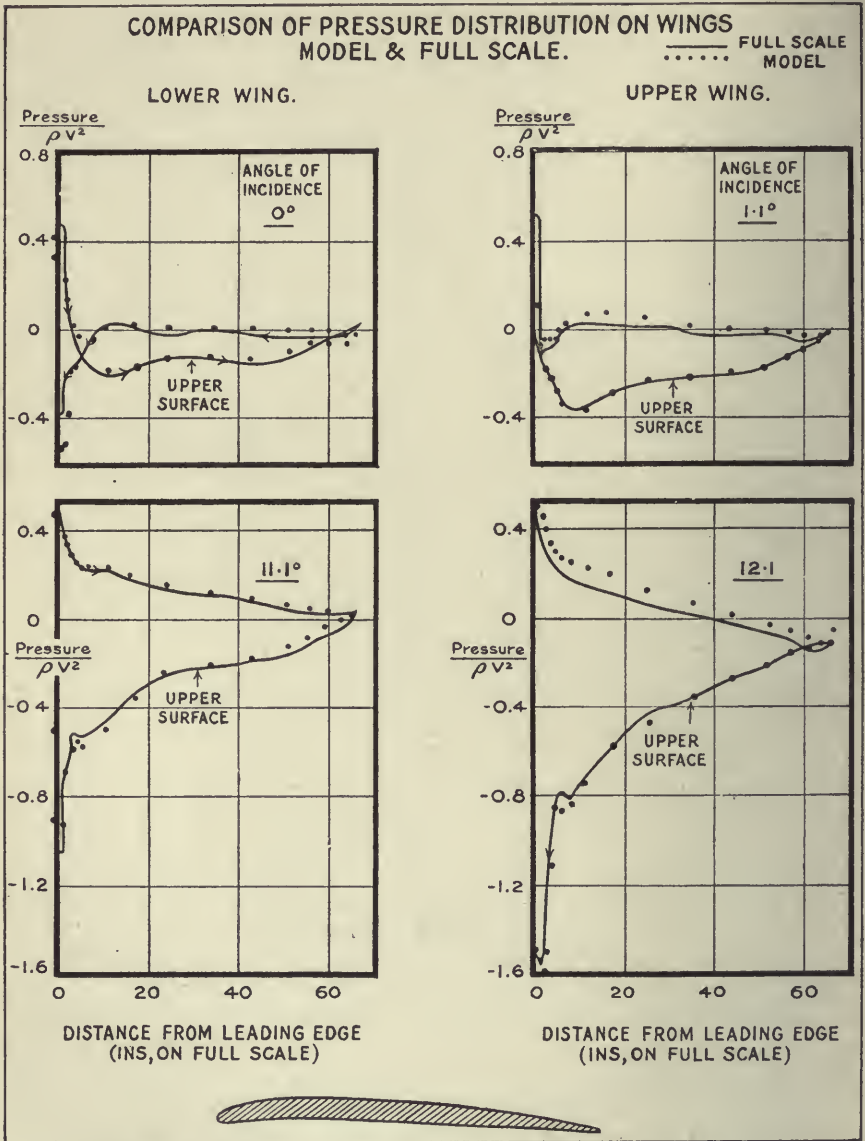

Fig. 198.—Comparison of wing characteristics on the model and full scales.

this measurement involves either a measure of angle of incidence, of gliding angle or of thrust. Of these the determination of gliding angle with air-screw stopped gives promise of earliest results of sufficient accuracy. For

drag an error of 1° in the angle of incidence means an error of 30 per cent., and a sufficient accuracy is not readily attained ; a reliable thrust meter has yet to be developed.   As the resultant force is nearly equal to the lift, this quantity can be deduced with little error from the pressure distribution and a rough measure of the angle of incidence, and the model and full scale agree.   This is not, however, a new check between full scale and model.

TABLE 2.—Changes of Lift, Drag and Moment on an Aerofoil over the Model Range of vl.

Angle of incidence.	Lift coefficient, k_L $vl = 30$	δk_L $vl = 20$	δk_L $vl = 10$	Drag coefficient, k_D $vl = 30$	δk_D $vl = 20$	δk_D $vl = 10$	Centre of gravity at 0·4 chord.		
							Moment coefficient, k_M $vl = 30$	δk_M $vl = 20$	δk_M $vl = 10$
−6°	−0·152	−0·003	−0·007	0·0352	0·0003	0·0016	−0·0710	+0·0002	0·0004
−4°	−0·047	−0·016	−0·025	0·0208	0·0004	0·0017	−0·0330	0·0010	0·0020
−2°	+0·062	−0·022	−0·054	0·0124	0·0008	0·0022	−0·0250	0·0015	0·0030
0°	+0·144	−0·005	−0·044	0·0099	0·0006	0·0023	−0·0143	0·0004	0·0010
2°	0·216	−0·002	−0·019	0·0113	0·0004	0·0021	−0·0028	−0·0001	−0·0002
4°	0·290	−0·002	−0·014	0·0146	0·0004	0·0020	+0·0109	−0·0001	−0·0002
6°	0·362	−0·002	−0·014	0·0206	0·0004	0·0020	+0·0225	−0·0001	−0·0002
8°	0·440	−0·003	−0·018	0·0279	0·0004	0·0023	0·0350	−0·0001	−0·0002
10°	0·512	−0·004	−0·022	0·0365	0·0004	0·0026	0·0441	−0·0001	−0·0003
12°	0·584	−0·007	−0·030	0·0456	0·0005	0·0030	0·0542	−0·0002	−0·0005
14°	0·630	−0·020	−0·050	0·0562	0·0006	0·0035	0·0628	−0·0003	−0·0007
16°	0·618	−0·025	−0·059	0·0742	0·0011	0·0043	0·0625	−0·0004	−0·0010
18°	0·576	−0·033	−0·067	0·1008	great	great	0·0267	—	—
20°	0·520	−0·025	−0·060	0·1475	great	great	0·0092	—	—

It is easily possible in a wind channel to make tests on wings of different sizes and at different speeds, but the tests throw little light on the behaviour of aeroplane wings since the variations of vl which are possible are so small. The smallest aeroplane is about five times the scale of the largest model, and travels at speeds which vary from being less than that of the air current in the channel to being twice as great.   For very favourable conditions the range of vl from model to full scale is 4 : 1.   Table 2 shows roughly how the values of the various resistance coefficients of a wing are affected by changes of vl over the wind channel range.   The wing section had an upper surface of similar shape to that shown in Fig. 198, but had no camber on the under surface.

The table shows the lift, drag and moment coefficients for $vl = 30$ for a range of angles of incidence together with the differences in these quantities due to a change from $vl = 30$ to $vl = 20$ and $vl = 10$.   An examination of the table will show that for the most useful range of flying angles, i.e. from 0° to 12°, the variations with vl are not very great, the minimum drag coefficient being the most seriously affected.   At angles of incidence less than 0° the lift coefficient is affected appreciably, whilst at large angles of incidence, 14°–20°, the effect of changing vl is appreciable on both the lift and drag coefficients.   It is in the latter case that recent extensions of model experiments will be of great value.

Judging from these results alone it might be expected that for efficient flight the model tests would be very accurate, but that at very high and very low speeds of flight, scale factors of appreciable magnitude would be necessary. At the present moment all that can be said is that full-scale experiments have not shown any obvious errors even at the extreme speeds. Something more than ordinary testing appears to be required if the corrections are to be evaluated, and for the present, wind channel tests at $vl = 30$ (*i.e.* 6″ chord and a wind speed of 60 ft.-s.) may be applied to full scale without any vl factor.

Variation of the Maximum Lift Coefficient in the Model Range of vl.— The variation of lift coefficient in the neighbourhood of the maximum varies very greatly from one wing section to another. For the form shown in Fig. 198 the changes are appreciable but not very striking in character. Changing to a much thicker section such as is used in airscrews the effect of change of speed is marked, and shows that the flow is very critical in the neighbourhood of the maximum lift coefficient. Fig. 199 shows a good example of this critical flow. The section is shown in the top left-hand corner of the figure, and the value of vl is the product of the wind velocity in feet per second and the maximum dimension of the section in feet. With $vl = 5$ the curve for lift coefficient reaches a maximum of 0·41 at an angle of incidence of 8°, and after a fall to 0·32 again rises somewhat irregularly to 0·43 at an angle of incidence of 40 degrees. At the other extreme of vl, *i.e.* 14·5, the first maximum has a value of 0·60 at 12°·5, followed by a fall to 0·45 at 15° and a very sharp rise to 0·78 at 16°·5. For greater angles of incidence the value of the lift coefficient falls to 0·43 at 40°, and agrees for the last 10 degrees of this range with the value for $vl = 5$. Intermediate curves are obtained for intermediate values of vl, and it appears probable that at a somewhat greater value of vl than 14·5 the first minimum would disappear, leaving a single maximum of nearly 0·8. The drag curves show less striking, but quite considerable, changes with change of vl.

The curves for all values of vl are in good agreement from the angle of no lift up to 6 or 8 degrees, and for the higher values of vl the region of appreciable change is restricted to about 4°. If the experiments had been carried to $vl = 30$, it appears probable that substantial independence of vl would have been attained. It is to this stage that model experiments should, if possible, be carried before application to full scale is made. There is, of course, no certainty that between the largest vl for the model and that for the aeroplane some different type of critical flow may not exist. There is, however, complete absence of any evidence of further critical flow, and much evidence tending in the reverse direction.

There are no experiments on aeroplane bodies or on airships and their models which indicate any instability of flow comparable with that shown for an aerofoil in Fig. 199. In all cases there is a tendency to lower drag coefficients as vl increases, the proportionate changes being greatest for the airship envelopes. Table 3 shows three typical results; in the first column is the speed of test, whilst in the others are figures showing the change of drag coefficient with change of speed, or, what is the same thing so long as the model is unchanged, with change of vl. The first model was

comparable in size with an aeroplane body, but its shape was one of much
lower resistance for a given cross-section.   The change of drag coefficient
over the range shown is about 8 per cent.   Comparison with actual airships
is difficult for lack of information, but it is clear that this rate of change is

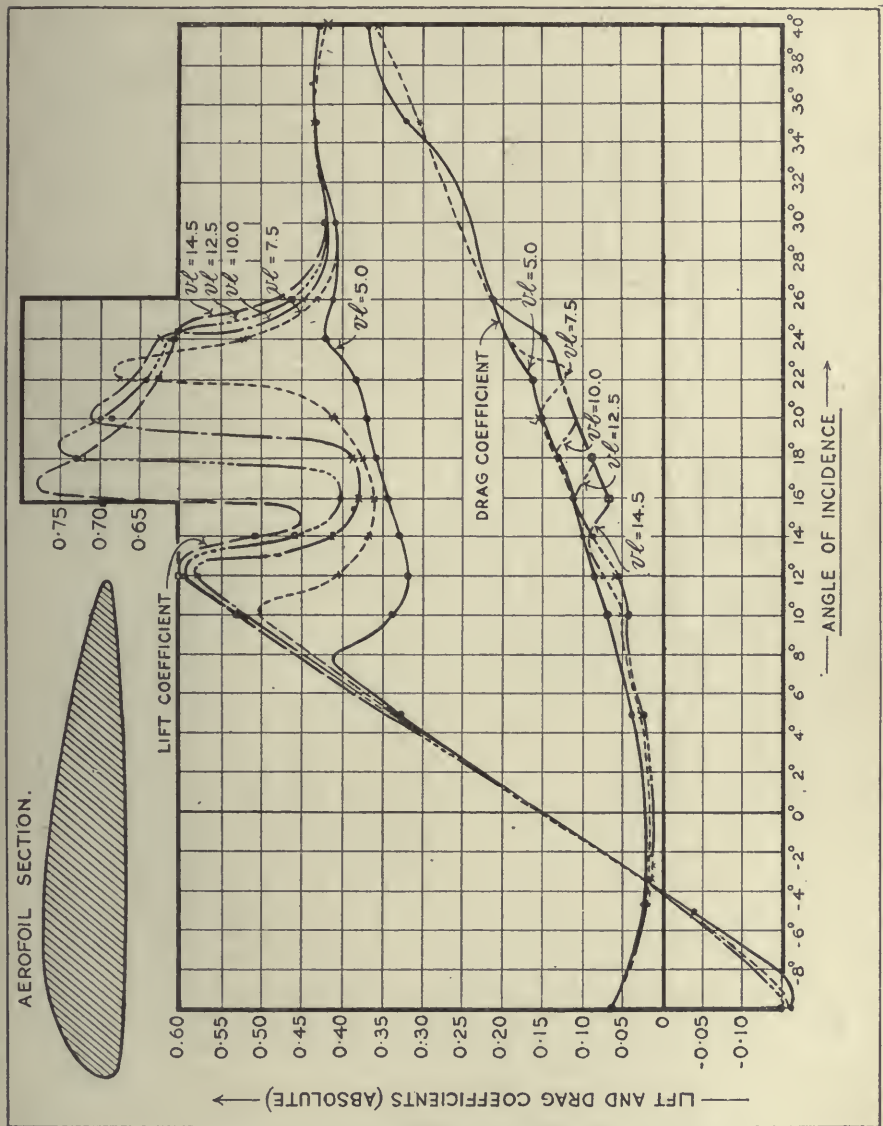Fig. 199.—Changes in force due to changes in type of flow at the critical angle of a wing.

not continued up to the *vl* suitable for airships, and it is probable that the
rate of change is a local manifestation of change of type of flow from which
it is impossible to draw reliable deductions for extrapolation.   As applied
to aeroplane bodies however, the range of *vl* covered is so great that the

slight extrapolation required may be made without danger. This conclusion is strengthened by the last two columns, which show that when rigging, wind screens, etc., are added to a faired body the drag coefficient changes less rapidly with vl, and the usual assumption that the drag coefficient of an aeroplane body is independent of vl is sufficiently accurate for present-day design.

TABLE 3.—Scale Effect on Aeroplane Bodies and Airship Models.

Velocity (ft.-s.).	Ratio of drag coefficients at various speeds to the drag coefficient at 60 ft.-s.		
	Model of rigid airship envelope, 1·5 ft. diameter, 15 ft. long.	Model of non-rigid airship envelope and rigging, 0·6 ft. diameter, 3 ft. long.	Model of aeroplane body, 1·5 ft. long.
40	1·05	1·02	1·00
50	1·01	1·01	1·00
60	1·00	1·00	1·00
70	0·99	1·00	1·00
80	0·97	1·00	0·99

The Resistance of Struts.—In describing the properties of aerofoils it was shown that the thickening of the section led to a critical type of flow

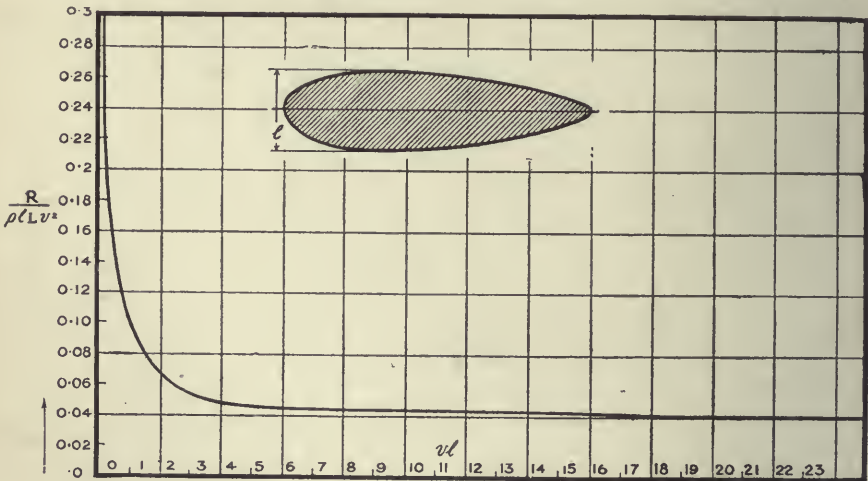Fig. 200.—Scale effect on the resistance of a strut.

R = resistance in lbs.
l = smaller dimension of cross-section in feet.
L = length of strut in feet.
v = speed in feet.

at certain angles of incidence. A further change of aerofoil section leads to a strut, and experiment shows that the flow is apt to become extremely critical, especially when the strut is inclined to the wind. Even when

symmetrically placed in the wind the resistance coefficient of a good form of strut changes very markedly with vl for small values (Fig 200).

Consider a strut of which the narrower dimension of the cross-section is $1\frac{1}{2}$ ins. or 0·125 ft. At 150 ft.-s. the value of vl is nearly 19 and the drag coefficient is 0·040. It is obvious from Fig. 200 that the exact value of vl is unimportant. Even had vl been as small as 6 the drag coefficient would still not have varied by as much as 20 per cent. If, on the other hand, the test of a model at 75 ft.-s. is considered, the scale being $\frac{1}{20}$th, the value of vl is about 0·5, and the corresponding resistance coefficient is 0·15. The variation from constancy is then great, and for this reason it is usual when testing complete model aeroplanes to cut down the number of inter-plane struts to a minimum and to eliminate the effect of the remainder before applying the results to full scale. The same precaution is taken in regard to wires.

Wheels.—The resistance of wheels varies very accurately as the square of the speed over the model range, and there is no difficulty in getting values of vl approaching those on the full scale. There is an appreciable mutual effect on resistance between the wheels and undercarriage and between the struts at the joints, and except for wires the complete under-carriage should be tested on a moderately large scale if the greatest accuracy is desired.

Aeroplane as a Whole.—It was shown when discussing the resistance of an aeroplane in detail that the whole may be divided into planes, structure, body, undercarriage and tail, and the resistance of these parts obtained separately; the results when added give a close approximation to the resistance of the whole. It may therefore be expected from the preceding arguments that the aeroplane as a whole will show the same characteristics on lift as are shown by the wings alone, and will have a less marked percentage change in drag with change in vl. The number of ex-periments on the subject is very small, but they fully bear out the above conclusion.

To summarise the position, it may be said that a model aeroplane complete except for wires and struts, having a wing chord of 6 ins., may be tested at a speed of 60 ft.-s., and the results applied to the full scale on the assumption that the flow round the model is exactly similar to that round the aeroplane.

Airscrews.—The airscrew is commonly regarded as a rotating aerofoil, and there is no difficulty on the model scale in obtaining values of vl much in excess of 30. The possibility of experiments by the use of a whirling arm also makes more full-scale observations available. Although the number of partial checks is very numerous, accurate comparison has not been carried out in a sufficient number of cases to make a quantitative statement of value. For normal aeroplane use the general conclusion arrived at is that the agreement between models and full scale is very close.

It has been pointed out that the compressibility of air begins to become evident at velocities of 500 or 600 ft.-s., and airscrews have been designed and satisfactorily used up to 800 ft.-s. At the higher speeds empirical correction factors were found to be necessary which had not appeared at

lower speeds. One experiment, a static test, has been carried out at speeds up to 1150 ft.-s. In the neighbourhood of the velocity of sound the type of flow changed rapidly, so that the slip stream was eliminated and the main outflow centrifugal. The noise produced was very great and discomfort felt in a short time. It is clear that no certainty in design at present exists for tip speeds in excess of 800 ft.-s.

Summary of Conclusions.—This *résumé* of the applications of the principles of dynamical similarity will have indicated a field of research of which only the fringes have yet been touched. So far as research has gone, the result is to give support to a reasonable application of the results of model experiments. This conclusion is important since model results are more readily and rapidly obtained than corresponding quantities on the full scale, and the progress of the science of aeronautics has been and will continue to be assisted greatly by a judicious combination of experiments on both the model and full scales.

CHAPTER IX

THE PREDICTION AND ANALYSIS OF AEROPLANE PERFORMANCE

THE PERFORMANCE OF AEROPLANES

THE term "performance" as applied to aeroplanes is used as an expression to denote the greatest speed at which an aeroplane can fly and the greatest rate at which it can climb. As flight takes place in the air, the structure of which is variable from day to day, the expression only receives precision if the performance is defined relative to some specified set of atmospheric conditions. As aeroplanes have reached heights of nearly 30,000 feet the stratum is of considerable thickness, and in Britain, aeronautical experiments and calculations are referred to a standard atmosphere which is defined in Tables 1 and 2.

TABLE 1.—STANDARD HEIGHT.

The pressure is in multiples of 760 mm. of mercury, and the density of 0·00237 slug per cubic ft.

Standard height (ft.).	Relative density. σ	Relative pressure. p	Temperature ° C.	Absolute temperature ° C.	Aneroid height (ft.).
0	1·025	1·000	9	282	0
1,000	·994	·964	7·5	280 5	1,000
2,000	·963	·929	6	279	2,010
3,000	·932	·895	4·5	277·5	3,020
4,000	·903	·861	3	276	4.040
5,000	·870	·829	1·5	274·5	5,070
6,000	·845	·798	0	273	6,100
7,000	·818	·768	−1·5	271·5	7,130
8,000	·792	·739	−3	270	8,180
9,000	·765	·711	−4·5	268·5	9,230
10,000	·740	·684	−6	267	10,290
11,000	·717	658	−8	265	11,360
12,000	·695	·632	−10	263	12,440
13,000	·673	·607	−12	261	13,520
14,000	·652	·583	−14	259	14,600
15,000	·630	·560	−16	257	15,700
16,000	·610	·538	−18	255	16,800
17,000	·590	·516	−20	253	17,900
18,000	·571	·496	−22	251	19,010
19,000	·553	·476	−24	249	20,140
20,000	·535	·456	−26	247	21,270
21,000	·515	·437	−28	245	22,410
22,000	·498	·419	−29·5	243·5	23,560
23,000	·481	·402	−31·5	241·5	24,720
24,000	·464	·385	−33	240	25,890
25,000	·448	·369	−35	238	27,060
26,000	·432	·353	−37	236	28,240
27,000	·417	·338	−38·5	234·5	29,430
28,000	·402	·324	−40·5	232·5	30,640
29,000	·388	·310	−42	231	31,860
30,000	·374	·296	−44	229	33,100

TABLE 2.—ANEROID HEIGHT.

The pressure is in multiples of 760 mm. of mercury, and the density of 0·00237 slug per cubic ft.

Aneroid height (ft.).	Relative pressure. p	Relative density. σ	Temperature °C.	Absolute Temperature °C.	Standard height (ft.).
0	1·000	1·025	9	282	0
1,000	·964	·994	7·5	280·5	1,000
2,000	·929	·962	6	279	1,990
3,000	·895	·933	4·5	277·5	2,980
4,000	·863	·904	3	276	3,960
5,000	·832	·876	1·5	274·5	4,940
6,000	·802	·849	0	273	5,900
7,000	·773	·822	—1·5	271·5	6,870
8,000	·745	·796	—3	270	7,830
9,000	·718	·771	—4	269	8,780
10,000	·692	·747	—5·5	267·5	9,730
11,000	·667	·724	—7·5	263·5	10,670
12,000	·643	·703	—9	264	11,600
13,000	·620	·683	—11	262	12,520
14,000	·597	·663	—13	260	13,440
15,000	·576	·644	—14·5	258·5	14,360
16,000	·555	·626	—16·5	256·5	15,270
17,000	·535	·607	—18·5	254·5	16,180
18,000	·516	·589	—20	253	17,090
19,000	·497	·571	—22	251	18,000
20,000	·480	·554	—24	249	18,880
21,000	·462	·537	—25·5	247·5	19,760
22,000	·445	·521	—27	246	20,650
23,000	·429	·506	—29	244	21,520
24,000	·414	·491	—30·5	242·5	22,380
25,000	·399	·477	—32	241	23,240
26,000	·384	·462	—33·5	239·5	24,110
27,000	·370	·448	—35	238	24,960
28,000	·357	·435	—36·5	236·5	25,800
29,000	·344	·422	—38	235	26,650
30,000	·332	·410	—39·5	233·5	27,480

The tables show the quantities of importance in the standard atmosphere with the addition of a quantity called "aneroid height." The term arises from the use of an aneroid barometer in an aeroplane, the divisions on which are given in thousands of feet and fractions of the main divisions. As a measure of height the instrument is defective, and it will be noticed from the table that an aneroid height of 33,100 feet corresponds with a real height of 30,000 feet in a standard atmosphere. In aeronautical work of precision the aneroid barometer is regarded solely as a pressure indicator, and the readings of aneroid height as taken, are converted into pressure by means of Table 2 before any use is made of the results. The term "aneroid height" is useful as a rough guide to the position of an aeroplane, and for this reason the aneroid barometer has never been displaced by an instrument in which the scale is calibrated in pressures directly.

The first column of Table 1 shows for a standard atmosphere the real height of a point above the earth (sea level), whilst the others show relative pressure, relative density and temperature, both Centigrade and absolute.

In trials, temperature is observed by reading a thermometer fixed on one
of the wing struts, and the density is calculated from the observed tem-
perature and the pressure deduced from the aneroid height.

An illustration is given in Fig. 201 of variations of temperature which
may be observed during performance trials. The curves cover the months
May to February, and contain observations for hot and cold days. Whilst
the general trend of the curves is to show a fall of temperature with height
there was one occasion on which a temperature inversion occurred at
about 3000 feet. The extreme difference of temperature shown at the
ground was over 25° C., and at 12,000 ft. the difference was 10° C. It
will be noticed that the curve for aneroid height which would follow from
Table 2 would fall amongst the curves shown, roughly in the mean position.

There are some atmospheric variations which affect performance, but
of which account can-
not yet be taken. If
the air be still no diffi-
culties arise, but if it
be in movement—ex-
cept in the case of
uniform horizontal
velocity—errors of ob-
servation will result.
To see this it is noted
that the natural gliding
angle of an aeroplane
may be 1 in 8, *i.e.* the
effect of gravity at such
an angle of descent is
as great as that of the
engine in level flight.
Suppose that an up-
current of 1 in 100

FIG. 201.—Atmospheric changes of temperature.

exists during a level flight, the aeroplane will be keeping at constant height
above the earth by means of the aneroid barometer, and consequently will
be descending through the air at 1 in 100. This is equivalent to an 8 per
cent. addition to the power of the engine and an increase of 3 miles per
hour on the observed speed. The flight speed being 200 ft.-s. the up-
current would have a velocity of 2 ft.-s., an amount which is much less
than the extremes observed. It is generally thought that up-currents are
less prevalent at considerable heights than near the ground, but no regular
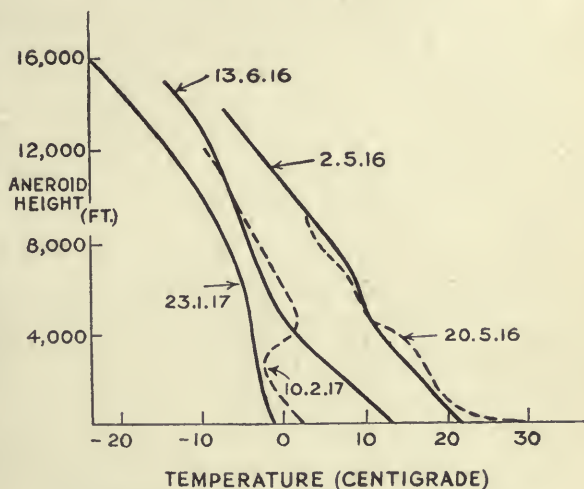means of estimating up-currents with the desired accuracy is available for use.

A variation of horizontal wind velocity with height introduces errors
into the observed rate of climb of an aeroplane due to the conversion of
kinetic energy of the aeroplane into potential energy. If, in rising 1000 ft.,
the wind velocity increases by 30 per cent. of the flying speed of an aero-
plane, the error may be ±8 per cent. dependent on whether flight is into
the wind or with the wind. This error can be eliminated by flying back-
wards and forwards over the same course.

Special care in regulating the petrol consumption to the atmospheric conditions is required ; without regulation the petrol-air mixture tends to become too rich as the height increases, with a consequent loss of engine power, and an increased petrol consumption. The following figures will show how important is the regulation of the petrol flow.

In a particular aeroplane the time to climb to 10,000 feet with un-controlled petrol was 25 mins., and this was reduced to 21·5 mins. by suitable adjustment. The increase of speed was from 84 m.p.h. to 91 m.p.h., and although this is probably an extreme case, it is clear that the use of some form of altitude control becomes essential for any accurate measurements of aeroplane performance. The revolution counter and the airspeed indicator afford the pilot a means of adjusting the petrol-air mixture to its best condition.

The prediction and reduction of aeroplane performance proceeds on the assumption that all precautions have been taken in the adjustment of the petrol supply to the engine, and that during a series of trials the prevalence of up-currents will obey the law of averages, so that the mean will not contain any errors which may have occurred in single trials.

The question of the calibration of instruments is not dealt with here, but in the section dealing with methods of measurements of the quantities involved in the study of aerodynamics.

Prediction of Aeroplane Performance

When the subject of prediction is considered in full detail, taking account of all the known data, it is found to need considerable knowledge and experience before the best results are obtained. A first approximation to the final result can, however, be made with very little difficulty, and this chapter begins with the material and basis of rapid prediction, and proceeds to the more accurate methods in later paragraphs.

Rapid Prediction.—An examination of numbers of modern aeroplanes will indicate to an observer that the differences in form and construction are not such as to mask the great general resemblances. Aeroplane bodies and undercarriages present perhaps the greatest individual characteristics, but a first generalisation is that all aeroplanes have sensibly the same external form. Aeroplanes to similar drawings but of different scale would be described as of the same form, and the similarity is extended to the airscrew. Even the change from a two-bladed airscrew to one with four blades is a secondary characteristic in rapid prediction.

The maximum horizontal speed of which an aeroplane is capable, its maximum rate of climb and its " ceiling," are all shown later to depend only on the ratio of horsepower to total weight, and the wing loading, so long as the external form of the aeroplane is constant. The generalisation as to external form suggests a method of preparing charts of performance, and such charts are given in Figs. 202–204.

Maximum Speed (Fig. 202).—The ordinate of Fig. 202 is the maximum speed of an aeroplane in m.p.h., whilst the abscissa is the standard horse-power per 1000 lbs. gross load of aeroplane. The standard horsepower is that on the bench at the maximum revolutions for continuous running.

To allow for loading, unless 7 lbs. $\square'$
Divide Standard B.H.P. available by $(\frac{w}{7})^{\frac{1}{2}}$
and read off the velocity on the diagram.
Multiply the velocity so read by $(\frac{w}{7})^{\frac{1}{2}}$ to
get the correct speed.

$W = Wt$ in lbs.

w is loading in lbs/$\square$

20000'

15000'

10000'

GROUND

6500'

STANDARD H.P./1000 LBS.

TOP SPEED M.P.H.
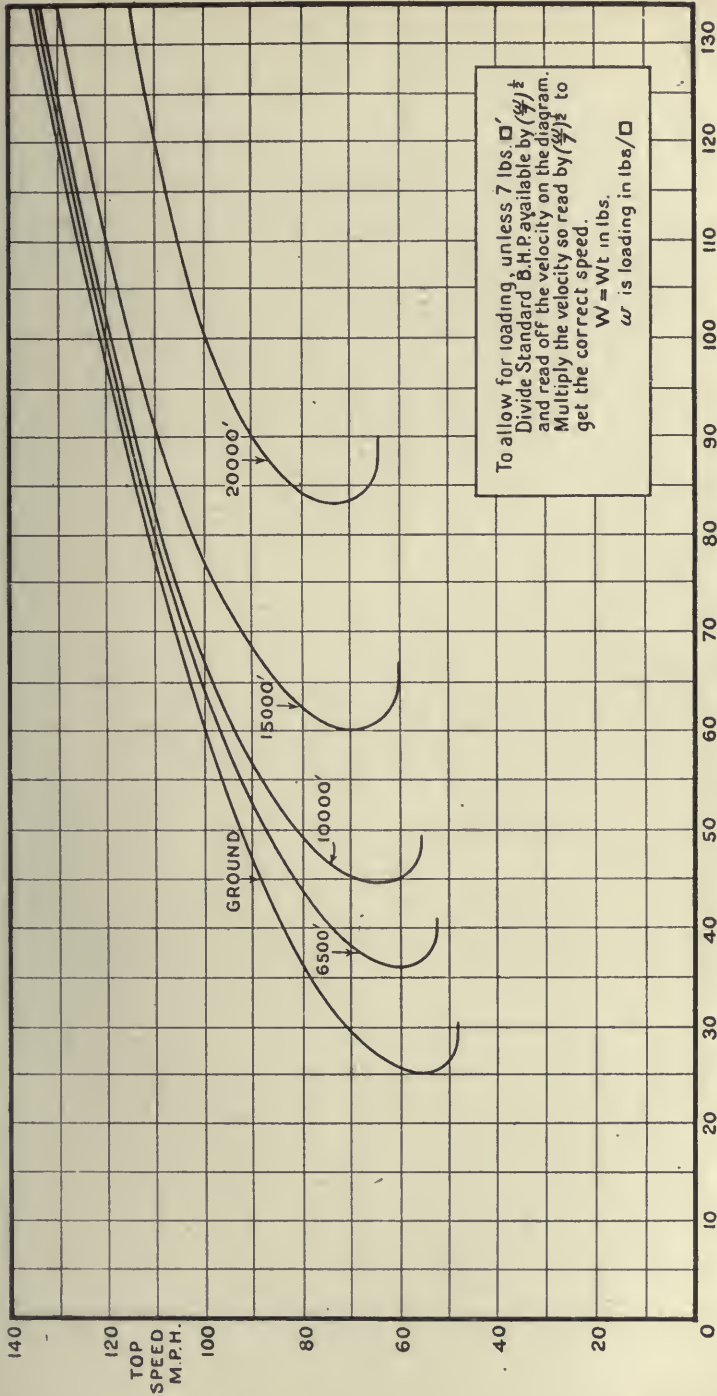
140

120

100

80

60

40

20

0

Fig. 202.—Speed and horsepower chart for rapid prediction.

A family of curves relating speed and power is shown, each curve of the family corresponding with a definitely chosen height. The curves may be used directly if the wing loading is 7 lbs. per sq. foot ; for any other wing loading the formula on the figure should be used.

Example 1.—Aeroplane weighing 2100 lbs., h.p. 220. Find the probable top speed at the ground, 6500 ft., 10,000 ft., 15,000 ft., and 20,000 ft., assuming that the engine may be run " all out " at each of these heights. The wing loading is to be 7 lbs. per sq. foot.

$$\text{h.p. per 1000 lbs.} = 105$$

and from Fig. 202 it is found that—

At ground	Top speed	= 124 m.p.h.
,, 6,500 ft.	,,	= 123 ,,
,, 10,000 ft.	,,	= 121 ,,
,, 15,000 ft.	,,	= 117 ,,
,, 20,000 ft.	,,	= 103 ,,

This example illustrates the general law, that the top speed of aeroplanes with non-supercharged engines, falls off as the altitude increases, slowly for low altitudes but more and more rapidly as the ceiling is approached.

Example 2.—The same aeroplane will be taken to have increased weight and horse-power, the wing loading being 10 lbs. per sq. foot instead of 7 lbs. per sq. ft., but the horsepower per 1000 lbs. as before.

By the rule on Fig. 202 find $\dfrac{105}{\sqrt{\dfrac{10}{7}}}$, *i.e.* 88.

On Fig. 202 read off the speeds for 88 h.p. per 1000 lbs. weight.

Ground	Speed for 88 h.p. per 1000 lbs. and 7 lbs. per sq. ft. . . .	= 117	Speed for 105 h.p. per 1000 lbs. and 10 lbs. per sq. ft.. . .	= 140 m.p.h.
6,500 ft.	,, ,,	= 115·5	,, ,,	= 138 ,,
10,000 ft.	,, ,,	= 114	,, ,,	= 136 ,,
15,000 ft.	,, ,,	= 109	,, ,,	= 130 ,,
20,000 ft.	,, ,,	= 88	,, ,,	= 105 ,,

To get the real speed for 105 h.p. per 1000 lbs. multiply the figures in the second column by $\sqrt{\dfrac{10}{7}}$. The results are given in the last column of the table, and the point of interest is the increase of top speed near the ground due to an increase in loading. The penalty for this increase in top speed is an increase in landing speed in the proportion of $\sqrt{10}$ to $\sqrt{7}$, *i.e.* of nearly 20 per cent. There are also losses in rate of climb and in ceiling.

Maximum Rate of Climb (Fig. 203).—The ordinate of the figure is the rate of climb in feet per minute, whilst the abscissa is still the standard horsepower per 1000 lbs. gross weight. The same aeroplanes as were used for Examples 1 and 2 will again be considered.

Example 3.—Find the rate of climb of an aeroplane weighing 2100 lbs. with an engine horsepower of 220, the loading of the wings being 7 lbs. per sq. foot.

The standard h.p. per 1000 lbs. is 105, and from Fig. 203 the following rates of climb are read off :—

Ground	Rate of climb	= 1530 ft.-min.
6,500 ft.	,,	= 1120 ,,
10,000 ft.	,,	= 890 ,,
15,000 ft.	,,	= 580 ,,
20,000 ft.	,,	= 270 ,,

The rapid fall of rate of climb with altitude is chiefly due to the loss of engine power with height, and it is here that the supercharged engine would make the greatest change from present practice.   The ceiling, or
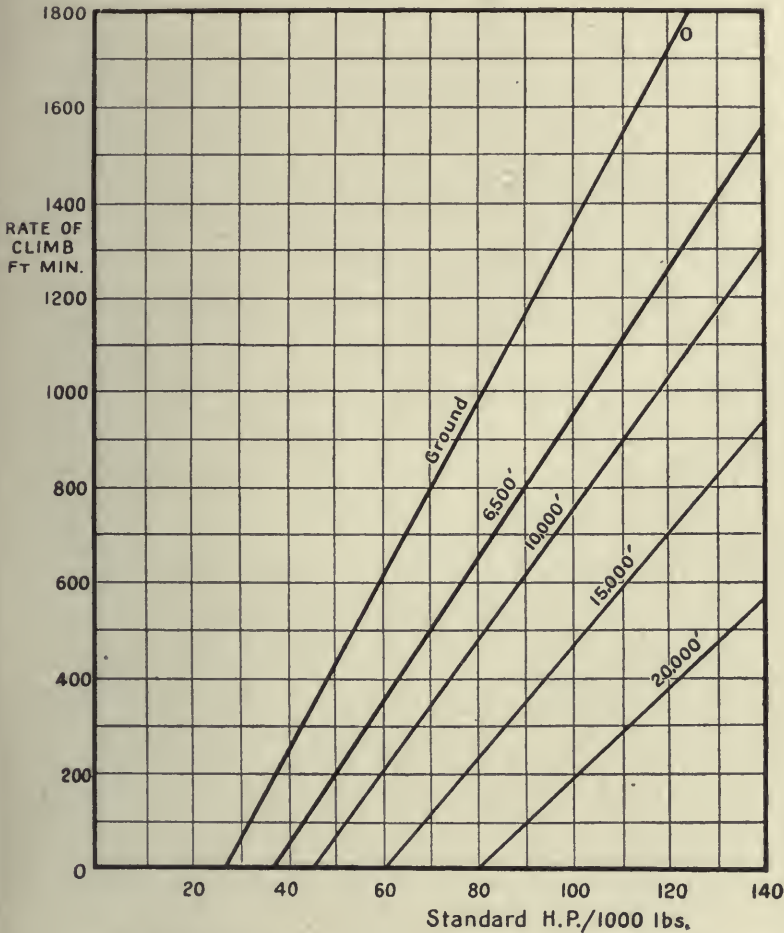

Fig. 203.—Rate of climb and horsepower chart for rapid prediction.

To allow for loading, unless 7 lbs./ft.²

Multiply Std. H.P./1000 lbs. when climb is zero by $\left(\dfrac{w}{7}\right)^{\frac{1}{4}}$, then subtract the excess of this over the value when $w = 7$ from the Std. H.P./1000 lbs.

$$W = \text{wt. in lbs.}   w = \text{loading in lbs./ft.}^2$$

height at which the rate of climb is zero, is seen to be just below 25,000 ft. A further diagram, Fig. 203a, is drawn to show this point more simply. and from it the ceiling is given as 24,000 ft.

Example 4.—Conditions as in Example 2, where the loading is 10 lbs. per sq foot.

The rule on Fig. 203 is applied below.

	(1) Std. h.p. at zero rate of climb.	(2) $(1) \times \sqrt{\frac{10}{7}}$	(3) $(2)-(1)$.	(4) 105 — numbers in (3).	(5) Rate of climb from (4) and Fig. 203.
Ground	26	31	5	100	1350
6,500 ft.	36	43	7	98	940
10,000 ft.	45	54	9	96	700
15,000 ft.	60	72	12	93	380
20,000 ft.	83	99	16	89	60
Ceiling	—	—	$-105 \times \sqrt{\frac{10}{7}} = 88$		$0 \dots$ ceiling 21,000 ft.

The effect of increasing the loading in the ratio 10 to 7 is seen to be a reduction in the rate of climb of nearly 200 ft. per minute, and a reduction of the ceiling of about 3000 ft.

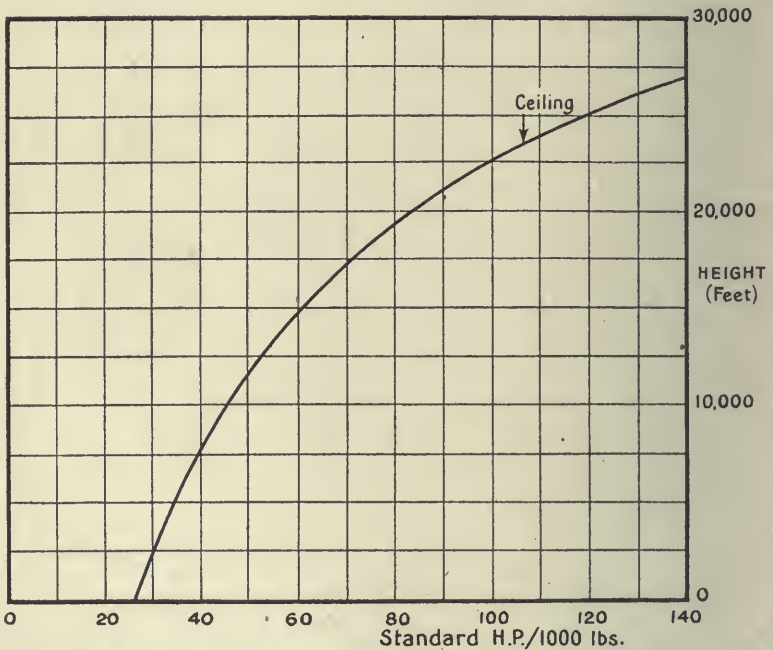The four examples illustrate a general rule in modern high-speed

FIG. 203A.—Ceiling and horsepower chart for rapid prediction.

The curve applies at a loading of 7 lbs./ft.².
An approximate formula which applies to all loadings is

$$\text{At ceiling,} \left(\frac{\sigma}{w}\right)^{\frac{1}{2}} f(h) = 0.010 \frac{W}{\text{Std. B.H.P.}}$$

W = wt. in lbs., σ = relative density, w = loading in lbs./ft.².

aeroplanes, that high speed is more economically produced with heavy wing loading than with light loading, whilst rapid climb and high ceiling are more easily attained with the light loading. The reasons for this appear from a study of the aerodynamics of the aeroplane, which shows

that the angle of incidence at top speed is usually much below that giving best lift/drag for the wings, so that an increase of loading leads to a better angle of incidence at a given speed. For climbing, the angle of incidence is usually that for best lift/drag for the whole aeroplane, and the horse-power expended in forward motion (not in climbing) is proportional to the speed of flight. To support the aeroplane, this speed of flight must be increased in the proportion of the square root of the increased loading to its original value. It is not possible in climbing to choose a better angle of incidence.

Rough Outline Design for the Aeroplane of Example 1.—In estimating the approximate performance the data used has been very limited, and no indication has been given of the uses to which such an aeroplane could be put. How much of the total weight of 2100 lbs. is required for the engine and the structure of the aeroplane? How much fuel will be required for a journey of 500 miles? What spare load will there be?

Structure Weight.—The percentage which the structure weight bears to the gross weight of an aeroplane varies from 27 to 32 as the aeroplane grows in size from a gross load of 1500 lbs. to one of 15,000 lbs. The smaller aeroplanes usually have a factor of safety greater than the large ones, and so for equal factor of safety the difference in the structure weights would be greater than that quoted above. For rough general purposes, the structure weight may be taken as 30 per cent. of the gross weight.

Engine Weight.—The representative figure is "weight per standard horsepower," and for non-supercharged motors the figure varies from about 2·0 lbs. per h.p. for a radial air-cooled engine to 3·0 lbs. per h.p. for a light water-cooled engine. For large power, water-cooled engines are the rule, whilst the smaller-powered engines may be either air-cooled or water cooled. As a general figure 3 lbs. per h.p. should be taken as the more representative value.

Weight of Petrol and Oil.—An air-cooled non-rotary engine or a water-cooled engine consumes approximately 0·55 lb. of petrol and oil per brake horse-power hour when the engine is all out.

The consumption of petrol varies with the height at which flight takes place roughly in proportion to the relative density σ. The general figure for fuel consumption is then

$$0\cdot55\sigma \text{ lb. per standard h.p. hour.}$$

Example 5.—Estimates of weight available for net load can now be made.

Total weight of aeroplane	2100 lbs.
Structure 2100 × 0·30	630 lbs.
Engine 220 × 3	660 lbs.
Fuel for 500 miles, *i.e.* 4 hrs. at a height of 10,000 ft.	
4 × 0·55 × 0·74 × 220	360 lbs.
For pilot passenger and useful load	450 lbs.

1650

Out of this 450 lbs. the pilot and passenger weigh 180 each on the average, leaving about 90 lbs. of useful load in a two-seater aeroplane, or 270 lbs. of useful load in a single-seater aeroplane.

In this way a preliminary examination of the possibilities of a design to suit an engine can be made before entering into great detail.

MORE ACCURATE METHOD OF PREDICTING AEROPLANE PERFORMANCE

In the succeeding paragraphs, a method of predicting aeroplane performance will be described and illustrated by an example. At the present time, knowledge of the fundamental data to which resort is necessary before calculations are begun has not the accuracy which makes full calculation advantageous. Simplifying assumptions will be introduced at a very early stage, but it will be possible for any one wishing to carry out the processes to their logical conclusions to pick up the threads and elaborate the method. Another reason for the use of simplifying assumptions is the possibility thereby opened up of reversing the process and analysing the results of a performance trial. It appears in the conclusion that the number of main factors in aeroplane performance is sufficiently small for effective analysis of aeroplane trials, with appeal only to general knowledge and not to particular tests on a model of the aeroplane.

In estimating the various items of importance in the design of an aeroplane as they affect achieved performance, it is convenient to group them under four heads :—

(a) The estimation of the resistance of the aeroplane as a glider without airscrew.

(b) The estimation of airscrew characteristics.

(c) The variation of engine-power with speed of rotation.

(d) The variation of engine power with height.

It is the connection of these four quantities when acting together which is now referred to as prediction of aeroplane performance. In the example chosen the items (a) to (d) are arbitrarily chosen, and do not constitute an effort at design. It is probable that the best design for a given engine will only be attained as the result of repetitions of the process now developed, the number of repetitions being dependent on the skill of the designer.

Of the four items, (a) and (b) are usually based on model experiments, of which typical results have appeared in other parts of the book. The third item is obtained from bench tests of the engine, whilst the fourth has hitherto been obtained by the analysis of aeroplane trials with support from bench tests in high-level test houses.

It has been shown that the resistance of an aeroplane may be very appreciably dependent on the slip stream from the airscrew, and for a single-seater aeroplane of high power the increased resistance during climb, of the parts in the slip stream may be three times as great as that when gliding. One of the first considerations in developing the formulae of prediction relates to the method of dealing with slip-stream effects.

Experiments on models of airscrews and bodies at the National Physical Laboratory have shown certain consistent effects of mutual interference. The effect of the presence of a body is to increase the experimental mean pitch and efficiency of an airscrew, whilst the effect of the airscrew slip stream is to increase the resistance of the body and tail very appreciably. The first point has been dealt with under Airscrews and the latter when dealing with tests on bodies. It is convenient to extract here a typical

instance of body resistance as affected by slip stream because the formulae developed depend essentially on the observed law of change.

For a single-engined tractor aeroplane the total resistance coefficient has a minimum value at moderately high speeds, say 100 m.p.h. near the ground, and of this total roughly 40 per cent. is due to parts in the slip stream. If R_i be the resistance of the parts in the slip-stream region, but with zero thrust, and R_i' the resistance of the same parts when the airscrew is developing a thrust T, then

$$\frac{R_i'}{R_i} = 0\cdot 85 + 1\cdot 2\,\frac{T}{\rho V^2 D^2} \quad . \quad . \quad . \quad . \quad . \quad (1)$$

is a typical relation between them. Without exception an equation of the form of (1) has been found to apply, variations in the combination of airscrew and body being represented by changes in the numerical factors. Using this knowledge of the generality of (1) leads to simplified formulae in which the airscrew thrust and efficiency have somewhat fictitious values corresponding with an equally fictitious drag for the aeroplane. It will be found that the efficiency of the airscrew and the drag of the aeroplane so used are not greatly different from those of the airscrew and aeroplane when the effects of interference are omitted.

A more detailed statement will make the assumptions clear. If T be the thrust, V the forward speed, W the weight of the aeroplane and V_c its rate of climb,

$$T = R + W\frac{V_c}{V} \quad . \quad . \quad . \quad . \quad . \quad . \quad (2)$$

on the justifiable hypothesis that the thrust is assumed always to act along the drag axis. The hypothesis which is admitted here is not admissible in calculations of stability because the pitching moment is there involved, and not only the drag and lift. Another assumption which will be made is that the inclination of the flight path is so small that the cosine of the angle is sensibly equal to unity.

The resistance R depends appreciably on the slip stream from the airscrew, but that fraction which is in the slip stream is not greatly affected by variations of the angle of incidence of the whole aeroplane. The part of the resistance which arises from the wings and generally the part not in the slip stream, is appreciably dependent on the angle of incidence and is related to the lift coefficient, k_L.

R may therefore be written as

$$R = R_0 + R_i' \quad . \quad . \quad . \quad . \quad . \quad . \quad (3)$$

where R_0 represents the resistance of parts outside the slip stream, and R_i' the resistance of the parts in the slip stream. Equation (1) is now used to express R_i' in terms of the resistance of the parts in the absence of slip stream. If R_i be the glider resistance of the parts,

$$R_i' = R_i\left\{a + b\left(\frac{V}{nD}\right)^{-2}k_T\right\} \quad . \quad . \quad . \quad . \quad (4)$$

where a and b are constants, and k_T is the thrust coefficient defined by

$$k_T = \frac{T}{\rho n^2 D^4} \quad . \quad . \quad . \quad . \quad . \quad . \quad (5)$$

" a " is usually less than unity apparently owing to the shielding of the body by the airscrew boss. Its value is seen to be 0·85 in equation (1), and this is a usual value for a tractor scout. " b " is more variable, and the tests on various combinations of body and airscrew must be examined in any particular case if the best choice is to be made.

Using the various expressions developed, equation (2) becomes

$$T = R_0 + R_i \left\{ a + b \left(\frac{V}{nD} \right)^{-2} k_T \right\} + W \frac{V_c}{V} \quad . \quad . \quad . \quad (6)$$

Equation (6) will now be converted to an expression depending on k_T, k_D, and k_L by dividing through by $\rho S V^2$, where S is the wing area. The value of $\frac{W}{\rho S V^2}$ is not strictly equal to k_L on account of the load on the tail, but the approximation is used in the illustration of method as sufficiently accurate for present purposes. With these changes equation (6) becomes

$$\left\{ \frac{D^2}{S} - b(k_D)_i \right\} \left(\frac{V}{nD} \right)^{-2} k_T = (k_D)_0 + a(k_D)_i + k_L \frac{V_c}{V} \quad . \quad . \quad . \quad (7)$$

The factor $\frac{D^2}{S} - b(k_D)_i$ in equation (7) will now be recognised as a constant for all angles of incidence, and it is convenient to introduce a fictitious thrust coefficient defined by

$$k_T' = \left\{ 1 - \frac{S}{D^2} b(k_D)_i \right\} k_T \quad . \quad . \quad . \quad . \quad . \quad (8)$$

The curve representing this overall thrust coefficient as a function of advance per revolution differs from that of the airscrew in the scale of its ordinates. To estimate the value of the multiplying factor for the new scale the following approximate values may be used :—

$$\frac{S}{D^2} = 5, \quad b = 1·2, \quad (k_D)_i = 0·01 \quad . \quad . \quad . \quad . \quad (9)$$

and the coefficient of k_T in (8) is 0·94. The new ordinate of thrust is then 6 per cent. less than that of the real thrust. As the effect of the body is to increase the airscrew thrust, it will be seen that the fictitious thrust coefficient is within 5 per cent. of that of the airscrew alone over the useful working range.

The term $(k_D)_0 + a(k_D)_i$ may be regarded as a fictitious drag coefficient for the aeroplane as a glider. The correct expression for the glider drag coefficient being $(k_D)_0 + (k_D)_i$, the departure of the coefficient " a " from unity is a measure of the difference between the fictitious and real values of the drag coefficient. From the numerical example quoted it will be found that the difference is 6 per cent. of the minimum drag coefficient

of the whole aeroplane. It has been previously remarked that this difference arises from the shielding of the body by the airscrew boss, and in any particular case the effect could be estimated with fair accuracy if required as a refinement in prediction.

The equation for forces which corresponds with (7) is

$$T' = D' + W\frac{V_c}{V} \quad . \quad . \quad . \quad . \quad . \quad . \quad (10)$$

where T' and D' may be regarded provisionally as the thrust of the airscrew and the drag of the aeroplane estimated separately.

Since D' depends only on the air speed of the aeroplane, it is possible to deduce from (10) a relation of a simple nature between thrust and climb, if flying experiments be made at the same air speed but at different throttle positions. The relation is

$$\delta T' = \frac{W}{V}\delta V_c \quad . \quad . \quad . \quad . \quad . \quad . \quad (11)$$

where δV_c is the increment in rate of climb corresponding with an increase of thrust $\delta T'$. Since $\frac{W}{V}$ and δV_c are measured during performance, equation (11) can be used in the reverse order to deduce $\delta T'$ from a trial.

The treatment of slip stream given above completes the special assumptions; at various places assumptions have been indicated which may become less accurate than the experimental data. The more accurate algebraic work which would then be required presents no serious difficulty.

Details of a Prediction Calculation

Calculations will be made on assumed data corresponding roughly with a high-speed modern aeroplane; although the actual numbers are generally representative of an aeroplane they have been taken from various sources on account of completeness, and not on account of special qualities as an efficient combination in an aeroplane.

Data required.

(1) Drag and lift coefficients of the aeroplane as a glider, corrected for shielding of airscrew boss.

(2) Thrust and torque coefficients of the airscrew as dependent on $\frac{V}{nD}$.

(For general analysis $\frac{V}{nP}$ has been preferred; if P and D be known the variables $\frac{V}{nD}$ and $\frac{V}{nP}$ are easily converted from one to the other.) The correction for slip-stream factor indicated in (8) is supposed to have been made.

(3) Engine horsepower as dependent on revolutions at standard density and temperature.

(4) Engine horsepower as dependent on height. A standard atmosphere is used.

The brake horsepower of the engine under standard conditions will be denoted by " Std. B.H.P.," whilst the factor expressing variation with height will be $f(h)$. At any height in the standard atmosphere the brake horsepower at given revolutions will be

$$(\text{B.H.P.})_h = f(h) \times \text{Std. B.H.P.} \quad . \quad . \quad . \quad . \quad (12)$$
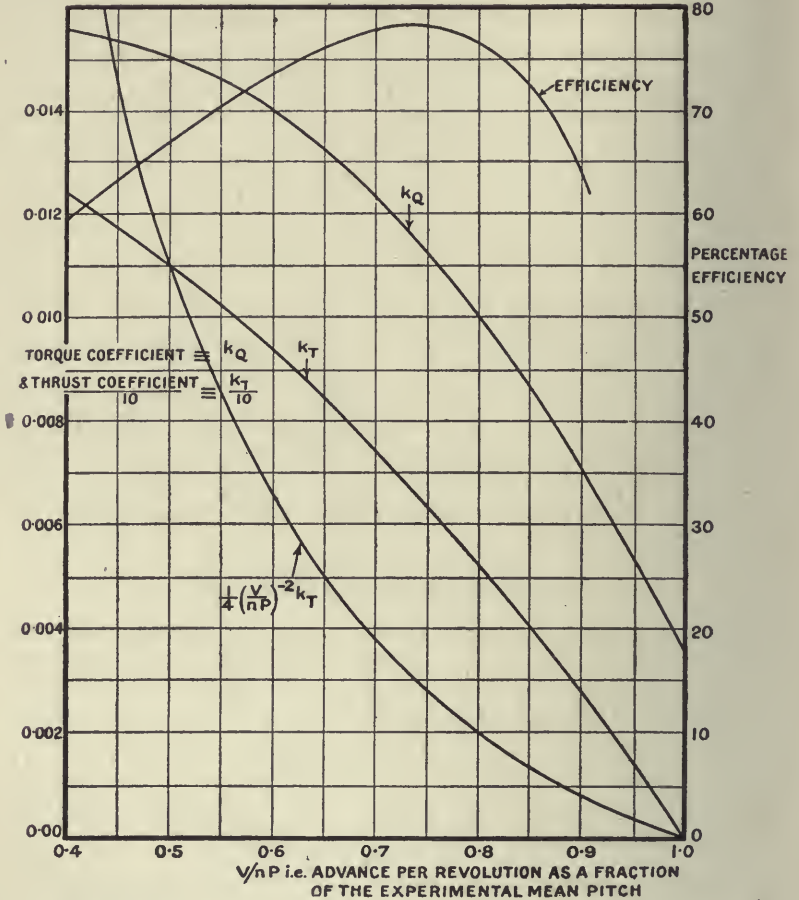

FIG. 204.—Airscrew characteristics used in example of prediction.

From the ordinary definition of torque, Q, and torque coefficient, $k_Q = \dfrac{Q}{\rho n^2 D^5}$, the expression

$$k_Q = \frac{550}{2\pi D^5} \cdot \frac{f(h)}{\rho n^3} \cdot \text{Std. (B.H.P.)} \quad . \quad . \quad . \quad . \quad (13)$$

is deduced.

It should be noticed from (13) that the value of $\dfrac{k_Q}{f(h)}$ is independent of

the aerodynamic properties of the aeroplane, and the revolutions of the engine and airscrew are therefore calculable for various speeds of flight
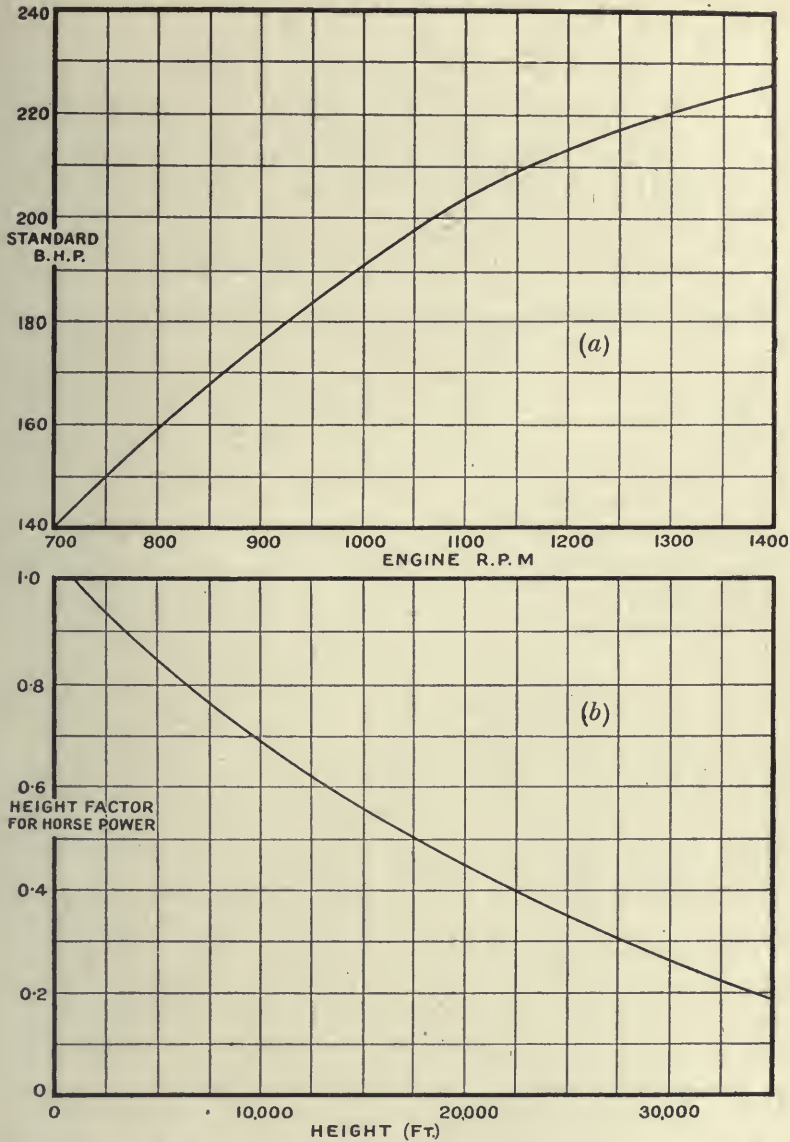

FIG. 205.—(a) Engine characteristics used in example of prediction.
(b) Variation of engine power with height used in example of prediction.

without knowledge of the drag and lift of the aeroplane.   This is the first step in the prediction.

Airscrew Revolutions and Flight Speed.—The data required are given in Figs. 204 and 205, to which must be added the diameter,

$D = 8 \cdot 75$ feet, and the pitch, $P = 10$ feet. For these data equation (13) leads to

$$k_Q = 156{,}000 \, \frac{f(h)}{\sigma} \cdot \frac{\text{Std. B.H.P.}}{(\text{r.p.m.})^3} \quad . \quad . \quad . \quad . \quad (14)*$$

The relative density, σ, is unity in a standard atmosphere at a height of about 800 feet, this value having been chosen to conform with the standards of the Aerodynamics laboratories throughout the world and with the average meteorological conditions throughout the year.

The following table is compiled from Figs. 204 and 205 and equation (14).

TABLE 3.

R.p.m.	Std. B.H.P.	$\dfrac{\text{Std. B.H.P.}}{(\text{r.p.m.})^3}$	k_Q				
			Ground.	5000 ft.	10,000 ft.	15,000 ft.	20,000 ft.
1400	226·0	$8 \cdot 23 \times 10^{-8}$	0·01245	0·01215	0·01175	0·01125	0·01080
1350	223·4	$9 \cdot 10 \times 10^{-8}$	0·01380	0·01345	0·01305	0·01245	0·01195
1300	220·0	$10 \cdot 00 \times 10^{-8}$	0·01510	0·01475	0·0145	0·01360	0·01315
1250	216·5	$11 \cdot 10 \times 10^{-8}$	—	—	—	0·01505	0·01460

From the values of k_Q and the curves of Fig. 204 the values of $\dfrac{V}{nP}$ can be read off and the value of V calculated, leading to Table 4.

TABLE 4.

R.p.m.	Ground.		5000 ft.		10,000 ft.		15,000 ft.		20,000 ft.	
	$\dfrac{V}{nP}$	V ft. per sec.	$\dfrac{V}{nP}$	V ft. per sec.	$\dfrac{V}{nP}$	V ft. per sec.	$\dfrac{V}{nP}$	V ft. per sec.	$\dfrac{V}{nP}$	V ft. per sec.
1400	0·692	161·5	0·705	165	0·728	170	0·750	175	0·768	179
1350	0·611	137·5	0·635	143	0·660	148·5	0·692	156	0·717	161·5
1300	0·420	91·0	0·496	107·5	0·545	118	0·622	135	0·652	141·5
1250	—	—	—	—	—	—	0·430	89·5	0·520	108·5

Table 4 shows the relation between the engine revolutions and the forward speed of airscrew for all altitudes, the engine being "all out." The relationship is shown diagrammatically in Fig. 206. The corresponding relation between $\dfrac{V}{nP}$ and the forward speed of the airscrew is also shown in Fig. 206.

The fall of revolutions with height which is observed in level flights

---

* Throughout the theoretical part of the book the units used have been the foot and second with forces measured in pounds. The unit of mass is then conveniently taken as that in a body weighing g lbs., and has been called the "slug." Common language has other units, speeds of flight being in miles per hour, rate of climb in feet per min., and rotation in revolutions per minute. Where the final results are required in the common language, early adoption often leads to a saving of labour.

is deducible from these observations and the properties of the aeroplane as below:—

The expression for lift coefficient in terms of weight is

$$k_{\text{L}} = \frac{\text{W}}{\text{S}} \cdot \frac{1}{\rho \text{V}^2}, \quad \cdots \quad \cdots \quad \cdots \quad (15)$$

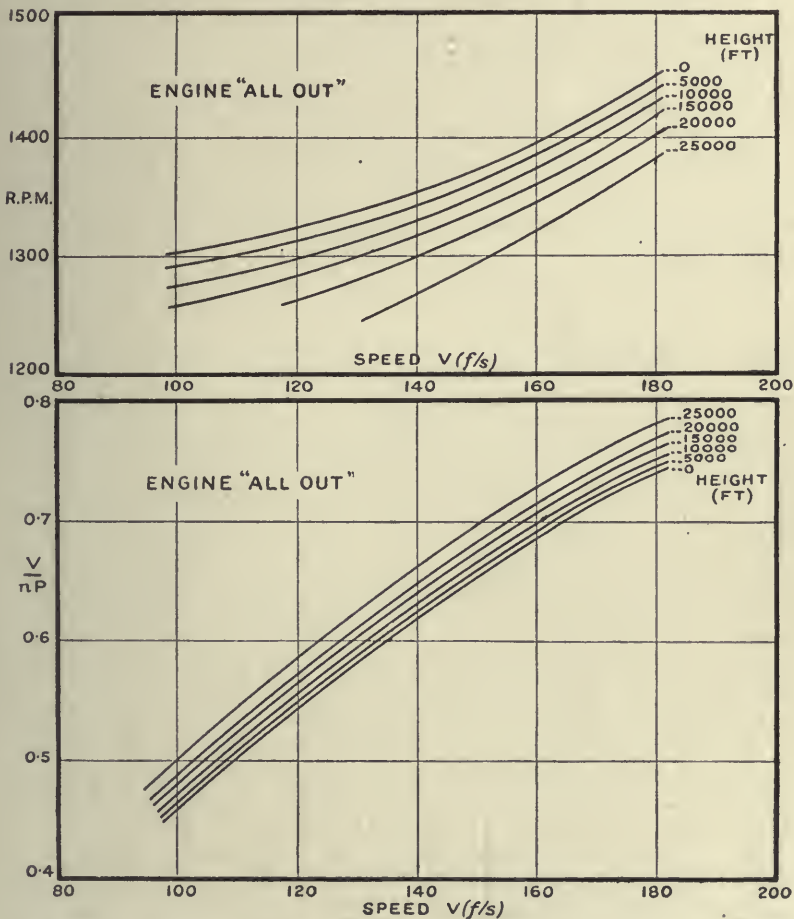and in the example the loading $\frac{\text{W}}{\text{S}}$ will be taken as 7 lbs. per square foot.

FIG. 206.—Calculated relations between forward speed, engine speed, and advance per revolution as a fraction of the pitch.

Converting to common units and particular values for the aeroplane leads to

$$k_{\text{L}} = \frac{1372}{\sigma (\text{V}_{\text{m.p.h.}})^2} \quad \cdots \quad \cdots \quad \cdots \quad (16)$$

The quantity $\sigma^{\frac{1}{2}}\text{V}$ is important and has been called indicated air

speed. Equation (16) shows that k_L depends on the indicated air speed and not on the true speed.

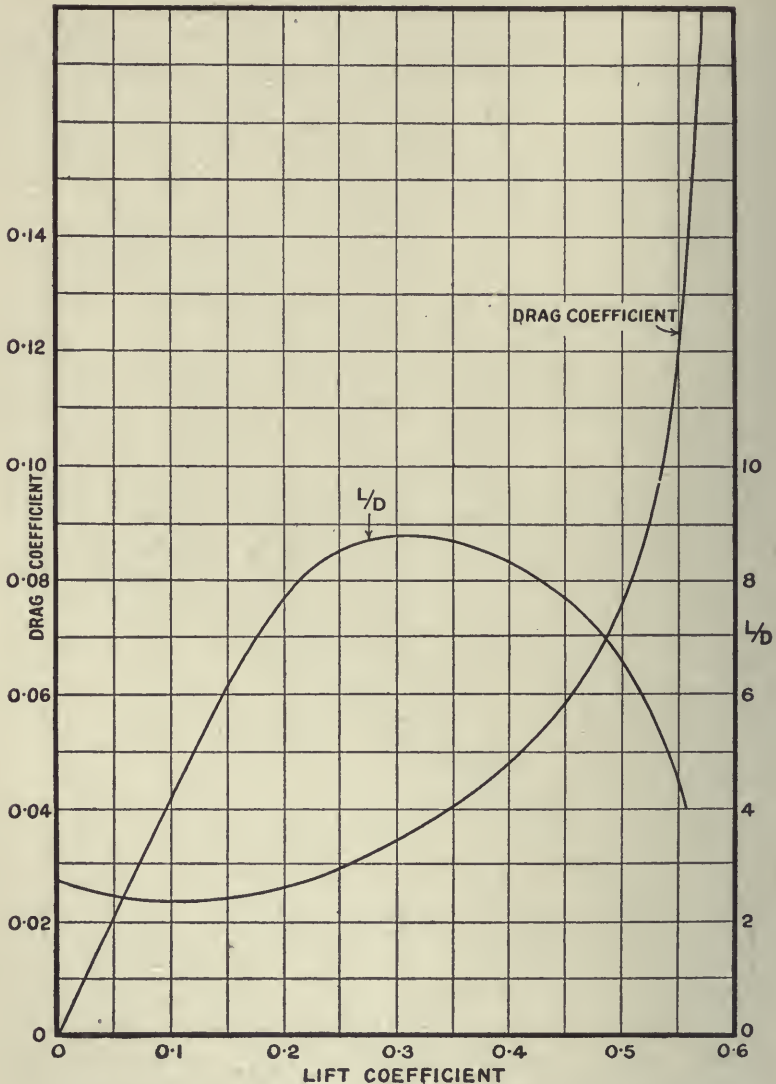Fig. 207 shows the value of drag coefficient for a particular aeroplane

FIG. 207.—Aeroplane glider characteristics used in example of prediction.

glider as dependent on lift coefficient, and hence with (16) leads to a knowledge of drag coefficient for any value of the indicated air speed.

The equivalent of equation (10) as applied to the relation between thrust, drag and lift coefficients is

$$\frac{D^2}{S}\left(\frac{V}{nD}\right)^{-2}k_T = k_D + k_L\frac{V_c}{V} \quad . \quad . \quad . \quad . \quad .(17)$$

and the determination of k_D and k_L for any angle of climb together with equation (17) leads to the estimation of $\frac{V}{nD}$ and k_T, since the latter is known when $\frac{V}{nD}$ is known. For convenience of use in connection with (17) a new curve has been prepared in Fig. 204, which shows the value of $\frac{1}{4}\left(\frac{V}{nP}\right)^{-2}k_T$ as dependent on $\frac{V}{nP}$, and equation (17) may be rewritten as

$$\frac{1}{4}\left(\frac{V}{nP}\right)^{-2}k_T = \frac{1}{4}\cdot\frac{P^2S}{D^4}\left(k_D + k_L\frac{V_c}{V}\right) \quad . \quad . \quad . \quad .(18)$$

It is now necessary to fix the area of the wings, S, or since $\frac{W}{S}$ has been taken as 7, the weight of the aeroplane. The value of S will be taken as 272 sq. feet, giving a gross weight of 1900 lbs. With P=10 and D=8·75, equation (18) becomes

$$\frac{1}{4}\left(\frac{V}{nP}\right)^{-2}k_T = 1\cdot16\left(k_D + k_L\frac{V_c}{V}\right). \quad . \quad . \quad . \quad .(19)$$

Level Flights.—For level flying V_c is zero, and the calculation of performance starts by assuming a value of indicated air speed $\sigma^{\frac{1}{2}}V_{m.p.h.}$, and calculating the corresponding value of k_L from (16). From the lift coefficient, the value of the drag coefficient is obtained by the use of Fig. 207, and equation (19) leads to the calculation of $\frac{1}{4}\left(\frac{V}{nP}\right)^{-2}k_T$. One of the curves of Fig. 204 gives $\frac{V}{nP}$ for any value of $\frac{1}{4}\left(\frac{V}{nP}\right)^{-2}k_T$, and from $\frac{V}{nP}$ and the curve for torque coefficient k_Q is obtained. From $\frac{V}{nP}$ the value of $\sigma^{\frac{1}{2}}$(r.p.m.) is calculated since $\sigma^{\frac{1}{2}}V$ and P are known. Finally from equation (14) and the known values of k_Q and $\sigma^{\frac{1}{2}}$(r.p.m.), the value of $\frac{\text{Std. B.H.P.}}{\text{r.p.m.}}f(h)$ is obtained as dependent on the airscrew.

A second value for this same quantity is obtained from the engine curve, and the indicated air speeds for which the two agree are those for steady horizontal flight. The detailed calculation is carried out in the table below.

For the values of indicated air speed chosen in column 1, Table 5, equation (16) has been used to determine the lift coefficient of column 2. The rest of the table follows as indicated above.

Columns 6 and 8 of Table 5 give a unique curve, PQ of Fig. 208, between $\sigma^{\frac{1}{2}}$r.p.m. and $f(h)\frac{\text{Std. B.H.P.}}{\text{r.p.m.}}$ for level flights. The relation between the two quantities has been derived wholly from the aerodynamics of the aeroplane, and will continue to hold if the engine be throttled down.

TABLE 5.

1	2	3	4	5	6	7	8
Indicated air speed.	Lift coefficient.	Drag coefficient.	$\frac{1}{4}\left(\frac{V}{nP}\right)^{-2}k_T$	$\frac{V}{nP}$	$\sigma^{\frac{1}{2}}.$ r.p.m.	k_Q	$f(h)\dfrac{\text{Std. B.H.P.}}{\text{r.p.m.}}$
$\sigma^{\frac{1}{2}}V$m.p.h.	k_L	k_D	From equation (19) and col. 3.	From col. 4 and curve for airscrew.	From cols. 1 and 5.	From col. 5 and curve for airscrew.	From cols. 6 and 7 and equation (14).
50	0·550	0·120	0·1390	0·457	962	0·0153	0·0903
52	0·507	0·079	0·0915	0·535	856	0·0148	0·0696
53	0·489	0·070	0·0811	0·558	837	0·0142	0·0651
54	0·470	0·0644	0·0747	0·577	826	0·0141	0·0626
56	0·437	0·0553	0·0642	0·606	815	0·0139	0·0598
58	0·408	0·0492	0·0570	0·627	815	0·0136	0·0580
60	0·381	0·0448	0·0520	0·646	818	0·0134	0·0578
65	0·325	0·0370	0·0429	0·682	838	0·0124	0·0560
70	0·280	0·0320	0·0371	0·707	872	0·0122	0·0595
80	0·214	0·0270	0·0313	0·733	960	0·0117	0·0691
90	0·169	0·0250	0·0290	0·747	1060	0·0115	0·0827
100	0·137	0·0244	0·0283	0·757	1163	0·0113	0·0990
110	0·113	0·0240	0·0278	0·759	1280	0·0113	0·1180
120	0·095	0·0240	0·0278	0·759	1395	0·0113	0·1405
130	0·081	0·0240	0·0278	0·759	1510	0·0113	0·1650

To calculate the top speed, use is made of a graphical method of finding when the engine horsepower is that required by the aerodynamics.

TABLE 6.

Height (ft.).	Relative density, σ.	Horse-power factor, $f(h)$.	$\sigma^{\frac{1}{2}}.$ (r.p.m.).			$\dfrac{\text{Std. B.H.P.}}{\text{r.p.m.}}f(h)$ from engine.		
			r.p.m. = 1500	r.p.m. = 1400	r.p.m. = 1300	r.p.m. = 1500	r.p.m. = 1400	r.p.m. = 1300
Ground	1·025	1·038	1520	1418	1314	0·1582	0·1680	0·1760
5,000	0·874	0·842	1402	1309	1216	0·1284	0·1365	0·1435
10,000	0·740	0·686	1290	1204	1118	0·1046	0·1112	0·1165
15,000	0·630	0·558	1190	1111	1032	0·0851	0·0902	0·0948
20,000	0·535	0·446	1097	1024	950	0·0680	0·0722	0·0758
25,000	0·445	0·352	1000	933	866	0·0537	0·0570	0·0599

The curves connecting $\sigma^{\frac{1}{2}}.$r.p.m. and $f(h)\dfrac{\text{Std. B.H.P.}}{\text{r.p.m.}}$ as deduced solely from the engine are plotted in Fig. 208 from the numbers of Table 6. The necessary calculations are simple, the necessary data being contained in Figs. 205 (a) and 205 (b).

The curve PQ of Fig. 208 is that obtained from aerodynamics alone, and applies at all heights. The separate short curves marked with the height are from the engine data. An intersection indicates balance between power available and power required for level flight. At 10,000 ft. the balance occurs when $\sigma^{\frac{1}{2}}.$r.p.m. = 1227. Since $\sigma = 0.74$ this gives the r.p.m. as 1427.

A further unique relation independent of the position of the engine throttle is given by columns 1 and 6 of Table 5. For any value of $\sigma^{\frac{1}{2}}$. r.p.m.
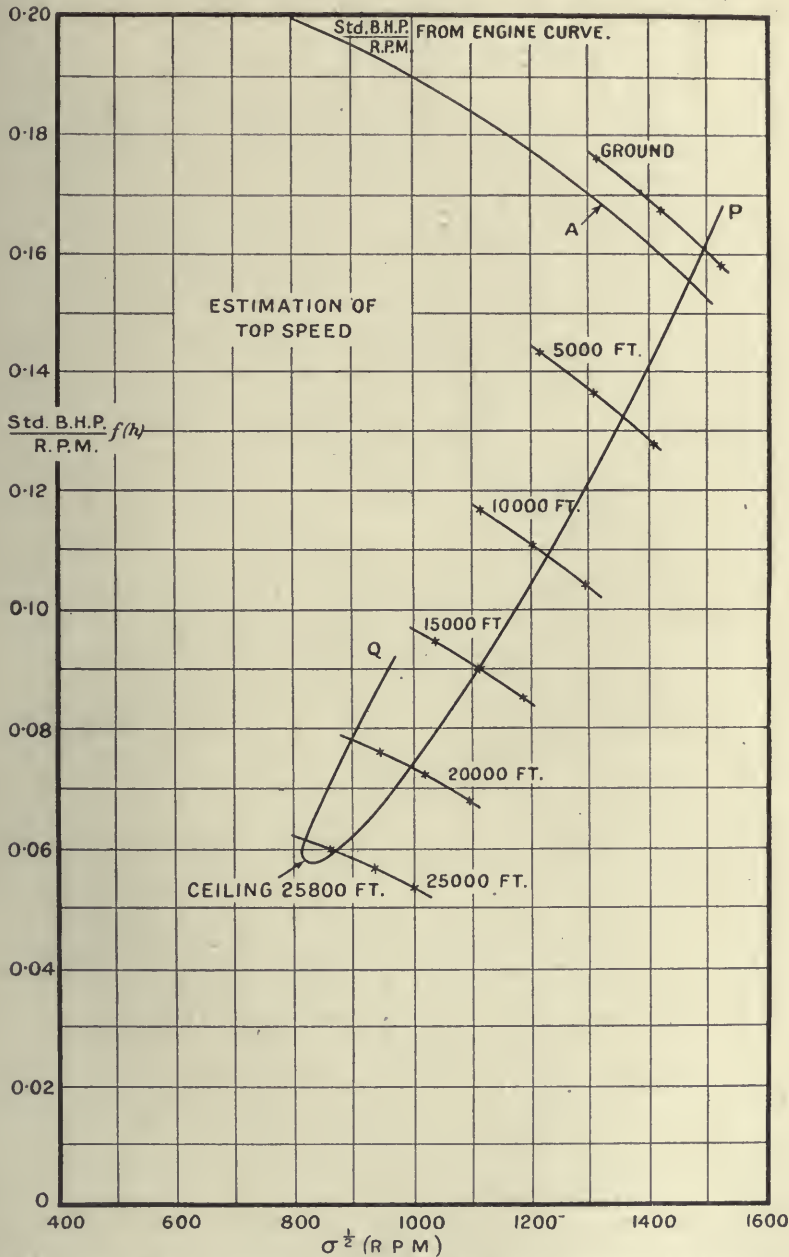

FIG. 208.—Calculated relation between horsepower and revolutions for steady horizontal flight.

the value of $\sigma^{\frac{1}{2}}V_{m.p.h.}$ is known (see Fig. 209). Full particulars of top speed of aeroplane are now obtained from the intersections of Fig. 208 and

the above relation between indicated air speed and revolutions. The results are collected in Table 7.
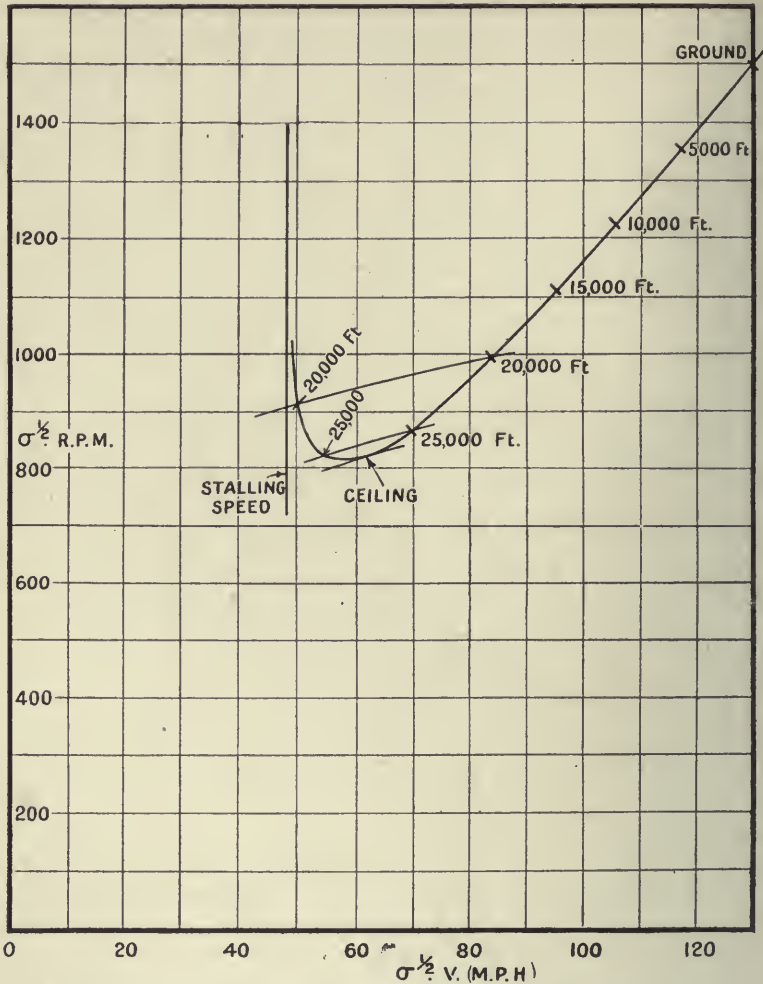

FIG. 209.—Calculated relation between forward speed and revolutions.

TABLE 7.

Height (ft.).	$\sigma^{\frac{1}{2}}$. r.p.m.	$\sigma^{\frac{1}{2}}V_{m.p.h.}$	$V_{m.p.h.}$	r.p.m.
Ground	1492	129	127·5	1472
5,000	1352	117	125	1448
10,000	1227	105·5	122·5	1427
15,000	1108	95	119·5	1398
20,000	996	83·5	114·2	1361
	(901)	(50·5)	(69)	(1232)
25,000	872	69·5	104·2	1307
	(820)	(55)	(82·5)	(1230)

Fig. 209, which shows the relation between indicated air speed and $\sigma^{\frac{1}{2}}$

r.p.m., indicates the most direct comparison between prediction and observations in level flight.

Maximum Rate of Climb.—It has already been shown that for the condition of " engine all out " there is relation between the speed of flight V and the quantity $\dfrac{V}{n\mathrm{P}}$. For certain specified heights this relation is shown in Fig. 206. Using this relation and the values of lift and drag coefficients of Fig. 207 it is possible to calculate the rate of climb V_c from
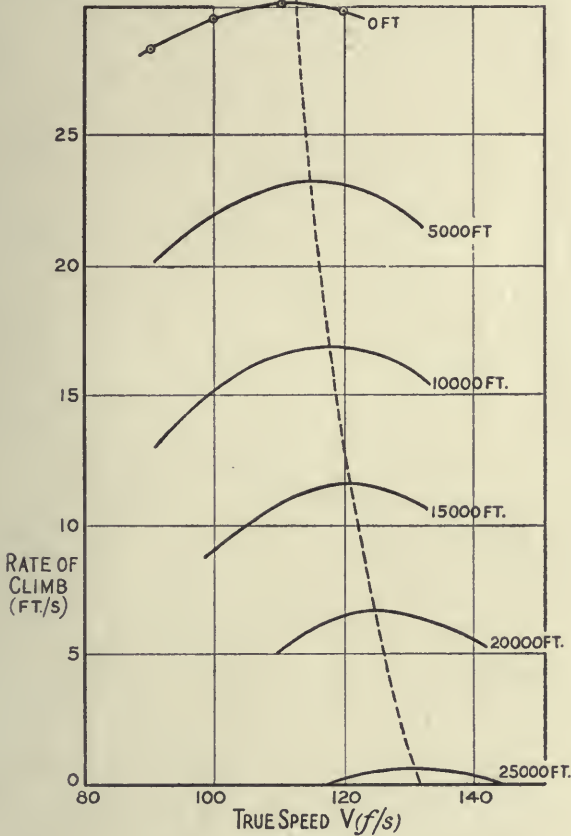

FIG. 210.—Calculated rate of climb.

equation (19) for any assumed value of V. The procedure followed is the calculation of the rate of climb for assumed air speeds and by the plotting of the results finding the condition of maximum climb. A sample table for ground level is given below.

After plotting in Fig. 210, the maximum rate of climb was found to be 30·2 ft.-s. or 1815 ft.-min. The speed was 110 ft.-s. or an indicated air speed of 76 m.p.h. The airscrew revolutions were 1320 p.m.

The calculation was repeated for other heights, and the results obtained are shown in Table 9 and Fig. 210.

2 E

TABLE 8.

1	2	3	4	5	6	7
V ft.-s.	k_L	k_D	$\dfrac{V}{nP}$	$\dfrac{1}{16}\left\{\dfrac{1}{4}\left(\dfrac{V}{nP}\right)^{-2}k_T\right\}$	Column 5 minus column 3.	V_c ft.-s.
90	0·356	0·0412	0·414	0·1531	0·1119	28·3
100	0·288	0·0328	0·459	0·1180	0·0852	29·6
110	0·238	0·0288	0·501	0·0940	0·0652	30·2
120	0·200	0·0264	0·542	0·0760	0·0496	29·8

TABLE 9.

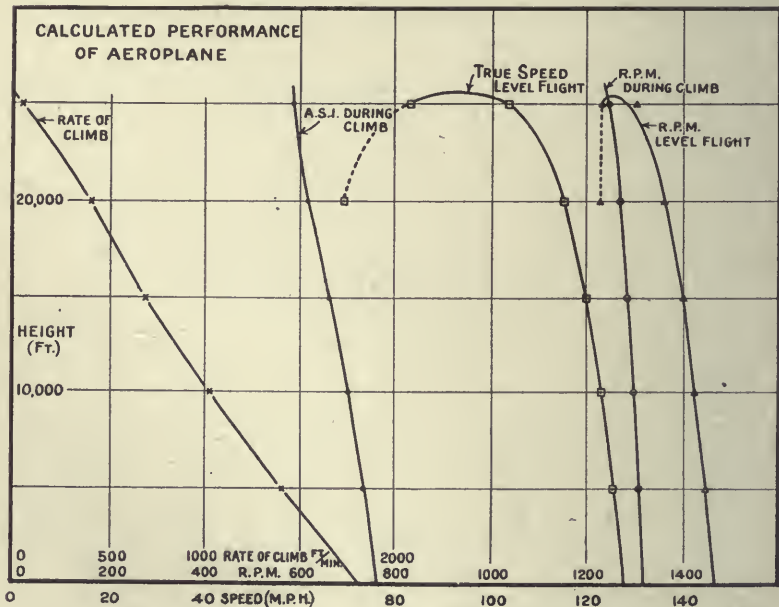| 1	2	3	4
Height (ft.).	Best indicated air speed (m.p.h.).	Maximum rate of climb (ft.-min.).	Airscrew revolutions (r.p.m.).
Ground	76·0	1815	1320
5,000	73·3	1400	1310
10,000	70·0	1020	1300
15,000	66·1	690	1285
20,000	61·2	400	1270
25,000	60·0	40	1245

Fig. 211.—Detailed results of performance calculations.

The well-known characteristics of variation of performance with height are shown in this table.   The maximum rate of climb decreases rapidly with height from 1815 ft.-min. near the ground to zero at a little more than 25,000 feet.   The best air-speed and airscrew revolutions both fall off as the height increases.

The results of the calculations of top speed and rate of climb are collected in Fig. 211, and illustrate typical performance curves.   As the data were not representative of any special aeroplane it is not possible to make a detailed comparison with any particular trials, but within the limits of general comparison the accuracy of the method of calculation is amply great.

Theory of the Reduction of the Observations of Aeroplane Performance from an Actual to a Standard Atmosphere

The problem is to find how to adjust observations under non-standard conditions so that the results will represent those which would have been obtained had the test been carried out in a standard atmosphere.   General theoretical laws govern the aerodynamics of the problem, and a relation between the power required by the airscrew and that available from the engine must be satisfied.

As in most aeronautical problems, the assumption is made that over the range of speeds possible in flight the resistances of the aeroplane for a given angle of incidence and advance per revolution of the airscrew vary as the square of the speed.   With the possible exception of airscrews having high tip speeds the assumption has great practical and theoretical sanction.

To develop the method, consider the forces acting on an aeroplane when flying steadily.   The weight is a force which, both in its direction and magnitude, is independent of the motion through the air.   The resultant air force must be equal and opposite to the weight if the flight is steady, but the magnitude and direction are fixed solely by motion relative to the air.   Fig. 212 helps towards the mathematical expression relating the weight and resultant air force.

A line, assumed parallel to the wing chord for convenience, is fixed arbitrarily in the plane of symmetry of the aeroplane.   The direction of motion makes an angle α with this datum line, and the velocity is V.   The airscrew revolutions are n, and if similarity of external form is kept and the dimension of the aeroplane defined by l, it is known experimentally that R and γ, the resultant force and its angular position, are dependent on α, V, n, l and the density of the air.   As was shown in discussing dynamical similarity, a limit to the form of permissible functions of connection is easily found.

The variable l will be departed from at once and will be replaced by two variables, S for l^2 and D for l.   The quantity $\dfrac{D^2}{S}$ must be kept

constant, but otherwise the use of the two leads to expressions of common form more readily than l.   The functional relations required are

$$R = \rho V^2 S f\left(a, \frac{V}{nD}\right) \quad . \quad . \quad . \quad . \quad . \quad (20)$$

$$\gamma = \quad . \quad F\left(a, \frac{V}{nD}\right) \quad . \quad . \quad . \quad . \quad . \quad (21)$$

the first giving the magnitude of R and the second its direction.
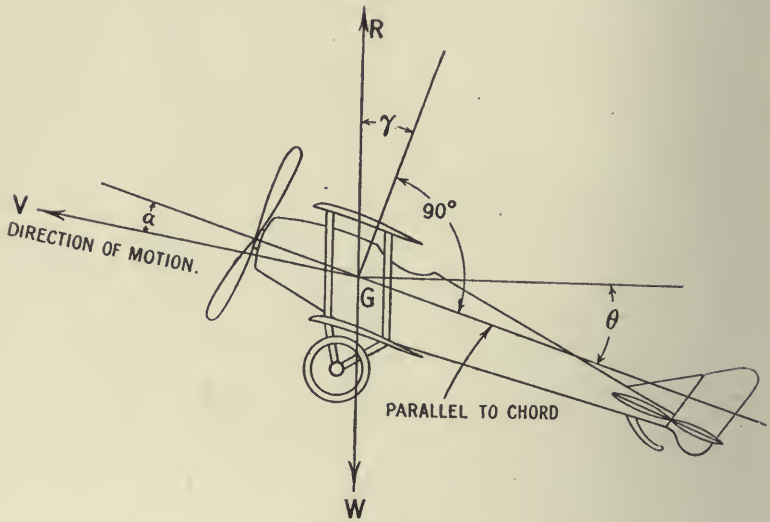
Fig. 212.

The conditions of steady motion are seen from Fig. 212 to be R=W and $\gamma = \theta$, and equations (20) and (21) become

$$\frac{W}{S} \cdot \frac{1}{\rho V^2} = f\left(a, \frac{V}{nD}\right) \quad . \quad . \quad . \quad . \quad . \quad (22)$$

$$\theta = F\left(a, \frac{V}{nD}\right) \quad . \quad . \quad . \quad . \quad . \quad (23)$$

These equations contain the fundamental formulae of reduction and are of great interest.   It will be noticed that the important variables are the loading per unit area, $\frac{W}{S}$, the air speed, $\sigma^{\frac{1}{2}} V$, the angle of climb $(\theta - a)$, the angle of incidence of the wings, a, and the advance per revolution as a fraction of diameter, $\frac{V}{nD}$.

Level Flight.—As the angle of climb is zero, θ is equal to a, and equation (23) shows that $\frac{V}{nD}$ is a function of a only.   Equation (22) then

shows that the angle of incidence is determined by the wing loading and air speed. For an aeroplane S is fixed and W varies so little during trials that it may be considered as constant, and the important conclusion is reached that the angle of incidence in level flight depends only on the air speed. No assumption has been made that the engine is giving full power.

For the same aeroplane carrying different loads inside the fuselage, equation (22) shows the relation between loading and air speed which makes flight possible at the same angle of incidence, and, given a test at one value of $\dfrac{W}{S}$, an accurate prediction for another value is possible. It is only necessary to introduce consideration of the engine for maximum speed. The details are given a little later in the chapter.

Climbing Flight.—For a given loading and air speed, equation (22) shows a relation between α and $\dfrac{V}{nD}$ which, used in equation (23), determines θ and hence the angle of climb, $\theta - \alpha$. Unless another condition be introduced, such as a limit to the revolutions of the engine or the knowledge that the throttle is fully open, both air speed and $\dfrac{V}{nD}$ can be varied at the pilot's wish. Before the subject can be pursued, therefore, the power output of the engine must be discussed.

Engine Power.—The engine power depends on many variables, but the only ones of which account is taken in reduction are the revolutions of the engine and the pressure and density of the atmosphere. The particular fuel used is clearly of great importance, as is also the condition of the engine as to regular running and efficient carburation. These points may be covered by bench tests, using the same fuel as in flight and by providing a control for the adjustment of the fuel-air mixture during flight. This latter adjustment can be used to give the maximum airscrew revolutions for a given air speed.

Unless the points mentioned receive adequate attention during test flights it is not possible to make rational reductions of the results.

At full power the expression

$$P = \phi(n, p, \rho) \quad . \quad . \quad . \quad . \quad . \quad . \quad (24)$$

is used to connect the power, revolutions and atmospheric pressure and density. The form of ϕ is determined by bench tests where the three variables are under control.

The torque of the engine, Q_e, is readily obtained as

$$Q_e = \frac{550}{2\pi n}\phi(n, p, \rho) \quad . \quad . \quad . \quad . \quad . \quad (25)$$

and this must balance the airscrew torque, which by the theory of dimensions has the form

$$Q_a = \rho n^2 D^5 \psi\left(\alpha, \frac{V}{nD}\right) \quad . \quad . \quad . \quad . \quad . \quad (26)$$

For known values of p and ρ the equality of the two values of Q gives a relation between n, a, $\dfrac{V}{nD}$ and D. In the early part of this chapter, when dealing with prediction the detailed interpretation of this relation was given, D being constant and ψ independent of a. Theoretically the present equations are more exact than those used before, but they are not yet in their most convenient form. Equating the two values of Q leads to

$$\phi(n, p, \rho) = \rho n^3 D^5 \cdot \frac{2\pi}{550} \cdot \psi\left(a, \frac{V}{nD}\right)$$

$$= \rho\left(\frac{nD}{V}\right)^3 \cdot V^3 S \cdot \frac{D^2}{S} \cdot \frac{2\pi}{550} \cdot \psi\left(a, \frac{V}{nD}\right)$$

$$= \frac{(\rho V^2 S)^{\frac{3}{2}}}{(\rho S)^{\frac{1}{2}}} \cdot \frac{D^2}{S} \frac{2\pi}{550} \cdot \left(\frac{nD}{V}\right)^3 \psi\left(a, \frac{V}{nD}\right) \quad . \quad . \quad (27)$$

The next step is to use equation (22) to substitute for $\rho V^2 S$ in terms of W, and equation (27) becomes

$$P \equiv \phi(n \cdot p \cdot \rho) = \frac{W^{\frac{3}{2}}}{(\rho S)^{\frac{1}{2}}} \cdot \frac{D^2}{S} \cdot \frac{2\pi}{550} \cdot \left(\frac{nD}{V}\right)^3 \cdot \frac{\psi\left(a \cdot \frac{V}{nD}\right)}{\left\{f\left(a, \frac{V}{nD}\right)\right\}^{\frac{3}{2}}} \quad . \quad . \quad (28)$$

If the loading per square foot, i.e. $\dfrac{W}{S}$, be denoted by w, and $\chi\left(a, \dfrac{V}{nD}\right)$ be written for the quantity beginning with $\dfrac{D^2}{S}$, equation (28) reduces to the important relation

$$\frac{P}{W} \cdot \sqrt{\frac{\rho}{w}} = \chi\left(a, \frac{V}{nD}\right) \quad . \quad . \quad . \quad . \quad . \quad . \quad (29)$$

The result of the analysis has been to introduce a variable which contains as a factor the horsepower per unit weight, a quantity well known to be of primary importance in the estimation of the performance of an aeroplane.

A combination of equations (22) and (29) shows that the angle of incidence and advance per revolution of the airscrew are fixed for all aeroplanes of the same external form if the quantities $\dfrac{P}{W}\sqrt{\dfrac{\rho}{w}}$ and $\dfrac{w}{\rho V^2}$ are known. In level flight it has been seen that the angle of incidence is a function of the advance per revolution and it now follows that $\dfrac{w}{\rho V^2}$ is a function of $\dfrac{P}{W}\sqrt{\dfrac{\rho}{w}}$. The angle α is rarely used in reduction, but $\dfrac{V}{nD}$ is of importance. The power P as used, has been the actual power and is equal to $f \cdot P_s$, where P_s is the standard horsepower and f the power factor which allows for changes of pressure and temperature from the standard condition.

A figure illustrating the relation between the quantities of importance in level flight is shown (Fig. 213). The units are feet and secs. where not otherwise specified. For international comparisons ρ would be better than σ, as the dimensions of the quantities are then zero and consequently the same for any consistent set of dynamical units.

For climbing flight, the form adopted needs development; since $\frac{P}{W}\sqrt{\frac{\rho}{w}}$ and $\frac{w}{\rho V^2}$ determine both a and $\frac{V}{nD}$, it follows from equation (23) that they also fix $\theta - a$, the angle of climb. The value of $\frac{V_o}{V}$ is equal
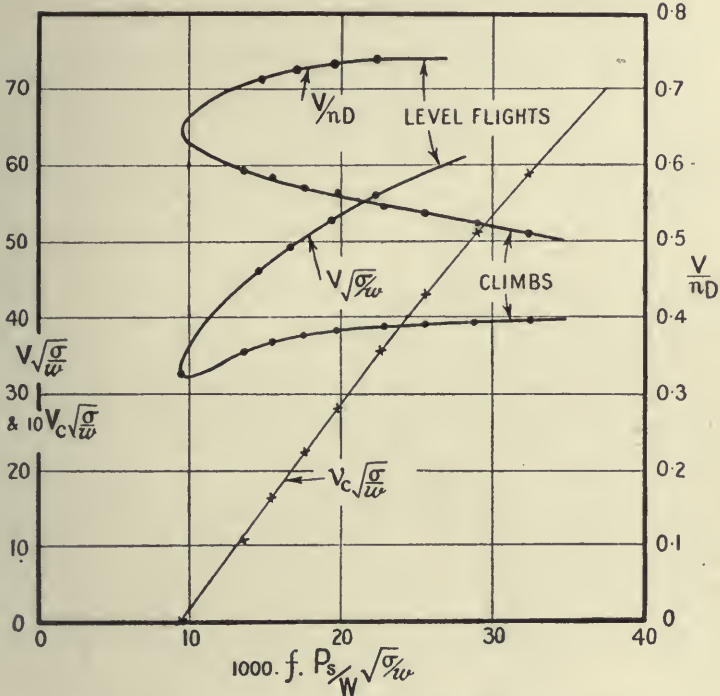

Fig. 213.—Fundamental curves of aeroplane performance.

to $\sin \theta$, and hence an equation for the rate of climb may be written as

$$V_c = V F_1\left(a, \frac{V}{nD}\right) \quad . \quad . \quad . \quad . \quad . \quad (30)$$

or, multiplying by $\sqrt{\frac{\rho}{w}}$ on both sides,

$$V_c\sqrt{\frac{\rho}{w}} = V\sqrt{\frac{\rho}{w}}F_1\left(a, \frac{V}{nD}\right) . \quad . \quad . \quad . \quad (31)$$

Equation (22) shows that $V\sqrt{\frac{\rho}{w}}$ is a function of a and $\frac{V}{nD}$, and hence it

follows from (31) that $V_c\sqrt{\dfrac{\rho}{w}}$ is also a function of α and $\dfrac{V}{nD}$, or as was seen above, of $\dfrac{P}{W}\sqrt{\dfrac{\rho}{w}}$ and $\dfrac{w}{\rho V^2}$.

The results obtained from a climbing test on an aeroplane are shown in Fig. 213, which now connects the variables $\dfrac{P}{W}\sqrt{\dfrac{\sigma}{w}}$, $V\sqrt{\dfrac{\sigma}{w}}$, $V_c\sqrt{\dfrac{\sigma}{w}}$ and $\dfrac{V}{nD}$ for both level and climbing flights. The condition that the rate of climb is to be a maximum converts $V\sqrt{\dfrac{\sigma}{w}}$ from an independent to a dependent variable. For a complete record of aeroplane performance $V\sqrt{\dfrac{\sigma}{w}}$ and $\dfrac{P}{W}\sqrt{\dfrac{\sigma}{w}}$ would need to be considered as independent variables, making an infinite series of curves of which the figure illustrates the two most important cases.

The general theorem has important applications in which all the variables are used. For the reduction of performance simplifications can be made, since in the process W, w and D are constant.

Application of the Formulae of Reduction to a Particular Case

Observations on a high-speed scout taken in flight are shown in Table 10.

TABLE 10.—(1) *Climb.*

Aneroid height, feet.	Time, min. sec.	Temperature, ° C.	Indicated air speed (m.p.h.).	R.p.m.
0	—	27	75	1490
4,000	0	18	75	1495
6,000	1 28	15	75	1500
8,000	3 12	11	75	1500
10,000	5 7	7	75	1505
12,000	7 4	3	70	1480
14,000	9 22	— 1	70	1485
15,000	10 41	— 2	70	1485
16,000	12 3	— 4	70	1485
17,000	13 38	— 6	70	1480
18,000	15 18	— 8	70	1485
19,000	17 4	—10	70	1480
20,000	18 50	—10	70	1480

(2) *Level Speeds.*

Aneroid height, feet.	Temperature, ° C.	Indicated air speed (m.p.h.).	R.p.m.
20,000	—10	87	1565
18,000	— 8	91	1580
16,000	— 4	98	1610
14,000	— 1	101	1620
12,000	3	107	1635
10,000	7	111	—

After preliminary tests to find the best air speed, the aeroplane was climbed to 20,000 feet, readings being taken of time, temperature of the air, indicated speed and engine revolutions at even values of height as shown by the aneroid barometer. The level flights with the engine all out were then taken at even values of the aneroid height by stopping at each height on the way down.

The bench tests of the engine are shown in Figs. 214 and 215, the first showing and the horsepower at standard pressure and temperature and the second the pressure and temperature factor for variations from the standard.

Aneroid Height.—The aneroid barometer is essentially an instrument for measuring pressure, the relation between the two quantities aneroid height and pressure being shown in columns 1 and 2 of Table 2. The aneroid height agrees with the true height only if the temperature be 10° C. Since the difference of pressure between two points arises from the weight of the air between them, *i.e.* depends on the relative density, it will follow that at any other temperature than 10° C. the relation between real height H and aneroid height h will be obtained from the equation

$$\frac{d\mathrm{H}}{dh} = \frac{273 + t}{283} \quad . \quad . \quad . \quad . \quad . \quad . \quad (32)$$

where t is the temperature Centigrade. This gives a relation which, in conjunction with the measurement of t, enables the real height H to be calculated for actual conditions. For present purposes this would not be important unless the day happened to be a standard day.

The pressures as shown in Tables 1 and 2 are based on a unit of 760 mm. of Hg at the ground, a temperature of 15°·6 C., and a relative density of unity. The relation between p, t and σ is then

$$\sigma = \frac{288 \cdot 6}{273 + t} \cdot p \quad . \quad . \quad . \quad . \quad . \quad . \quad (33)$$

From the observations and figures, Table 11 is now prepared.

TABLE 11.

1	2	3	4	5	6	7
Aneroid height (ft.).	Relative pressure. (atmos.).	Temperature, ° C.	Height factor for power, f	Relative density, σ	$\sigma^{\frac{1}{2}}$	$\sigma^{\frac{1}{2}}$ r.p.m.
20,000	0·480	−10	0·489	0·530	0·728	1140
18,000	0·516	− 8	0·525	0·564	0·751	1185
16,000	0·555	− 4	0·565	0·600	0·775	1247
14,000	0·597	− 1	0·605	0·637	0·798	1292
12,000	0·643	3	0·646	0·677	0·822	1344
10,000	0·692	7	0·695	0·719	0·847	—

The second column of Table 11 is obtained from the first by the use of the relation between aneroid height and pressure shown in Table 2.
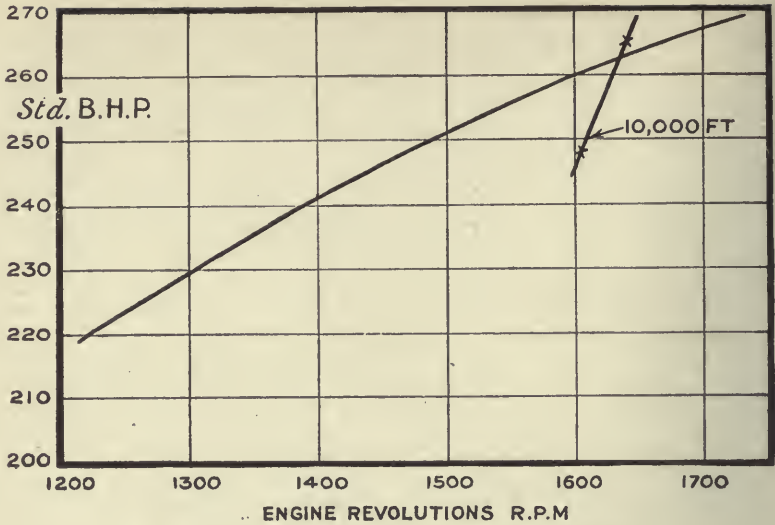
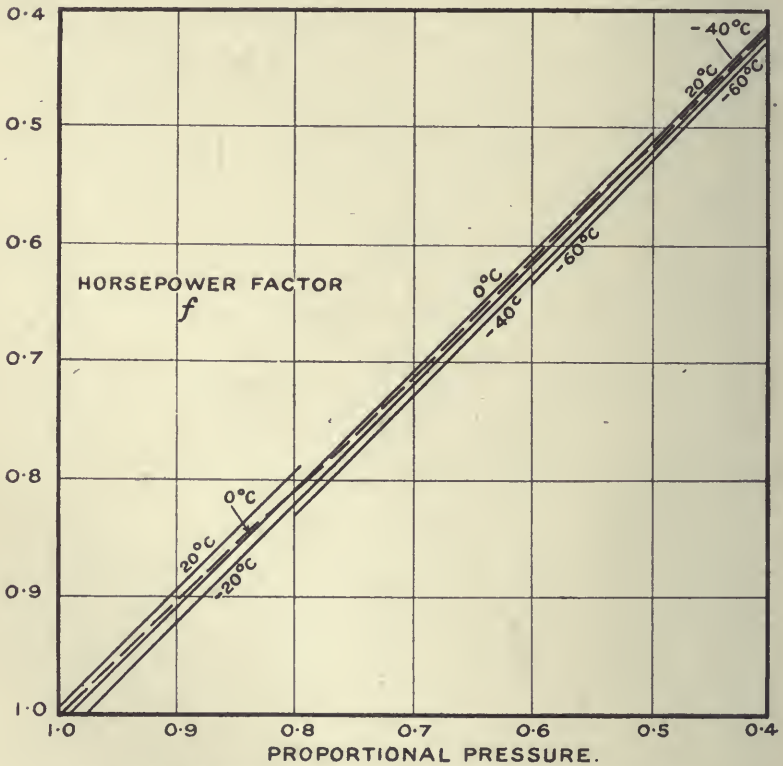FIG. 214.—Standard horsepower and revolutions.

FIG. 215.—Variation of horsepower with pressure and temperature.

Column 3 was observed, and 4 then follows from Fig. 215.   The relative density σ was calculated from columns 2 and 3 by use of equation (33), and the last column follows from column 6 and the observations of revolutions.

Further calculation leads to the required fundamental data of reduction.

<div align="center">TABLE 12.</div>

Aneroid height (ft.).	R.p.m.	Standard horsepower, P_s	$f \cdot P_s \sqrt{\sigma}$	$\dfrac{V_{m.p.h.}}{r.p.m.}$
20,000	1565	257	91·5	0·0766
18,000	1580	258	101·7	0·0768
16,000	1610	260·5	114·2	0·0786
14,000	1620	261	126·0	0·0782
12,000	1635	262·5	139·2	0·0798
10,000	—	264 ?	151 ?	—

The first two columns of Table 12 are observations ; the third is obtained from the second and Fig. 214, and the fourth and fifth are calcu-
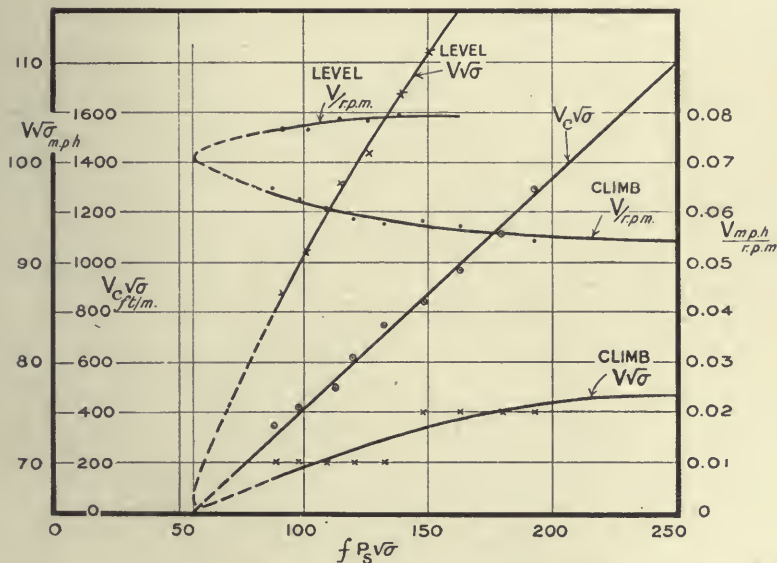

FIG. 216.—Standard curves of performance reduction.

lated using the figures in Tables 10 and 11.   The results are plotted in Fig. 216, and are now standard reductions of maximum speed.

To find the performance in a standard atmosphere the process is reversed as follows.   From the definition of a standard atmosphere and the law of variation of horsepower with pressure and temperature as given in Table 1 the calculation proceeds as for Table 11, except for the last column.

TABLE 13.

1	2	3	4	5	6
Standard height (ft.).	Relative pressure (atmos.).	Temperature, ° C.	Height factor for power, f	Relative density, σ	$\sigma^{\frac{1}{2}}$
20,000	0·456	−26	0·470	0·535	0·732
18,000	0·496	−22	0·512	0·571	0·756
16,000	0·538	−18	0·549	0·610	0·781
14,000	0·583	−14	0·595	0·652	0·808
12,000	0·632	−10	0·642	0·695	0·834
10,000	0·684	− 6	0·693	0·740	0·861

From the standard curves of Fig. 216 are then obtained the following numbers :—

TABLE 14.

$\sigma^{\frac{1}{2}}V$	$\dfrac{V}{\text{r.p.m.}}$	$f . P_s \sqrt{\sigma}$
85	0·0756	88·6
90	0·0767	98·4
95	0·0777	108·6
100	0·0785	120·5
105	0·0790	133·6
110	0·0795	148·5
113	0·0795	158·4

The final figures for performance in a standard atmosphere are obtained by finding that solution of Tables 13 and 14 which is consistent with full power of the engine. The calculation is simple, and at 10,000 ft. is found by assuming values of 110 and 113 for $\sigma^{\frac{1}{2}}V$ and calculating the values of r.p.m. and P_s.

$$\left.\begin{array}{l} \sigma^{\frac{1}{2}}V = 110, \quad \text{r.p.m.} = 1605, \quad P_s = 248 \\ \sigma^{\frac{1}{2}}V = 113, \quad \text{r.p.m.} = 1640, \quad P_s = 265 \end{array}\right\} \quad . \quad . \quad . \quad (34)$$

These figures are readily obtained by calculation from numbers already tabulated. The two values of r.p.m. and P_s are then plotted in Fig. 214 and joined by a straight line. The intersection with the real horsepower curve occurs where the revolutions are 1635, and the real speed in m.p.h. is $1635 \times 0.0795 = 130$ m.p.h. By a repetition of the process the final performance during level flight in a standard atmosphere is found, see Table 15.

TABLE 15.

Standard height (ft.).	Maximum true speed in level flight (m.p.h.).	Engine speed (r.p.m.).
20,000	113	1500
18,000	120	1560
16,000	125	1600
14,000	127	1615
12,000	129	1625
10,000	130	1635

Maximum Climb.—The observations are the times taken to climb to given aneroid heights, and the times depend on the state of the atmosphere at all points through which the aeroplane has passed. The quantity which depends on the local conditions is the rate of climb, and it is necessary to carry out a differentiation. The accuracy of observation is not so great that special refinement is possible, and a suitable process is to plot height against time on an open scale and read off the time at each thousand feet. The rate of climb at 10,000 feet say, may then be taken as the mean between 9000 and 11,000 feet. In this way the observed results give the second column of Table 16 for the aneroid rate of climb. To convert to real rate of climb these figures must be multiplied by $\dfrac{dH}{dh}$ as given by equation (32) and tabulated in column 4. The relative density, σ, is obtained from equation (33). The last column is calculated from the two preceding columns.

TABLE 16.

Aneroid height (ft.).	Aneroid rate of climb (ft.-m.).	t ° C.	$\dfrac{dH}{dh}$	Real rate of climb (ft.-m.).	σ	$\sigma^{\frac{1}{2}}V_C$ (ft.-m.).
4,000	1370	18	1·015	1390	0·860	1290
6,000	1230	15	1·010	1240	0·808	1115
8,000	1120	11	1·000	1120	0·760	975
10,000	1020	7	0·990	1010	0·719	855
12,000	935	3	0·975	910	0·677	750
14,000	815	— 1	0·960	780	0·637	620
16,000	660	— 4	0·950	625	0·600	485
18,000	590	— 8	0·935	550	0·564	415
20,000	530	—10	0·930	490	0·530	355

The rest of the calculation for climb follows exactly as for level flying, and the table of results is given without further comment.

TABLE 17.

Aneroid height (ft.).	Height factor for power, f.	Indicated air speed, $\sigma^{\frac{1}{2}}V_{m.p.h.}$	R.p.m.	Standard horsepower, P_s	$f \cdot P_s \sqrt{\sigma}$	$\dfrac{V_{m.p.h.}}{r.p.m.}$
4,000	0·859	75	1495	250·5	193	0·0542
6,000	0·800	75	1500	251	180	0·0556
8,000	0·745	75	1500	251	163	0·0573
10,000	0·695	75	1505	251	148	0·0588
12,000	0·646	70	1480	249	132·5	0·0575
14,000	0·605	70	1485	249·5	120	0·0590
16,000	0·565	70	1485	249·5	109	0·0608
18,000	0·525	70	1485	249·5	98	0·0627
20,000	0·489	70	1480	249	88·5	0·0650

The results are plotted in Fig. 216 together with those for level flights.

The procedure followed in calculating the rate of climb in a standard atmosphere is exactly analogous to that for level flights until the engine revolutions and horsepower have been found. After this the values of $f \cdot P_s \sqrt{\sigma}$ are calculated, and $V\sqrt{\sigma}$ and $V_0\sqrt{\sigma}$ read from the standard

curves of Fig. 216. V and V_0 are then readily calculated. The results are shown in Table 18.

TABLE 18.

Standard height (ft.).	Rate of climb (ft.-min.).	Time to climb (mins.).	Indicated air speed (m.p.h.).	Engine revolutions (r.p.m.).
0	1740	0	76·5	1385
2,000	1570	1·21	76·5	1415
4,000	1430	2·54	76	1435
6,000	1295	4·02	75·5	1460
8,000	1160	5·75	74·5	1475
10,000	1020	7·49	73·5	1490
12,000	865	9·63	72·5	1495
14,000	735	12·15	71·5	1490
16,000	615	15·12	70	1480
18,000	505	18·70	69	1460
20,000	370	23·30	68	1430

The third column of the above table is obtained by taking the reciprocals of the numbers in the second column and plotting against the standard height, $i.e.$ plotting $\dfrac{dt}{dH}$ against H. The integral, obtained by any of the standard methods, gives the value of t up to any height H.

Remarks on the Reduction.—The observations used for the illustrative example were taken directly from a pilot's report. In some respects, particularly for the indicated air-speed readings, the analysis shows that improvement of observation would lead to rather better results. On the other hand, it is known, both practically and theoretically, that the best rate of climb is not greatly affected by moderate changes of air speed and the primary factor is not thereby appreciably in error.

The procedure followed is very general in character, and may be applied to any horsepower factor which depends on pressure and density, no matter what the law. It is shown later in the chapter that flying experiments may be so conducted that a check on the law of variation with height is obtained from the trials themselves, the essential observations including a number of flights near the ground with the engine "all out," the conditions ranging from maximum speed level to maximum rate of climb, As the flight experiments can only give the power factor for the particular relation between p and t which happens to exist, it is still necessary to appeal to bench tests for the corrections from standard conditions, but not for the main variation.

The standard method of reduction of British performance trials has up to the present date been based on the assumption that the engine horsepower depends only on the density. Questions are now being raised as to the strict validity of this assumption, and the law of dependence of power on pressure and temperature is being examined by means of specially conducted experiments. The extreme differences from the more elaborate assumption do not appear to be very great, and affect comparative results only when the actual atmosphere differs greatly from the standard atmo-

sphere. It appears that a stage has been reached at which the differences come within the limits of measurement, and the rather more complex law will then be needed.

If the horsepower depends on the atmospheric density only, the reduction of observations is simplified, for the height in the standard atmosphere is then fixed by the density alone and all observations of speed and revolutions apply at this standard height irrespective of the real height at the time of observation. For level speeds only the 1st, 2nd, 3rd and 5th columns of Table 11 are required. From the values of σ and Table 1 the values of the standard height are obtained, and using these as abscissae the indicated air speeds and the revolutions of the engine are plotted. This is now the reduced curve, and at even heights the standard values of air speed and revolutions are read from the curve.

For climbs the first six columns of Table 16 are required, and the real rate of climb is then plotted against the standard height as determined by σ. The remaining processes follow as for level flights.

By whatever means the calculations are carried out, the results of the reduction of performance to a standard serves the purpose of comparison between various aeroplanes and engines in a form which is especially suitable when their duties are being assigned.

For some purposes, such as the calculation of the performance of a weight-carrying aeroplane or a long-distance machine in which the weight of petrol consumed is important, the standard reduction is appreciably less useful than the intermediate stage represented by Tables 12 and 17, or preferably by curves obtained from them and the loading to give the form of Fig. 213. The loading, w, was 8·5 lbs. per square foot.

Examples of the Use of Standard Curves of the Type shown in Fig. 213

Aerodynamic Merit.—The first point to be noticed is that the curves are essentially determined by the aerodynamics of the aeroplane and airscrew, and do not depend on the engine used. This will have been appreciated from the fact that a special calculation was necessary to ensure that the engine was giving full power in any particular condition of flight.

The variables $V\sqrt{\dfrac{\rho}{w}}$, $V\sqrt{\dfrac{\rho}{w}}$ against $\dfrac{P}{W}\cdot\sqrt{\dfrac{\rho}{w}}$, $i.e.\left(f\cdot\dfrac{P_s}{W}\sqrt{\dfrac{\rho}{w}}\right)$ are non-dimensional coefficients which for the aeroplane and airscrew play the same part as the familiar lift and drag coefficients for wing forms. Using either σ or ρ, two sets of curves for different aeroplanes may be superposed and their characteristics compared directly. If for a given value of $\dfrac{P}{W}\sqrt{\dfrac{\sigma}{w}}$ one aeroplane gives greater values of $V\sqrt{\dfrac{\sigma}{w}}$ and $V_o\sqrt{\dfrac{\sigma}{w}}$ than another, the aerodynamic design of the former is the better. In this connection it should be remarked that the measure of power is the torque dynamometer on the engine test bed, and that the engine is used as an intermediary standard. It is unfortunately not a thoroughly good inter-

mediary, and the accuracy of the curves is usually limited to that of a knowledge of the engine horsepower in flight. All aeroplanes give curves of the same general character, the differences being similar in proportionate amount to those between the lift and drag curves of good wing sections.

Change of Engine without Change of Airscrew.—Since the aerodynamics of the aeroplane is not changed by the change of engine, it follows that the standard curves are immediately applicable. The only effect of the change is to introduce a new engine curve to replace the old one in order to satisfy the condition that the engine is fully opened up during level flights or maximum climb.

Change of Weight carried.—Again the aerodynamics is not changed, and the curves are applicable as they stand. As an example, consider the effect of changing the weight of an aeroplane from 2000 lbs. and a loading
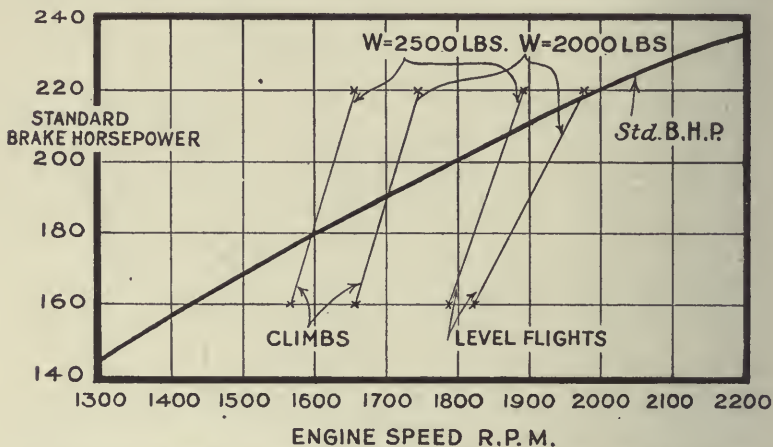
Fig. 217.—Balance of horsepower required and horsepower available when the gross load is changed.

of 8 lbs. per sq. foot to a weight of 2500 lbs. and a loading of 10 lbs. per sq. foot, the height being 10,000 ft.

The value of σ at a height of 10,000 ft. in a standard atmosphere is 0·740, and the horsepower factor will be taken as $f = 0·68$. The engine curve of standard horsepower is shown in Fig. 217.

To begin the calculation, two values of standard horsepower, P_s, are assumed, and the curve of Fig. 217 shows that 160 and 220 are reasonable values. Greater accuracy would be attained by taking three values.

Taking one loading as example, the procedure is as follows:—

(1) $P_s = 220$, $f \cdot \dfrac{P_s}{W} \cdot \sqrt{\dfrac{\sigma}{w}} = 22·7$ from the data given.

(2) From the standard curves of Fig. 213 read off, for the above value of 22·7 as abscissae, the ordinates to get

$$\frac{V}{nD} = 0\cdot736, \quad \text{and } V\sqrt{\frac{\sigma}{w}} = 56\cdot4 \text{ for level flight ;}$$

$$\text{and } \frac{V}{nD} = 0\cdot548, \quad \text{and } V\sqrt{\frac{\sigma}{w}} = 38\cdot7 \text{ for maximum rate of climb}$$

With $D = 7\cdot87$ feet and the given values of σ and w the values of $n \times 60$ from the above are 1975 and 1820 r.p.m., it being noted that the standard figure uses V in ft.-s. and n in revolutions per second.

(3) For $P_s = 160$, $f \cdot \dfrac{P_s}{W} \cdot \sqrt{\dfrac{\sigma}{w}} = 16\cdot5$, and proceeding as before the revolutions are found to be 1744 r.p.m. for level flight and 1655 for climbing flight.

The two values of P_s and r.p.m. are plotted in Fig. 217 and the points joined by a straight line (or curve if three values were used). The intersection of the line with the standard horsepower curve gives the condition that the engine is developing maximum power for the assumed conditions. The results for both loadings are

loading $\dfrac{8 \text{ lbs.}}{\text{sq. ft.}}$ $\begin{cases} P_s = 217 \text{ and r.p.m.} = 1980 \text{ for level flight.} \\ P_s = 190 \text{ and r.p.m.} = 1700 \text{ for climbing flight.} \end{cases}$

loading $\dfrac{10 \text{ lbs.}}{\text{sq. ft.}}$ $\begin{cases} P_s = 208 \text{ and r.p.m.} = 1870 \text{ for level flight.} \\ P_s = 179 \text{ and r.p.m.} = 1595 \text{ for climbing flight.} \end{cases}$

The balance of engine and airscrew having been found, $f \cdot \dfrac{P_s}{W} \cdot \sqrt{\dfrac{\sigma}{w}}$ can be calculated, and the corresponding values of $V\sqrt{\dfrac{\sigma}{w}}$ and $V_o\sqrt{\dfrac{\sigma}{w}}$ read from the standard curves, Fig. 213. The results, converted to speeds in m.p.h. and rates of climb in feet per min. are

loading $\dfrac{8 \text{ lbs.}}{\text{sq. ft.}}$ weight 2000 lbs. $\Big\}$ Maximum speed 129 m.p.h.
Maximum rate of climb 575 ft.-min. at A.S.I. of 75 m.p.h.

loading $\dfrac{10 \text{ lbs.}}{\text{sq. ft.}}$ weight 2500 lbs. $\Big\}$ Maximum speed 119 m.p.h.
Maximum rate of climb 230 ft.-min. at A.S.I. of 75·5 m.p.h.

The result of the addition of 500 lbs. to the load carried is seen to be a loss of 10 m.p.h. on the maximum speed at 10,000 feet, and a loss of nearly 350 ft.-min. on the rate of climb.

The point should again be noted here, that although the rate of climb calculated for the increased loading is a possible one, it does not follow that it is the best except from the general knowledge that rate of climb when near the maximum is not very sensitive to changes of air-speed indicator reading. The necessary experiments for a more rigid application can always be made when greater accuracy is desired.

2 F

Separation of Aeroplane and Airscrew Efficiencies

In the previous reduction and analysis of aeroplane performance no separation of the efficiencies of the aeroplane and airscrew has been attempted, and the analysis has been based on very strong theoretical ground. The proposal now before us is the reversal of the process followed in the detailed prediction of aeroplane performance, and in order to proceed at all it is necessary to introduce data from general knowledge. In the chapter on Airscrews it was pointed out that all the characteristics of airscrews can be expressed approximately by a series of standard curves applicable to all. The individual characteristics of each airscrew can be represented by four constants, and the analysis shows how these constants may be determined from trials in flight. The determination of these four constants also leads to the desired separation of aeroplane and airscrew efficiencies.

The principles involved have been dealt with in the earlier section on detailed prediction where the fundamental equations were developed. The analysis will therefore begin immediately with an application to an aeroplane.

The aeroplane chosen for illustration was a two seater-aeroplane with water-cooled engine. The choice was made because the flight observations available were more complete than usual. The observations reduced to a standard atmosphere are given in Table 19 below, whilst the standard engine horsepower as determined on the bench will be found in a later table.

TABLE 19.

Level flights.			Maximum climb.			
Relative density.	Speed (m.p.h.).	Engine (r.p.m.).	Relative density.	Speed (m.p.h.).	Engine (r.p.m.).	Rate of climb (ft.-min.).
0·833	134	1935	0·963	77·6	1700	1265
* ,,	115	1700	0·903	78·0	1700	1145
* ,,	98	1500	0·845	79·0	1700	1025
* ,,	80	1300	0·792	80·2	1695	905
			0·740	81·4	1690	780
0·717	132·5	1910	0·695	81·6	1685	660
* ,,	115	1720	0·652	81·7	1675	540
* ,,	100	1565	0·610	82·0	1660	420
* ,,	80	1360				
0·611	126	1860				
* ,,	100	1595				
* ,,	80	1400				
0·740	133	1915				
0·673	130·5	1895				
0·630	128	1870				
0·600	125	1855				

* These level flights were made with throttled engine.

The revolutions of the airscrew were less than those of the engine, the gearing ratio being 0·6 to 1.   Further particulars are :

$$
\left.
\begin{array}{llll}
\text{Gross weight of aeroplane} & : & . & . & 3475 \text{ lbs.} \\
\text{Wing area} & . & . & . & 436 \text{ sq. ft.} \\
\text{Airscrew diameter} & . & . & . & 10·13 \text{ ft.}
\end{array}
\right\} \quad . \quad . \quad (35)
$$

It will be found that it is possible to deduce from the data given—
(1) The pitch of the airscrew.
(2) The variation of engine power with height.
(3) The efficiency of the airscrew.
(4) The resistance of the aeroplane apart from its airscrew.

Determination of the Pitch of the Airscrew.—The pitch of the airscrew is deduced from the torque coefficient of the airscrew as shown by the standard

FIG. 218.—Standard airscrew curves used in the analysis of aeroplane performance.

curves of Fig. 218 and the bench tests on the power of the engine as follows.   From the numbers in Table 19 and equation (13) the value of $\dfrac{k_Q}{f(h)}$ can be calculated from bench tests of the engine.   The speed of the aeroplane, the engine revolutions and gearing and the airscrew diameter being known, the value of $\dfrac{V}{nD}$ as shown in Table 20 is easily calculated.

Using equation (13) and putting in the numerical values of the example

$$
\frac{k_Q}{f(h)} = 341{,}000 \; \frac{\text{Std. B.H.P.}}{\sigma (\text{r.p.m.})^3_{\text{engine}}} \quad . \quad . \quad . \quad . \quad (36)
$$

and the values given in the last column of Table 20 are calculated from this formula.　Table 20 shows that at the same height two values of $\dfrac{k_Q}{f(h)}$ are obtained, one from the maximum level speed and the other from the test for maximum rate of climb.　The particulars in Table 21 were extracted from columns 1, 6 and 7 of Table 20.

TABLE 20.—Experiments with Engine "all out."

Height (ft.).	Relative density.	Speed (m.p.h.).	Engine (r.p.m.).	Standard (B.H.P.).	$\dfrac{V}{nD}$	$\dfrac{k_Q}{f(h)}$
6,500	0·833	134	1935	354	1·005	0·0201
11,000	0·717	132·5	1910	353	1·004	0·0242
16,000	0·611	126	1860	351	0·978	0·0304
10,000	0·740	133	1915	354	1·005	0·0232
13,000	0·673	130·5	1895	353	1·000	0·0263
15,000	0·630	125	1855	351	0·978	0·0297
16,500	0·600	128	1870	351	0·994	0·0306
2,000	0·963	77·6	1700	338	0·661	0·0244
4,000	0·903	78·0	1700	338	0·664	0·0260
6,000	0·845	79·0	1700	338	0·672	0·0278
8,000	0·792	80·2	1695	338	0·687	0·0299
10,000	0·740	81·4	1690	338	0·700	0·0324
12,000	0·695	81·6	1685	337	0·701	0·0345
14,000	0·652	81·7	1675	336	0·706	0·0373
16,000	0·610	82·0	1660	334	0·716	0·0408

TABLE 21.

Height (ft.).	Level flight.		Maximum climb.	
	$\dfrac{V}{nD}$	$\dfrac{k_Q}{f(h)}$	$\dfrac{V}{nD}$	$\dfrac{k_Q}{f(h)}$
6,000	1·005	0·0198	0·672	0·0278
10,000	1·005	0·0232	0·700	0·0324
14,000	0·998	0·0278	0·706	0·0373

For each row of the table $f(h)$ is constant, and a relation between k_Q and $\dfrac{V}{nD}$ is obtained.　This relation is sufficient to determine the pitch of the airscrew if use be made of the standard curves of Fig. 218.　As shown in the chapter on Airscrews the ordinates and abscissae of these curves are undetermined, but the shape is determined when the pitch diameter ratio $\dfrac{P}{D}$, is known.

The value of $\dfrac{P}{D}$ is found as follows.

Assume $\frac{P}{D} = 1\cdot0$. From Table 21, this leads to $\frac{V}{nP} = 1\cdot005$ at 6000 ft. for level flight. The value of $Q_0 k_Q$ from the standard airscrew curves is $0\cdot365$, and by combination with Table 21 $Q_0 f(h)$ is found as $18\cdot5$. For the climbing trial the corresponding number is $30\cdot6$; had the assumed value of $\frac{P}{D}$ been appropriate to the experiment this latter number would have agreed with that deduced from level flights. To attain the condition of agreement the calculation is repeated for other values of $\frac{P}{D}$ with the results shown in Table 22.

TABLE 22.

Height.	Pitch diameter ratio, $\frac{P}{D}$	$Q_0 f(h)$	
		Level flight.	Climbing flight.
6000 ft.	$\begin{cases}1\cdot0 \\ 1\cdot2 \\ 1\cdot4\end{cases}$	18·5 30·6 38·9	30·6 35·8 36·5

Inspection of the figures in the two last columns will show that equality occurs at $\frac{P}{D}$ equal to about $1\cdot3$. The actual value was obtained by plotting the two values of $Q_0 f(h)$ on a base of $\frac{P}{D}$ and reading off the intersection. In this way a number of $1\cdot32$ was found for $\frac{P}{D}$. Repeating the process for observations at 10,000 feet gave $1\cdot30$, and at 14,000 feet, $1\cdot33$.

It will thus be seen that the observations give consistent results, and that the analysis is capable of giving full value to the observations.

The mean value of $\frac{P}{D}$ being $1\cdot32$ and the diameter $10\cdot13$, the pitch is $13\cdot3$ feet.

Variation of Engine Power with Height and the Value of Q_0.— In calculating the pitch of the airscrew it was also shown incidentally how the value of $Q_0 f(h)$ could be determined, and an extension of the calculations is all that is necessary to determine both quantities when once it is noted that $f(h)$ is unity when σ is unity. The values of $Q_0 f(h)$ if plotted against σ will give a curve which can be produced back to unit σ with accuracy, and the value of Q_0 is thereby determined. Since Q_0 is independent of height the value of $f(h)$ is then readily deduced. The calculations for all observations with the engine all out are given in Table 23.

The first, second and fourth columns of Table 23 are taken from the first, second and last columns of Table 20. The value of $\frac{V}{nP}$ is obtained

from $\dfrac{V}{nD}$ of Table 20 by the use of the pitch diameter ratio, 1·32, already found. $Q_Q k_Q$ is read from the standard curves for airscrews for the values
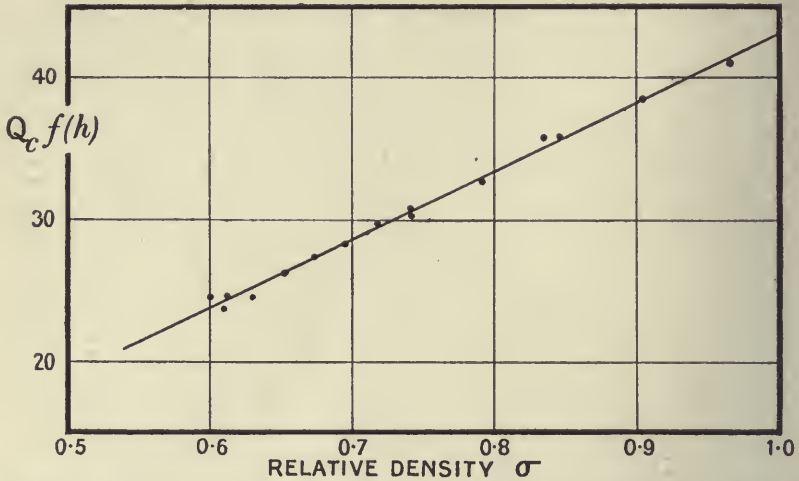
Fɪɢ. 219.—Calculated variation of horsepower with height from observations in flight.

of $\dfrac{V}{nP}$ in column 3, the particular values for $\dfrac{P}{D} = 1·32$ being interpolated between those for $\dfrac{P}{D} = 1·2$ and $\dfrac{P}{D} = 1·4$. Column 6 follows by division of the numbers in column 5 by those in column 4.

TABLE 23.

1	2	3	4	5	6	7
Height (ft.).	Relative density, σ	$\dfrac{V}{nP}$	$\dfrac{k_Q}{f(h)}$	$Q_Q k_Q$ $\dfrac{P}{D} = 1·32$	$Q_Q f(h)$	$\dfrac{f(h)}{Q_C = 43}$
6,500	0·833	0·761	0·0201	0·715	35·6	0·83
11,000	0·717	0·761	0·0242	0·715	29 6	0·69
16,000	0·611	0·740	0·0304	0·747	24·6	0·57
10,000	0·740	0·761	0·0232	0·715	30·8	0·72
13,000	0·673	0·758	0·0263	0·720	27·4	0·64
15,000	0·630	0·753	0·0297	0·728	24·5	0·57
16,500	0·600	0·740	0·0306	0·747	24·4	0·57
2,000	0·963	0·501	0·0244	1·000	41·0	0·95
4,000	0·903	0·503	0·0260	0·999	38·4	0·89
6,000	0·845	0·509	0·0278	0·995	35·8	0·83
8,000	0·792	0·520	0·0299	0·988	33·0	0·77
10,000	0·740	0·530	0·0324	0·982	30·3	0·70
12,000	0·695	0·531	0·0345	0·982	28·4	0·66
14,000	0·652	0·534	0·0373	0·978	26·2	0·61
16,000	0·610	0·542	0·0408	0·972	23·8	0·55

The values of $Q_0 f(h)$ in column 5 are then plotted in Fig. 219 with σ as a base. The points lie on a straight line which intersects the ordinate at $\sigma = 1$ at the value 43. Since $f(h)$ is then unity, this value determines Q_0 for the airscrew, column 7 of Table 23 is obtained by division and shows the variation of engine power with height.

The law of variation as thus deduced empirically may be expressed as

$$f(h) = \frac{\sigma - 0\cdot12}{0\cdot88} \quad . \quad . \quad . \quad . \quad . \quad . \quad (37)$$

and shows that the brake horsepower falls off appreciably more rapidly than the relative density.

In the course of the calculation of $f(h)$ it has been shown that

$$Q_0 = 43 \quad . \quad . \quad . \quad . \quad . \quad . \quad . \quad (38)$$

TABLE 24.

Speed (m.p.h.).	Relative density.	$\dfrac{V}{nP}$	k_L	$k_L \dfrac{V_0}{V}$
134	0·833	0·761	0·105	0
*115	,,	0·744	0·142	0
* 98	,,	0·718	0·196	0
* 80	,,	0·676	0·295	0
132·5	0·717	0·761	0·125	0
*115	,,	0·735	0·156	0
*100	,,	0·703	0·219	0
* 80	,,	0·647	0·343	0
126	0·611	0·740	0·162	0
*100	,,	0·689	0·257	0
* 80	,,	0·628	0·402	0
133	0·740	0·761	0·120	0
130·5	0·673	0·758	0·137	0
128	0·630	0·753	0·152	0
125	0·600	0·740	0·168	0
77·6	0·963	0·501	0·270	0·0500
78·0	0·903	0·503	0·285	0·0476
79·0	0·845	0·509	0·297	0·0440
80·2	0·792	0·520	0·308	0·0395
81·4	0·740	0·530	0·320	0·0350
81·6	0·695	0·531	0·339	0·0313
81·7	0·652	0·534	0·361	0 0272
82·0	0·610	0·542	0·382	0·0224

Determination of the Aeroplane Drag and the Thrust Coefficient Factor, T_c.—To determine the aeroplane drag and thrust coefficient factor T_0, use is made of equation (18), two values of $\dfrac{V}{nP}$ for the same air speed being extracted from the observations, so that the drag coefficient may be eliminated as indicated in producing equation (11). The

* Engine throttled.

lift coefficient, k_L, is now an important variable, and giving the particular values of the example to the quantities of equation (15), shows that

$$k_L = \frac{1570}{\sigma V^2_{\text{m.p.h.}}} \quad . \quad . \quad . \quad . \quad . \quad . \quad (39)$$

With this formula and the rates of climb given in Table 19 the values of k_L and $k_L\dfrac{V_0}{V}$ can be calculated. The results are given in Table 24.

From the numbers in Table 24, $\dfrac{V}{nP}$ for level flight is plotted on a base of k_L in order that values of $\dfrac{V}{nP}$ may be extracted for values of the air
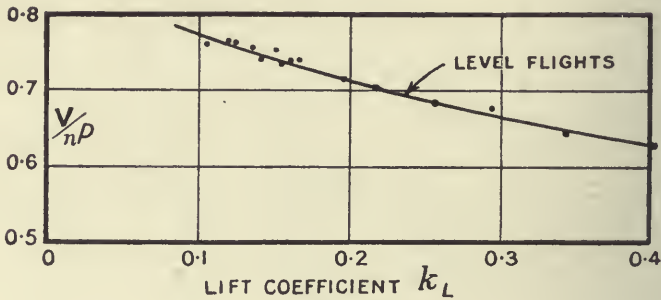
Fig. 220.

speed intermediate between observations. The condition required is that values of $\dfrac{V}{nP}$ from the curve for level flights shall be taken at the same air speed as for climbing. Constant air speed means constant k_L. From Fig. 220, Table 25 is compiled, part of the data being taken directly from Table 24.

TABLE 25.

Lift coefficient, k_L	$k_L\dfrac{V_0}{V}$	$\dfrac{V}{nP}$	
		Climbing flight.	Level flight.
0·270	0·0500	0·501	0·680
0·320	0·0350	0·530	0·660
0·382	0·0224	0·542	0·634

The formula which leads to the thrust coefficient factor, T_c, is obtained from equation (18), and may be written as

$$\frac{1}{4}\left(\frac{V}{nP}\right)^{-2} T_c k_T = \frac{1}{4} \cdot \frac{P^2 S}{D^4} T_c\left(k_D + k_L\frac{V_0}{V}\right). \quad . \quad . \quad (40)$$

The left-hand side of (40) is known for any value of $\dfrac{V}{nP}$ from one of the standard airscrew curves, Fig. 218. For each value of k_L in Table 25 sufficient information is now given from which to calculate T_0 and k_D.

The particular value of $\dfrac{1}{4} \cdot \dfrac{P^2 S}{D^4}$ for the example is 1·85, and for level flight with $\dfrac{V}{nP} = 0·680$ the value of $\dfrac{1}{4}\left(\dfrac{V}{nP}\right)^{-2} T_0 k_T = 0·366$, and equation (40) becomes

$$0·366 = 1·85 T_0 (k_D) \quad . \quad . \quad . \quad . \quad . \quad (41)$$

For climbing at the same value of k_L the resulting equation is

$$1·000 = 1·85 T_0 (k_D + 0·050) \quad . \quad . \quad . \quad . \quad (42)$$

From the two equations T_0 is found as

$$T_0 = \frac{1·000 - 0·366}{1·85 \times 0·050} = 6·86 \quad . \quad . \quad . \quad . \quad (43)$$

TABLE 26.

1	2	3	4	5	6
$\dfrac{V}{nP}$	$\dfrac{1}{4}\left(\dfrac{V}{nP}\right)^{-2}T_c k_T$	$k_D + k_L \dfrac{V_c}{V}$	$k_L \dfrac{V_c}{V}$	k_D	k_L
0·761	0·189	0·0146	—	0·0146	0·105
0·744	0·244	0·0188	—	0·0188	0·142
0·718	0·290	0·0224	—	0·0224	0·196
0·676	0·372	0·0288	—	0·0288	0·295
0·761	0·189	0·0146	—	0·0146	0·125
0·735	0·260	0·0201	—	0·0201	0·156
0·703	0·317	0·0245	—	0·0245	0·219
0·647	0·440	0·0340	—	0·0340	0·343
0·740	0·250	0·0193	—	0·0193	0·162
0·689	0·347	0·0268	—	0·0268	0·257
0·628	0·490	0·0378	—	0·0378	0·402
0·761	0·189	0·0146	—	0·0146	0·120
0·758	0·222	0·0164	—	0·0164	0·137
0·753	0·230	0·0178	—	0·0178	0·152
0·740	0·250	0·0193	—	0·0193	0·168
0·501	1·000	0·0773	0·0500	0·0273	0·270
0·503	0·985	0·0761	0·0476	0·0285	0·285
0·509	0·953	0·0736	0·0440	0·0296	0·297
0·520	0·896	0·0692	0·0395	0·0297	0·308
0·530	0·845	0·0652	0·0350	0·0303	0·320
0·531	0·840	0·0649	0·0313	0·0336	0·339
0·534	0·825	0·0637	0·0272	0·0365	0·361
0·542	0·793	0·0613	0·0224	0·0389	0·382

The other values of k_L yield $T_0 = 6.72$ and $T_0 = 7.56$, and the consistency of the reduction is seen to be only moderate. An examination of equation (40) shows why, the differences on which T_0 depends being smaller and smaller as the rate of climb diminishes. In meaning the observations, due weight is given to the relative accuracy if the numerators and denominators of the fractions for T_0 be added before division. The result in the present instance is to give

$$T_0 = 7.0 \quad . \quad . \quad . \quad . \quad . \quad . \quad . \quad (44)$$

In tests carried out with a view to applying the present line of analysis the evidence of glides would be included, and the accuracy of reduction appreciably increased.

Aeroplane Drag.—T_0 having been determined, equation (40) is a
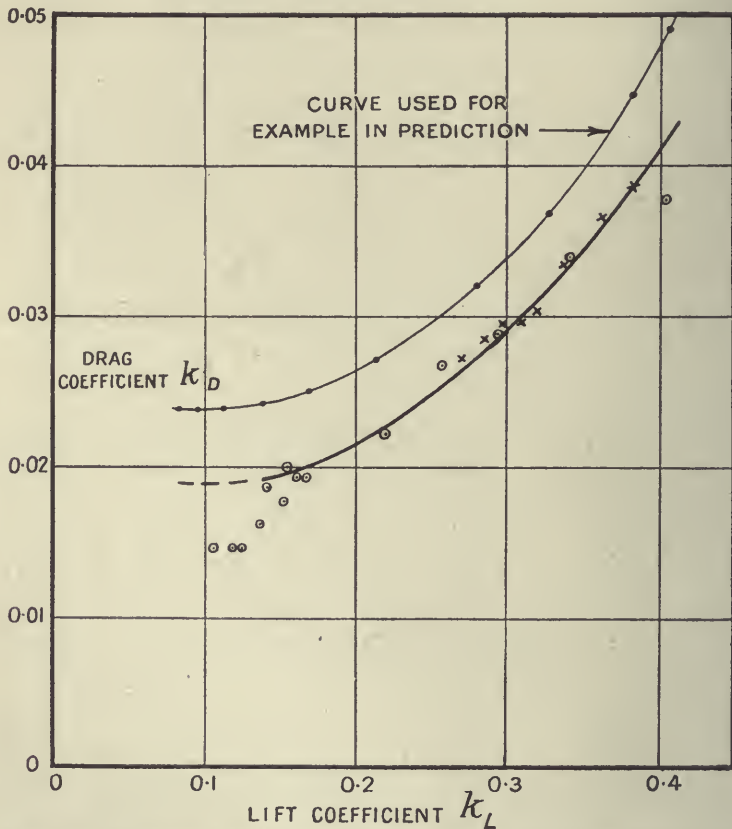
Fig. 221.—Aeroplane glider drag as deduced by analysis of performance trials.

relation between the drag coefficient k_D and known quantities. The calculation is given in Table 26, using figures from Table 24 as a basis.

Column 1 is taken from Table 24, and column 2 is deduced from it by

use of one of the standard airscrew curves, Fig. 218; column 3 then follows from equation (40). The fourth and sixth columns are also taken from Table 24, whilst the fifth column is deduced from columns 3 and 4.

The curve showing k_D as dependent on k_L is given in Fig. 221, together with the curve which was previously used in the example of prediction. For values of the lift coefficient below 0·15 the calculated points fall much below the curve drawn as probable. A discussion of this result is given a little later; as an example of analysis the drag as deduced will be found to represent the observations.

Airscrew Efficiency.—The analysis is practically complete as already given, but as the airscrew efficiency is one of the quantities used in describing the performance of an airscrew its value will be calculated. The formula in convenient terms is

$$\eta = \frac{1}{2\pi} \cdot \frac{P}{D} \cdot \frac{Q_0}{T_0} \cdot \frac{V}{nP} \cdot \frac{T_0 k_T}{Q_0 k_Q} \quad . \quad . \quad . \quad . \quad (45)$$

or, in the example

$$\eta = 1 \cdot 29 \frac{V}{nP} \cdot \frac{T_0 k_T}{Q_0 k_Q} \quad . \quad . \quad . \quad . \quad . \quad (46)$$

From the standard airscrew curves the efficiency at various values of $\frac{V}{nP}$ (or $\frac{V}{nD}$ if required) is easily obtained as in Table 27.

TABLE 27.

$\frac{V}{nP}$	$T_0 k_T$	$Q_0 k_Q$	η per cent.
0·5	1·000	1·000	64·5
0·6	0·823	0·922	69·1
0·7	0·629	0·804	70·5
0·8	0·421	0·652	66·5
0·9	0·209	0·472	51·5
1·0	0	0·263	0

The maximum airscrew efficiency is seen to be 70·5 per cent.

Remarks on the Analysis.—The analysis should be regarded as a tentative process which will become more precise if regular experiments be made to obtain data with the requisite accuracy. The standard airscrew curves may need minor modification, but it is obvious that a further step could be taken which replaces them in a particular instance. From the drawings of the airscrew the form of the standard curve could be calculated by the methods outlined in the chapter on Airscrews. It is not then necessary that the calculations of efficiency, thrust or torque as made from drawings shall be relied on for absolute values of the four airscrew constants determined as now outlined, but only for the general shape of the airscrew curves.

Both the drag of the aeroplane and the efficiency of the airscrew as

deduced by analysis are less than those used in prediction in an earlier part of the chapter, and the differences are mutually corrective. The actual values depend primarily on T_0, and for this purpose large differences of rate of climb are required if accuracy is to be attained. This object can be achieved by a number of judiciously chosen glides.

The Shape of the Drag Coefficient—Lift Coefficient Curve at Small Values of the Lift Coefficient.—The difference between the result of analysis and that of direct observation on a model is, in the example, so striking that further attention is devoted to the point. The model curve as used in prediction, Fig. 207, shows a minimum for k_D at about
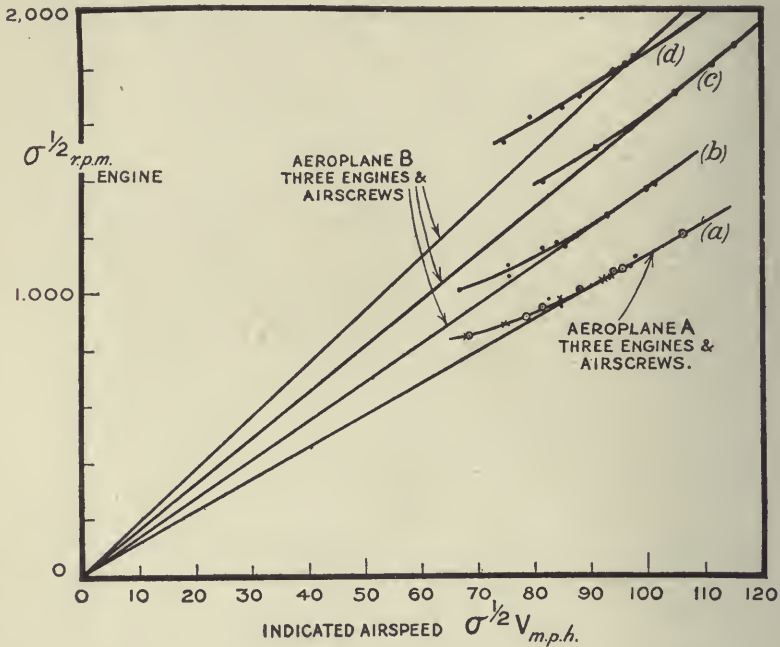
FIG. 222.

$k_L = 0.10$, and no great increase in value occurs up to $k_L = 0.15$. It is possible to make a very direct examination for the constancy of k_D over a limited range of k_L, which is independent of the standard curves for airscrews. It has been shown in equation (20) that the drag coefficient of an aeroplane is dependent on α and $\dfrac{V}{nD}$ only, and the new limitation removes the dependence on α. Similarly the thrust coefficient of an aeroplane is fixed by $\dfrac{V}{nD}$ and is not appreciably dependent on α. It then follows that constant drag coefficient involves constant advance per revolution for the airscrew. Advantage is taken of this relation in plotting Fig. 222. The ordinates are the values of $\sigma^{\frac{1}{2}}$ r.p.m. for the engine, and the abscissae are

the air speeds for the aeroplane. A line from the origin to a point on any of the curves is inclined to the vertical at an angle whose tangent is $\dfrac{V}{n}$, and if such a line happens to be tangential to the curves, $\dfrac{V}{n}$ is constant, and hence k_D is constant by the preceding argument.

Experiments for two aeroplanes were chosen. In aeroplane A the airscrew speed was that of the engine and about 1250 r.p.m. With an airscrew diameter of 9 feet the tip speed is nearly 600 ft.-s. Aeroplane B was fitted with engines of different gearing and engine speed, and the tip speeds of the airscrew were roughly 650 ft.-s., 600 ft.-s. and 700 ft.-s. for the curves b, c and d of Fig. 222.

An examination of the curves of Fig. 222 shows that in three out of the four, lines from the origin through the points for high speeds lie amongst the points within the limits of accuracy of the observations for an appreciable range. Curve d is a marked exception. Taking the values of indicated air speed from the parts of the curves which coincide with the lines shows the values below.

AEROPLANE A.	AEROPLANE B.
Loading 6 lbs. per sq. ft.	Loading 7 lbs. per sq. ft.
$\sigma^{\frac{1}{2}}V$ varies from 90 m.p.h. to 107 m.p.h. in curve a.	$\sigma^{\frac{1}{2}}V$ varies from 90 m.p.h. to 103 m.p.h. in curve b, and from 100 m.p.h. to 115 m.p.h. in curve c.
k_L varies from 0·10 to 0·15 for curve a.	k_L varies from 0·13 to 0·17 for curve b, and from 0·10 to 0·14 for curve c.

The values of k_L as calculated from the observed air speeds for which $\dfrac{V}{n}$ is sensibly constant are in very good agreement with observations on models, a range of k_L from 0·10 to 0·17 being indicated over which the drag coefficient varies very little.

Since curves b, c and d all refer to the same aeroplane, it is not permissible to assume that the drag coefficient can sometimes depend appreciably on air speed and at other times be independent of it over the same range. The figures given for the tip speeds of the various airscrews show that they are above half the velocity of sound, and that the greatest discrepancy occurs at the highest tip speed. In the example for which detailed analysis was given the tip speed was about 600 ft.-s., and the ratio of the tip speed to the velocity of sound varies little at high speeds, since the velocity of sound falls as the square root of the absolute temperature and tends to counteract the fall of revolutions with height. The evidence for an effect of compressibility is therefore very weak.

A more probable source for the difference is the twisting of the airscrew blades under load. An examination of the formulae for thrust and lift coefficients will show that for a constant drag coefficient (or advance per

revolution of the airscrew) the thrust is inversely proportional to the lift coefficient. Between $k_L=0.15$ and $k_L=0.10$ there is a 50 per cent. increase in force, and if the blade is liable to twist under load the result will be a change in experimental pitch and a departure from the assumption that an airscrew is sensibly rigid.

It may then be that failure to obtain a standard type of curve as a result of analysis is an indication of twisting of the airscrew blades. At any rate, the result has been to suggest further experiments which will remove the uncertainty. It will be appreciated that the sources of error now discussed do not appear in the test of an aeroplane which is gliding down with the airscrew stopped. The analysis of such experiments may be expected to furnish definite information as to the constancy of k_D at high speeds. Flying experiments will then give information as to the effects of twisting and compressibility, and the advantages of research in this direction do not need further emphasis.

CHAPTER X

THE STABILITY OF THE MOTIONS OF AIRCRAFT

PART I.

General Introduction to the Problems covered by the term Stability.—The earlier chapters of this book have been chiefly occupied by considerations of the steady motions of aircraft. This is a first requisite. The theory of stability is the study of the motions of an aeroplane about a steady state of flight when left to its own devices, either with controls held or abandoned

Figs. 223 and 224 show observations on two aeroplanes in flight, the speeds of which as dependent on time were photographically recorded. One aeroplane was stable and the other unstable, and the differences in record are remarkable and of great importance. The flights occurred in good ordinary flying weather, and no serious error will arise in supposing that the air was still.

Stable Aeroplane (Fig. 223).—A special clutch was provided by means of which the control column could be locked ; the record begins with the aeroplane flying at 62 m.p.h., and the lock just put into operation. As the steady speed was then 73 m.p.h., the aeroplane, being stable, commenced to dive and gain speed. Overshooting the mark, it passed to 83 m.p.h. before again turning upwards ; there is a very obvious dying down of the oscillation, and in a few minutes the motion would have become steady. The record shows that after a big bump the aeroplane controlled itself for more than two miles without any sign of danger.

Unstable Aeroplane.—The next record, Fig. 224, is very different and was not so easily obtained, since no pilot cares to let an unstable aeroplane attend to itself. No positive lock was provided, but by gently nursing the motion it was found possible to get to a steady flying speed with the control column against a stop. Once there the pilot held it as long as he cared to, and the clock said that this was less than a minute. After a few seconds the nose of the aeroplane began to go up, loss of speed resulted and stalling occurred. Dropping its nose rapidly the aeroplane began to gather speed and get into a vertical dive, but at 80 m.p.h. the pilot again took control and resumed ordinary flight. The aeroplane in this condition is top heavy.

A stalled aeroplane has been shown, Chap. V., to be liable to spin, and the ailerons become ineffective. Near the ground an accidental stalling may be disastrous. The importance of a study of stability should need no further support than is given by the above illustration.

In all probability difficulties in respect to stability limited the duration of the early flights of Santos Dumont, Farman, Bleriot, etc. It may be said that the controls were imperfect before the Wright Bros. introduced their system of wing-warping in conjunction with rudder action, and that this deficiency in control would be sufficient to account for the partial failures of the early aviators. Although this objection may hold good, it is obvious that a machine which is totally dependent on the skill of the
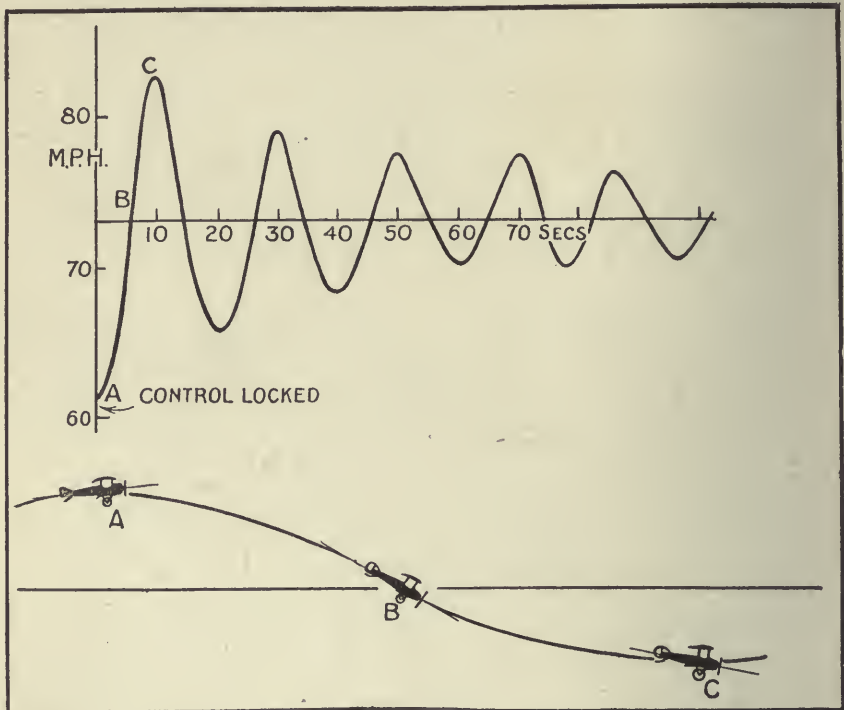
Fig. 223.—The uncontrolled motion of a stable aeroplane.

pilot for its safety is not so good as one which can right itself without the pilot's assistance.

Definition of a Stable Aeroplane.—A stable aeroplane may be defined as one which, from any position in the air into which it may have got either as the result of gusts or the pilot's use of the controls, shall recover its correct flying position and speed when the pilot leaves the machine to choose its own course, with fixed or free controls, according to the character of the stability.

Sufficient height above the ground is presumed to allow an aeroplane to reach a steady flying state if it is able to do so. The more rapidly the aeroplane recovers its flying position the more stable it may be said to be. If a pilot is necessary in order that an aeroplane may return to its normal flight position, then the aeroplane itself cannot be said to be stable
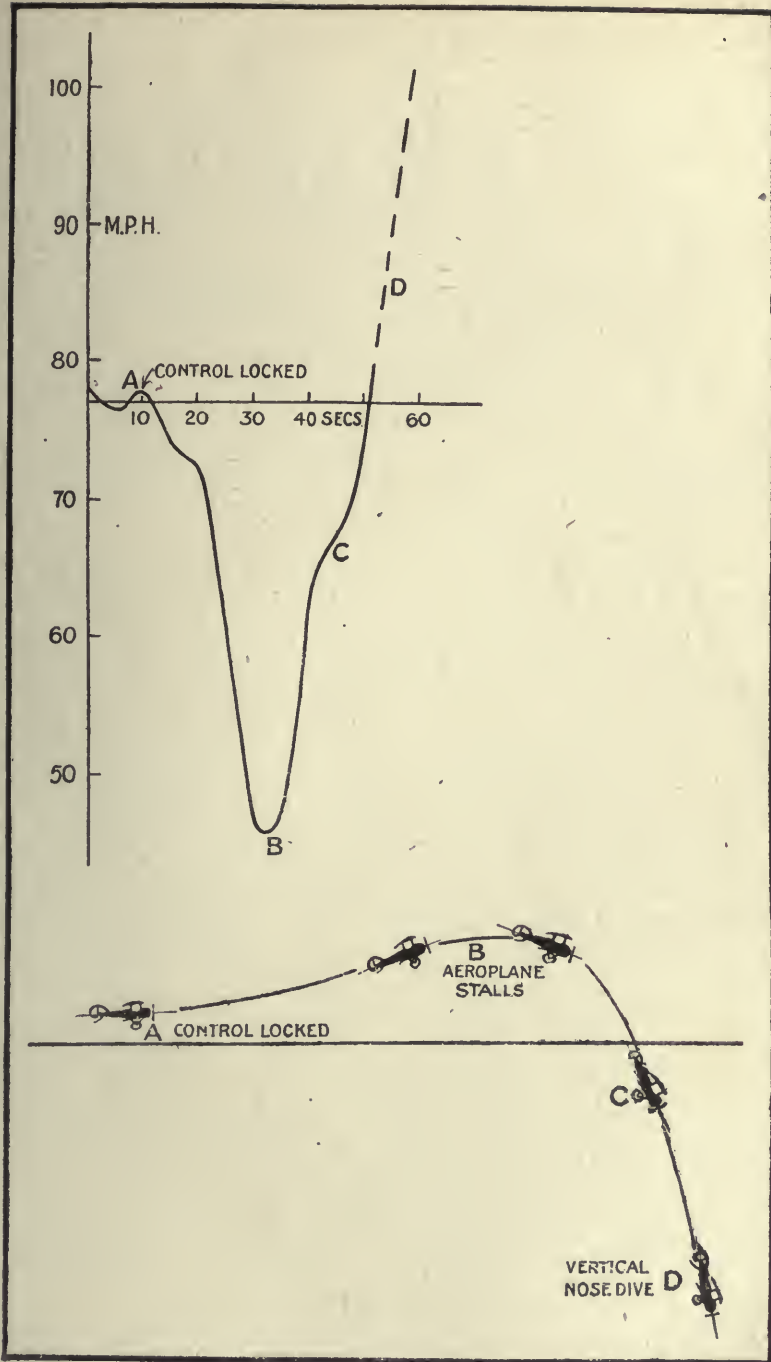
FIG. 224.—The uncontrolled motion of an unstable aeroplane.

although the term may be applied to the combination of aeroplane and pilot.

A subdivision of stability is desirable, the terms " inherent " and " automatic " being already in use. An aeroplane is said to be " inherently stable " if, when the controls are placed in their normal flying position whilst the aeroplane is in any position and flying at any speed, the result is to bring the machine to its normal flying position and speed. " Automatic stability " is used to describe stability obtained by a mechanical device which operates the controls when the aeroplane is not in its correct flying attitude.

Although the subject of stability may be thus subdivided, it will be found that the methods used for producing inherent stability throw light on the requirements for automatic stability devices. Before a designer is in a completely satisfactory position he must have information which will enable him to find the motion of an aeroplane under any conceivable set of circumstances. The same information which enables him to calculate the inherent stability of an aeroplane is also that which he uses to design effective controls, and the same as that required for any effective development of automatic stability devices.

A designer cannot foretell the detailed nature of the gusts which his aeroplane will have to encounter, and therefore cannot anticipate the consequences to the flying machine. In this respect he is only in the usual position of the engineer who uses his knowledge to the best of his ability and, admitting his limitations, provides for unforeseen contingencies by using a factor of safety.

Effect of Gusts.—The aeroplane used as an indication of what may be expected of an inherently stable machine had the advantage of flying in comparatively still air. It is not necessary during calulations to presume still air and neglect the existence of gusts. For instance, the mathematical treatment includes a term for the effects of side slipping of the aeroplane. Exactly the same term applies if the aeroplane continues on its course but receives a gust from the side. A head gust and an upward wind are similarly contemplated by the mathematics, and even for gusts of a complicated nature the mechanism for examining the effects on the motion of an aeroplane is provided.

Before entering on the formal mathematical treatment of stability a further illustration of full-scale measurement will be given, and a series of models will be described with their motions and their peculiarities of construction. The series of models corresponds exactly with the outstanding features of the mathematical analysis.

The Production of an Unstable Oscillation.—An aeroplane has many types of instability, one of the more interesting being illustrated in Fig. 225. which incidentally shows that an aeroplane may be stable for some conditions of flight and unstable for others. The records were taken by the equivalent of a pin-hole camera carried by the aeroplane and directed towards the sun. In order to record the pitching oscillations the pilot arranged to fly directly away from the sun by observing the shadow of the wing struts on the lower wing. The pilot started the predominant

oscillations by putting the nose of the aeroplane up or down and then
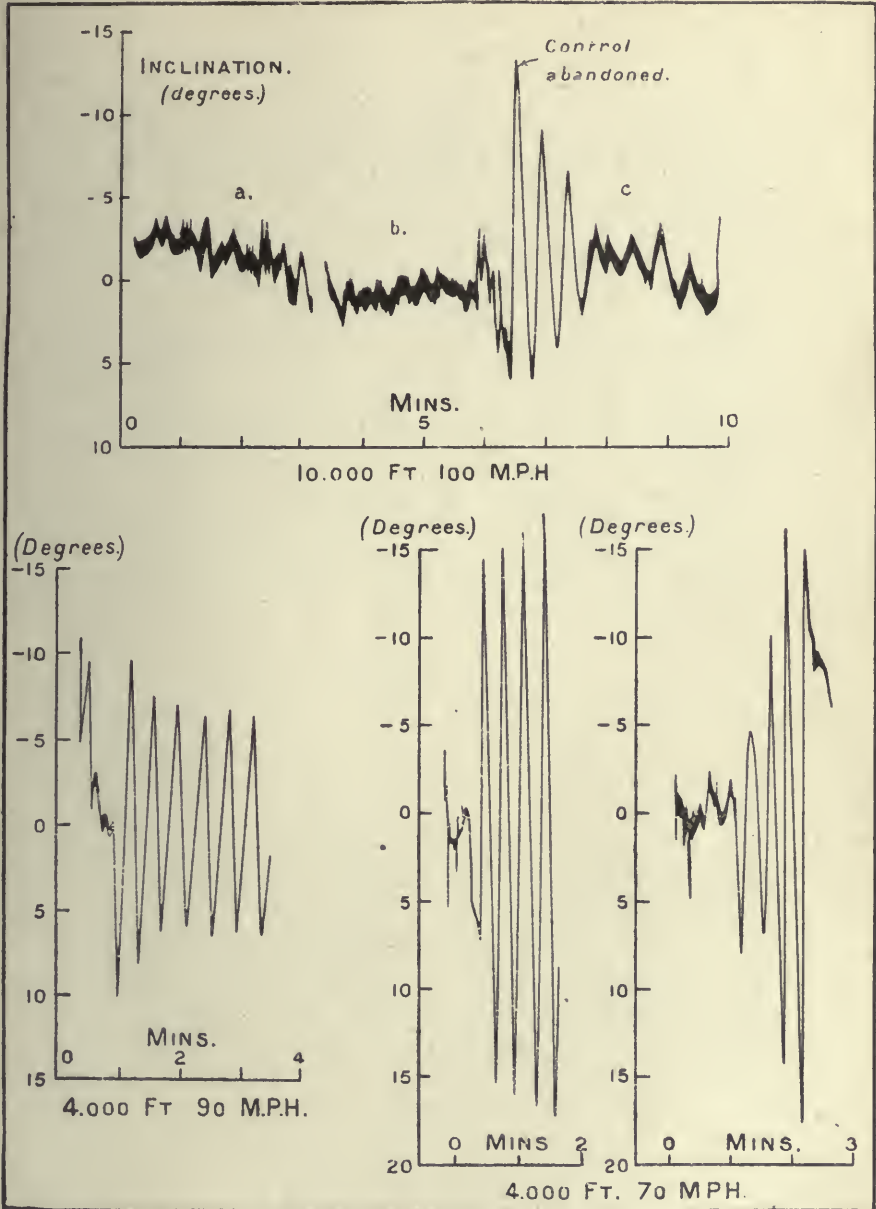
Fig. 225.—The uncontrolled motion of an aeroplane, showing that stability depends
on the speed of flight.

abandoning the control column.   A scale of angles is shown by the side
of the figure.   The upper diagram shows that at a speed of 100 m.p.h. and a

height of 10,000 ft. the aeroplane was stable. During the period " a " the pilot did his best to fly level, whilst for " b " the aeroplane was left to its own devices and proved to be a good competitor to the pilot. At the end of " b " the pilot resumed control, put the nose down and abandoned the column to get the oscillation diagram which gives a measure of the stability of the aeroplane. At a speed of 90 m.p.h. at 4000 feet one of the lower diagrams of Fig. 225 shows an oscillation which dies down for the first few periods and then becomes steady. The stability was very small for the conditions of the flight, and a reduction of speed to 70 m.p.h. was sufficient to produce an increasing oscillation. Two records of the latter are shown, the more rapidly increasing record being taken whilst the aero-plane was climbing slightly.

The motions observed are calculable, and the object of this chapter is to indicate the method. The mathematical theory for the aeroplane as now used was first given by Professor G. H. Bryan, but has since been combined with data obtained by special experiments. The present limita-tions in application are imposed by the amount of the experimental data and not by the mathematical difficulties, which are not serious.

The records described have been concerned either with the variation of speed of the aeroplane or of its angle to the ground, *i.e.* with the longi-tudinal motion. There are no corresponding figures extant for the lateral motions, and the description of these will be deferred until the flying models are described in detail.

Flying Models to illustrate Stability and Instability

Model showing Complete Stability (Fig. 226).—The special feature of the model is that, in a room 20 feet high and with a clear horizontal travel of 30 feet, it is not possible so to launch it that it will not be flying correctly before it reaches the ground. The model may be dropped upside down, with one wing down or with its tail down, but although it will do different manoeuvres in recovering from the various launchings its final attitude is always the same.

The appearance of the little model is abnormal because the stability has been made very great. Recovery from a dive or spin when assisted fully by the pilot may need 500 feet to 1000 feet on an aeroplane, and although the model is very small it must be made very stable if its characteristics are to be exhibited in the confines of a large lecture hall.

Distinguishing Features on which Stability of the Model depends.—In a horizontal plane there are two surfaces, the main planes and the tail plane, which together account for longitudinal stability. The angle of incidence of the main planes is greater than that of the tail, and the centre of gravity of the model lies one-third of the width of the main plane from its leading edge.

In the vertical plane are two fins; the rear fin takes the place of the usual fin and rudder, but the forward fin is not represented in aeroplanes by an actual surface. It will be found that a dihedral angle on the wings is equivalent in some respects to this large forward fin.
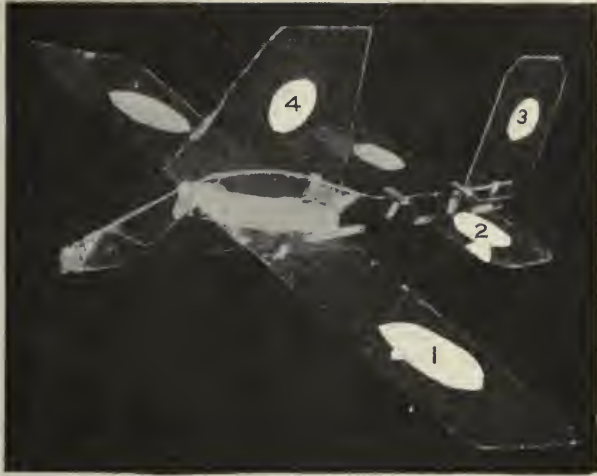
Fig. 226.—Very stable model.

(1) Main plane.   (2) Elevator fin.   (3) Rudder fin.   (4) Dihedral fin.

Fig. 227.—Slightly stable model.

Centre of pressure changes produce the effects of fins.

All the changes of stability which occur can be accounted for in terms of the four surfaces of this very stable model. The changes and effects will be referred to in detail in the succeeding paragraphs.

A flying model may be completely stable with only one visible surface, the main plane. Such a model is shown in Fig. 227. It has, however, properties which introduce the equivalents of the four surfaces.

The simplest explanation of stability applies to an ideal model in which the main planes produce a force which always passes through the centre
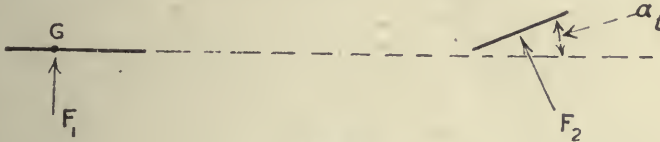
FIG. 228.

of gravity of the aeroplane model. In any actual model, centre of pressure changes exist which complicate the theory, but Fig. 228 may be taken to represent the essentials of an ideal model in symmetrical flight.

In the first example imagine the model to be held with its main plane horizontal just before release. At the moment of release it will begin to fall, and a little later will experience a wind resistance under both the main plane and the tail plane. Two things happen : the resistance tends to stop the falling, and the force F_2 on the tail plane acting at a considerable distance from G tends to put the nose of the model down.

Now consider the motion if the model is held with the main plane vertical just before release. There will be no force on the main plane due to the fall, but as the tail plane is inclined to the direction of motion it will experience a force F_2 tending to put the nose of the model up. The model cannot then stay in either of the attitudes illustrated. Had there not been an upward longitudinal dihedral angle between the main plane and tail plane there would have been no restoring couple in the last illustration, and it will be seen that the principle of the upward longitudinal dihedral angle is fundamental to stability. It is further clear that the model cannot stay in any attitude which produces a force on the tail, and ultimately the steady motion must lie along the tail plane, and since the angle to the main planes is fixed, the angle of incidence of the latter must be α_t when the steady state of motion has been reached.
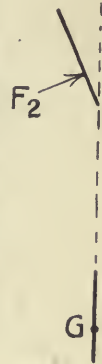
FIG. 229.

From the principles of force measurement, etc., it is known that the direction of the resultant force on an aerofoil depends only on its angle of incidence, and as the force to be counteracted must be the weight of the model, this resultant force must be vertical in the steady motion. This leads directly to the theorem that the angle of glide is equal to the angle whose tangent is the drag/lift of the aerofoil.

Although the direction of the resultant force on an aerofoil is determined solely by the angle of incidence, the magnitude is not and increases as the

square of tho speed. In a steady state the magnitude of the resultant force must be equal to the weight of the model, and the speed in the glide will increase until this state is reached. The scheme of operations is now complete, and is

(a) The determination of the angle of incidence of the main planes by the upward setting of the tail-plane angle.

(b) As a consequence of (a) the angle of glide is fixed.

(c) As a consequence of (a) and (b) the velocity of glide is fixed.

Further application of the preceding arguments will show that any departure from the steady state of flight given by (a), (b), and (c) introduces a force on the tail to correct for the disturbance.

Degree of Stability.—No assumptions have been made as to the size of the tail plane necessary for stability, nor of the upward tail setting. In the ideal model any size and angle are sufficient to ensure stability. It is, however, clear that with a very small tail the forces would be small and the correcting dive, etc., correspondingly slow ; such a model would have small stability. If the tail be large and at a considerable angle to the main plane, the model will switch round quickly as a result of a disturbance and will be very stable. It will be seen, then, that stability may have a wide range of values depending on the disposition of the tail.

Centre of Pressure Changes are Equivalent to a Longitudinal Dihedral Angle.—Fig. 227 shows a stable model without a visible tail plane. In the case just discussed the force F_1 on the main planes was supposed to act through the centre of gravity at all angles of incidence. This is equivalent to no change of centre of pressure on the wings, a case which does not often occur. The model of Fig. 227 is such that when the angle of incidence falls below its normal value the air pressure acts ahead of the centre of gravity, and *vice versâ*. The couple, due to this upward air force through the centre of pressure and the downward force of weight through the centre of gravity, tends to restore the original angle of incidence. The small mica model has an equivalent upward tail-setting angle in contradistinction to most cambered planes, for which the equivalent angle is negative and somewhat large. Tail-planes are therefore necessary to balance this negative angle before they can begin to act as real stabilising surfaces. The unstable aeroplane for which the record is given in Fig. 224 had either insufficient tail area or too small a tail angle.

The equivalent tail-setting angle of an aeroplane is not easily recognisable for other reasons than those arising from changes of the centre of pressure. Tail planes are usually not flat surfaces, but have a plane of symmetry from which angles are measured. The lift on such a tail plane is zero when the wind blows along the plane of symmetry. The main planes, on the other hand, do not cease to lift until the chord is inclined downwards at some such angle as 3°. If the plane of symmetry of the tail plane is parallel to the chords of the wings there is no geometrical dihedral angle, but aerodynamically the angle is 3°.

A complication of a different nature arises from the fact that the tail plane is in the downwash of the main planes.

Although all the above considerations are very important, they do not traverse the correctness of the principles outlined by the ideal model.

Lateral Stability.—Suppose the very stable model to be held, prior to release, by one wing tip so that the main plane is vertical. At the moment of release there will be a direct fall which will shortly produce wind forces on the fins, but not on the main plane or tail plane. On the front fin the force F_3, Fig. 230, in addition to retarding the fall, tends to roll the aeroplane so as to bring A round towards the horizontal. The air force F_4 on the tail fin tends to put the nose of the aeroplane down to a dive and so gets the axis into the direction of motion. Both actions continue, with the result that the main planes and tail plane are affected by the air forces and the longitudinal stability is called into play. It is not until the aeroplane is on an even keel that the fins cease to give restoring couples. Any further adjustments are then covered by the discussion of longitudinal stability already given.

FIG. 230.

Lateral stability involves rolling, yawing and side slipping of the aeroplane, all of which disappear in steady flight. The mica model Fig. 227 has rolling and yawing moments, due to centre of pressure changes when side slipping occurs. The equivalent fins are very small, and the stability so slight that small inaccuracies of manufacture lead to curved paths and erratic motion.

The large central fin of the very stable model is never present in an aeroplane, as it is found that a dihedral angle between the wings is a more convenient equivalent.

Fig. 231 shows a model which flies extremely well and which has no front fin. The dihedral angle between the wings is not great, each of them being inclined by about 5° to the line joining the tips. The properties of a lateral dihedral angle have been referred to in Chaps. IV. and V.

Unstable Models.—Two cases of unstable aeroplanes have been mentioned, and both instabilities can be reproduced in models. The tail plane of the model shown in Fig. 232 will be seen to be small, whilst the balancing weight which brings the centre of gravity into the correct place is small and well forward, so putting up the moment of inertia of the model for pitching motions.

To reproduce the type motion of Fig. 224 the tail plane would be set down at the back to make a slight negative tail-setting angle and the model launched at a high speed. It would rise at first and lose speed, after which the nose would fall and a dive ensue; with sufficient height the model would go over on to its back, and except for the lateral dihedral angle would stay there. The righting would come from a rolling over of the model, and the process would repeat itself until the ground was reached.
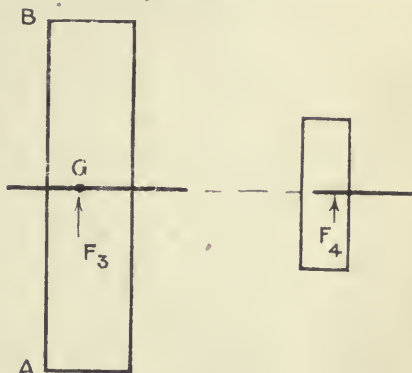
As illustrated the tail plane is set so that the model takes up an increasing oscillation similar to that shown in Fig. 225. The rear edge of the tail plane is higher than for the nose dive, and there is a small upward angle between the main plane and the tail plane, which tends to restore the position of the model when disturbed Owing to the smallness of the restoring couple, the heavy parts carry the wings too far and hunting occurs. About an axis through the centre of gravity the model would exhibit weathercock stability, whilst with the centre of gravity free the motion is unstable.

If the tail plane be further raised at its rear edge the model becomes stable, and if launched at a low speed would take a path similar to that of the aeroplane for which the record is given in Fig. 223.

Lateral Instability.—A model which illustrates three types of lateral instability is shown in Fig. 233. As illustrated the model when flown develops a lateral oscillation as follows : the model flies with the larger fin forward, because the distance from the centre of gravity is less than that of the rear fin, but if held as a weathercock with the axis through the centre of gravity there will be a small couple tending to keep the model straight. Due to an accidental disturbance the model sideslips to the left, the pressure on the fins turns it to the left, but since the centre of the fins is high there is also a tendency to a bank which is wrong for the turn. This goes on until the lower wing is moving so much faster on the outer part of the circle as to counteract and overcome the direct rolling couple, and the model returns to an even keel, but is still turning. Overshooting the level position the sideslipping is reversed and the turning begins to be checked. As in the longitudinal oscillation, hunting then occurs.

A second type of instability is produced by removing the front fin, the result being that the model travels in a spiral. Suppose that a bank is given to the model, the left wing being down ; sideslipping will occur to the left and the pressure on the rear fin will turn the aeroplane to the left and tend to raise the left wing. On the other hand, the outer wing will be the right wing, and as it will travel faster than the inner wing due to turning the extra lift will tend to raise the right wing still further. There is no dihedral angle on the main plane and the proportions of the model are such that the turning lifts the right wing more than the sideslipping lowers it. The result is increased bank, increased sideslipping and increased turning, and the motion is spiral.

The third instability is shown by the model if the front fin be replaced and the rear one removed. The model does not then possess weathercock stability, and in free flight may travel six or ten feet before a sufficient disturbance is encountered. The collapse is then startlingly rapid, and the model flutters to the ground without any attempt at recovery,

Remarks on Applications.—Aeroplanes are often in the condition of gliders, and their motions then correspond with the gliding models. When the airscrew is running new forces are called into play, and the effects on stability may be appreciable. The additional forces do not in any way change the principles but only the details of the application, and the

Fig. 231.—Stable model with two real fins.
The dihedral fin is not actually present, but an equivalent effect is
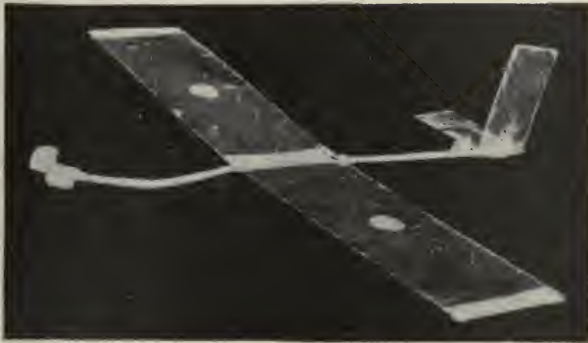produced by the dihedral angle between the wings.

Fig. 232.—Model which develops an unstable phugoid oscillation. Large
moment of inertia fore and aft with small restoring couple.

Fig. 233.—Model which illustrates lateral instabilities.
(1) With front fin removed: spiral instability.   (2) As shown: unstable
lateral oscillation.   (3) With rear fin removed: spin instability.

description of stable and unstable motion just concluded applies to the stable and unstable motions of an aeroplane flying under power.

From the short descriptions given it will have been observed that the simple motions of pitching, falling, change of speed are interrelated in the longitudinal motions, whilst the lateral motions involve sideslipping, rolling and yawing. The object of a mathematical theory of stability is to show exactly how these motions are related.

MATHEMATICAL THEORY OF STABILITY

The theory will be taken in the order of longitudinal stability, lateral stability, and stability when the two motions affect each other.

LONGITUDINAL STABILITY

The motions with which longitudinal stability deals all occur in the plane of symmetry of an aircraft. Changes of velocity occur along the
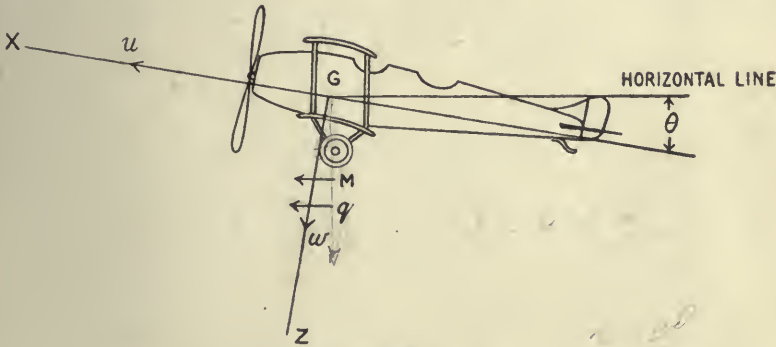
FIG. 234.

axes of X and Z whilst pitching is about the axis of Y. Axes fixed in the body (Fig. 234) are used, although the treatment is not appreciably simpler than with fixed axes, except as a link with the general case.

The equations of motion are

$$\begin{aligned}
\dot{u} + wq &= X' \\
\dot{w} - uq &= Z' \\
\dot{q}B &= M
\end{aligned}\Bigg\} \qquad \cdots \cdots \cdots \quad (1)^*$$

* The group of equations shown in (1) has valid application only if gyroscopic couples due to the rotating airscrew are ignored; the conditions of the mathematical analysis assume that complete symmetry occurs in the aircraft, and that the steady motion is rectilinear and in the plane of symmetry. This point is taken up later.

A point of a different kind concerns the motion of the airscrew relative to the aircraft, and would most logically be dealt with by the introduction of a fourth equation of motion—

$$2\pi I\dot{n} + Q_a = Q_e \qquad \cdots \cdots \cdots \cdots \quad (1a)$$

where I is the moment of inertia of the airscrew, Q_a is the aerodynamic torque, and Q_e is the torque in the engine shaft. All present treatments of aeroplane stability make the assumption, either explicitly or implicitly, that I is zero.

Mathematically this is indefensible as an equivalent of (1a), but the assumption is

The forces mX' and mZ' depend partly on gravitational attraction and partly on air forces. M, the pitching moment, depends only on motion through the air.

Gravitational Attractions.—The weight of the aircraft, mg, is the only force due to gravity, and the components along the axes of X and Z are

$$-g \sin \theta \text{ and } g \cos \theta \quad . \quad . \quad . \quad . \quad . \quad (2)$$

Air Forces.—Generally, the longitudinal force, normal force, and pitching moment depend on u, w and q. An exception must be made for lighter-than-air craft at this point, and the analysis confined to the aeroplane. The expressions for X, Z and M are

$$\begin{aligned}
X &= f_X(u, \ w \ \ q) \\
Z &= f_Z(u, \ w, \ q) \\
M &= f_M(u, \ w, \ q)
\end{aligned} \Bigg\} \quad . \quad . \quad . \quad . \quad . \quad . \quad (3)$$

Restatement of the Equations of Motion as applied to an Aeroplane.— Substituting for X, Z and M in (1) leads to the equations

$$\begin{aligned}
\dot{u} + wq &= -g \sin \theta + f_X(u, w, q) \\
\dot{w} - uq &= \ \ \ g \cos \theta + f_Z(u, w, q) \\
\dot{q}B &= \ \ \ \ \ \ \ \ \ \ \ \ \ \ f_M(u, w, q)
\end{aligned} \Bigg\} \quad . \quad . \quad . \quad (4)$$

In the general case, which would cover looping, these equations cannot be solved exactly. For such solutions it has been customary to resort to step-to-step integration, an example of which has been given in Chapter V.

The particular problem dealt with under stability starts with a steady motion, and examines the consequences of small disturbances.

If u_o, w_o, θ_o be the values of u, w and θ in the steady motion, equations (4) become

$$\begin{aligned}
0 &= -g \sin \theta_o + f_X(u_o, w_o, 0) \\
0 &= \ \ \ g \cos \theta_o + f_Z(u_o, w_o, 0) \\
0 &= \ \ \ \ \ \ \ \ \ \ \ \ \ f_M(u_o, w_o, 0)
\end{aligned} \Bigg\} \quad . \quad . \quad . \quad . \quad (5)$$

Since $q = \dot{\theta}$, it follows that q must be zero in any steady longitudinal motion, θ being constant.

The third equation of (5) shows that the pitching moment in the steady motion must be zero. The first two equations express the fact that the resultant air force on the aeroplane must be equal and opposite to the weight of the aeroplane. There is no difficulty in satisfying equations (5), and the problems relating to them have been dealt with in Chapter II.

---

nevertheless satisfactory in the present state of knowledge. The damping of any rotational disturbance of an airscrew is rapid, whilst changes of forward speed of an aeroplane are slow and are the only changes of appreciable magnitude to which the airscrew has to respond.

The extra equation of motion does not lead to any serious change of method, but it adds to the complexity of the arithmetical processes, and the simplification which results from the assumption $I=0$ appears to be more valuable than that of the extra accuracy of retaining it.

A little later in the chapter, is given a numerical investigation of the validity of the assumption, but it is always open to a student to recast the equations of stability so as to use the variables u, w, q and n instead of confining attention to u, w and q only.

Small Disturbances.—Suppose that u becomes $u_o + \delta u$, w becomes $w_o + \delta w$, θ becomes $\theta_o + \delta\theta$, and q becomes δq instead of zero. Equations (4) will apply to the disturbed motion so produced. If δu, δw, δq be made very small, equations (4) can be modified very greatly, the resulting forms admitting of exact solution. To find these forms the new values of u, etc., are substituted in (4), and the terms expanded up to first-order terms in δu, δw, etc. In the case of the first equation of (4) the expanded form is

$$\delta\dot{u} + w_o\delta q = -g\sin\theta_o + f_{\mathrm{x}}(u_o, w_o, 0)$$

$$-g\cos\theta_o . \delta\theta + \delta\dot{u}\frac{\partial f_{\mathrm{x}}}{\partial u} + \delta w\frac{\partial f_{\mathrm{x}}}{\partial w} + \delta q\frac{\partial f_{\mathrm{x}}}{\partial q} \quad . \quad . (6)$$

From the conditions for steady motion, equation (5), the value of $-g\sin\theta_o + f_{\mathrm{x}}(u_o, w_o, 0)$ is seen to be zero, and (6) becomes

$$\delta\dot{u} + w_o\delta q = -g\cos\theta_o\delta\theta + \delta u\frac{\partial f_{\mathrm{x}}}{\partial u} + \delta w\frac{\partial f_{\mathrm{x}}}{\partial w} + \delta q\frac{\partial f_{\mathrm{x}}}{\partial q} \quad . \quad . (7)$$

Resistance Derivatives.—The quantities $\dfrac{\partial f_{\mathrm{x}}}{\partial u}$, $\dfrac{\partial f_{\mathrm{x}}}{\partial w}$, $\dfrac{\partial f_{\mathrm{x}}}{\partial q}$, etc., are called resistance derivatives, and as they occur very frequently are written more simply as X_u, X_w, X_q, etc.

A further simplification commonly used is to write u instead of δu. With this notation the equations of disturbed motion become

$$\left.\begin{array}{l} \dot{u} + w_o q = -g\cos\theta_o . \theta + uX_u + wX_w + qX_q \\ \dot{w} - u_o q = -g\sin\theta_o . \theta + uZ_u + wZ_w + qZ_q \\ B\dot{q} = \qquad\qquad uM_u + wM_w + qM_q \end{array}\right\} \quad . \quad . \quad . (8)$$

In these equations $q = \dot{\theta}$, and the equations are linear differential equations with constant coefficients. Between the three equations any two of the variables u, w and q may be eliminated by substitution, leading to an equation of the form

$$\mathrm{F(D)} . u = 0 \quad . \quad . \quad . \quad . \quad . \quad . (9)$$

where $\mathrm{F(D)}$ is a differential operator. For longitudinal stability $\mathrm{F(D)}$ contains all powers of D up to the fourth.

The standard solution of (9) is

$$u = u_1 e^{\lambda_1 t} + u_2 e^{\lambda_2 t} + u_3 e^{\lambda_3 t} + u_4 e^{\lambda_4 t} \quad . \quad . \quad . \quad . (10)$$

where λ_1, λ_2, λ_3, and λ_4 are the roots of the algebraic equation $\mathrm{F}(\lambda) = 0$, and u_1, u_2, u_3, and u_4 are constants depending on the initial values of the disturbance. There are similar relations for w and q with the same values for λ_1, λ_2, λ_3, and λ_4.

For each term of the form $ue^{\lambda t}$, etc., the value of $\dot{u}$ is λu, $\dot{w} = \lambda w$, etc., where λ may take any one of its four values, and in finding the expansion for $\mathrm{F}(\lambda)$ this relation is first used to change equations (8) to

$$\left.\begin{array}{l} (\lambda - X_u)u \qquad - X_w w + (w_o\lambda - X_q\lambda + g\cos\theta_o)\theta = 0 \\ - Z_u u + (\lambda - Z_w)w + (-u_o\lambda - Z_q\lambda + g\sin\theta_o)\theta = 0 \\ - M_u u \qquad - M_w w \qquad\quad + (B\lambda^2 - M_q\lambda)\theta = 0 \end{array}\right\} \quad . \quad (11)$$

and the elimination of any two of the variables u, w and θ leads to the stability equation

$$F(\lambda) = \begin{vmatrix} \lambda - X_u & -X_w & w_0\lambda - X_q\lambda + g\cos\theta_o \\ -Z_u & \lambda - Z_w & -u_0\lambda - Z_q\lambda + g\sin\theta_o \\ -M_u & -M_w & B\lambda^2 - M_q\lambda \end{vmatrix} = 0 \quad . \quad (12)$$

The coefficient of the highest power of λ, $i.e.$ λ^4, is B, and in order to arrive at an expression for which the coefficient is unity it is convenient to divide through everywhere by B. This is effected if $\dfrac{M_u}{B}$ is written instead of M_u, $\dfrac{M_w}{B}$ instead of M_w, and $\dfrac{M_q}{B}$ instead of M_q in a new determinant otherwise the same as (12).

The expansion of $\dfrac{F(\lambda)}{B}$ in powers of λ is easily achieved, and the results are given below.

Coefficient of λ^4, 1

$A_1 \equiv$ Coefficient of λ^3, $-X_u - Z_w - \dfrac{1}{B}M_q$

$B_1 \equiv$ Coefficient of λ^2, $\dfrac{1}{B}\begin{vmatrix} Z_w & u_0+Z_q \\ M_w & M_q \end{vmatrix} + \dfrac{1}{B}\begin{vmatrix} X_u & -w_0+X_q \\ M_u & M_q \end{vmatrix} + \begin{vmatrix} X_u & X_w \\ Z_u & Z_w \end{vmatrix}$

$C_1 \equiv$ Coefficient of λ^1, $-\dfrac{1}{B}\begin{vmatrix} X_u & X_w & -w_0+X_q \\ Z_u & Z_w & u_0+Z_q \\ M_u & M_w & M_q \end{vmatrix} + \dfrac{g}{B}\begin{vmatrix} M_u & -\sin\theta_o \\ M_w & \cos\theta_o \end{vmatrix}$

$D_1 \equiv$ Coefficient of λ^0, $\dfrac{g}{B}\begin{vmatrix} X_u & X_w & \cos\theta_o \\ Z_u & Z_w & \sin\theta_o \\ M_u & M_w & 0 \end{vmatrix} \quad . \quad . \quad . \quad . \quad . \quad . \quad (13)$

The conditions for stability are given by Routh, and are that the five quantities A_1, B_1, C_1, D_1 and $A_1B_1C_1 - C_1^2 - A_1^2D_1$ shall all be positive.

Example I.—For an aeroplane weighing about 2000 lbs. and

$$u_0 = 122\cdot4 \qquad w_0 = -4\cdot3 \qquad \theta_0 = -2°\cdot6$$

the following approximate values of the derivatives may be used :—

$$\left. \begin{array}{lll} X_u = -0\cdot159 & X_w = 0\cdot081 & X_q = 0 \\ Z_u = -0\cdot68 & Z_w = -4\cdot67 & Z_q = -0\cdot60 \\ \dfrac{1}{B}M_u = -0\cdot0047 & \dfrac{1}{B}M_w = -0\cdot130 & \dfrac{1}{B}M_q = -9\cdot8 \end{array} \right\} \quad . \quad (14)$$

Substituting the values of (14) in (13) leads to

$$A_1 = 14\cdot8, \quad B_1 = 62\cdot0, \quad C_1 = 9\cdot80, \quad D_1 = 2\cdot16$$

All these quantities are positive.

$$A_1B_1C_1 - C_1^2 - A_1^2D_1 = 8420$$

and the motion is completely stable.

Some further particulars of the motion are obtained by solving the biquadratic equation in λ.

The equation $\quad \lambda^4 + 14\cdot 8\lambda^3 + 62\cdot 0\lambda^2 + 9\cdot 80\lambda + 2\cdot 16 = 0$ has the factors

$$(\lambda + 7\cdot 34 \pm 2\cdot 45i)(\lambda + 0\cdot 075 \pm 0\cdot 170i) = 0 \qquad . \quad . \ (15)^*$$

All the roots are complex. A pair of complex roots indicates an oscillation. The real part of a complex root gives the damping factor, and the imaginary part has its numerical value equal to 2π divided by the periodic time of the oscillation. In the above case the first pair of factors indicates an oscillation with a period of $2\cdot 57$ secs. and a damping factor of $7\cdot 34$, whilst the second pair of complex factors corresponds with a period of $37\cdot 0$ secs. and a damping factor of $0\cdot 075$.

The meaning of damping factor is often illustrated by computing the time taken for the amplitude of a disturbance to die to half magnitude. If

$$u = u_1 e^{-\lambda_1 t}$$

u will be half the initial value u_1 when

$$e^{-\lambda_1 t} = \tfrac{1}{2}$$

Taking logarithms,

$$-\lambda_1 t = -\log_e 2 = -0\cdot 69$$

and $\qquad\qquad \therefore t$ to half amplitude $= \dfrac{0\cdot 69}{\lambda_1}$

In the illustration the more rapid oscillation dies down to half value in less than $\tfrac{1}{10}$th second, whilst the slower oscillation requires $9\cdot 2$ seconds.

It will be readily understood from this illustration that after a second or so only the slow oscillation will have an appreciable residue. The resemblance to the curve, shown in Fig. 223, of the oscillations of an aeroplane will be recognised without detailed comparison.

Airscrew Inertia as affecting the Last Example

A numerical investigation can now be made of the importance of the assumption that the motion of an aeroplane is not much affected by the inertia of the airscrew. Corresponding with the data of the example are the two following equations for aerodynamic torque and engine torque:—

$$Q_a = 1\cdot 004n^2 - 0\cdot 0018\frac{u^3}{n} \qquad . \quad . \quad . \quad . \quad . \ (15a)$$

$$\text{and } Q_e = 875 - 14\cdot 6n \qquad . \quad . \quad . \quad . \quad . \quad . \ (15b)$$

Solving the equation, $Q_a = Q_e$, for $u = 122\cdot 4$ leads to the value $n = 25\cdot 2$.

Substituting $n_o + n$ for n and $u_o + u$ for u in equations (15a) and (15b) and separating the parts corresponding with disturbed motion from those for steady motion converts equation 1a into

$$\dot{n} + \left(1\cdot 16 + 0\cdot 160n_o + 0\cdot 000143\frac{u_o^3}{n_o^2}\right)n = \frac{0\cdot 000429u_o^2}{n_o}u \quad . \quad . \ (15c)$$

or with $u_o = 122\cdot 4$ and $n_o = 25\cdot 2$

$$\dot{n} + 5\cdot 59n = 0\cdot 256u \qquad . \quad . \quad . \quad . \quad . \ (15d)$$

* For method of solution, see Appendix to this chapter.

Before any solution of (15d) can be obtained u must be known as a function of n and t. In equation (15) a value of u was found of the form $u_1 e^{\lambda_1 t}$, but this assumes a definite relation between n and u for all motions whether disturbed or steady. The value $u_1 e^{\lambda_1 t}$ so found may be used in (15d) and the result examined to see whether any fundamental assumptions on which it was based are violated. A solution of (15d) is now

$$n = n_1 e^{5 \cdot 59 t} + \frac{0 \cdot 256 u_1 e^{\lambda_1 t}}{\lambda_1 + 5 \cdot 59} \quad . \quad . \quad . \quad . \quad . \quad . \quad (15e)$$

except in the case where $\lambda_1 = -5 \cdot 59$, when the solution is

$$n = e^{-5 \cdot 59 t}\{n_1 + 0 \cdot 256 u_1 t\} \quad . \quad . \quad . \quad . \quad . \quad . \quad (15f)$$

λ_1 is frequently complex, and following the usual rule $h + ik$ is written for λ_1 and $h - ik$ for the complementary root λ_2, and the two roots are considered together. For an oscillation, equation (15e) is replaced by

$$n = n_1 e^{-5 \cdot 59 t} + \frac{0 \cdot 256 e^{ht}}{\sqrt{\overline{h + 5 \cdot 59}^2 + k^2}}\{u_1 \cos (kt + \gamma) + u_2 \sin (kt + \gamma)\} \quad . \quad (15g)$$

where $\qquad \cos \gamma = \dfrac{h + 5 \cdot 59}{\sqrt{\overline{h + 5 \cdot 59}^2 + k^2}}$ and $\sin \gamma = \dfrac{-k}{\sqrt{\overline{h + 5 \cdot 59}^2 + k^2}}$

The first term of (15e) and (15g) is reduced to 1 per cent. of its initial value in less than one second. In the case of (15f) the maximum value of the second term occurs at $t = 0 \cdot 18$ sec. and is $0 \cdot 125 u_1$, and like the first term becomes unimportant in about a second.

Had the inertia of the airscrew been neglected the relation obtained from (15d) would have been

$$n = \frac{0 \cdot 256 u}{5 \cdot 59} \quad . \quad . \quad . \quad . \quad . \quad . \quad . \quad . \quad (15h)$$

Instead of which the more accurate equation (15e) gives after 1 sec.

$$n = \frac{0 \cdot 256 u}{\lambda_1 + 5 \cdot 59} \quad . \quad . \quad . \quad . \quad . \quad . \quad . \quad (15i)$$

and it is seen immediately that if λ_1 be real, equation (15h) may be used instead of (15i) if λ_1 is small compared with 5·59. If 50 per cent. of the motion is to persist after 1 sec., λ_1 cannot exceed 0·69, and in the more important motions of an aeroplane λ_1 is much less. In such cases the assumption is justified that the relation between airscrew revolutions and forward speed is substantially independent of the disturbance of the steady motion.

In the case of an oscillation the motion shown by (15g) involves both a damping factor and a phase difference. The damping factor corresponding with (15i) is

$$n = \frac{0 \cdot 256 u}{\sqrt{\overline{h + 5 \cdot 59}^2 + k^2}} \quad . \quad . \quad . \quad . \quad . \quad (15j)$$

whilst the phase difference is

$$\tan \gamma = \frac{-k}{h + 5 \cdot 59} \quad . \quad . \quad . \quad . \quad . \quad . \quad (15k)$$

Applied to Example I. (15j) and (15k) give

Rapid oscillation $\qquad h = -7 \cdot 34 \qquad k = 2 \cdot 90$
$\qquad\qquad\qquad\qquad n = -0 \cdot 075 u$ and $\gamma = 240°$

whilst the approximate formula (15h) gives

$$n = 0 \cdot 046 u \text{ and } \gamma = 0$$

It is clear, therefore, that the approximation I=0 must not be applied to the first second of the motion without further consideration.

Phugoid oscillation $h = -0.075$ and $k = 0.170$
                               $n = 0.046u$ and $\gamma = 1°.8$

whilst the approximate formula gives

$$n = 0.046u \text{ and } \gamma = 0$$

In this case it is equally clear that the approximation I=0 is quite satisfactory.

It may therefore be concluded that any investigation of the early stages of disturbed motion should start with the four equations of motion, whilst any investigation for the later periods can be made by the use of three only.

VARIATION OF THRUST DUE TO CHANGE OF FORWARD SPEED

Whilst dealing with the subject of the airscrew it may be advantageous to supplement the equation for Q_a by the corresponding expression for the thrust, viz.

$$T = 1.25n^2 - 0.0222u^2 \quad . \quad . \quad . \quad . \quad . \quad . \quad (15l)$$

Using equation (15h) and remembering that n and u are small quantities, the change of revolutions with change of forward speed is

$$\frac{\partial n}{\partial u} = \frac{\text{``} n \text{''}}{u} = 0.0458$$

Differentiating in equation (15l) leads to

$$\frac{\partial T}{\partial u} = 2.50n_o \frac{\partial n}{\partial u} - 0.0444u_o \quad . \quad . \quad . \quad . \quad (15m)$$

With $n_o = 25.2$ and $u_0 = 122.4$, the value of $\frac{\partial T}{\partial u}$ is -2.64 lbs. per foot per sec. The mass of the aeroplane being 62.1 slugs, the contribution of the airscrew to the value of X_u is seen to be $-\frac{2.64}{62.1}$, *i.e.* -0.043. This is rather more than one-quarter of the total as shown in (14).

Effect of Flight Speed on Longitudinal Stability.—The effect of variation of flight speed is obtained by repeating the process previously outlined, and as there are many common features in aeroplanes a set of curves is given showing generally how the resistance derivatives of an aeroplane vary with the speed of flight.

The stalling speed assumed was 58.6 ft.-s. (40 m.p.h.), and it will be noticed that near the stalling speed most of the derivatives change very rapidly with speed. For lateral stability as well as longitudinal stability it will be found that marked changes occur in the neighbourhood of the stalling speed, and that some of the instabilities which then appear are of the greatest importance in flying.

The derivatives illustrated in Figs. 235–238, correspond with an aeroplane which is very stable longitudinally for usual conditions of flight.

Not all the derivatives are important, and X_q is often ignored. The periods and damping factors corresponding with the derivatives are of interest as showing how stability is affected by flight speed. A table of results is given (Table 1).
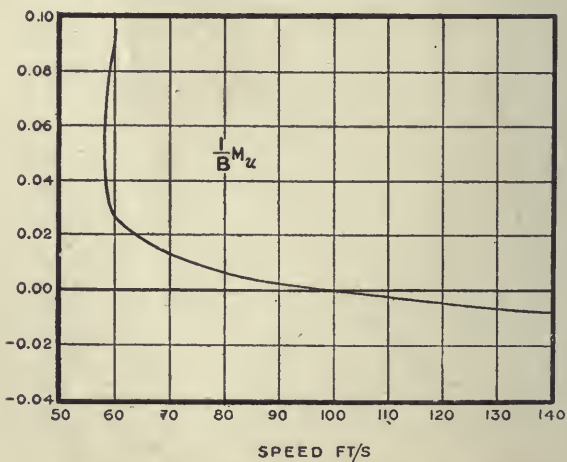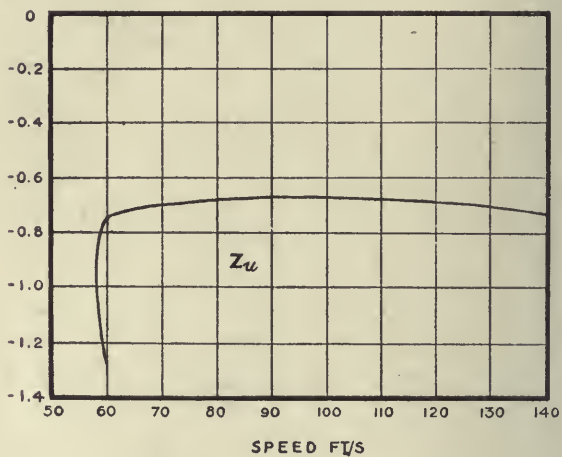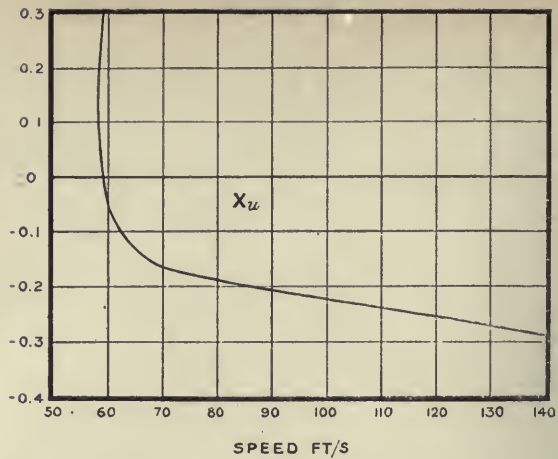
Fig. 235.—Resistance derivatives for changes of longitudinal velocity.
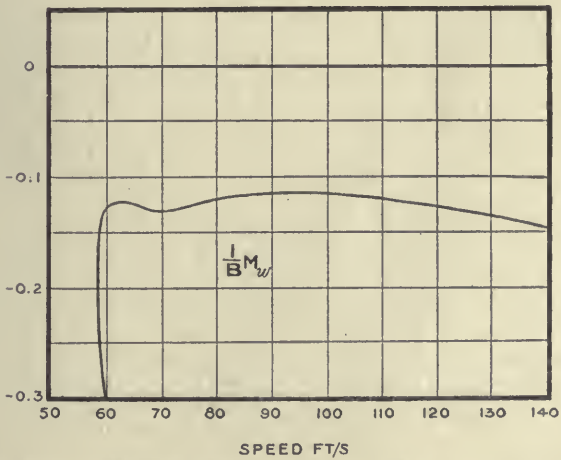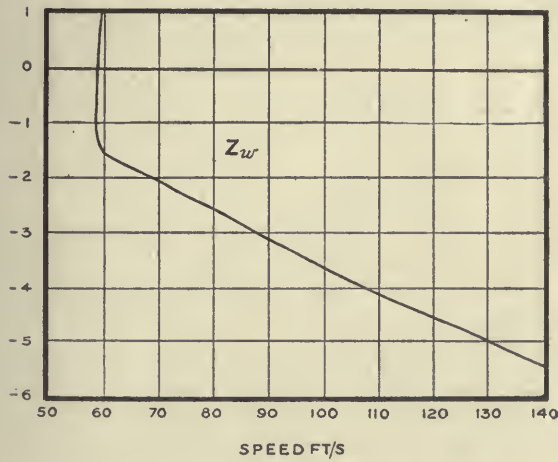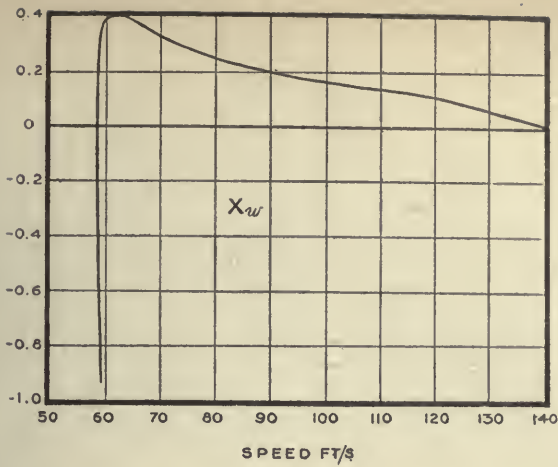
Fig. 236.—Resistance derivatives for changes of normal velocity.
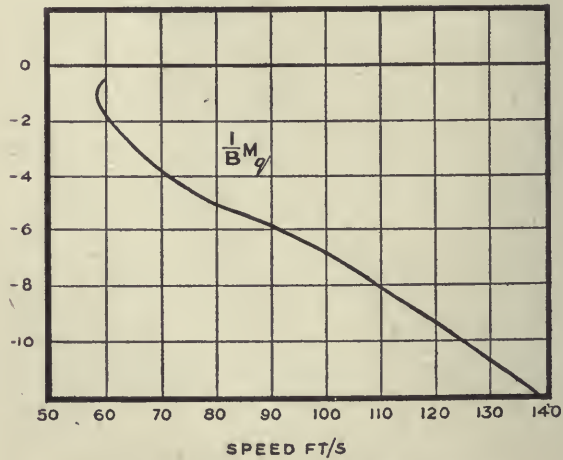
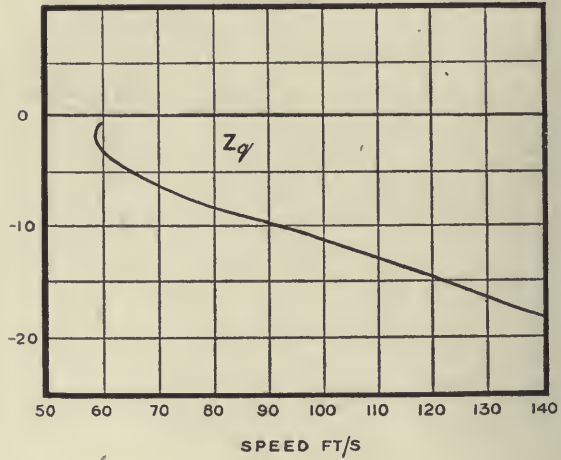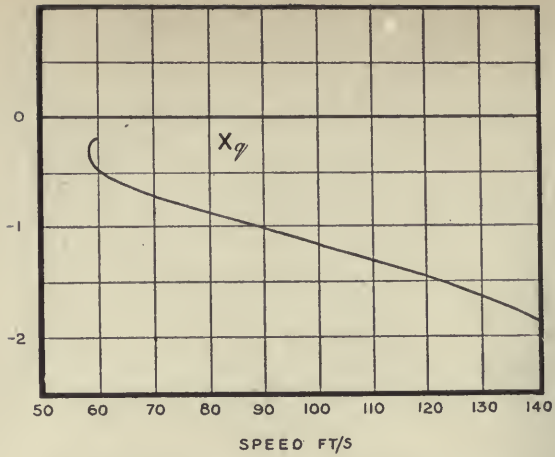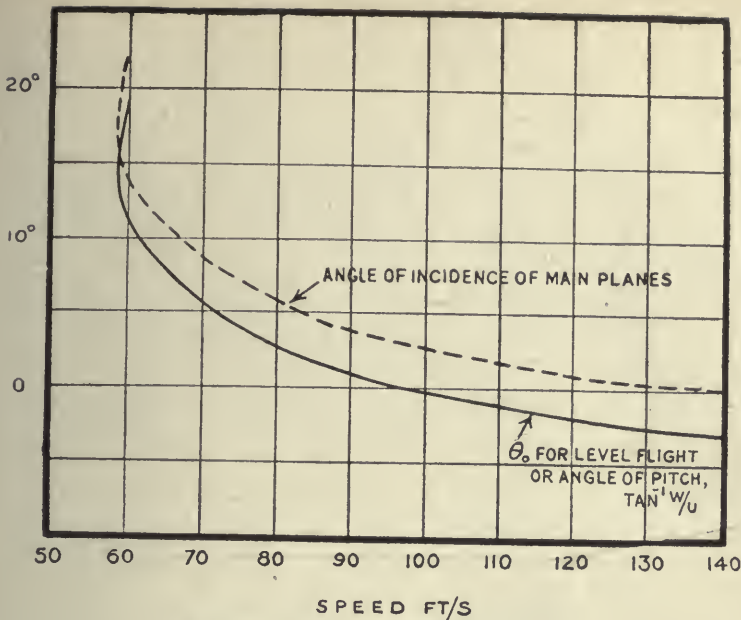FIG 237.—Resistance derivatives for pitching.

Fig. 238.—Angle of pitch and flight speed.

TABLE 1.

Flight speed ft.-s.	Rapid oscillation.			Phugoid oscillation.		
	Periodic time (secs.).	Damping factor.	Time to half disturbance (secs.).	Periodic time (secs.).	Damping factor.	Time to half disturbance (secs.).
59·2	1·67	−0·01	(Doubles in 70 secs.)	8·5	0·170	4·0
58·6	2·05	+0·99	0·70	8·3	0·051	13·5
60·0	2·22	1·45	0·47	9·3	0·031	22·2
70·0	2·21	2·97	0·23	13·3	0·037	18·6
80·0	2·25	3·85	0·18	17·0	0·044	15·7
90·0	2·23	4·55	0·15	21·1	0·051	13·5
100·0	2·16	5·34	0·13	25·4	0·058	11·9
122·5	2·57	7·34	0·095	37·0	0·075	9·2
247·0	5·24	16·27	0·042	Aperiodic and 0·028	0·272	2·54 and 24·6

Throughout the range of speed possible in rectilinear steady flight the disturbed motion naturally divides into a rapid motion, which in this case is an oscillation, and a slower motion which is an oscillation except at a very high speed. This latter motion was called a " phugoid oscillation " by Lanchester, and the term is now in common use.

At stalling angle the short oscillation becomes unstable, and a critical examination will show that the change is due to change of sign of Z_w and X_w. Physically it is easily seen that above the stalling angle falling

increases the angle of incidence, further decreases the lift, and accentuates the fall.

At the higher speeds the damping of the rapid oscillation is great, and in later chapters it is shown that the motion represents (as a main feature) the adjustment of angle of incidence to the new conditions.

The slow oscillation in this instance does not become unstable, but is not always vigorously damped ; at 60 ft.-s. the damping factor is only 0·031. A modification of aeroplane such as is obtained by moving the centre of gravity backwards will produce a change of sign of this damping factor, and an increasing phugoid oscillation is the result.

At high speeds the period of the phugoid oscillation becomes greater, and ultimately the oscillation gives place to two subsidences. In a less stable aeroplane the oscillation may change to a subsidence and a divergence, in which case the aeroplane would behave in the manner illustrated in Fig. 224.

All the observed characteristics of aeroplane stability are represented in calculations similar to those above. Many details require to be filled
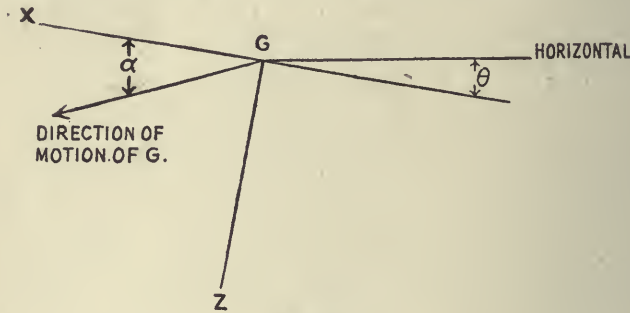
Fig. 239.

in before the calculations become wholly representative of the disturbed motion of an aeroplane. The details are dealt with in the determination of the resistance derivatives.

Climbing and Gliding Flight.—The effect of cutting off the engine or of opening out is to alter the airscrew race effects on the tail of an aeroplane. The effects on the steady motion may be considerable, so that each condition of engine must be treated as a new problem. The derivatives are also changed. The effect of climbing is to reduce the stability of an aeroplane at the same speed of flight if we make the doubtful assumption that the changes of the derivatives due to the airscrew are unimportant.

There is not, in the analysis so far given, any expression for the inclination of the path of the centre of gravity, G. Referring to Fig. 239, it is seen that the angle of pitch α is involved as well as the inclination of the axis of X to the horizontal. The angle of ascent Θ is $-\alpha + \theta$, or in terms of the quantities more commonly used in the theory of stability

$$\Theta = \theta - \tan^{-1}\frac{w}{u}$$

In level flight Θ is zero, and the value of θ differs from the angle of incidence of the main planes by a constant.

Whether climbing, flying level or gliding, the angle of pitch, i.e. $\tan^{-1}\frac{w}{u}$, is almost independent of the inclination of the path; it is markedly a function of speed. The curve in Fig. 238 marked "θ_0 for level flight or angle of pitch, $\tan^{-1}\frac{w}{u}$" is most satisfactorily described as "angle of pitch."

Variation of Longitudinal Stability with Height and with Loading.— When discussing aeroplane performance, i.e. the steady motion of an aeroplane, it was shown that the aerodynamics of motion near the ground could be related to the motion for different heights and loadings if certain functions were chosen as fundamental variables. In particular it was shown that similar steady motions followed if

$$\frac{\rho V^2 S}{W} \text{ and } \frac{V}{nD}$$

were kept constant for the same or for similarly shaped aeroplanes. $\left(\frac{W}{S}\right.$ is now used for the wing loading, to avoid the double use of w in the same formula.) It was found to be unnecessary to consider the variation of engine power with speed of rotation and height, except when it was desired to satisfy the condition of maximum speed or maximum rate of climb.

In order to develop the corresponding method for stability it is necessary to examine more closely the form taken by the resistance derivatives. In equation (3) the forces and moments on an aeroplane were expressed in the form

$$X = f_x(u, w, q)$$

with n a known function of u, w, and q. No assumption was made that for a given density, attitude and advance per revolution, the forces and moments were proportional to the square of the speed.

If appeal be made to the principle of dynamical similarity it will be found that one of the possible forms of expression for X is

$$mX = \rho l^2 V^2 F\left\{\frac{w}{V}, \frac{lq}{V}, \frac{nl}{V}\right\} \quad . \quad . \quad . \quad . \quad . \quad (16)$$

where ρ is the density of the fluid, V is the resultant velocity of the aeroplane, and l is a typical length which for a given aeroplane is constant.

The arguments $\frac{w}{V}, \frac{lq}{V}, \frac{nl}{V}$ are of the nature of angles; $\frac{w}{V}$ is a measure of the angle of incidence of the aeroplane as a whole, $\frac{lq}{V}$ represents local changes of angle of incidence, and $\frac{nl}{V}$ defines the angle of attack of the airscrew blades.

Since V is the resultant velocity,

$$V^2 = u^2 + w^2 \quad . \quad . \quad . \quad . \quad . \quad . \quad (17)$$

and
$$\frac{\partial V}{\partial u_{w\,=\,const.}} = \frac{u}{V}, \text{ and } \frac{\partial V}{\partial w_{u\,=\,const.}} = \frac{w}{V}$$

Proceeding now to find one of the derivatives by differentiation of X with respect to u, whilst w and q are constant, leads to

$$X_u = \frac{\rho l^2}{m} 2V \frac{\partial V}{\partial u} F(\ldots) + \frac{\rho l^2 V^2}{m} \frac{\partial V}{\partial u} \left\{ -\frac{w}{V^2} \frac{\partial F}{\partial \frac{w}{V}} - \frac{lq}{V^2} \cdot \frac{\partial F}{\partial \frac{lq}{V}} + \frac{\partial}{\partial V}\left(\frac{nl}{V}\right)\frac{\partial F}{\partial \frac{nl}{V}} \right\} \quad (18)$$

or $X_u = \frac{\rho l^2 V}{m} \left\{ 2F - \frac{w}{V} \cdot \frac{\partial F}{\partial \frac{w}{V}} - \frac{lq}{V} \cdot \frac{\partial F}{\partial \frac{lq}{V}} + V \frac{\partial}{\partial V}\left(\frac{nl}{V}\right)\frac{\partial F}{\partial \frac{nl}{V}} \right\} \cdot \frac{u}{V} \quad . \quad . \quad . \quad (19)$

If now, during changes of ρ and m, $\frac{w}{V} = $ const., equation (17) shows

that $\frac{u}{V} = $ const. Further, make $\frac{lq}{V} = $ const., and $\frac{nl}{V} = $ const., and ex-

amine (19). The partial differential coefficients $\frac{\partial F}{\partial \frac{w}{V}}, \frac{\partial F}{\partial \frac{lq}{V}}$ and $\frac{\partial F}{\partial \frac{nl}{V}}$ have the

same value for variations under the restricted conditions. The outstanding term which does not obviously satisfy the condition of constancy is

$$V \frac{\partial}{\partial V}\left(\frac{nl}{V}\right) . \quad . \quad . \quad . \quad . \quad . \quad . \quad (20)$$

and this must be examined further; it will be found to vary in a more complex manner than the other quantities.

The airscrew torque may be expressed as

$$\phi_a = \rho n^2 l^5 \chi \left\{ \frac{w}{V}, \frac{lq}{V}, \frac{nl}{V} \right\} \quad . \quad . \quad . \quad . \quad (21)$$

and the engine torque as

$$\phi_e = \phi(h) . \psi(n) \quad . \quad . \quad . \quad . \quad . \quad (22)$$

In a standard atmosphere ρ is a known function of the height h. Equating ϕ_o and ϕ, putting $\phi(h) = \phi_,(\rho)$ gives

$$\rho n^2 l^5 \chi \left\{ \frac{w}{V}, \frac{lq}{V}, \frac{nl}{V} \right\} = \phi_,(\rho)\psi(n) \quad . \quad . \quad . \quad . \quad (23)$$

Differentiating partially with $\frac{w}{V}$ and $\frac{lq}{V}$ constant leads to

$$2\rho n l^5 \frac{\partial n}{\partial V}\chi + \rho n^2 l^5 \frac{\partial}{\partial V}\left(\frac{nl}{V}\right)\frac{\partial \chi}{\partial \frac{nl}{V}} = \phi_,(\rho)\psi'(n)\frac{\partial n}{\partial V} \quad . \quad . \quad (24)$$

Since in changes the $\dfrac{nl}{V} =$ const. there is a relation between the changes of n and V given by

$$\frac{\partial n}{\partial V} = \frac{n}{V}$$

and equation (24) becomes after rearrangement of terms

$$V\frac{\partial}{\partial V}\left(\frac{nl}{V}\right) = \frac{-2\chi + \dfrac{\phi_{\prime}(\rho)\psi'(n)}{\rho n l^5}}{\dfrac{\partial\chi}{\partial\dfrac{nl}{V}}} \quad . \quad . \quad . \quad . \quad . \quad (25)$$

χ and $\dfrac{\partial\chi}{\partial\dfrac{nl}{V}}$ are both constant during the changes of density and load, and

the complex expression

$$\frac{\phi_{\prime}(\rho)\psi'(n)}{\rho n l^5} \quad . \quad . \quad . \quad . \quad . \quad . \quad (26)$$

is the only one requiring further consideration.

Equation (23) shows that $\dfrac{\phi_{\prime}(\rho)\psi(n)}{m}$ is constant for our restricted conditions, and again utilising the condition that $\dfrac{\rho n^2 l^2}{m}$ and l^2 are constant,

$$\frac{\psi'(n)}{\psi(n)} = \frac{\text{const.}}{n} \quad . \quad . \quad . \quad . \quad . \quad . \quad (27)$$

is an equation to be satisfied by the torque curve of an engine if the value for $V\dfrac{\partial}{\partial V}\left(\dfrac{nl}{V}\right)$ is to take simple form. This equation can be integrated to give

$$\psi(n) = An^B \quad . \quad . \quad . \quad . \quad . \quad . \quad (28)$$

where A and B are constants. The only member of this family of curves which approaches an actual torque curve for an aero-engine is with $B = 0$, and this assumption is often made in approximate calculations. A more usual form for $\psi(n)$ is

$$\psi(n) = a - bn \quad . \quad . \quad . \quad . \quad . \quad . \quad (29)$$

where the approximation to a torque curve can be made to be very good over the working range, and where bn will not exceed $\frac{1}{3}$rd of a. Using (29) the value of $\dfrac{\phi_{\prime}(\rho)\psi'(n)}{\rho n l^5}$ may be estimated as compared with -2χ, for equation (23) gives

$$\frac{\phi_{\prime}(\rho)\psi(n)}{\rho n^2 l^5} = \chi$$

and
$$\therefore -2\chi\left\{1 - \frac{\phi_{,}(\rho)\psi'(n)}{2\rho n l^5 \chi}\right\} = -2\chi\left\{1 - \frac{n\psi'(n)}{2\psi(n)}\right\}$$
$$= -2\chi\left\{1 + \frac{bn}{2(a-bn)}\right\}. \quad . \quad (30)$$

The second term in the bracket is seen to be one-quarter of the first in the extreme case.

It may then be taken, as a satisfactory approximation, that $V\frac{\partial}{\partial V}\left(\frac{nl}{V}\right)$ is constant for the conditions of similar motions, and the resistance derivative X_u varies with weight (mg) and density (ρ) according to the law

$$X_u \propto \frac{\rho l^2 V}{m} \quad . \quad . \quad . \quad . \quad . \quad (31)$$

The same expression follows for the other force derivatives. For the moment derivatives,

$$\frac{M_u}{m} \propto \frac{\rho l^2 V}{m} \quad \text{and} \quad \therefore \frac{M_u}{B} \propto \frac{\rho l^2 V}{m} \cdot \frac{1}{k^2}$$

where k is the radius of gyration. The necessary theorem for the relation between stability at a given height and a given loading and the stability at any other height and loading can now be formulated.

Let ρ_0, V_0 and $\frac{W_0}{S}$ be one set of values of density, velocity and loading for which the conditions of steady motion have been satisfied and the resistance derivatives determined.

For another state of motion in which the density, velocity and loading are ρ_1, V_1 and $\frac{W_1}{S}$, the conditions for steadiness will be satisfied if

$$\frac{\rho_1 V_1{}^2}{W_1} = \frac{\rho_0 V_0{}^2}{W_0} \quad . \quad . \quad . \quad . \quad . \quad (32)$$

and the advance per revolution of the airscrew be made the same as before by an adjustment of the engine throttle.

The derivatives in the new steady motion are obtained from the values in the original motion by multiplying them by the ratio $\frac{\rho_1 V_1}{W_1} \cdot \frac{W_0}{\rho_0 V_0}$ for forces and by $\frac{\rho_1 V_1}{\rho_0 V_0}$ for couples. The first ratio is equal to $\frac{V_0}{V_1}$ or to $\sqrt{\frac{W_0}{W_1} \cdot \frac{\rho_1}{\rho_0}}$, as may be seen by use of (32).

If the derivatives of (13) be identified with density ρ_0 and loading $\frac{W_0}{S}$ a new series of coefficients for the stability equation can be written down in terms of them, but for density ρ_1 and loading $\frac{W_1}{S}$. They are

Coefficient of λ_1^4, 1

$A_1' \equiv$ coefficient of λ_1^3,

$$\left(\frac{W_0}{W_1}\cdot\frac{\rho_1}{\rho_0}\right)^{\frac{1}{2}}\left(-X_u - Z_w - \frac{1}{B}\frac{k_0^2}{k_1^2}M_q\right)$$

$B_1' \equiv$ coefficient of λ_1^2,

$$\left(\frac{W_0}{W_1}\cdot\frac{\rho_1}{\rho_0}\right)\left\{\frac{1}{B}\frac{k_0^2}{k_1^2}\begin{vmatrix} Z_w & u_0\frac{W_1}{W_0}\cdot\frac{\rho_0}{\rho_1}+Z_q \\ M_w & M_q \end{vmatrix} + \frac{1}{B}\frac{k_0^2}{k_1^2}\begin{vmatrix} X_u & -w_0\frac{W_1}{W_0}\cdot\frac{\rho_0}{\rho_1}+X_q \\ M_u & M_q \end{vmatrix} + \begin{vmatrix} X_u & X_w \\ Z_u & Z_w \end{vmatrix}\right\}$$

$C_1' \equiv$ coefficient of λ_1^1,

$$-\frac{1}{B}\left(\frac{W_0}{W_1}\cdot\frac{\rho_1}{\rho_0}\right)^{\frac{1}{2}}\frac{k_0^2}{k_1^2}\begin{vmatrix} X_u & X_w & -w_0\frac{W_1\rho_0}{W_0\rho_1}+X_q \\ Z_u & Z_w & u_0\frac{W_1\rho_0}{W_0\rho_1}+Z_q \\ M_u & M_w & M_q \end{vmatrix} + \frac{g}{B}\left(\frac{W_0\rho_1}{W_1\rho_0}\right)^{\frac{1}{2}}\frac{k_0^2}{k_1^2}\begin{vmatrix} M_u & -\sin\theta_0 \\ M_w & \cos\theta_0 \end{vmatrix}$$

$D_1' \equiv$ coefficients of λ_1^0,

$$\frac{g}{B}\left(\frac{W_0}{W_1}\cdot\frac{\rho_1}{\rho_0}\right)\frac{k_0^2}{k_1^2}\begin{vmatrix} X_u & X_w & \cos\theta_0 \\ Z_u & Z_w & \sin\theta_0 \\ M_u & M_w & 0 \end{vmatrix} \quad . \quad . \quad . \quad . \quad (33)$$

It will be seen from (33) that several modifications are introduced into the stability equation by the changes of loading and density.

For changes of density only, $k_1 = k_0$. If the weight of an aeroplane be changed it will usually follow that the radius of gyration will be changed, as the added weight will be near the centre of gravity. If the masses are so disposed during a change of loading that $k_1 = k_0$, and the height is so chosen that $\frac{W_0}{W_1}\cdot\frac{\rho_1}{\rho_0} = 1$, (33) leads to the simple form of equation

$$\lambda_1^4 + A_1\lambda_1^3 + B_1\lambda_1^2 + C_1\lambda_1 + D_1 = 0 \quad . \quad . \quad . \quad (34)$$

and the stability is exactly that of the original motion. The condition $\frac{W_0}{W_1}\cdot\frac{\rho_1}{\rho_0} = 1$ is not easily satisfied, since the heavy loading in one case may involve the use of too great a height in the corresponding lightly loaded condition.

The factor $\frac{1}{B}\begin{vmatrix} M_u & -\sin\theta_0 \\ M_w & \cos\theta_0 \end{vmatrix}$ which occurs in (33) represents the quantity $\frac{M_v}{B}$, i.e. the change of $\frac{M}{B}$ due to change of flight speed at constant altitude. Apart from the airscrew this quantity would always be zero since M is then zero for all speeds. For an aeroplane with twin engines so far apart that the tail plane does not project into the tail races the value of $\frac{M_v}{B}$ will be very small.

As an example of the use of (33) it will be assumed that $\frac{k_1}{k_0} = 1$, $\frac{W_1}{W_0}$ $=1\cdot20$, and $\frac{\rho_1}{\rho_0} = 0\cdot74$, $i.e.$ the loading has been increased by 20 per cent. and the flight is taking place at 10,000 ft. instead of near the ground. The least stable condition of the aeroplane has been chosen. Table 1 shows that it occurs for $V_0 = 60$ ft.-s. The conditions lead to

$$\sqrt{\frac{W_1}{W_0} \cdot \frac{\rho_0}{\rho_1}} = 1\cdot27 \quad \text{and} \quad V_1 = 1\cdot27V_0 = 76\cdot4 \text{ ft.-s.}$$

In the original example, page 467, the values of the coefficients of the stability equation were

$$A_1 = 2\cdot80, \ B_1 = 10\cdot0, \ C_1 = 1\cdot86 \quad \text{and} \ D_1 = 4\cdot39$$

With $u_0 = 60$, $w_0 = 12$ and the values of the derivatives given in Figs. 235–237, the new equation for stability becomes

$$\lambda^4 + 2\cdot21\lambda^3 + 7\cdot00\lambda^2 + 0\cdot96\lambda + 2\cdot82 = 0$$

and a solution of it is

$$(\lambda + 1\cdot105 \pm 2\cdot31i)(\lambda + 0\cdot001 \pm 0\cdot655i) = 0 \qquad . \quad . \quad . \ (35)$$

The second factor shows that the motion is only just stable.

The new and original motions are compared in the Table below.

TABLE 2.

	Original motion near the ground.	New motion at 10,000 feet with an increase of 20 per cent. in the load carried.
Flight speed	60 ft.-s.	76·4 ft.-s.
Period of rapid oscillation	2·22 secs.	2·72 secs.
Damping factor	1·45	1·10
Time to half disturbance	0·47 sec.	0·63 sec.
Period of phugoid oscillation	9·3 secs.	9·6 secs.
Damping factor	0·031	0·001
Time to half disturbance	22 secs.	700 secs.

The general effect of the increased loading and height is seen to be an increase in the period of the oscillations and a reduction in the damping. The tendency is clearly towards instability of the phugoid oscillation.

Approximate Solutions of the Biquadratic Equation for Longitudinal Stability.—If the period and damping of the rapid oscillation be very much greater than those of the phugoid oscillation, the biquadratic can be divided into two approximate quadratic factors with extreme rapidity. The original equation being

$$\lambda^4 + A_1\lambda^3 + B_1\lambda^2 + C_1\lambda + D_1 = 0$$

the approximate factors are

$$\lambda^2 + A_1\lambda + B_1 = 0$$

and

$$\lambda^2 + \left(\frac{C_1}{B_1} - \frac{A_1 D_1}{B_1{}^2}\right)\lambda + \frac{D_1}{B_1} = 0 \qquad . \quad . \quad . \quad . \ (36)$$

An example, see (15), gave

$$(\lambda + 7\cdot34 \pm 2\cdot45i) = 0$$

and

$$(\lambda + 0\cdot075 \pm 0\cdot170i) = 0$$

as a solution of

$$\lambda^4 + 14\cdot8\lambda^3 + 62\cdot0\lambda^2 + 9\cdot80\lambda + 2\cdot16 = 0$$

Applied to this equation (36) gives one factor as

$$\lambda^2 + 14\cdot8\lambda + 62\cdot0 = 0$$

or

$$(\lambda + 7\cdot4 \pm 2\cdot68i) = 0$$

which substantially reproduces the more accurate solution for the rapid oscillation.

The factor for the phugoid oscillation is

$$\lambda^2 + 0\cdot150\lambda + 0\cdot0332 = 0$$

or

$$\lambda + 0\cdot075 \pm 0\cdot165i = 0$$

a factor which again approaches the correct solution with sufficient closeness for many purposes.

A second example is provided in (35), the approximate factors being

$$(\lambda + 1\cdot105 \pm 2\cdot40i) \quad \text{and} \quad (\lambda + 0\cdot005 \pm 0\cdot635i)$$

instead of the more accurate

$$(\lambda + 1\cdot105 \pm 2\cdot35i) \quad \text{and} \quad (\lambda + 0\cdot001 \pm 0\cdot655i)$$

of (35). The approximation is again good.

Lateral Stability

The theory of lateral stability follows lines parallel to those of longitudinal stability, and some of the explanatory notes will be shortened in developing the formulæ.

The motions with which lateral stability deals are asymmetrical with respect to the aeroplane. Side slipping occurs along the axis of Y, whilst angular velocities in roll and yaw occur about the axes of X and Z. Axes fixed in the aeroplane are again used.

The equations of motion are—

$$\left.\begin{array}{l} \dot{v} + ur = Y' \\ \dot{p}A - \dot{r}E = L \\ \dot{r}C - \dot{p}E = N \end{array}\right\} \quad \cdots \cdots \quad (37)$$

The force mY depends partly on gravitational attraction and partly on air forces. The rolling moment L and the yawing moment N depend only on the motion through the air.

In the steady motion each of the three quantities Y, L and N is zero. v_0, p_0 and r_0 are also zero.

GRAVITATIONAL ATTRACTION

The component of the weight of the aeroplane along the axis of Y is

$$mg \cos \theta_0 . \sin \phi \quad . \quad . \quad . \quad . \quad . \quad . \quad (38)$$

where ϕ is a small angle. The approximation $\sin \phi = \phi$ will be used.

AIR FORCES

Generally, the lateral force, rolling moment and yawing moment depend on v, p and r. With a reservation as to lighter-than-air craft, Y, L and N take the forms

$$\left.\begin{array}{l} Y = f_Y(v,\, p,\, r) \\ L = f_L(v,\, p,\, r) \\ N = f_N(v,\, p,\, r) \end{array}\right\} . \quad . \quad . \quad . \quad . \quad . \quad (39)$$

There are no unsteady motions exclusively lateral, such as that of looping for longitudinal motion. Such motions as turning and spinning, although steady, cannot theoretically be treated apart from the longitudinal motion. For these reasons Y, L and M do not contain terms of zero order in v, p and r, and expansion of (39) leads immediately to the derivatives. Expanding by Taylor's theorem,

$$Y = \delta v \frac{\partial f_Y}{\partial v} + \delta p \frac{\partial f_Y}{\partial p} + \delta r \frac{\partial f_Y}{\partial r} \quad . \quad . \quad . \quad . \quad (40)$$

etc., or with a notation similar to that employed for longitudinal derivatives

$$Y = vY_v + pY_p + rY_r . \quad . \quad . \quad . \quad . \quad (41)$$

with similar expressions for L and N.

Forming the equations for small oscillations from (37) and (41) leads to

$$\left.\begin{array}{l} \dot{v} + u_0 r = g \cos \theta_0 . \phi + vY_v + pY_p + rY_r \\ \dot{p}A - \dot{r}E = \qquad\qquad vL_v + pL_p + rL_r \\ \dot{r}C - \dot{p}E = \qquad\qquad vN_v + pN_p + rN_r \end{array}\right\} \quad . \quad . \quad .. \quad (42)$$

Before equations (42) can be used as simultaneous equations in v, p and r, it is necessary to express ϕ in terms of p and r.

To obtain the position denoted by θ_0, ϕ, ψ the standard method is to rotate the aeroplane about GZ through ψ, then about GY through θ_0, and finally about GX through ϕ. The initial rotation about GZ has a component about GX (Fig. 240), and consequently $\dot{\phi}$ is not equal to p. The two modes of expressing angular velocities lead to the relations—

$$\left.\begin{array}{l} p = \dot{\phi} - \dot{\psi} \sin \theta_0 \\ r = \qquad \dot{\psi} \cos \theta_0 \end{array}\right\} \quad . \quad . \quad . \quad . \quad (43)$$

Combining the two equations, we have

$$\dot{\phi} = p + r \tan \theta_0 \quad . \quad . \quad . \quad . \quad . \quad (44)$$

Equations (43) might be used to convert equations (42) to the variables v, ϕ and ψ. The alternative and equivalent method is to use the knowledge that $\dot{\phi} = \lambda\phi$ in order to express ϕ in terms of p and r. Equations (42) become

$$
\left.
\begin{aligned}
\dot{v} - u_0 r &= g\cos\theta_0\frac{p}{\lambda} + g\sin\theta_0\frac{r}{\lambda} + vY_v + pY_p + rY_r \\
\dot{p}A - \dot{r}E &= \hphantom{xxxxxxxxxxx} vL_v + pL_p + rL_r \\
\dot{r}C - \dot{p}E &= \hphantom{xxxxxxxxxxx} vN_v + pN_p + rN_r
\end{aligned}
\right\} \quad . \quad (45)
$$

The solution of (45) is obtained by the substitutions

$$
\dot{v} = \lambda v, \quad \dot{p} = \lambda p, \quad \dot{r} = \lambda r \quad . \quad . \quad . \quad . \quad . \quad (46)
$$

where v_1, p_1 and r_1 are the initial values of the disturbance.
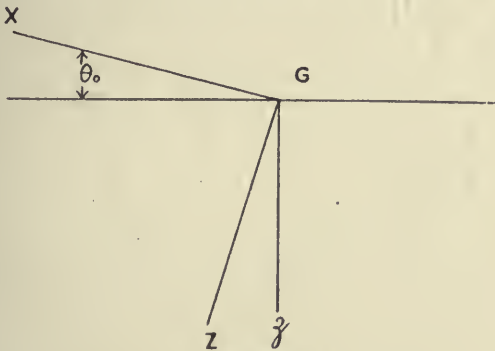
Fig. 240.

Equations (45) become—

$$
\left.
\begin{aligned}
(\lambda - Y_v)v + &\left(\frac{-g\cos\theta_0}{\lambda} - Y_p\right)p + \left(\frac{-g\sin\theta_0}{\lambda} - Y_r + u_0\right)r = 0 \\
-L_v v + &(\lambda A - L_p)p + (-\lambda E - L_r)r \hphantom{xxxxx} = 0 \\
-N_v v + &(-\lambda E - N_p)p + (\lambda C - N_r)r \hphantom{xxxxxx} = 0
\end{aligned}
\right\} (47)
$$

The elimination of any two of the quantities v, p and r leads to the equation from which λ is determined, i.e. to

$$
\begin{vmatrix}
\lambda - Y_v & -\dfrac{g\cos\theta_0}{\lambda} - Y_p & -\dfrac{g\sin\theta_0}{\lambda} - Y_r + u_0 \\[2mm]
-L_v & \lambda A - L_p & -\lambda E - L_r \\[2mm]
-N_v & -\lambda E - N_p & \lambda C - N_r
\end{vmatrix} = 0
\quad . \quad . \quad (48)
$$

If the first row be multiplied by λ to clear the denominators the equation will be seen to be a biquadratic in λ, the coefficient of the first term being $AC - E^2$.

For the purposes of comparison of results it is convenient to divide all coefficients of powers of λ by AC by dividing the second row by A and the third by C. The coefficients obtained, after these changes, by expansion of (48) in powers of λ are

Coefficient of λ^4, $1 - \dfrac{E^2}{AC}$

$A_2 \equiv$ coefficient of λ^3, $-Y_v - \dfrac{1}{A}L_p - \dfrac{1}{C}N_r$

$$+ \dfrac{E}{AC}(EY_v - L_r - N_p)$$

$B_2 \equiv$ coefficient of λ^2,

$$\dfrac{1}{A}\begin{vmatrix} Y_v & Y_p \\ L_v & L_p \end{vmatrix} + \dfrac{1}{C}\begin{vmatrix} Y_v & -u_0 + Y_r \\ N_v & N_r \end{vmatrix} + \dfrac{1}{AC}\begin{vmatrix} L_p & L_r \\ N_p & N_r \end{vmatrix}$$

$$+ \dfrac{E}{AC}\left\{ \begin{vmatrix} Y_v & Y_p \\ N_v & N_p \end{vmatrix} + \begin{vmatrix} Y_v & -u_0 + Y_r \\ L_v & L_r \end{vmatrix} \right\}$$

$C_2 \equiv$ coefficient of λ,

$$-\dfrac{1}{AC}\begin{vmatrix} Y_v & Y_p & -u_0 + Y_r \\ L_v & L_p & L_r \\ N_v & N_p & N_r \end{vmatrix} - \dfrac{g}{AC}\begin{vmatrix} L_v & -A\sin\theta_0 \\ N_v & C\cos\theta_0 \end{vmatrix}$$

$$- \dfrac{gE}{AC}\begin{vmatrix} L_v & -\cos\theta_0 \\ N_v & \sin\theta_0 \end{vmatrix}$$

$D_2 \equiv$ coefficient of λ^0,

$$-\dfrac{g}{AC}\begin{vmatrix} L_v & L_p & L_r \\ N_v & N_p & N_r \\ 0 & \cos\theta_0 & \sin\theta_0 \end{vmatrix} \quad . \quad . \quad . \quad . \quad (49)$$

It is clear that (49) is greatly simplified in form if the axes of X and Z are chosen so as to coincide with principal axes of inertia, since E is then zero. It appears from a comparison of the magnitudes of the various terms that those containing E as a factor are never important for any usual choice of axes.

The terms of (49) which do not contain E show a strong general similarity of form to those for longitudinal stability.

The conditions for stability are that A_2, B_2, C_2, D_2 and $A_2B_2C_2 - C_2^2 - A_2^2D_2$ shall all be positive.

Example—

$$\left. \begin{array}{lll} u_0 = 90 \text{ ft.-s.,} & \theta_0 = 0°\cdot9, & E = 0 \\ Y_v = -0\cdot105, & Y_p = -0\cdot90, & Y_r = 15 \\ \dfrac{1}{A}L_v = -0\cdot051, & \dfrac{1}{A}L_p = -8\cdot6, & \dfrac{1}{A}L_r = 3\cdot40 \\ \dfrac{1}{A}N_v = 0\cdot0142, & \dfrac{1}{C}N_p = -0\cdot032, & \dfrac{1}{C}N_r = -0\cdot40 \end{array} \right\} \quad . \quad . \quad . \quad (50)$$

Substituting the values of (50) in (49) leads to

$$A_2 = 9\cdot10, \ B_2 = 5\cdot52, \ C_2 = 11\cdot26, \ D_2 = -0\cdot960$$

D_2 is negative and indicates instability.

The equation

$$\lambda^4 + 9 \cdot 10\lambda^3 + 5 \cdot 52\lambda^2 + 11 \cdot 26\lambda - 0 \cdot 960 = 0$$

has the factors

$$(\lambda + 8 \cdot 60)(\lambda^2 + 0 \cdot 570\lambda + 1 \cdot 36)(\lambda - 0 \cdot 082) = 0 \qquad \cdot \quad \cdot \quad \cdot \ (51)$$

The roots are partly real and partly complex, and this is the common case. The instability is shown by the last factor, and it will be seen later that the aeroplane is spirally unstable. The first factor represents a very rapid subsidence, chiefly of the rolling motion. The remaining factor has complex roots and the corresponding oscillation is well damped.

The time of reduction of the rolling subsidence to half its initial value is 0·08 sec., whilst the instability leads to a double disturbance in about $8\frac{1}{2}$ secs. The period of the oscillation is $5\frac{1}{2}$ secs., and damps down to half value in $2\frac{1}{2}$ secs.

Effect of Flight Speed on Lateral Stability

The procedure followed for longitudinal stability is again adopted and typical curves for lateral derivatives are given (Figs. 241–243). The stalling speed has been kept as before, and the values of θ_0 may be taken from Fig. 238.

Unlike the longitudinal motion, which was usually very stable, the illustration shows instability to be the common feature, and later this will be traced to the choice of $\frac{1}{B}L_v$ and $\frac{1}{C}N_v$, which are largely at the designer's disposal.

The periods and damping factors at various speeds corresponding with the derivatives of Figs. 241–243 are given in Table 3 and are of great interest.

TABLE 3.

Flight speed (ft.-s.).	Rolling subsidence.		Lateral oscillation.			Spiral subsidence.	
	Damping factor.	Time to half disturbance (secs.).	Periodic time (secs.).	Damping factor.	Time to half disturbance (secs.).	Damping factor.	Time to half disturbance (secs.).
59·2	0·652	1·0	6·25	−1·31	−0·53	+1·53	0·45
58·6	2·0	0·35	5·48	−0·48	−1·4	+0·42	1·6
60	3·07	0·22	6·41	+0·19	+3·6	+0·03	23·0
70	6·50	0·11	7·00	0·35	2·0	−0·16	−4·3
80	7·50	0·09	6·25	0·31	2·2	−0·12	−5·7
90	8·60	0·08	5·55	0·28	2·5	−0·08	−8·6
100	9·60	0·07	4·91	0·28	2·5	−0·05	−14·0
122·5	11·81	0·06	3·95	0·31	2·2	−0·01	−70·0
140	13·50	0·05	3·46	0·35	2·0	+0·003	+230

Negative values occurring in the above table indicate instability, and the expression " time to half disturbance " when associated with a negative sign should be interpreted as " time to double disturbance."

Throughout the speed range of steady flight the stability equation

for the lateral motion has two real roots and one pair of complex roots. When the aeroplane is stalled or overstalled the oscillation becomes very unstable, and stalling is a common preliminary to an involuntary spin. For speeds between 70 ft.-s. and 100 ft.-s. the oscillation is very stable, and neither the period nor the damping shows much change.

The damping of the rolling subsidence is compared below with the value of $\frac{1}{A}L_p$ on account of the remarkable agreement at speeds well above the minimum possible.

TABLE 4.

Flight speed (ft.-s.).	Damping factor of rolling subsidence.	$-\frac{1}{A}L_p$
59·2	0·65	−1·5
58·6	2·0	+0·5
60	3·07	2·7
70	6·50	6·0
80	7·50	7·5
90	8·60	8·6
100	9·60	9·6
122·5	11·8	11·8
140	13·5	13·4

The agreement suggests that $(\lambda + \frac{1}{A}L_p)$ is commonly a factor of the biquadratic for stability except near stalling speed. The motion indicated is the stopping of the downward motion of a wing due to the increase of angle of incidence. This is the nearest approach to simple motion in any of the disturbances to which an aeroplane is subjected. It is possible that the first two terms entered under spiral subsidence really belong to the rolling subsidence. as the analysis up to this point does not permit of discrimination when the roots are roughly of the same magnitude. In either case the discrepancy between $-\frac{L_p}{A}$ and the damping factor at 59·2 ft.-s. is great, and in itself indicates a much less simple motion for an aeroplane which is overstalled and then disturbed. ·

Over a considerable range of speeds (70 ft.-s. to 130 ft.-s.) instability is indicated in what has been called the " spiral subsidence." This is not a dangerous type of instability, and has been accepted for the reason that considerable rudder control has many advantages for rapid manoeuvring, as in aerial fighting, and the conditions for large controls are not easily reconciled with those for stability.

For navigation, such instability is undesirable, since, as the name implies, the aeroplane tends to travel in spirals unless constantly corrected. This motion can be analysed somewhat easily so as to justify the description " spiral."

As was indicated in equation (51), spiral instability is associated with a change in sign of D_2 from positive to negative, whilst C_2 is then
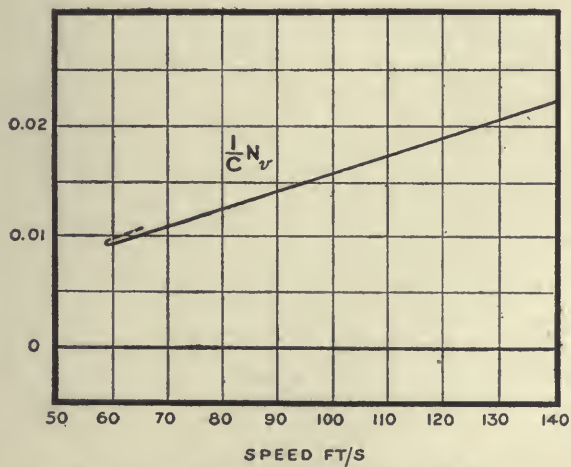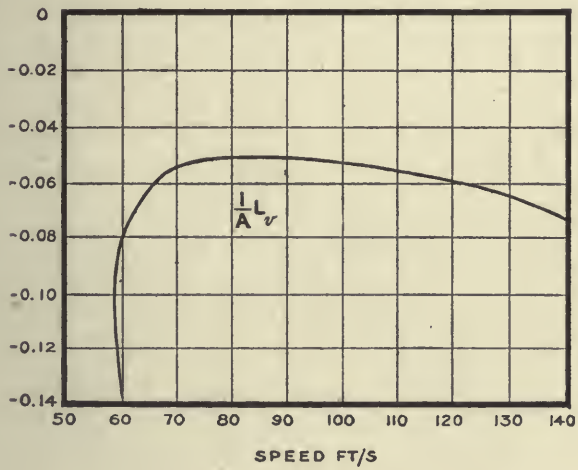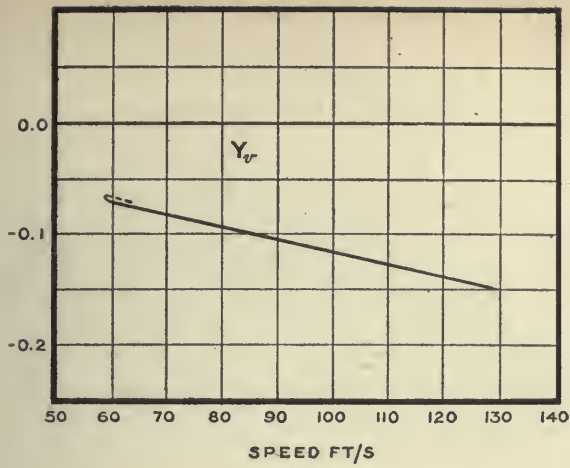
FIG. 241.—Resistance derivatives for sideslipping.
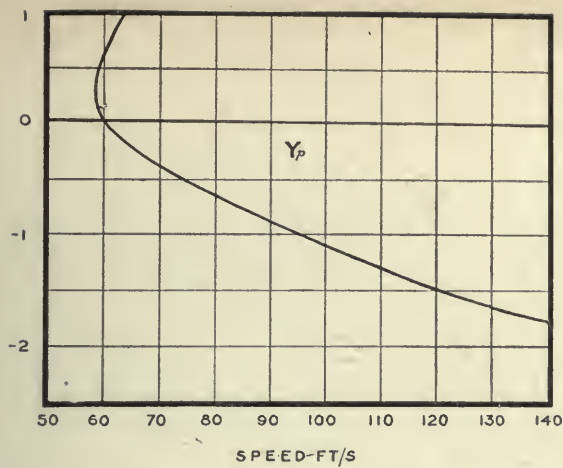
482
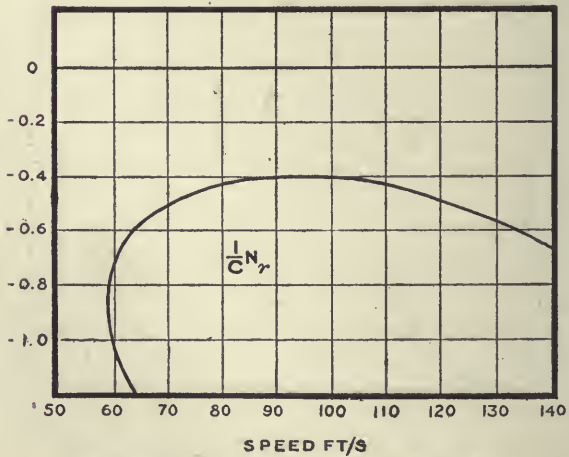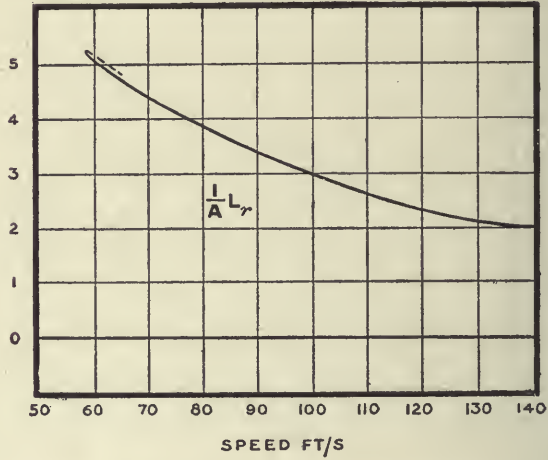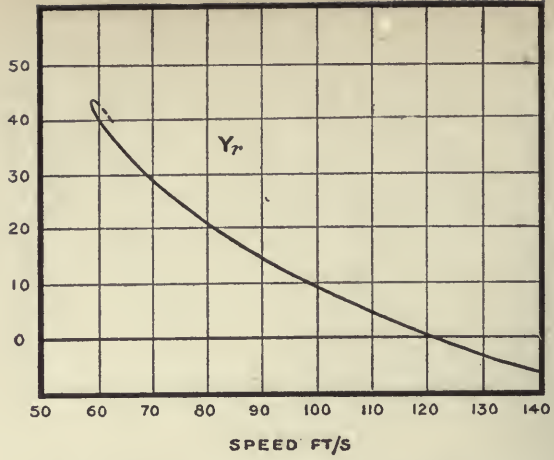
Fig. 242.—Resistance derivatives for rolling.
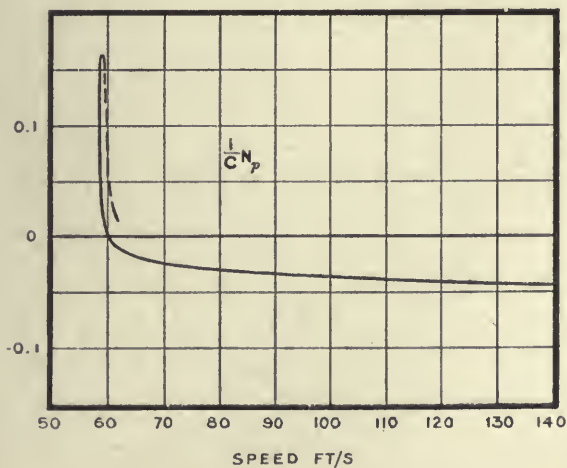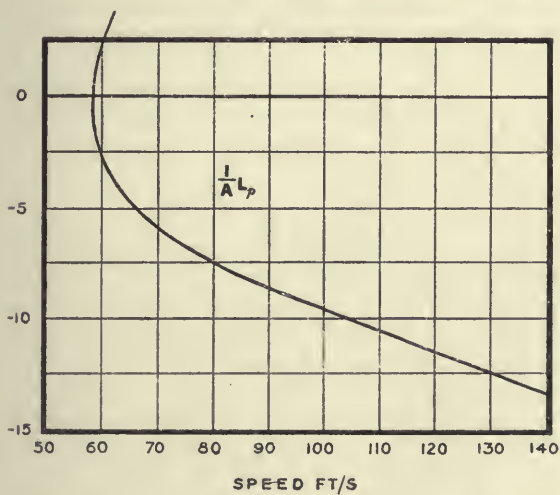
FIG. 243.—Resistance derivatives for yawing.

moderately large. If D_2 is very small the root of the biquadratic corresponding with the spiral subsidence is

$$\lambda + \frac{D_2}{C_2} = 0 \quad . \quad . \quad . \quad . \quad . \quad . \quad (52)$$

θ_0 is zero between 90 ft.-s. and 100 ft.-s., and equation (49) shows that when θ_0 is zero

$$D_2 = \frac{g}{AC} \begin{vmatrix} L_v & L_r \\ N_v & N_r \end{vmatrix} \quad . \quad . \quad . \quad . \quad . \quad (53)$$

and D_2 depends on the rolling moments and yawing moments due to sideslipping and turning, and changes sign when N_vL_r is numerically greater than L_vN_r.

Consider the motion of the aeroplane when banked but not turning : the aeroplane begins to sideslip downwards, and the sideslipping acting through the dihedral angle produces a rolling couple L_v tending to reduce the bank. At the same time the sideslipping acting on the fin and rudder produces a couple N_v turning the aeroplane towards the lower wing. The upper wing travels through the air faster than the lower as a result of this turning, and produces a couple L_r tending to increase the bank. The turning is damped by the couple N_r.

There are then two couples tending to affect the bank in opposite directions, and the aeroplane is stable if the righting couple preponderates. If, on the other hand, the aeroplane is unstable it overbanks, sideslips in more rapidly, and so on, the result being a spiral. There is a limit to the rate of turning, but the more formal treatment of disturbed motion must be deferred to a later part of the chapter. Enough has been said to justify the terms used.

Climbing and Gliding Flight

Owing to the twist in the airscrew race the effect of variation of thrust on the position of the rudder may be very considerable. The derivatives also change because of the change of speed of the air over the fin and rudder. An airscrew which has a velocity not along its axis experiences a force equivalent to that on a fin in the position of the airscrew. Yawing and sideslipping produce moments as well as forces, and the calculation of stability must in general be approached by the estimation of new conditions of steady motion and new derivatives.

Variation of Lateral Stability with Height and Loading

The derivatives change with density and loading according to the law already deduced for longitudinal stability, where it was shown that the force derivatives and the moment derivatives divided by the mass of the aeroplane varied as $\frac{\rho V}{m}$, if the quantities $\frac{\rho V^2 S}{W}$ and $\frac{V}{nD}$ were kept

constant in the steady motions. If $\dfrac{W_0}{S}$ and ρ_0 correspond with loading and density for one steady motion and $\dfrac{W_1}{S}$ and ρ_1 with loading and density for another, then the force derivatives in the second motion are obtained from those in the first by multiplying by $\sqrt{\dfrac{W_0}{W_1} \cdot \dfrac{\rho_1}{\rho_0}}$. For the moment derivatives the multiplying factor is $\sqrt{\dfrac{W_1}{W_0} \cdot \dfrac{\rho_1}{\rho_0}}$, or more conveniently $\dfrac{m_1}{m_0} \sqrt{\dfrac{W_0}{W_1} \cdot \dfrac{\rho_1}{\rho_0}}$.

In writing down the coefficients of the biquadratic for stability it will be assumed that the axes of X and Z have been chosen to be principal axes of inertia, so that E is zero. The coefficients are:

Coefficient of $\lambda_1{}^4$, 1

$$A_2{}^1 \equiv \text{coefficient of } \lambda_1{}^3, \; \left(\frac{W_0}{W_1} \cdot \frac{\rho_1}{\rho_0}\right)^{\frac{1}{2}} \left\{ -Y_v - \frac{1}{A}\left(\frac{k_0{}^2}{k_1{}^2}\right)_A L_p - \frac{1}{C}\left(\frac{k_0{}^2}{k_1{}^2}\right)_C N_r \right\}$$

$B_2{}^1 \equiv$ coefficient of $\lambda_1{}^2$,

$$\left(\frac{W_0}{W_1} \cdot \frac{\rho_1}{\rho_0}\right) \left\{ \frac{1}{A}\left(\frac{k_0{}^2}{k_1{}^2}\right)_A \begin{vmatrix} Y_r & Y_p \\ L_v & L_p \end{vmatrix} + \frac{1}{C}\left(\frac{k_0{}^2}{k_1{}^2}\right)_C \begin{vmatrix} Y_v & -u_0\dfrac{W_1}{W_0} \cdot \dfrac{\rho_0}{\rho_1} + Y_r \\ N_v & N_r \end{vmatrix} \right.$$
$$\left. + \frac{1}{AC}\left(\frac{k_0{}^2}{k_1{}^2}\right)_A\left(\frac{k_0{}^2}{k_1{}^2}\right)_C \begin{vmatrix} L_p & L_r \\ N_p & N_r \end{vmatrix} \right\}$$

$C_2{}^1 \equiv$ coefficient of λ_1,

$$-\frac{1}{A}\left(\frac{k_0{}^2}{k_1{}^2}\right)_A \frac{1}{C}\left(\frac{k_0{}^2}{k_1{}^2}\right)_C \left\{ \left(\frac{W_0}{W_1} \cdot \frac{\rho_1}{\rho_0}\right)^{\frac{3}{2}} \begin{vmatrix} Y_v & Y_p & -u_0\dfrac{W_1}{W_0} \cdot \dfrac{\rho_0}{\rho_1} + Y_r \\ L_v & L_p & L_r \\ N_v & N_p & N_r \end{vmatrix} \right.$$
$$\left. + g\left(\frac{W_0}{W_1} \cdot \frac{\rho_1}{\rho_0}\right)^{\frac{1}{2}} \begin{vmatrix} L_v & -\sin\theta_0 \\ N_v & \cos\theta_0 \end{vmatrix} \right\}$$

$D_2{}^1 \equiv$ coefficient of $\lambda_1{}^0$,

$$-\frac{g}{AC}\left(\frac{k_0{}^2}{k_1{}^2}\right)_A\left(\frac{k_0{}^2}{k_1{}^2}\right)_C \left(\frac{W_0}{W_1} \cdot \frac{\rho_1}{\rho_0}\right)_2 \begin{vmatrix} L_v & L_p & L_r \\ N_v & N_p & N_r \\ 0 & \cos\theta_0 & \sin\theta_0 \end{vmatrix} . \quad (54)$$

If $\dfrac{W_0}{W_1} \cdot \dfrac{\rho_1}{\rho_0} = 1$, $\left(\dfrac{k_0{}^2}{k_1{}^2}\right)_A = 1$ and $\left(\dfrac{k_0{}^2}{k_1{}^2}\right)_C = 1$, the stability is again the same as the original stability.

It has been pointed out that spiral instability occurs when D_2 changes sign, and from (54) it is clear that the new factors will not change the

condition although they may affect the magnitude. It follows that spiral instability cannot be eliminated or produced by changes of height or loading.

Example.—Increase of loading 20 per cent. and the height 10,000 feet, where $\dfrac{\rho_1}{\rho_0} = 0.740$. Speed 60 ft.-s., $\left(\dfrac{k_0{}^2}{k_1{}^2}\right)_A = 1$, $\left(\dfrac{k_0{}^2}{k_1{}^2}\right)_c = 1$, $\theta_0 = 11^\circ$

$$\sqrt{\frac{W_1 \cdot \rho_0}{W_0 \cdot \rho_1}} = 1.27 \quad \text{and} \quad V_1 = 1.27 V_0 = 76.4 \text{ ft.-s.}$$

For the loading w_0 and ρ_0 the values of the coefficients of the biquadratic which correspond with Table 3 are

$$A_2 = 3.48, \; B_2 = 2.33, \; C_2 = 3.12, \; D_2 = 0.104$$

and from (54) the values for the increased loading and height are found as

$$A_2' = 2.74, \; B_2' = 1.45, \; C_2' = 1.83, \; D_2' = 0.0645$$

The biquadratic equation with these coefficients has been solved, the factors being

$$(\lambda + 2.45)(\lambda^2 + 0.255\lambda + 0.728)(\lambda + 0.0362) = 0$$

or

$$(\lambda + 2.45)(\lambda + 0.127 \pm 0.852i)(\lambda + 0.0362) = 0 \qquad (55)$$

The new and original motions are compared in the Table below : —

TABLE 5.

	Original motion near ground.	New motion at 10,000 ft. with an increased loading of 20%.
Flight speed	60 ft.-s.	76.4 ft.-s.
Damping factor of rolling subsidence . .	3.07	2.45
Time to half disturbance	0.22 sec.	0.28 sec.
Period of lateral oscillation	6.41 secs.	7.37 secs.
Damping factor	0.19	0.063
Time to half disturbance	3.6 secs.	11 secs.
Damping factor of spiral subsidence . . .	0.03	0.036
Time to half disturbance	23 secs.	19 secs.

The rolling subsidence is somewhat less heavily damped for the increased loading and height, whilst the spiral subsidence is more heavily damped. The period of the lateral oscillation is increased and its damping much reduced.

In both longitudinal and lateral motions the most marked effect of reduced density and increased loading has been the decrease of damping of the slower oscillations.

STABILITY IN CIRCLING FLIGHT

The longitudinal and lateral stabilities of an aeroplane can only be considered separately when the steady motion is rectilinear and in the plane of symmetry, and it is now proposed to deal with those cases in which the separation cannot be assumed to hold with sufficient accuracy.

The analytical processes followed are the same as before, but the quantities involved are more numerous and the expressions developed more complex. In order to keep the simplest mathematical form it has been found advantageous to take as axes of reference the three principal axes of inertia of the aeroplane.

The equations of motion have been given in Chapter V., and in reference to principal axes of inertia take the form—

$$
\left.
\begin{aligned}
\dot{u} + wq - vr &= X \\
\dot{v} + ur - wp &= Y \\
\dot{w} + vp - uq &= Z \\
\dot{p}A - rq(B - C) &= L \\
\dot{q}B - pr(C - A) &= M \\
\dot{r}C - qp(A - B) &= N
\end{aligned}
\right\} \quad . \quad . \quad . \quad . \quad . \quad (56)
$$

The axes are indicated in Fig. 106, Chapter IV., whilst in Chapter V. various expressions are used for the angular positions relative to the ground. Of the alternatives available, the expressions in terms of direction cosines n_1, n_2 and n_3 for the position of the downwardly directed vertical relative to the body axes will be used.

Gravitational Attractions.—The values of X, Y and Z depend partly on the components of gravitational attraction and partly on motion through the air. The former are respectively

$$
n_1 g, \quad n_2 g \quad \text{and} \quad n_3 g \quad . \quad . \quad . \quad . \quad (57)
$$

Air Forces.—In an aeroplane the forces and moments are taken to be determined wholly by the relative motion, and each of them is typified by the expression

$$
X = f_X(u, v, w, p, q, r). \quad . \quad . \quad . \quad . \quad (58)
$$

Before the stability of a motion can be examined, the equations of steady motion must be satisfied, *i.e.*

$$
\left.
\begin{aligned}
w_0 q_0 - v_0 r_0 &= X_0 \\
u_0 r_0 - w_0 p_0 &= Y_0 \\
v_0 p_0 - u_0 q_0 &= Z_0 \\
-r_0 q_0 (B - C) &= L_0 \\
-p_0 r_0 (C - A) &= M_0 \\
-q_0 p_0 (A - B) &= N_0
\end{aligned}
\right\} \quad . \quad . \quad . \quad . \quad . \quad (59)
$$

must be solved. It has already been pointed out (Chapter V.) that steady motions can only occur if the resulting rotation of the aircraft is about the vertical, in which case

$$
p_0 = n_1 \Omega \qquad q_0 = n_2 \Omega \qquad r_0 = n_3 \Omega \quad . \quad . \quad . \quad (60)
$$

where Ω represents the resultant angular velocity. Some problems connected with the solution of equations (59) have been referred to in Chapter V.

Small Disturbances.—As in the case of longitudinal stability, the quantities $\dfrac{\partial f}{\partial u}$, $\dfrac{\partial f_X}{\partial v}$, etc., are spoken of as resistance derivatives, and their

values are determined experimentally. The shorter notation X_u, X_v introduced by Bryan is also retained. If $u_0 + u$ be written for u, $v_0 + v$ for v, etc., in equations (56) and the expansions of $X \ldots N$ up to first differential coefficients used instead of the general functions, the equations can be divided into parts of zero and first order. The terms of zero order vanish in virtue of the conditions of steady motion as given by (59), and there remain the first-order terms as below :—

$$
\begin{aligned}
\dot{u} + wq_0 + w_0 q - vr_0 - v_0 r &= gdn_1 + uX_u' + vX_v' + wX_w' \\
&\quad + pX_p' + qX_q' + rX_r' \\
\dot{v} + ur_0 + u_0 r - wp_0 - w_0 p &= gd\dot{n}_2 + uY_u' + vY_v' + wY_w' \\
&\quad + pY_p' + qY_q' + rY_r' \\
\dot{w} + vp_0 + v_0 p - uq_0 - u_0 q &= gdn_3 + uZ_u' + vZ_v' + wZ_w' \\
&\quad + pZ_p' + qZ_q' + rZ_r' \\
A\left\{\dot{p} + \frac{C-B}{A}(rq_0 + r_0 q)\right\} &= \quad uL_u' + vL_v' + wL_w' \\
&\quad + pL_p' + qL_q' + rL_r' \\
B\left\{\dot{q} + \frac{A-C}{B}(pr_0 + p_0 r)\right\} &= \quad uM_u' + vM_v' + wM_w' \\
&\quad + pM_p' + qM_q' + rM_r' \\
C\left\{\dot{r} + \frac{B-A}{C}(qp_0 + q_0 p)\right\} &= \quad uN_u' + vN_v' + wN_w' \\
&\quad + pN_p' + qN_q' + rN_r'
\end{aligned}
\right\} \quad . \ (61)
$$

In these equations u, v, w, p, q and r represent the small disturbances, whilst the same letters with the suffix zero apply to the steady

FIG. 244.

motion, and are therefore constant during the further calculations. The dashes used to the letters $X \ldots N$ indicate that the parts due to air only are involved; the derivatives are all experimentally known constants.

Evaluation of dn_1, dn_2 **and** dn_3 **in terms of** p, q **and** r.— Before progress can be made with equations (61) it is necessary to reduce all the quantities to dependence on p, q and r. In developing the relation, three auxiliary small angles α, β and γ are used which represent displacements from the original position, and expressions for p, q and r and dn_1, dn_2 and dn_3 will be written down in terms of α, β, γ, and the rotations in the steady motion.
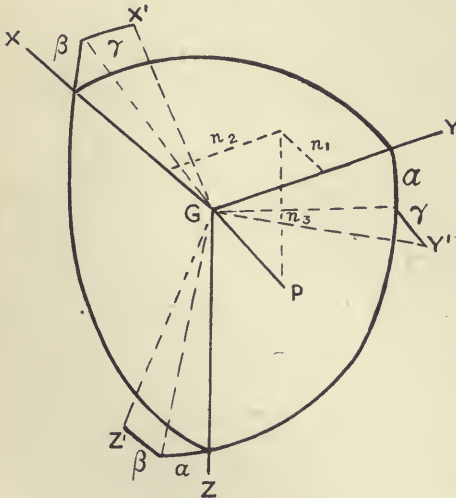
If GP of Fig. 244 represent the downwardly directed vertical defined by the direction cosines n_1, n_2 and n_3 before displacement and by $n_1 + dn_1$, etc., afterwards, it is readily deduced from the figure that

$$n_1 + dn_1 = n_1 - n_3\beta + n_2\gamma \quad . \quad . \quad . \quad . \quad . \quad (62)$$

with similar expressions for n_2 and n_3. The changes of direction cosines are therefore

$$\left.\begin{array}{l} dn_1 = -n_3\beta + n_2\gamma \\ dn_2 = -n_1\gamma + n_3\alpha \\ dn_3 = -n_2\alpha + n_1\beta \end{array}\right\} \quad . \quad . \quad . \quad . \quad . \quad (63)$$

The resultant velocity being made up of Ω about the vertical and $\dot{\alpha}$, $\dot{\beta}$ and $\dot{\gamma}$ about the axes of X, Y and Z, the changes from p_0, q_0 and r_0 can be obtained by resolution along the new axes, and hence

$$\left.\begin{array}{l} p = \dot{\alpha} - n_3\Omega\beta + n_2\Omega\gamma \\ \quad = \dot{\alpha} - r_0\beta + q_0\gamma \\ q = r_0\alpha + \dot{\beta} - p_0\gamma \\ r = -q_0\alpha + p_0\beta + \dot{\gamma} \end{array}\right\} \quad . \quad . \quad . \quad . \quad (64)$$

In the case of small oscillations it is known from the general type of solution that

$$\dot{\alpha} = \lambda\alpha \qquad \dot{\beta} = \lambda\beta \qquad \dot{\gamma} = \lambda\gamma . \quad . \quad . \quad . \quad (65)$$

and using these values in (64) reduces the equations to simultaneous linear form for which the solution is

$$\frac{\alpha}{\begin{vmatrix} -r_0 & q_0 & p \\ \lambda & -p_0 & q \\ p_0 & \lambda & r \end{vmatrix}} = \frac{-\beta}{\begin{vmatrix} \lambda & q_0 & p \\ r_0 & -p_0 & q \\ -q_0 & \lambda & r \end{vmatrix}} = \frac{\gamma}{\begin{vmatrix} \lambda & -r_0 & p \\ r_0 & \lambda & q \\ -q_0 & p_0 & r \end{vmatrix}} = \frac{1}{\begin{vmatrix} \lambda & -r_0 & q_0 \\ r_0 & \lambda & -p_0 \\ -q_0 & p_0 & \lambda \end{vmatrix}} . \quad (66)$$

The determinant in the denominator of the last expression is easily evaluated and found to be $\lambda(\Omega^2 + \lambda^2)$. and from (63) and (66) it can be deduced that

$$dn_1 = \begin{vmatrix} \lambda & n_1 & p \\ r_0 & n_2 & q \\ -q_0 & n_3 & r \end{vmatrix} \Big/ (\Omega^2 + \lambda^2) \quad . \quad . \quad . \quad . \quad (67)$$

$$= \frac{1}{\Omega^2 + \lambda^2}\{(1 - n_1{}^2)\Omega p - (n_1 q_0 + n_3\lambda)q - (n_1 r_0 - n_2\lambda)r\} \quad . \quad (68)$$

Similar expressions for dn_2 and dn_3 follow from symmetry by the ordinary laws of cyclic changes.

It is convenient to make temporary use of a quantity μ defined by

$$\mu = \frac{g}{\Omega^2 + \lambda^2} \quad . \quad . \quad . \quad . \quad . \quad (69)$$

With the aid of the relations developed it is now possible to rewrite equations (61) in more convenient form as

$$
\left.
\begin{aligned}
&(X_u{}' - \lambda)u + (X_v{}' + r_0)v + (X_w{}' - q_0)w \\
&+ \{X_p{}' + \mu\Omega(1 - n_1{}^2)\}p + \{X_q{}' - w_0 - \mu(n_1 q_0 + \lambda n_3)\}q + \{X_r{}' + v_0 - \mu(n_1 r_0 - \lambda n_2)\}r = 0 \\[4pt]
&(Y_u{}' - r_0)u + (Y_v{}' - \lambda)v + (Y_w{}' + p_0)w \\
&+ \{Y_p{}' + w_0 - \mu(n_2 p_0 - \lambda n_3)\}p + \{Y_q{}' + \mu\Omega(1 - n_2{}^2)\}q + \{Y_r{}' - u_0 - \mu(n_2 r_0 + \lambda n_1)\}r = 0 \\[4pt]
&(Z_u{}' + q_0)u + (Z_v{}' - p_0)v + (Z_w{}' - \lambda)w \\
&+ \{Z_p{}' - v_0 - \mu(n_3 p_0 + \lambda n_2)\}p + \{Z_q{}' + u_0 - \mu(n_3 q_0 - \lambda n_1)\}q + \{Z_r{}' + \mu\Omega(1 - n_3{}^2)\}\ r = 0 \\[6pt]
&\frac{L_u{}'u}{A} \qquad\qquad\quad + \frac{L_v{}'v}{A} \qquad\qquad\quad + \frac{L_w{}'w}{A} \\
&+ \left(\frac{L_p{}'}{A} - \lambda\right)p \qquad + \left(\frac{L_q{}'}{A} + \frac{B - C}{A}r_0\right)q + \left(\frac{L_r{}'}{A} + \frac{B - C}{A}q_0\right)r \qquad = 0 \\[6pt]
&\frac{M_u{}'u}{B} \qquad\qquad\quad + \frac{M_v{}'v}{B} \qquad\qquad\quad + \frac{M_w{}'w}{B} \\
&+ \left(\frac{M_p{}'}{B} + \frac{C - A}{B}q_0\right)p + \left(\frac{M_q{}'}{B} - \lambda\right)q \qquad + \left(\frac{M_r{}'}{B} + \frac{C - A}{B}p_0\right)r \qquad = 0 \\[6pt]
&\frac{N_u{}'u}{C} \qquad\qquad\quad + \frac{N_v{}'v}{C} \qquad\qquad\quad + \frac{N_w{}'w}{C} \\
&+ \left(\frac{N_p{}'}{C} + \frac{A - B}{C}q_0\right)p + \left(\frac{N_q{}'}{C} + \frac{A - B}{C}p_0\right)q + \left(\frac{N_r{}'}{C} - \lambda\right)r \qquad = 0
\end{aligned}
\right\} \cdot \ (70)
$$

An examination of the equations will show that certain constants may be grouped together and treated as new derivatives. The table below will be convenient for reference to the equivalents used.

	u	v	w	p	q	r
X	$X_u{}'$	$X_v{}' + r_0$	$X_w{}' - q_0$	$X_p{}'$	$X_q{}' - w_0$	$X_r{}' + v_0$
Y	$Y_u{}' - r_0$	$Y_v{}'$	$Y_w{}' + p_0$	$Y_p{}' + w_0$	$Y_q{}'$	$Y_r{}' - v_0$
Z	$Z_u{}' + q_0$	$Z_v{}' - p_0$	$Z_w{}'$	$Z_p{}' - v_0$	$Z_q{}' + u_0$	$Z_r{}'$
L	$\dfrac{L_u{}'}{A}$	$\dfrac{L_v{}'}{A}$	$\dfrac{L_w{}'}{A}$	$\dfrac{L_p{}'}{A}$	$\dfrac{L_q{}'}{A} + \dfrac{B - C}{A}r_0$	$\dfrac{L_r{}'}{A} + \dfrac{B - C}{A}q_0$
M	$\dfrac{M_u{}'}{B}$	$\dfrac{M_v{}'}{B}$	$\dfrac{M_w{}'}{B}$	$\dfrac{M_p{}'}{B} + \dfrac{C - A}{B}r_0$	$\dfrac{M_q{}'}{B}$	$\dfrac{M_r{}'}{B} + \dfrac{C - A}{B}p_0$
N	$\dfrac{N_u{}'}{C}$	$\dfrac{N_v{}'}{C}$	$\dfrac{N_w{}'}{C}$	$\dfrac{N_p{}'}{C} + \dfrac{A - B}{C}q_0$	$\dfrac{N_q{}'}{C} + \dfrac{A - B}{C}p_0$	$\dfrac{N_r{}'}{C}$

(71)

Table (71) needs little explanation; it indicates that in the further work an expression such as X_v is used instead of the longer one $X_v{}' + r_0$, and so on.

If now the variables p, q, r, u, v and w be eliminated from equations (70), the stability equation in λ is obtained, and in determinantal form is given by (72).

$$
\begin{vmatrix}
X_u - \lambda & X_v & X_w & X_p + \mu\Omega(1 - n_1{}^2) & X_q - \mu(n_1 q_0 + n_3\lambda) & X_r - \mu(n_1 r_0 - n_2\lambda) \\
Y_u & Y_v - \lambda & Y_w & Y_p - \mu(n_2 p_0 - n_3\lambda) & Y_q + \mu\Omega(1 - n_2{}^2) & Y_r - \mu(n_2 r_0 + n_1\lambda) \\
Z_u & Z_v & Z_w - \lambda & Z_p - \mu(n_3 p_0 + n_2\lambda) & Z_q - \mu(n_3 q_0 - n_1\lambda) & Z_r + \mu\Omega(1 - n_3{}^2) \\
L_u & L_v & L_w & L_p - \lambda & L_q & L_r \\
M_u & M_v & M_w & M_p & M_q - \lambda & M_r \\
N_u & N_v & N_w & N_p & N_q & N_r - \lambda
\end{vmatrix} = (0)
$$

(72)

The further procedure consists in an application of (72), and the point at which analytical methods are used before introducing numerical values is at the choice of a worker. The analysis has elsewhere been carried to the stage at which the coefficients of λ have all been found in general form,

but the expressions are very long. It would be possible to make the substitution in (72) and expand in powers of λ by successive reduction of the order of the determinant, and from the simplicity of the first three columns it would be expected that this would not be difficult. The presence of μ is a complication, and perhaps the following form, in which it has been eliminated, represents the best stage at which to make a beginning of the numerical work :—

$$
\lambda^2 \begin{vmatrix}
X_u-\lambda & X_v & X_w & X_p & X_q-\dfrac{gn_3}{\lambda} & X_r+\dfrac{gn_2}{\lambda} \\[2mm]
Y_u & Y_v-\lambda & Y_w & Y_p+\dfrac{gn_3}{\lambda} & Y_q & Y_r-\dfrac{gn_1}{\lambda} \\[2mm]
Z_u & Z_v & Z_w-\lambda & Z_p-\dfrac{gn_2}{\lambda} & Z_q+\dfrac{gn_1}{\lambda} & Z_r \\[2mm]
L_u & L_v & L_w & L_p-\lambda & L_q & L_r \\
M_u & M_v & M_w & M_p & M_q-\lambda & M_r \\
N_u & N_v & N_w & N_p & N_q & N_r-\lambda
\end{vmatrix}
$$

$$
-g\Omega \begin{vmatrix}
X_u-\lambda & X_v & X_w & -(1-n_1{}^2) & X_q & X_r \\
Y_u & Y_v-\lambda & Y_w & n_1 n_2 & Y_q & Y_r \\
Z_u & Z_v & Z_w-\lambda & n_1 n_3 & Z_q & Z_r \\
L_u & L_v & L_w & 0 & L_q & L_r \\
M_u & M_v & M_w & 0 & M_q-\lambda & M_r \\
N_u & N_v & N_w & 0 & N_q & N_r-\lambda
\end{vmatrix}
$$

$$
-g\Omega \begin{vmatrix}
X_u-\lambda & X_v & X_w & X_p & n_1 n_2 & X_r \\
Y_u & Y_v-\lambda & Y_w & Y_p & -(1-n_2{}^2) & Y_r \\
Z_u & Z_v & Z_w-\lambda & Z_p & n_2 n_3 & Z_r \\
L_u & L_v & L_w & L_p-\lambda & 0 & L_r \\
M_u & M_v & M_w & M_p & 0 & M_r \\
N_u & N_v & N_w & N_p & 0 & N_r-\lambda
\end{vmatrix} \quad . \ (73)
$$

$$
-g\Omega \begin{vmatrix}
X_u-\lambda & X_v & X_w & X_p & X_q & n_1 n_3 \\
Y_u & Y_v-\lambda & Y_w & Y_p & Y_q & n_2 n_3 \\
Z_u & Z_v & Z_w-\lambda & Z_p & Z_q & -(1-n_3{}^2) \\
L_u & L_v & L_w & L_p-\lambda & L_q & 0 \\
M_u & M_v & M_w & M_p & M_q-\lambda & 0 \\
N_u & N_v & N_w & N_p & N_q & 0
\end{vmatrix}
$$

$$
+\Omega^2 \begin{vmatrix}
X_u-\lambda & X_v & X_w & X_p & X_q & X_r \\
Y_u & Y_v-\lambda & Y_w & Y_p & Y_q & Y_r \\
Z_u & Z_v & Z_w-\lambda & Z_p & Z_q & Z_r \\
L_u & L_v & L_w & L_p-\lambda & L_q & L_r \\
M_u & M_v & M_w & M_p & M_q-\lambda & M_r \\
N_u & N_v & N_w & N_p & N_q & N_r-\lambda
\end{vmatrix} = 0
$$

The equation proves to be of the eighth degree, the term which appears to be of order λ^{-1} having a zero coefficient. The expressions which occur when the longitudinal and lateral motions are separable are underlined in the first determinant of equation (73), which therefore contains the octic

$$(\lambda^4 + A_1\lambda^3 + B_1\lambda^2 + C_1\lambda + D_1)(\lambda^4 + A_2\lambda^3 + B_2\lambda^2 + C_2\lambda + D_2) \quad . \quad (74)$$

If $C_{1_{g=0}}$ be written for C_1 when the g terms are neglected, it is obvious that the second determinant contains a term

$$\Omega^2(\lambda^3 + A_1\lambda^2 + B_1\lambda + C_{1_{g=0}})(\lambda^3 + A_2\lambda^2 + B_2\lambda + C_{2_{g=0}}) \quad . \quad (75)$$

From the third and fifth determinant can be obtained the term

$$n_2\Omega(\lambda^3 + A_1\lambda^2 + B_1\lambda + C_{1_{g=0}})\left\{ \begin{vmatrix} 0 & gn_1 & gn_3 \\ L_v & L_p & L \\ N_v & N_p & N_r \end{vmatrix} - g\lambda \begin{vmatrix} L_v & n_3 \\ N_v & -n_1 \end{vmatrix} \right\} \quad (76)$$

The fourth determinant furnishes a similar term :

$$n_2\Omega(\lambda^3 + A_2\lambda^2 + B_2\lambda + C_{2_{g=0}})\left\{ \begin{vmatrix} X_u & X_w & gn_1 \\ Z_u & Z_w & gn_3 \\ M_u & M_u & 0 \end{vmatrix} - g\lambda \begin{vmatrix} n_3 & -n_1 \\ M_u & M_w \end{vmatrix} \right\} \quad (77)$$

The remaining terms of (73) are too complicated to analyse in a general way, but from one or two numerical examples it would appear that the more important items are shown in (74) . . . (77).

The factors of (74) are exactly those which would be used if the motions were separable, but with the derivatives having the values for the curvilinear motion.

Example of the Calculation of the Stability of an Aeroplane when turning during horizontal flight.

Initial conditions of the steady motion :—

$$n_1 = 0 \qquad n_2 = 0\cdot707 \qquad n_3 = 0\cdot707$$

i.e. the axis of X is horizontal and the aeroplane banked at 45°.

$$u_0 = 113\cdot5 \text{ ft.-s.} \qquad v_0 = 0 \qquad w_0 = 0$$

i.e. the flight speed is 113·5 ft.-s., and there is no sideslipping or normal velocity. The last condition constitutes a special case in which the resultant motion has been chosen as lying along one of the principal axes of inertia

$$\Omega = 0\cdot284 \text{ rads.-sec.}$$

i.e. one complete turn in about 22 secs.

$$\theta_0 = 0 \qquad \phi_0 = 45° \text{ as deduced from } n_1, n_2 \text{ and } n_3$$

(78)

The only condition above which requires specific reference to the equations of motion for its value is that which gives Ω. The second equation of (59) is

$$u_0 r_0 - w_0 p_0 = Y_0 \quad . \quad . \quad . \quad . \quad . \quad . \quad . \quad (79)$$

and for the condition of no sideslipping Y_0 depends only on gravitational attraction and is equal to $n_2 g$; since $r_0 = n_3\Omega$, whilst w_0 and p_0 are zero, equation (79) becomes

$$u_0\Omega = \frac{n_2}{n_3}g \quad . \quad . \quad . \quad . \quad . \quad . \quad (80)$$

a relation between Ω and quantities defined in (78) which must be satisfied. The other equations of (59) must be satisfied, and the subject is dealt with in Chapter V. Since there are only four controls at the disposal of the pilot, some other automatic adjustment besides (80) is required, and is involved above in the statement that $u_0 = 113\cdot5$ ft.-s. when $w_0 = 0$. The state of steady motion is fixed by equations (59), and the small variations of $u \ldots r$ about this steady state lead to the resistance derivatives. In the present state of knowledge it is apparently sufficient to assume that derivatives are functions of angle of incidence chiefly and little dependent on the magnitude of v_0, p_0, q_0 and r_0. Progress in application of the laws of motion depends on an increase in knowledge of the aerodynamics.

With these remarks interposed as a caution, the derivatives for an aeroplane of about 2000 lbs. weight flying at an angle of incidence of 6° may be typically represented by the fol owing derivatives.

Resistance Derivatives (see Table (71)).

	u	v	w	p	q	r	
X	$-0\cdot111$	$0\cdot201$	$-0\cdot020$	0	0	0	
Y	$-0\cdot201$	$-0\cdot128$	0	$-1\cdot07$	0	$-109\cdot8$	
Z	$-0\cdot598$	0	$-2\cdot89$	0	$102\cdot6$	0	(81)
L/A	0	$-0\cdot0333$	0	$-7\cdot94$	$-0\cdot088$	$2\cdot48$	
M/B	0	0	$-0\cdot1051$	$0\cdot088$	$-8\cdot32$	0	
N/C	0	$+0\cdot0145$	0	$0\cdot594$	0	$-1\cdot023$	

The values of A, B and C occur only in the derivatives, and the use of $\dfrac{L}{A}$, $\dfrac{M}{B}$ and $\dfrac{N}{C}$ in (73) does not affect the condition for stability. The whole of the quantities in (81) are essentially experimental and must therefore be obtained from the study of design data. When the effects of airscrew slip stream are included the deduction from general data is laborious and needs considerable experience if serious error is to be avoided.

The numerical values of the derivatives as given in (81) can be substituted in (73) and the determinants reduced successively until the octic has been determined. It is desirable to keep a somewhat high degree of accuracy in the process in order to avoid certain errors of operation which affect the solution to a large extent. The final result obtained in the present example is

$$\lambda^8 + 20\cdot4\lambda^7 + 151\cdot3\lambda^6 + 490\lambda^5 + 687\lambda^4 + 719\lambda^3 + 150\lambda^2 + 109\lambda + 6\cdot87 = 0 \quad . \quad (82)$$

This equation has two real roots only, which can be extracted if desired by Horner's process. A general method for all roots has been given by Graeffe, and as this does not appear in the English text-books an account of its application to (82), is given as an appendix to this chapter. By use of the method it was found that equation (82) has the factors

$$(\lambda^2 + 11\cdot25\lambda + 35\cdot1)(\lambda^2 - 0\cdot006\lambda + 0\cdot171)(\lambda + 7\cdot79)(\lambda + 0\cdot067)(\lambda^2 + 1\cdot33\lambda + 2\cdot19) = 0 \quad . \quad (83)$$

and the disturbed motion consists of three oscillations, one of which is unstable, and two subsidences.

A careful examination of (83) in the light of the separable cases of longitudinal and lateral disturbances shows that the factors in the order given correspond with (a) Rapid longitudinal oscillation; (b) Phugoid oscillation (unstable); (c) Rolling subsidence; (d) Spiral subsidence; and (e) Lateral oscillation. It appears from further calculations that at an angle of incidence of 6° the effect of turning shows chiefly in the phugoid oscillation and in the spiral subsidence, the former becoming less stable and the latter more stable. At or near the stalling angle changes of a completely different kind may be expected, but the motion has not been analysed.

Comparison of Straight Flying and Circling Flight.—For reasons given earlier as to the inadequacy of the data for calculating derivatives, too much weight should not be attached to the following tables as representative of actual flight. They do, however, illustrate points of importance in the effect of turning on stability. Four conditions are considered :—

    (1) Horizontal straight flight.
    (2) Gliding straight flight.
    (3) Horizontal circling.
    (4) Spiral gliding.

The data is based on the assumption that the airscrew gives a thrust only, and therefore ignores the effects of slip stream on the tail which modify the moment coefficients in both the longitudinal and lateral motions. A recent paper by Miss B. M. Cave-Browne-Cave shows that our knowledge is reaching the stage at which the full effects can be dealt with on somewhat wide general grounds. The tables are based on flight in all cases at an angle of 6°, and the speed has been varied to maintain that condition.

The angle of bank in turning has been taken as 45°.

Rapid longitudinal oscillation.—

	Horizontal straight.	Gliding straight.	Horizontal circling.	Spiral gliding	
Damping factor . . .	4·71	4·67	5·62	5·53	
Modulus	4·97	4·92	5·92	5·82	(84)
Damping factor ÷ velocity.	0·0495	0·0494	0·0495	0·0494	
Modulus ÷ velocity . .	0·0521	0·0520	0·0522	0·0520	

The damping factors for curvilinear flights are both appreciably greater than those for rectilinear flight, and it will be seen from the third row of the table that the increase is entirely accounted for by the change of speed.

Phugoid oscillation.—

	Horizontal straight.	Gliding straight.	Horizontal circling.	Spiral gliding.	
Damping factor . . .	0·0465	0·0555	−0·003	0·026	
Modulus	0·28	0·28	0·41	0·41	(85)
Damping factor ÷ velocity.	0·000488	0·000586	−0·00003	0·000201	
Modulus ÷ velocity . .	0·0029	0·0030	0·0036	0·0037	

The damping factors for curvilinear flight are very much less than those for rectilinear motion, whilst the moduli are greater. The oscillation is, therefore, rather more rapid, but less heavily damped, whilst the effect of descending is of the same character for both straight and curved flight paths, and descent gives increased stability in all cases.

Rolling subsidence.—

	Horizontal straight.	Gliding straight.	Horizontal circling.	Spiral gliding.	
Damping factor . . .	6·55	6·50	7·79	7·76	(86)
Damping factor ÷ velocity .	0·0686	0·0687	0·0686	0·0694	

As in the case of the rapid longitudinal oscillation, the changes in the damping coefficient of the rolling subsidence are accounted for by changes of speed, as may be seen from the second row of (86).

Spiral motion.—

	Horizontal straight.	Gliding straight.	Horizontal circling.	Spiral gliding.	
Damping factor . . .	−0·0069	0·044	0·067	0·092	(87)
Damping factor ÷ velocity .	−0·00007	0·00047	0·00059	0·00082	

The effect of the turning has been to increase very considerably the damping factor of the spiral motion, and the change appears to be closely associated with the opposite change noted in connection with the phugoid oscillation. Here, as in that case, the changes of speed do not account for the changes of damping factor.

Lateral oscillation.—

	Horizontal straight.	Gliding straight.	Horizontal circling.	Spiral gliding.	
Damping factor . . .	0·550	0·525	0·665	0·633	(88)
Modulus	1·27	1·23	1·48	1·43	
Damping factor ÷ velocity .	0·00576	0·00555	0·00586	0·00566	
Modulus ÷ velocity . .	0·0133	0·0130	0·0130	0·0128	

The changes of modulus are seen to be almost entirely accounted for by the changes of speed. A considerable part of the change in the damping factors is also accounted for in the same way, although in this case the influence of other changes is indicated.

General Remarks on the Tables.—So far as the oscillations are involved, the tables indicate a tendency for the product of the velocity and the periodic time to remain constant. The rapid lateral and longitudinal oscillations remain practically independent of each other. An important interaction, which probably occurs in the circular flight of all present-day aeroplanes, connects the spiral and phugoid motions. It appears that turning increases the damping factor of the spiral motion whilst simultaneously reducing the stability of the phugoid oscillation. In one of the examples here given, the motion has changed from a stable phugoid oscillation and an unstable spiral motion in horizontal straight flight to an unstable phugoid oscillation and a stable spiral motion for a horizontal banked turn.

Effect of Changes of the Important Derivatives on the Stability of Straight and Circling Horizontal Flight.—The derivatives considered were M_w, L_v and N_v with consequential changes of M_q and N_r, and are important in different respects. M_w can be varied by changing the position of the centre of gravity and the tail-plane area, L_v by adjustment of the lateral dihedral angle, and N_v by change of fin and rudder area. All are appreciably at the choice of a designer, and the following calculations give some idea of the possible effects which may be produced. At a given angle of incidence resistance derivatives are proportional to velocity, and simplicity of comparison has been assisted by a recognition of this fact.

Variations of M_w. L_v and N_v constant.

Rapid longitudinal oscillation.—

$100 \div M_w/B \times$ velocity.		−0·264	−0·176	−0·093	−0·042	0	0·044	0·0884	
$10^2 \times$ damping factor $\div$ velocity	Horizontal straight	6·24	5·58	4·95	{5·04 {4·07	5·92 2·52	6·55 1·27	6·60 0·57	(89)
	Horizontal circling	6·23	5·56	4·95	{4·91 {4·08	5·43 3·07	6·27 1·51	6·56 0·42	
$10^2 \times$ modulus $\div$ velocity	Horizontal straight	7·02	6·17	5·21	(4·53)*	(3·86)	(2·89)	—	
	Horizontal circling	6·98	6·15	5·20	(4·46)	(3·90)	3·08)	—	

The range given to M_w is particularly large, and the most noticeable feature of (89) is the small effect of turning on the rapid longitudinal oscillation. The figures in brackets correspond with a pair of real roots, viz. $(4·53)^2 = (5·04 \times 4·07)$, and it will be seen that the motion represented is always stable but not always an oscillation. For a very unstable aeroplane as represented oy the lowest value of M_w there is some indication of a complex interchange between the longitudinal and lateral motions, which would need further investigation before its meaning could be clearly estimated.

Phugoid oscillation.—

$100\, M_w/B \times$ velocity.		−0·264	−0·176	−0·093	−0·042	0	0·044	0·0884	
$10^4 \times$ damping factor $\div$ Velocity	Horizontal straight	4·3	4·5	4·9	5·6	{14·5 {0·0	56·0 −24·4	56·8 −46·9	(90)
	Horizontal circling	0·39	0·14	−0·25	−0·69	−1·26	−2·78	− 9·48	
$10^3 \times$ modulus $\div$ velocity	Horizontal straight	3·66	3·40	2·92	2·26	—	—	—	
	Horizontal circling	3·82	3·74	3·64	3·56	3·34	2·94	2·11	

The differences for stability between straight and circling flight are here very marked. The former shows stability at all positive values of M_w, and the change from stability of the oscillation to instability in a nose-dive occurs without the intermediate stage of an unstable oscillation. In circling flight, however, the general result of a reduction of M_w is to produce in increasing oscillation. In all cases the damping is very small in circling motion at an angle of bank of 45° as compared with that in straight flying, and a greater value of M_w is needed for stability. In

straight flying there is indicated a limit to the degree of damping of the phugoid oscillation which can be attained.

Spiral motion.—

100 M_w/B × velocity.		$-0\cdot264$	$-0\cdot176$	$-0\cdot093$	$-0\cdot042$	0	$+0\cdot044$	
10^4 × damping factor ÷ velocity	Horizontal straight	$-0\cdot72$	$-0\cdot72$	$-0\cdot72$	$-0\cdot72$	$-0\cdot72$	$-0\cdot72$	(91)
	Horizontal circling	$4\cdot78$	$5\cdot18$	$5\cdot93$	$6\cdot89$	$8\cdot52$	$13\cdot8$	

In rectilinear flight the spiral motion is unaffected by changes of M_w, and the negative value indicates instability. The effect of turning is to convert a small instability into a marked stability which is dependent for a secondary order of variation on the magnitude of M_w.

Rolling Subsidence and Lateral Oscillation.—It appears that neither of these quantities is appreciably affected by either the variation of M_w or of circling, beyond the changes which are proportional to the velocity of flight. The expressions corresponding with those used in (90) are then constants for the conditions now investigated. For the rolling subsidence " damping factor/velocity " has the value $0\cdot0686$, whilst for the lateral oscillation " damping factor/velocity " is equal to $5\cdot85 \times 10^{-3}$, whilst "modulus/velocity " has the value $1\cdot31 \times 10^{-2}$.

Variations of L_v and N_v. M_w Constant.—The changes of rapid longitudinal oscillation due to change of lateral derivatives are inappreciable, and the differences between straight flying and circling are produced only by the changes in the velocity of flight. Similar remarks apply to the rolling subsidence, as might have been expected from the very simple character of the motion and the fact that the only important variable of the motion, *i.e.* L_p, has not been subjected to change.

Phugoid oscillation.   Circling flight.—

	N_v/C × 10^4/velocity.								
L_v/A × velocity	$-0\cdot5$	0	$+0\cdot5$	$+1\cdot28$	$-0\cdot5$	0	$+0\cdot5$	$+1\cdot28$	
	Damping factor × 10^4/velocity				Modulus × 10^3/velocity				
0	—	$2\cdot16$	$-3\cdot88$	$-3\cdot34$	—	$2\cdot75$	$3\cdot36$	$3\cdot60$	(92)
$-0\cdot0002935$	$1\cdot54$	$4\cdot84$	$0\cdot86$	$-0\cdot25$	$4\cdot16$	$3\cdot64$	$3\cdot56$	$3\cdot64$	
$-0\cdot001$	$29\cdot9$	$12\cdot0$	$7\cdot4$	$4\cdot71$	$3\cdot71$	$3'73$	$3\cdot61$	$3\cdot62$	

Straight flight.   Damping factor × 10^4/velocity = $4\cdot9$
and   Modulus × 10^3/velocity = $2\cdot92$ for all values of L_v and N_v.

For the numerically smallest values of L_v and N_v the centrifugal terms introduced by turning, convert a stable phugoid to an unstable one. Increase in the dihedral angle has a counterbalancing effect, and the phugoid becomes stable over the range of N_v covered by the table. The longitudinal stability of rectilinear motion is of course unchanged by a dihedral angle or by the size of the fin and rudder, which are the parts of the aeroplane which primarily determine L_v and N_v.

2 κ

Spiral motion.—

$L_v/A \times$ velocity		-0.5	0	$+0.5$	$+1.28$	$+2.00$	
		Damping factor $\times 10^4$/velocity.					
			$N_v/C \times 10^4$/velocity.				
0	Horizontal straight	127	0	-8.33	-9.70	-10.15	(93)
	Horizontal circling	—	10.7	7.05	6.70	—	
-0.0002935	Horizontal straight	106	26.9	6.61	-0.72	-3.15	
	Horizontal circling	—	4.01	5.56	5.94	—	
-0.00075	Horizontal straight	69.2	32.8	17.7	9.05	5.40	
	Horizontal circling	—	—	—	—	—	
-0.001	Horizontal straight	54.8	31.7	20.65	12.72	9.06	
	Horizontal circling	1.44	2.57	3.93	4.69	—	

The value of N_v changes sign when the aeroplane, regarded as a weathercock rotating about the axis of Z, just tends to turn tail first. In the absence of a dihedral angle the steady state is neutral in straight flight, but becomes stable on turning. For both straight flying and turning, stability may be produced in an aeroplane showing weathercock instability by the use of a sufficiently large dihedral angle. It is not known how far this conclusion may be applied at other angles of incidence.

Lateral oscillation.—

$L_v/A \times$ velocity		Damping factor $\times 10^3$/velocity.					Modulus $\times 10^2$/velocity.					
		-0.5	0	0.5	1.28	2.00	-0.5	0	0.5	1.28	2.00	
0	Horizontal straight	-1.76 / $+12.7$	1.13 / 8.83	5.80	6.50	7.10	—	—	0.836	1.24	1.514	(94)
	Horizontal circling	—	1.07	5.76	6.35	—	—	—	0.850	1.223	—	
-0.0002935	Horizontal straight	-0.98 / $+10.6$	2.90 / 4.69	4.79	5.76	6.48	—	—	0.946	1.326	1.59	
	Horizontal circling	—	4.47	5.23	5.90	—	—	0.574	0.946	1.304	—	
-0.00075	Horizontal straight	—	2.65	3.80	4.86	5.61	—	0.906	1.170	1.486	1.724	
	Horizontal circling	—	—	—	—	—	—	—	—	—	—	
-0.001	Horizontal straight	$+0.92$	2.48	3.42	4.45	5.21	0.828	1.066	1.286	1.576	1.80	
	Horizontal circling	-1.44 / $+1.26$	0.26 / 3.26	4.05	4.91	—	0.680	0.967	1.216	1.52	—	

The figures in (94) show that the lateral oscillation is very dependent on the size of the dihedral angle and little dependent on the rate of turning except when the aeroplane is devoid of weathercock stability, *i.e.* $N_v \gtrless 0$.

General Remarks on the Numerical Results.—Although all the calculations refer to one angle of incidence (6°) and to circling at an angle of bank of 45° when turning is present, they have nevertheless shown that the

stability of the slower movements of an aeroplane, *i.e.* the phugoid oscillation, the spiral motion and the lateral stability, is markedly affected by the details of design and by the centrifugal terms. The theory of stability in non-rectilinear flight is therefore important, and methods of procedure for further use should be considered. It was found that the approximation indicated in (74) . . . (77) sufficed to bring out the salient changes in the examples tried, and it may be permissible to use the form generally if occasional complete checks be given by the use of (73). The reduction of labour is the justification for such a course. Such indications as the change from spiral instability to stability by reason of turning can be deduced in more general form from the approximation, since it is only necessary to discuss the change of sign of the term independent of λ.

Further data relating to the above tables may be found in the " Annual Report of the Advisory Committee for Aeronautics," pages 189–223 1914–15, by J. L. Nayler, Robert Jones and the author.

Gyroscopic Couples and their Effect on Straight Flying.—If P be the angular velocity of the rotating parts of the engine and airscrew, and the moment of inertia be I, there will be couples about the axes of Y and Z due to pitching and yawing which can be deduced from the equations of motion as given in (56). There are certain oscillations which occur with two blades which are not present in the case of four blades, but the average effect is the same. Putting $A = I$, $B = C = 0$, and taking the steady effects of rotation only, leads to

$$M = + I \cdot P \cdot r \quad . \quad . \quad . \quad . \quad . \quad (95)$$
$$N = - I \cdot P \cdot q \quad . \quad . \quad . \quad . \quad . \quad (96)$$

for the couples needed to rotate the airscrew with angular velocities r and q. There will therefore be couples of reversed sign acting on the aeroplane which may be expressed in derivative form by

$$M_r = - I \cdot P, \qquad N_q = I \cdot P \quad . \quad . \quad . \quad . \quad (97)$$

and these are the only changes from the previous consideration of the stability of straight flying. Equation (73) takes simple form since the last four determinants disappear-when Ω is zero, whilst in the first determinant only the terms underlined together with M_r and N_q have any value, and the equation becomes

$$\lambda^2 \begin{vmatrix} X_u - \lambda & 0 & X_w & 0 & X_q - \dfrac{gn_3}{\lambda} & 0 \\ 0 & Y_v - \lambda & 0 & Y_p + \dfrac{gn_3}{\lambda} & 0 & Y_r - \dfrac{gn_1}{\lambda} \\ Z_u & 0 & Z_w - \lambda & 0 & Z_q + \dfrac{gn_1}{\lambda} & 0 \\ 0 & L_v & 0 & L_p - \lambda & 0 & L_r \\ M_u & 0 & M_w & 0 & M_q - \lambda & M_r \\ 0 & N_v & 0 & N_p & N_q & N_r - \lambda \end{vmatrix} = 0 \quad . \quad . \quad (98)$$

This determinant is easily reduced to

$$(\lambda^4 + A_1\lambda^3 + B_1\lambda^2 + C_1\lambda + D_1)(\lambda^4 + A_2\lambda^3 + B_2\lambda^2 + C_2\lambda + D_2)$$

$$-M_r N_q \lambda^2 \begin{vmatrix} X_u - \lambda & X_w \\ Z_u & Z_w - \lambda \end{vmatrix} \times \begin{vmatrix} Y_v - \lambda & Y_p + \dfrac{gn_3}{\lambda} \\ L_v & L_p - \lambda \end{vmatrix} = 0 \quad . \quad (99)$$

where the quantities $A_1 \ldots D_1$, $A_2 \ldots D_2$ are those for longitudinal and lateral stability when gyroscopic couples are ignored.

An examination of (99) in a particular case showed that the coefficients of powers of λ in the gyroscopic terms were all positive and small compared with the coefficients obtained from the product of the biquadratic factors. The rapid motions, longitudinal and lateral, will therefore be little affected. It appears, further, that the change in the phugoid oscillation is a small increase in stability. Since the gyroscopic terms do not contain one independent of λ, the above remark as to signs of the coefficients shows that a spirally stable or unstable aeroplane without rotating airscrew will remain stable or unstable when gyroscopic effects are added. In any case of importance, however, equation (99) is easy to apply, and the conclusion need not be relied upon as more than an indicative example.

The Stability of Airships and Kite Balloons

The treatment of the stability of lighter-than-air craft differs from that for the aeroplane in several particulars, all of which are connected with the estimation of the forces acting. The effect of the buoyancy of the gas is equivalent to a reduction of weight so far as forces along the co-ordinate axes are concerned, but the combined effect of weight and buoyancy introduces terms into the equation of angular motion which were not previously present. The mooring of an airship to a cable or the effect of a kite wire introduces terms in both the force and moment equations.

The mathematical theory is developed in terms of resistance derivatives without serious difficulty, but the number of determinations of the latter of a sufficiently complete character is so small that the applications cannot be said to be adequate. This is in part due to the lack of full-scale tests on which to check calculations, and in part to the fact that the air forces and moments on the large bulk of the envelopes of lighter-than-air craft depend not only on the linear and angular velocities through the air, but also on the linear and angular accelerations. In a simple example it would appear that the lateral acceleration of an airship is little more than half that which would be calculated on the assumption that the lateral resistance is determined only by the velocities of the envelope.

The new terms arising from buoyancy will be developed generally and the terms arising from a cable, left to a separate section, since they do not affect the free motion of an airship. The separation into longitudinal and lateral stabilities will be adopted, and the general case left until such time as it appears that the experimental data are sufficiently advanced as to permit of their use.

Gravitational and Buoyancy Forces.—If the upward force due to buoyancy be denoted by F, the values of the component forces along the axes are

$$mX = n_1(mg - F) \quad mY = n_2(mg - F) \quad mZ = n_3(mg - F) \ . \ (100)$$

For an airship in free flight $mg - F$ is zero and the component forces vanish. In the kite balloon reserve buoyancy is present and is balanced by the vertical component of the pull in the kite wire.

Gravitational and Buoyancy Couples.—The centre of gravity of lighter-than-air craft is usually well below the centre of buoyancy, *i.e.* below the centre of volume of the displaced air. The latter point will vary with the condition of the ballonets and must be separately evaluated in each case as part of the statement of the conditions of steady motion. Both the centres of gravity and buoyancy will be taken to lie in the plane of symmetry, and the co-ordinates of the latter are denoted by x and z relative to the body axes through the centre of gravity. The buoyancy force F acts vertically upwards, and the components of force at (x, o, z) are therefore

$$-n_1F \quad -n_2F \quad \text{and} \quad -n_3F \ . \quad . \quad . \quad . \ (101)$$

Taking moments about the body axes shows that on this account the components are

$$L = n_2F \cdot z, \qquad M = (n_3x - n_1z)F, \qquad N = -n_2F \cdot x \quad . \ (102)$$

Air Forces and Moments.—To meet the new feature that the forces and moments depend on accelerations as well as on velocity, it is assumed that in longitudinal motion the quantities X, Z and M have the typical form

$$X = f_x(u, w, q, \dot{u}, \dot{w}, \dot{q}) \quad . \quad . \quad . \quad . \quad . \ (103)$$

as a result of motion through the air ; following the previous method X is expanded as

$$X = f_x(u_0, w_0, q_0) + uX_u + wX_w + qX_q + \dot{u}X_{\dot{u}} + \dot{w}X_{\dot{w}} + \dot{q}X_{\dot{q}} \ . \ (104)$$

The number of derivatives introduced is twice as great as that for the longitudinal stability of an aeroplane.

Changes of Gravitational and Buoyancy Forces and Couples.—These changes depend on the variations of the direction cosines n_1, n_2 and n_3 arising from displacements of the axes, and may be determined directly or from the general form given in (68) by putting Ω, p_0, q_0, r_0 and n_2 equal to zero. The changes of the direction cosines are

$$dn_1 = -\frac{n_3q}{\lambda}, \quad dn_2 = -\frac{n_1r}{\lambda} + \frac{n_3p}{\lambda}, \quad dn_3 = \frac{n_1q}{\lambda} \quad . \ (105)$$

of which the first and last refer only to longitudinal stability and the second to lateral stability.

Division of (56) into Equations of Steady Motion and Disturbed Motion. —Using the separate expressions for forces due to gravity, buoyancy and air, equations (56) become

$$
\left.
\begin{aligned}
\dot{u} + wq &= n_1\Big(g - \frac{F}{m}\Big) + f_{\mathrm{x}}(u,\, w,\, q,\, \dot{u},\, \dot{w},\, \dot{q}) \\
\dot{w} - uq &= n_3\Big(g - \frac{F}{m}\Big) + f_{\mathrm{z}}(u,\, w,\, q,\, \dot{u},\, \dot{w},\, \dot{q}) \\
\dot{q}\mathrm{B} &= (n_3 x - n_1 z)\mathrm{F} + f_{\mathrm{M}}(u,\, w,\, q,\, \dot{u},\, \dot{w},\, \dot{q})
\end{aligned}
\right\} \quad . \quad (106)
$$

In steady motion, $\dot{u}$, $\dot{w}$, $\dot{q}$, and q are zero, and hence (106) becomes

$$
\left.
\begin{aligned}
0 &= n_1\Big(g - \frac{F}{m}\Big) + f_{\mathrm{x}}(u_0,\, w_0,\, q_0) \\
0 &= n_3\Big(g - \frac{F}{m}\Big) + f_{\mathrm{z}}(u_0,\, w_0,\, q_0) \\
0 &= (n_3 x - n_1 z)\mathrm{F} + f_{\mathrm{M}}(u_0,\, w_0,\, q_0)
\end{aligned}
\right\} \quad . \quad . \quad . \quad (107)
$$

If in (106) $u_0 + u$ is written for u, etc., $n_1 + dn_1$, for n_1, etc., the equations of disturbed motion are obtained, the terms of zero order being those of (107), and therefore independently satisfied ; the first-order terms are

$$
\left.
\begin{aligned}
\dot{u} + w_0 q &= -\frac{n_3}{\lambda}\Big(g - \frac{F}{m}\Big)q + u\mathrm{X}_u + w\mathrm{X}_w + q\mathrm{X}_q \\
&\qquad + \dot{u}\mathrm{X}_{\dot{u}} + \dot{w}\mathrm{X}_{\dot{w}} + \dot{q}\mathrm{X}_{\dot{q}} \\
\dot{w} - u_0 q &= \frac{n_1}{\lambda}\Big(g - \frac{F}{m}\Big)q + u\mathrm{Z}_u + w\mathrm{Z}_w + q\mathrm{Z}_q \\
&\qquad + \dot{u}\mathrm{Z}_{\dot{u}} + \dot{w}\mathrm{Z}_{\dot{w}} + \dot{q}\mathrm{Z}_{\dot{q}} \\
\dot{q}\mathrm{B} &= \mathrm{F}(n_1 x + n_3 z)\frac{q}{\lambda} + u\mathrm{M}_u + w\mathrm{M}_w + q\mathrm{M}_q \\
&\qquad + \dot{u}\mathrm{M}_{\dot{u}} + \dot{w}\mathrm{M}_{\dot{w}} + \dot{q}\mathrm{M}_{\dot{q}}
\end{aligned}
\right\} \quad . \quad (108)
$$

Collecting these terms in accordance with the note made in (10) and carried out for the aeroplane in equations (11) and (12) leads to

$$
\left.
\begin{aligned}
(\mathrm{X}_u + \lambda\mathrm{X}_{\dot{u}} - \lambda)u + (\mathrm{X}_w + \lambda\mathrm{X}_{\dot{w}})w + \Big\{\mathrm{X}_q + \lambda\mathrm{X}_{\dot{q}} - w_0 - \frac{n_3}{\lambda}\Big(g - \frac{F}{m}\Big)\Big\}q = 0 \\
(\mathrm{Z}_u + \lambda\mathrm{Z}_{\dot{u}})u + (\mathrm{Z}_w + \lambda\mathrm{Z}_{\dot{w}} - \lambda)\dot{w} + \Big\{\mathrm{Z}_q + \lambda\mathrm{Z}_{\dot{q}} + u_0 + \frac{n_1}{\lambda}\Big(g - \frac{F}{m}\Big)\Big\}q = 0 \\
(\mathrm{M}_u + \lambda\mathrm{M}_{\dot{u}})u + (\mathrm{M}_w + \lambda\mathrm{M}_{\dot{w}})w + \Big\{\mathrm{M}_q + \lambda\mathrm{M}_{\dot{q}} - \mathrm{B}\lambda + \frac{F}{\lambda}(n_1 x + n_3 z)\Big\}q = 0
\end{aligned}
\right\} \quad (109)
$$

Comparing (109) with (11) shows that the changes consist of the writing of $g - F/m$ for g, $\mathrm{X}_u + \lambda\mathrm{X}_{\dot{u}}$ for X_u, etc., except that in the case of M_q the expression $\mathrm{M}_q + \lambda\mathrm{M}_{\dot{q}} + (n_1 x + n_3 z)\mathrm{F}/\lambda$ is written instead of M_q.

Eliminating u, w and q from the three equations of disturbed motion leads to an equation in λ which is of the fourth degree as in the case of the aeroplane. Except for the term independent of λ the coefficients in the

equation contain terms depending on accelerations. In particular the coefficient of λ^4 is made up of the moment of inertia B and acceleration terms; the first two lines are most easily appreciated by multiplying by m, when it is seen that $mX_{\dot u}$, $mZ_{\dot w}$, etc., are compared directly with the mass m. This analytical result is the justification for a common method of expressing the results of forces due to acceleration of the fluid motion as virtual additions to the mass of the moving body.

One type of instability may be made evident by a change of sign of the last term of the biquadratic equation for stability, but this is not so likely to occur in longitudinal as in lateral motion. The criterion for this type of stability is independent of the acceleration of the fluid motion, as may be seen from the coefficients of the biquadratic equation given below.

Coefficient of λ^4,

$$
\begin{vmatrix}
X_{\dot u}-1 & X_{\dot w} & X_{\dot q} \\
Z_{\dot u} & Z_{\dot w}-1 & Z_{\dot q} \\
M_{\dot u} & M_{\dot w} & M_{\dot q}-B
\end{vmatrix}
$$

Coefficient of λ^3,

$$
\begin{vmatrix}
X_{\dot u}-1 & X_{\dot w} & X_q-w_0 \\
Z_{\dot u} & Z_{\dot w}-1 & Z_q+u_0 \\
M_{\dot u} & M_{\dot w} & M
\end{vmatrix}
+
\begin{vmatrix}
X_{\dot u}-1 & X_w & X_{\dot q} \\
Z_{\dot n} & Z_w & Z_{\dot q} \\
M_{\dot u} & M_w & M_{\dot q}-B
\end{vmatrix}
+
\begin{vmatrix}
X_u & X_{\dot w} & X_{\dot q} \\
Z_u & Z_{\dot w}-1 & Z_{\dot q} \\
M_u & M_{\dot w} & M_{\dot q}-B
\end{vmatrix}
$$

Coefficient of λ^2,

$$
\begin{vmatrix}
X_u & X_w & X_{\dot q} \\
Z_u & Z_w & Z_{\dot q} \\
M_u & M_w & M_{\dot q}-B
\end{vmatrix}
+
\begin{vmatrix}
X_u & X_{\dot w} & X_q-w_0 \\
Z_u & Z_{\dot w}-1 & Z_q+u_0 \\
M_u & M_{\dot w} & M_{\dot q}
\end{vmatrix}
$$

$$
+
\begin{vmatrix}
X_{\dot u}-1 & X_w & X_q-w_0 \\
Z_{\dot u} & Z_w & Z_q+u_0 \\
M_{\dot u} & M_w & M_q
\end{vmatrix}
+
\begin{vmatrix}
X_{\dot u}-1 & X_{\dot w} & -n_3(g-F/m) \\
Z_{\dot u} & Z_{\dot w}-1 & n_1(g-F/m) \\
M_{\dot u} & M_w & F(n_1x+n_3z)
\end{vmatrix}
$$

Coefficient of λ,

$$
\begin{vmatrix}
X_u & X_w & X_q-w_0 \\
Z_u & Z_w & Z_q+u_0 \\
M_u & M_w & M_q
\end{vmatrix}
+
\begin{vmatrix}
X_u & X_{\dot w} & -n_3(g-F/m) \\
Z_u & Z_{\dot w}-1 & n_1(g-F/m) \\
M_u & M_{\dot w} & F(n_1x+n_3z)
\end{vmatrix}
+
\begin{vmatrix}
X_{\dot u}-1 & X_w & -n_3(g-F/m) \\
Z_{\dot u} & Z_w & n_1(g-F/m) \\
M_{\dot u} & M_w & F(n_1x+n_3z)
\end{vmatrix}
$$

Coefficient independent of λ,

$$
\begin{vmatrix}
X_u & X_w & -n_3(g-F/m) \\
Z_u & Z_w & n_1(g-F/m) \\
M_u & M_w & F(n_1x+n_3z)
\end{vmatrix}
\quad . \quad . \quad . \quad . \quad (110)
$$

Lateral Stability.—The results of the steps only will be given, since the method has been illustrated previously. After substitution in (56) for the parts due to gravity and buoyancy and those arising from motion through the air, the equations of lateral motion become for principal axes of inertia

$$
\left.
\begin{aligned}
\dot v + ur &= dn_2\left(g-\frac{F}{m}\right) + f_{\mathrm{Y}}(v,\, p,\, r,\, \dot v,\, \dot p,\, \dot r) \\
\dot p \mathrm{A} &= dn_2\mathrm{F}z + f_{\mathrm{L}}(v,\, p,\, r,\, \dot v,\, \dot p,\, \dot r) \\
\dot r \mathrm{C} &= -dn_2\mathrm{F}x + f_{\mathrm{N}}(v,\, p,\, r,\, \dot v,\, \dot p,\, \dot r)
\end{aligned}
\right\}
\quad . \quad . \quad (111)
$$

where dn_2 only appears because n_2 is zero as a condition of the separate consideration of the lateral and longitudinal motions. Similarly v_0, p_0 and r_0 are zero, and the equations of equilibrium are automatically satisfied by the forces and couples due to the air being also zero from the symmetry of the motion. The value of dn_2 has already been given, and the three equations of disturbed motion in terms of v, p and r are

$$
\left.\begin{aligned}
\dot{v}+u_0 r &=\left(-\frac{n_1 r}{\lambda}+\frac{n_3 p}{\lambda}\right)\left(g-\frac{F}{m}\right)+v Y_v+p Y_p+r Y_r \\
&\qquad\qquad\qquad\qquad\quad +\dot{v} Y_{\dot{v}}+\dot{p} Y_{\dot{p}}+\dot{r} Y_{\dot{r}} \\
\dot{p} A &=\left(-\frac{n_1 r}{\lambda}+\frac{n_3 p}{\lambda}\right) F z \quad +v L_v+p L_p+r L_r \\
&\qquad\qquad\qquad\qquad\quad +\dot{v} L_{\dot{v}}+\dot{p} L_{\dot{p}}+\dot{r} L_{\dot{r}} \\
\dot{r} C &=\left(\frac{n_1 r}{\lambda}-\frac{n_3 p}{\lambda}\right) F x \quad +v N_v+p N_p+r N_r \\
&\qquad\qquad\qquad\qquad\quad +\dot{v} N_{\dot{v}}+\dot{p} N_{\dot{p}}+\dot{r} N_{\dot{r}}
\end{aligned}\right\} . \quad (112)
$$

Arranging the terms as factors of v, p and r leads to

$$
\left.\begin{aligned}
(Y_v+\lambda Y_{\dot{v}}-\lambda)v+\left\{Y_p+\lambda Y_{\dot{p}}+\frac{n_3}{\lambda}\left(g-\frac{F}{m}\right)\right\}p+\left\{Y_r+\lambda Y_{\dot{r}}-u_0-\frac{n_1}{\lambda}\left(g-\frac{F}{m}\right)\right\}r&=0 \\
(L_v+\lambda L_{\dot{v}})v+\left(L_p+\lambda L_{\dot{p}}-\lambda A+\frac{n_3}{\lambda}F z\right)p+\left(L_r+\lambda L_{\dot{r}}-\frac{n_1}{\lambda}F z\right)r&=0 \\
(N_v+\lambda N_{\dot{v}})v+\left(N_p+\lambda N_{\dot{p}}-\frac{n_3}{\lambda}F x\right)p+\left(N_r+\lambda N_{\dot{r}}-\lambda C+\frac{n_1}{\lambda}F x\right)r&=0
\end{aligned}\right\}(113)
$$

The elimination of v, p and r from equations (113) gives a biquadratic equation with the following coefficients :—

Coefficient of λ^4,

$$
\begin{vmatrix}
Y_{\dot{v}}-1 & Y_{\dot{p}} & Y_{\dot{r}} \\
L_{\dot{v}} & L_{\dot{p}}-A & L_{\dot{r}} \\
N_{\dot{v}} & N_{\dot{\cdot}} & N_{\dot{r}}-C
\end{vmatrix}
$$

Coefficient of λ^3,

$$
\begin{vmatrix}
Y_v & Y_{\dot{p}} & Y_{\dot{r}} \\
L_v & L_{\dot{p}}-A & L_{\dot{r}} \\
N_v & N_{\dot{p}} & N_{\dot{r}}-C
\end{vmatrix}
+\begin{vmatrix}
Y_{\dot{v}}-1 & Y_p & Y_{\dot{r}} \\
L_{\dot{v}} & L_p & L_{\dot{r}} \\
N_{\dot{v}} & N_p & N_{\dot{r}}-C
\end{vmatrix}
+\begin{vmatrix}
Y_{\dot{v}}-1 & Y_{\dot{p}} & Y_r-u_0 \\
L_{\dot{v}} & L_{\dot{p}}-A & L_r \\
N_{\dot{v}} & N_{\dot{p}} & N_r
\end{vmatrix}
$$

Coefficient of λ^2,

$$
\begin{vmatrix}
Y_v & Y_{\dot{p}} & Y_r-u_0 \\
L_v & L_{\dot{p}}-A & L_r \\
N_v & N_{\dot{p}} & N_r
\end{vmatrix}
+\begin{vmatrix}
Y_v & Y_p & Y_{\dot{r}} \\
L_v & L_p & L_{\dot{r}} \\
N_v & N_p & N_{\dot{r}}-C
\end{vmatrix}
+\begin{vmatrix}
Y_{\dot{v}}-1 & Y_p & Y_r-u_0 \\
L_{\dot{v}} & L_p & L_r \\
N_{\dot{\cdot}} & N_p & N_r
\end{vmatrix}
$$

$$
+n_1\begin{vmatrix}
Y_{\dot{v}}-1 & Y_{\dot{p}} & -(g-F/m) \\
L_{\dot{v}} & L_{\dot{p}}-A & -F z \\
N_{\dot{v}} & N_{\dot{p}} & F x
\end{vmatrix}
+n_3\begin{vmatrix}
Y_{\dot{v}}-1 & g-F/m & Y_{\dot{r}} \\
L_{\dot{v}} & F z & L_{\dot{r}} \\
N_{\dot{v}} & -F x & N_{\dot{r}}-C
\end{vmatrix}
$$

Coefficient of λ,

$$\begin{vmatrix} Y_v & Y_p & Y_r-u_0 \\ L_v & L_p & L_r \\ N_v & N_p & N_r \end{vmatrix} +n_1 \begin{vmatrix} Y_v & Y_{\dot p} & -(g-F/m) \\ L_v & L_{\dot p}-A & -Fz \\ N_v & N_{\dot p} & Fx \end{vmatrix} +n_3 \begin{vmatrix} Y_v & g-F/m & Y_r \\ L_v & Fz & L_r \\ N_v & -Fx & N_r-C \end{vmatrix}$$

$$+n_1 \begin{vmatrix} Y_{\dot v}-1 & Y_p & -(g-F/m) \\ L_{\dot v} & L_p & -Fz \\ N_{\dot v} & N_p & Fx \end{vmatrix} +n_3 \begin{vmatrix} Y_{\dot v}-1 & g-F/m & Y_r-u_0 \\ L_{\dot v} & Fz & L_r \\ N_{\dot v} & -Fx & N_r \end{vmatrix}$$

Coefficient independent of λ,

$$n_1 \begin{vmatrix} Y_v & Y_p & -(g-F/m) \\ L_v & L_p & -Fz \\ N_v & N_p & Fx \end{vmatrix} +n_3 \begin{vmatrix} Y_v & g-F/m & Y_r-u_0 \\ L_v & Fz & L_r \\ N_v & -Fx & N_r \end{vmatrix} \quad . \quad (114)$$

The formula of which most use has hitherto been made in airship stability is deduced from (114) by considering horizontal flight with the axis of the envelope horizontal; n_1 is then zero. The reserve buoyancy is zero, *i.e.* $g-F/m=0$, and the centre of buoyancy is vertically above the centre of gravity so that x is zero. The coefficient independent of λ is then

$$n_3 Fz \begin{vmatrix} Y_v & Y_r-u_0 \\ N_v & N_r \end{vmatrix} \quad . \quad . \quad . \quad . \quad . \quad . \quad (115)$$

and if this quantity changes sign there is a change from stability to instability, the latter corresponding with a positive sign under usual conditions. For an airship to be laterally stable the condition becomes

$$Y_v N_r > (Y_r - u_0)N_v$$

Examples of the use of the Equations of Disturbed Airship Motion.— The further remarks will be confined to horizontal flight, in which case $n_1=0$. The numerical data are not all that could be desired, and use must as yet be made of general ideas.

Remarks on the Values of the Derivatives.—For an airship of any type in present use, there is approximate symmetry not only about a vertical plane, but also about a horizontal plane through the centre of buoyancy. There are then some simple relations between the forces and couples due to rising and falling and those due to sideslipping. It may be expected that the forces on an airship will not be affected appreciably by a slow rotation about the axis of the envelope, and if this assumption be made it is easily seen that the relationship between derivatives due to rolling and derivatives due to sideslipping is simple. The relations which may be simply deduced as a result of the above hypotheses are :—

$$X_w = X_v = 0 \quad . \quad . \quad . \quad . \quad . \quad (116)$$

i.e. there is no change of resistance for slight inclinations of the axis of the airship to the wind.

$$Z_w = Y_v \quad . \quad . \quad . \quad . \quad . \quad . \quad (117)$$

This relation expresses the fact that the lift and lateral force on the airship

have the same value for the same inclinations of the axis of X to the wind in pitch and yaw respectively.

$$X_q = X_r - zX_u' = -zX_u' \quad . \quad . \quad . \quad . \quad (118)$$

where X_q, the variation of resistance due to pitching, differs from X_r, the variation of resistance due to yawing, because the axis of X lies at a distance z below the centre of buoyancy whilst the axis of Z passes through that point. Symmetry about a vertical plane is sufficient to ensure that X_r is zero.

As the car and airscrew are near the centre of gravity, X'_u will be almost wholly due to the resistance of the envelope in its fore and aft motion due to pitching about the axis of Y. The change of resistance of the whole airship due to a change of forward speed u will be greater than X'_u, partly on account of the additional resistance of the car, but also because of reduced thrust from the airscrew.

$$Z_q = -Y_r \quad . \quad . \quad . \quad . \quad . \quad . \quad (119)$$

The variations of normal force due to pitching and lateral force due to yawing will be roughly related as shown in (119). Both are associated directly with u_0 in the conditions of stability, and their value is not known with any degree of accuracy. There is a possibility that Y_r may be half as great as u_0.

$$Z_u = 0 \quad . \quad . \quad . \quad . \quad . \quad . \quad (120)$$

Since the lift due to wind is zero, the rate of change of Z with change of forward speed will also be zero.

The pitching moment due to change of forward speed, i.e. M_u, may not be zero. If the airscrews are at the level of the car, and therefore near the C.G., it would appear that the change of airscrew thrust with change of forward speed will not greatly affect M. It can then be stated as probable that

$$M_u = mzX'_u$$

and $\qquad M_q = N_r + mz^2X'_u \quad . \quad . \quad . \quad . \quad (121)$

Equation (121) gives a relation between the damping derivatives in pitch and yaw, assuming equal fin areas horizontally and vertically; the term $mz^2X'_u$ occurs because the axis of X is below the centre of buoyancy.

$$M_w = -N_v \quad . \quad . \quad . \quad . \quad . \quad . \quad (122)$$

is a further relation which assumes equal fin areas. Both M_w and N_v are greatly dependent on the area and disposition of the fins, and are two of the more important derivatives.

The approximate relation

$$L_v = -mzY_v \quad . \quad . \quad . \quad . \quad . \quad (123)$$

can be deduced from the consideration that the lateral force on the car is unimportant compared with that on the envelope, and that the rotation

of the envelope about its own axis produces no lateral force. Further relations of a similar character are

$$\left.\begin{array}{c} Y_p = -zY_v \\ L_p = -zL_v \\ N_p = -zN_v \end{array}\right\} \quad . \quad . \quad . \quad . \quad . \quad . \quad . \quad (124)$$

The rolling moment due to yawing will often be small, and the derivative L_r may be negligible in its effects as compared with the large restoring couple in roll due to buoyancy and weight.

Of the three moments of inertia the order of magnitude will clearly be A, C, B.

The value of $X_{\dot{u}}$ has been determined in a few cases and appears to range from $-0 \cdot 15$ to $-0 \cdot 25$. $Z_{\dot{w}}$ and $Y_{\dot{v}}$ both have values of the order of -1. Up to the present the other derivatives have not been determined, and in calculations their existence has been ignored.

Approximate Analysis of Airship Motions.—Using all the simplifications indicated previously, the equations of disturbed motion given in (108) and (111) take simple form, and the results of an examination of them are useful as a guide to the importance of the terms involved. The longitudinal group becomes

$$\left.\begin{array}{l} \{X_u - \lambda(1 - X_{\dot{u}})\}u - zX'_u q \qquad\qquad = 0 \\ \{Z_w - \lambda(1 - Z_{\dot{w}})\}w + (u_0 + Z_q)q \qquad = 0 \\ mzX'_u u + M_w w + \{(M_q - B\lambda) + Fz/\lambda\}q = 0 \end{array}\right\} \quad . \quad (125)$$

whilst the lateral group is—

$$\left.\begin{array}{l} \{Y_v - \lambda(1 - Y_v)\}v - zY_v p - (u_0 - Y_r)r = 0 \\ - mzY_v v + (-zL_v - \lambda A + Fz/\lambda)p \qquad = 0 \\ N_v v - zN_v p + (N_r - \lambda C)r \qquad\qquad = 0 \end{array}\right\} \quad . \quad (126)$$

In this form the dissimilarity of the longitudinal and lateral disturbances is shown, and since the derivatives have been based on symmetry of the envelope the conclusion may be drawn that the difference is due to the fact that the axis of Z passes through the centre of buoyancy, whilst the axis of Y is some distance below that point.

Critical Velocities.—It has already been shown that for a given attitude of a body in the air the resistance derivatives due to change of linear or angular velocity are proportional to the wind speed. A similar theorem shows that the acceleration effects are independent of the wind speed so long as the resistance varies as the square of the speed. Without using any approximations, therefore, it will be seen from (110) that for longitudinal stability the biquadratic equation takes the form

$$k_1\lambda^4 + k_2 V\lambda^3 + (k_3 V^2 + k_4)\lambda^2 + (k_5 V^2 + k_6)V\lambda + k_7 V^2 = 0 \quad . \quad (127)$$

whilst the lateral stability leads to an exactly similar form. Instability occurs when any one of the coefficients changes sign, and equation (127) shows two possibilities with change of speed if k_3 and k_4 or k_5 and k_6 happen to have opposite signs. There is the further condition given by

Routh's discriminant which might lead to a new critical speed, but the further analysis will be confined to an examination of the approximate equations (125) and (126). The first of these has the stability biquadratic

$$\{X_u - \lambda(1 - X_{\dot{u}})\} \begin{vmatrix} Z_w - \lambda(1 - Z_{\dot{w}}) & u_0 + Z_q \\ M_w & (M_q - B\lambda) + Fz/\lambda \end{vmatrix}$$

$$- \{Z_{\dot{w}} - \lambda(1 - Z_{\dot{w}})\} mz^2(X'_u)^2 = 0 \quad . \quad . \quad . \quad . \quad (128)$$

It is not strictly legitimate to say that resistance derivatives due to changes of velocity vanish when V=0, since slight residual terms of higher order are present, but in accordance with the theory of small oscillations as developed this will be the case, and with the airship stopped, equation (128) reduces to

$$\lambda^2 B - Fz = 0 \quad . \quad . \quad . \quad . \quad . \quad (129)$$

Since z is negative, whilst B and F are positive, this is the equation of an undamped oscillation of period—

$$2\pi\sqrt{-\frac{B}{Fz}} \quad . \quad . \quad . \quad . \quad . \quad (130)$$

If, as appears probable, we may neglect $mz^2(X'_u)^2$ in comparison with $X_u M_q$, equation (128) has one root given by

$$\lambda = \frac{X_u}{1 - X_{\dot{u}}} \quad . \quad . \quad . \quad . \quad . \quad (131)$$

which indicates that a variation of forward speed is damped out aperiodically. The neglected terms are those arising from changes of drag of the envelope due to pitching about an axis below the centre of figure.

Approximate Criterion for Longitudinal Stability.—Equation (128) now takes the form

$$\begin{vmatrix} Z_w - \lambda(1 - Z_{\dot{w}}) & u_0 + Z_q \\ M_w & (M_q - B\lambda) + Fz/\lambda \end{vmatrix} = 0 \quad . \quad . \quad (132)$$

and by a consideration of the terms, using the theory of equations, an important approximate discriminant for longitudinal stability is obtained. The equation is a cubic in λ, and must therefore have at least one real root. The product of the roots is $\dfrac{-zFZ_w}{B(1 - Z_{\dot{w}})}$, the value of which is essentially negative and important. This follows from general knowledge, for z is negative, F positive, Z_w and $Z_{\dot{w}}$ negative and B positive in all aircraft contemplated. If only one real root occurs it must therefore be negative, whilst if all the roots are real they must either all be negative or two positive and one negative. A change of sign of a real root can only occur by a passage through zero, and in the present instance this does not occur since the product of the roots cannot be zero. The cubic may represent a subsidence and an oscillation, and the only possibility of instability arises from an increase in the amplitude of the latter.

The condition for change of sign of the damping coefficient of the oscillation can easily be deduced, for the sum of the roots is

$$M_q/B + Z_w/(1 - Z_{\dot{w}}) \quad . \quad . \quad . \quad . \quad . \quad (133)$$

and the damping of the oscillation will be zero if the real root is equal to this value. Making the substitution for λ in equation (132) leads to the criterion for stability:

$$\begin{vmatrix} M_q & u_0 + Z_q \\ M_w & Z_w - \dfrac{Fz(1 - Z_{\dot{w}})^2/B}{M_q(1 - Z_{\dot{w}})/B + Z_w} \end{vmatrix} > 0 \qquad . \quad . \quad (134)$$

The periodic time of the oscillation at the critical change is found from the product and sum of the roots, and is

$$T = 2\pi \sqrt{ -\frac{B}{Fz}\left\{ 1 + \frac{M_q(1 - Z_{\dot{w}})}{BZ_w} \right\} } \quad . \quad . \quad . \quad (135)$$

Since the second term in the bracket is always positive, comparison of (135) with (130) shows that the oscillation in critical motion is slower than that at rest. The critical velocity above which the motion is unstable is easily determined from (134), and a knowledge of the manner of variation of the derivatives with change of speed. If u_c be the critical velocity and u_0 the velocity for which the derivatives were calculated, the expression for $(u_c/u_0)^2$ is

$$\begin{vmatrix} M_q & u_0 + Z_q \\ M_w & Z_w - \left(\dfrac{u_0}{u_c}\right)^2 \dfrac{Fz(1 - Z_{\dot{w}})^2/B}{M_q(1 - Z_{\dot{w}})/B + Z_w} \end{vmatrix} = 0 \qquad . \quad . \quad (136)$$

From equation (136) can be seen the condition given by Crocco (see page 41, "Technical Report of the Advisory Committee for Aeronautics, 1909–10") for the non-existence of a critical velocity, i.e. $u_c = \infty$. Converted into present notation, Crocco's condition is

$$\begin{vmatrix} M_q & u_0 + Z_q \\ M_w & Z_w \end{vmatrix} = 0 \quad . \quad . \quad . \quad . \quad . \quad (137)$$

except that Crocco assumed that Z_q was negligible in comparison with u_0. His expression for lateral stability has an exactly analogous form.

$u_0 + Z_q$ is positive, whilst M_q, Z_w and z are negative, and the remaining terms are positive with the exception of M_w. If M_w be negative, i.e. if a restoring moment due to the wind is introduced by angular displacement, expression (136) shows that the airship's motion is stable at all speeds. It will be seen, however, that stability may be obtained with M_w positive, and this is the usual state owing to constructional difficulties in attaching large fins.

Approximate Criterion for Lateral Stability.—The biquadratic equation for stability which is obtained from equation (126) is

$$\begin{vmatrix} Y_v - \lambda(1 - Y_{\dot{v}}) & -zY_v & -u_0 + Y_r \\ -mzY_v & -zL_v - \lambda A + Fz/\lambda & 0 \\ N_v & -zN_v & N_r - \lambda C \end{vmatrix} = 0 \qquad . \quad (138)$$

If the motion through the air is very slow, the derivatives due to changes of velocity become zero, and (138) reduces to

$$\lambda^2 - Fz/A = 0 \quad . \quad . \quad . \quad . \quad . \quad (139)$$

and arising from the expression containing p clearly refers to an oscillation in roll. It appears that no airship is provided with controls which affect the rolling, and an oscillation in roll may be expected at all flight speeds. This suggests that the term $-mzY_v$ is usually unimportant, in which case the oscillation in flight is given by

$$\lambda^2 + \frac{zL_v}{A} - \frac{Fz}{A} = 0 \quad . \quad . \quad . \quad . \quad . \quad (140)$$

and is seen to have a damping term due to the motion. The remaining factor of the stability equation is then

$$\begin{vmatrix} Y_v - \lambda(1 - Y_{\dot v}) & -u_0 + Y_r \\ N_v & N_r - \lambda C \end{vmatrix} = 0 \quad . \quad . \quad . \quad (141)$$

The sum of the roots of equation (141) is $\dfrac{N_r}{C} + \dfrac{Y_v}{1 - Y_{\dot v}}$, and is negative in each term for all airships. If equation (141) has complex roots, therefore, the real part must be negative and the corresponding oscillation stable. Lateral instability can then only occur by a change in the sign of the term independent of λ, and the criterion for stability is

$$\begin{vmatrix} Y_v & -u_0 + Y_r \\ N_v & N_r \end{vmatrix} > 0 \quad . \quad . \quad . \quad . \quad (142)$$

As Y_v and N_r are both negative, it is an immediate deduction from (142) that a restoring moment about a vertical axis through the C.G. due to wind forces, i.e. a positive value for N_v, is not an essential for stability. Moreover, combined with the condition that equally effective fins be used both vertically and horizontally, (142) is sufficient to ensure the complete stability of an airship at all speeds.

In the criterion of stability, Y_v and Y_r are inversely proportional to m, the mass of the airship, and it is interesting to examine the possibilities of variation of Y_v and Y_r at various heights, i.e. when m varies. It has been assumed in the preceding analysis that the mass of the airship included that of the hydrogen, i.e. that the hydrogen moved as a solid with the envelope. This is obviously only an approximation to the truth, as internal movements of the gas are clearly possible, but, so far as it holds good, the mass concerned in the motion is that of the air displaced by the airship. This mass is independent of the condition of the hydrogen or the amount of air in the ballonets; on the other hand, it is proportional to the density of the air and therefore varies with height. The forces on the airship at the same velocity also vary directly as the air density, and hence Y_v and Y_r are independent of height. The stability of an airship is not affected by height, at least to a first approximation.

Illustration in the Case of the N.S. Type of Airship of the Values of the Derivatives with Different Sizes of Fin.—Photographs of this type of airship are shown in Fig. 9, Chapter I. ; Fig. 245, showing the dimensions of the model tested and the fins used, is given in connection with the derivatives. The figures should be regarded only as first approximations to the truth, to be replaced at a later stage of knowledge by data obtained under more favourable conditions than those existing during the war. They however served their purpose in that the fins selected as a result of these calculations were satisfactory in the first trial flight, and so aided in the rapid development of the type. The airship was designed at the
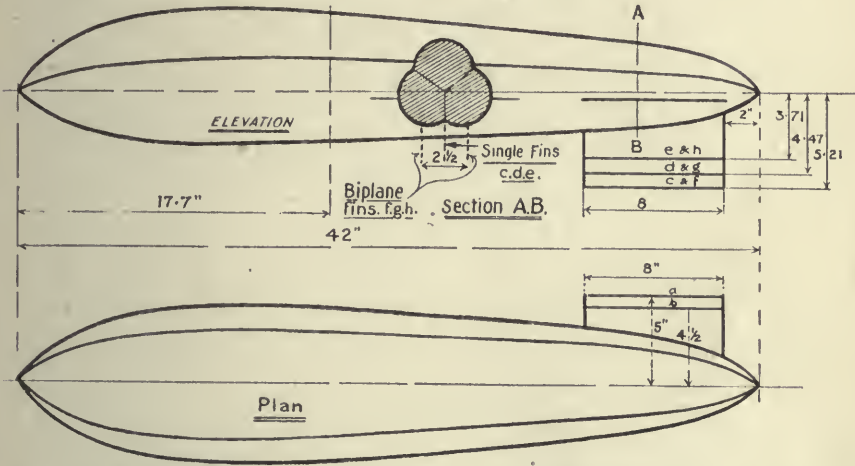
FIG. 245.—Model of a non-rigid airship used in the determination of resistance derivatives.

R.N. Airship Station, Kingsnorth, and the model experiments were made at the National Physical Laboratory. The data obtained were

		Symbol in calculations.
Volume	360,000 cubic feet . . .	—
Length	260 ft.	—
Speed	75 ft.-s.	u_0
Total lift	23,500 lbs.	F
Wt. of hydrogen . . .	2,500 lbs.	—
Wt. of displaced air . .	26,000 lbs.	—
Mass	$\dfrac{26,000}{32 \cdot 2} = 800$ slugs approx.	m
Height of centre of buoyancy above the centre of gravity	10 ft.	$-z$
Moments of inertia—		
About longitudinal axis	4×10^5 slug-ft.^{2}	A
About lateral axis . .	$2 \cdot 1 \times 10^6$,,	B
About normal axis . .	$1 \cdot 9 \times 10^6$,,	C

Horizontal fins are denoted in Fig. 245 by a and b.

Vertical fins are denoted in Fig. 245 by c, d, e, f, g and h.

Of the vertical fins f, g and h were arranged as biplanes. The presence of the horizontal fins was found not to affect appreciably the forces on the vertical fins, and *vice versâ*.

Derivatives.

	No fins.	Fins b.	Fins a.
mX'_u	-32	-32	-32
mX_u	-50	-50	-50
mZ_w	-300	-390	-490
mZ_q	—	-35	-35
M_w	4.7×10^4	2.5×10^4	2.1×10^4
M_q	$+2.0 \times 10^5$	-7.5×10^6	-7.9×10^6
X'_u	-0.25	-0.25	-0.25
Z'_w	-1.0	-1.0	-1.0

	No fins.	Monoplane fins.			Biplane fins.		
		c	d	e	f	g	h
mY_v	-300	-350	-260	-220	-450	-350	-290
mY_r	—	$+40$	$+35$	$+35$	$+40$	$+40$	$+40$
N_v	-4.7×10^4	-2.7×10^4	-3.3×10^4	-3.8×10^4	-1.7×10^4	-2.5×10^4	-3.3×10^4
N_r	—	-7.1×10^6	-5.9×10^6	-5.4×10^6	-7.8×10^6	-7.3×10^6	-6.9×10^6

Owing to the shielding of the fins by the body of the envelope the numerical value of Y_v is less for symmetrical flight than when yawed.
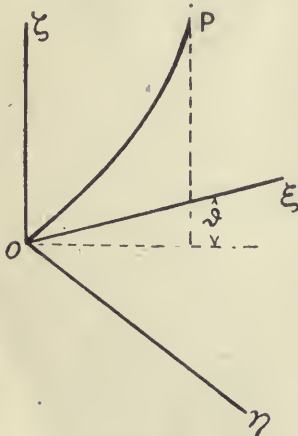
Fig. 246.

It is probable, therefore, that turning tends to produce greater stability as it introduces sideslipping. The additional terms can be introduced as required, and some discussion of the subject has already been given by Jones and Nayler. The mathematical theory is well ahead of its applications, and no difficulty in extending it as required have as yet appeared.

Forces in a Mooring Cable or Kite Balloon Wire due to its Weight and the Effect of the Movement of the Upper End.—The axes $O\xi$, $O\eta$ and $O\zeta$ (Fig. 246) are chosen as fixed relative to the earth, the cable or wire being fixed at O. The point of attachment of the cable to the aircraft is P, and may have movement in various directions.

Forces at P due to the Wire.—If the stiffness of the wire and the wind forces on it be neglected, the form of the wire will be a catenary, and it is

clear that the forces in it will not be affected by rotations about the axis of ζ. The problem, so far as it affects the forces at P due to the kite wire, can then be completely solved by considering deflections of P in a plane. In any actual case it is certain that waves will be transmitted along the wire, but the above assumptions would appear to represent those of primary importance.

If k be the horizontal component of the tension in the wire (constant at all points when wind forces are neglected), the equation to the catenary can be shown to be

$$\zeta = \frac{k}{w} \cosh \frac{w}{k}(\xi + \xi_0) - \frac{k}{w} \cosh \frac{w}{k}\xi_0 \quad . \quad . \quad . \quad (143)$$

w is the weight of the wire per unit length, and ξ_0 is a constant of integration so chosen that $\zeta = 0$ when $\xi = 0$. From the geometry of the catenary it will readily be seen that ξ_0 is the distance from the point of attachment of the wire to the vertex of the catenary, the distance being measured along the negative direction of ξ. This follows from the fact that $\frac{\delta\zeta}{\delta\xi} = 0$ when $\xi = -\xi_0$.

It is convenient to use, as a separate expression, the length of wire from the point P to the ground. If s be used to denote this length, then

$$s = \frac{k}{w} \sinh \frac{w}{k}(\xi + \xi_0) - \frac{k}{w} \sinh \frac{w}{k}\xi_0 \quad . \quad . \quad . \quad (144)$$

Equations (143) and (144) define k, the horizontal component of the tension in the wire, and the length s, in terms of the position of the point P and the weight of unit length of wire. In the case of an aircraft the co-ordinates of P may be changed by a gust of wind, and it is now proposed to find the variations of k which result from any arbitrary motion of P in the plane of the wire. A further approximation will be made here in that the extensibility of the wire will be neglected. As the problem mathematically will be considered as one of small oscillations, this assumption falls within the limitations usually imposed by such analysis.

Since the length of the wire is constant in the motions of P under consideration, it follows by differentiation of (144) that

$$0 = dk\left\{\frac{s}{k} - \frac{w\xi_0}{k_2}\zeta - \frac{\zeta}{k} \cosh \frac{w}{k}(\xi + \xi_0)\right\}$$
$$+ d\xi \cosh \frac{w}{k}(\xi + \xi_0) + d\xi_0 \frac{w\zeta}{k} \quad . \quad . \quad . \quad (145).$$

It will be obvious from the definition of ξ_0 given previously that any variation in P will produce a corresponding change in ξ_0, and although a constant of integration when P is fixed, its variations must be included in the present calculations.

Differentiating equation (143) gives an expression corresponding to (145)

$$d\zeta = dk\left\{\frac{\zeta}{k} - \frac{w\xi_0}{k^2}s - \frac{\xi}{k}\sinh\frac{w}{k}(\xi + \xi_0)\right\}$$

$$+ d\xi \sinh\frac{w}{k}(\xi + \xi_0) + d\xi_0\frac{ws}{k} \quad . \quad . \quad . \quad (146)$$

Eliminating $d\xi_0$ between equations (145) and (146) the relation

$$dk = \frac{\zeta d\zeta + \dfrac{k}{w}\sinh\dfrac{w\xi}{k}d\xi}{\dfrac{2k}{w^2}\left(1 - \cosh\dfrac{w\xi}{k}\right) + \dfrac{\xi}{w}\sinh\dfrac{w\xi}{k}} \quad . \quad . \quad . \quad (147)$$

is obtained, which gives the variations of horizontal force dk in terms of the movements of the upper end of the wire.

To find the variation of the vertical component of the tension of the wire as a consequence of changes $d\xi$ and $d\zeta$ in the position of the point P, it is useful to employ equations (147) and (145). The slope of the wire at the point P can be obtained from equation (143) by differentiation, giving

$$\frac{d\zeta}{d\xi} = \sinh\frac{w}{k}(\xi + \xi_0) \quad . \quad . \quad . \quad . \quad (148)$$

and therefore the vertical component of the tension T_1 is

$$T_1 = k\sinh\frac{w}{k}(\xi + \xi_0) \quad . \quad . \quad . \quad . \quad (149)$$

In the displaced position of the point P the vertical component of the tension, T_2, will be given by

$$T_2 = T_1 + dk\left\{\sinh\frac{w}{k}(\xi + \xi_0) - \frac{w(\xi + \xi_0)}{k}\cosh\frac{w}{k}(\xi + \xi_0)\right\}$$

$$+ w\cosh\frac{w}{k}(\xi + \xi_0).(d\xi + d\xi_0) \quad . \quad . \quad . \quad . \quad (150)$$

Using the value of $d\xi_0$, which may be obtained from (145), equation (150) becomes

$$T_2 = T_1 + dk\left[\sinh\frac{w}{k}(\xi + \xi_0) + w\cosh\frac{w}{k}(\xi \mp \xi_0)\right.$$

$$\left.\left\{\frac{\xi}{w\zeta}\cosh\frac{w}{k}(\xi + \xi_0) - \frac{\xi}{k} - \frac{s}{w\zeta}\right\}\right]$$

$$+ d\xi.w\cosh\frac{w}{k}(\xi + \xi_0)\left\{1 - \frac{k}{w\zeta}\cosh\frac{w}{k}(\xi + \xi_0)\right\} \quad . \quad (151)$$

Substituting in equation (151) the value of dk obtained from equation (147) an expression for $T_2 - T_1$ in terms of $d\xi$ and $d\zeta$ is obtained.

The forces *acting on the aircraft* at P along the axes of ξ and ζ are

$$-(k + \mu d\zeta + \nu d\xi) \quad . \quad . \quad . \quad . \quad . \quad . \quad (152)$$

and

$$-\left\{ k \sinh \frac{w}{k}(\xi + \xi_0) + \mu\mu_1 d\zeta + (\nu\mu_1 + \nu_1)d\xi \right\} \quad . \quad . \quad (153)$$

where

$$\mu = \frac{\zeta}{\dfrac{2k}{w^2}\left(1 - \cosh \dfrac{w}{k}\xi\right) + \dfrac{\xi}{w}\sinh \dfrac{k}{w\xi}}$$

$$\nu = \frac{\dfrac{k}{w}\sinh \dfrac{w\xi}{k}}{\dfrac{2k}{w^2}\left(1 - \cosh \dfrac{w}{k}\xi\right) + \dfrac{\xi}{w}\sinh \dfrac{k}{w\xi}}$$

$$\mu_1 = \frac{\xi}{\zeta}\cosh \frac{w}{k}(\xi + \xi_0)\cosh \frac{w}{k}\xi_0 - \frac{k}{w\zeta}\sinh \frac{w}{k}\xi$$

$$\nu_1 = w \cosh \frac{w}{k}(\xi + \xi_0)\left\{1 - \frac{k}{w\zeta}\cosh \frac{w}{k}(\xi + \xi_0)\right\}$$

$$\left.\rule{0pt}{120pt}\right\} \quad . \quad (154)$$

The expressions μ, μ_1 and ν are always positive, and ν_1 negative.

All the above relations have been developed on the assumption that the rope lies entirely in the plane $\xi O \zeta$. In the case of the disturbed position of an aircraft, especially if more than one wire is used, it will be necessary to consider the components of the tension along the axes of ξ, η and ζ when the plane of the wire makes an angle θ with the plane $\xi O \zeta$.

If ξ, η and ζ are the co-ordinates of P, then the angle θ is such that

$$\tan \theta = \frac{\eta}{\xi} \quad . \quad . \quad . \quad . \quad . \quad (155)$$

The values of ξ, ξ_0 and $d\xi$ in the previous expressions must now be replaced by $\xi \sec \theta$, $\xi_0 \sec \theta$, and $d\xi \sec \theta$ respectively. If the point of attachment of the wire for a second rope is not at the point (o, o, o) but at the point $(\xi_1, \eta_1\ o)$, then instead of (155) there will be the relation

$$\tan \theta_1 = \frac{\eta - \eta_1}{\xi - \xi_1} \quad . \quad . \quad . \quad . \quad . \quad (156)$$

and the values of ξ, ξ_0 and $d\xi$ in (152), (153) and (154) will need to be replaced by

$$(\xi - \xi_1)\sec \theta_1, \quad (\xi_0 - \xi_{01})\sec \theta_1 \quad \text{and} \quad d\xi \sec \theta_1. \quad . \quad (157)$$

By means of (156) and (157) any number of wires connected together at P can be considered. The conditions relating to equilibrium will indicate some relation between the angles θ, θ_1, θ_2, etc., since the force on the aircraft along the axis of η must then be zero from considerations of symmetry.

If the wires are not all brought to the same point P, the relations given above can be used if, instead of the co-ordinates of P (ξ, η, ζ), the co-ordinates of Q, the new point of attachment, are used. In the case of more

than one point of attachment at the aircraft, it will be possible to have equilibrium without having the plane of symmetry in the vertical plane containing the wind direction. If, however, symmetry is assumed, it will be necessary to arrange that the moment about any axis parallel to $O\zeta$ shall be zero.

With the aid of the above equations it is possible to determine both the conditions of equilibrium for a captive aircraft and the derivatives due to the swaying of the rope.

CHAPTER X

THE STABILITY OF THE MOTIONS OF AIRCRAFT

PART II.—THE DETAILS OF THE DISTURBED MOTION OF AN AEROPLANE

IN developing the mathematical theory of stability it was shown that the periods and damping factors of oscillations could be obtained together with the rates of subsidence or divergence of non-periodic motions. It was not, however, possible by the methods developed to show how the resultant motion was divided between forward motion, vertical motion and pitching for longitudinal disturbances, or between sideslipping, rolling and yawing for lateral disturbances.

It is now proposed to take up the further mathematical analysis in the case of separable motions and to illustrate the theory by a number of examples, including flight in a natural wind. The subject includes the consideration of the effect of controls and the changes which occur as an aeroplane is brought from one steady state to another. It is possible that the method of attack will be found suitable for investigations relating to the lightness of controls and the development of automatic stability devices.

Reference to the equations of disturbed motion, (8) and (45), will show that three equations are defined for longitudinal and three for lateral motion, and that in each case a combination of them has led to a single final equation for stability. There are left two other relations which can be used to find the relative proportions in the disturbance of the various component velocities and angular velocities.

Longitudinal Disturbance.—The condition for stability was obtained by eliminating u, w and q from the equations of motion and determined values of λ from which the periods and damping factors were calculated. The method of solution of the differential equation depends on the knowledge of the fact that

$$u = ae^{\lambda t} \qquad w = be^{\lambda t} \qquad q = ce^{\lambda t} \quad . \quad . \quad . \quad (158)$$

are expressions which when introduced into the differential equations of disturbed motion reduce them to algebraic equations. a, b and c are the initial values of the disturbances in u, w and q which correspond with the chosen value of λ. An examination of the stability equation shows that there are four values of λ in the case of an aeroplane, some of which are complex and others real. Using (158) the equations of disturbed motion become

$$(X_u - \lambda)a + X_w b + \left(X_q - w_0 - g\frac{n_3}{\lambda}\right)c = 0$$

$$Z_u a + (Z \ - \lambda)b + \left(Z_q + u_0 + g\frac{n_1}{\lambda}\right)c = 0 \qquad \cdot \quad \cdot \ (159)$$

$$M_u a + M_w b + (M_q - B\lambda)c = 0$$

Since λ is known from one combination of these three equations, only two of them can be considered as independent relations between a, b and c, and choosing the first two, a solution of (159) is

$$
\frac{a}{\begin{vmatrix} X_w & X_q - w_0 - g\dfrac{n_3}{\lambda} \\[2mm] Z_w - \lambda & Z_q + u_0 + g\dfrac{n_1}{\lambda} \end{vmatrix}}
= \frac{b}{\begin{vmatrix} X_q - w_0 - g\dfrac{n_3}{\lambda} & X_u - \lambda \\[2mm] Z_q + u_0 + g\dfrac{n_1}{\lambda} & Z_u \end{vmatrix}}
= \frac{c}{\begin{vmatrix} X_u - \lambda & X_w \\[2mm] Z_u & Z_w - \lambda \end{vmatrix}}
\qquad (160)
$$

and the ratios b/a and c/a are determined. This is essentially the solution required, and for real values of λ the form is suitable for direct numerical application. If, however, λ be complex, it is necessary to consider a pair of corresponding roots and to separate the real and imaginary parts of (160) before computation is possible.

If the roots be $\lambda_1 = h + ik$ and $\lambda_2 = h - ik$, the two values of such a term as u group together as

$$u = e^{ht}(a_1 e^{ikt} + a_2 e^{-ikt}) \quad \cdot \quad \cdot \quad \cdot \quad \cdot \ (161)$$

or in terms of sines and cosines instead of exponentials,

$$u = e^{ht}\{(a_1 + a_2) \cos kt + i(a_1 - a_2) \sin kt\} \quad \cdot \quad \cdot \ (162)$$

and from equations (160) it is desired to find the values of $a_1 + a_2$ and of $i(a_1 - a_2)$ in order to give u the real form of a damped oscillation.

On substituting $h + ik$ for λ in equations (160) the expressions become complex and of the form

$$a_1(\mu_1 + i\nu_1) = b_1(\mu_2 + i\nu_2) = c_1(\mu_3 + i\nu_3) . \quad \cdot \quad \cdot \ (163)$$

with a corresponding expression for the root $h - ik$, which is

$$a_2(\mu_1 - i\nu_1) = b_2(\mu_2 - i\nu_2) = c_2(\mu_3 - i\nu_3) . \quad \cdot \quad \cdot \ (164)$$

where the values of μ_1, μ_2, μ_3, ν_1, ν_2 and ν_3 are found from

$$
\frac{\mu_1}{\sqrt{\mu_1{}^2 + \nu_1{}^2}} = \begin{vmatrix} X_w & X_q - w_0 - \dfrac{gn_3 h}{h^2 + k^2} \\[2mm] Z_w - h & Z_q + u_0 + \dfrac{gn_1 h}{h^2 + k^2} \end{vmatrix} - \frac{gn_3 k^2}{h^2 + k^2}
$$

$$
\frac{\nu_1}{\sqrt{\mu_1{}^2 + \nu_1{}^2}} = k\left\{ \begin{vmatrix} X_w & -\dfrac{gn_3}{h^2 + k^2} \\[2mm] Z_w - h & +\dfrac{gn_1}{h^2 + k^2} \end{vmatrix} - \left(X_q - w_0 - \dfrac{gn_3 h}{h^2 + k^2}\right) \right\}
\qquad \cdot \ (165)
$$

$$\frac{\mu_2}{\sqrt{\mu_2{}^2 + \nu_2{}^2}} = \left. \begin{array}{cc} X_q + w_0 - \dfrac{gn_3h}{h^2 + k^2} & X_u - h + \dfrac{gn_1k^2}{h^2 + k^2} \\[2ex] Z_q + u_0 + \dfrac{gn_1h}{h^2 + k^2} & Z_u \end{array} \right.$$

$$\frac{\nu_2}{\sqrt{\mu_2{}^2 + \nu_2{}^2}} = k \left\{ \begin{array}{cc} -\dfrac{gn_3}{h^2 + k^2} & X_u - h \\[2ex] +\dfrac{gn_1}{h^2 + k^2} & Z_u \end{array} \left| -\left(Z_q + u_0 + \dfrac{gn_1h}{h^2 + k^2} \right) \right\} \right. \qquad (166)$$

$$\frac{\mu_3}{\sqrt{\mu_3{}^2 + \nu_3{}^2}} = \left| \begin{array}{cc} X_u - h & X_w \\ Z_u & Z_w - h \end{array} \right| - k^2 \qquad \cdots \cdots \quad (167)$$

$$\frac{\nu_3}{\sqrt{\mu_3{}^2 + \nu_3{}^2}} = k(X_u + Z_w - 2h)$$

and are directly calculable from known values of h, k and the derivatives of the aeroplane. From the expressions connecting a, b and c with μ and ν it is easily deduced that

$$b_1 + b_2 = \frac{\mu_1\mu_2 + \nu_1\nu_2}{\mu_2{}^2 + \nu_2{}^2}(a_1 + a_2) - \frac{\mu_1\nu_2 - \mu_2\nu_1}{\mu_2{}^2 + \nu_2{}^2}i(a_1 - a_2)$$

and $\quad i(b_1 - b_2) = \dfrac{\mu_1\mu_2 + \nu_1\nu_2}{\mu_2{}^2 + \nu_2{}^2}i(a_1 - a_2) + \dfrac{\mu_1\nu_2 - \mu_2\nu_1}{\mu_2{}^2 + \nu_2{}^2}(a_1 + a_2) \qquad (168)$

with similar expressions for $c_1 + c_2$ and $i(c_1 - c_2)$.

If A and B be used instead of $a_1 + a_2$ and $i(a_1 - a_2)$ the expressions for a disturbed oscillation become

$$u = e^{ht}(A \cos kt + B \sin kt)$$

$$w = \frac{e^{ht}}{\mu_2{}^2 + \nu_2{}^2}[\{(\mu_1\mu_2 + \nu_1\nu_2)A - (\mu_1\nu_2 - \mu_2\nu_1)B\} \cos kt$$
$$+ \{(\mu_1\nu_2 - \mu_2\nu_1)A + (\mu_1\mu_2 + \nu_1\nu_2)B\} \sin kt]$$

$$q = \frac{e^{ht}}{\mu_3{}^2 + \nu_3{}^2}[\{(\mu_1\mu_3 + \nu_1\nu_3)A - (\mu_1\nu_3 - \mu_3\nu_1)B\} \cos kt$$
$$+ \{(\mu_1\nu_3 - \mu_3\nu_1)A + (\mu_1\mu_3 + \nu_1\nu_3)B\} \sin kt] \quad (169)$$

In actually calculating the motion of an aeroplane the integrals of u, w and q may be required. From (161) it will be seen that

$$\int u\,dt = \frac{a_1}{h + ik}e^{(h + ik)t} + \frac{a_2}{h - ik}e^{(h - ik)t} \quad \cdots \quad (170)$$

Expressed in terms of sines and cosines, (170) is

$$\int u\,dt = \frac{e^{ht}}{\sqrt{h^2 + k^2}}\left\{\frac{A}{\mu_1}\cos(kt - \gamma) + \frac{B}{\nu_1}\sin(kt - \gamma)\right\} \quad (171)$$

where $\sin \gamma = \dfrac{k}{\sqrt{h^2 + k^2}}$, and $\cos \gamma = \dfrac{h}{\sqrt{h^2 + k^2}}$, the positive value of $\sqrt{h^2 + k^2}$ being always taken.

Similar expressions follow for w and q. In the case of rectilinear motion in the plane of symmetry and in still air, $q = \dot{\theta}$, a$^\cdot$ hence integration gives the value of θ, *i.e.* the inclination of the axis of X to the horizontal.

Equal Real Roots.—It appears that it may be necessary to deal with equal or nearly equal roots, and the method outlined above then breaks down. Following the usual mathematical method, it is assumed that

$$u = (C + Dt)e^{\lambda t} \qquad . \quad . \quad . \quad . \quad . \quad (172)$$

From (160) $b = a\phi(\lambda)$ and the solution for w is

$$w = \{(C + Dt)e^{\lambda t}\phi(\lambda) + De^{\lambda t}\phi'(\lambda)\} \qquad . \quad . \quad . \quad (173)$$

It is therefore necessary in the case of equal real roots to find the value of $\phi'(\lambda)$ as well as that of $\phi(\lambda)$. The differentiation presents no serious difficulties and does not occur sufficiently often for the complete formulæ to be reproduced.

Example.—The derivatives assumed to apply in a particular case are :—

$$
\left.
\begin{array}{lll}
X_u = -0.14 & Z_u = -0.80 & M_u = 0 \\[4pt]
X_w = 0.19 & Z_w = -2.89 & \dfrac{1}{B}M_w = -0.106 \\[4pt]
X_q = 0 & Z_q = -9 & \dfrac{1}{B}M_q = -8.40
\end{array}
\right\} \quad . \quad . (174)
$$

$$n_1 = 0 \qquad n_3 = 1 \qquad w_0 = 0 \qquad u_0 = 80 \quad . \quad . \quad . \quad . \quad (175)$$

From (175) it will be seen that flight is horizontal with the axis of X in the direction of flight. Proceeding to the biquadratic for stability and its solutions, shows that

$$\lambda_1 = -5.62 \qquad \lambda_2 = -5.62 \qquad \lambda_3 \text{ and } \lambda_4 = -0.075 \pm 0.283i \quad . \quad (176)$$

Applying the formulae of (165) . . . (167) leads to

$$
\left.
\begin{array}{ll}
\mu_1 = +0.000639 & \nu_1 = -0.00313 \\
\mu_2 = -0.00396 & \nu_2 = +0.0143 \\
\mu_3 = 0.350 & \nu_3 = -1.12
\end{array}
\right\} \quad . \quad . \quad . \quad (177)
$$

and

$$
\left.
\begin{array}{ll}
\phi_b(\lambda) = 177 & \phi_b'(\lambda) = 204 \\
\phi_c(\lambda) = -6.92 & \phi_c'(\lambda) = -5.53
\end{array}
\right\} \quad . \quad . \quad . \quad . \quad (178)
$$

and by substitution in equations (158) and (169)

$$u = e^{-0.075t}\{A \cos 0.283t + B \sin 0.283t\} + e^{-5.62t}(C + Dt)$$

where A, B, C and D are arbitrary constants to be fixed presently by the initial conditions of the motion.

$$w = e^{-0.075t}\{(-0.214A + 0.0147B) \cos 0.283t - (0.0147A + 0.214B) \sin 0.283t\}$$
$$+ e^{-5.62t}(177c + 204D + 177Dt)$$

$$q = e^{-0.075t}\{(0.00274A - 0.000277B) \cos 0.283t + (0.000277A + 0.00274B) \sin 0.283t\}$$
$$- e^{-5.62t}(6.92C + 5.53D + 6.92Dt)$$

$$\theta = \frac{e^{-0.075t}}{0.292}\{(0.00274A - 0.000277B) \cos (0.283t - \gamma)$$

$$+ (0.000277A + 0.00274B) \sin (0.283t - \gamma)\}$$

$$+ \frac{e^{-5.62t}}{5.62}\Big\{6.92C + 5.53D + 6.92D\Big(t + \frac{1}{5.62}\Big)\Big\} \quad . \quad . \quad . \quad . \quad (179)$$

where $\cos \gamma = -0.257$ and $\sin \gamma = 0.966$.

Initial conditions.—Let u_1, w_1, q_1, and θ_1 be the values of u, w, q and θ when $t=0$, then

$$\left.\begin{array}{l}u_1 = \quad A + C \\ w_1 = -0\cdot214A + 0\cdot0147B + 177C + 204D \\ q_1 = \quad 0\cdot00274A - 0\cdot000277B - 6\cdot92C - 5\cdot53D \\ \theta_1 = -0\cdot00333A - 0\cdot00883B + 1\cdot23C + 1\cdot204D\end{array}\right\} \quad . \quad . \quad . \quad (180)$$

and four linear equations are produced to give A, B, C and D in terms of the initial values of components of the disturbance. Illustrations of the motion are given in Fig. 247 for the four simple initial disturbances in u, w, q and θ. For the first of these, where

$$u_1 = u \quad w_1 = 0 \quad q_1 = 0 \quad \text{and} \quad \theta_1 = 0, \text{ when } t = 0$$

the values of A . . . D are

$$\left.\begin{array}{l}A = \quad 1\cdot001u_1 \\ B = -0\cdot265u_1 \\ C = -0\cdot00147u_1 \\ D = \quad 0\cdot00235u_1\end{array}\right\} \quad . \quad . \quad . \quad . \quad . \quad (181)$$

The substitution of these in (179) gives the analytical expressions for the disturbed motion due to meeting a head-on gust. The completed formulae are shown in (182), and the curves of Fig. 247 (*a*) were obtained from them.

$$u = u_1 e^{-0\cdot075t}(1\cdot001 \cos 0\cdot283t - 0\cdot265 \sin 0\cdot283t) + u_1 e^{-5\cdot62t}(-0\cdot00147 + 0\cdot00235t)$$

$$w = u_1 e^{-0\cdot075t}(-0\cdot220 \cos 0\cdot283t + 0\cdot042 \sin 0\cdot283t) + u_1 e^{-5\cdot62t}(0\cdot220 + 0\cdot416t)$$

$$q = u_1 e^{-0\cdot075t}(0\cdot00281 \cos 0\cdot283t - 0\cdot00045 \sin 0\cdot283t) - u_1 e^{-5\cdot62t}(0\cdot00281 + 0\cdot0163t)$$

$$\theta = u_1 e^{-0\cdot075t}(-0\cdot00104 \cos 0\cdot283t + 0\cdot00970 \sin 0\cdot283t)$$
$$- u_1 e^{-5\cdot62t}(-0\cdot00104 - 0\cdot0029t) \quad . \quad . \quad . \quad (182)$$

Effect of the Movement of a Control.—If an aeroplane be flying steadily under given conditions and the elevator be moved or the engine throttle adjusted, it will begin to move to some new condition of equilibrium if the aeroplane is stable. The disturbances of motion may then be regarded as the differences between the original steady motion and the final steady motion, and if small can be covered by the theory of small oscillations. A movement of the elevator will be denoted by μ and a change of thrust by ν; the changes in the forces and moments which result will be assumed to be proportional to μ and ν. Equation (5) then becomes—

$$0 = -g \sin \theta_0 + f_x(u_0, w_0, 0) - g \cos \theta_0 . \theta + u X_u + w X_w + \mu X_\mu + \nu X_\nu \quad (183)$$

where u_0, w_0 and θ_0 still apply to the original motion and the first two terms are therefore zero, whilst u, w and θ are the changes in the steady motion which arise from the elevator movement μ and the thrust change ν. Three equations are obtained which define the disturbances u, w and θ in terms of μ and ν, and are—

$$\left.\begin{array}{l}-g \cos \theta_0 . \theta + u X_u + w X_w + \mu X_\mu + \nu X_\nu = 0 \\ -g \sin \theta_0 . \theta + u Z_u + w Z_w + \mu Z_\mu + \nu Z_\nu = 0 \\ \qquad\qquad u M_u + w M_w + \mu M_\mu + \nu M_\nu = 0\end{array}\right\} \quad . \quad . \quad (184)$$

The solution of these equations presents no difficulty and leads to

$$\frac{\theta}{\begin{vmatrix} X_u & X_w & \mu X_\mu + \nu X_\nu \\ Z_u & Z_w & \mu Z_\mu + \nu Z_\nu \\ M_u & M_w & \mu M_u + \nu M_\nu \end{vmatrix}} = \frac{-\begin{vmatrix} g \cos \theta_0 & X_w & \mu X_\mu + \nu X_\nu \\ g \sin \theta_0 & Z_w & \mu Z_\mu + \nu Z_\nu \\ 0 & M_w & \mu M_\mu + \nu M_\nu \end{vmatrix}}{}$$

$$= \frac{w}{-\begin{vmatrix} g \cos \theta_0 & X_u & \mu X_\mu + \nu X_\nu \\ g \sin \theta_0 & Z_u & \mu Z_\mu + \nu Z_\nu \\ 0 & M_u & \mu M_\mu + \nu M_\nu \end{vmatrix}} = \frac{-1}{-\begin{vmatrix} g \cos \theta_0 & X_u & X_w \\ g \sin \theta_0 & Z_u & Z_w \\ 0 & M_u & M_w \end{vmatrix}} \quad . \quad . \quad (185)$$

The motion of the aeroplane is found for changes of elevator and thrust on the assumption that the old steady conditions persisted whilst X_μ, N_μ, etc., were measured, this being the usual assumption underlying the calculation of derivatives.

Example : Use of Elevator only.—In addition to the derivatives previously given in this section it is necessary to have the values

$$X_\mu = 0 \qquad Z_\mu = -0·2 \qquad \frac{1}{B}M_\mu = -3 \ . \ . \ . \ . \ . \ (186)$$

in order to calculate the elementary disturbances in u, w, q and θ which are equivalent to a movement of the elevator. Equations (185) then lead to

$$u_1 = 95·9\mu \qquad w_1 = -28·2\mu \qquad q_1 = 0 \qquad \theta = -0·581\mu \ . \ . \ (187)$$

and these values together with equations (180) serve to determine the values of A, B, C and D, which are

$$A = 95·7\mu \qquad B = 28·5\mu \qquad C = 0·221\mu \qquad D = -0·231\mu \ . \ . \ (188)$$

and suffice to determine the whole motion from equations (179). As calculated, the values of u, etc., refer to the final steady motion ; they can be used relative to the original steady motion by adding constants to make the initial disturbances in u, w, q and θ zero. This was the procedure followed in producing Fig. 248 from the analytical expressions.

Change of Airscrew Thrust only.—In order to give X_ν a value it would be necessary to define ν as some quantity depending on the position of the throttle, viz. the revolutions of the airscrew. If, however, a simple example be taken, it is permissible to write

$$+m\nu X_\nu = \delta T \qquad Z_\nu = 0 \qquad M_\nu = 0 \ . \ . \ . \ . \ (189)$$

where δT represents the increment of thrust which constitutes the disturbance. Since the original steady motion was horizontal, $\theta_0 = 0$, and the component disturbances are

$$u_1 = 0 \qquad w_1 = 0 \qquad q_1 = 0 \qquad \theta = \frac{\delta T}{mg} \ . \ . \ . \ . \ (190)$$

and a reduction of thrust leads primarily to a descent and not to a change of speed. The diagram corresponding with (190) is the typical simple disturbance shown in Fig. 247 (d).

Description of Figs. 247 and 248 illustrating the Results of the Calculations of Longitudinal Disturbances

Gust in the Direction of Flight.—The result is shown in Fig. 247 (a), the ordinates of which are proportional to the magnitude of the increase of wind speed, u_1, and the abscissae the times in seconds after entering the gust. (Variations of gust with time are dealt with later.) The speed through the air is seen to fall rapidly from $u = u_1$ at $t = 0$ to zero in less than five seconds, and to continue its fall to $u = -0·5u_1$ in nearly 10 secs. The record is that of a damped oscillation of insignificant amplitude at the end of one minute. The value of w at first falls rapidly, showing a rapid adjustment of angle of incidence to the new conditions, and is accompanied by a very similar but oppositely disposed curve for the angular velocity q. The inclination of the aeroplane axis to the ground is seen to vary considerably, and to have its maximum and minimum nearly a quarter of a period later than the velocity, whilst that of w is a half-period later and q almost in phase. This relation constitutes a characteristic of the phugoid oscillation, and applies to the later parts of all the diagrams. The fact can be deduced from

the analytical expressions by any one used to the manipulation of the formulae relating to damped oscillations.
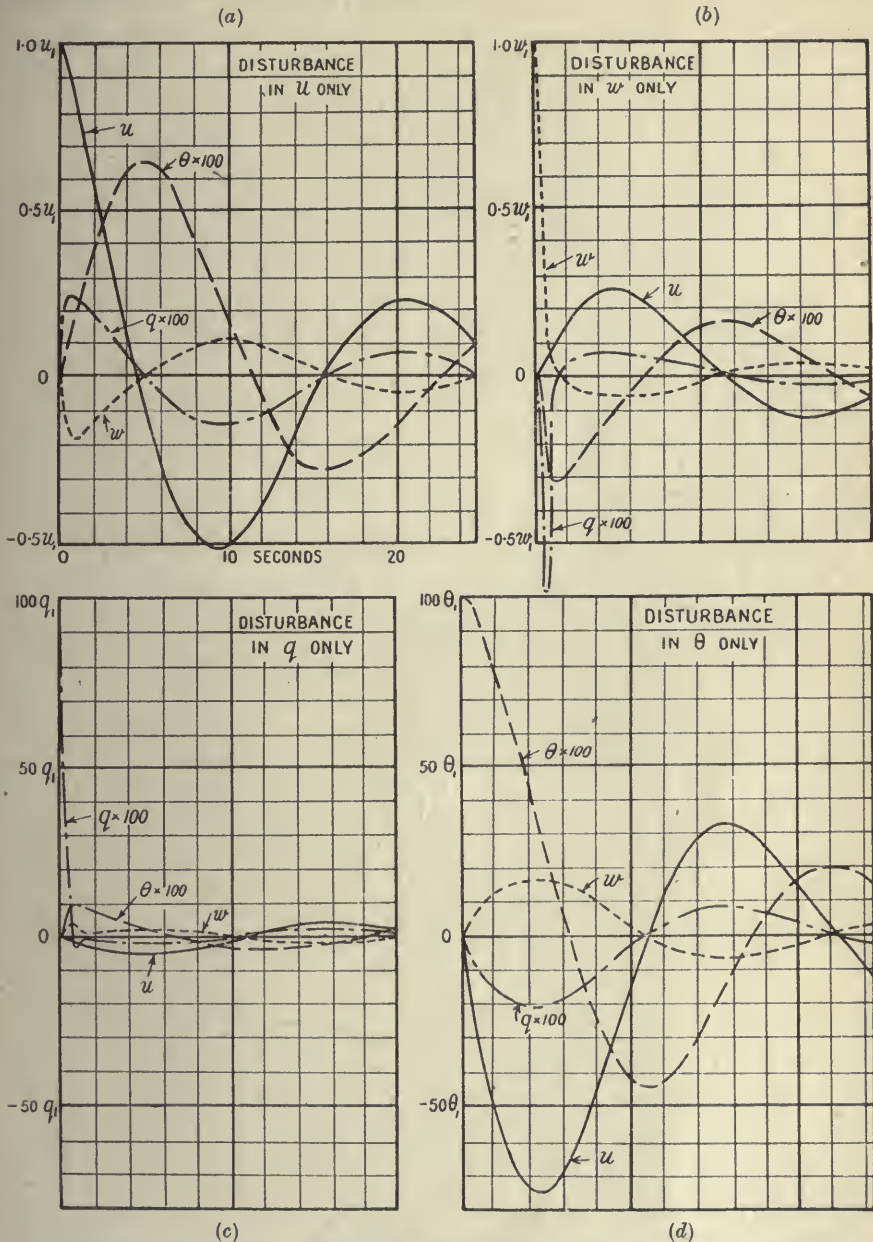
FIG. 247.—The effect of simple longitudinal disturbances. (Aeroplane stable.)

Up-current.—The first effect of running into an up-current is an increase of normal velocity and therefore of angle of incidence. The

aeroplane gets an angular velocity very rapidly and loses it almost equally
rapidly, so that the angle of incidence has adjusted itself at an early stage
to the value suitable for the residual phugoid oscillation.

Disturbance of Angular Velocity.—A horizontal whirlwind is the only
means of producing such an effect, and could not continue without producing
permanent inclination. The only valid deduction to be drawn from a
disturbance in q is that it will be taken up with extreme rapidity and will
leave a phugoid of small amplitude.
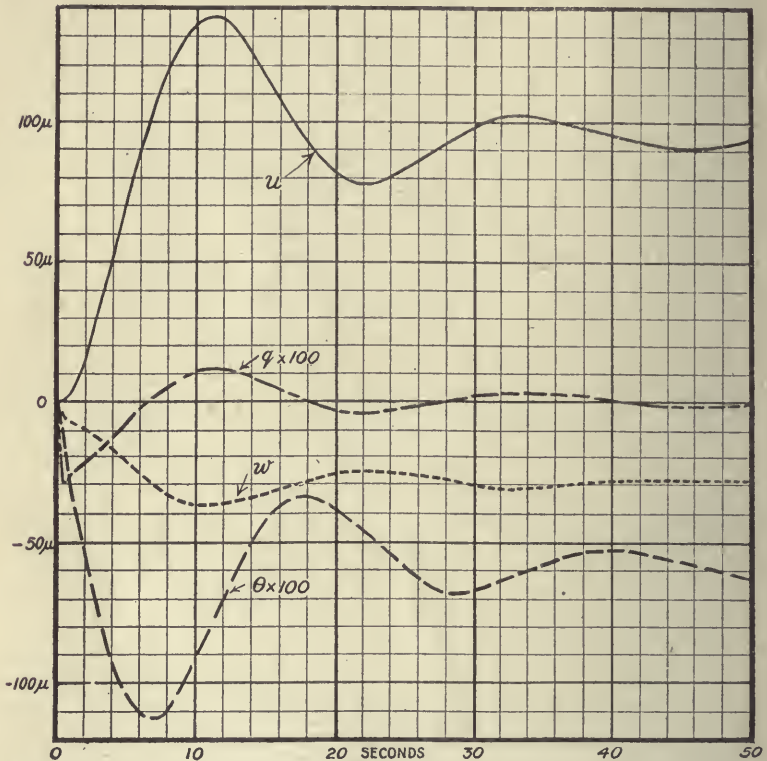
Fig. 248.—Disturbance due to the movement of an elevator. (Aeroplane stable.)

Disturbance of Path.—Change of thrust is the nearest equivalent to
this disturbance, which is mainly phugoid. Since the value of $e^{-5.62t}$ is
small at the end of half a second, the analytical expressions show that the
subsequent motion in all cases consists of the phugoid oscillation with an
amplitude which depends both on the magnitude of the disturbing cause
and on its type.

Movement of the Elevator.—Fig. 248 shows the result of giving a positive
movement to the elevator; this corresponds with the control column
forward and the elevator down. The result is a rapid angular velocity
which raises the tail and reduces the angle of incidence; the aeroplane

dives and gains speed. After the damping of the oscillation is complete, the aeroplane has no angular velocity, a reduced angle of incidence, an increased speed and a downward path. The final motion was indicated by the simpler methods of Chapter II., but the present result shows exactly how the new state is reached.

DISTURBANCES OF LATERAL MOTION

The arguments followed are those already dealt with, and much of the detail will therefore be omitted. If the disturbances be

$$v = ae^{\lambda t} \qquad p = be^{\lambda t} \qquad r = ce^{\lambda t} \quad . \quad . \quad . \quad . \quad (191)$$

the values of a, b and c are given by the relations

$$\frac{a}{\begin{vmatrix} L_p - \lambda A & L_r \\ N_p & N_r - \lambda C \end{vmatrix}} = \frac{b}{\begin{vmatrix} L_r & L_v \\ N_r - \lambda C & N_v \end{vmatrix}} = \frac{c}{\begin{vmatrix} L_v & L_p - \lambda A \\ N_v & N_p \end{vmatrix}} \quad (192)$$

where principal axes of inertia have been chosen so that E is zero. If λ be real, the values of b/a and c/a are obtained from (192), whilst if complex, the procedure is that followed in connection with longitudinal stability.

The expressions for v, p and r for complex roots and therefore for oscillations, will be given somewhat different form, but are essentially similar to those given in (169).

$$\left. \begin{array}{l} v = \alpha e^{ht} \cos (kt + \beta) \\[2mm] p = \dfrac{\alpha}{\mu_2{}^2 + \nu_2{}^2} e^{ht} \{ (\mu_1 \mu_2 + \nu_1 \nu_2) \cos (kt + \beta) + (\mu_1 \nu_2 - \mu_2 \nu_1) \sin (kt + \beta) \} \\[2mm] r = \dfrac{\alpha}{\mu_3{}^2 + \nu_3{}^2} e^{ht} \{ (\mu_1 \mu_3 + \nu_1 \nu_3) \cos (kt + \beta) + (\mu_1 \nu_3 - \mu_3 \nu_1) \sin (kt + \beta) \} \end{array} \right\} \quad (193)$$

Values of ϕ and ψ as required are determined from the relations

$$\left. \begin{array}{l} \dot{\phi} = p + r \tan \theta_0 \\ \dot{\psi} = r \sec \theta_0 \end{array} \right\} \quad . \quad . \quad . \quad . \quad . \quad (194)$$

The values of μ_1, μ_2, etc., are given below as—

$$\left. \begin{array}{l} \dfrac{\mu_1}{\sqrt{\mu_1{}^2 + \nu_1{}^2}} = \begin{vmatrix} L_p - hA & L_r \\ N_p & N_r - C \end{vmatrix} - k^2 AC \\[3mm] \dfrac{\nu_1}{\sqrt{\mu_1{}^2 + \nu_1{}^2}} = -k \left\{ \begin{vmatrix} L_p - hA & 0 \\ N_p & -C \end{vmatrix} - A(N_r - hC) \right\} \\[3mm] \dfrac{\mu_2}{\sqrt{\mu_2{}^2 + \nu_2{}^2}} = \begin{vmatrix} L_r & L_v \\ N_r - hC & N_v \end{vmatrix}, \quad \dfrac{\nu_2}{\sqrt{\mu_2{}^2 + \nu_2{}^2}} = -kCL_v \\[3mm] \dfrac{\mu_3}{\sqrt{\mu_3{}^2 + \nu_3{}^2}} = \begin{vmatrix} L_v & L_p - hA \\ N_v & N_p \end{vmatrix}, \quad \dfrac{\nu_3}{\sqrt{\mu_3{}^2 + \nu_3{}^2}} = -kAN_v \end{array} \right\} \quad (195)$$

Example.—The derivatives assumed to apply in a particular case are :

$$Y_v = -0.25 \qquad \frac{1}{A}L_v = -0.0332 \qquad \frac{1}{C}N_v = 0.0154$$

$$Y_p = 1 \qquad \frac{1}{A}L_p = -8.0 \qquad \frac{1}{C}N_p = 0.80$$

$$Y_r = -3 \qquad \frac{1}{A}L_r = 2.60 \qquad \frac{1}{C}N_r = -1.06 \qquad \Bigg\} \quad (196)$$

$$n_1 = 0 \qquad n_2 = 0 \qquad n_3 = 1 \qquad w_0 = 0 \qquad u_0 = 80$$

The solution of the biquadratic for stability gives to λ the values

$$\lambda_1 = 0.0157 \qquad \lambda_2 = -8.26 \qquad \lambda_3 \text{ and } \lambda_4 = -0.526 \pm 0.984i$$

The first value of λ is positive, and the aeroplane is therefore unstable.
For $\lambda_1 = 0.0157$ equations (192) give

$$b/a = 0.00069 \qquad c/a = -0.0149 \quad \Bigg\}$$

whilst for $\lambda_2 = -8.26$

$$b/a = -2.24 \qquad c/a = -0.246 \quad \Bigg\} \qquad (197)$$

For the complex roots λ_3 and λ_4

$$\mu_1 = 0.0000170 \qquad \nu_1 = -0.000144 \quad \Bigg\}$$
$$\mu_2 = 0.0164 \qquad \nu_2 = 0.0238 \qquad \Bigg\} \qquad (198)$$
$$\mu_3 = 0.0125 \qquad \nu_3 = -0.00213 \quad \Bigg\}$$

Using expressions corresponding with those for longitudinal disturbances,

$$v = e^{-0.526t}(A \cos 0.984t + B \sin 0.984t) + Ce^{0.0157t} + De^{-8.26t}$$

$$p = e^{-0.526t}\{(-0.00376A - 0.00332B) \cos 0.984t$$
$$+ (0.00332A - 0.00376B) \sin 0.984t\} + 0.00069Ce^{0.0157t} - 2.24De^{-8.26t}$$

$$r = e^{-0.526t}\{(0.00324A - 0.0110B) \cos 0.984t$$
$$+ (0.0110A + 0.00324B) \sin 0.984t\} + 0.0149Ce^{0.0157t} + 0.246De^{-8.26t}$$

$$\phi = \int p\,dt \text{ since } \theta_0 = 0$$
$$= e^{-0.526t}\{(-0.00338A - 0.00298B) \cos (0.984t - \gamma)$$
$$+ (0.00298A - 0.00338B) \sin (0.984t - \gamma) + 0.0440Ce^{0.0157t} + 0.271De^{-8.26t}$$

where
$$\cos \gamma = -0.472 \qquad \sin \gamma = 0.882 \quad . \quad . \quad . \quad . \quad . \quad (199)$$

Initial conditions.—Let v_1, p_1, r_1, and ϕ_1 be the values of v, p, r and ϕ when $t=0$,
then

$$v_1 = A + C + D$$
$$p_1 = -0.00376A - 0.00332B + 0.00069C - 2.24D$$
$$r_1 = 0.00324A - 0.0110B + 0.0149C + 0.246D \quad \Bigg\} \quad (200)$$
$$\phi_1 = -0.00103A + 0.00439B + 0.0440C + 0.271D$$

Illustrations of the four simple types of initial disturbance are given in Fig. 249. For
the first of these

$$v_1 = v \qquad p_1 = 0 \qquad r_1 = 0 \qquad \phi_1 = 0$$

and the values of A ... D are

$$A = 0.992v_1$$
$$B = 0.258v_1 \quad \Bigg\}$$
$$C = 0.0104v_1 \qquad . \quad . \quad . \quad . \quad . \quad . \quad (201)$$
$$D = -0.00205v_1$$

The analytical expressions for the disturbance can be obtained by using these values
in equations (199).

Effect of the Movement of a Control.—If ϑ and η be used to denote the
angles through which the ailerons and rudder are moved and these angles
be restricted to be small quantities for which the moments and forces are
proportional to the angle of aileron and rudder, the effect on the motion

can be represented by derivatives X_{ϑ}, X_n, etc., and the equations of small oscillations applied. Following the same procedure as for elevators and thrust shows that the equivalent elementary disturbances are—

$$
\begin{vmatrix}
-\phi_1 g \cos \theta_0 & & \\
Y_v & Y_r - Y_p \tan \theta_0 - u_0 & \vartheta Y_\vartheta + \eta Y_n \\
L_v & L_r - L_p \tan \theta_0 & \vartheta L_\vartheta + \eta L_n \\
N_v & N_r - N_p \tan \theta_0 & \vartheta N_\vartheta + \eta N_n
\end{vmatrix}
=
\begin{vmatrix}
v_1 & & \\
L_r - L_p \tan \theta_0 & \vartheta L_\vartheta + \eta L_n \\
N_r - N_p \tan \theta_0 & \vartheta N_\vartheta + \eta N_n
\end{vmatrix}
$$

$$
=
\begin{vmatrix}
-r_1 & \\
L_v & \vartheta L_\vartheta + \eta L_n \\
N_v & \vartheta N_\vartheta + \eta N_n
\end{vmatrix}
=
\begin{vmatrix}
1 & \\
L_v & L_r - L_\vartheta \tan \theta_0 \\
N_v & N_r - N_\vartheta \tan \theta_0
\end{vmatrix} \quad . \quad (202)
$$

The denominator of the last of these expressions is equal to $D_2/g \cos \theta_0$, where D_2 is the coefficient independent of λ in the biquadratic equation for lateral stability. Sensitivity of control is then seen to be greatest when the aeroplane is just not spirally unstable.

Example : Use of rudder only.—The additional quantities required are dependent on the area of the rudder, but it may be taken that

$$Y_n = -0.06 N_n \quad \text{and that} \quad L_n = 0 \quad . \quad . \quad . \quad . \quad (203)$$

in which case the curves can be drawn to an arbitrary ordinate as shown in Fig. 250 where ηN_n has been chosen to give v_n some arbitrary value.

If the conditions of turning require that there should not be any sideslipping, equations (202) show that

$$
\begin{vmatrix}
L_r - L_p \tan \theta_0 & \vartheta L_\vartheta + \eta L_n \\
N_r - N_p \tan \theta_0 & \vartheta N_\vartheta + \eta N_n
\end{vmatrix} = 0 \quad . \quad . \quad . \quad . \quad (204)
$$

must be satisfied, and this cannot be the case for rudder only unless

$$\frac{L_n}{L_r - L_p \tan \theta_0} = \frac{N_n}{N_r - N_p \tan \theta_0} \quad . \quad . \quad . \quad . \quad (205)$$

This condition varies with the inclination of the axis of X to the horizontal. The ratios depend on the design of the aeroplane, and it would not appear to be possible to approximate to the condition of turning without sideslipping by the use of the rudder only, since L_n is always very small. In general the effect of turning without sideslipping is produced by using the ailerons in conjunction with the rudder, and the practical possibilities are known to cover the requirements of lateral balance.

Description of Figs. 249 and 250 illustrating the Results of the Calculations of Lateral Disturbances

Lateral Gust.—Fig. 249 (a) shows that the preliminary adjustments to new conditions occur very rapidly. A positive value of v corresponds with sideslipping to the right or a gust from the right. The gust starts a turn to the right temporarily with the wrong bank, but after about 3 secs. this is corrected. At the end of 10 secs. the conditions are those for a right-hand turn with sideslipping inwards, and due to instability the turn gets more rapid. It has been seen from the treatment of the stability of circling flight that this type of instability ultimately disappears and a steady turn results. Here is one of the known limitations to the application of the theory of small oscillations.
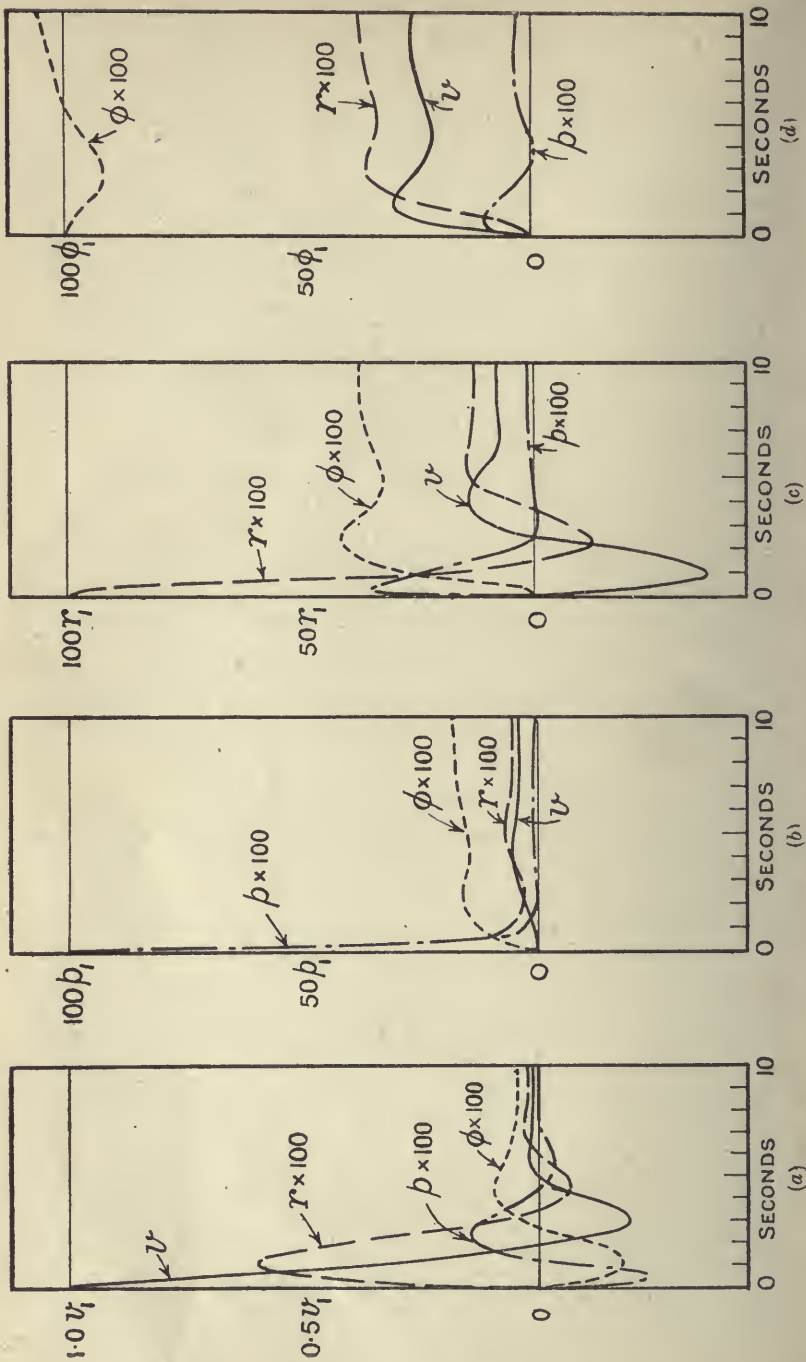
Fig. 249.—The effect of simple lateral disturbances. (Aeroplane unstable.)

Rolling due to Up-gust striking the Left Wing.—The rolling is stopped with great rapidity (Fig. 249 (b)), and leaves the aeroplane with a small bank; sideslipping then occurs, and the aeroplane finishes with a spiral turn as for a lateral gust.

Yawing due to a Gust which strikes the Tail from the Right.—The effect of turning is to increase the velocity of the left wing and increase its lift, causing a bank for a right-hand turn. The bank reaches its maximum in about 2 secs. Under the action of centrifugal forces the aeroplane begins to sideslip to the left, and until the bank is sufficient to reverse this effect the changes are rapid. The aeroplane reaches an unstable turn of appreciable magnitude.

Effect of a Sudden Bank.—The preliminary rapid movements are towards the final spiral turn of large magnitude; the aeroplane with its left wing up, begins to sideslip inwards and to turn to the right.
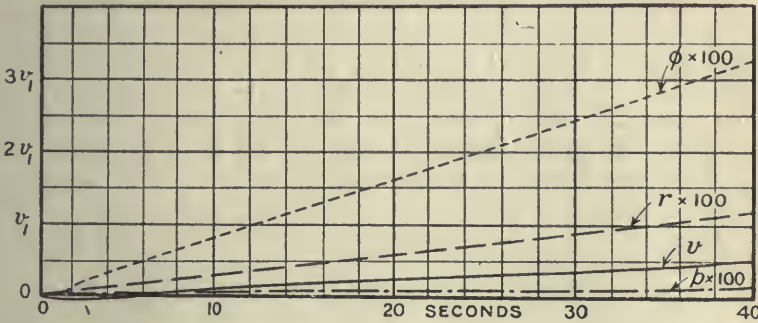
Fig. 250.—Disturbance due to the movement of a rudder. (Aeroplane unstable.)

In all cases the only important disturbances existing at the end of 10 secs. are those of the unstable spiral turn.

The Effect of a Movement of the Rudder is seen from Fig. 250 to be the initiation of a spiral turn, and the control of such an aeroplane involves the pilot as an essential feature. The ordinate of the curves is arbitrary, but is proportional to the movement of the rudder.

The Mathematical Theory of Disturbed Motion and Control when the Disturbing Causes are Variable with Time

The general theory of the solution of differential equations of the type met with in problems of the stability of small oscillations shows that the effects of two simple disturbances coexist as though independent of each other. It is therefore permissible to regard the new problem as a search for a method of adding a number of elementary disturbances due to gusts or to movements of the controls which may occur at any time.

For any aeroplane subject to disturbance it has already been shown that the motion can be expressed in a number of terms of the type

$$u = Ae^{\lambda_1 t} + Be^{\lambda_2 t} + Ce^{\lambda_3 t} + De^{\lambda_4 t} \quad . \quad . \quad . \quad (206)$$

2 M

where u has its usual meaning of change of velocity along the axis of X. The coefficients A, B, C and D are, in general, linear functions of the disturbing causes. If, for instance, a horizontal gust of velocity u_1 is encountered, A, B, etc., are all proportional to u_1. It is convenient to have a shortened notation for (206) and it is proposed to denote it by

$$u = u_1 (uu)_t. \quad . \quad . \quad . \quad . \quad . \quad (207)$$

Similarly an expression

$$w = u_1 (uw)_t \quad . \quad . \quad . \quad . \quad . \quad (208)$$

is written for the effect of a horizontal gust of magnitude u_1 at $t=0$ on the normal velocity w. Similar expressions follow for q and θ.

$(uu)_t$, $(uw)_t$, $(uq)_t$ and $(u\theta)_t$ are all definite functions of t for a given aeroplane, and examples have been given in Fig. 247 (a).

It is now necessary to define a second time τ and to explain its relation to t. The expressions $(uu)_t$, etc., give the magnitude of a disturbance t secs. after the disturbing cause operated. It will be evident that in a succession of gusts the final disturbance at time t will be the sum of the effects of disturbing causes at all previous times, and τ is used to distinguish the time at which the disturbance occurred. The expression $(uu)_{t-\tau}$ represents the disturbance factor at time t from a disturbance at τ, the magnitude of which can be represented by the element $f'(\tau) . d\tau$. By means of this definition it will be seen that $f(\tau)$ represents a continuous disturbing cause over any range of time whatever, and that the residual disturbance in u is

$$u = \int_0^t (uu)_{t-\tau} f'(\tau) d\tau \quad . \quad . \quad . \quad . \quad (209)$$

$f(t)$ may be a record of horizontal velocity as obtained from an anemometer, and in that case the differentiation to find $f'(t)$ becomes laborious. The necessity for the operation may be avoided by a partial integration which leads to

$$u = -(uu)_t f(0) + (uu)_0 f(t) - \int_0^t \frac{\partial}{\partial \tau} (uu)_{t-\tau} f(\tau) d\tau . \quad . \quad (210)$$

The differentiation of the known algebraic expression $(uu)_{t-\tau}$ presents no serious difficulty, and this latter form is in many ways preferable to the former.

In the case of w, q and θ the integrals at the limits are zero for a horizontal gust, whilst for u the quantity $(uu)_0 = 1$ and $f(o)$ is zero if continuity in u is assumed as an initial condition. In the latter case, as $f(t)$ is the change in velocity of the wind over the ground at time t and u is the change of velocity of the aeroplane relative to the air in the same interval of time, it can be seen that

$$- \int_0^t \frac{\partial}{\partial \tau} (uu)_{t-\tau} f(\tau) d\tau \quad . \quad . \quad . \quad . \quad (211)$$

is the change of the velocity of the aeroplane relative to the ground.

The evaluation of (211) is easily carried out graphically, and one method of arranging the work is shown in Fig. 251. The full curve of the upper
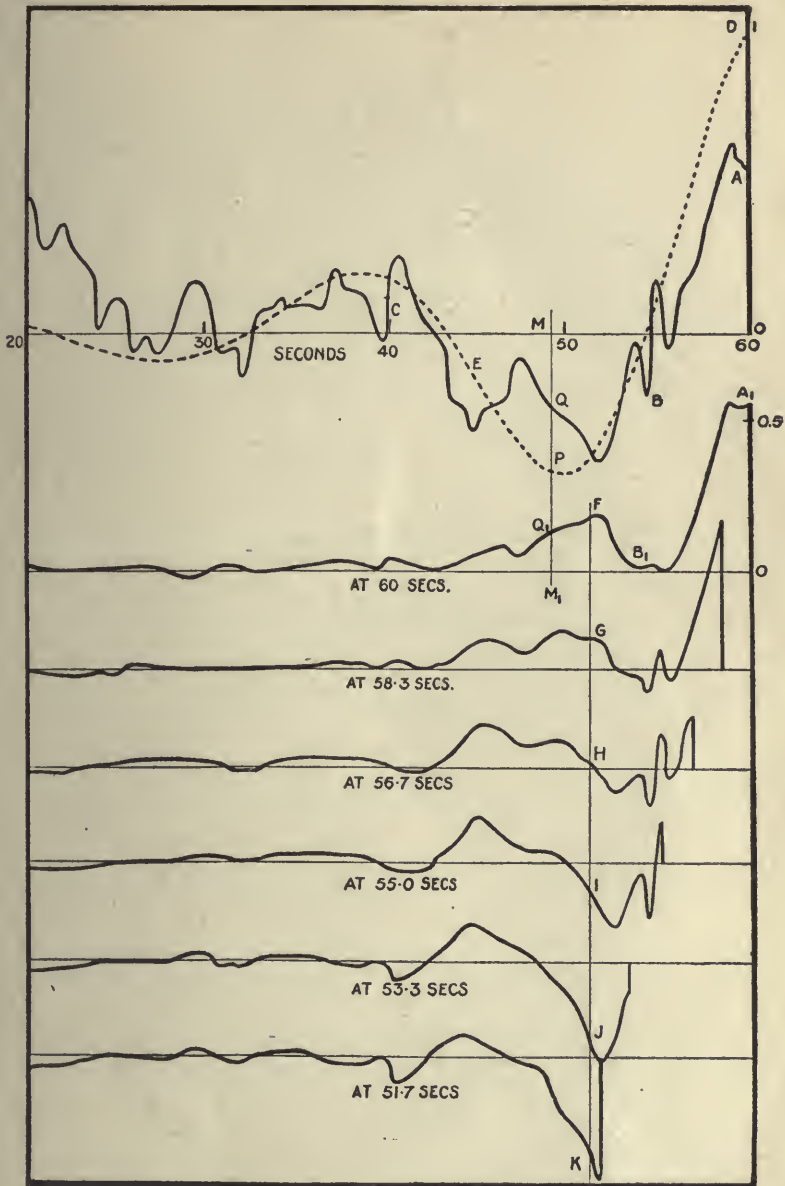
FIG. 251.—Disturbances due to a natural wind. (Aeroplane stable.)

diagram being taken to represent an anemometer record,* shows wind

velocity as ordinate on a time base and covers a period of about 40 secs. The dotted curve represents $\frac{\partial}{\partial \tau}(uu)_{t-\tau}$, except that the scale of τ has been reversed for convenience. When $t = 49$ secs., *i.e.* at M, Fig. 251, the value of $f(\tau)$ is MQ, whilst the value of $\frac{\partial}{\partial \tau}(uu)_{t-\tau}$ is MP owing to the special arrangement. The product of MQ and MP then represents an element of the integral of (211), and is plotted as $Q_1 M_1$ in the figure below. Points at other times similarly obtained complete the lower curve, the area of which represents the total disturbance " at 60 secs." due to passage through gusty air. Further curves are shown for other times to emphasize the fact that the effect of a gust depends markedly on the time which has elapsed since it was encountered. A large effective increase shown by F at 60 secs. becomes zero at 56·7 secs. at H, and has a considerable negative value at K at 51·7 secs. The total areas show somewhat similar characteristics.

A repetition of the calculations, using $(uw)_t$, $(uq)_t$ and $(u\theta)_t$ would lead to the determination of w, q and θ as functions of time. In effect (see footnote) * this has been done, and the more important items are shown in

open time scale, and was made at Kew Observatory, using a **Dines Recording Anemometer.** The part reproduced on a time base of 60 secs. occupied 240 secs. in the taking, the average wind speed being 20 ft.-s. Since no better information is available it has been assumed that the gusts met by an aeroplane travelling 80 ft. through the air are the same as those registered during the passage of 80 ft. of air over the observatory instrument.

* The dotted curve of Fig. 251 was not equal to $\frac{\partial}{\partial \tau}(uu)_{t-\tau}$, but to a portion only of it, since a saving of labour was thereby effected. It represents the value of

$$e^{-0·075t} \cos 0·283t \quad . \quad . \quad . \quad . \quad . \quad . \quad . \quad (212)$$

By a change of the time epoch to the point at which this dotted line cuts the axis of time, it is clear that the multiplying factor

$$ke^{-0·075t} \sin 0·283t$$

is simultaneously applied, k being a known constant equal to the value of $e^{-0·075}t$ at the expiration of a quarter of a period. Two curves representing

$$\int_0^t f(\tau)e^{-0·075(t-\tau)} \cos 0·283(t-\tau)a\tau$$

and

$$\int_0^{t·} f(\tau)e^{-0·075(t-\tau)} \sin 0·283(t-\tau)a\tau \quad . \quad . \quad . \quad . \quad . \quad (213)$$

were obtained as continuous functions of t in this way.

In addition calculations were made for the rapid oscillations, and it was found that to a sufficient degree of accuracy the integrals

$$\int_0^t f(\tau)e^{-5·62(t-\tau)(t-\tau)}d\tau$$

and

$$\int_0^t f(\tau)e^{-5·62(t-\tau)}(t-\tau)d\tau \quad . \quad . \quad . \quad . \quad . \quad . \quad (214)$$

were proportional to $f(\tau)$, the values being $0·177 f(\tau)$ and $0·0308 f(\tau)$ respectively. Physically this means that the motion of the aeroplane represented by (214) is so rapid that the disturbance is a comparatively exact counterpart of the gust.

The curves of disturbance in u, w, q and θ can be obtained from the above curves by addition in various proportions determined by the arbitrary constants A, B, C and D.

Fig. 252. One of the quantities estimated has been the variation of height above the ground, and involves the relations

$$\dot{h} = u_0\theta - w \left. \right\} \qquad \cdots \cdots \quad (215)$$
$$h = \int \dot{h}\,dt \left. \right\}$$

the form having a special character since in the steady motion the axis of X is along the direction of flight and is horizontal.

Description of Fig. 252.—The upper curve shows the wind record from 0 to 60 seconds. The aeroplane was supposed to have a flying speed of 80 ft.-s. in its steady state, and to have this velocity relative to the air at $t=0$. Its velocity over the ground was then 60 ft.-s., and the wind speed of 20 ft.-s. against the aeroplane's motion. The full curve marked " variation of air speed " was calculated at the points indicated, whilst the dotted curve shows the variation of ground speed. The difference between the curves shown by the shaded area is equal to the variation of the wind from 20 ft.-s., *i.e.* the ordinates are equal to those of the upper diagram. It will be noticed that the inertia of the aeroplane is great enough to average out all the more rapid changes of wind speed, and shows the advantage of speed of flight as a means of producing average steadiness. It will be seen that variations of speed of ± 12 ft.-s. are indicated, and these may be considered too large to come within the definition of small oscillations. Certain other approximations will have been noticed by a careful student which could be met by more rigorous treatment if desired. The advantages of the present methods are however thought to be sufficiently great to warrant their use.

The curve marked $u_0\theta$ represents the rate of climb due to inclination of the axis of X, whilst w shows the change of normal velocity. The ordinates of the shaded area then represent the total rate of climb $\dot{h}$. Integration with respect to t then leads to the last curve for " rise and fall." On the whole the aeroplane gains height, the maximum gain being 40 feet ; in one place a fall below the original level of about 15 feet is shown. It is possible that the aeroplane shown would just be able to land itself, as the vertical downward velocity due to the gusts is not more than 5 ft.-s.

THE EFFECTS OF CONTINUOUS USE OF CONTROLS, AND THE CALCULATION OF THE MOVEMENTS NECESSARY TO COUNTER THE EFFECTS OF A GUST

The first problem to be attacked will be the finding of an elevator movement of a continuous character which will eliminate the effects of an isolated gust. By a method analogous to that following in adding the effects of gusts it is clearly possible to calculate the motion of an aeroplane which results from a prescribed motion of the elevator. The problem now considered is the converse of this, since it is proposed to find the elevator movement which corresponds with a prescribed aeroplane motion.

It has been seen in the discussion of disturbed motion that changes in u, w, q and θ which arise from isolated disturbing causes in any of the
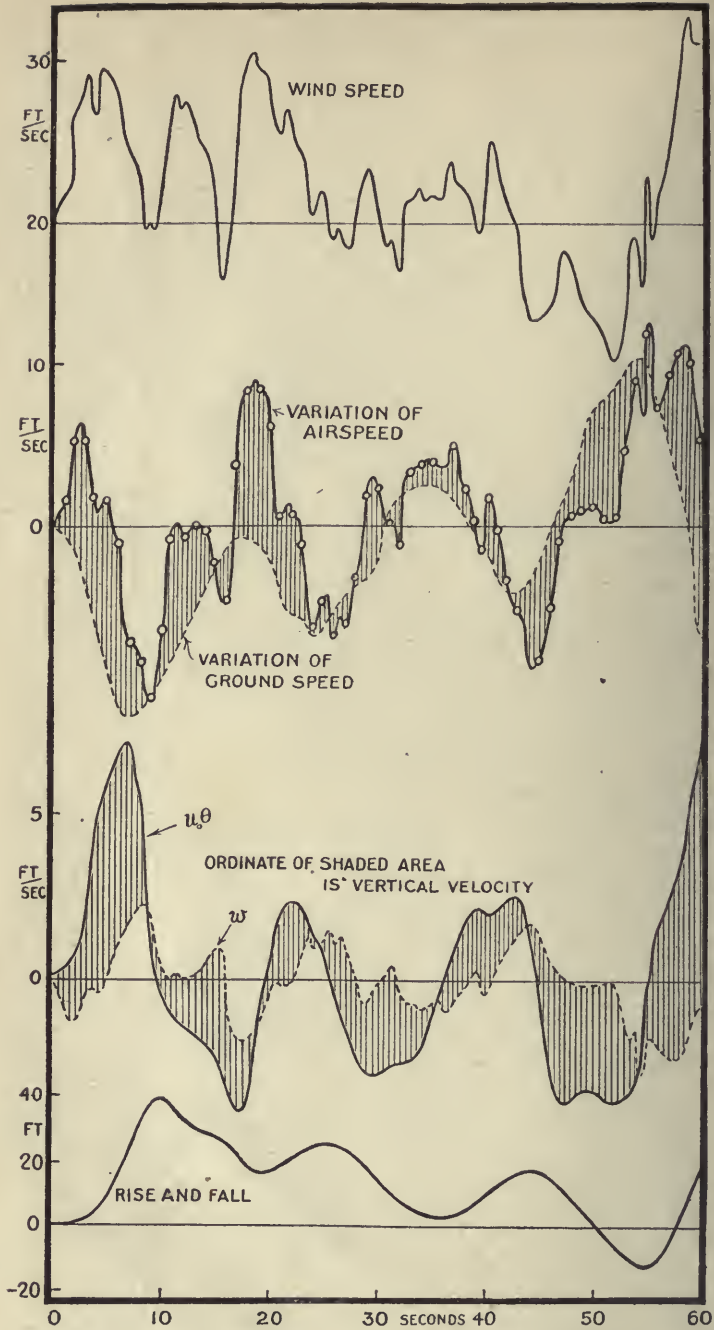
Fig. 252.—Uncontrolled flight in a natural wind. (Aeroplane stable.)

quantities have a common analytical form with four or sometimes five constants peculiar to the disturbance considered. The same analytical form applies to disturbances of v, p, r and ϕ, and the disturbances produced by the controls. The general problem can therefore be approached by the consideration of any quantity Ξ defined by

$$\Xi = Ae^{\lambda_1 t} + Be^{\lambda_2 t} + Ce^{\lambda_3 t} + De^{\lambda_4 t} + E \quad . \quad . \quad . \quad (216)$$

where Ξ may be u, v, w, p, q, r, θ or ϕ, and suffixes such as μ, ν, ς and η may be used in addition to $u \ldots \phi$ to signify the initial disturbing cause. As an example Ξ_μ would be a disturbance due to change of elevator position, whilst Ξ_u would be a disturbance due to a gust in the direction of the axis of X.

It is now proposed to show that any disturbance such as Ξ can be eliminated (practically if not theoretically) by the use of controls. Stability is a means of reduction of a disturbance to zero, but needs time for its operation. Whereas a phugoid oscillation may take one or two minutes for extinction by inherent stability, the use of the controls can reduce the time required to a few seconds.

In order to assist the explanation of the method it will be supposed, in the first instance, that Ξ is the vertical velocity of an aeroplane, and is produced by the addition of elementary disturbances Ξ_μ occurring at different times from the progressive movement of the elevator. The disturbance of vertical velocity due to a horizontal gust at time $t=0$ is Ξ_u, and it is desired to make the continuous use of the elevator eliminate Ξ_u. Ξ is of course equal to $(u_0\theta - w)$ by the definition of vertical velocity.

By the theorem in addition developed in connection with a variable wind it will be found that the resultant vertical velocity due to the elevator, i.e. Ξ, is made up from its parts by the integral.

$$\Xi_{\text{(continuous use of elevator)}} = \int_0^t F'(\tau)(\Xi_\mu)_{t-\tau}d\tau \quad . \quad . \quad . \quad . \quad . \quad (217)$$

where $F(t)$ is the angular position of the elevator at time t.

By a proper choice of $F(t)$, Ξ can be made to have almost any desirable form. It is convenient to integrate by parts to avoid infinite differential coefficients due to a sudden change of elevator position, and the expression becomes

$$\Xi_{\text{(continuous use of elevator)}} = \left\{ F(\tau)(\Xi_\mu)_{t-} \right\}_0^t - \int_0^t F(\tau)\frac{\partial}{\tau\partial}(\Xi_\mu)_{t-\tau}d\tau \quad . \quad (218)$$

If before the elevator is put over the aeroplane is flying steadily, the value of $(\Xi_\mu)_0$ is zero since there is no immediate change in u, w, q or θ by reason of the putting over of the control. Also if movements of the elevator are measured from the position in the steady motion, $F(o)$ is zero, and the partial integration leads to

$$\Xi_{\text{(continuous use of elevator)}} = -\int_0^t F(\tau)\frac{\partial}{\partial\tau}(\Xi_\mu)_{t-\tau}d\tau \quad . \quad . \quad . \quad . \quad (219)$$

If the rate of change of the particular disturbance due to putting over the elevator is zero when $t = 0$, then the rate of change of Ξ must also be zero. In any practical case the rate of change may be small, and it is then necessary to determine some limit to the elevator movement which is permitted. This imposes some slight limitation to the values of Ξ which can be produced.

If, due to a horizontal gust, a disturbance Ξ_u has been given, the final motion is

$$\Xi \text{ (continuous use of elevator and isolated horizontal gust)} = \Xi_u - \int_0^t \mathrm{F}(\tau)\frac{\partial}{\partial\tau}(\Xi_\mu)_{t-\tau}d\tau \quad . \quad . \quad . \quad (220)$$

and the condition of no residual motion is clearly that the right-hand side (220) shall be zero.

Solution of Equation (220).—A solution of this equation can always be found by a process of trial and error, even when limitations are given to the motions of the controls. In some cases an analytical expression can be found, for an examination of (220) when $\Xi = 0$ and Ξ_u and Ξ_μ have the form of (216) shows that $\mathrm{F}(t)$ must be a sum of exponential terms of the type—

$$\mathrm{F}(t) = \mathrm{A}_1 e^{\mathrm{K}_1 t} + \mathrm{B}_1 e^{\mathrm{K}_2 t} + \mathrm{C}_1 e^{\mathrm{K}_3 t} + \mathrm{D}_1 \quad . \quad . \quad . \quad (221)$$

Assuming the result it will be shown that the expression is correct, and that $\mathrm{A}_1 \ldots \mathrm{D}_1$ and K_1, K_2 and K_3 can be determined.

Writing down the expressions for Ξ_μ and Ξ_u in accordance with (216) gives—

$$\frac{\partial}{\partial t}\Xi_\mu = \mathrm{A}_2 e^{\lambda_1 t} + \mathrm{B}_2 e^{\lambda_2 t} + \mathrm{C}_2 e^{\lambda_3 t} + \mathrm{D}_2 e^{\lambda_4 t}. \quad . \quad . \quad (222)$$

for the rate of change of vertical velocity at time t due to an elevator moment at time 0, and

$$\Xi_u = \mathrm{A}_3 e^{\lambda_1 t} + \mathrm{B}_3 e^{\lambda_2 t} + \mathrm{C}_3 e^{\lambda_3 t} + \mathrm{D}_3 e^{\lambda_4 t} + \mathrm{E}_3 \quad . \quad . \quad (223)$$

for the vertical velocity at time t due to a horizontal gust at time $t=0$ (actually E_3 is zero in the case supposed, but would have had a value if the disturbance had been due to a change in engine speed).

The terms of equation (220) are now specified, and the integration presents little difficulty. The result is to obtain

$$\mathrm{A}_3 e^{\lambda_1 t} + \mathrm{B}_3 e^{\lambda_2 t} + \mathrm{C}_3 e^{\lambda_3 t} + \mathrm{D}_3 e^{\lambda_4 t} + \mathrm{E}_3$$
$$= \mathrm{A}_2 e^{\lambda_1 t}\left(\frac{\mathrm{D}_1}{\lambda_1} - \frac{\mathrm{A}_1}{\mathrm{K}_1 - \lambda_1} - \frac{\mathrm{B}_1}{\mathrm{K}_2 - \lambda_1} - \frac{\mathrm{C}_1}{\mathrm{K}_3 - \lambda_1}\right) - \frac{\mathrm{A}_2 \mathrm{D}_1}{\lambda_1} + \frac{\mathrm{A}_2 \mathrm{A}_1}{\mathrm{K}_1 - \lambda_1}e^{\mathrm{K}_1 t} + \frac{\mathrm{A}_2 \mathrm{B}_1}{\mathrm{K}_2 - \lambda_1}e^{\mathrm{K}_2 t} + \frac{\mathrm{A}_2 \mathrm{C}_1}{\mathrm{K}_3 - \lambda_1}e^{\mathrm{K}_3 t}$$
$$+ \mathrm{B}_2 e^{\lambda_2 t}\left(\frac{\mathrm{D}_1}{\lambda_2} - \frac{\mathrm{A}_1}{\mathrm{K}_1 - \lambda_2} - \frac{\mathrm{B}_1}{\mathrm{K}_2 - \lambda_2} - \frac{\mathrm{C}_1}{\mathrm{K}_3 - \lambda_2}\right) - \frac{\mathrm{B}_2 \mathrm{D}_1}{\lambda_2} + \frac{\mathrm{B}_2 \mathrm{A}_1}{\mathrm{K}_1 - \lambda_2}e^{\mathrm{K}_1 t} + \ldots$$
$$+ \quad . \quad . \quad . \quad . \quad . \quad . \quad . \quad . \quad . \quad . \quad . \quad . \quad . \quad . \quad (224)$$

as an identical relation. The coefficient of $e^{\mathrm{K}_1 t}$ in the identity gives the equation

$$0 = \frac{\mathrm{A}_2}{\mathrm{K}_1 - \lambda_1} + \frac{\mathrm{B}_2}{\mathrm{K}_1 - \lambda_2} + \frac{\mathrm{C}_2}{\mathrm{K}_1 - \lambda_3} + \frac{\mathrm{D}_2}{\mathrm{K}_1 - \lambda_4} \quad . \quad . \quad (225)$$

and two similar expressions follow for K_2 and K_3. It will then be seen that K_1, K_2 and K_3 are determined by the solutions of the cubic equation in K—

$$0 = \frac{A_2}{K - \lambda_1} + \frac{B_2}{K - \lambda_2} + \frac{C_2}{K - \lambda_3} + \frac{D_2}{K - \lambda_4} \quad . \quad . \quad . \quad (226)$$

Equating the coefficients of $e^{\lambda_1 t}$, $e^{\lambda_2 t}$ . . . (224) gives

$$A_3 = A_2 \Big(\frac{D_1}{\lambda_1} - \frac{A_1}{K_1 - \lambda_1} - \frac{B_1}{K_2 - \lambda_1} - \frac{C_1}{K_3 - \lambda_1} \Big)$$

$$B_3 = B_2 \Big(\frac{D_1}{\lambda_2} - \frac{A_1}{K_1 - \lambda_2} - \frac{B_1}{K_2 - \lambda_2} - \frac{C_1}{K_3 - \lambda_2} \Big)$$

. . . .

$$E_3 = -D_1 \Big(\frac{A_2}{\lambda_1} + \frac{B_2}{\lambda_2} + \frac{C_2}{\lambda_3} + \frac{D_2}{\lambda_4} \Big) \quad . \quad . \quad . \quad . \quad . \quad (227)$$

or apparently five equations from which to determine the four quantities A_1, B_1, C_1 and D_1. Adding the equations together, however, it will be seen that there is obtained the expression

$$A_3 + B_3 + C_3 + D_3 + E_3 = 0 \quad . \quad . \quad . \quad . \quad (228)$$

and this is often intrinsically satisfied. In that case $A_1 \ldots D_1$ can be determined. If E_3 be zero then D_1 is zero, and the addition of the equations still requires that

$$A_3 + B_3 + C_3 + D_3 = 0 \quad . \quad . \quad . \quad . \quad (229)$$

if a solution is to be possible.

The values of K_1, K_2, and K_3 must all be negative if the aeroplane is to be permanently controllable, otherwise the elevator angle will increase to the permissible limit and failure will then occur.

Some physical ideas illustrate the value of the restrictions (228) and (229). It is, for example, not possible to eliminate all the effects of a head-on gust of initial amplitude u_1, for E is then zero and the value of $A + B + C + D$ is unity. It is clear that nothing short of an infinite force could neutralise the assumed instantaneous increase in u_1. The same objection does not apply to w, q and θ, but for the former of these it is readily seen that the amplitude of the elevator movement would be prohibitive in the initial stages. The operation attempted would be that of producing a change of down load on the tail equal to the change of up load on the wings. $\dot{q}$ and q are both zero as a result of the gust, whilst $\dot{q}$ may be given a large value by use of the elevator. Either q or θ is therefore a suitable quantity for complete elimination by the use of the elevator. In relation to the figures previously given for an elevator it appears that a solution which leads to the elimination of θ is

$$K_1 = 0 \qquad K_2 = -0 \cdot 192 \qquad K_3 = -2 \cdot 62$$
$$A_1 = -B_1 \quad C_1 = 0 \qquad D_1 = 0 \qquad \Big\} \quad . \quad . \quad (230)$$

so that the elevator starts from its zero position at time t and returns there when t is great. The condition $K_1 = 0$ introduces some little difficulty in

interpretation and appears to involve the condition $A_1 = -B_1$ as a fundamental consequence, so that in the case for which $A_2 + B_2 + C_2 + D_2 = 0$, it is probable that a further identical relation holds.

Approximate Solution of Equation (220).—The necessity for dealing with partial elimination leads to a substitution of a graphical method for the exact analytical expressions just given. The process of finding
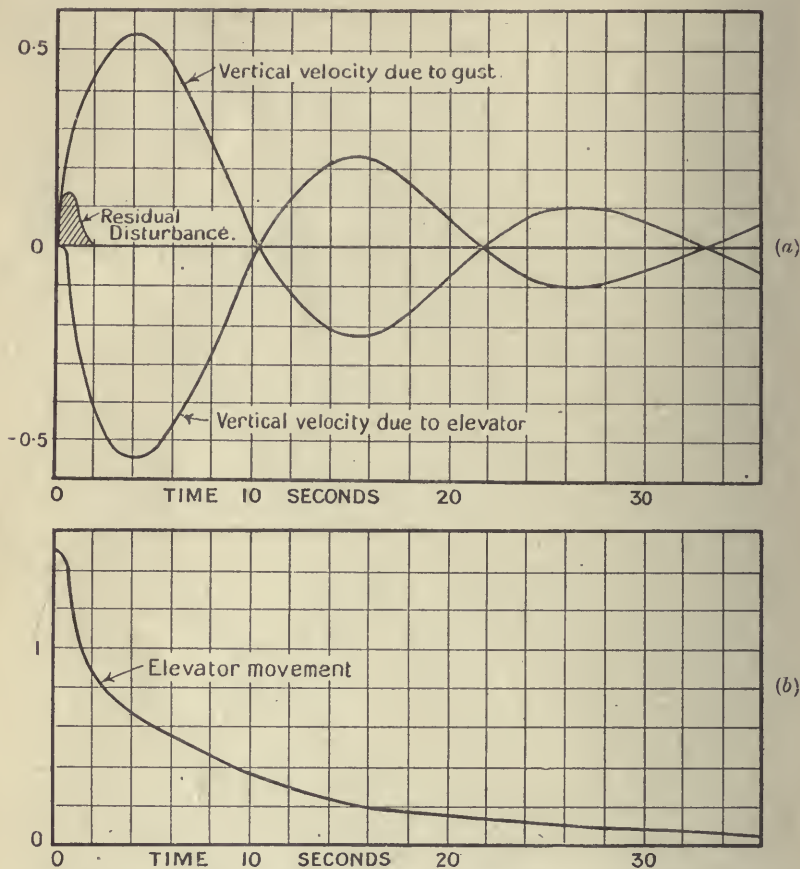
FIG. 253.—Use of the elevator to eliminate a disturbance.   (Aeroplane stable.)

the elevator movement is one of trial and error, but presents no serious difficulties. It has already been pointed out that equation (217) provides the means of calculating the disturbance due to an elevator when its movement is known ; the process of trial and error assumes a curve for a short time, beginning at some arbitrary limit (1·5 in Fig. 253 (b)) and this suffices for a calculation of the motion. The result is compared with the motion it is desired to repeat and corrected accordingly. If small steps of time are taken at the beginning, the calculation will be well established and can proceed more rapidly in the later stages. The resulting movement

is shown in Fig. 253 (b), the scale being arbitrary and proportional to the elevator angle. The vertical velocity corresponding with this elevator movement is shown in Fig. 253 (a), together with the vertical velocity which would result from a horizontal gust in the absence of control. The two curves are seen to be almost exact mirror images about the line of zero ordinates, and the small residual disturbance when the two are combined is due to the limitation placed on the initial angle of the elevator. The ordinates of the curves are proportional to the strength of the gust in one case and to the angle of the elevator in the other. The actual values of u_1 and μ_1 are of little present interest.

Examination of the Residual Disturbances in u, w, q and θ when Equation (220) has been satisfied for Vertical Velocity

It has been seen that the elevator can be used so as to make $(u_0\theta - w)$ very small in the case of meeting a horizontal gust. It is necessary to consider what is the effect of the same elevator movement on the flight speed and angle of path. An equation similar to (217) shows that all the motions are fully determined, and it will appear that they are of reduced magnitude. The general investigation leads to apparently complex expressions, but it is hoped that an illustration will make it clear that the residual errors in u, w and q can be obtained with little difficulty. Some of the equations previously used will be collected here in the form most suitable for the present purpose.

It has been shown previously that all possible disturbances of the motion of an aeroplane can be expressed by exponential and trigonometrical functions, rigidly so in the case of small oscillations, and very nearly so for the real motion of an aeroplane in approximately rectilinear flight. The following particular forms are equivalent to those given on p. 519 :—

$$u = ae^{ht}\cos(kt+\beta) + (\gamma+\delta t)e^{\lambda_1 t} + \zeta_1 \quad . \quad . \quad . \quad . \quad (231)$$

$$w = \frac{a}{\mu_2{}^2+\nu_2{}^2}e^{ht}\{(\mu_1\mu_2+\nu_1\nu_2)\cos(kt+\beta)$$
$$+ (\mu_1\nu_2-\mu_2\nu_1)\sin(kt+\beta)\}$$
$$+ \eta_1(\gamma+\delta t)e^{\lambda_1 t} + \xi_1\delta e^{\lambda_1 t} + \zeta_2 \quad . \quad . \quad . \quad (232)$$

$$q = \frac{a}{\mu_3{}^2+\nu_3{}^2}e^{ht}\{(\mu_1\mu_3+\nu_1\nu_3)\cos(kt+\beta)$$
$$+ (\mu_1\nu_3-\mu_3\nu_1)\sin(kt+\beta)\}$$
$$+ \eta_2(\gamma+\delta t)e^{\lambda_1 t} + \xi_2\delta e^{\lambda_1 t} + \zeta_3 \quad . \quad . \quad . \quad (233)$$

$$\theta = \int q\, dt = \frac{\alpha}{\mu_4{}^2+\nu_4{}^2}e^{ht}\{(\mu_1\mu_4+\nu_1\nu_4)\cos(kt+\beta)$$
$$+ (\mu_1\nu_4-\mu_4\nu_1)\sin(kt+\beta)\}$$
$$+ \eta_3(\gamma+\delta t)e^{\lambda_1 t} + \xi_3\delta e^{\lambda_1 t} + \zeta_4 \quad . \quad . \quad . \quad (234)$$

In these expressions the arbitrary constants are α, β, γ and δ, whilst $\mu_1, \mu_2. \ldots \nu_1, \nu_2, \ldots \eta_1, \eta_2$, etc., are known from equations (165) $\ldots$ (167).

If the disturbance contemplated (at present all disturbances are considered as isolated and sustained) is a change in the wind, then ζ_1, ζ_2, ζ_3 and ζ_4 are all zero, and the aeroplane ultimately settles down to the same steady motion relative to the new wind. If the disturbance is due to an internal cause, such as a movement of the elevator, we have $u=0$, $w=0$, $q=0$, $\theta=0$, when $t=0$. The values of α, β, γ and δ are found as indicated in equations (180), and finally, to satisfy the initial conditions just given,

$$\zeta_1 = -(\alpha \cos \beta + \gamma)$$
$$\zeta_2 = -\left(\alpha\frac{\mu_1\mu_2 + \nu_1\nu_2}{\mu_2^2 + \nu_2^2}\cos\beta + \alpha\frac{\mu_1\nu_2 - \mu_2\nu_1}{\mu_2^2 + \nu_2^2}\sin\beta + \eta_1\gamma + \xi_1\delta\right) \quad (235)$$

etc.

Unless rotations in the wind are assumed to occur ζ_3 will be zero.

It will be seen from equations (231) . . . (234) that the phase differences between the oscillations in u, w, q and θ are independent of the values of α and β, and no matter what the nature of the disturbance, the motions in u, w, q and θ will follow each other in the same order, with the same phase differences and the same relative amplitudes. This relation between the oscillations can be clearly seen from the curves of Fig. 247, since the other terms are vanishingly small at the end of 2 secs.

The terms in $e^{\lambda_1 t}$ can be divided into two parts, the relations between the disturbances in u, w, q, and θ for the parts being independent of γ and δ.

The relations between the oscillations just referred to will be found later to simplify the analysis of motions due to an elevator. It is clear that to an exceedingly high degree of approximation, all simple disturbances rapidly tend to become similar damped oscillations of phugoid type, and it appears that only the dissimilar portions, limited to a time of about 5 secs. in the worst case, need special treatment in passing from variation of vertical velocity say, to that of variation of flight speed, etc.

The elevator movement $F(t)$ having been chosen so that there is no resultant vertical velocity, it is now desired to find the change of flight speed due to gust and elevator. The value is

$$u_u + \int_0^t F'(\tau)(u_\mu)_{t-\tau}\,d\tau \quad . \quad . \quad . \quad . \quad (236)$$

but for the general problem u_u will be replaced by Ξ'_u, where Ξ' is any linear combination of the variations u, w, q and θ.

From equations (231) . . . (234) the values of Ξ'_u and Ξ'_μ may clearly be expressed respectively as

$$\Xi'_u = a_1 e^{ht}\{a'\cos(kt+\beta_1) + b'\sin(kt+\beta_1)\} + \eta'_1(\gamma_1 + \delta_1 t)e^{\lambda_1 t} + \xi'_1\delta_1 e^{\lambda_1 t} \quad . \quad (237)$$

and $\quad \Xi'_\mu = a_2 e^{ht}\{a'\cos(kt+\beta_2) + b'\sin(kt+\beta_2)\} + \eta'_1(\gamma_2 + \delta_2 t)e^{\lambda_1 t} + \xi'_1\delta_2 e^{\lambda_1 t} + \zeta'_1 \quad . \quad (238)$

where $a_2 a' \cos\beta_2 + a_2 b'\sin\beta_2 + \eta'_1\gamma_2 + \xi_1\delta_2 + \zeta_1 = 0$

Ξ' differs from Ξ in being some different linear function of u, w, q

and θ; the values of α_1, β_1, γ_1 and δ_1 are therefore the same for both Ξ' and Ξ, but a, b, η, etc., have been changed to a', b', η', etc.

If
$$\frac{a'}{\sqrt{a'^2 + b'^2}} = \cos n', \quad \frac{b'}{\sqrt{a'^2 + b'^2}} = -\sin n' \quad \text{and} \quad \sqrt{\frac{\overline{a^2 + b^2}}{a'^2 + b'^2}} = m \quad (238a)$$

the value of Ξ'_μ becomes

$$\Xi'_\mu = \frac{a_2 m}{\sqrt{a^2 + b^2}} e^{ht} \cos (kt + \beta_2 + n') + \eta'_1(\gamma_2 + \delta_2 t)e^{\lambda_1 t} + \xi'_1 \delta_2 e^{\lambda_1 t} + \zeta'_1 \quad . \quad (239)$$

with a somewhat similar expression for Ξ'_u.

The value of the integral $\int_0^t F'(\tau)(\Xi_\mu)_{t-\tau} d\tau$, which is the disturbance of vertical velocity due to the elevator, has already been determined (Fig. 253). It is now proposed to make the integral $\int_0^t F'(\tau)(\Xi'_\mu)_{t-\tau} d\tau$ depend on the known integral, which for brevity will sometimes be referred to as $f(t)$. Its value in the complete notation above is

$$f(t) = \int_0^t F'(\tau)\Bigg[\frac{a_2}{\sqrt{a^2 + b^2}} e^{h(t-\tau)} \cos \{k(t - \tau) + \beta_2 + n\}$$
$$+ \eta_1\{\gamma_2 + \delta_2(t - \tau)\}e^{\lambda_1(t-\tau)} + \xi_1 \delta_2 e^{\lambda_2(t-\tau)} + \zeta_1 \Bigg]d\tau \quad . \quad . \quad (240)$$

and t cannot be negative in this integral.

It has already been pointed out that after the lapse of a short interval of time all curves for isolated sustained disturbances are similar in general character, but differ in the phase and amplitude of the oscillation. Changes in phase and amplitude will therefore be introduced successively into the expression (240). The phase difference between the oscillations in Ξ' and in Ξ is seen to be $n' - n$, or is equivalent to a time phase of $\frac{(n' - n)}{k}$ secs. If then $t + \frac{n' - n}{k}$ is substituted for t in (240), a suitable correction will have been made for the phase difference. As a result of this substitution, (240) becomes

$$f\left(t + \frac{n'-n}{k}\right) = \int_0^{t+\frac{n'-n}{k}} F'(\tau)\Bigg[\frac{a_2}{\sqrt{a^2+b^2}} e^{h\left(t-\tau+\frac{n'-n}{k}\right)} \cos \{k(t-\tau)+\beta_2+n'\}$$
$$+ \eta_1\left\{\gamma_2 + \delta_2\left(t-\tau+\frac{n'-n}{k}\right)\right\} e^{\lambda_1\left(t-\tau+\frac{n'-n}{k}\right)} + \xi_1 \delta_2 e^{\lambda_1\left(t-\tau+\frac{n'-n}{k}\right)} + \zeta_1 \Bigg]d\tau \quad . \quad (241)$$

The integral required for the disturbance of flight speed, Ξ', is

$$\int_0^t F'(\tau)(\Xi'_\mu)_{t-\tau} d\tau \equiv \int_0^t F'(\tau)\Bigg[\frac{m a_2}{\sqrt{a^2+b^2}} e^{h(t-\tau)} \cos \{k(t-\tau)+\beta_2+n'\}$$
$$+ \eta'_1\{\gamma_2 + \delta_2(t-\tau)\}e^{\lambda_1 t} + \xi'_1 \, _2 e^{\lambda_1(t-\tau)} + \zeta_1 \Bigg]d\tau \quad . \quad (242)$$

and on comparison with (241) it will be seen that the phases of the oscillations of Ξ' and Ξ which refer to flight speed and vertical velocity respectively, due to use of the elevator only, have been brought into

agreement, but the amplitudes are still different. Agreement of amplitude can be produced by multiplying both sides of (241) by $me^{\frac{-h(n'-n)}{k}}$ and the equation then becomes

$$
me^{\frac{-h(n'-n)}{k}}f\left(t+\frac{n'-n}{k}\right)=\int_0^{t+\frac{n'-n}{k}}F'(\tau)\frac{ma_2}{\sqrt{a^2+b^2}}e^{h(t-\tau)}\cos\left\{k(t-\tau)+\beta_2+n'\right\}d\tau
$$

$$
+\int_{-\frac{n'-n}{k}}^{t}F\left(\tau+\frac{n'-n}{k}\right)\left[me^{\frac{-h(n'-n)}{k}}\eta_1\{\gamma_2+\delta_2(t-\tau)\}+\xi_1\delta_2e^{\lambda_1(t-\tau)}+m\zeta_1e^{\frac{-h(n'-n)}{k}}\right]d\tau \quad (243)
$$

In this expression the second integral has been obtained by a substitution of $\tau+(n'-n)k$ for τ in that arising from the separation of the integral of (241) into two parts.

From (242) and (243) an expression can be written down for $\int_0^t F'(\tau)(\Xi'\mu)_{t-\tau}d\tau$ in terms of $f(t)$ and residual integrals.

$$
\int_0^t F'(\tau)(\Xi'\mu)_{t-\tau}d\tau=me^{\frac{-h(n'-n)}{k}}f\left(t+\frac{n'-n}{k}\right)
$$

$$
-\int_t^{t+\frac{n'-n}{k}}F'(\tau)\frac{ma_2}{\sqrt{a^2+b^2}}e^{h(t-\tau)}\cos\left\{k(t-\tau)+\beta_2+n'\right\}d\tau
$$

$$
+\int_0^{-\frac{n'-n}{k}}F'\left(\tau+\frac{n'-n}{k}\right)\left\{me^{\frac{-h(n'-n)}{k}}[\eta_1\{\gamma_2+\delta_2(t-\tau)\}+\xi_1\delta_2]e^{\lambda_1(t-\tau)}+m\zeta_1e^{\frac{-h(n'-n)}{k}}\right\}d\tau
$$

$$
-\int_0^t F'\left(\tau+\frac{n'-n}{k}\right)\left\{(m\eta_1e^{\frac{-h(n'-n)}{k}}-\eta'_1)\{\gamma_2+\delta_2(t-\tau)\}e^{\lambda_1(t-\tau)}\right.
$$

$$
\left.+\left(m\xi_1e^{\frac{-h(n'-n)}{k}}-\xi'_1\right)\delta_2e^{\lambda_1(t-\tau)}+m\zeta_1e^{\frac{-h(n'-n)}{k}}-\zeta'_1\right\}d\tau \quad . \quad (244)
$$

By a few simple transformations, such as the substitution of $t-\tau$ for τ in the first integral of the right-hand side, (244) becomes

$$
\int_0^t F'(\tau)(\Xi'\mu)_{t-\tau}d\tau=me^{\frac{-h(n'-n)}{k}}f\left(t+\frac{n'-n}{k}\right)
$$

$$
+\int_0^{-\frac{n'-n}{k}}F'(t-\tau)\left\{\frac{ma_2}{\sqrt{a^2+b^2}}e^{h\tau}\cos(k\tau+\beta_2+n')\right\}d\tau
$$

$$
+\int_0^{-\frac{n'-n}{k}}F'\left(\tau+\frac{n'-n}{k}\right)\left\{me^{\frac{-h(n'-n)}{k}}[\eta_1\{\gamma_2+\delta_2(t-\tau)\}+\xi_1\delta_2]e^{\lambda_1(t-\tau)}+m\zeta_1e^{\frac{-h(n'-n)}{k}}\right\}d\tau
$$

$$
-\int_0^t F'\left(\tau+\frac{n'-n}{k}\right)\left[\left(m\eta_1e^{\frac{-h(n'-n)}{k}}-\eta'_1\right)\{\gamma_2+\delta_2(t-\tau)\}e^{\lambda_1(t-\tau)}\right.
$$

$$
\left.+\left(m\xi_1e^{\frac{-h(n'-n)}{k}}-\xi'_1\right)\delta_2e^{\lambda_1(t-\tau)}+\left(m\zeta_1e^{\frac{-h(n'-n)}{k}}-\zeta'_1\right)\right]d\tau \quad . \quad . \quad . \quad (245)
$$

The interpretation of (245) is not difficult. The first term on the right-hand side, i.e. $me^{\frac{h(n'-n)}{k}}f\left(t+\frac{'-n}{k}\right)$ shows that part of the disturbance in Ξ' (or flight speed) is proportional to the disturbance in Ξ (or vertical velocity) and differs in phase by a time $\frac{n'-n}{k}$. This part of the

integral is then easily evaluated from the previously determined vertical motion. The two integrals first occurring on the right-hand side have definite limits, and the whole of the integration involved is limited to a time equal to the time difference in phase, which can be arranged so as not to exceed one-half the period of the oscillation, in this case about 11 secs. The last integral is taken between more general limits, but the terms involving $e^{\lambda_1(t-\tau)}$ as a factor rapidly become negligibly small, say at the end of 2 secs., whilst the remaining terms are easily integrated and give the value of a motion which is proportional to the elevator movement.

Comparison between the changes of flight speed and vertical velocity due to a gust and the corresponding changes due to continuous use of the elevator.

Considering the change of flight speed during a gust and the change of vertical velocity due to the gust, it will now be shown that a somewhat similar relation holds between Ξ'_u and Ξ_u as between Ξ' and Ξ. $\mathrm{F}(t)$ having been chosen so as approximately to satisfy equation (220), that equation can be modified by the use of $f(t)$, giving rise to

$$f(t) + \Delta f(t) + \Xi_u = 0 \quad . \quad . \quad . \quad . \quad (246)$$

where $\Delta f(t)$ is a small term depending on the degree of approximation to an exact solution of (220). Substituting for Ξ_u from the equivalent of (237) and using (238a),

$$f(t) = -\Delta f(t) - \frac{a_1 e^{ht}}{\sqrt{a^2 + b^2}} \cos (kt + \beta_1 + n) - e^{\lambda_1 t}\{\eta_1(\gamma_1 + \delta_1 t) + \xi_1 \delta_1\} \quad . \quad (247)$$

and further, directly from (237) and (238a)

$$-\Xi'_u = -\frac{ma_1}{\sqrt{a^2 + b^2}} e^{ht} \cos (kt + \beta_1 + n') - e^{\lambda_1 t}\{\eta'_1(\gamma_1 + \delta_1 t) + \xi'_1 \delta_1\} \quad . \quad (248)$$

An expression is easily obtained which differs from (247) in phase and amplitude, giving

$$me^{\frac{-h(n'-n)}{k}} f\left(t + \frac{n'-n}{k}\right) = -me^{\frac{-h(n'-n)}{k}} \Delta f\left(t + \frac{n'-n}{k}\right) - \frac{ma_1 e^{ht}}{\sqrt{a^2+b^2}} \cos (kt + \beta_1 + n')$$

$$-me^{\lambda_1 t + \frac{(\lambda_1-h)(n'-n)}{k}}\left[\eta_1\left\{\gamma_1 + \delta_1\left(t + \frac{n'-n}{k}\right)\right\} + \xi_1 \delta_1\right] \quad . \quad (249)$$

The form of the term involving cosines is now identical with the corresponding term in (248). Equation (249), however, applies until $t + \dfrac{n'-n}{k}$ is zero, whilst (248) is limited to positive values of t. If $\dfrac{n'-n}{k}$ is positive, the part of (249), which corresponds with negative values of t in the cosine term, will not be eliminated by subtracting (249) from (248), and there will be a corresponding remainder in Ξ'_u for positive values of t when $\dfrac{n'-n}{k}$

is negative. If we call this difference χ, then by combination of (249) and (248)

$$\Xi'_u = \chi - me^{\frac{-h(n'-n)}{k}} f\left(t + \frac{n'-n}{k}\right) - me^{\frac{-h(n'-n)}{k}} f\left(t + \frac{n'-n}{k}\right)$$
$$+ e^{\lambda_1 t}\{\eta'_1(\gamma_1 + \delta_1 t) + \xi_1'\delta_1\}$$
$$- e^{\lambda_1 t + \frac{(\lambda_1 - h)(n'-n)}{k}} m\left[\eta_1\left\{\gamma_1 + \delta_1\left(t + \frac{n'-n}{k}\right)\right\} + \xi_1\delta_1\right] . \quad (250)$$

where χ represents the value of $(-\Xi_u)$ from 0 to $-\dfrac{n'-n}{k}$ if $n'-n$ is positive and Ξ'_u from 0 to $-\dfrac{n'-n}{k}$ if $n'-n$ is negative.

The motion of the aeroplane in Ξ', *i.e.* the variation of flight speed, as the result of both the wind and elevator movements is

$$\Xi'_{\text{(continuous use of elevator and isolated horizontal gust)}} = \Xi'_u + \int_C^t F'(\tau)(\Xi'_\mu)_{t-\tau}d\tau \quad . \quad . \quad . \quad . \quad (251)$$

an exactly similar expression to that for Ξ from which $F(t)$ was originally found. By an examination of the terms in (245) and (250) it will be seen that the term depending on $f(t)$ vanishes from the expression for Ξ'. The remainder of the terms in Ξ'_u are easily evaluated. $me^{\frac{-h(n'-n)}{k}}\Delta f\left(t + \frac{n'-n}{k}\right)$ can be plotted from the known value of $\Delta f(t)$, whilst the remaining terms involve only calculations for times up to 2 secs., when they become negligible.

Adding (245) and (250) together the value of Ξ' is seen to be

$$\Xi' \equiv \Xi'_u + \int_0^t F'(\tau)(\Xi'_\mu)_{t-\tau}d\tau = \chi - me^{\frac{-h(n'-n)}{k}}\Delta f\left(t + \frac{n'-n}{k}\right)$$
$$+ e^{\lambda_1 t}\left\{\eta'_1(\gamma_1 + \delta_1 t) + \xi_1'\delta_1 - me^{\frac{(\lambda_1-h)(n'-n)}{k}}\left[\eta_1\left\{\gamma_1 + \delta_1\left(t + \frac{n'-n}{k}\right)\right\} + \xi_1\delta_1\right]\right\}$$
$$+ \int_0^{-\frac{n'-n}{k}} F'(t-\tau)\frac{ma_2}{\sqrt{a^2+b^2}}\cos(k\tau + \beta_2 + n')e^{h\tau}d\tau$$
$$+ \int_0^{-\frac{n'-n}{k}} F'\left(\tau + \frac{n'-n}{k}\right)\left\{me^{\frac{-h(n'-n)}{k}}[\eta_1\{\gamma_2 + \delta_2(t-\tau)\} + \xi_1\delta_2]e^{\lambda_1(t-\tau)} + m\zeta_1 e^{\frac{-h(n'-n)}{k}}\right\}d\tau$$
$$- \int_0^t F'\left(\tau + \frac{n'-n}{k}\right)\left\{\left(m\eta_1 e^{\frac{-h(n'-n)}{k}} - \eta'_1\right)\{\gamma_2 + \delta_2(t-\tau)\}e^{\lambda_1(t-\tau)}\right.$$
$$\left. + \left(m\xi_1 e^{\frac{-h(n'-n)}{k}} - \xi'_1\right)\delta_2 e^{\lambda_1(t-\tau)} + \left(m\zeta_1 e^{\frac{-h(n'-n)}{k}} - \zeta_1'\right)\right\} \quad . \quad (252)$$

When $n' = n$, $m = 1$, $\eta_1' = \eta$, etc., (252) reduces to

$$\Xi_u + \int_0^t F'(\tau)(\Xi_\mu)_{t-\tau}d\tau + \Delta f(t) = 0 \quad . \quad . \quad . \quad (253)$$

In any case in which $n'-n$ exceeds π it would be advantageous to take $(n'-n)$ as the excess over π instead of over zero. This is equivalent to changing the sign of m and proceeding as before.

Illustration of the Mathematical Processes of Equations (241) to (252) by Reference to a Particular Case.—The assumed elevator movement will be that indicated in Fig. 253, and is one which practically eliminates variations of vertical velocity of the aeroplane when moving through an isolated horizontal gust. In this case $\Xi = u_0\theta - w$, and the variation of vertical velocity due to the gust whilst the elevator remains fixed is $(u_0\theta-w)_u=\Xi_u$ and is shown in one of the curves of Fig. 253. The almost similar motion produced by the movements of the elevator alone with no wind is also shown in the same figure and is the value of $\int_0^t \mathrm{F}'(\tau)(\Xi_\mu)_{t-\tau}d\tau$. The difference between the two curves has been indicated in the same figure and corresponds with the mathematical expression $\Delta f(t)$ of equation (246). The variation of vertical velocity due to a horizontal gust, *i.e.* $(u_0\theta-w)_u$ is identical with $f(t)$ of the same equation.

It is now desired to find the variation of forward speed of the aeroplane relative to the air. Ξ' of the mathematical equations is then u. The variation of the velocity of the aeroplane due to the wind alone is mainly a damped phugoid and is shown in Fig. 247 (a). The variation of velocity will be modified by the elevator movement, and the value of Ξ'_μ, *i.e.* the variation of velocity due to a single sudden movement of the elevator is represented by the curve marked u in Fig. 254 (c); since the elevator movement is known,

$$\Xi' =u = \Xi'_u + \int_0^t \mathrm{F}'(\tau)(\Xi'_\mu)_{t-\tau}d\tau \quad . \quad . \quad . \quad . \quad (254)$$

and the integral for u which gives the curve of Fig. 254 could have been determined without any reference to the fact that $\mathrm{F}(\tau)$ was chosen to ensure the elimination of $(u_0\theta + w)$. It is, however, already clear that some such relationship exists, and in finding the value of u from (254) the results were so arranged as to indicate this relationship.

In the actual working it was found to be convenient to transform (254) by a partial integration, obtaining

$$\Xi' =u = \Xi_u + \int_0^t \mathrm{F}()\frac{d}{d\tau}(\Xi'_\mu)_{t-\tau}d\tau \quad . \quad . \quad . \quad (255)$$

The curve $(\dot{u}_\mu)$ is drawn in Fig. 254 (a), and from this curve and the elevator movement in Fig. 253 the value of the integral of (255) has been found. The ordinate SQ of the curve RQMNP, Fig. 254 (a), is plotted in a manner similar to that previously adopted for determining the elevator movement $\mathrm{F}(t)$, *i.e.* the elevator position at 12 secs. obtained from Fig. 253 is multiplied by the ordinate of the curve u_μ of Fig. 254 (a) for a time $(15\cdot3-12)$ secs. to obtain the element SQ of the integral representing the disturbance at $15\cdot3$ secs. The area of the figure RQMNP is then the disturbance at $15\cdot3$ secs. which results from the movement of the elevator alone, and the complete disturbance at any time due to elevator alone is represented by the curve ABCD of Fig. 254 (b). The curve u_u of the same figure is the disturbance due to wind alone, and the disturbance of the machine as a consequence of both wind and elevator

movement is obtained by simple addition of the separate effects and is given by the curve EBF. The curve has the general characteristics of the curve in Fig. 253, *i.e.* the variations in u are roughly proportional to the elevator movement in this case of simple initial disturbance.
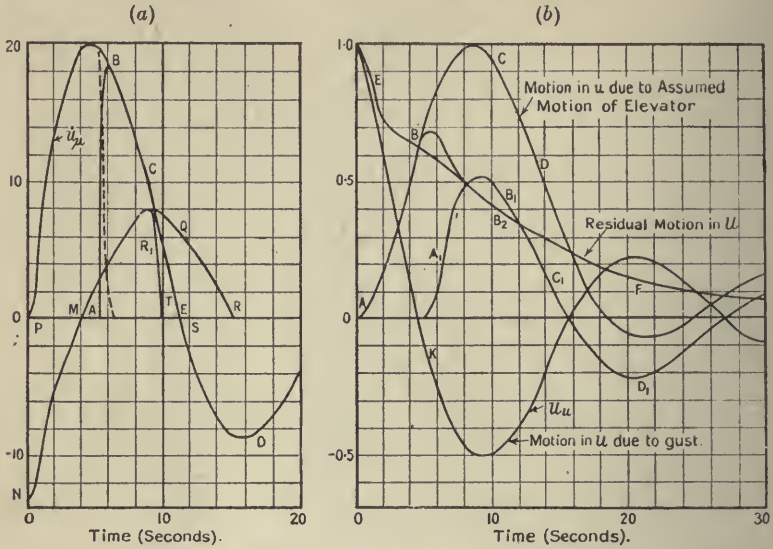
Resultant Disturbance of an Aeroplane after choosing
Elevator Movement to Eliminate Variations of Vertical Velocity
which would otherwise be caused by a sudden Horizontal Gust.
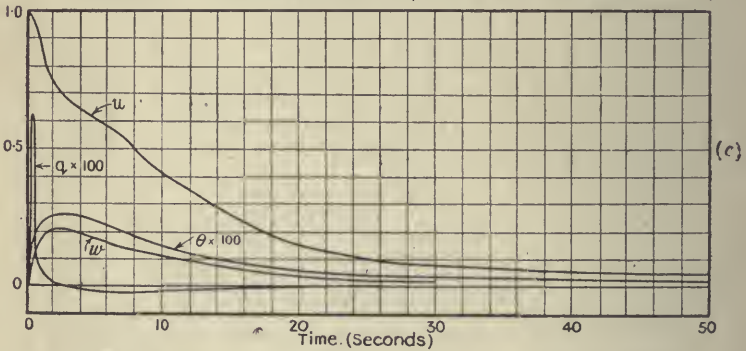
FIG. 254.—Residual disturbances of a controlled aeroplane when full use of the elevator is made in maintaining level flight.

Returning to a consideration of Fig. 254 (*a*), it will be seen that a curve ABCED has been drawn which coincides with $\dot{u}_\mu$ for all points after B. The part ABCED is a reproduction to another scale of the curve for $(u_0\theta - \dot{w})_\mu$, but has been moved along the axis of time so that the point K of Fig. 254 (*b*) coincides with the point E of Fig. 254 (*a*). The change of time is equivalent to substituting $t + \dfrac{n' - n}{k}$ for t as was done to obtain equation (241), whilst

the multiplication by 0·940 to make the ordinates agree corresponds with the multiplier $me^{\frac{-h(n'-n)}{k}}$ used in obtaining equation (240). If now the curve ABCED of Fig. 254 (a) be used instead of PBCE, a new curve TR_1MNP is obtained, which encloses part of the area RQMNP. This area is proportional to $(u_0\theta-w)$ as plotted in Fig. 253 (a). The actual values of all such areas are plotted in Fig. 253 (a) as $A_1B_1C_1D_1$, which then represents

$$me^{\frac{-h(n'-n)}{k}}f\left(t+\frac{n'-n}{k}\right)+me^{\frac{-h(n'-n)}{k}}\Delta f\left(t+\frac{n'-n}{k}\right)$$

of equation (250). A reference to Fig. 254 (b) shows that for times greater than 6 secs. this curve is almost symmetrical with u_u, and hence, on adding the disturbances, the oscillation after about 6 secs. is completely eliminated. The elimination of disturbance here indicated corresponds with the elimination of the term in $f\left(t+\frac{n'-n}{k}\right)$ by the addition of equations (245) and (250).

The residual disturbance is seen to depend to an appreciable extent on the integral corresponding with the area RQR_1T_1, Fig. 254 (a), and since the elevator movement is approximately an exponential curve, the residual motion on this account is after a few seconds nearly proportional to the elevator movement. This follows from the figures, since the effect of multiplying the ordinates of RQR_1T, Fig. 254 (a), by an exponential is to produce figures which differ from one another only in the scale of the ordinates. This does not apply for times less than 6 secs., i.e. for times less than the base of the figure RQR_1T. The curve obtained from the values of the areas of RQR_1T at all times is shown in Fig. 254 (b) as ABB_2F, and is the graphical representation of the integrals on the right-hand side of (252).

There remains to be considered the portion of the curve u_u which was not eliminated by subtracting $A_1B_1C_1D_1$. The part from K onwards with increasing time has been already dealt with as $\Delta f\left(t+\frac{n'-n}{k}\right)$ to a new scale. The part from $t = 0$ up to K, Fig. 254 (b), i.e. the value of u_u up to K corresponds with the χ of equation (252), and χ is thus seen to be of some appreciable importance in certain cases, but ceases to increase in value after an interval of time which need not exceed one-quarter of the phugoid period.

There is then, for disturbances in u, w, q and θ, a period of not more than 8 or 10 secs., during which the character of the motion is somewhat complicated owing to its being made up of two or three relatively important components. After this, however, the motion in each case is very nearly a copy of the elevator movement, and it appears that the motion is not oscillatory.

Curves corresponding with those of Fig. 248 are drawn in Fig. 254 (c) for the continuous movement of the elevator given in Fig. 253 instead of for a single sudden movement. The ordinates are given as fractions of u_1, the variation of speed in the gust.

Extension to Motion in a Natural Wind.—The process to be followed from this point onwards is identical with that described in the previous section, on the disturbed longitudinal motion of an aeroplane flying in a natural wind (pages 529–533). The difference in the initial assumptions is covered completely if the curves of Fig. 254 (c) are used in the new calculations in every case in which the curve of Fig. 247 (a) were used in the earlier calculations.

A brief reference to the results and a comparison with those previously obtained for an uncontrolled aeroplane will show how different the disturbances may be. The importance of the results appears to lie not in the demonstration that such reduction of disturbance is possible, but in indicating a method for the systematic investigation and design of automatic devices for aeroplanes. The results also show that there is a possibility of getting more and more advantage from the use of inherent stability without the attendant disadvantages of violent motion in winds, if in addition some mechanical device can be invented which will operate the controls so as to reduce the disturbances which the inherent stability has to eliminate.

In considering the results of the calculations referring to the longitudinal motion of an aeroplane in a natural wind, it should be remembered that the calculation has been carried out on the assumption that a perfect pilot has instantaneous knowledge of the variations in the wind and is able to make the necessary correct movement. An actual pilot would produce a less exact approximation, and in particular would probably not attempt to give such complicated movements to his elevator. This introduces a further modification, and it will be interesting later to find the effect of a slow elevator movement which averages out rapid fluctuations ; it is, however, a question of order of approximation and not of principle.

The elevator movement requisite to cut out the variations of vertical velocity due to the wind described in the previous section is given in Fig. 255, together with the anemogram.

Its general characteristics follow those of the wind somewhat closely. There is, however, a superposed variation which does not bear any simple relation to the wind at the instant and is, in fact, dependent to a large extent on previous history during the last minute.

The residual variation in vertical velocity has been plotted to ten times the scale of the corresponding diagram for the uncontrolled machine, as otherwise it would have been too small to see clearly. The residual vertical velocity is shown in Fig. 255, together with the vertical velocity of the uncontrolled aeroplane. The maximum vertical velocity when the aero-plane is controlled as assumed is only a fraction of a foot per second instead of the 10 ft.-s. previously found at the end of a minute. This indicates the practical elimination of the vertical velocity and is the best which can be done under any circumstances.

In a similar way, the elevator movement might have been chosen so as practically to eliminate the variation of speed over the ground or the inclination of the axis of the aeroplane. With the elevator movement assumed, which was not primarily arranged to reduce anything but the

FIG. 255.—Controlled flight in a natural wind (aeroplane stable) compared with uncontrolled flight of same aeroplane.

vertical velocity, the variations of horizontal speed are greatly reduced, as will be seen by reference to Fig. 255.

One of the curves of this figure shows the variation of horizontal velocity of the aeroplane in the natural wind for the elevator movements shown above, *i.e.* when the aeroplane is controlled. The variations of speed are not great, and vary between an increase of 2 ft.-s. and a decrease of 4 ft.-s. The comparative curve of velocity is reproduced from the previous section, and shows a speed of flight over the ground varying from an increase of 10 ft.-s. to a decrease of 12 ft. s.

APPENDIX

Introduction.—The conditions for the stability of an aeroplane in the general case involve as part of the analysis the solution of an algebraic equation of the eighth degree. The roots may commonly consist of two real roots and three complex pairs, and it was found on reference to the English text-books available that no general method of solution was indicated which did not involve almost prohibitive labour in the arithmetical calculations. In a book by H. von Sanden, issued in Germany last year, a method of solution is described which appeared to have the required generality; information on one point of importance in relation to complex roots being missing, reference was made for fuller information to a paper by C. Runge in the *Ency. Math. Wissen.*, 1898–1900. It was there found that a method of solution of a completely general character was devised by Graeffe in 1837 and described by Runge as the best method known at the time of writing the above article (at least, when all the roots are required); Runge further describes a method of dealing with complex roots, developed by Encke.

Another paper, by Jelinek, referred to by Burnside and Panton, deals with the same problem, and, although written in German in 1869, is not mentioned by Runge. As a method of finding approximate values of the roots, that proposed by Jelinek appears to be much less useful than Graeffe's, but may possibly be of considerable value in obtaining a continuous increase in the accuracy of any root, *i.e.* the method may bear somewhat the same relation to complex roots that Horner's process does to real roots. Graeffe's method appears to be much more convenient than Sturm's for finding the approximate position of real roots, and has the further advantage of giving approximate values for the complex pairs of roots.

As the solution of equations is of some importance in calculations of stability, and as the methods mentioned above have not yet appeared in the English text-books, it has been thought advisable to give an account of them in some detail, and in particular to show how they have been applied.

Solution of a Biquadratic Equation.[*]—Taking the example given in longitudinal stability which lead to equation (15), p. 461, the detailed arithmetical process of finding the roots will be shown. The equation is

$$\lambda^4 + 14 \cdot 8\lambda^3 + 62 \cdot 0\lambda^2 + 9 \cdot 80\lambda + 2 \cdot 16 = 0 \quad . \quad . \quad . \quad . \quad (1)$$

and for the purposes of explanation the coefficients will be defined by writing the equation as

$$a_4\lambda^4 + a_3\lambda^3 + a_2\lambda^2 + a_1\lambda + a_0 = 0 \quad . \quad . \quad . \quad . \quad . \quad (2)$$

[*] The more complete explanation of the method occurs in the illustration of the solution of an equation of the eighth degree.

· The process followed isthat of multi plying two equations together, the second of which differs from the first in that the sign of λ has been changed. The work is simply arranged as

$$a_4 +\ a_3\ \ +\ a_2\ \ +\ a_1\ \ +a_0$$
$$+\qquad -\qquad +$$
$$\overline{a_4{}^2\qquad a_3{}^2\ +\ a_2{}^2\ -\ a_1{}^2\ +a_0{}^2}$$
$$+2a_2a_4 - 2a_1a_3 + 2a_0a_2$$
$$2a_0a_4$$

$$. \quad . \quad . \quad . \quad . \quad . \quad . \quad . \quad . \quad . \quad (3)$$

and the addition of the results leads to the product required. In a numerical example the process is repeated until $2a_0a_4$ is very small and until the second line is devoid of consecutive terms. Separation of the roots has then been effected. If a_1a_3 becomes small whilst a_2a_4 and a_0a_2 are not negligible, the presence of two pairs of complex roots is indicated. If a_1a_3, on the other hand, is left as important two real roots are indicated and one complex root, and so on.

In the numerical example above the process is carried out as below :—

$$1 + 1^{1 \cdot}48 + 6^{1 \cdot}20\ +\ 9 \cdot 80\ + 2 \cdot 16$$
$$-\qquad +\qquad -\qquad +$$
$$\overline{1 - 2^{2 \cdot}19 + 3^{3 \cdot}84\ - 9^{1 \cdot}60\ + 4 \cdot 66}$$
$$+1 \cdot 24\ - 0 \cdot 29\ + 26 \cdot 8$$
$$0 \cdot 00$$

2nd power of roots
$$\overline{1 - 9^{1 \cdot}5\ + 3^{3 \cdot}55\ + 1^{2 \cdot}72\ + 4 \cdot 66}$$
$$+\qquad +\qquad -\qquad +$$
$$\overline{1 - 9^{3 \cdot}02 + 1^{7 \cdot}260 - 2^{4 \cdot}96\ + 2^{1 \cdot}17}$$
$$+7 \cdot 10\ + 0 \cdot 000\ + 3 \cdot 30$$
$$-$$

The separation is proved by the last line to have been complete at the second power, and the moduli of the roots are found as $\sqrt{3^{3 \cdot}55}$ and $\sqrt{\dfrac{4 \cdot 66}{3^{3 \cdot}55}}$. The convenient arrangement for working is

	Log.	Diff. of logs.	Diff./2.	Antilog.	
$3^{3 \cdot}53$	$3 \cdot 550$	$3 \cdot 550$	$1 \cdot 775$	$59 \cdot 6$	. . . . . r_1
$4 \cdot 66$	$0 \cdot 668$	$\bar{3} \cdot 118$	$\bar{2} \cdot 559$	$0 \cdot 0362$	. . . r_2

If p_1 and p_2 be the coefficients of λ in the quadratic factors they can be obtained from the formula

$$p = \frac{a_3 - \dfrac{a_1}{r}}{a_4 - \dfrac{a_0}{r^2}} \qquad . \quad . \quad . \quad . \quad . \quad . \quad (4)$$

The values are $p_1 = 14 \cdot 64$ and $0 \cdot 158$, and the factors of (1) are

$$\lambda^2 + 14 \cdot 64\lambda + 59 \cdot 6 = 0 \quad \text{and} \quad \lambda^2 + 0 \cdot 158\lambda + 0 \cdot 0362 = 0 . \quad . \quad (5)$$

These factors differ a little from those given in equation (15), p. 461, but, as will be shown later, an accurate answer can always be obtained from any

approximation whenever it is required, and for many purposes high accuracy is not required.

Illustration of the Solution of a Numerical Equation of the Eighth Degree by Graeffe's Method.—The equation to be solved will be taken as equation (82), p. 493, and is

$$\lambda^8 + 20{\cdot}4\lambda^7 + 151{\cdot}3\lambda^6 + 490\lambda^5 + 687\lambda^4 + 719\lambda^3 + 150\lambda^2 + 109\lambda + 6{\cdot}87 = 0 \quad . \ (6)$$

The roots are known to be partly real and partly complex, but this knowledge is not of assistance in the application of the method. Graeffe forms the equation whose roots are the squares of the roots of (6), and treating the new equation in the same way, forms the equation whose roots are the fourth power of those of (6). After continuing the process for a number of times (n) the roots will have been raised to the $(2n)$th power, and it is almost obvious without formal proof that this will lead to a separation of the roots, at any rate when they are real and unequal. One point is, however, worthy of notice here, and that is, the suppression of sign which takes place on squaring. This leads to no great difficulty when taking the $(2n)$th root of a real quantity, but introduces the necessity for special consideration of complex roots. In the case of real roots the signs must be found by trial if necessary, but the use of Descartes' rule of signs may render trial unnecessary.

To find the equation whose roots are the squares of (6) it is only necessary to change the sign of λ to form a new equation and then to multiply this new equation by equation (6). The method of arranging the multiplication is of some importance, and the form adopted by Graeffe is as follows :—

Suppose the original equation is

$$a_n x^n + a_{n-1}x^{n-1} + a_{n-2}x^{n-2} + a_{n-3}x^{n-3} \ldots = 0 \quad . \quad . \quad . \ (7)$$

Write down only the coefficients, and beneath them the signs of the new coefficients formed by changing the sign of x. The multiplication process is then readily seen to follow as below :—

$$
\begin{array}{cccc}
a_n & a_{n-1} & a_{n-2} & a_{n-3} \\
+ & - & + & -
\end{array}
$$

$$
\begin{array}{cccc}
(a_n)^2 & - (a_{n-1})^2 & + (a_{n-2})^2 & - (a_{n-3})^2 \\
& 2(a_n)(a_{n-2}) & - 2(a_{n-1})(a_{n-3}) & + 2(a_{n-2})(a_{n-4}) \\
& & 2(a_n)(a_{n-4}) & - 2(a_{n-1})(a_{n-5}) \\
& & & + 2(a_n)(a_{n-6}) \quad . \quad . \quad . \ (8)
\end{array}
$$

The products are continued in successive rows as far as possible, and the sums of the columns give the new equation whose roots are the squares of the roots of equation (6). After repetition it will be noticed in a numerical example that the terms in the lowest rows soon become very small, and if all the roots are real and unequal, the process rapidly leads to all the terms in the second and succeeding rows becoming negligible, and the separation of the roots is then complete. If a complex pair occurs, one of the products in the second row will not become unimportant, and the calculation is stopped when the terms immediately to the right and left of it become negligible. More than one complex pair leads to more than one important term in the second row, but in the absence of repeated roots these terms can never be contiguous.

The process presumes the existence of a limit of accuracy of calculation

and in the work which follows, this limit will be taken to be that which can be obtained by a 20-inch slide-rule. The exact limit taken affects the accuracy of determination of the roots, but it would probably not be advantageous to get high accuracy directly, but to do this as a second and entirely separate calculation. One other point of convenience remains : it will readily be seen that the raising of numbers to high powers will lead to the introduction of extremely large and extremely small numbers in the final equation. It is a convenience therefore to have some means of readily indicating powers of 10. The notation used by Von Sanden will be adopted, and this expresses a number such as 1.323×10^6 by 1.323^6. The notation is not unobjectionable, but no better alternative suggests itself. Proceeding now to solve equation (6) the first step corresponding with (8) is

x^8	x^7	x^6	x^5	x^4	x^3	x^2	x	
1	2.04^2	1.513^2	4.901^2	6.87^2	7.19^2	1.50^2	1.09^2	6.87
+	−	+	−	+	−	+	−	+
1	-4.161^2	$+2.290^4$	-2.402^5	$+4.719^5$	-5.168^5	$+2.250^4$	-1.188^4	$+4.719^1$
	$+3.026$	-2.000	$+2.080$	-7.050	$+2.060$	-15.67	$+0.206$	
		$+0.137$	-0.293	$+0.454$	-1.068	$+0.94$		
			$+0.003$	-0.044	$+0.021$			
				$+0.001$				

2nd power—

1	-1.135^2	$+4.27^3$	-6.12^4	-1.925^5	-4.155^5	-1.248^5	-9.82^3	$+4.719^1$
								$=0$ . . (9)

Equation (9) is the equation whose roots are the squares of the roots of equation (6), the powers of x at the head of each column being supposed to apply all down the column. The numbers in the fourth and fifth rows are small, and in continuing to the fourth powers of the roots it will be found that they become negligible. The sequence of signs due to changing x to $-x$ in (9) is given as the next row, and the multiplication is then continued for two sequences :—

+	+	+	+	−	+	−	+	+
1	-1.288^4	$+1.823^7$	-3.745^9	$+3.705^{10}$	-1.726^{11}	$+1.557^{10}$	-9.642^7	$+2.227^3$
	$+0.854$	-1.389	-1.644	-5.083	$+0.480$	-0.816	-1.177	
		-0.038	-0.094	-0.107	$+0.011$	-0.002		

4th power—

1	-4.34^3	$+3.96^6$	-5.483^9	-1.485^{10}	-1.235^{11}	$+7.39^9$	-1.082^8	$+2.227^3$
+	+	+	+	−	+	+	+	+
								. . . . (10)

1	-1.883^7	$+1.568^{13}$	-3.008^{19}	$+2.205^{20}$	-1.525^{22}	$+5.461^{19}$	-1.171^{16}	$+4.959^6$
	0.792	-4.760	-0.012	-3.55	-0.022	-2.991	$+0.003$	
		-0.003	$*$	$*$	$*$	$*$	$*$	

8th power—

1	-1.091^7	-3.195^{13}	-3.020^{19}	-1.135^{21}	-1.547^{22}	$+2.470^{19}$	-1.168^{16}	$+4.959^6$
								. . . . (11)

In the process of finding the equations with roots of the 8th power from that with roots of the 4th, it will be noticed that only one term, and that a very small one, occurs in the third row. In the second row the 3rd, 5th and 7th terms are very small and will disappear in the process of finding the 16th powers. This indicates that a considerable degree of separation of the roots has already been

effected, although the occurrence of two important terms in the second and third columns shows that the separation is not complete. Replace (11) by a general equation as in (8) and proceed to the next step, putting zero for the terms which are seen to vanish from a consideration of (11).

1	a_7	a_6	a_5	a_4	a_3	a_2	a_1	a_0
+	−	+	−	+	−	+	−	+
1	$-(a_7)^2$	$+(a_6)^2$	$-(a_5)^2$	$+(a_4)^2$	$-(a_3)^2$	$+(a_2)^2$	$-(a_1)^2$	$+(a_0)^2$
	$+2a_6$	$-2a_7 \cdot a_5$	0	$2a_5a_3$	0	$2a_3a_1$	0	

$$(4) \qquad\qquad (3) \qquad (2) \qquad (1)$$
$$. \quad . \quad . \quad . \ (12)$$

The sequence in the second row now indicates that separation has not been obtained for the terms bracketed (4) whilst separation has been obtained for the rest, there being complex pairs to be obtained from the quadratic factors bracketed (3) and (2), and a real root to be obtained from the linear equation (1). After separation to the extent shown has been obtained the further arithmetic can be confined to the first four columns. Reverting to (11), the next sequence of signs, etc., is

+		+		−		+
1	$-1 \cdot 191^{14}$	+	$1 \cdot 020^{27}$		$-9 \cdot 120^{38}$	
	$-0 \cdot 639$	−	$0 \cdot 659$			

$$16\text{th power} \quad 1 \quad -1 \cdot 830^{14} \quad + \quad 3 \cdot 61^{26} \quad -9 \cdot 120^{38} \qquad . \quad . \quad . \ (13)$$

	+		+		+		+
1	$-3 \cdot 350^{28}$	+	$1 \cdot 303^{53}$		$-8 \cdot 32^{77}$	
	$+0 \cdot 072$	−	$3 \cdot 337$			

$$32\text{nd power} \quad 1 \quad -3 \cdot 278^{28} \quad - \quad 2 \cdot 034^{53} \quad -8 \cdot 32^{77} \quad . \quad . \quad . \quad . \ (14)$$

$$\underbrace{\qquad}_{4b} \qquad \underbrace{\qquad}_{4a}$$

The separation of (4) is indicated when obtaining the equation of 32nd powers from the 16th. The first term on the second row is seen to be small in comparison with that above it, whilst the second term of the row is important. At the 32nd power the process has been carried far enough, and (4) has been divided into a linear and a quadratic factor. The original equation has then two real roots and three pairs of complex roots.

The larger of the two real roots is now obtained from 4b, (14), since the root of the equation

$$x = 3 \cdot 278^{28} \quad . \quad . \quad . \quad . \quad . \quad . \quad . \ (15)$$

is the 32nd power of the larger real root of the original equation. The 32nd root is easily extracted, leaving an ambiguity of sign which can be removed by a trial division of the original equation. Since all the signs of the original equation are positive, it follows in this case from Descartes' rule of signs that the root is negative.

The largest pair of complex roots is obtained from the solution of—

$$-3 \cdot 278^{28}x^2 - 2 \cdot 034^{53}x - 8 \cdot 32^{77} = 0 \quad . \quad . \quad . \quad . \ (16)$$

and by making use of De Moivre's theorem the 32nd root can be taken. There are now, however, 32 ambiguities corresponding with the 32 roots of unity, and as all the roots are complex, no simple means of determining the final answer is immediately apparent. The method proposed by Graeffe in such a case is to solve (16) as a quadratic equation, obtaining one ambiguity only, *i.e.* with a positive or negative sign for the real part of the root. By trial in (13) one of these will be found to be inadmissible. Extracting the square root a further ambiguity occurs which can be removed by trial in (11), and so on.

The method will be seen to be perfectly general, but it is not the only method by which the complex factors can be extracted. It will be noticed that directly from (16) the value of the modulus of the root of the original equation can be obtained as the 32nd root of $8 \cdot 3277/3 \cdot 278^{28}$, and the sign to be taken is necessarily the positive one. There is then a factor of the original equation of the form (x^2+px+r), where r is known but p is to be found. If the original equation is divided by this factor a remainder which is linear in x will be left, and since r is known, the coefficients of x and the coefficient independent of x give two equations from which to determine p. This may be effected by the process of finding the common factor. It will be shown later that much of the division can be carried out generally, and in any particular case the highest power of p to be dealt with in the detailed arithmetical division is not greater than $\dfrac{n+1}{2}$, where n is the highest power of x in the original equation. For equations up to and including the 6th order the whole division has been carried out generally, giving the following formulæ for p.

For a cubic the value can be obtained from the sum of the roots and the value of the real root.

If the coefficients have the significance given to them in equation (7), the formulæ for p are—

Biquadratic
$$p = \frac{a_3 - \dfrac{a_1}{r}}{a_4 - \dfrac{a_0}{r^2}} \qquad \dots \qquad \dots \qquad \dots \quad (17)$$

Quintic
$$p = \frac{a_5\left(a_4 - \dfrac{a_2}{r}\right) + \dfrac{a}{r^3}\left(a_3 \quad \dfrac{a_1}{r}\right)}{a_5\left(a_5 - \dfrac{a_1}{r^2}\right) + \dfrac{a_0}{r^3}\left(a_4 - \dfrac{a_0}{r^2}\right)} \qquad \dots \quad (18)$$

Sextic :—write β for $a_6 - \dfrac{a_0}{r^3}$; γ for $a_5 - \dfrac{a_1}{r^2}$; δ for $a_4 - \dfrac{a_2}{r}$

then
$$p = \frac{\left(a_5 - a_6\dfrac{\gamma}{\beta}\right)\left(\dfrac{\delta}{\beta} - r\right) - \left(a_3 - \gamma r - \dfrac{2a_1}{r}\right)}{\dfrac{\gamma}{\beta}\left(a_5 - a_6\dfrac{\gamma}{\beta}\right) - \left\{r(\beta - 2a_6) - a_6\dfrac{\delta}{\beta} + a_4\right\}} \qquad \dots \quad (19)$$

For equations of higher degrees the formula gets appreciably longer and may not be advantageous. The formulae given above cover the usual cases occurring for the stability of an aeroplane, as in general two of the roots of the octic equation are real.

To apply the foregoing analysis to equation (6) the moduli are required, and these can be obtained at the same time as the numerical value of the real roots. The further calculations are given below in a form suggested by H. von Sanden,

the numbers in the first column being obtained directly from equations (14) and (11).

	Log.	Diff. of logs.	$\frac{\text{Diff.}}{32}$	Antilog.		
$3\cdot278^{28}$	$28\cdot516$	$28\cdot516$	$0\cdot892$	$7\cdot80$		real negative root.
$8\cdot32^{77}$	$77\cdot920$	$49\cdot404$	$1\cdot545$	$35\cdot07$	r_1	modulus of complex root.
$3\cdot020^{19}$	$19\cdot480$	—	Diff./8			
$1\cdot547^{22}$	$22\cdot189$	$2\cdot709$	$0\cdot3385$	$2\cdot18$	r_2	,, ,,
$1\cdot168^{16}$	$16\cdot067$	$\overline{7}\cdot878$	$\overline{1}\cdot2348$	$0\cdot172$	r_3	,, ,,
$4\cdot959^{6}$	$6\cdot695$	$\overline{10}\cdot628$	$\overline{2}\cdot8285$	$0\cdot0674$		real negative root . (20)

The process does not need detailed description, as it is the same as that followed in extracting the nth root by means of logarithms.

The original equation will now be reduced to one of the 6th degree by dividing through by the factors $\lambda + 7\cdot80$ and $\lambda + 0\cdot0674$ obtained from the values of the real roots. The original equation is represented by its coefficients in the first line, and the second and third give the figures obtained for the successive quotients and remainders when dividing by $\lambda + 7\cdot80$.

1	$2\cdot04^1$	$1\cdot513^2$	$4\cdot901^2$	$6\cdot87^2$	$7\cdot19^2$	$1\cdot50^2$	$1\cdot09^2$	$6\cdot87$. (21)
1	$1\cdot259$	$0\cdot531$	$0\cdot765$	$0\cdot900$	$0\cdot1746$	$0\cdot1386$	$0\cdot00881$	—
—								
	$7\cdot81$	$9\cdot82^1$	$4\cdot136^2$	$5\cdot97^2$	$7\cdot015^2$	$1\cdot361^2$	$1\cdot081^2$	

The terms underlined give the seventh degree equation required, and the first term in the third row, viz. $7\cdot81$, shows that the root is approximately correct. It is essential for success that the division by large roots should begin from the term independent of λ, and for small roots should begin at the term containing the highest power of λ.

Dividing by $(\lambda + 0\cdot0674)$ and working in the ordinary decimal notation

1	$12\cdot59$	$53\cdot1$	$76\cdot5$	$90\cdot0$	$17\cdot46$	$13\cdot86$	$0\cdot881 = 0$ (22)
	$0\cdot07$	$0\cdot84$	$3\cdot53$	$4\cdot9$	$5\cdot74$	$0\cdot79$	$0\cdot881$

$$\lambda^6 + 12\cdot52\lambda^5 + 52\cdot3\lambda^4 + 72\cdot97\lambda^3 + 85\cdot1\lambda^2 + 11\cdot72\lambda + 13\cdot07 \qquad = 0 \quad (23)$$

The last line is a sextic with three pairs of complex roots. Using the formula given in (19) with $r_1 = 35\cdot07$, the value of p is obtained as below :—

$$\beta = 1 \qquad \lambda = 12\cdot52 \qquad \delta = 49\cdot9$$
$$p = \frac{72\cdot97 - 12\cdot52 \times 35\cdot07 - 0\cdot67}{-35\cdot07 - 49\cdot9 + 52\cdot3} = 11\cdot22 \quad . \quad . \quad . \quad (24)$$

One quadratic factor is therefore $\lambda^2 + 11\cdot22\lambda + 35\cdot07$ . . . . . . (25)

Divide out by this factor, remembering that it is a large root—

1	$12\cdot52$	$52\cdot3$	$72\cdot97$	$85\cdot1$	$11\cdot72$	$13\cdot07$	
1	$1\cdot322$	$2\cdot350$	$0\cdot2150$	$0\cdot370$	$4\cdot18$	. . . . . (26)
=	$11\cdot20$	$49\cdot95$	$72\cdot96$	$84\cdot73$	$7\cdot54$	
		$14\cdot83$	$26\cdot38$	$2\cdot31$		
		$35\cdot12$	$46\cdot38$	$82\cdot42$		

The quotient is indicated by the figures which are doubly underlined, and the approximate correctness of the factor is indicated by the agreement of the first numbers in the third and fifth rows with those in the quadratic factor.

The biquadratic (26) can now be solved, using formula (17).

$$r_2 = 2\cdot18 \qquad p = \frac{1\cdot32 \times 2\cdot18 - 0\cdot215}{2\cdot18 - \dfrac{0\cdot370}{2\cdot18}} = 1\cdot325 \quad . \qquad . \qquad . \qquad (27)$$

and $r_3 = 0\cdot172$

$$p = \frac{1\cdot32 \times 0\cdot172 - 0\cdot215}{-2\cdot01} = -0\cdot0059 \quad . \qquad . \qquad . \qquad (28)$$

and the two remaining quadratic factors are

$$(\lambda^2 + 1\cdot325\lambda + 2\cdot18) \quad . \qquad . \qquad . \qquad . \qquad . \qquad (29)$$

and

$$(\lambda^2 - 0\cdot0059\lambda + 0\cdot172) \quad . \qquad . \qquad . \qquad . \qquad . \qquad (30)$$

The whole calculation to this stage can be carried out to slide-rule accuracy by two computers in about 3 hours. It is necessary to work independently for successive steps and to make comparisons at the end of each step. When the powers of 10 in the later stages become great, considerable discrepancies in the significant figures occur and seem to indicate want of accuracy. This is not usually the case, and the roots ultimately deduced by both computers will be found to agree even when the discrepancies mentioned above appear to be very great. The reason for this is obvious when column 2 in table (20) is examined.

Method of obtaining Any Result more accurately.—In examining the stability of a particular aeroplane it is probable that the roots thus obtained are sufficiently accurate for all practical purposes. In an investigation concerning the effect of certain modifications of detail, higher accuracy is desirable, and methods will be described for increasing the accuracy of any complex root progressively, without the necessity for a knowledge of the remaining roots.* The procedure is as follows : Divide the original equation by the approximate quadratic factor, obtaining a remainder of the form $R_1 x + R_0$, and a quotient. Again divide this quotient by the approximate quadratic factor, leaving a remainder $R_3 x + R_2$. If the approximate quadratic factor be $x^2 + px + r$, then the corrected quadratic factor is $x^2 + (p + \delta p)x + r + \delta r$, where

$$\delta p = \frac{\begin{vmatrix} R_1 & R_3 \\ R_0 & R_2 \end{vmatrix}}{\begin{vmatrix} R_3 & pR_3 - R_2 \\ R_2 & rR_3 \end{vmatrix}} \quad . \qquad . \qquad . \qquad . \qquad . \qquad (31)$$

$$\text{and } \delta r = \frac{\begin{vmatrix} R_1 & pR_3 - R_2 \\ R_0 & rR_3 \end{vmatrix}}{\begin{vmatrix} R_3 & pR_3 - R_2 \\ R_2 & rR_3 \end{vmatrix}} \quad . \qquad . \qquad . \qquad . \qquad . \qquad (32)$$

The process can be repeated to give any desired degree of accuracy. It is probable that the values of R_2 and R_3 once obtained will be sufficiently accurate for use in several successive divisions.

Numerical Illustration of the Use of the Above Method of Successive Approximation.—The factor given by (29), *i.e.* $\lambda^2 + 1\cdot325\lambda + 2\cdot18$, is known to be an approximate solution of equation (123). It is desired to find a factor which is a more accurate solution. The slide-rule is here replaced by a calculating machine on which both the multiplications and subtractions required are

---

* For real roots, Newton's and Horner's methods as described in English text-books are available.

carried out, and some of the steps in a division such as that in (26) do not appear in the working, the calculating machine rendering the writing of them unnecessary. The full working is given below :—

1	20·4	151·3	490	687	719	150	109	6·87
	19·075	149·12	448·42	417·02	99·182	62·163	9·166	3·634
		123·85	284·32	40·292	45·796	1·4844	7·199	

and continuing to a second division by the same factor—

$$17{\cdot}750 \quad 121{\cdot}67 \quad 245{\cdot}62 \quad -173{\cdot}67 \quad -206{\cdot}17 \quad 713{\cdot}93$$
$$98{\cdot}15 \quad 115{\cdot}58 \quad -326{\cdot}81 \quad +226{\cdot}86 \quad . \quad . \quad . \quad . \quad . \quad (33)$$

The remainders are :—

$$R_0 - 3{\cdot}634 ; \ R_1 = 7{\cdot}199 ; \ R_2 = 713{\cdot}93 \text{ and } R_3 = 226{\cdot}86 \quad . \quad (34)$$

and from these it is found that

$$\begin{vmatrix} R_1 & R_3 \\ R_0 & R_2 \end{vmatrix} = 4315 ; \quad \begin{vmatrix} R_1 & pR_3 - R_2 \\ R_0 & rR_3 \end{vmatrix} = 5060, \quad \text{and} \quad \begin{vmatrix} R_3 & pR_3 - R_2 \\ R_2 & rR_3 \end{vmatrix} = 407{,}300$$
$$. \quad . \quad . \quad (35)$$

Using these values in (31) and (32)

$$\delta p = + 0{\cdot}01060 \quad \text{and} \quad \delta r = + 0{\cdot}01243 \quad . \quad . \quad . \quad (36)$$

and a new approximation to the quadratic factor is

$$\lambda^2 + 1{\cdot}3356\lambda + 2{\cdot}19243 \quad . \quad . \quad . \quad . \quad . \quad (37)$$

Repeating the process, keeping more figures in the calculation, the following numbers are obtained :—

20·4	151·3	490	687	719	150
19·0644	149·10757	448·20264	415·91664	98·40603	66·99719
	123·64516	283·06216	37·85882	47·84179	3·09969

109	6·87
4·11022	0·07415
−0·02973	

From which

$$R_0 = 0{\cdot}07415 \quad \text{and} \quad R_1 = - 0{\cdot}02973 \quad . \quad . \quad . \quad (38)$$

In the calculation of δp and δr the values of R_2 and R_3 will be taken to be those in (151)

$$\begin{vmatrix} R_1 & R_3 \\ R_0 & R_2 \end{vmatrix} = - 38{\cdot}04 \qquad \begin{vmatrix} R_1 & pR_3 - R_2 \\ R_0 & rR_3 \end{vmatrix} = 15{\cdot}69$$

and

$$\delta p = - 0{\cdot}0000934, \qquad \delta r = 0{\cdot}0000385 \quad . \quad . \quad . \quad (39)$$

The new approximation to the quadratic factor is

$$\lambda^2 + 1{\cdot}3355066\lambda + 2{\cdot}1924685 \quad . \quad . \quad . \quad . \quad (40)$$

The degree of accuracy is now approaching that with which the calculating machine can be used directly, and one further calculation brings the numerical values correct to eight significant figures.

20·4	151·3	490	687	719
19·0644934	149·1075315	448·2017	415·90833	98·3766
	123·6467755	283·0706	37·86566	47·8068

150	109	6·87
66·98073	4·18518	−0·002266
3·13449	−0·000949	

R_0 is now —0·002266 and R_1 is —0·000949 as compared with the —3·634 and 7·199 of (34).

$$\begin{vmatrix} R_1 & R_3 \\ R_0 & R_2 \end{vmatrix} = -0·164 \qquad \begin{vmatrix} R_1 & pR_3 - R_2 \\ R_0 & rR_3 \end{vmatrix} = -1·404$$

$$\text{and } \delta p = -0·00000040, \ \delta r = -0·0000034 \quad . \quad . \quad . \ (41)$$

The quadratic factor is

$$\lambda^2 + 1·3355062\lambda + 2·1924651 \quad . \quad . \quad . \quad . \quad . \ (42)$$

with an accuracy which probably extends to the last digit.

The method of approximation will be seen to correspond with Newton's method of approximation to the value of real roots, and it is greatly assisted by the use of a calculating machine. No counterpart of Horner's process for real roots is known, the nearest approach to it being one described by Jelinek. All such methods require special consideration in the case of repeated roots, but such cases are not of sufficiently common occurrence to make a detailed discussion necessary.

INDEX

                                            2 o

THE END